DOWNWARD PARTICLE FLUXES AND SEDIMENT ACCUMULATION RATES RELATED TO THE ORGANIC CARBON AND BIOGENIC SILICA CYCLES IN THE GERLACHE AND WESTERN BRANSFIELD STRAITS, ANTARCTICA

INSTITUTO DE CIENCIAS
DEL MAR DE BARCELONA
(C.S.I.C.)

UNIVERSIDAD POLITÉCNICA
DE CATALUÑA

UNIVERSIDAD DE
BARCELONA

PROGRAMA DE DOCTORADO EN CIENCIAS DEL MAR

DOWNWARD PARTICLE FLUXES AND SEDIMENT ACCUMULATION RATES RELATED TO THE ORGANIC CARBON AND BIOGENIC SILICA CYCLES IN THE GERLACHE AND WESTERN BRANSFIELD STRAITS, ANTARCTICA

Enrique Isla

Memoria para optar al título de Doctor en Ciencias del Mar por la Universidad Politécnica de Cataluña, bajo la dirección del Doctor Albert Palanques Monteys, del Instituto de Ciencias del Mar de Barcelona (C.S.I.C.)

Barcelona, Junio de 2001

A la casa y a Núria

Hay que inventar, hay que hablar, hay que crear, aun a riesgo de hacer locuras y disparates o de rasparse las rodillas y el alma. Eso es lo que vale la pena.

Eduardo Galeano

AGRADECIMIENTOS

En primer lugar quiero agradecer al Dr. Albert Palanques por haber dirigido este trabajo y por su constante apoyo a lo largo de todo este proceso. Agradezco también la confianza que desde el principio depositó en mi y que me ha permitido trabajar con completa libertad de decisión y acción. Su visión global del medio marino y su postura abierta a la discusión han sido valiosas guías para ayudarme a entrar al interesante estudio de la dinámica sedimentaria en los océanos.

A todos mis compañeros de la Unidad de Geología Marina del Instituto de Ciencias Marinas que siempre me dieron su ayuda y consejos en cuanto los necesite. Empiezo especialmente por Ana. Mi gran compañera de tesis que me aguanto en el despacho y en el laboratorio todos estos años. Ella me enseñó, entre muchas cosas más, a cuantificar sílice biogénica. Su apoyo moral y físico fue siempre incondicional y absoluto, los momentos más difíciles e incómodos habrían sido mucho más ásperos sin su compañía y solidaridad. Al Dr. Pere, el "veterano" que me enseñó las técnicas para analizar las muestras de las trampas de sedimento y que me dió muy útiles consejos para empezar con el pie derecho en este estudio. También le debo el descubrimiento del extraño mundo del "carajillo Pujol". A Jorge por hacer que invariablemente, campañas oceanográficas, discusiones científicas y pláticas informales tuvieran un agradable ambiente de buen humor. Además por ayudar a mejorar notablemente el alcance de nuestros trabajos con su peculiar punto de vista. A Bene, que me dio la bienvenida al laboratorio de sedimentología y que hizo análisis granulométricos hasta que el sedigraph nos dejó. También por su apoyo, compañerismo y por siempre estar animándome y aconsejándome para no distraerme y terminar con este estudio. A Neus, "News", que siempre con buen humor, compartió conmigo las explosiones del LECO. A Mohamed mi otro compañero de despacho que me aguantó y me ayudó más de lo que él cree. A Belén, a Gemma, a Marcel.lí y a Jesús por su amable ayuda siempre que la necesite. A Graziella, Ferrán, David, Fernando, Susana, Ludovic, Annick, Belén, Luis, María José, Sandra, Marta y los "nuevos fichajes" del despacho Marc y Jacobo. Entre todos hicieron una ambiente de trabajo muy agradable durante estos años.

A todo el personal del Instituto de Ciencias del Mar, que siempre amable y eficazmente me ayudaron y me facilitaron cualquier tarea.

A los Doctores Pere Masqué y Joan Albert Sánchez Cabeza y su grupo del Laboratorio de Radioactividad Ambiental de la Universidad Autónoma de Barcelona que realizaron los análisis del ^{210}Pb y cuyos comentarios ayudaron a mejorar el contenido de nuestros trabajos.

A la Dra. Mª de los Angeles Bárcena de la Universidad de Salamanca por los análisis de micropaleontología.

A la Dra. Martha Ferrario de la Universidad Nacional de La Plata por la identificación de las diatomeas.

Al Dr. Josep Mª Gili por compartir conmigo su rica visión multidisciplinar de los procesos marinos e invitarme a colaborar con él. También por enseñarme una postura incansable y positiva ante situaciones adversas.

A Martha, Nuria y el Dr. Cross por sus correcciones a mi inglés.

A Nuria por su ayuda en los análisis estadísticos y sus sutiles sugerencias en el estilo y presentación del manuscrito. También por dejarme trabajar en su laboratorio y facilitarme todo lo que necesité. L'aigua fresca al camp del pagès.

A Joan por sus valiosos consejos que me ahorraron días de trabajo usando el word y por sus elegantes sugerencias en el formato del manuscrito.

A Juanita por su compañerismo, por admitirme en su laboratorio y por prestarme su máquina cuando emprendí la campaña alemana.

A Cova por tenerme de "okupa" en su despacho y además por hacer de éste un apretado ambiente agradable.

To Andreas, that kindly allowed me to work in his office.

To Fidane and Hubertus for receiving me in their office and make me feel, as it was mine. They together with Lucie, José, Johannes, Katja, Sabine, and Astrid made my stay at Bremerhaven very pleasant.

Very especially to Dieter for allowed me to work at the AWI and for make my stay there pleasant and productive. His kind comments were very helpful as well. Viele danke.

A Victoria y Alfonso por respaldarme siempre y especialmente para conseguir la beca que me permitió desarrollar este estudio.

A Aida, su madre, Eduardo y Octavio, por recibirme como un miembro de la familia.

A mi familia, mi puerto seguro.

A Diego y Kalin, mis brújulas.

A Hugo, Aramis, Octavio, Eduardo y Ramón por suavizar mi aterrizaje en Barcelona y en el Instituto, también por los cafés de las 11. También a Margarita, los Güeros, Alex, César, Roberto, Enrique, Pepe, los Blasco, los Bigorra, Miren, Maricarmen y Ernesto.

A María del Mar, por su compañía y apoyo constantes y sólidos y todas sus enseñanzas.

A Joan "gregario mayor", gran amigo y compañero por esa genial e inolvidable travesía que al parecer apenas empieza.

A Eulalia y Claudio por estar siempre ahí.

A Antonio, Antonia, Estrella y Juan Carlos y por hacerme sentir badiano.

A Rosa y Julio por aguantar las historias de Tupac Amaru.
A Alex, el discípulo del capitán Garfio, por ayudar siempre que fué necesario.

A Genoveva e Isabel de la Universidad Politécnica de Catalunya por su gran ayuda.

Al Dr. Ricardo Anadón, jefe del proyecto FRUELA, dentro del cual está enmarcado este estudio.

A los proyectos de investigación: REF. ANT94-1010. Flujo de carbono en un área de elevada productividad: cuenca occidental del Estrecho de Bransfield y Estrecho de Gerlache, Antártida. y MAR96-1781-CO2-01. Flujos sedimentarios asociados al intercambio en zonas de mares semicerrados y frentes. Financiados por la CIRIT.

Al Consejo Nacional de Ciencia y Tecnología (CONACYT) de México por concederme una beca doctoral para realizar este estudio.

A la tripulación del buque oceanográfico "Hespérides" sin cuya colaboración no se habría podido realizar esta investigación.

PROLOGUE

The biogeochemical cycle of the carbon in the oceans rules the fate of the gaseous carbon dioxide (CO_2) that is increasing the temperature in the earth's atmosphere. The carbon cycle is as variable as any other nature's expression and its spatial and temporal changes make this complex system difficult to analyse. The introduction of mathematical models trying to simulate this structure is enhancing the knowledge of the relations between gaseous CO_2 in the atmosphere and its final storage in the bottom sediment of the oceans. The connection of the model results with the real systems behaviour is linked to the amount and qualities of the data, which are used to build and calibrate these models. Taking into account, the area and diversity of the global ocean the particular and detailed information about the cycle of carbon in relatively small areas is still poor.

Since the beginning of the last century, particular areas of the Antarctic Ocean as the Antarctic Peninsula margin have been identified as highly productive zones. In this area, primary production supports a large biologic activity. Thus, carbon fluxes from the ocean surface to the deep sea may bear a special interest. Nevertheless, research on the cycle of carbon in this part of the ocean is still limited. The aim of the present study is to contribute with detailed information of the biogeochemical cycles of carbon and biogenic silica in an area where these kind of measurements is scarce.

This study has been structured in several parts and it has been written in the English language in order to make the access to its findings easier to the potential readers that, due to the international status of the study area, may be attracted from many countries.

In Part I, includes a description of the study area and the biochemical cycles of carbon and biogenic silica in the Antarctic Ocean. The description of the study area is focused in the primary productivity and the sedimentary processes along with the water circulation.

In the Part II, it is explained the methodology to obtain the samples on the field and the posterior treatment in the lab. The location of the sampled sites within the study area is presented with a Table and a map.

Part III is divided in two chapters. In the first chapter a detailed description of the sediment cores is given along with figures of each measured variable. At the end a brief summary and a detailed Table with information about sediment accumulation rates complete the chapter. The second chapter describes the temporal variations and the constituents of the settling particle fluxes at two sites in the study area. The end of the chapter includes five Tables that complete the information of every sampling period.

In Part IV the interpretation of the results through its relation to the primary productivity, the bottom topography and the water circulation pattern is explained in two chapters. The first chapter is devoted to the bottom sediment and the second to the settling particulate matter.

The Part V is composed by a summary of the main findings, the final conclusions, and a section where ideas for future research are proposed in order to improve the knowledge of this Antarctic system. At the end of the summary one figure illustrates an approach to the organic carbon and biogenic silica budget in the study area.

Part VI contains the list of the literature referenced in this study.

Part VII is a section with all the articles related to this study.

INDEX

PART I. INTRODUCTION

¿Porqué no pones el título de los capítulos en letra algo más grande y centrado?

1. CARBON AND BIOGENIC SILICA FLUXES IN THE ANTARCTIC MARINE ENVIRONMENT

Since 1800 the carbon dioxide (CO_2) concentration in the atmosphere has increased exponentially (Fig 1.1). This phenomenon is mainly due to the combustion of fossil fuels and deforestation (Siegenthaler and Sarmiento, 1993). The temperature of the earth atmosphere has been increasing as well because the CO_2, as other green house gasses, absorbs the infrared radiation emitted by the Sun and it does not allow it to leave the Planet. Therefore, the study of the carbon cycle is a main key to better understand the global climatic change. During the last three decades the advance in the knowledge of the carbon cycle has grown substantially (McCarthy, 2000). Nevertheless, it is still necessary to improve on more accurate estimates for essential reservoirs and fluxes within this biogeochemical structure (Fig. 1.2).

In the oceans, photosynthesis, or primary production, reduces the partial pressure of the CO_2 in surface waters by converting the gaseous CO_2 into particulate and dissolved organic carbon. This carbon is transported through different means from the euphotic zone to the deep ocean, where is finally buried in the bottom sediment. The reduction of the CO_2 partial pressure due to the uptake of gaseous carbon by primary producers and its exportation to the deep ocean is known as the “biological pump”.

The Southern Ocean (south of 50°S) plays a special role in this context. In this area, primary production is generally not restricted to the availability of nutrients (Wefer and Fischer, 1991), and it occupies a special place in the control of atmospheric CO_2 due to its great area, about one fifth of the World Ocean. The ocean surrounding Antarctica has a high potential to extract gaseous CO_2 from the atmosphere when, during the austral spring and summer, primary production and organic carbon flux out of the surface layers zone increase (Wefer et al., 1988; Wefer and Fischer, 1991). In order to estimate the magnitude of these processes in the Southern Ocean within the global carbon cycle, primary production rates and the organic carbon export production out of the euphotic zone has to be known.

Up to the date, the best way to measure the fluxes of organic matter along the water column is with sediment traps. These tools allow to measure organic matter fluxes at different depths and to establish their temporal differences.

During the last decade several studies with sediment traps were carried out in the Bransfield Strait (Wefer et al., 1988; Karl and Asper, 1990; Karl et al., 1991; Wefer and Fischer, 1991) and in the Ross Sea (DeMaster et al, 1991; DeMaster et al., 1992; Nelson et al., 1996). Nevertheless, the information obtained by sediment traps in the Bransfield and Gerlache Straits was rarely complemented with primary production measurements and sediment cores studies.

The FRUELA project “Flujo de carbono en una area de elevada productividad: Cuenca Occidental del Estrecho de Bransfield y Estrecho de Gerlache, Antártida.” is focused into analyse and describe the carbon flux in an area that, despite its very high primary productivity has not been studied in detail (Anadón and Estrada, in press). There are no studies where the connection between the surface waters (primary productivity) and the bottom sediment (organic mater finally buried) of these areas is described.

a)

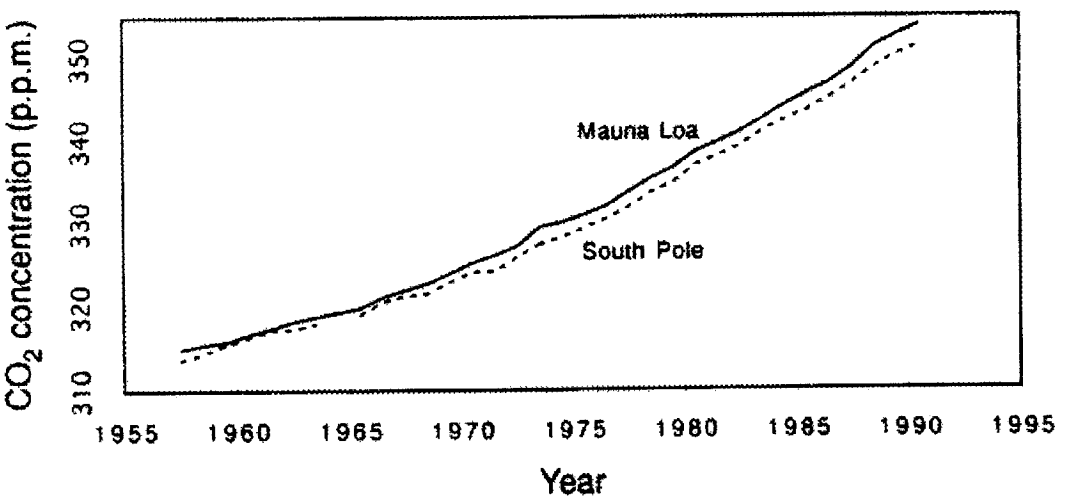

b)

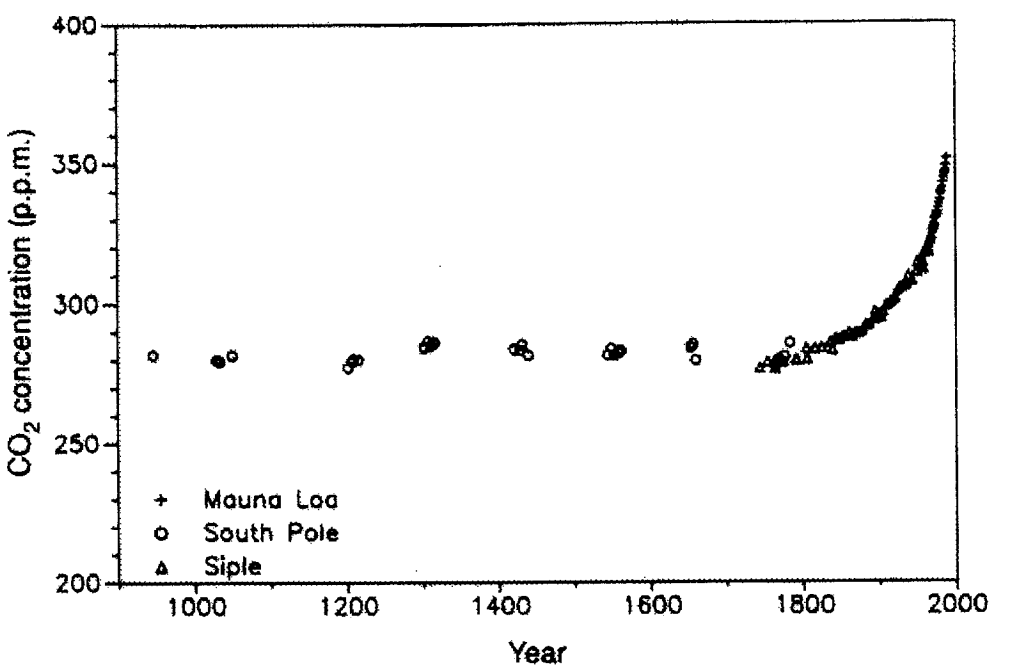

Fig. 1.1. a) Atmospheric CO_2 measurement at Mauna Loa, Hawaii and at the South Pole. b) Record of atmospheric CO_2 for the past 1000 yr, given by direct atmospheric observations at Mauna Loa (+) and measurements on Antarctic ice cores from Siple station (△) and South Pole (O). Taken from Siegenthaler and Sarmiento (1993).

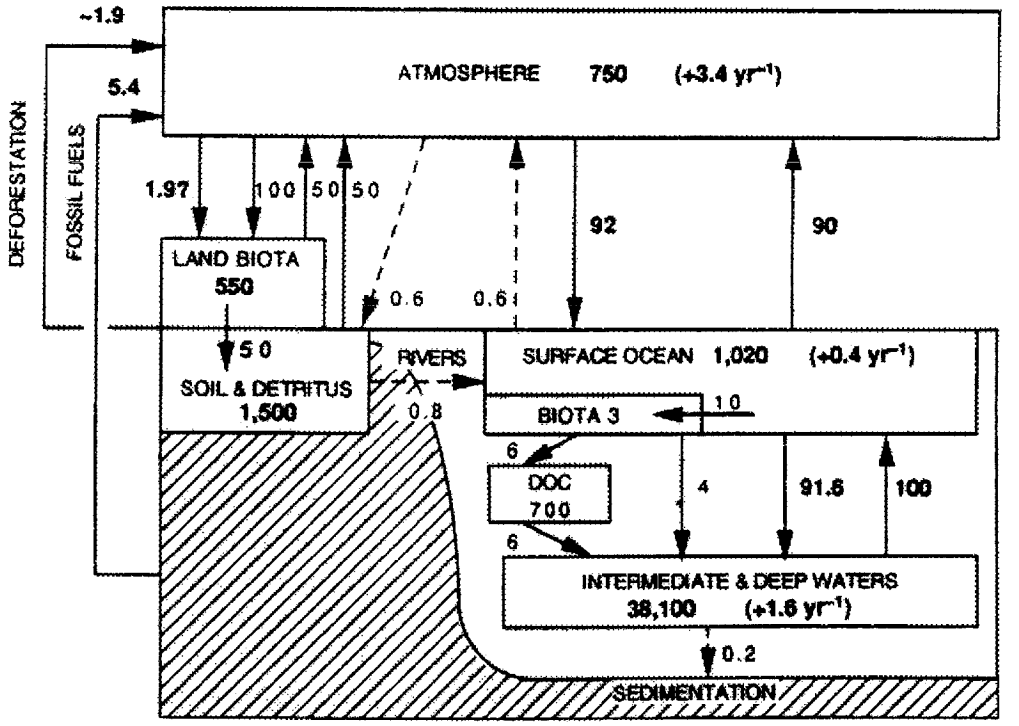

Fig. 1.2. The 1980-89 global carbon cycle reservoirs and fluxes. Units are Gt C and Gt C yr^{-1} (1Gt C = 10^{15} g C). Taken from Siegenthaler and Sarmiento (1993).

Studies about the carbon cycle in the Southern Ocean have shown that the bottom sediment in this area of the world ocean is really conserving no more than 9% of the primary produced organic carbon (Nelson, 1988; DeMaster et al, 1991). Nevertheless, this percentage accounts for less than 1% of the global budget while the same area is keeping between 50 and 75% of the biogenic silica that enters the marine environment (DeMaster et al., 1992; Tréguer et al., 1995). Therefore, the biogeochemical cycle of silica (SiO_2) in the Southern Ocean occupies a special place in the global context.

The cycle of Si (Fig. 1.3) in the marine environment initiates when the primary production activity takes dissolved silica, as silicic acid, and transforms it into particulate biogenic silica. At this point the cycle of Si is linked to that of the carbon (Tréguer et al., 1995). Diatoms, radiolaria, siliceous sponges and silicoflagellates utilise silicon to grow and to build up their solid structures. Thus, high primary productivity areas should be connected to high biogenic silica deposition in the bottom sediments.

The high BSi content in the bottom sediment related to the apparent mean annual low productivity in the surface waters of the Southern Ocean is known as the "opal paradox". This fact has been explained by the good preservation of BSi in the bottom sediment promoted at least in part by low temperatures (DeMaster et al., 1996). Nevertheless, a recent proposal (Pondaven et al., 2000) suggests that opal production has been underestimated and opal accumulation rates overestimated.

Due to the major importance of diatoms in the biological pump in the Southern Ocean and to the presence of silica-rich sediments, opal (amorphous biogenic silica) has a strong potential as a proxy for paleoproductivity reconstruction. However, the high spatial variation in biogenic silica preservation and in the magnitude of decoupling between Si and C cycles in the marine environment has stopped paleoreconstructions after biogenic silica analysis. Thus, in order to obtain a better calibration of this proxy more information about the budgets of biogenic silica and its relation with the carbon cycle is still required.

This study is focused in the western Bransfield and Gerlache Straits. These areas have been identified as high primary productive marine environments (Burkholder and Sieburth, 1961; v. Bodungen, 1986; Huntley et al., 1991; Karl et al., 1991; Anadón and Estrada, in press). Therefore, they are supposed to have high organic matter downward fluxes and accumulation rates when compared with other regions of the Southern Ocean.

Western Bransfield Strait basin is a water masses mixing area, close to volcanic activity spots (Deception Island) and is the natural end of the Orleans Trough which might be acting as a natural sediment trap. This basin could be reflecting sedimentary processes above it and along the trough. Due to its location it brings the possibility to identify differences between vertical and lateral particle inputs. The latter may play an important role in redistributing organic matter from highly productive areas.

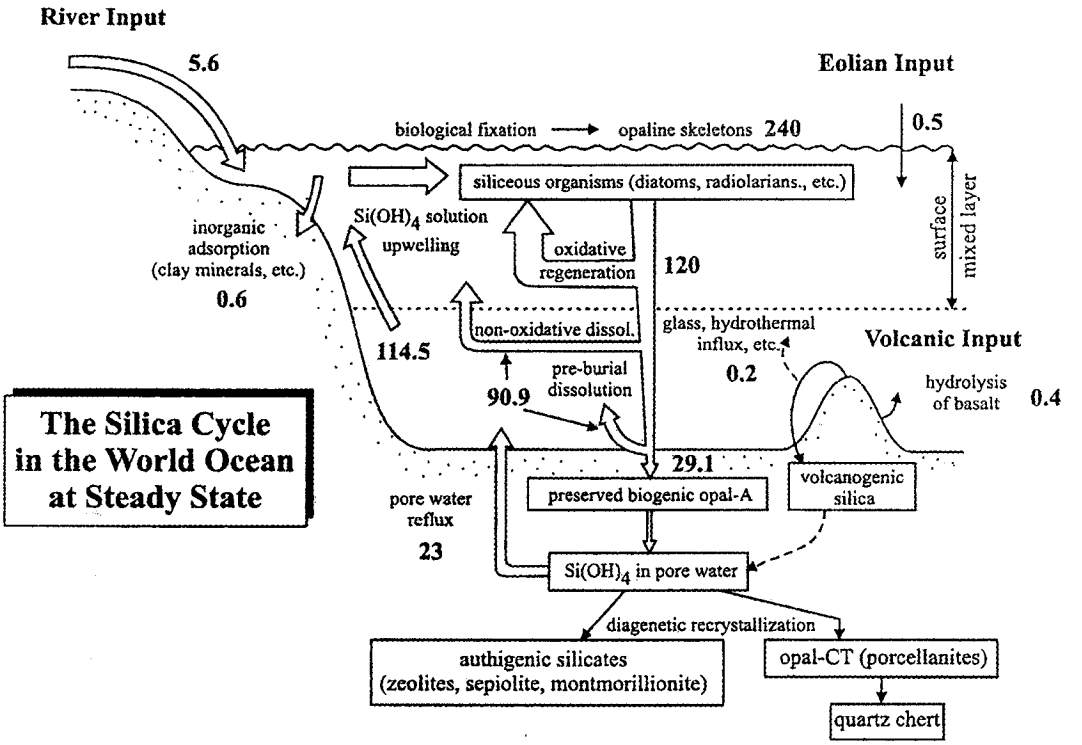

Fig. 1.3. Biogeochemical cycle of silica in the world ocean at steady state. Taken from Rickert (2000) after Tréguer et al. (1995).

2. STUDY AREA

The study area comprises the western Bransfield and Gerlache Straits and their confluence with the Bellingshausen Sea.

2.1. BRANSFIELD STRAIT

The Bransfield Strait owes its name to the British explorer Edward Bransfield who, in 1820 discovered the northwestern coast of the Antarctic Peninsula.

The Bransfield Strait is a narrow (approximately 100 km wide), elongated ENE-WSW basin located approximately between 54° W 61° S and 63° W 64° S (Fig. 2.1). It is limited by the northern margin of the Antarctic Peninsula and the southern margin of the South Shetland Archipelago. It extents for approximately 460 km from the Clarence Island vicinities towards Low Island at the southwest. The Bransfield Strait is a Cenozoic, extensional back-arc basin with hydrothermal (Schlosser, et al., 1988) seismic and volcanic activity (Pelayo and Wiens, 1989). The only active subaerial volcanism in the region occurs in Deception Island, though there is evidence of recent activity in Penguin and Bridgeman Islands (Jeffers and Anderson, 1990). The western margin of the Strait has the steep slope of the South Shetland Islands, which is incised by six troughs. The eastern margin has four troughs that cut the broad shallow shelf of the Trinity Peninsula to a depth of 750 m. The U-shaped cross-sectional profiles of these troughs suggest that they are glacially carved features. They appear to connect with glacial drainage systems onshore (Jeffers and Anderson, 1990). The shelf brake occurs at about 250 m depth, and a second platform deepens gradually from 750 at the outlets of the troughs to about 900 m depth. A steeper slope leads to the basin floor, which deepens from 1300 at the southwest end of the central subbasin to more than 2000 m southeast King George Island. The margins of the eastern basin are free of the large troughs seen farther to the southwest. The Bransfield Strait is divided in three sub-basins: western, central, and eastern, each of them separated by the highs of Deception and Bridgeman islands respectively (Fig. 2.2). The western sub-basin is the shallowest within the Strait, with a maximum depth of about 1500-m, it is adjacent to landmasses with large glacial drainage systems. In this sub-basin the bottom topography is extremely rugged at depths shallower than 500 m (Jeffers and Anderson, 1990).

The coast of the Bransfield Strait is abrupt and shows a high number of bays with different shapes. A small bay of the western part of the Strait, the Johnson's Dock, has been studied. Johnson's Dock is a semi-enclosed small bay located in Livingston Island's South Bay (South Shetland Islands), next to the Spanish Antarctic Base (Fig. 2.3) (approximately 60° 22.5'W, 62° 39.3'S and 60° 21.75'W, 62° 39.6'S). This dock is approximately 750-m long and 550-m wide. It has several depressions of more than 20-m depth that are confined by the till deposits of the frontal morraine of the Johnson's glacier. It is connected to Livingston Island's South Bay through a small mouth about 75-m wide and 40-cm deep.

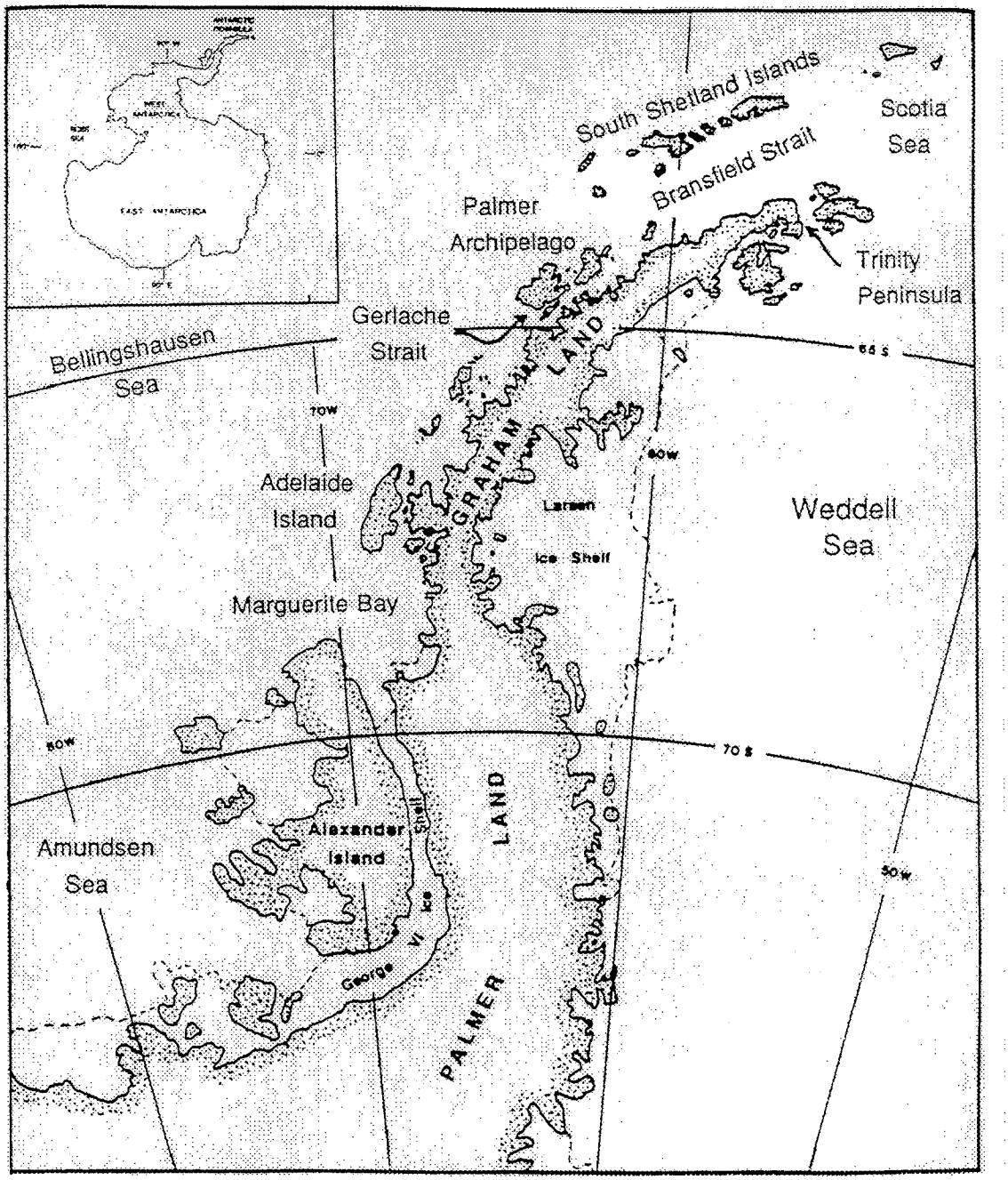

Fig 2.1. Location of the Bransfield and Gerlache Straits in the Antarctic Continent. Taken from Harden et al., 1992.

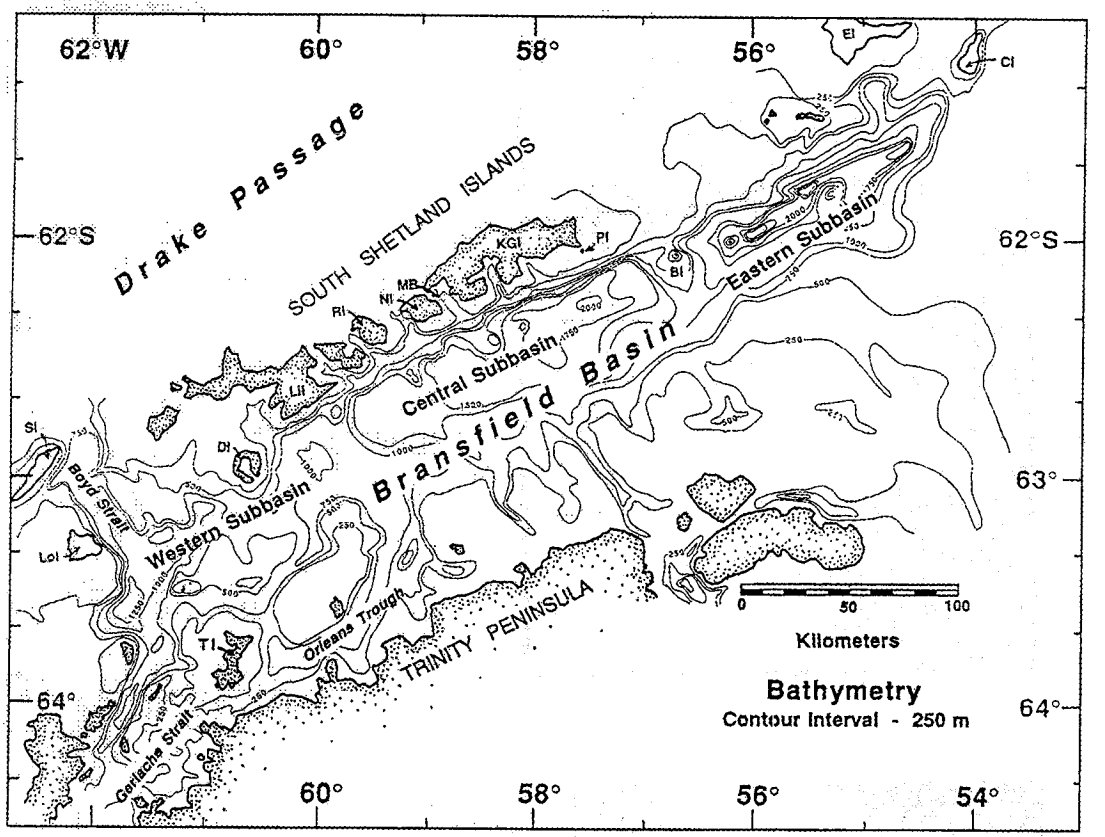

Fig. 2.2. Bathymetry of the Bransfield Strait, showing locations of western, central, and eastern sub-basins. Contour interval 250 meters. BI= Bridgeman Island, CI= Clarence Island, DI= Deception Island, EI= Elephant Island, KGI= King George Island, LII= Livingston Island, LoI= Low Island, MB= Maxwell Bay, NI= Nelson Island, PI= Penguin Island, RI= Robert Island, SI= Smith Island, TI= Trinity Island. Taken from Jeffers and Anderson (1990).

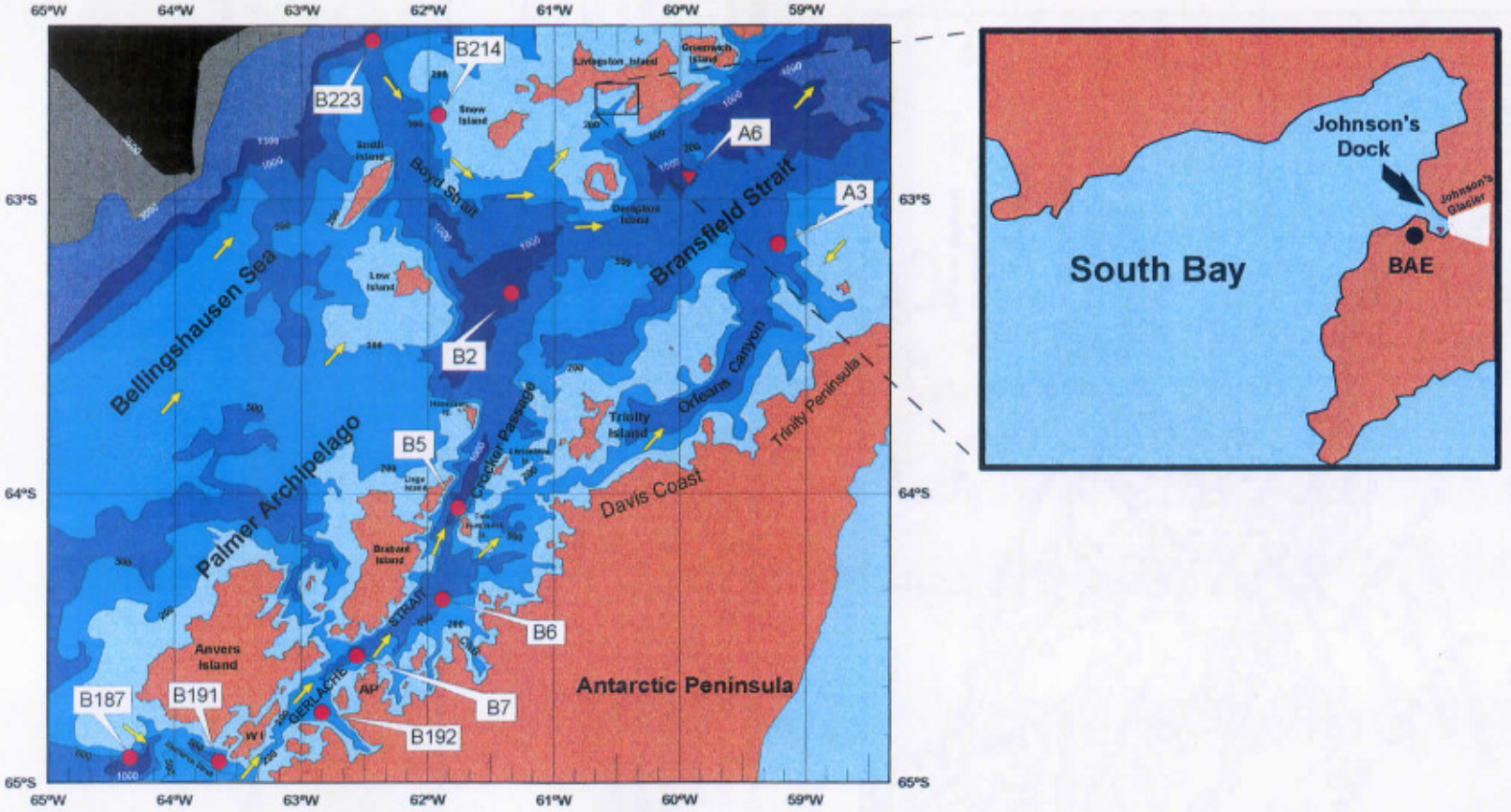

Fig. 2.3. Area of study. Yellow arrows indicate the main surface circulation pattern. Arctowski Peninsula is indicated as AP, Charlotte bay as ChB, and Wiencke Island as WI. The Spanish Antarctic Base, Juan Carlos I is indicated as BAE. Red circles indicate sediment core sampling sites and red triangles sediment trap and core sites.

2.1.1. Sedimentology and sediment accumulation rates

Present day settling particle matter all over the strait is a mixture of terrigenous and biogenic material. The latter account for approximately 20% of the total dry weight and is composed mainly by biogenic silica and organic carbon (Dunbar et al., 1985; DeMaster, 1987, Gersonde and Wefer, 1987; DeMaster, et al., 1991; Yoon et al., 1994; Palanques et al, in press). As in the present days, during the glacial cycles the terrigenous sediment was supplied mainly by glacial-marine processes (Anderson et al., 1980; Drewry and Cooper, 1981; Domack et al., 1994; McGinnis et al., 1997; Prieto et al., 1999).

Jeffers and Anderson (1990) give the best description of the Strait's sedimentary processes.

The fine material settled at depths shallower than 250 m is intensely scoured by currents. Singer, (1987) found textural evidence of winnowing by marine currents exceeding 0.11 cm/s. Just coarse ice rafted debris and volcanic lapilli remains at these areas. The current effect diminishes with depth making the slope deeper than 250 m the deposition site of the current derived sand and silt eroded from shallower depths and of the material that bypasses the shelf entirely. Mostly these deposits are muddy sands and sandy muds, with a general tendency to fine as water depth increases. Ice rafted pebbles are also present, but clearly less than in shallower sediments. Sediment gravity flow deposits are present on steeper slopes. Proximal facies are preserved as well. Poorly graded gravels, coarse sands and unsorted conglomerates are typical deposits. On the basin floor the dominant biogenic component is the biosiliceous material, mostly diatom tests and their fragments. The main part of the terrigenous fraction, is quartz silt, which is more abundant near the base of the slopes. The volcanic component includes ash from subaerial and submarine eruptions, this material occurs mostly disseminated throughout the sediments and as discrete ash layers, sometimes several centimetres thick (Jeffers and Anderson, 1990). Clay mineral data from cores in the King George Island indicate a decreasing importance of volcanic activity through time (Yoon et al., 1994). Typical basin floor deposits are ashes bearing diatomaceous muds and oozes. Volcanic material from recent subaerial eruptions is abundant near Deception Island (Jeffers and Anderson, 1990).

Bays and associated canyons of the South Shetland Islands margin are potential conduits for delivery of terrigenous material to the fanlike depositional lobes on the basin floor. Maxwell Bay, in King George Island, is the only capable to deliver large volumes of sediment to the basin and it has overfilled its bathymetric sill (Griffith and Anderson, 1989; Jeffers and Anderson, 1990). The other bays may deliver suspended sediment through water plumes of glacial origin. Trinity Peninsula Shelf troughs do not appear to carry significant amounts of terrigenous material to the basin. They are filled with diatomaceous mud and oozes like those on the basin floor. Slumping of the canyon walls may account for the occasional coarse-grained material in cores recovered from the troughs (Jeffers and Anderson, 1990).

Glaciers on the peninsula side of the strait do not produce sediment laden melt water in large volumes as those of the islands because glaciers from the Trinity Peninsula

are not exposed to high precipitation regimes relative to those experienced at the South Shetland Archipelago (Griffith and Anderson, 1989).

During the austral summer the sea bed of the strait receives mainly biogenic material due to the high primary production activity in the surface water (Yoon et al., 1994).

In the western sub-basin there is little evidence of substantial sediment accumulation at depths shallower than 800 m. There are sediments delivered, perhaps glacially, to the basin through the Orleans Trough during glacial maximum periods (Jeffers and Anderson, 1990).

Sediment accumulation rates in the Strait have been identified via ^{210}Pb and ^{14}C radiometric analysis. These results ranged between 0.02 and 0.5 cm/y along the Strait (Nelson, 1988; Harden et al., 1992). Harden and collaborators (1992) suggested that sedimentation processes have been more or less constant on 100 and 1000-yr time scales.

2.1.2. Water masses, circulation, and sea-ice coverage

The Bransfield Strait is a semi-enclosed sea. Its water exchanges with the oceanic surroundings are limited by the local bathymetry. At the western end, depth exceeds 500-m only at the passage called Boyd Strait, between Smith and Snow Islands. At the eastern boundary, the channels connecting the eastern basin with the Southern Ocean around Clarence Island are less than or very close to 1000-m depth. Thus, the waters of the basins have no direct communication with the open ocean at depths much below 1000-m (Gordon and Nowlin, 1978). Intermediate and deep waters, such as the Circumpolar Deep Water (CDW) have a difficult access to the Strait (Sievers, 1982).

In the upper 500-m cold (less than 0°C), salty (34.1-34.6 psu) and weakly stratified Weddell Sea Water (WSW), enters the Strait over the broad continental shelf around D'Urville and Joinville Islands. It flows southwestward along the Trinity Peninsula margin. At the north of Tower Island and between Trinity and Tower Islands the WSW apparently converges with warmer (2.25°C), fresher (33.5 psu), and vertically stratified water from the Gerlache Strait. These waters make a front and a stream that flows northward and joins the Bransfield Current (BC) (Niiler, et al., 1991; García, et al., 1994). The BC transports the warm (0.5-3.0°C), fresh (33.1-33.9 psu) and stratified Bellingshausen Sea Antarctic Superficial Water (BSW) that flows northeastward along the South Shetland Islands southern margin and around Deception Island with an important speed (Sievers, 1982). At the same it is changing its original properties due to, at least in part, the melting of the ice during the summer (Gordon and Nowlin, 1978). The BSW enters the Strait between the Snow and Smith Islands over the Boyd Strait and between Smith and Low islands making a front with the WSW approximately at the middle of the Strait. This front is essentially a surface feature and it has an important interannual variability; it can move toward the north about 50-60 km (García, et al., 1994). Below the mixed layer, a slope front is present at each side of the Strait. The sharpest front occurs along the South Shetland Islands slope. It is associated with the relative strong BC geostrophic flow toward northeast. On the Antarctic Peninsula slope the front is weak formed by a counter-current that flows

slowly toward southwest (García, et al., op. cit.). Between 300 and 500 m depth Circumpolar Deep Water (CDW) gets into the Strait through the eastern side of the Boyd Strait. This warm water makes a band that flows along the South Shetland Islands margin and leave the strait by the north end (Capella, et al., 1992).

Clowes (1934) found that deep and bottom waters of the Bransfield Strait were unlike those of the adjacent deep oceans and he concluded that the bottom water inside the strait is originated within the Strait. Bottom waters of the three subbasins of the strait are colder, fresher, with more dissolved oxygen and less nutrients than those of their oceanic vicinities (Gordon and Nowlin, 1978). These authors found that there are important convection events that transport cold winter water from the upper layers to the deepest part of the basin (2600 m approximately). During the austral summer the upper ocean in the strait is too warm and fresh to be considered as a deep-water formation source (Gordon and Nowlin, op. cit.). During the winter, due to the thermohaline alteration, all the water of the shelf and part of the continental rise is practically homogeneous (Sievers, 1982). The deep and bottom water formed in the Strait apparently does not leave the basin since there is no influence of it in the adjacent oceanic waters of similar density (Gordon and Nowlin, 1978).

On a regional scale, sea ice generally undergoes seasonal growth and decay, controlling surface water primary productivity. During the winter (July-October) the Strait remains ice covered with limited primary productivity, whereas during the summer (December-April) the area is completely ice free, giving rise to increased phytoplanktonic activity (Griffith and Anderson, 1989; Yoon et al., 1994).

The Johnson's Dock is a stratified system during summer with a low-salinity surface layer due to the ice melting inputs. Wind activity (mainly from the first quadrant) can produce vertical mixing by convection (Isla et al., 2001).

2.1.3. Productivity

The western coast of the Antarctic Peninsula is among the most productive areas of the world ocean like those rich upwelling coasts of Africa and Southamerica, though it experiences a strong seasonal variation (Steemann Nielsen, 1975; Raymont, 1980) (Fig. 2.4).

During the 1920's and 1930's British scientists gave the first extensive literature on the biology of the Bransfield Strait based on the results of the Discovery expeditions promoted by the whaling industry over the Southern Ocean (Huntley et al. 1991). Studies on krill as the principal whale food, had preceded research all over the trophic chain, and the Bransfield Strait has been identified as an area with high biological productivity in the euphotic surface waters (Burkholder and Sieburth, 1961; v. Bodungen, 1986; Huntley et al., 1991; Karl et al., 1991; Anadón and Estrada, in press). This high productivity has an annual variation with an intense phytoplankton bloom developed mainly in December and January, during the Austral summer (Wefer et al., 1988; Holm-Hansen and Mitchell, 1991; Huntley et al., 1991), and an abrupt decay from February to March (Wefer et al., 1988; Holm-Hansen and Mitchell, 1991).

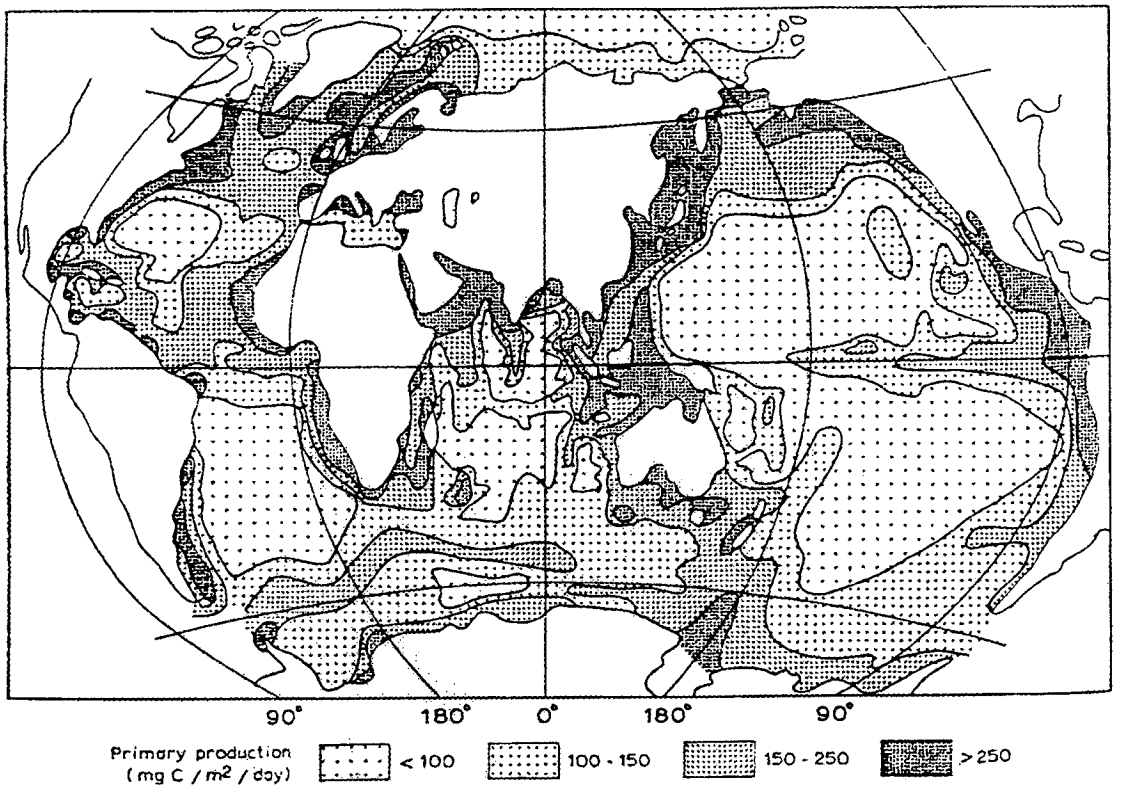

Fig. 2.4. Distribution of primary production in the World Ocean. Taken from Raymont (1980).

Light and both micro and macro nutrients do not appear to be the major factors responsible of the phytoplankton decline but probably sinking and advective transport processes and/or grazing (Holm-Hansen and Mitchell, 1991). V. Bodungen et al. (1986) identified copepods as the most important grazers. In specific areas their grazing pressure was equivalent to approximately the 50% of daily primary production. Nevertheless, krill grazing pressure could have local intensity but little importance on controlling blooms development in a wider range (v. Bodungen, 1986; v. Bodungen et al., 1986).

Although sinking of resting spores counts for much of the phytoplankton biomass below the euphotic zone, this process removes less than the 50 % of the bloom biomass (Holm-Hansen and Mitchell, 1991). V. Bodungen et al. (1986) suggest that sinking of viable cells or resting spores is strongly related to bottom topography and hydrodynamic features and these associations are a factor of major importance on the development of the bloom demise but also on its build-up.

Rapid sinking of phytoplankton cells as resting spores not only accompanies the cessation of growth but also has been identified as a survival strategy, because this flux transports to the bottom of the shelf the seed to develop the following bloom (Smetacek, 1985; v. Bodungen et al. 1986; Karl et al., 1991). It has ecological implications as well because such transports to deeper zones make those environments a richer organic matter source over a longer period of the year than the water column (v. Bodungen et al. 1986).

Strong vertical mixing may promote diatoms grew over dinoflagellates, this indicates that among other factors the mixing regime could be of importance for species selection (v. Bodungen, 1986). Therefore, important in determining the quality of the material supplied to the bottom as well.

The resuspension of resting spores from the sea floor depends directly on current intensity and bottom depth, since each species has different resuspension and spore development conditions. Bottom topography and dispersion by currents determine the differences between species and areas of influence (v. Bodungen et al. 1986).

The southwestern portion of the Bransfield Strait and its proximity to the Gerlache Strait and the front between Weddell Sea and Bellingshausen Sea waters appear to be the areas of the Strait identified with the highest chlorophyll-a -as biomass- and primary productivity values. The northeastern half of the strait, the South Shetland Islands surroundings, excluding Deception Island, and the oceanic regions have the lowest values (Burkholder and Sieburth, 1961; Mandelli and Burkholder, 1966; v. Bodungen, 1986; Holm-Hansen and Mitchell, 1991; Huntley et al., 1991; Berdalet et al., 1997; Basterretxea and Arístegui, 1999; Hernández-León et al., 1999). The values of integrated chlorophyll-a (0-50 m depth) vary between 11 mg m^{-2} in the oceanic regions of the Bellingshausen Sea on the western side of the South Shetland Islands (Mandelli and Burkholder, 1966) to 550 mg m^{-2} on the Antarctic Peninsula continental shelf, close to the Gerlache Strait (Holm-Hansen and Mitchell, 1991). Primary productivity values range between 120 mg C $m^{-2}d^{-1}$ in the oceanic regions in the Bellingshausen Sea, (Mandelli and Burkholder, 1966) and more than 3000 mg C m^{-2} d^{-1} on the Antarctic Peninsula continental shelf (Holm-Hansen and Mitchell, 1991).

2.2. GERLACHE STRAIT

In January of 1898, the Belgian RV "Belgica" arrived to the coast of Graham Land, Antarctic Peninsula, and started a slow work on the string of islands on the opposite coast. The 29 year old captain of the ship, Adrien de Gerlache, named the passage between both coasts as Belgica Strait, today we now it as Gerlache Strait in honour to its discoverer.

The strait is located approximately between 61° W, 64° S and 64° W, 65° S. It is a very narrow passage between the northern margin of the Antarctic Peninsula and the southern margin of the Palmer Archipelago (Fig. 2.1). It extends from Hoseason and Trinity Islands and Davis Coast of the Antarctic Peninsula on the north to Wiencke and Anvers Islands and Antarctic Peninsula at Bismarck Strait on the south. It is about 180 km long and between 8 and 60 km wide. Several small islands are present throughout the strait. The Palmer Archipelago margin is steeper than that of the Antarctic Peninsula where four major bays incise the continental shelf. Because of their shape these bays were probably glacially developed. The troughs of three of them descend until 500-m depth to an almost flat central basin, with an isolated depression of about 1100-m between Liege and Two Hummock Islands. The continental slope on the peninsula margin is clearly narrower and curved than in the Bransfield Strait. The southern half of the strait has a mean depth of approximately 300-m. The Crocker Passage between Liege, Christiania and Two Hummock islands at the northeastern end is the deepest access to the strait with more than 1000-m depth.

2.2.1. Sedimentology and sediment accumulation rates

Griffith (1988) found that the bottom floor close to Palmer Archipelago is mainly composed by terrigenous mud (< 15% of biogenic silica content), whereas on the Antarctic Peninsula margin the diatomaceous fraction of the sea bed material is larger (≥ 15% of biogenic silica content). A substantial fraction of the total terrigenous input is deposited quickly and is not transported outside the Strait.

In the Gerlache Strait the input of terrigenous sediment comes mainly from basal or subglacial debris associated to glaciers grounded below the sea surface. In the Bransfield Strait the terrigenous material supply to the bottom comes mainly from sediment laden surface plumes associated to glaciers grounded above the sea level (Griffith,1988; Griffith and Anderson, 1989). As in the Bransfield Strait biogenic sedimentation and glacial deposition act as the main material suppliers.

Harden et al. (1992) using excess ^{210}Pb chronologies found a sediment accumulation rate that ranged from 0.15 to 0.51 cm/y. With ^{14}C analysis the values varied between 0.01 and 0.08 cm/y. This difference suggests that due to bioturbation events ^{210}Pb chronologies are too high or real differences in sediment accumulation rates have occurred in the Gerlache Strait between 100-yr and 1000-yr time scales (Masquè et al., in press)

2.2.2. Water masses, circulation, and sea-ice coverage

Niiler et al. (1990) discussed the surface circulation and found that there is a persistent current in the middle of the strait with a velocity of about 10–18 cm s^{-1}. This current transports water northeastward to the Bransfield Strait. They found the presence of mesoscale features on both sides of the current increasing water residence time on the sheltered bays of the Antarctic Peninsula.

García et al. (1999) suggested for the austral summer a typical water column composed by an upper layer described as Transitional Zonal Water with Bellingshausen Sea influence (TBW) that replaces Antarctic Surface Water which enters the strait over Bismarck Strait. The near-bottom layer of Transitional Zonal Water with Weddell Sea influence (TWW) takes the place of Lower Circumpolar Deep Water. This TWW hardly enters the strait over the shallow western end. Limited intermediate intrusions of Circumpolar Deep Water getting into the Strait either by the east or by the west are pointed as well. Local TBW is less saline and colder than in the Bransfield Strait due to local glaciers freshwater inputs. They proposed that no Bransfield Deep Water should be present because the western end of the strait is just about 300-m deep.

The strait is normally completely ice-covered from July to November when the ice retreats. The ice-free period is between January and April (Griffith and Anderson, 1989).

2.2.3. Productivity

Biomass and primary productivity values in the Gerlache Strait are even higher than those in the Bransfield Strait (Burkholder and Sieburth, 1961; Mandelli and Burkholder, 1966; Holm-Hansen and Mitchell, 1991; Basterretxea and Arístegui, 1999). Cochlan et al. (1993) summarise the results for surface waters in a range between 500-700 mg Chl-a m^{-2} and primary productivity values in the euphotic zone between 2-5 g C m^{-2} d^{-1}.

The high primary productivity is apparently related to the development of eddies in the sheltered coastal embayments of the Antarctic Peninsula that increase water residence time up to several months (Niiler et al., 1990). The nutrient-rich waters of the Peninsula coast become nursery grounds, from where substantial quantities of dissolved and particulate organic matter are transported outside the strait to the western Bransfield Strait and downwards. Specially to those regions where water depth is less than or equal to 250 m (Karl et al., 1991). The intense phytoplankton bloom in the Gerlache Strait during mid-December and January is followed by an abrupt decline in February (Clarke, 1988; Karl et al., 1991). This bloom demise generates a rain of non-living cells and resting spores that enriches deeper zones with organic matter (v. Bodungen et al., 1986).

There are differences in primary productivity within the Gerlache Strait during bloom conditions. The northeastern half is the most productive area (Burkholder and Sieburth, 1961; Mandelli and Burkholder, 1966; Holm-Hansen and Mitchell, 1991) but after the bloom demise it holds the lowest values as well (Karl et al., 1991). Other

areas of the Strait do not experience the same variability but show nearly identical average seasonal (December to March) values (Karl et al., 1991). These authors suggested that total annual primary production and particle flux values may be very similar along the Strait but the sea floor of the northeastern half should receive better-defined and concentrated pulses of organic matter.

PART II. METHODOLOGY

3. OCEANOGRAPHIC SURVEYS, INSTRUMENTS, AND METHODS

3.1. FIELD WORK

Three oceanographic expeditions were carried out during the 1995-96 period on board the Spanish RV "Hepérides", as part of the project, "Flujo de carbono en un area de elevada productividad (Cuenca occidental del Estrecho de Bransfield y Estrecho de Gerlache, Antártida)", (Carbon flux in a high productivity area (Western Bransfield Strait basin and Gerlache Strait, Antarctica) (Anadón and Estrada, in press).

Bottom sediment was sampled by means of a multiple corer (Bowers and Connelly) and a conventional gravity corer. Six multicores were taken along the Gerlache Strait, three in the western basin of the Bransfield Strait and two in the proximity of the Bellingshausen Sea with the neighbouring western Bransfield Strait. In addition, two gravity cores (points A3 and A6) were extracted from the western basin of the Bransfield Strait (Fig. 2.3, Table 3.1).

Settling particulate matter was sampled by sediment traps deployed at a coastal region and at a deep basin. One sediment trap was moored in Johnson's Dock, Livingston Island during summer time, from December 1997 to February 1998. Another two traps were deployed the previous summer in the western basin of the Bransfield Strait and they were recovered after one-year sampling period, from March 1995 to February 1996. The locations of the sampling sites are illustrated in Figure 2.3.

3.1.1. Sediment cores

The multicorer allow to get a maximum simultaneous extraction of 8, 10-cm diameter, sediment cores with a maximum length of 50 cm. This appliance has a guillotine-like mechanism that causes very little disturbance to the surface sediments. The acrylic tubes containing the sediment core are placed on a revolving base that works as a piston pushing the sediment upward. The sampled multicores were cut in 0.5-cm slices the upper 10 cm (top), 1-cm slices until cm 30 and then 2-cm slices until the end of it. Each slice was separated in two parts: the perimeter of the sediment core (in contact with the acrylic tube) and the inner mass, in order to remove the exterior ring which might have been mixed with the material of the adjoining levels during sampling. Both parts of the slice were stored at –14ºC in separated bags.

Gravity cores were only used with 5-m long lances with an inner diameter of 7.5 cm. The cores were stored at 4ºC until they were sampled at the Marine Sciences Institute-CSIC, Sedimentology Lab. These cores were analysed each 5 cm.

Table 3.1. Sampling sites and techniques in the study area. The water depth at which the sediment cores were taken is expressed in metres (m) and core length in centimetres (cm). For sediment traps date of deployment is indicated. Gravity corer is denoted as gravity and sediment trap as sed. trap. BAE means Base Antártica Española.

core	sampling technique	date	latitude (S)	longitude (W)	water depth (m)	core length (cm)
A3	multicorer	18/01/96	63º 10.27'	59º 19.49'	790	35
	gravity	18/01/96	63º 10.06'	59º 18.13'	810	435
A6	multicorer	17/01/96	62º 55.55'	59º 59.46'	1066	34
	gravity	29/01/96	62º 54.71'	59º 58.21'	1066	135
	sed. trap	1/03/95	62º 54.60'	59º 58.20'	1066	
B2	multicorer	6/02/96	63º 20.03'	61º 23.19'	1135	41
B5	multicorer	19/01/96	64º 03.05'	61º 45.60'	1008	33
B187	multicorer	19/01/96	64º 54.05'	64º 27.52'	714	36
B191	multicorer	04/02/96	64º 56.47'	63º 33.37'	560	34
B192	multicorer	04/02/96	64º 45.21'	62º 51.44'	283	17
B6	multicorer	20/01/96	64º 22.38'	61º 53.23'	553	35
B7	multicorer	20/01/96	64º 33.53'	62º 33.49'	830	34
B214	multicorer	27/01/96	62º 46.12'	61º 53.22'	192	34
B223	multicorer	27/01/96	62º 27.57'	62º 26.03'	1180	16.5
BAE	sed. trap	10/12/97	62º 39,50'	60º 23.20'	19.5	

3.1.2. Sediment Traps

Sediment traps are used to collect samples of settling particles in order to study temporal series of downward fluxes. This technique allow to analyse lithogenic and biogenic fluxes through the water column as for example in v. Bodungen, 1986; Stein, 1990; Abelmann and Gersonde, 1991; Leventer, 1991; Wefer and Fischer, 1991; Dunbar et al., 1998; Puig and Palanques, 1998; Thunell, 1998.

In this study the sediment traps Technicap model PPS 3 were used. The main body of this traps is composed by a cylindrical hull 100 cm height with an inner diameter of 40 cm (aspect ratio H/D= 2.5, collecting area = 0.125 m^2) and a conical lower part with a height of 54 cm and an included cone angle of 34°, which ends in a 10 cm long connecting cylinder with a 5 cm inner diameter (Fig. 3.1). In the lower part a 12 receiving cups rotary carousel is screwed on (Fig. 3.2). A programmable motor that allows the pre-setting of variable sampling intervals for each of the 12 sample cups controls the carousel (Heussner et al., 1990) (Fig. 3.3). Before deployments, each 250 ml capacity polypropylene tube, was rinsed and filled with a 5% (~ 1.7 M) formalin solution prepared from Carlo Erba formaldehyde (analytical grade 40%), mixed with 0.2 µm filtered seawater. The solution was buffered (pH ~7.5-8) with Carlo Erba analytical grade sodium borate. Formaldehyde was chosen because it appears to be a more effective poison than azide and chloroform for inhibiting microbial activity on organic material and grazing by swimmers (Knauer et al., 1984; Gundersen, 1988; Gundersen and Wassmann, 1990). After recovery, the pH was checked to ensure that the solutions remained buffered. The tubes were stored at 4°C.

3.1.3. Moorings

One line equipped with two Technicap PPS 3 sediment traps was moored at point A6 1066-m below the water surface. The deepest trap was approximately 30 meters above bottom (mab) and the other at 530 mab approximately (Fig. 3.4a). This mooring was sampling from the 1st of March 1995, to the 16th of February 1996.

Site A6 is one of the deepest points in the central basin of Bransfield Strait. This point is close to a volcanic spot and is the natural end of two glacial canyons. It is close to the Livingston and Deception Islands southeastern margin as well. Above location A6 a hydrographic front, described in the study area section, is usually developed.

Two other sediment traps were deployed at site A3 and B2 along with current meters. Unfortunately they were not recovered.

One Technicap model PPS 4 trap was moored in Johnson's Dock, Livingston Island (BAE site) (Fig. 3.4b). This trap has the same shape of model PPS 3 but different size, 62.5 cm height and 25 cm inner diameter, keeping the aspect ratio H/D=2.5. It was moored at 19.5 m water depth, 4.5 mab coupled to a current meter with turbidity sensor at 1.5 mab. Sampling periods for the sediment trap were six-seven days from 10th of December 1997 to the 26th of February 1998.

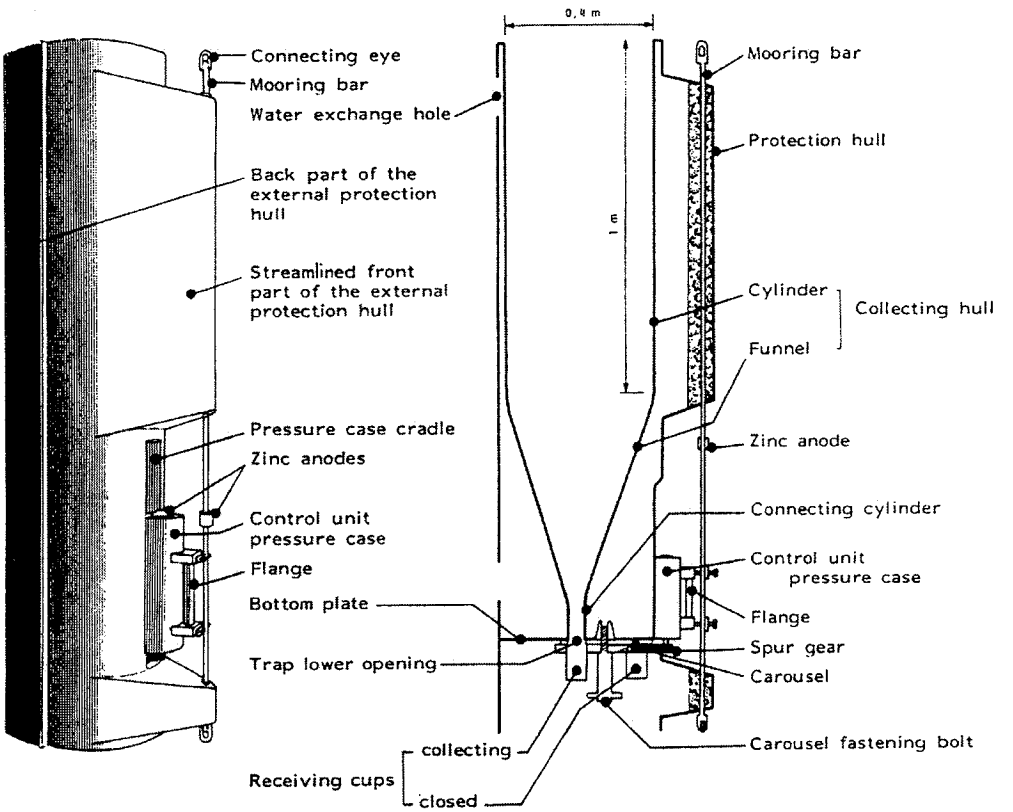

Fig. 3.1. a) General view and b) section draws to scale of the PPS 3 sediment trap. Taken from Heussner et al. (1990).

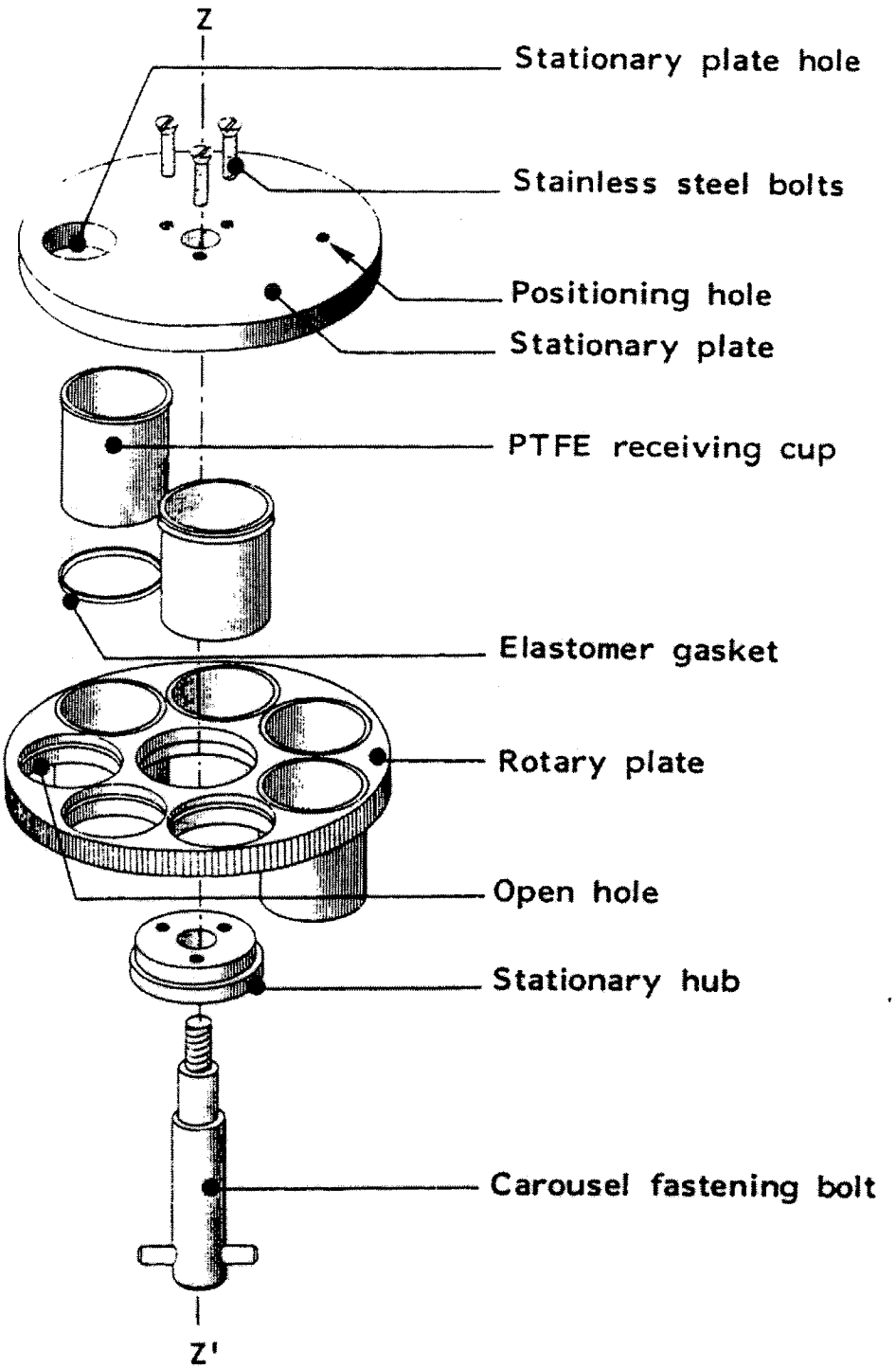

Fig. 3.2. Expanded draws of a 6-cup rotary carousel. Four Teflon cups are inserted in proper position into the rotary plate. The rotation axis is indicated by Z-•-Z'. PETP means polyethyleneterephtalate. Taken from Heussner, et al. (1990).

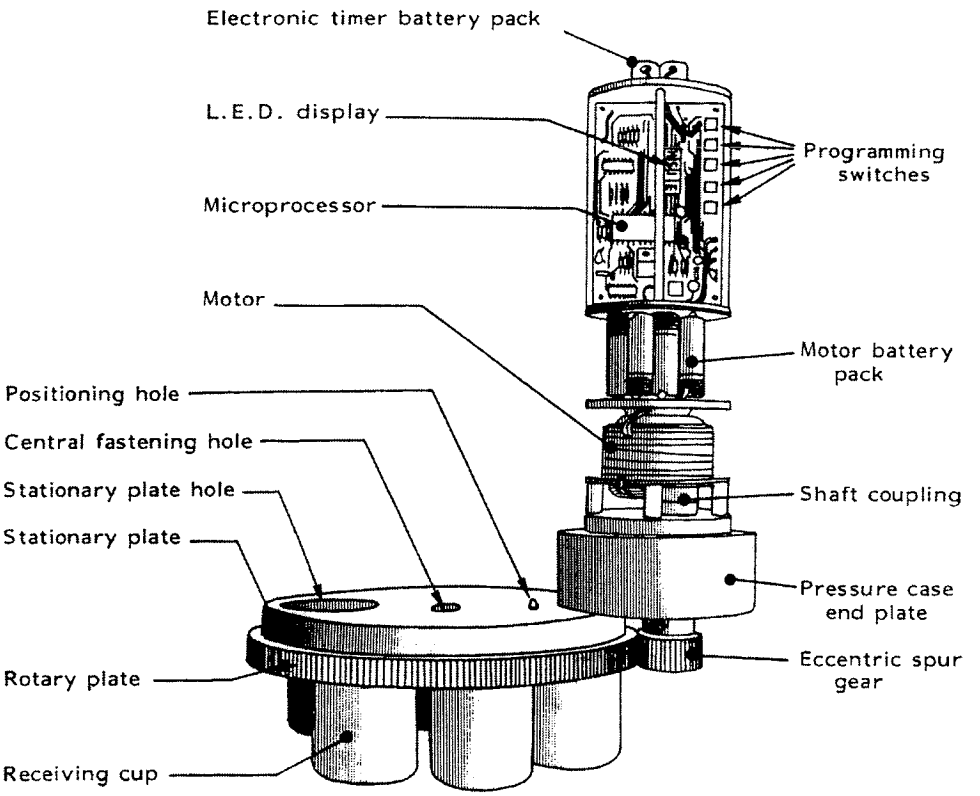

Fig. 3.3. The electronic timer/motor assembly connected to the carousel. Taken from Heussner et al. (1990).

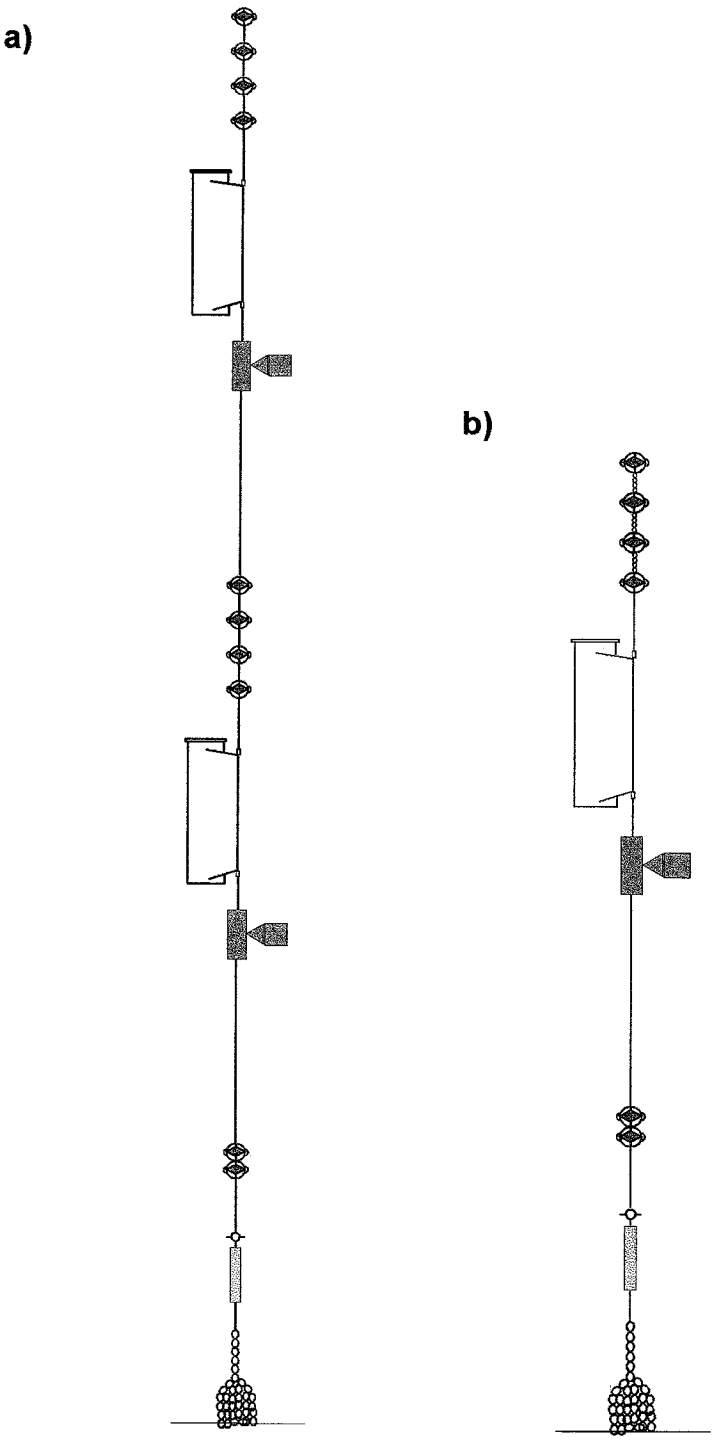

Fig. 3.4. Diagram of the moorings at a) Bransfield Strait (site A6) and b) Johnson's Dock (site BAE).

3.2. LABORATORY WORK

All the samples were treated at the Sedimentology Laboratory of the Marine Sciences Institute-CSIC.

3.2.1. Treatment of sediment trap samples

Before the sample treatment, several litres of 0.2 µm filtered seawater and two kinds of filters were prepared. 47 mm diameter glass microfibre Whatmann GF/F filter of approximately 45 µm mesh (GFF) and 47 mm diameter, 45 µm mesh nitro-cellulose white HAWP Millipore filter (NF). Before its use, the GFF were rinsed with distilled water and then placed for 24 h in an oven at 550° C where they were allowed to cool for another 24 h. Finally they were pre-weighed after 24 h more in a desiccation bowl. The NF filters were rinsed with distilled water and dried at 40°C for 24 h, then they were placed 24 h in a desiccation bowl. They were pre-weighed after this procedure.

The sediment trap samples were processed in the laboratory according to the method described by Heussner et al., (1990).

After its recovery from the sea each carousel was kept at 4°C until samples treatment in the lab. The particles in the collection tubes must settle completely before their treatment. Once all particles were completely settled after a period of repose and the solution above the material was crystal clear the liquid was removed and stored at 4°C. Each tube was rinsed with 0.2 µm-filtered seawater over a 1-mm plastic mesh in order to remove „swimmers". Swimmers are not related with passive-sinking flux. They are considered those large zooplankters that have swum into the trap sample tube and then poisoned. The sieved material was poured in a 2000-ml flask and filled with 0.2 µm-filtered seawater. The flask was placed in a shaking table in order to keep the material suspended and homogenised to guarantee equality when taking aliquots. The whole sample was equally fractionated and distributed with a peristaltic Jencons pump and a robot "xy" arm in to several flasks (Fig. 3.5). The entire sample was divided in order to get 10 fractions of 50 mg (for elemental analysis) and several of 250 mg (for ^{210}Pb and plankton analysis). The remaining sample was stored in glass containers at 4°C with formalin solution.

Sample total dry mass weight was calculated as the average of the dry mass weight of three subsamples filtered onto NF filters multiplied by the fraction filtered. The total mass flux was determined from the total mass weight, the collecting trap area (square meters) and the sampling interval (days) and expressed as mg m^{-2} d^{-1}.

3.2.2. Total carbon and total nitrogen

All the sediment trap and the core samples were stove dried at 40°C until constant weight were obtained before the elemental analysis were performed. After 24 h in a desiccation bowl each core sample was ground in a mechanic Agate mortar for 3 min. Sediment trap samples were treated on the filters.

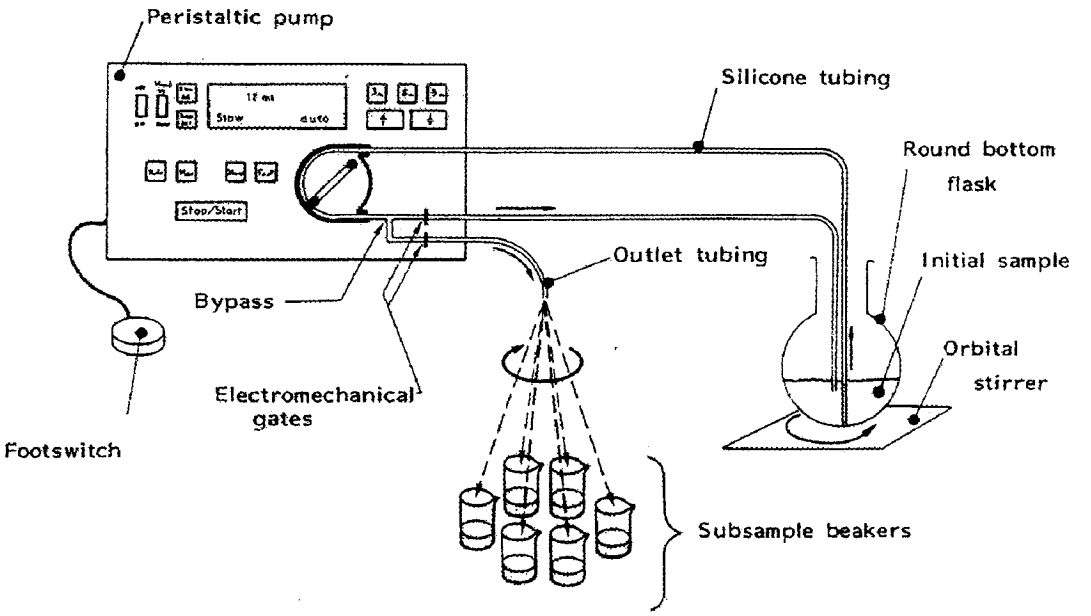

Fig. 3.5. The subsampling set for wet sediment trap samples. Taken from Heussner et al. (1990).

Total carbon (C) and nitrogen (N) were measured in a LECO CN-2000 auto-analyser. According to the user's manual provided by the manufacturer the next procedure was followed.

For the cores samples 100 mg of dry and grounded sediment (due to the little amount of some samples) was weighed on the sample container. The dry sediment trap samples filters were put into the sample container as they were before. Then, the container is placed into an electric furnace in a 1050°C environment where the sample is combusted after an oxygen injection. The gases produced in this reaction flow through steel wool and fibreglass filters in order to remove ashes. After flowing through a thermoelectric cooler where humidity is condensed and removed, the flux goes to a ballast tank where it is aloud to equilibrate. An aliquot of the homogenised gas flows through an infrared radiation (IR) emission cell where the produced CO_2 absorbs the IR energy. The difference in IR energy between emission and reception cells is converted to a voltage, which is transform via the calibration curve, to a TC percentage. A flow of „100%" oxygen (99.9999% Linde pure oxygen) before each analysis gives the value for no absorption or baseline.

The gasses used to calculate the N percentage follow a different way. Since the combustion of the sample produces not only N_2 but also several nitrogen oxides (NO_x), after the aliquot, the sample gas flux goes through a catalyst heater column filled with cooper wire at 750°C, this environment reduces all the nitrogen oxides to N_2. Once this procedure is done, the flux continues through a column with sodium hydroxide and magnesium perchlorate that removes CO_2 and moisture (H_2O), respectively. This reduced and clean gas flows through a measurement thermoconductivity cell, parallel to a reference cell through which only runs the carrier gas, helium (He). Both were already heated at 50°C. When the sample gas runs through the measurement cell the temperature of it increases because nitrogen has a lower thermal conductivity than helium. This temperature difference produce a voltage output that is converted into N %.

3.2.3. Organic and inorganic carbon, calcium carbonate and organic matter

Inorganic carbon (IC) analysis was performed with a LECO CC-100 analyser attached to the CN-2000. A weighed fraction of the same sample, or a filter, used in TC analysis is wrapped up with paper and then is released in a 6 M HCl solution for 40 sec. The CO_2 produced is conducted as the CO_2 in the C-N procedure and then this value is associated to the IC. Organic carbon (OC) value is the difference between IC and TC values.

Calcium carbonate content ($CaCO_3$) was calculated by multiplying IC% by 8.33 (Wefer and Fischer, 1991) and organic matter as twice OC percentage.

3.2.4. Biogenic silica

The procedure followed to measure the biogenic silica (BSi) was that of Mortlock and Froelich (1989). The sediment samples, or the filters, were prepared with a 30 min 5 ml bath with 10% H_2O_2 followed by a 30 sec sonication session with 5 ml of 10 % HCl.

The samples were allowed to react for 30 min. They were rinsed with double distilled water. Centrifugation (5 min at 5000 rpm) and oven dried pre-set the samples for the alkaline extraction. After sonication for 5 min within 40 ml of 2M Na_2CO_3 the samples were placed on an 85ºC bath for 5 h with vortex shaking every 2 h. At the end of the bath the samples were centrifuged for 5 min at 5000 rpm. A clear aliquot of each sample was taken.

17.5 ml of ammonium molybdate solution were added to every aliquot and after 20 min the addition of 7.5 ml of a reducing solution with sodium metol-sulfite, oxalic and sulphuric acids complete the reagents to produce the blue chromophore read on the spectrophotometer at 815 nm.

The following expression is used to calculate the SiO_2 %:

$$SiO_2\ \% = \frac{112.4 * Cs}{\text{sample weight (mg)}}$$

where:

Cs= (average samples absorbance – average blanks absorbance)* f

where:

f= calibration curve slope/1000 (mM/abs)

Then, the biogenic silica % is calculated like:

biogenic silica %= SiO_2 %* 2.4

3.2.5. Grain size analysis of the bottom sediment

The sand percentage was obtained by sifting a pre-weighed (dry, not ground), 20% peroxide attacked (in order to remove organic matter) sub-sample through a 63-µm mesh sieve using sodium pyrophosphate to rinse it. The material collected on the sieve was rinsed with distilled water and then placed in an oven at 90ºC for 24 h. Once the sample reached equilibrium with room temperature was weighed again and the difference with the initial dry weight was used to calculate the sand and silt+clay percentage.

3.2.6. Radiometric analysis

The ^{210}Pb analysis was done at the Radioactivity Laboratory of the Physics Department at the Universitat Autònoma de Barcelona by Dr. P. Masquè and J.A. Sánchez-Cabeza following the technique described by Sánchez-Cabeza et al, (1998). This work was performed to all multicorer samples and to the first 50 cm of the gravity cores A3 and A6.

^{14}C AMS analysis were performed by Beta Analytic Inc. to three samples, (top, middle and bottom) from core A3 and two samples from (top and bottom) core A6.

^{210}Pb concentration profiles in the sediment cores were used as a basis for determining the apparent sediment accumulation rates (SAR) onto the seabed during the last ca. 100 years. The ^{210}Pb analyses of the sediment samples were performed by total digestion of 200-300 mg sample aliquots. ^{209}Po were added to each sample before digestion as internal tracer. After digestion, samples were made 1 N HCl and ^{209}Po and ^{210}Po were deposited onto silver disks at 60-70 °C for 8 hours while stirring. α-spectrometers equipped with low background SSB detectors (EG&G Ortec) were used for counting polonium isotopes. The elapsed time span between sediment sampling and analyses, allowed ^{210}Pb to be in radioactive equilibrium with ^{210}Po (half-life = 138 d) in the sediment samples. For each batch of 10 samples, a reagent blank analysis was also carried out and subtracted for activity determination.

Excess ^{210}Pb was obtained by subtracting the supported ^{210}Pb calculated from the deeper parts of each core, where ^{226}Ra and ^{210}Pb are in equilibrium, assuming that it is constant along the core. This procedure is relatively usual in the literature (Langone et al., 1998) and was recently checked by Masqué et al. (in press) in the neighbouring Bransfield Strait by determining the ^{226}Ra concentrations along several sediment cores by gamma spectrometry, obtaining a good agreement between both approaches.

3.2.7. Apparent mean accumulation rates and surface mixed layer

Mean accumulation rates during the last ca. 100 years were obtained by multiplying the average content value of each variable within the SML and below it by the mean sediment accumulation rates derived from ^{210}Pb profiles.

The surface mixed layer (SML) is commonly defined as the upper sediment column with constant ^{210}Pb activity. Within this zone both mixing and accumulation control the ^{210}Pb profile. The depth of the SML was determined from the slope change in the ^{210}Pb-concentration profile along each core. Below this layer the sediment accumulation term has more importance in determining the shape of the ^{210}Pb profile. It is assumed that within the SML the most-recent sediment is mixed with that already settled so we found no way to establish differences between both kinds of material. In the present work the sediment below the SML is considered as buried. The SML was calculated as described in Masqué et al. (in press).

3.2.8. Burial efficiencies

The burial efficiency was calculated as the percentage of the surface mean accumulation flux that finally remains in the sediment column below the SML.

3.2.9. Micropaleontological analysis

Diatom counting routines were performed by Dr. María de los Angeles Bárcena at Geology and Paleontology Department, from the Sciences Faculty at the University of Salamanca, following the methodologies described by Schrader and Gersonde (1978). This procedure was applied to gravity core A3 each 10 cm and to gravity core A6 each 5 cm.

3.2.10. Statistical analysis

One-way analysis of variance (ANOVA) was performed to test for differences in the mean concentration of OC, N, BSi, and the OC/N ratio within the SML layer and below it. The squared root of the OC, N, BSi content, and OC/N ratio values was used in order to apply this parametric test.

PART III. RESULTS

4. CARBON, BIOGENIC SILICA, AND ACCUMULATION RATES IN BOTTOM SEDIMENT

This chapter shows a complete description of the sediment cores taken in the western Bransfield and Gerlache Straits and in the vicinities of the Bellingshausen Sea with the western Bransfield Strait along with the measured variables and some associations between them. The chapter is completed with the statistical analysis results section and a summary of the sediment cores description.

The description is divided in three subareas: Bransfield Strait, Gerlache Strait and Bellingshausen Sea. The cores from each subarea are described in two sections, *description of constituents* and *associations between variables*.

4.1. BRANSFIELD STRAIT

In the Bransfield Strait two gravity cores (sites A3 and A6) and three multicores were taken (sites A3, A6, and B2). One small core was taken at the Johnson's Dock in the Livingston Island (Fig. 2.3).

4.1.1. Multicore A3

4.1.1.1. Major biogenic constituents, SAR, and sand content

This 34-cm long core was taken at 790-m water depth at the natural end of the Orleans trough (Fig. 2.3). The core was composed mainly by dark green mud.

TC content varied between 1.07 and 1.33% with an average value of 1.19 ± 0.07% and a variation coefficient equal to 0.06 (Fig. 4.1a). There was a clear diminishing trend towards the bottom below cm 2. Between cm 11 and 19 this trend was more evident. The highest value was at cm 1.5 and the lowest at cm 19.

IC changed from <0.003 to 0.02%, the mean value was 0.01 ± 0.006% (Fig. 4.1b). IC profile had seven obvious minimum values that increased the variation coefficient up to 0.45. $CaCO_3$ content varied between 0 and 0.13%, the average was 0.11 ± 0.05% (Fig. 4.1c).

OC was more than 98% the TC. OC content values ranged between 1.07 to 1.33% (Fig. 4.1d). The average was 1.18 ± 0.07% and the variation coefficient 0.06.

N content minimum and maximum values were 0.14 and 0.19%, respectively and the average was 0.17 ± 0.01% (Fig. 4.1e). N content profile described a downcore-diminishing trend until cm 30. Between cm 10 and 20 this tendency was more evident. Whole core variation coefficient was 0.08.

BSi values varied between 16.14 and 21.25% (Fig. 4.1f). The mean value was 18.65 ± 1.33% and the variation coefficient 0.07. This variable showed an increasing trend towards the bottom. This pattern was not followed along the interval between

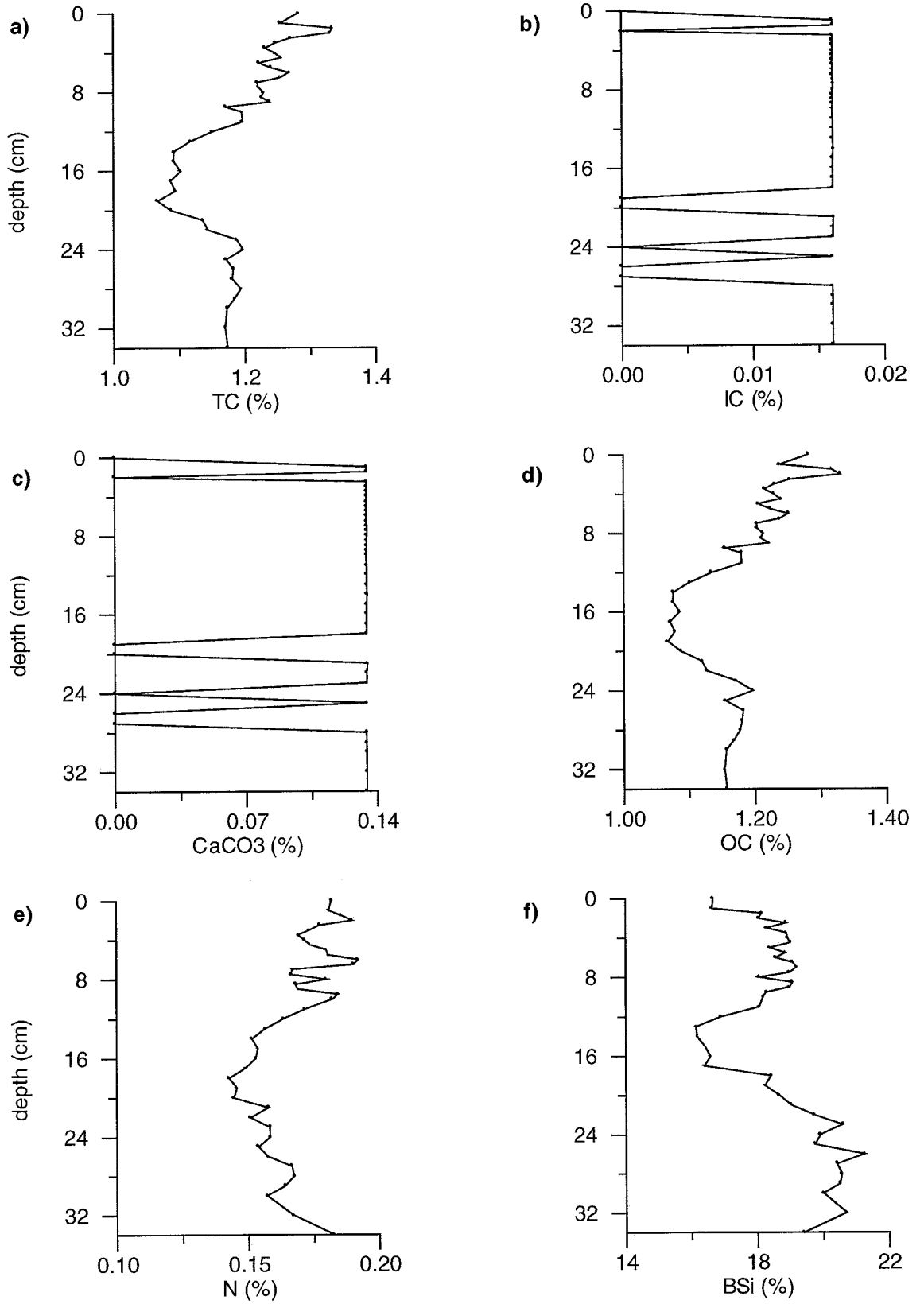

Fig. 4.1. (a) Total carbon (TC), (b) inorganic carbon (IC), (c) calcium carbonate (CaCO3), (d) organic carbon (OC), (e) nitrogen (N) and (f) biogenic silica (BSi) concentrations along multicore A3 in central Bransfield Strait.

centimetres 9 and 17, where an increasing trend was observed. This trend was only observed in the OC profile.

Excess ^{210}Pb analysis revealed a 12-cm thick surface mixed layer (SML) (Table 4.1). The OC, N, $CaCO_3$, and BSi averages within it were 1.23 ± 0.05, 0.18 ± 0.01, 0.12 ± 0.04 and 18.38 ± 0.77%, respectively. The averages below the SML, in the same order were 1.13 ± 0.05, 0.16 ± 0.01, 0.1 ± 0.06 and 18.95 ± 1.73%. The mean sediment accumulation rate (SAR) was 600 ± 30 g $m^{-2}y^{-1}$ or 1.17 ± 0.05 mm y^{-1}. SAR for each biogenic variable and burial efficiency percentages are listed in Table 4.1. $CaCO_3$ accumulation rate was higher below the SML than within it.

Sand percentage changed between 1.83 and 8.98 with an average of 3.1 ± 1.38% (Fig. 4.2a). It showed a clear diminishing trend towards the bottom and quite constant values after cm 2.5. It had a variation coefficient equal to 0.45.

4.1.1.2. Associations between variables

OC was well related to N (R^2= 0.68). Atomic OC/N ratio was always above 7.31 and below 8.83 (Fig. 4.2c). The average value was 8.24 ± 0.38 and the variation coefficient 0.05.

BSi was not clearly related to any other variable and it was the only measured constituent that showed an increasing downcore trend.

BSi/OC weight ratio varied between 13.01 and 17.98 with a mean value of 15.85 ± 1.27 and a variation coefficient equal to 0.08 (Fig. 4.2d). BSi was better preserved in the bottom sediment than the N and this latter better than the OC (Table 4.1).

The low sand percentage did not influenced any variable, even when it reached it's maximum –8.98%– at cm 1.5, where OC, BSi, and N had an increase as well. The determination coefficient (R^2) between sand and the other variables had always a value below 0.28.

4.1.2. Gravity core A3

4.1.2.1. Major biogenic constituents, diatom valves, SAR, and sand content

This core was taken at 810-m water depth at the natural end of the Orleans trough (Fig. 2.3). The core was 435-cm long and it was composed mainly by dark green mud with several black spots along the core. Several bioturbation signals were found from cm 253 until the bottom.

Total carbon (TC) content varied from 0.66 to 1.23% with an average of 1.05 ± 0.08% (Fig. 4.3a). This variable kept a quite constant value around 1% (variation coefficient 0.07).

Inorganic carbon (IC) content ranged from 0 to 0.04% with a mean of 0.01 ± 0.01% (Fig. 4.3b). The highest inorganic carbon (IC) values were associated to the samples

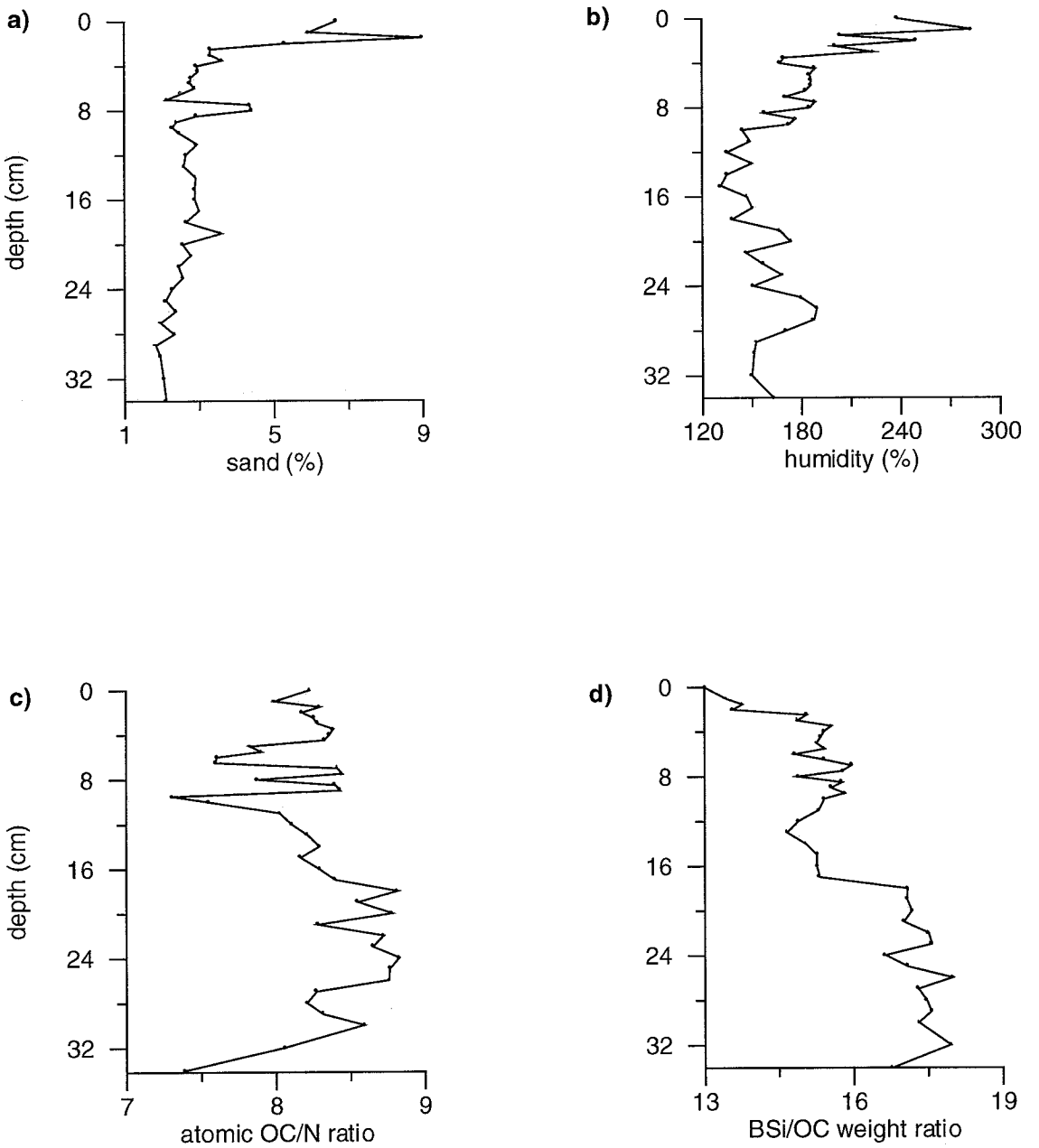

Fig. 4.2. (a) Sand and (b) humidity contents and (c) atomic organic carbon to nitrogen (OC/N) and (d) biogenic silica to organic carbon (BSi/OC) weight ratios along multicore A3 in central Bransfield Strait.

of the bottom and the lowest to those of the middle of the core. Calcium carbonate ($CaCO_3$) values varied between 0 and 0.31%, with an average of 0.11 ± 0.08% (Fig. 4.3c). Both variables had a variation coefficient of 0.76.

Organic carbon (OC) content values ranged between 71 and 96% of the TC. OC minimum and maximum values were 0.62 and 1.21%, respectively. The mean value was 1.03 ± 0.08% (Fig. 4.3d) and the variation coefficient 0.08. The OC curve followed the same constant trend of the TC.

Total nitrogen (N) content varied from 0.09 to 0.17% with an average of 0.14 ± 0.01% (Fig. 4.3e). The variation coefficient was 0.08. N profile was similar to that of the TC.

Biogenic silica (BSi) content minimum and maximum values were 17.32 and 25.49%, respectively, with a mean of 21.66 ± 1.83% (Fig. 4.3f). The variation coefficient was 0.09. BSi curve had a slight increasing tendency towards the bottom.

Diatom valves content per gram (DV) changed from $2.1x10^7$ to $7x10^8$ valves g^{-1} (v g^{-1}) with an average of $2x10^8 \pm 1.4x10^8$ v g^{-1} and a variation coefficient of 0.55 (Fig. 4.4a). DV showed a clear increasing trend towards the bottom, markedly from cm 170, with a maximum peak at cm 370. *Chaetoceros sp.* valves accounted for more than 73% of the total diatoms assemblages number at every sample, *Thalassiosira antarctica* valves ranged between 1.96 and 9.60%, remaining valves corresponded to the *Sea-ice taxa* group. Sea-ice taxa group was composed by species such as *Fragilariopsis curta* (V. Heurck) Hasle, *F. cylindrus* (Grun.), *F. vanheurckii* Hasle. *Thalassiosira antarctica* Comber/*T. scotia* Fryxell and Hoban in the spore stage (RS), were another constituents of the assemblage (Bárcena et al., in press).

^{14}C analysis yielded a corrected age of 3960 ± 50 years before present (BP) for the top of the core, 5090 ± 50 for cm 300 and 5990 ± 50 for the bottom, which means a linear sedimentation rate of 208 cm kyr^{-1}. After corrections, an age of 1968 yr BP has been associated to the bottom of the core (Bárcena et al., in press).

The ^{210}Pb activity and the diatom evidence in the top of the core suggest that the samples from this portion are related to the last sixty years (Bárcena et al., in press). It is also proposed a reduction in primary siliceous productivity within the last 2000 yr due to a cooling trend towards the present.

Bárcena et al., (in press) applied spectral analysis to the OC, diatom and BSi curves and they found a high frequency cyclic period of approximately 200-300 yr, which might be related to 200 yr solar cycles.

Sand content percentage ranged between 1.29 and 22.52% with an average of 3 ± 2.59%, the variation coefficient was 0.86 (Fig. 4.4b). Isolated peaks, like that on the sample from cm 405, increased the average. The sand content profile did not show a clear pattern.

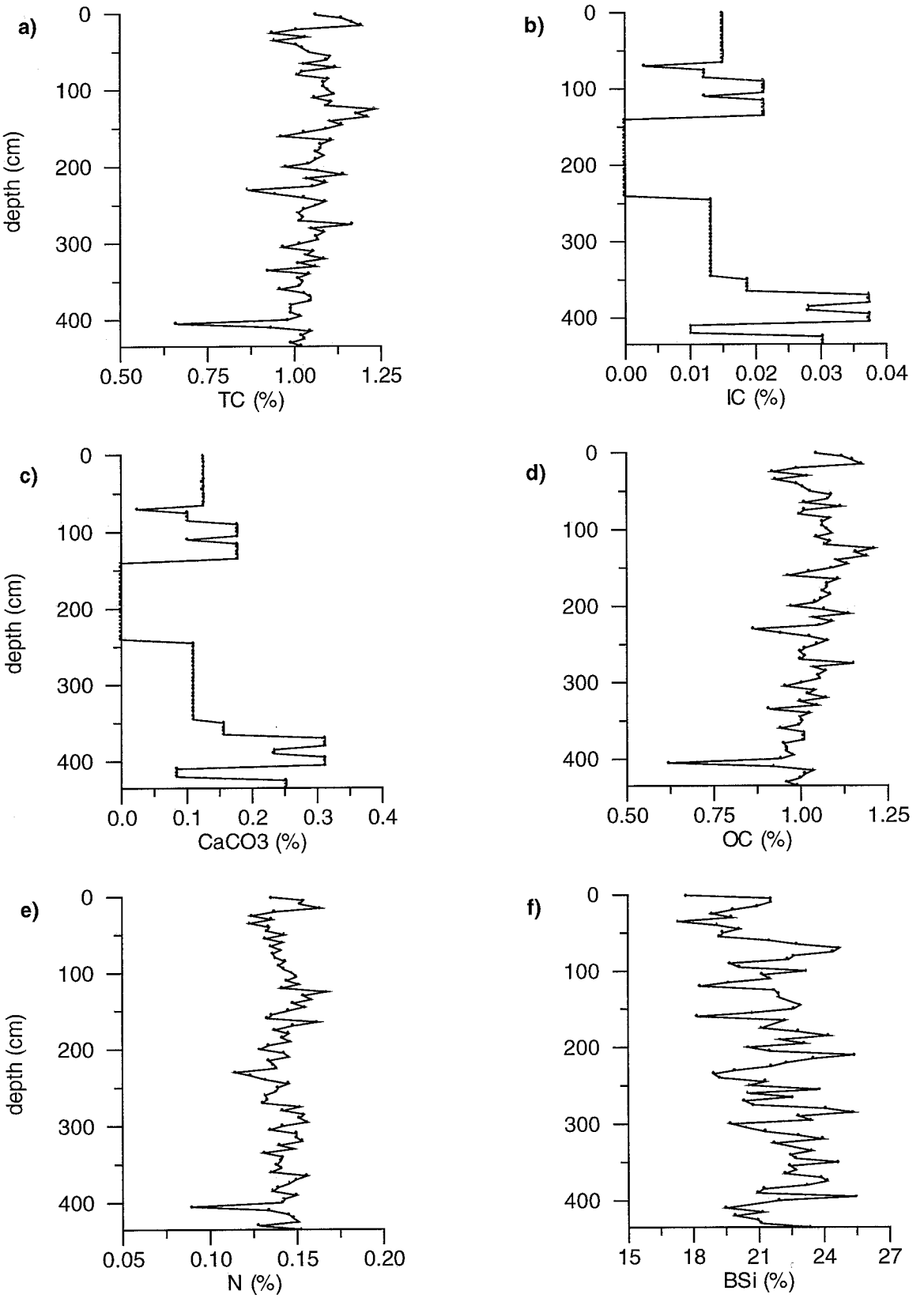

Fig. 4.3. (a) Total carbon (TC), (b) inorganic carbon (IC), (c) calcium carbonate (CaCO3), (d) organic carbon (OC), (e) nitrogen (N) and (f) biogenic silica (BSi) concentrations along gravity core A3 in central Bransfield Strait.

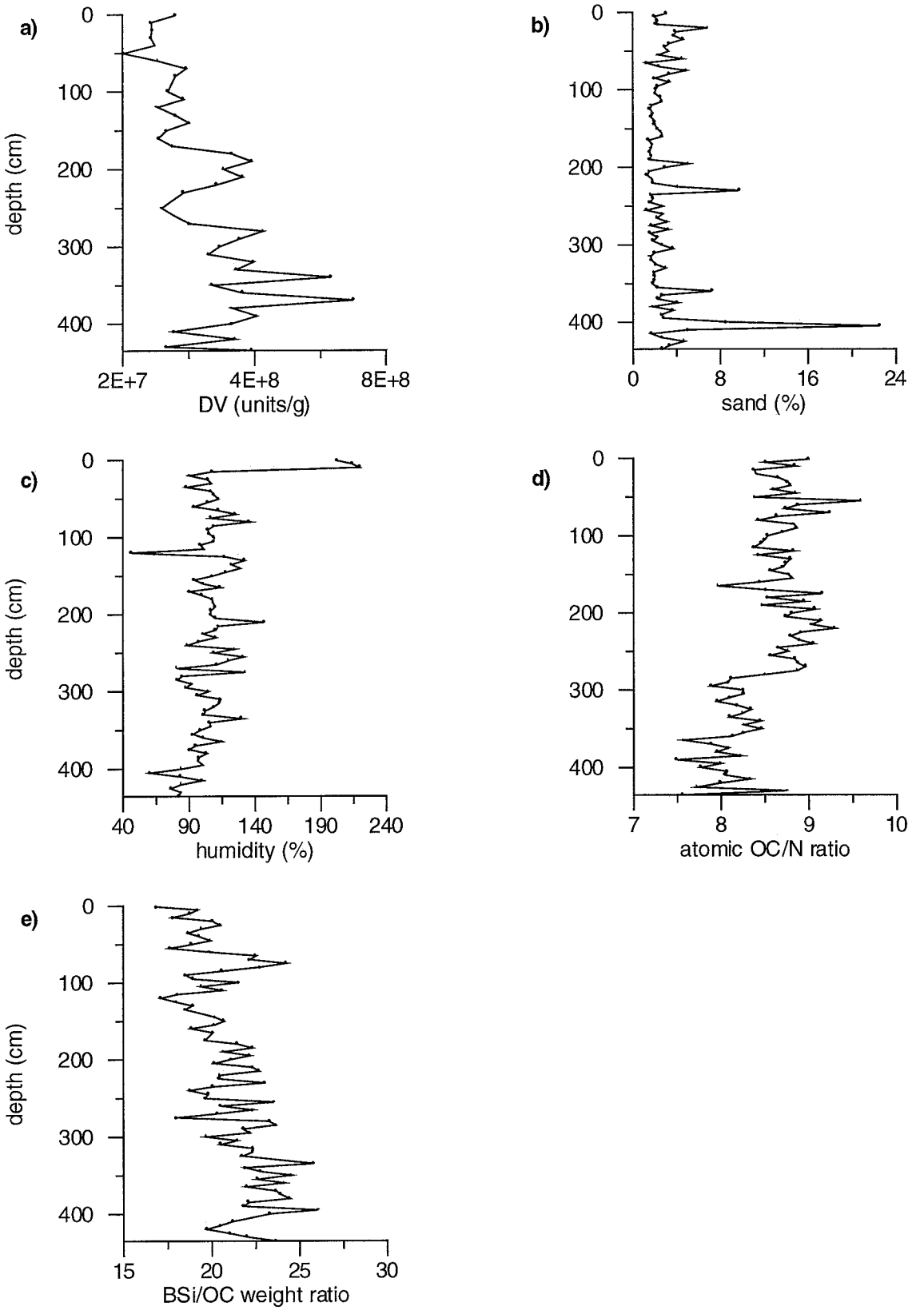

Fig. 4.4. (a) Diatom valves (DV), (b) sand and (c) humidity contents and (d) atomic organic carbon to nitrogen (OC/N) and (e) biogenic silica to organic carbon (BSi/OC) weight ratios along gravity core A3 in central Bransfield Strait.

4.1.2.2. Associations between variables

OC and N values were closely related (R^2= 0.62). Atomic OC/N ratio was above 7.5 and below 9.6 (Fig 4.4d). The atomic OC/N ratio average was 8.51 ± 0.42. It had the very low variation coefficient of 0.05. The decrease at cm 285 was due to a slight increase in the N content.

BSi showed no clear relation to OC content (R^2= 0.04) neither to N (R^2= 0.13). The BSi/OC weight ratio showed an increasing trend towards the bottom (Fig. 4.4e). It ranged from 16.90 to 26.03 with an average of 21 ± 2. The variation coefficient was 0.1. The increasing trend showed by the DV was not clearly reflected on the BSi or on the OC content profiles.

OC had an inverse relation to sand content (R^2= 0.5). This relation was particularly evident on cm 405, where sand percentage increased obviously. Sand content peaks were related to evident decreases in the concentration of the other measured variables but in that of IC. IC concentration was too little along the core, and it showed not a clear relation to OC, N, BSi or sand content. Nevertheless, both the highest $CaCO_3$ and sand content coesxisted in sample of cm 405.

The abundance pattern of the Sea-ice taxa group showed an inverse relation to the *Chaetoceros sp.* valves profile.

4.1.3. Multicore A6

4.1.3.1. Major biogenic constituents, SAR, and sand content

This core was taken at 1066-m water depth in a basin close to the volcanic spot of the Deception Island (Fig. 2.3). The core had 32-cm long and it consisted mainly of mud.

TC content varied between 0.40 and 1.30%, the mean value was 0.80 ± 0.21% and the variation coefficient 0.26 (Fig. 4.5a). The highest value was registered on the surface sample. TC profile had a diminishing trend towards the bottom, this tendency is more evident along the top two centimetres and from cm 15 to 21.

IC values ranged from <0.003 to 0.3% with a mean value of 0.02 ± 0.01% and a variation coefficient equal to 0.55 (Fig. 4.5b). IC profile showed an increasing trend towards the bottom. $CaCO_3$ content varied between 0 and 0.23% with an average value of 0.13 ± 0.07% (Fig. 4.5c).

OC was always more than 93% the TC. OC content minimum and maximum values were 0.38 and 1.30%, respectively and the average value along the core was 0.79 ± 0.22% with a variation coefficient equal to 0.28 (Fig. 4.5d).

Nitrogen content minimum and maximum values were 0.05 and 0.22%, respectively; the average was 0.11 ± 0.03% and the variation coefficient 0.32 (Fig. 4.5e). The top sample had the highest N content as it happened with the OC. The whole profile showed a decreasing trend towards the bottom.

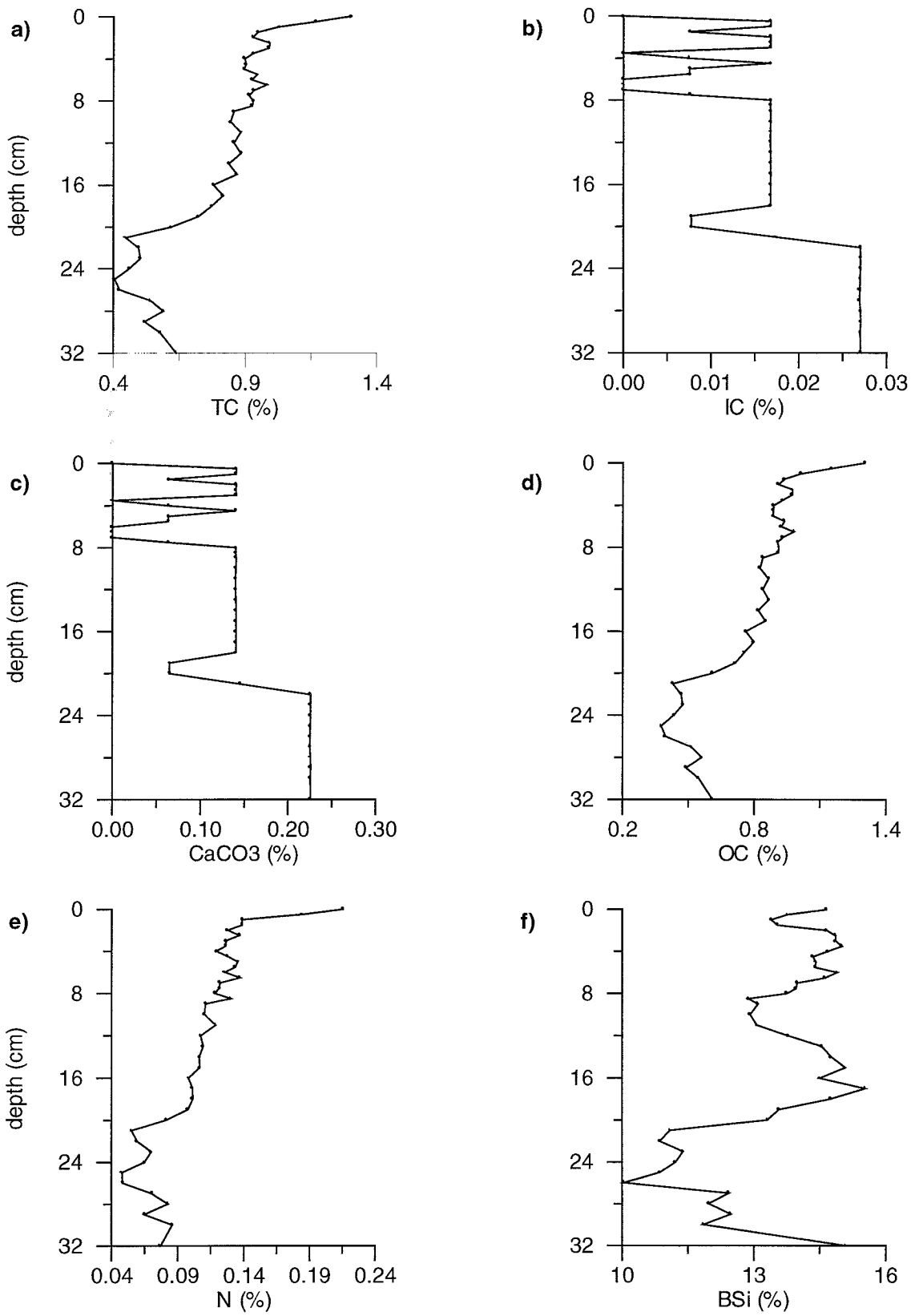

Fig. 4.5. (a) Total carbon (TC), (b) inorganic carbon (IC), (c) calcium carbonate (CaCO3), (d) organic carbon (OC), (e) nitrogen (N) and (f) biogenic silica (BSi) concentrations along multicore A6 in central Bransfield Strait.

BSi content was more constant than the other biogenic variables, it had a variation coefficient of 0.11, and it did not show the same diminishing trend towards the bottom. The lowest value was 10.04% and the highest 15.54%; the mean value was 13.54 ± 1.42% (Fig. 4.5f).

The SAR (Table 4.1) was 351 ± 10 g $m^{-2}y^{-1}$ or 0.57 ± 0.02 mm y^{-1}. The SML was 8.5 cm thick. Content averages (%) for OC, N, $CaCO_3$, and BSi within the SML were 0.96 ± 0.11, 0.14 ± 0.02, 0.08 ± 0.06 and 14.27 ± 0.61, respectively. The mean values for the rest of the core were 0.65 ± 0.18, 0.09 ± 0.02, 0.17 ± 0.05 and 12.97 ± 1.61% in the same order. Burial efficiencies and accumulation rate for each biogenic variable are showed in Table 4.1.

Sand content values ranged from 3.73 to 39.46% with an average of 17.02 ± 8.74% (Fig. 4.6a). There was a sand content increment from cm 19 until cm 30; the rest of the samples were constant around the mean value.

4.1.3.2. Associations between variables

N and OC content were strongly related. Atomic OC/N ratio showed an increasing trend towards the bottom. It varied between 7.06 and 9.55 with a mean value of 8.56 ± 0.59 (Fig. 4.6c). The variation coefficient was 0.07.

OC and BSi were strongly related (R^2=0.9). BSi/OC weight ratio profile showed an increasing trend towards the bottom. It ranged from 11.25 to 24.7 with an average of 18.38 ± 4.38 (Fig. 4.6d). The variation coefficient was 0.24.

BSi was inversely related to sand (R^2= 0.68). BSi was better preserved in the bottom sediment than the OC and this last better than the N.

The evident increment in the sand content towards the bottom of the core influenced inversely the rest of the measured variable contents. IC and sand content had their maximum values towards the bottom of the core.

4.1.4. Gravity core A6

4.1.4.1. Major biogenic constituents, diatom valves, SAR, and sand content

Site A6 is located at 1066-m water depth inside a depression between Deception Island and a volcanic structure (Fig. 2.3).

The core was 130-cm long and it consisted in green-grey and sandy mud. There were found black sand lens-shaped intrusions in the upper 26 cm and in the last 25 cm. There was a black sand segment between cm 26 and 38 and an erosive contact towards the base.

TC content ranged from 0.22 to 0.85% with a mean value of 0.52 ± 0.13% (Fig. 4.7a). There were two peaks at cm 15 and 45 and an evident decrease at cm 30. TC content

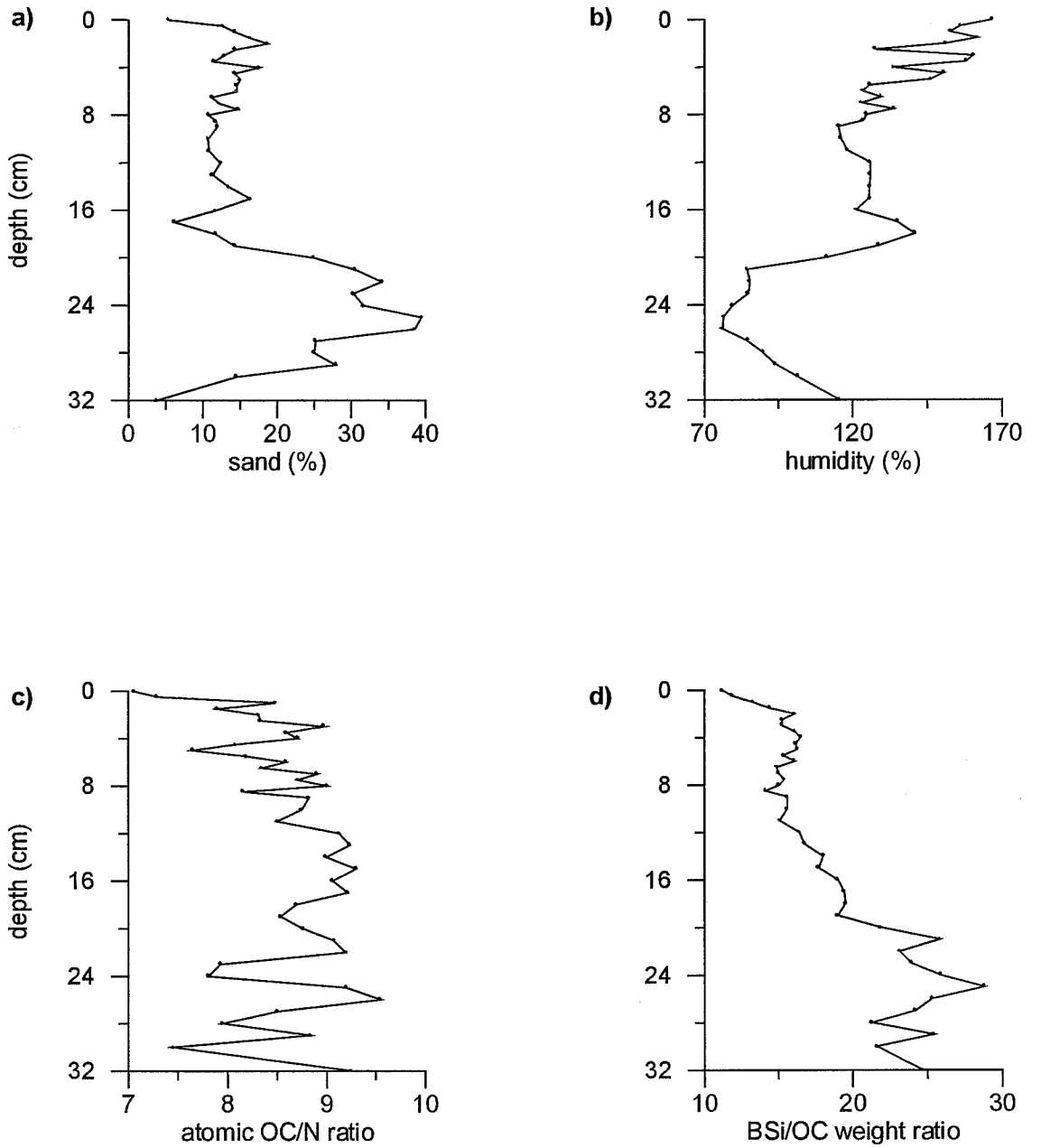

Fig. 4.6. (a) Sand and (b) humidity contents and (c) atomic organic carbon to nitrogen (OC/N) and (d) biogenic silica to organic carbon (BSi/OC) weight ratios along multicore A6 in central Bransfield Strait.

variation coefficient was 0.25. TC content values were quite constant around the mean value after cm 50.

IC content varied between 0.03 and 0.15% with an average of 0.04 ± 0.03% (Fig. 4.7b). IC content curve was quite constant, there were only three peaks along the core. The maximum value was associated to the bottom sample. Variation coefficient was 0.72 because of these three peaks. $CaCO_3$ minimum and maximum values were 0.24 and 1.23% with an average of 0.36 ± 0.26% (Fig. 4.7c).

OC content values ranged from 0.19 to 0.8% with a mean value of 0.47 ± 0.13% (Fig. 4.7d). Variation coefficient was 0.27. OC content accounted for more than 76% of the TC.

N content varied between 0.02 and 0.09% with an average of 0.06 ± 0.02% (Fig. 4.7e). Variation coefficient was 0.28.

BSi minimum and maximum values were 7.85 and 15.33%, respectively with an average of 12.87 ± 1.92% (Fig. 4.7f). Variation coefficient was 0.15. BSi content most evident changes occurred in the top 35-cm of the core.

DV values ranged from $5.4x10^7$ to $1.4x10^9$ v g^{-1} with an average of $4.7x10^8 \pm 3.1x10^8$ v g^{-1} (Fig. 4.8a). There were two important peaks at the middle of the core and one towards the bottom, none of them were related to any peak of the other variables. There was a slight downcore-increasing trend. Variation coefficient was 0.66. Chaetoceros sp. valves accounted for more than 75% of DV content in every sample. Sea-Ice Taxa was composed by the same species that those found in gravity core A3. This group showed an exceptional high concentration at the top of the core related to a Chaetoceros sp. minimum (Bárcena et al., in press).

^{14}C AMS chronology yielded an older age than expected equal to 3410 ± 50 yr BP for top sediment and an age of 5070 ± 50 for the bottom sample. This means a linear sedimentation rate of approximately 115 cm kyr^{-1}.

^{210}Pb and other radioactive nuclides coexisted in equilibrium in the top 10-cm, since there were no ^{210}Pb excess in the top of the core the most recent sediment should be lost, probably during core recovering (Bárcena et al., in press). In addition, these authors suggested that the lost portion is approximately equal to the last 200 yr, when a Little Ice Age was developing (Lamb, 1965). They related the exceptionally high concentration of the Sea-Ice Taxa group in the top of the core to colder climatic conditions than in the present day. Thus, extrapolating with the linear sedimentation rate and their conclusions, they proposed that the bottom of the core would have an age of 1860 yr BP.

As in core A3G, Bárcena et al., (in press) applied spectral analysis to the OC, diatom and BSi profiles and they found a high frequency cyclic period of approximately 200-300 yr, which might be related to 200 yr solar cycles.

Sand percentage values varied between 0.12 and 58 with a mean value of 14.2 ± 18.36% (Fig. 4.8b). Sand content profile showed evident changes, the variation

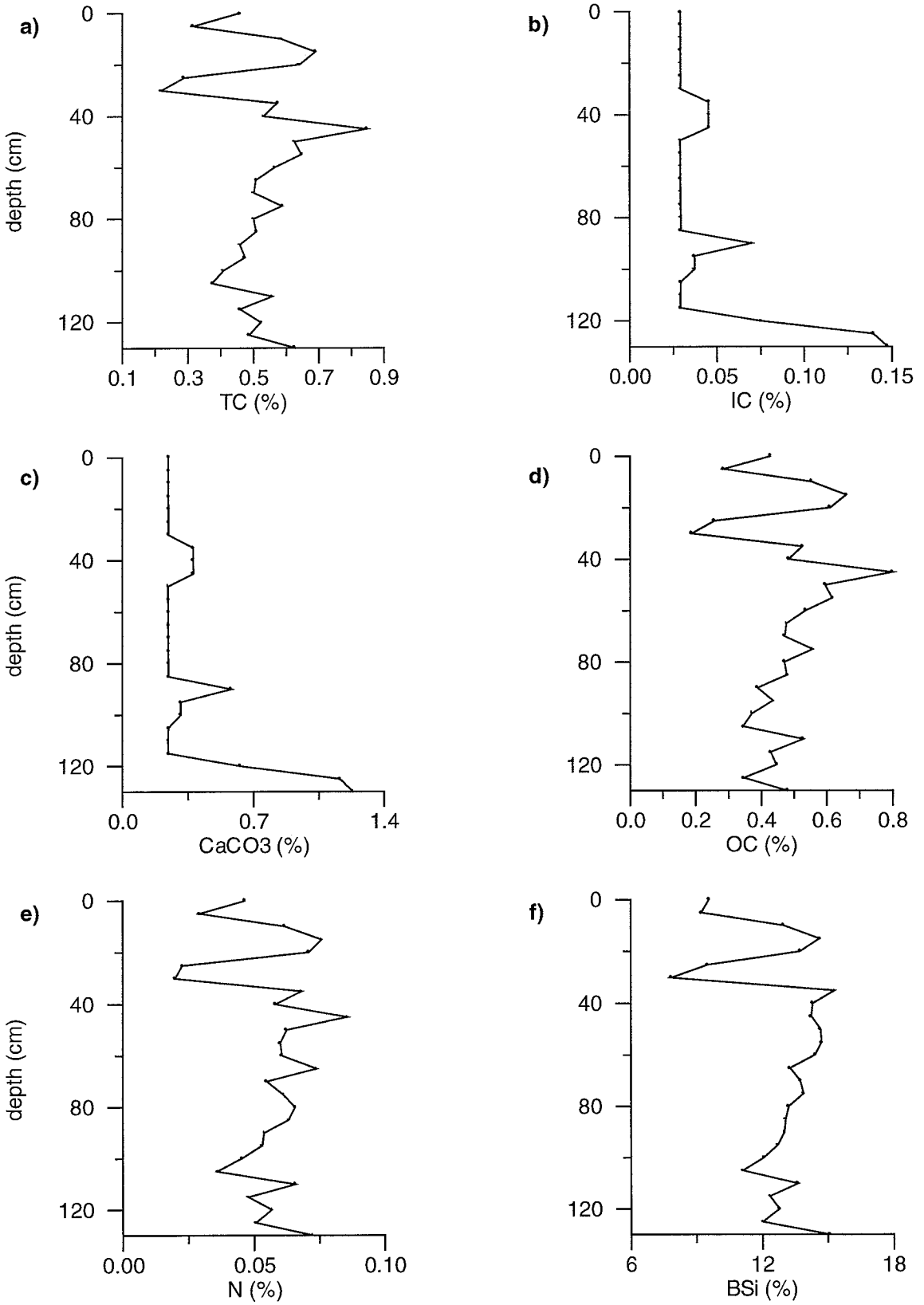

Fig. 4.7. (a) Total carbon (TC), (b) inorganic carbon (IC), (c) calcium carbonate (CaCO3), (d) organic carbon (OC), (e) nitrogen (N) and (f) biogenic silica (BSi) concentrations along gravity core A6G in central Bransfield Strait.

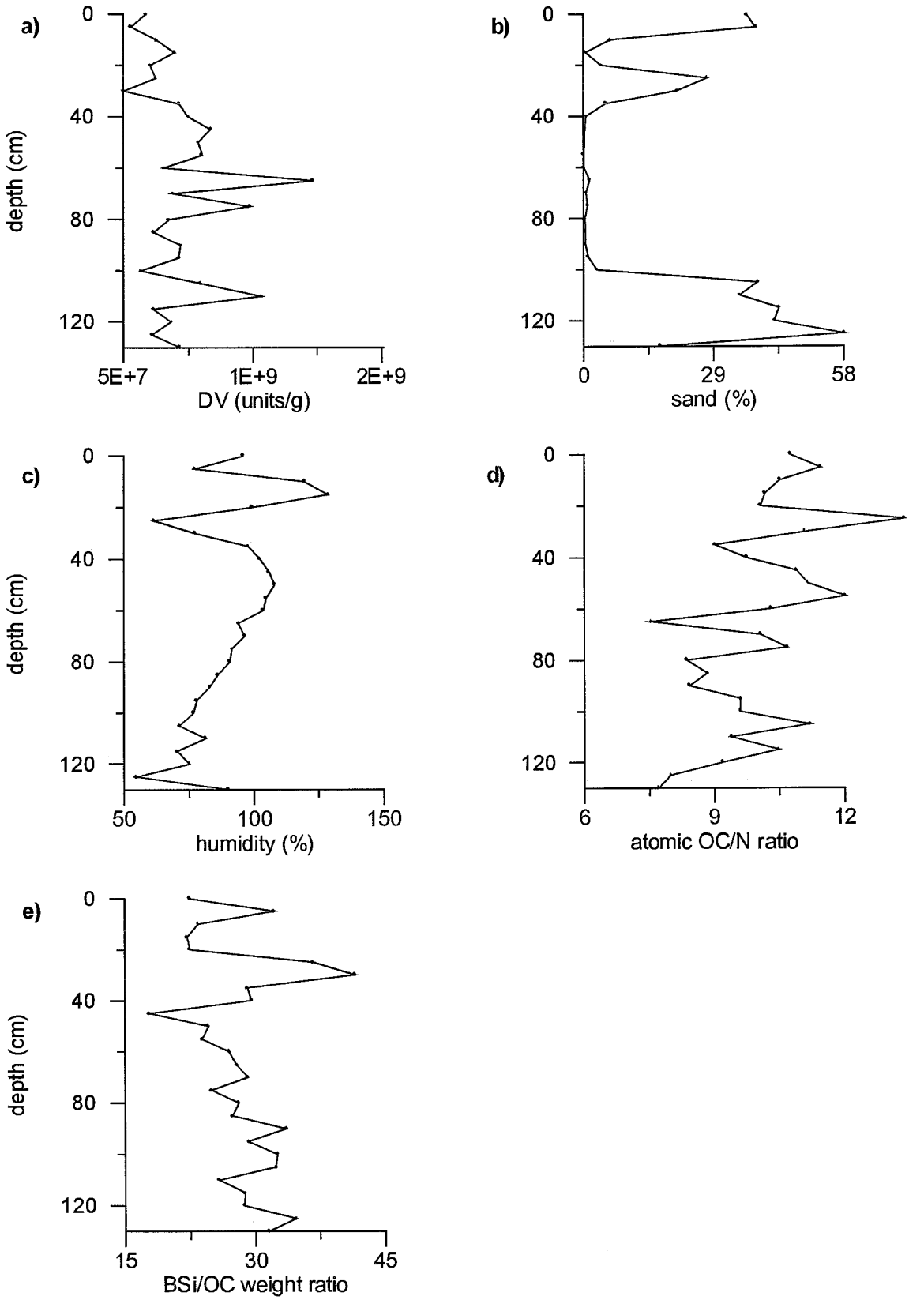

Fig. 4.8. (a) Diatom valves (DV), (b) sand and (c) humidity contents and (d) atomic organic carbon to nitrogen (OC/N) and (e) biogenic silica to organic carbon (BSi/OC) weight ratios along gravity core A6 in central Bransfield Strait.

coefficient was equal to 1.29. The highest values, between 34 and 58%, occurred at both the top and the bottom of the core.

4.1.4.2. Associations between variables

OC was closely related to N and BSi (R^2 = 0.79 and 0.64, respectively).

Atomic OC/N ratio had an average of 9.99 ± 1.36 and a variation coefficient of 0.14 (Fig. 4.8d). Its maximum value was 13.37 and the minimum 7.55.

BSi/OC weight ratio varied from 17.83 to 41.59, with an average of 28.41 ± 5.09 (Fig. 4.8e). It showed an increasing trend towards the bottom and also a variation coefficient equal to 0.18.

There were clear changes on DV values between cm 40 to 100 not reflected on the OC or BSi content profiles.

Sand influence was obvious along the top 40 cm and below cm 105. The sand content had an inverse relation to OC, N and BSi along the top 40 cm. Bottom samples had the higher IC values and high sand content. This correlation was not observed in the top samples, where very low IC content values were measured. IC had no clear relation to any other variable. From cm 40 to 100 sand content was almost null and no clear influence was reflected on OC or N profiles. Samples at cm 45 and 75 had an increment in OC, N, and DV not experienced by BSi. BSi was more related to sand percentage than OC.

4.1.5. Multicore B2

4.1.5.1. Major biogenic constituents, SAR, and sand content

This core was taken at 1135-m water depth at the western basin of the Bransfield Strait (Fig. 2.3). It consisted totally in mud and it was 38-cm long.

TC content values varied between 0.57 and 1.02%. The average was 0.75 ± 0.13% and the variation coefficient 0.17 (Fig. 4.9a). TC content profile showed a slight diminishing trend towards the bottom.

IC profile followed quite constant trend until sample at cm 27 where a sharp increasing trend was noticed. Minimum and maximum content values were <0.003 and 0.04%, respectively. The mean value was 0.013 ± 0.011%; the variation coefficient was 0.82 (Fig. 4.9b). $CaCO_3$ content varied between 0 and 0.36%. The average value was 0.11 ± 0.09% (Fig. 4.9c).

OC content was more than 92% of the TC. OC content values ranged from 0.53 to 1.02%. They averaged 0.75 ± 0.13% with a variation coefficient equal to 0.17 (Fig. 4.9d).

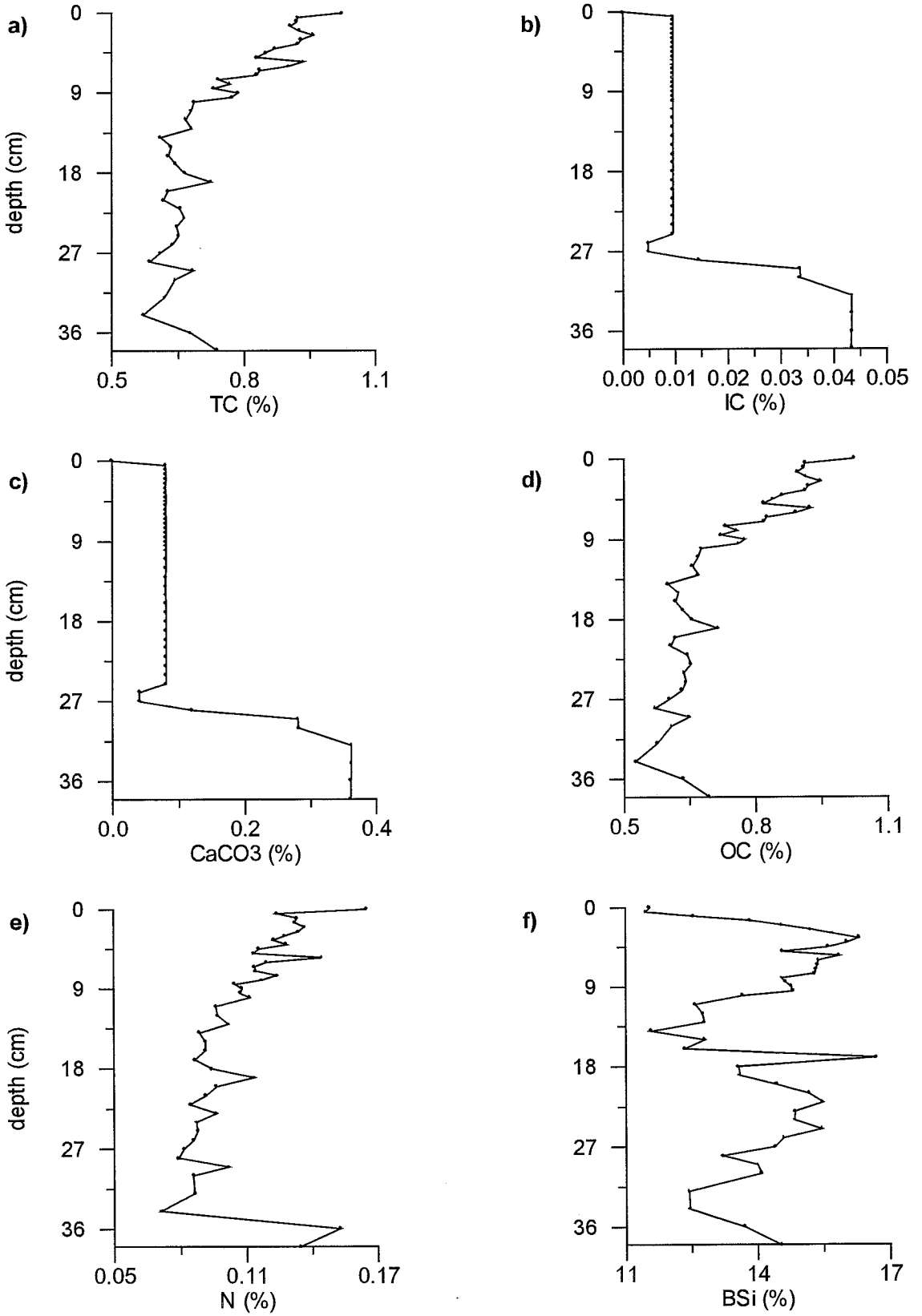

Fig. 4.9. (a) Total carbon (TC), (b) inorganic carbon (IC), (c) calcium carbonate (CaCO3), (d) organic carbon (OC), (e) nitrogen (N) and (f) biogenic silica (BSi) concentrations along multicore B2 in western Bransfield Strait.

N content profile was quite constant with an evident increase at the bottom. Its values varied between 0.07 and 0.15%. The mean value was 0.11 ± 0.02% and the variation coefficient 0.2 (Fig. 4.9e).

BSi content averaged 14.22 ± 1.34% with a variation coefficient of 0.09. Minimum and maximum values were 11.47 and 16.70%, respectively (Fig. 4.9f).

The SAR was 930 ± 30 g $m^{-2}y^{-1}$ or 1.56 ± 0.05 mm y^{-1} (Table 4.1). SML was 10 cm thick. The SAR for the biogenic variables and the associated burial efficiency are listed in Table 4.1. The mean values for the OC, $CaCO_3$, N, and BSi content within the SML were 0.85 ± 0.09, 0.08 ± 0.02, 0.12 ± 0.01, and 14.63 ± 1.35%, respectively. The average content values below this layer were 0.63 ± 0.04, 0.14 ± 0.12, 0.1 ± 0.02, and 13.85 ± 1.24% in the same order.

Sand content values ranged from 1.24 to 2.5%. The mean value was 1.73 ± 0.37% and the variation coefficient 0.21 (Fig. 4.10a). The sand content profile was quite constant.

4.1.5.2. Associations between variables

The average of IC-$CaCO_3$ content within the SML was lower than below it.

Atomic OC/N ratio averaged 7.96 ± 0.74. Minimum and maximum values were 4.85 and 8.92, respectively. The variation coefficient was 0.09 (Fig. 4.10c).

BSi/OC weight ratio ranged from 11.3 to 24.96. The mean value was 19.87 ± 3.24 and the variation coefficient 0.16 (Fig. 4.10d). This profile showed an increasing trend towards the bottom. BSi was better preserved in the sediment than the OC or the N.

4.1.6. Johnson's Dock

An 8-cm core was taken from the Johnson's Dock in the South Bay of Livingston Island (Fig. 2.3).

4.1.6.1. Major biogenic constituents

The OC content in the bottom sediment varied between 0.28 and 1.38%, with an average value of 0.42 ± 0.26% (Fig. 4.11). OC was more than 74% of the TC.

N content ranged from 0.03 to 0.15%, the average was 0.05 ± 0.03% (Fig. 4.11).

The $CaCO_3$ content varied between <0.003 to 0.86%, with a mean value of 0.51 ± 0.26% (Fig. 4.11). The OC content remained quite constant in the upper centimetres of the sediment record and it showed an evident decreasing trend below cm 6.

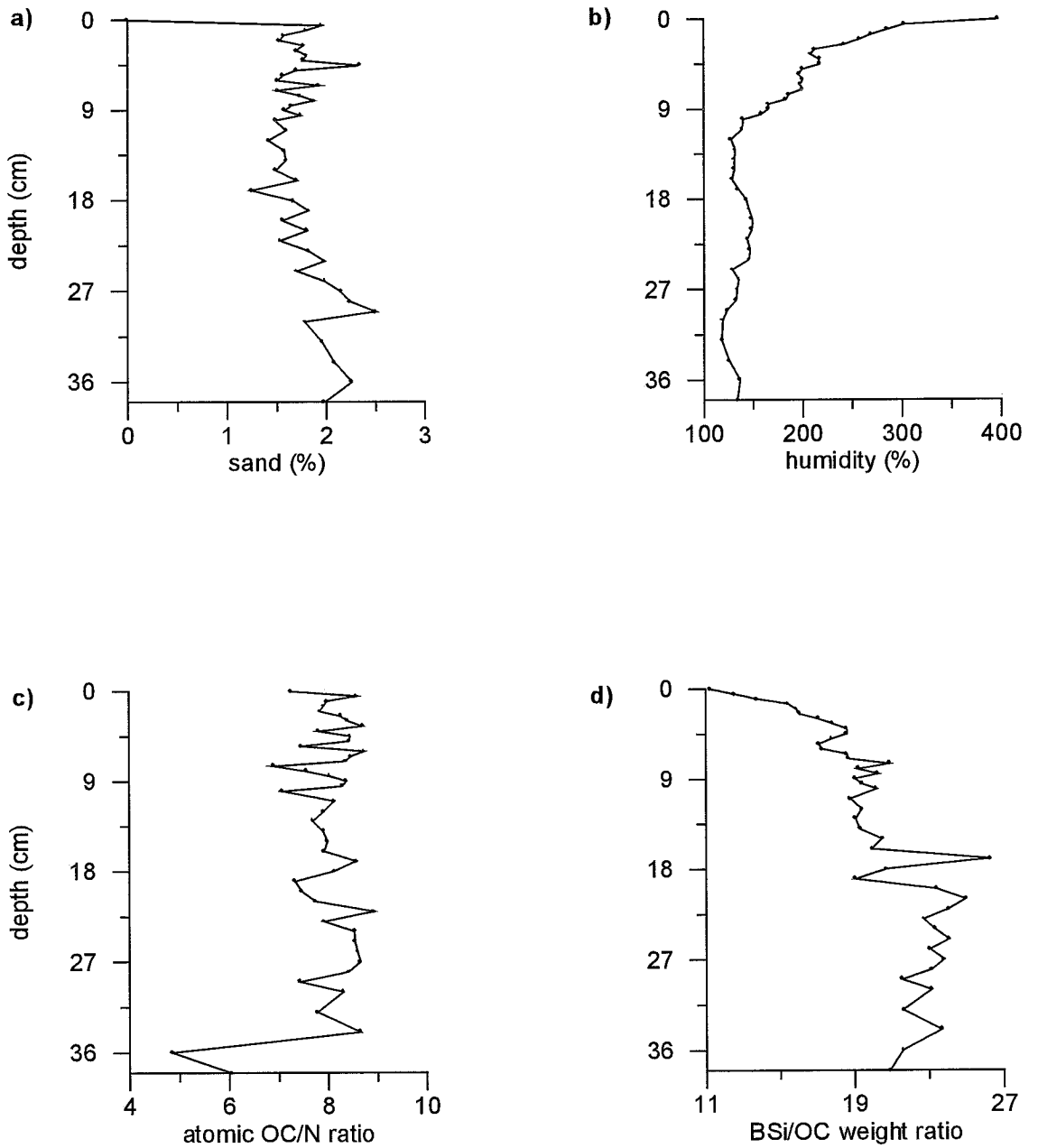

Fig. 4.10. (a) Sand and (b) humidity contents and (c) atomic organic carbon to nitrogen (OC/N) and (d) biogenic silica to organic carbon (BSi/OC) weight ratios along multicore B2 in western Bransfield Strait.

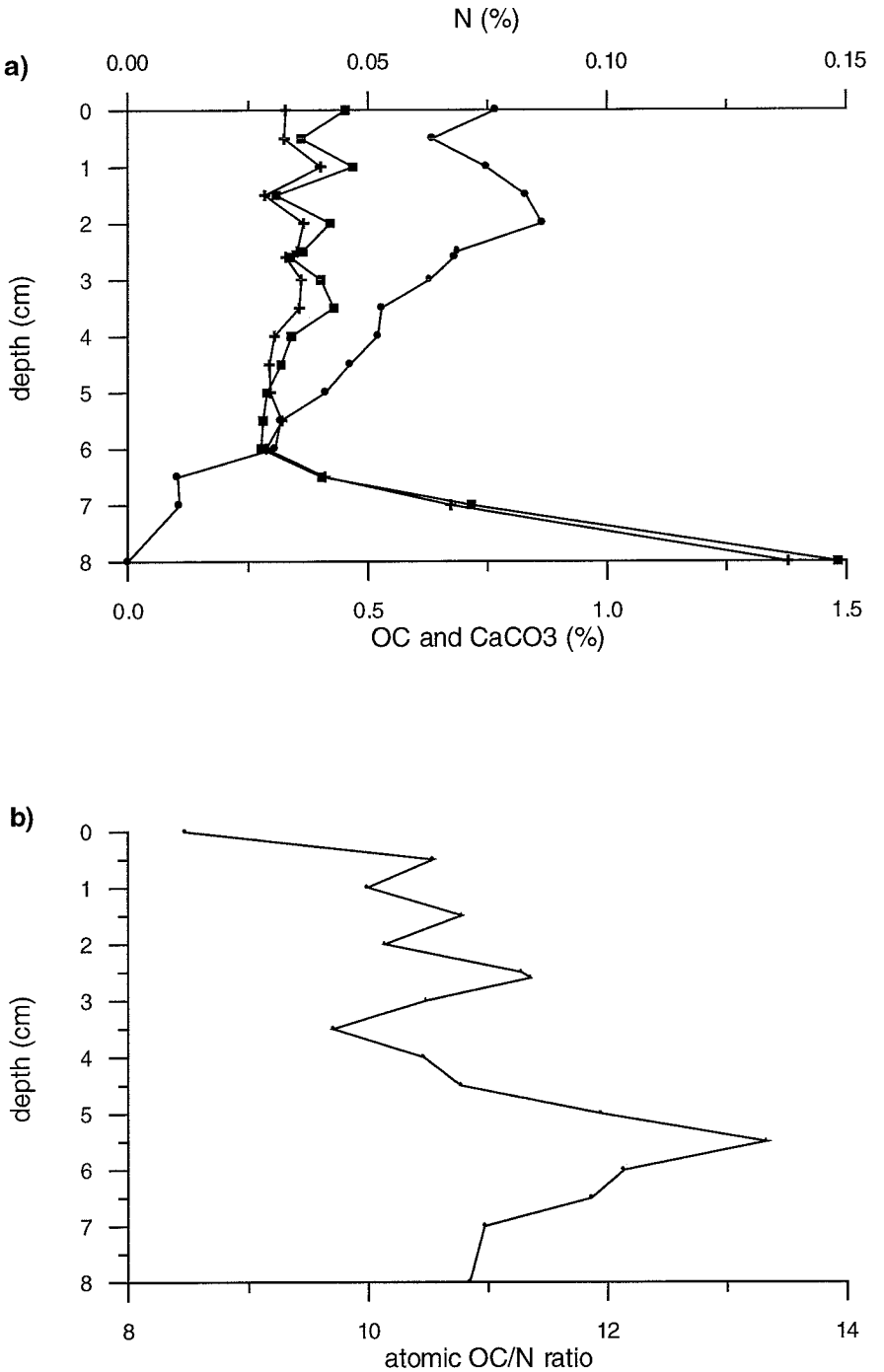

Fig. 4.11. a) Vertical profile of organic carbon (crosses), calcium carbonate (filled circles) and nitrogen (squares) content and b) atomic organic carbon (OC) to nitrogen (N) ratio in the bottom sediment at Johnson's Dock, Livingston Island.

4.2. GERLACHE STRAIT

In the Gerlache Strait six multicores were taken (B187, B191, B192, B5, B6, B7).

4.2.1. Multicore B187

4.2.1.1. Major biogenic constituents, SAR, and sand content

It was taken at 714-m water depth in a muddy bottom in a basin at the western extreme of the Gerlache Strait (Fig. 2.3). It was 34-cm long.

TC content varied between 0.83 and 1.26% with an average value of 1 ± 0.11% and a variation coefficient of 0.11 (Fig. 4.12a). TC profile followed a decreasing trend towards the bottom, which was more evident at cm 12.

IC content ranged from <0.003 to 0.01% (Fig. 4.12b); the average was 0.01 ± 0.003% and the variation coefficient 0.41. It was noticed an evident peak just below the surface sample. Two evident patterns -divided by the sample at cm 9- could be noticed along the IC profile. $CaCO_3$ content varied between 0 and 0.11%, it averaged 0.06 ± 0.02% with a variation coefficient equal to 0.41 (Fig. 4.12c).

OC was more than 98% the TC. Its minimum value was 0.82 and the maximum 1.26%, the mean value was 1 ± 0.11% (Fig. 4.12d). The variation coefficient was 0.11.

N content minimum and maximum values were 0.11 and 0.31%, respectively. The average was 0.14 ± 0.03%; the variation coefficient was 0.23 (Fig. 4.12e). One peak is obvious at cm 11. Although the profile was quite constant a slight decreasing trend was noticed.

BSi varied between 17.06 and 23.25%. The mean value was 20.39 ± 1.34% and the variation coefficient 0.07 (Fig. 4.12f). An increasing trend was evident until sample at cm-12, then the profile decreased towards the bottom.

No surface mixed layer (SML) was found in this material. The mean sediment accumulation rate (Table 4.1) for this core was 640 ± 30 g $m^{-2}y^{-1}$ or 1.71 ± 0.07 mm y^{-1}. The mean sediment accumulation rates at the surface sediment for OC, $CaCO_3$, N, and BSi were 7.56 ± 0.003, 0, 1.2 ± 0.003, and 121.02 ± 1.34 g $m^{-2}y^{-1}$, respectively. $CaCO_3$ burial efficiency could not be calculated because no IC was detected in the surface sediment.

Sand content ranged from 0.49 to 3.20%, the average was 1.1 ± 0.72%; the variation coefficient was 0.65 (Fig. 4.13a). This profile showed an increasing trend towards the bottom. There was an evident peak between cm 8 and 12.

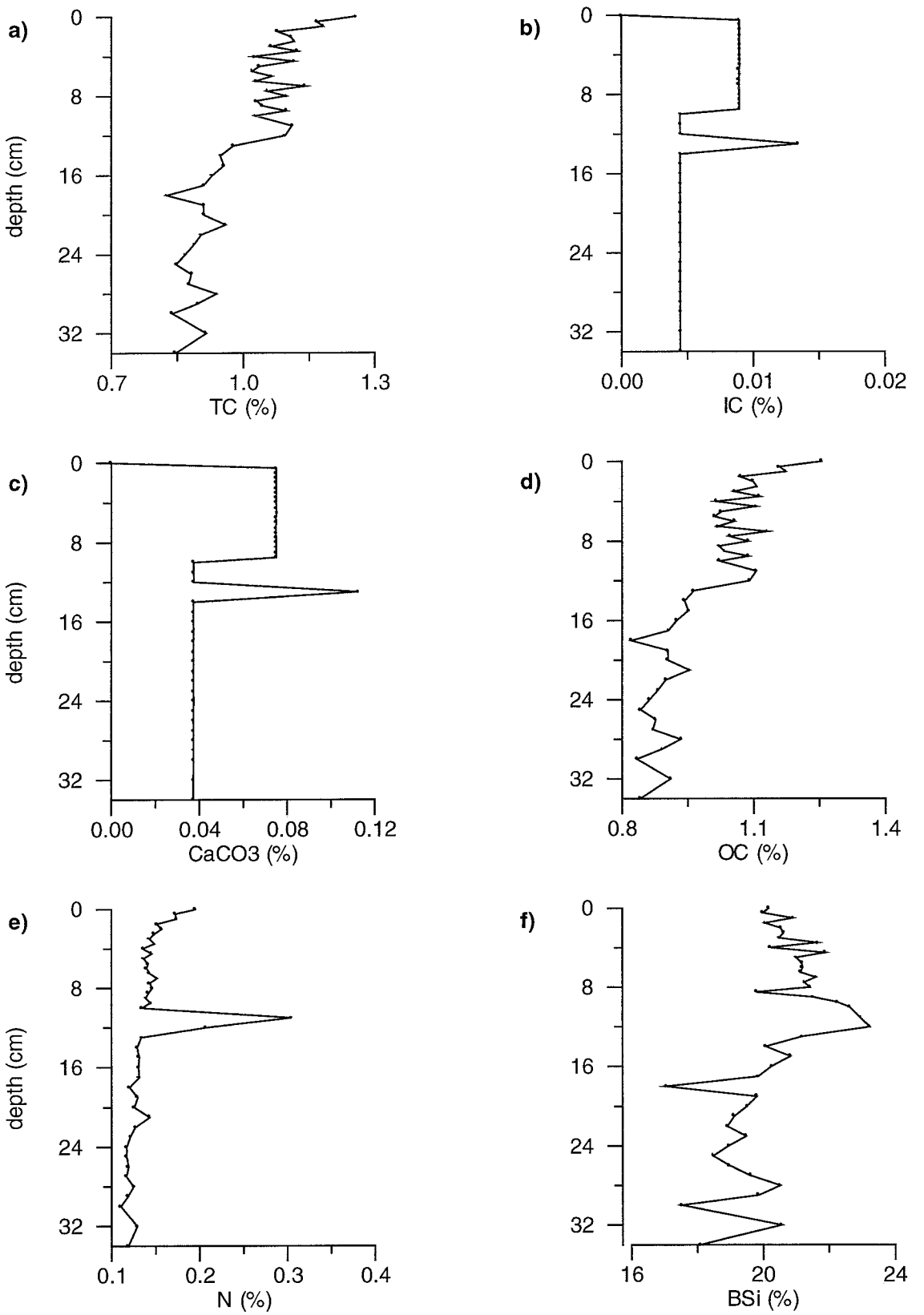

Fig. 4.12. (a) Total carbon (TC), (b) inorganic carbon (IC), (c) calcium carbonate (CaCO3), (d) organic carbon (OC), (e) nitrogen (N) and (f) biogenic silica (BSi) concentrations along multicore B187 in western Gerlache Strait.

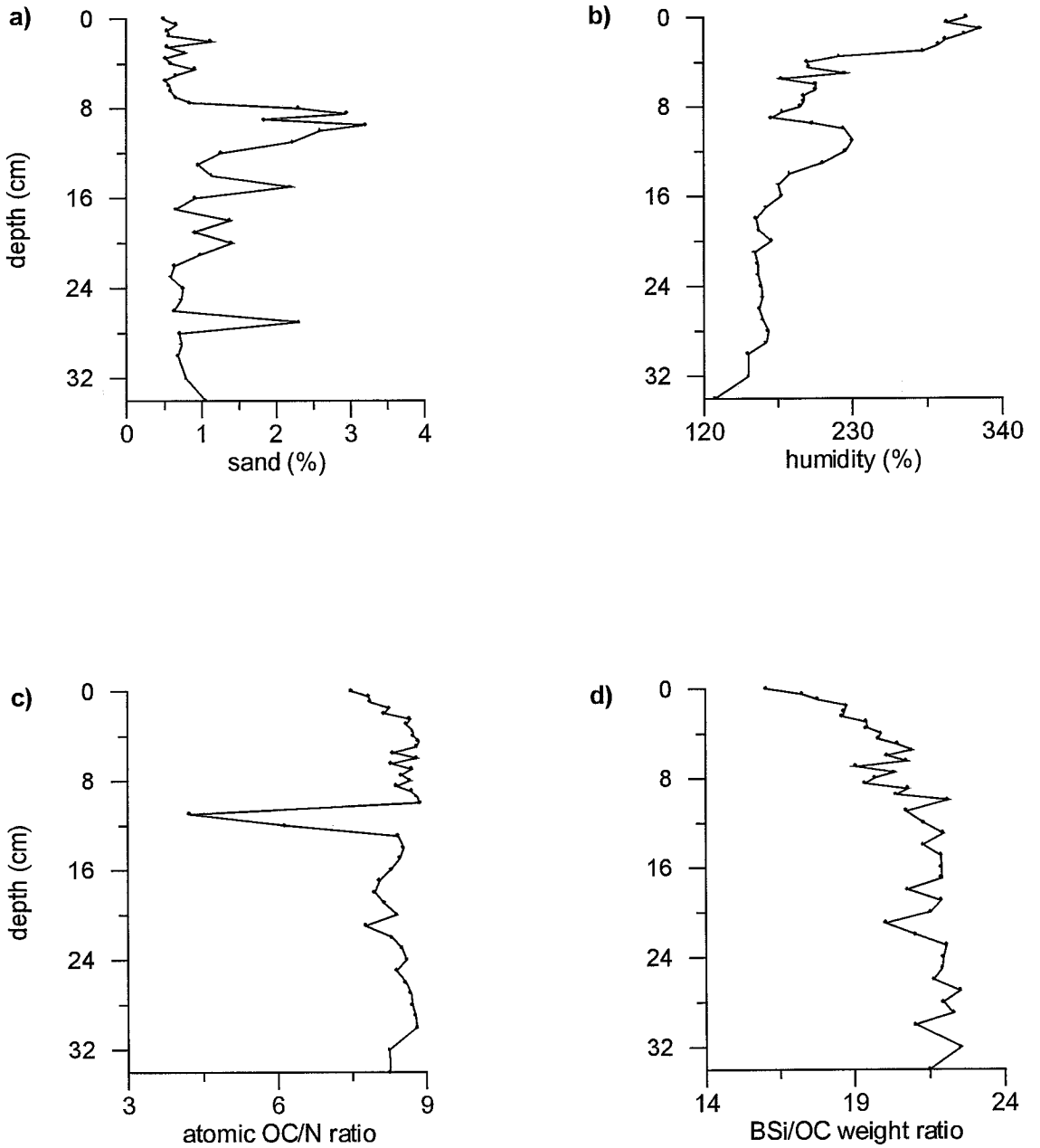

Fig. 4.13. (a) Sand and (b) humidity contents and (c) organic carbon to nitrogen (OC/N) and (d) biogenic silica to organic carbon (BSi/OC) weight ratios along multicore B187 in western Gerlache Strait.

4.2.1.2. Associations between variables

Atomic OC/N ratio minimum and maximum values were 4.27 and 8.87, respectively (Fig. 4.13c), the minimum value was due to an isolated N content increment in sample at cm 11. The atomic OC/N ratio average was 8.29 ± 0.79 with a variation coefficient of 0.1.

OC and BSi were not strongly related (R^2= 0.48). BSi/OC weight ratio ranged from 16.06 to 21.5, the mean value was 20.6 ± 1.49 and the variation coefficient was 0.24 (Fig. 4.13d). BSi/OC weight ratio showed an increasing trend towards the bottom.

BSi was not clearly related to any variable. The most evident association was with OC profile. BSi was the best-preserved variable.

No association between sand content and any other variable was found.

4.2.2. Multicore B191

4.2.2.1. Major biogenic constituents, SAR, and sand content

This 32-cm long core was taken from a muddy sea floor at 560-m water depth. This site was located between Anvers and Wiencke Islands, over the Bismarck Strait on the western part of the Gerlache Strait (Fig. 2.3). Several samples had clasts bigger than 30 mm in diameter that increased the sand content percentage.

TC content ranged from 0.6 to 0.91%; the average value was 0.7 ± 0.08% and the variation coefficient was equal to 0.12 (Fig. 4.14a). This profile showed a decreasing trend towards the bottom.

The minimum and maximum IC content values were <0.003 and 0.02%, respectively (Fig. 4.14b). The mean value was 0.01 ± 0.006% and the variation coefficient 0.52. A slight increasing trend towards the bottom was noticed. $CaCO_3$ content varied between 0 and 0.2%, it averaged 0.09 ± 0.05% (Fig. 4.14c).

OC content was more than 96% of the TC. It ranged from 0.59 to 0.89% with a mean value of 0.7 ± 0.08% (Fig. 4.14d). The variation coefficient was 0.11.

N content values varied between 0.07 and 0.13% and averaged 0.1 ± 0.01%; the variation coefficient was 0.15 (Fig. 4.14e). N content profile showed a slight decreasing trend towards the bottom.

BSi content values ranged from 9.84 to 12.21% (Fig. 4.14f). The mean value was 11.05 ± 0.66% and the variation coefficient 0.06. The top 7-cm concentrated samples with high BSi content. Below cm 10, the opal content increased again.

The SML was 2 cm thick (Table 4.1). The mean sedimentation rate was 930 ± 50 g $cm^{-2}y^{-1}$ or 1.17 ± 0.07 mm y^{-1}. This leaded to an OC accumulation rate of 7.81 ± 0.42 g $m^{-2}y^{-1}$ within the SML and 6.23 ± 0.33 g $m^{-2}y^{-1}$ below it. The OC burial efficiency at this site was 80%. The accumulation rate for $CaCO_3$ within the SML was 0.97 ± 0.05 g

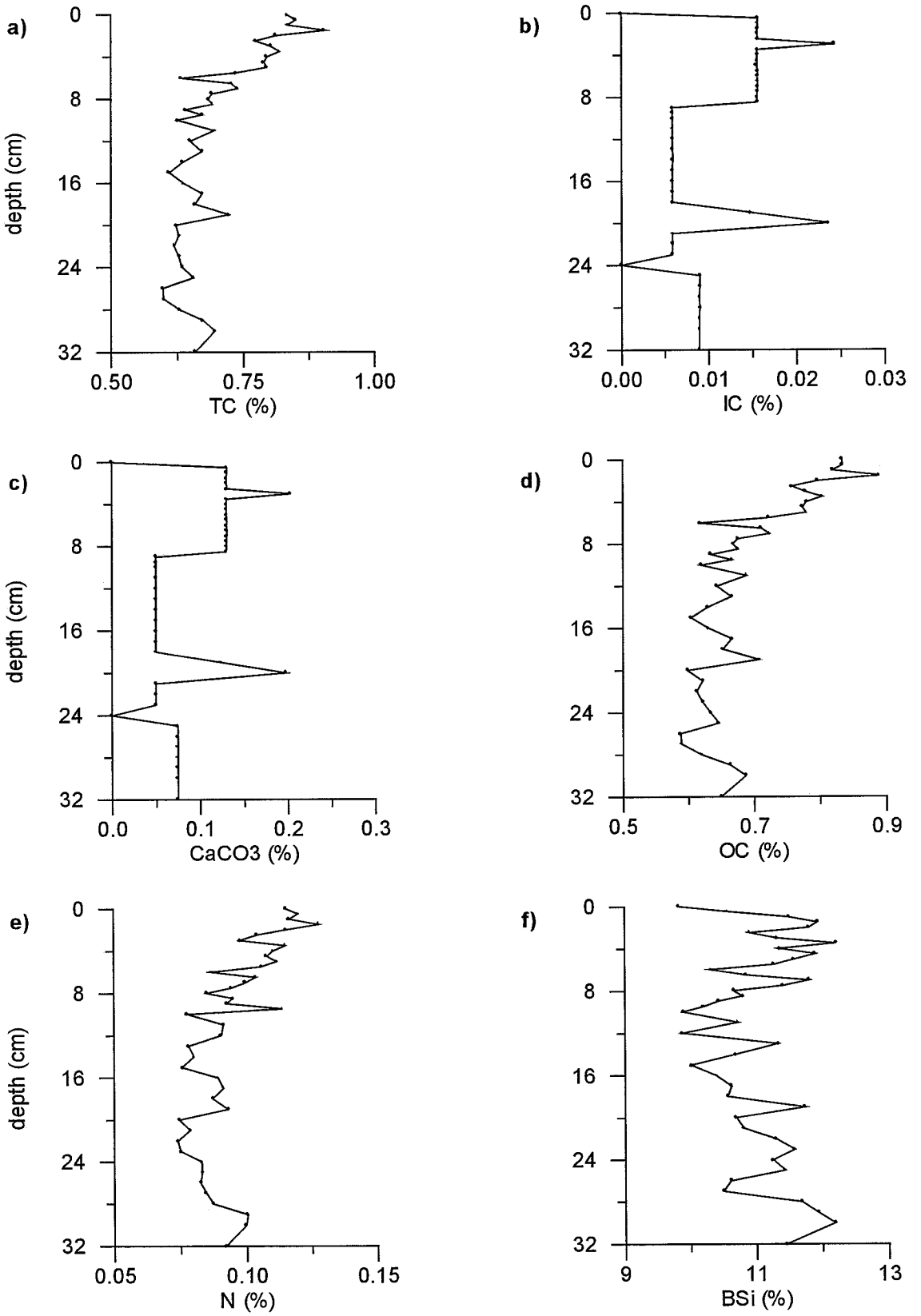

Fig. 4.14. (a) Total carbon (TC), (b) inorganic carbon (IC), (c) calcium carbonate (CaCO3), (d) organic carbon (OC), (e) nitrogen (N) and (f) biogenic silica (BSi) concentrations along multicore B191 in western Gerlache Strait.

$m^{-2}y^{-1}$ and below it 0.83 ± 0.05 g $m^{-2}y^{-1}$. The burial efficiency was 90%. N accumulation rate was 1.12 ± 0.06 g $m^{-2}y^{-1}$ within the SML and 0.84 ± 0.05 g $m^{-2}y^{-1}$ below it. The N burial efficiency was 75%. The BSi accumulation rate within the SML was 103.51 ± 5.57 g $m^{-2}y^{-1}$ and below it 102.67 ± 5.52 g $m^{-2}y^{-1}$. BSi burial efficiency was 99%. Averages content values for each biogenic variable within and below the SML are listed in Table 4.1.

Sand content values were among the highest within all the cores due to the presence of particles bigger than 1-mm diameter found in different layers. These values ranged between 16.80 and 49.93%, they averaged 22.87 ± 5.28%; the variation coefficient was 0.23 (Fig. 4.15a). The sand content profile showed a slight increasing trend towards the bottom.

4.2.2.2. Associations between variables

Atomic OC/N ratio minimum and maximum values were 6.83 and 9.93, respectively and the average 8.55 ± 0.62, the variation coefficient 0.07 (Fig. 4.15c).
OC and BSi contents were not well related (R^2= 0.15). The BSi/OC weight ratio ranged from 11.81 to 18.86, the mean value was 16.16 ± 1.59 and the variation coefficient 0.1 (Fig. 4.15d).
BSi was not clearly related to any other variable, though it was the best-preserved material.

Although sand percentage had high values, its influence was not evident in the biogenic variable contents and no clear relations were found.

4.2.3. Multicore B192

4.2.3.1. Major biogenic constituents, SAR, and sand content

This core had 16-cm length. It was taken at 283-m below the sea surface in a muddy bottom at the centre of the Gerlache Strait (Fig. 2.3).

TC content varied between 0.53 and 0.88%. The average was 0.73 ± 0.12% and the variation coefficient 0.16 (Fig. 4.16a). This profile showed a decreasing trend towards the bottom.

IC content values ranged from 0.01 to 0.11%. The IC content values averaged 0.07 ± 0.03% and they had a variation coefficient of 0.39 (Fig. 4.16b). $CaCO_3$ content values varied between 0.1 and 0.94%, they had a mean value of 0.59 ± 0.23% and a variation coefficient of 0.39 (Fig. 4.16c).

OC content minimum and maximum values were 0.42 and 0.85%, respectively; the mean value was 0.66 ± 0.12% and the variation coefficient 0.19 (Fig. 4.16d). OC was more than 78% of the TC.

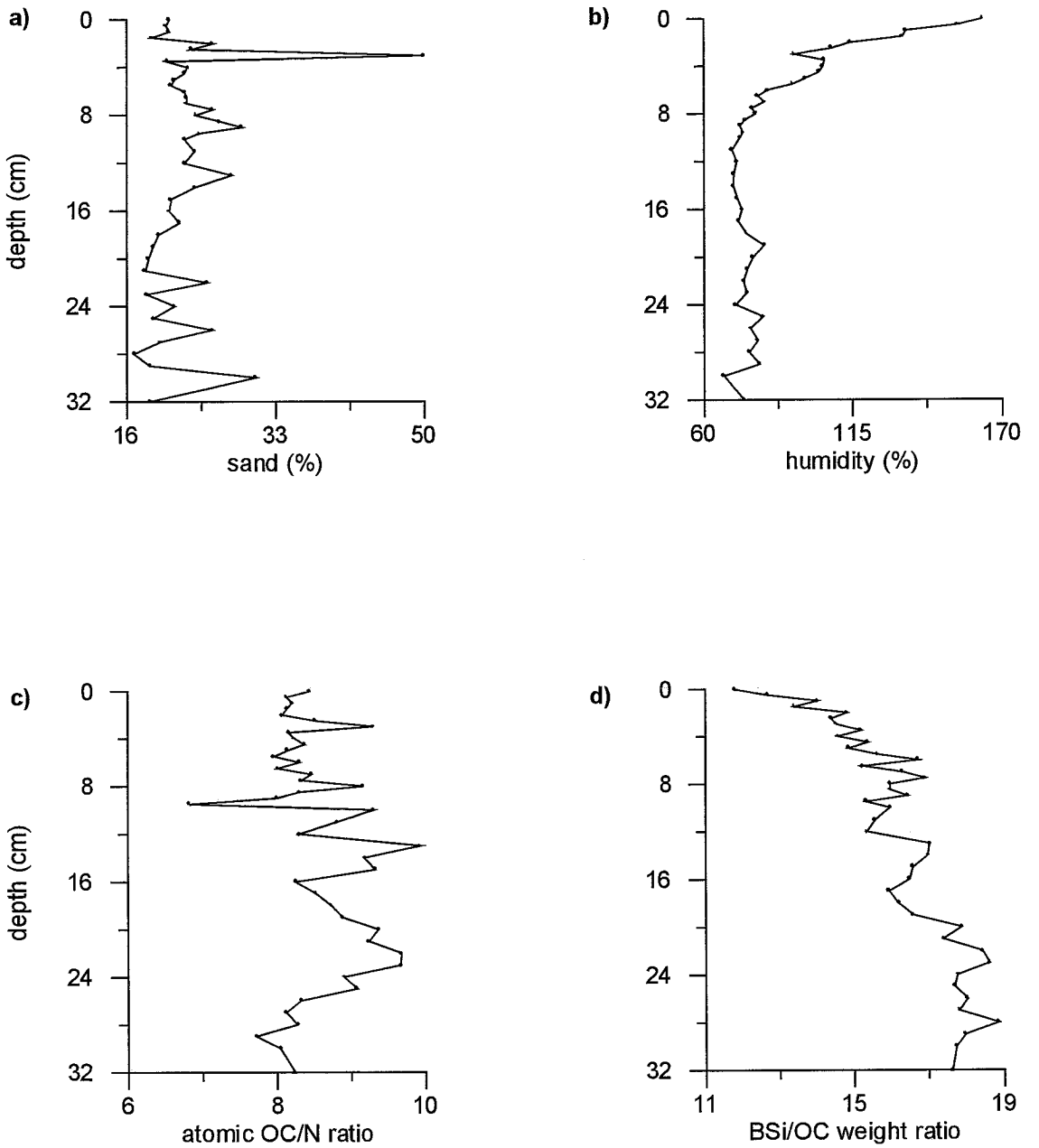

Fig. 4.15. (a) Sand and (b) humidity contents and (c) atomic organic carbon to nitrogen (OC/N) and (d) biogenic silica to organic carbon (BSi/OC) weight ratios along multicore B191 in western Gerlache Strait.

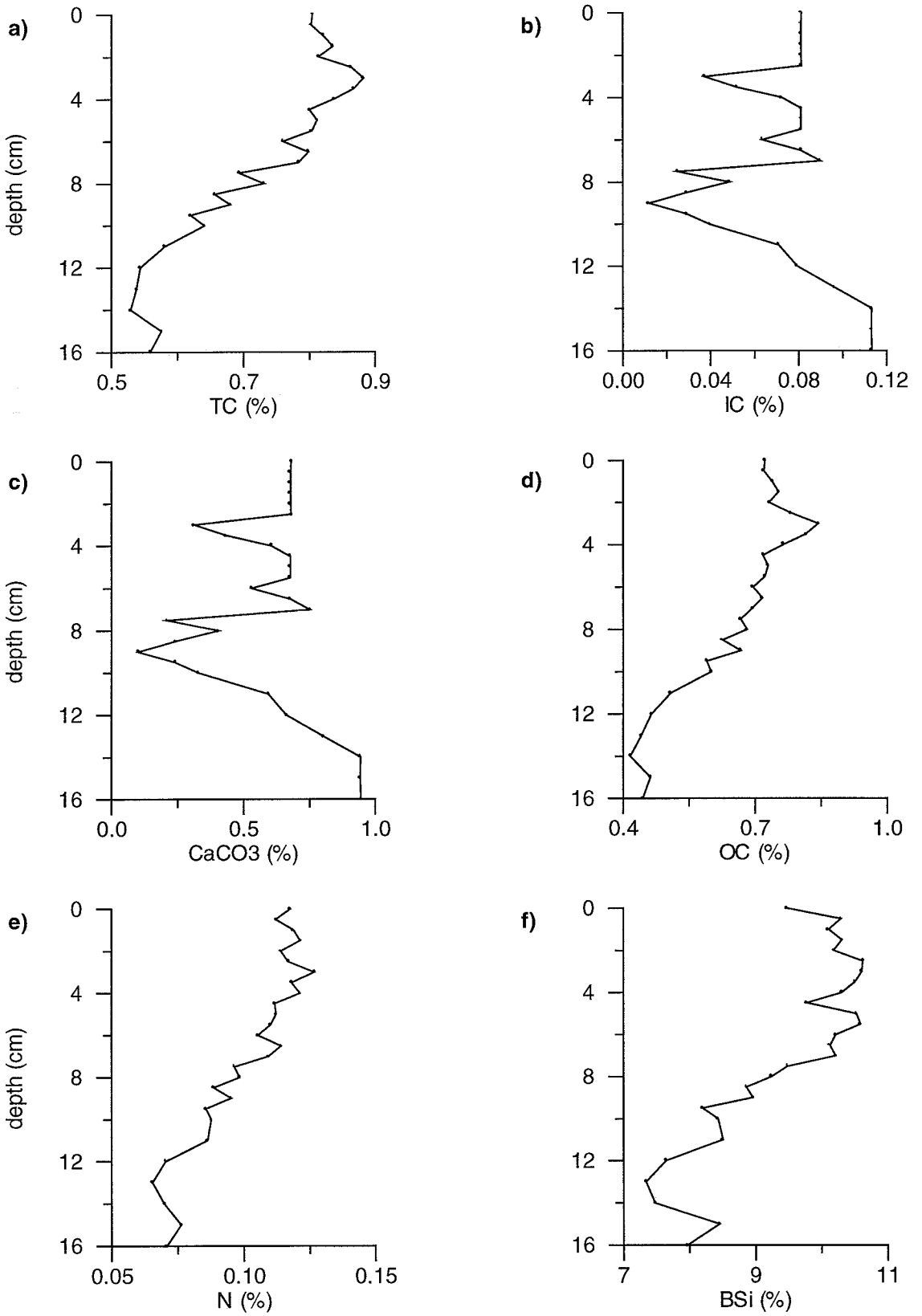

Fig. 4.16. (a) Total carbon (TC), (b) inorganic carbon (IC), (c) calcium carbonate (CaCO3), (d) organic carbon (OC), (e) nitrogen (N) and (f) biogenic silica (BSi) concentrations along multicore B192 in central Gerlache Strait.

N content values followed a decreasing trend towards the bottom. They ranged from 0.07 to 0.13% with an average of 0.1 ± 0.02%. The variation coefficient was 0.19 (Fig. 4.16e).

BSi content average was 9.43 ± 1.08% with a variation coefficient equal to 0.11. The decreasing trend followed towards the bottom varied between 7.34 and 10.63% (Fig. 4.16f).

The SAR was 630 ± 30 g $m^{-2}y^{-1}$ or 0.65 ± 0.03 mm y^{-1} (Table 4.1). The apparent mean OC accumulation rate within the SML was 4.73 ± 0.22 g $m^{-2}y^{-1}$ and below it 3.53 ± 0.17 g $m^{-2}y^{-1}$. The burial efficiency was 75%. The apparent mean $CaCO_3$ accumulation rate was 3.89 ± 0.19 g $m^{-2}y^{-1}$ within the SML and 3.47 ± 0.17 g $m^{-2}y^{-1}$ below it. The burial efficiency was 89%. The apparent mean N accumulation rate was 0.76 ± 0.04 g $m^{-2}y^{-1}$ within the SML and 0.57 ± 0.03 g $m^{-2}y^{-1}$ below it. The burial efficiency was 75%. The apparent mean BSi accumulation rate within the SML was 64.70 ± 3.08 g $m^{-2}y^{-1}$ and below it 53.74 ± 2.56 g $m^{-2}y^{-1}$. The burial efficiency was 83%. The mean values for the biogenic variables content within and below the SML are listed in Table 4.1.

Sand content showed an increasing trend towards the bottom that ranged from 18.81 to 62.52%. The mean value was 29.10 ± 11.26% and the variation coefficient 0.39 (Fig. 4.17a).

4.2.3.2. Associations between variables

Atomic OC/N ratio averaged 7.61 ± 0.39 with a variation coefficient of 0.05. Minimum and maximum values were 6.88 and 8.26, respectively (Fig. 4.17c).

The correspondence between OC and BSi values was strong (R^2= 0.87). BSi/OC ratio ranged from 12.57 and 18.32, the mean value was 14.62 ± 1.61 and the variation coefficient 0.11 (Fig. 4.17d). BSi/OC weight ratio values increased towards the bottom.

OC and sand content profiles had an opposite trend and a weak correspondence between their values (R^2= 0.45). Sand percentage did not clearly influence biological variables although it showed an evident inverse downcore trend.

4.2.4. Multicore B5

4.2.4.1. Major biogenic constituents, SAR, and sand content

This 32-cm long core was taken at 1008-m water depth over the Crocker Passage at the eastern extreme of the Gerlache Strait (Fig. 2.3). It consisted mainly in mud.

TC content ranged from 0.78 to 1.25%. The mean value was 1.03 ± 0.14% and the variation coefficient was equal to 0.13 (Fig. 4.18a). TC content profile showed a diminishing trend towards the bottom.

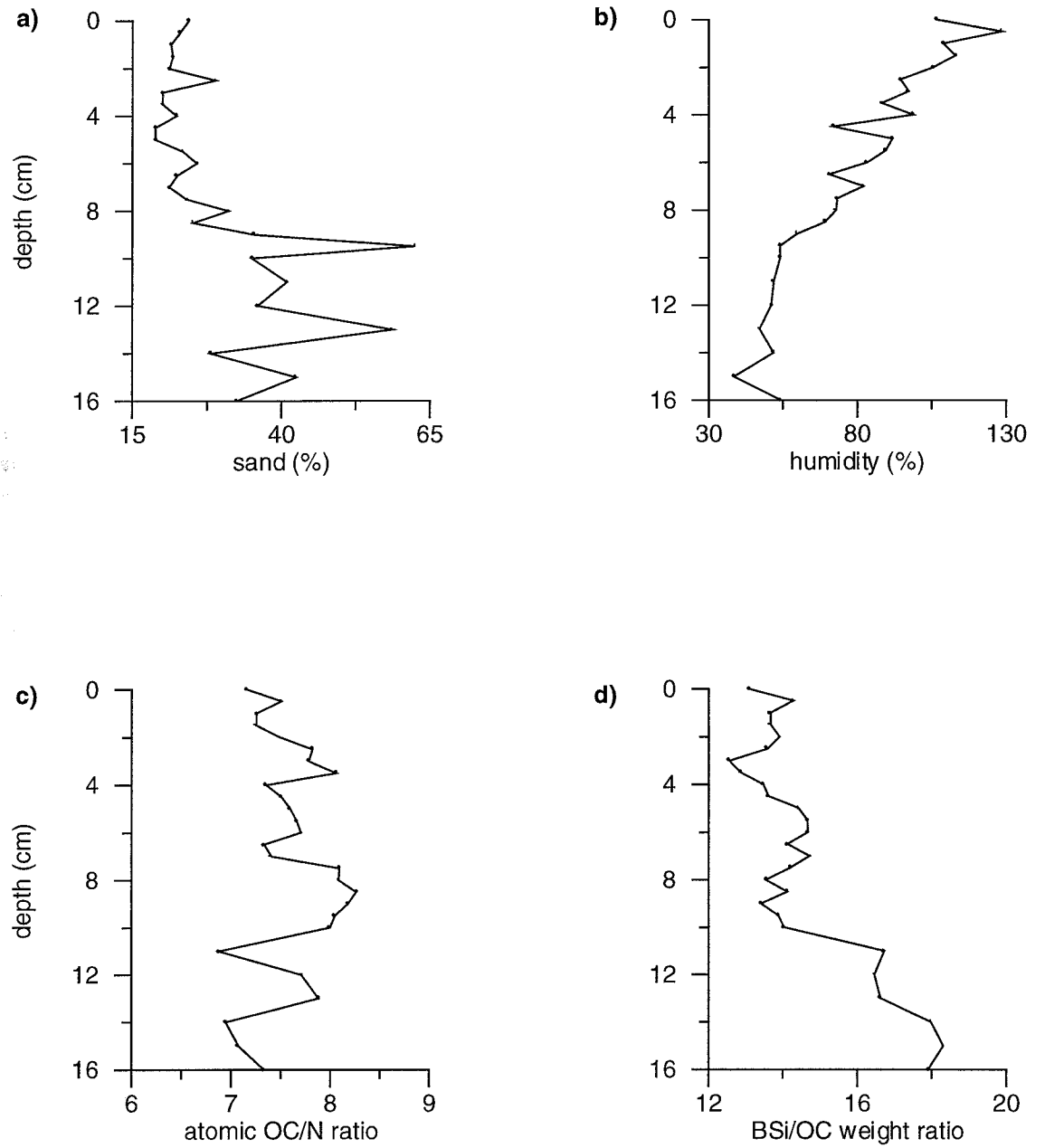

Fig. 4.17. (a) Sand and (b) humidity contents and (c) atomic organic carbon to nitrogen (OC/N) and (d) biogenic silica to organic carbon (BSi/OC) weight ratios along multicore B192 in central Gerlache Strait.

IC content varied between <0.003 and 0.01%. The average was 0.009 ± 0.004% and the variation coefficient 0.49 (Fig. 4.18b). The highest values corresponded to the samples from the extremes of the core. CaCO3 content minimum and maximum values were 0 and 0.11%, respectively. The mean was 0.08 ± 0.04% and the variation coefficient 0.49 (Fig. 4.18c).

OC content ranged from 0.76 to 1.25%. The average was 1.02 ± 0.14% and the variation coefficient 0.13 (Fig. 4.18d). OC accounted for more than 98% of the TC.

N content varied between 0.1 and 0.18%. The mean value was 0.13 ± 0.02% and the variation coefficient 0.14 (Fig. 4.18e). N content profile showed a clear diminishing trend towards the bottom, markedly along the top 7-cm.

BSi content profile followed a slight increasing trend towards the bottom. It ranged from 15.12 to 18.8%. The average value was 17.18 ± 0.83% and the variation coefficient 0.05 (Fig. 4.18f).

The SAR was 1110 ± 120 g $m^{-2}y^{-1}$ or 1.8 ± 0.2 mm y^{-1} (Table 4.1). The SML was 11 cm thick. Mean OC, N, $CaCO_3$, and BSi content values within the SML were 1.13 ± 0.07, 0.14 ± 0.02, 0.08 ± 0.04, and 17.39 ± 0.88%, respectively. In the same order mean values below this layer were 0.91 ± 0.09, 0.12 ± 0.01, 0.07 ± 0.03, and 16.96 ± 0.74%. SAR for each biogenic variable and the associated burial efficiencies are listed in Table 4.1.

Sand content values varied between 1.71 and 16.54%. The mean was 5.41 ± 4.14% and the variation coefficient 0.77 (Fig. 4.19a). There was a slight increasing tendency towards the bottom.

4.2.4.2. Associations between variables

Atomic OC/N ratio showed a slight increment towards the bottom. This tendency was more evident along the top 6 cm. The minimum and maximum values were 7.85 and 11.18, respectively. The mean value was 9.34 ± 0.87 and the variation coefficient 0.09 (Fig. 4.19c). BSi/OC ratio values ranged from 12.25 to 21.18. The average value was 17.1 ± 2.25, the variation coefficient was 0.13 (Fig. 4.19d). The BSi/OC weight ratio followed an increasing trend towards the bottom. BSi was the best-preserved variable in the sediment.

Sand content was not clearly related to any variable. Nevertheless, the sample with the highest sand content (16.54%) showed an increase in OC, N, and BSi contents as well.

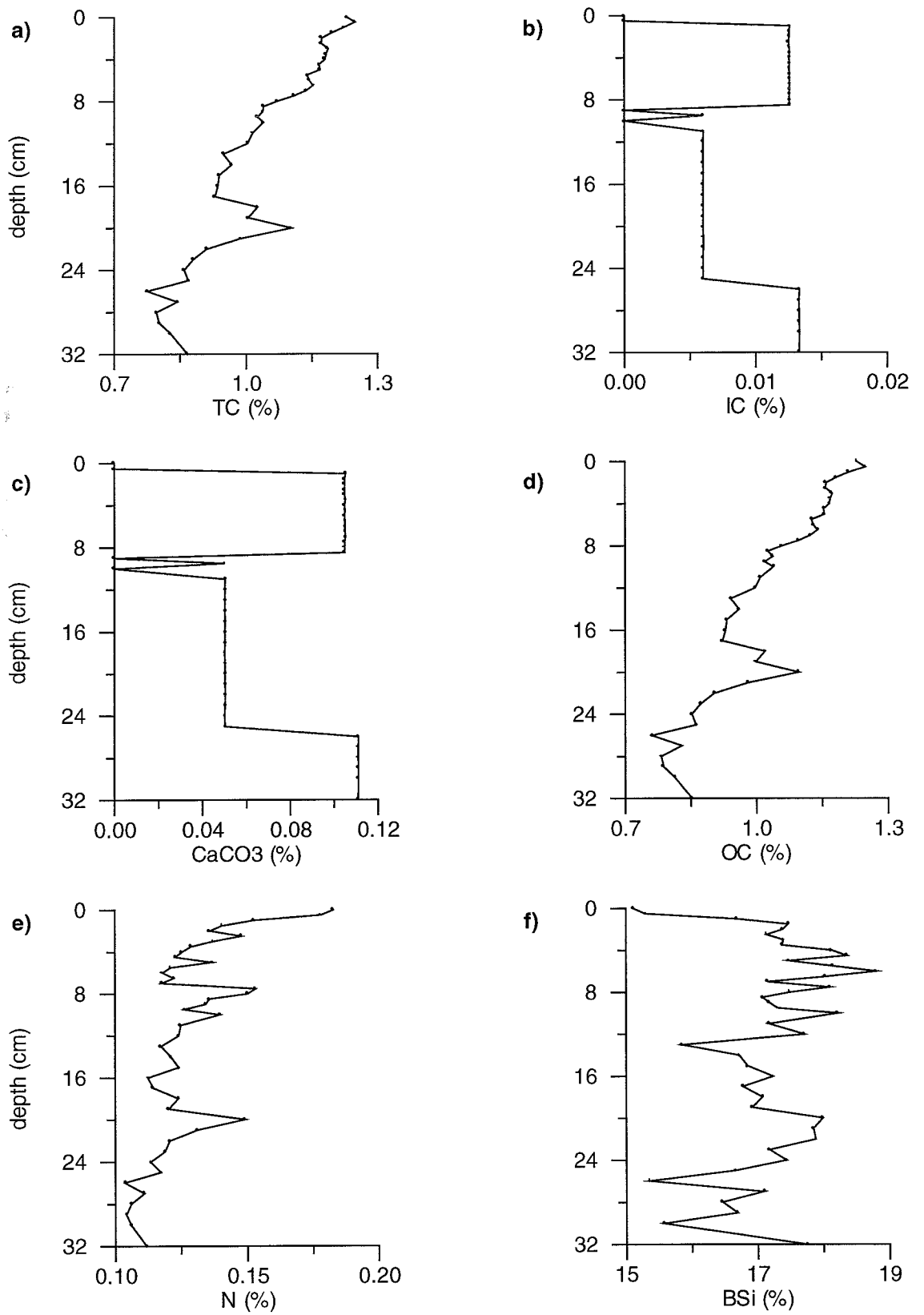

Fig. 4.18. (a) Total carbon (TC), (b) inorganic carbon (IC), (c) calcium carbonate (CaCO3), (d) organic carbon (OC), (e) nitrogen (N) and (f) biogenic silica (BSi) concentrations along multicore B5 in eastern Gerlache Strait.

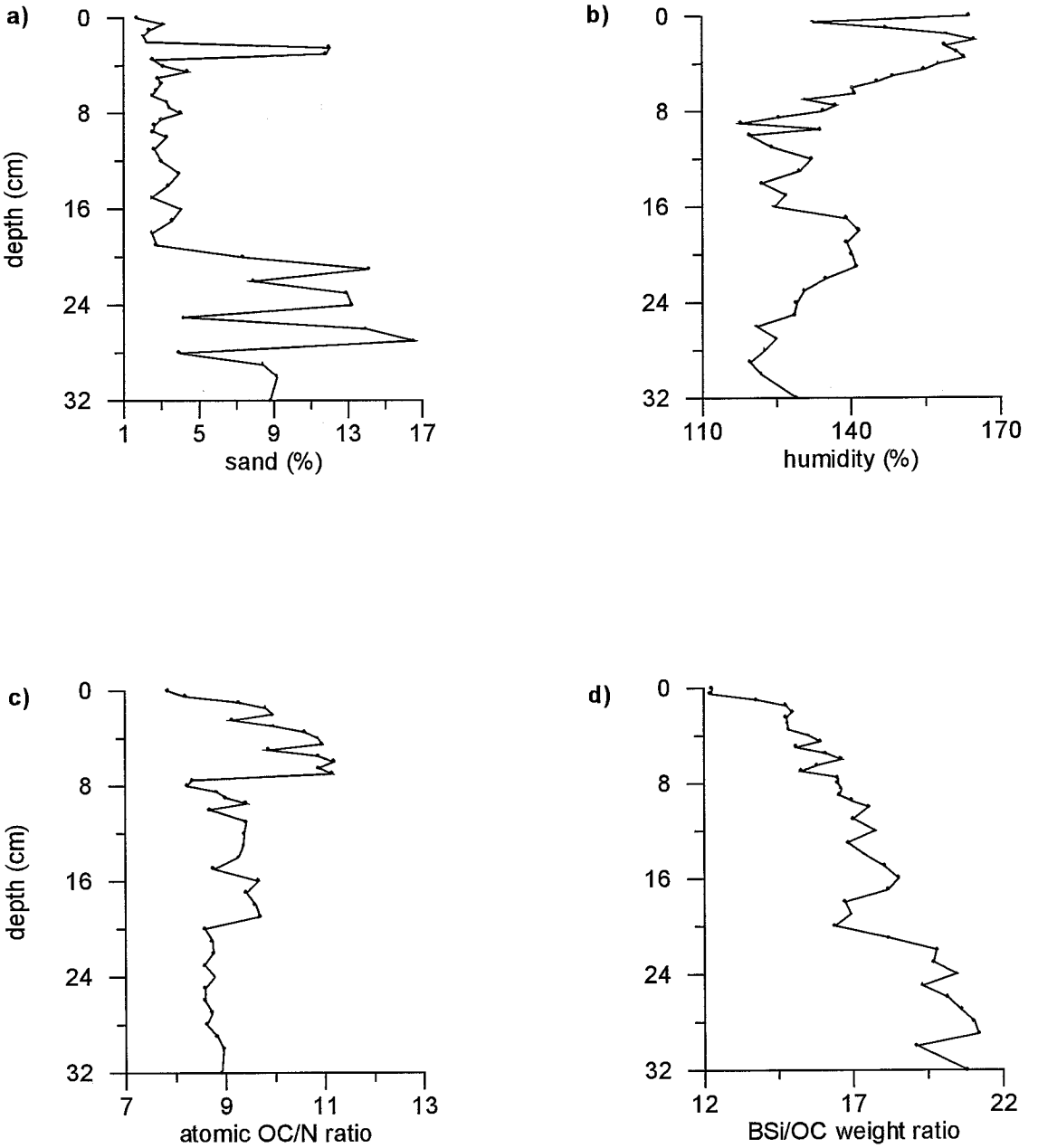

Fig. 4.19. (a) Sand and (b) humidity contents and (c) atomic organic carbon to nitrogen (OC/N) and (d) biogenic silica to organic carbon (BSi/OC) weight ratios along multicore B5 in eastern Gerlache Strait.

4.2.5. Multicore B6

4.2.5.1. Major biogenic constituents, SAR, and sand content

It was recovered at 553-m depth at the eastern part of the Gerlache Strait (Fig. 2.3). It was 34-cm long and it consisted mainly in mud.

TC content ranged from 0.74 to 1.61%. The average value was 1.01 ± 0.2% and the variation coefficient 0.2 (Fig. 4.20a). This profile showed a slight decreasing tendency towards the bottom.

The minimum and maximum IC content values were <0.003 and 0.02%, respectively (Fig. 4.20b). The mean was 0.01 ± 0.007% and the variation coefficient was equal to 0.54. An increasing trend was observed along the top 7 cm. $CaCO_3$ content varied between 0 and 0.2%. The average was 0.11 ± 0.06% (Fig. 4.20c).

OC content was more than 97% of the TC. It varied between 0.68 and 1.61%. The mean value was 1 ± 0.2 and the variation coefficient 0.2 (Fig. 4.20d).

N content values followed a slight decreasing tendency that ranged from 0.09 to 0.21%. The average was 0.13 ± 0.03% and the variation coefficient 0.21 (Fig. 4.20e).

BSi content values varied between 11.45 and 17.60%. The mean was 15.04 ± 1.72% and the variation coefficient 0.12 (Fig. 4.20f). The BSi profile showed a diminishing trend towards the bottom.

The SAR at this site was 1100 ± 90 g $cm^{-2}y^{-1}$ or 1.57 ± 0.13 mm y^{-1} (Table 4.1). The SML was 3 cm thick. The average content values for OC, N, $CaCO_3$, and BSi within the SML were 1.32 ± 0.13, 0.17 ± 0.02, 0.06 ± 0.05, and 17.03 ± 0.37%, respectively. In the same order the mean content values below the SML were 0.94 ± 0.14, 0.12 ± 0.02, 0.12 ± 0.06, and 14.65 ± 1.61%. SAR for each variable and the associated burial efficiency values are listed in Table 4.1.

Sand content minimum and maximum values were 2.68 and 31.93%, respectively (Fig. 4.21a). The average was 6.66 ± 5.15 and the variation coefficient 0.77. There was an evident increase of the sand content between cm 12 and 21 that increased the average and the variation coefficient.

4.2.5.2. Associations between variables

Atomic OC/N ratio ranged from 8.33 to 9.68. The average was 8.99 ± 0.25 and the variation coefficient 0.03 (Fig. 4.21c). This ratio profile did not show any evident tendency. BSi/OC weight ratio followed an increasing trend towards the bottom. BSi/OC minimum and maximum values were 10.47 and 18.14, respectively (Fig. 4.21d). The average was 15.29 ± 1.39 and the variation coefficient 0.09.

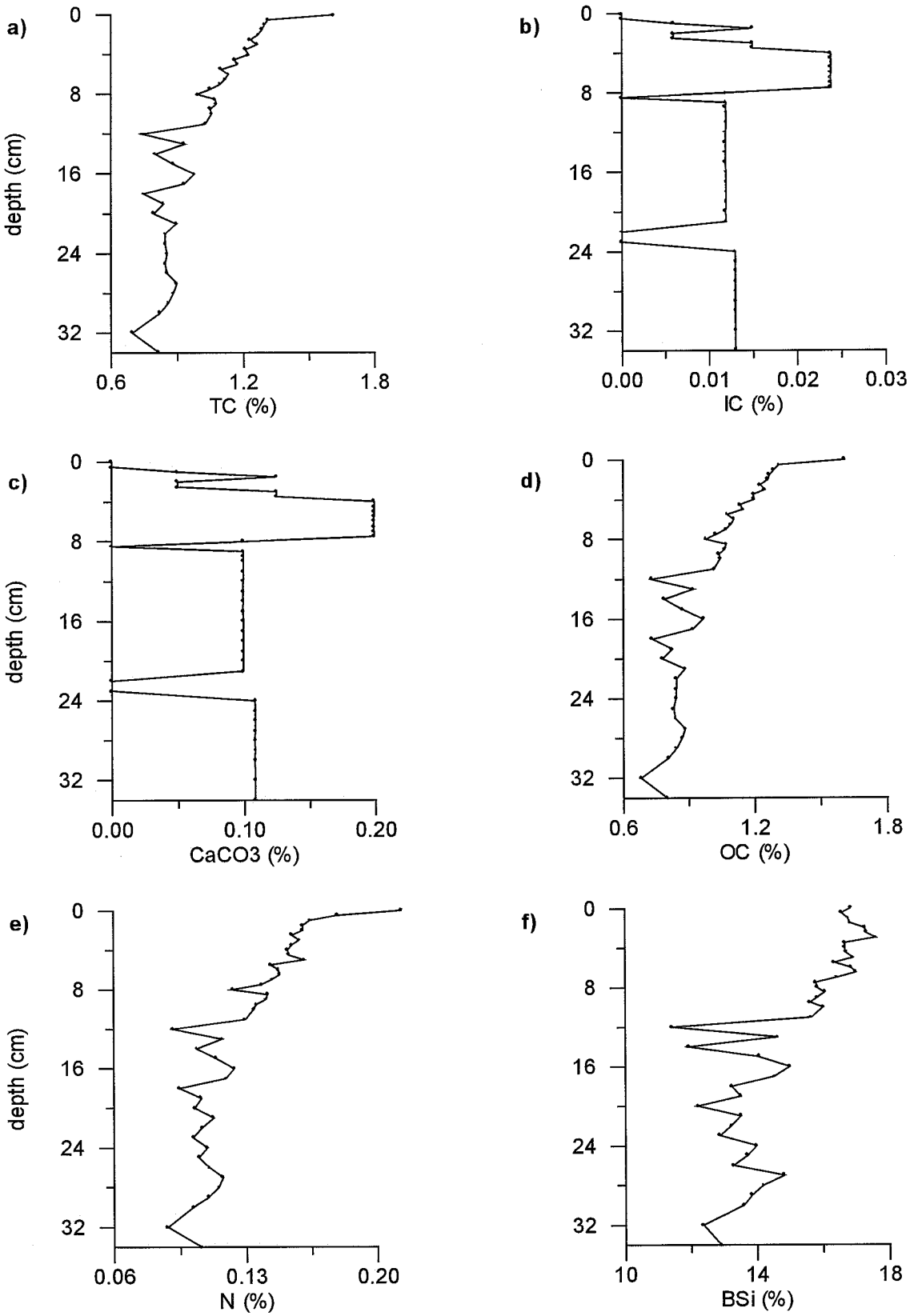

Fig. 4.20. (a) Total carbon (TC), (b) inorganic carbon (IC), (c) calcium carbonate (CaCO3), (d) organic carbon (OC), (e) nitrogen (N) and (f) biogenic silica (BSi) concentrations along multicore B6 in eastern Gerlache Strait.

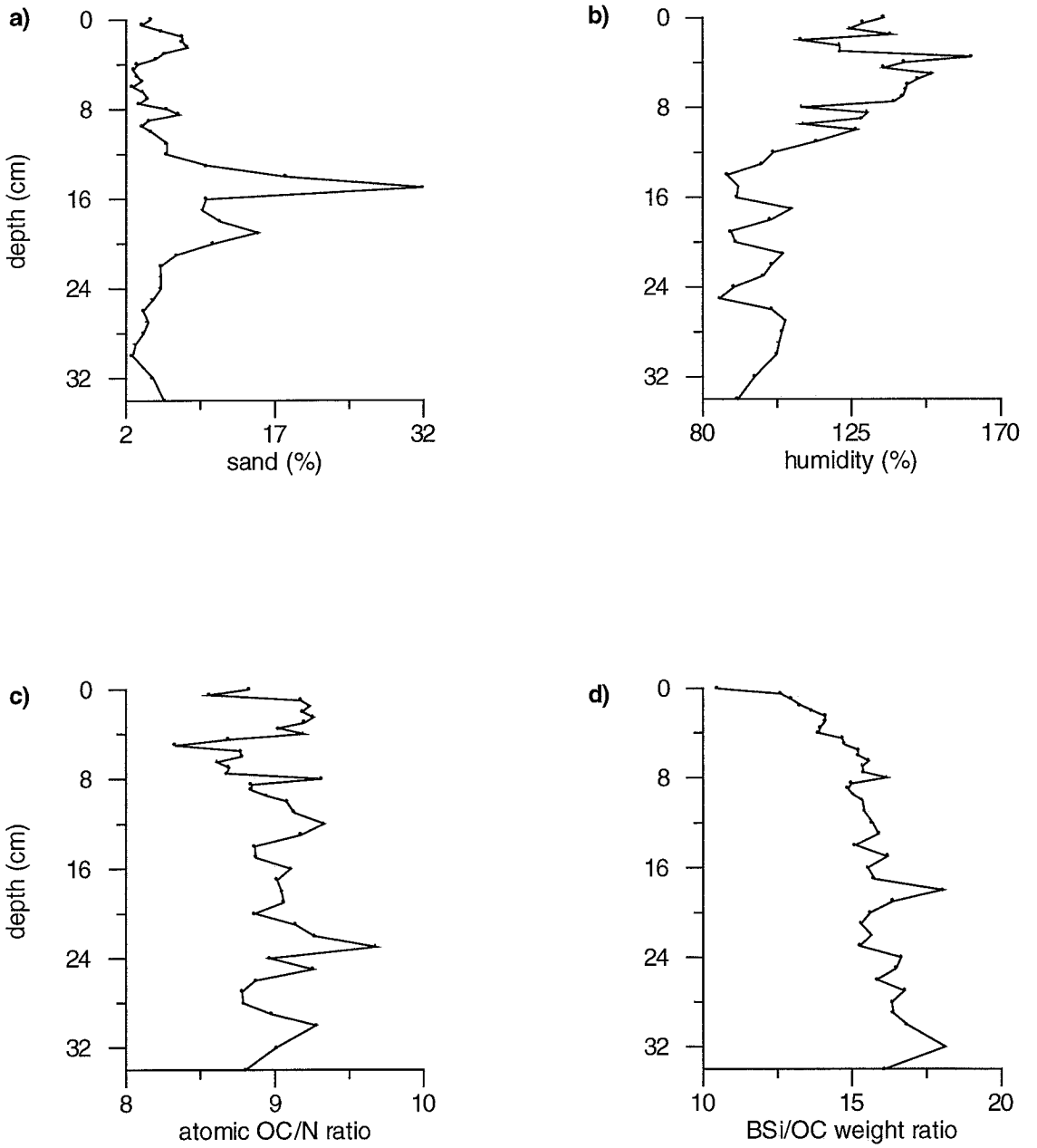

Fig. 4.21. (a) Sand and (b) humidity contents and (c) atomic organic carbon to nitrogen (OC/N) and (d) biogenic silica to organic carbon (BSi/OC) weight ratios along multicore B6 in eastern Gerlache Strait.

BSi was the variable that showed the highest burial efficiency percentage.
Sand content was not clearly related to any variable. Although there was a peak higher than 20% at cm 15, its influence was not noticed in the biogenic variables content.

4.2.6. Multicore B7

4.2.6.1. Major biogenic constituents, SAR, and sand content

This core was taken at 830-m water depth at the centre of the Gerlache Strait, between Arctowski Peninsula and the Brabant Island (Fig. 2.3). It was 32-cm long and it consisted mainly in sandy mud.

TC content ranged from 1.03 to 1.52 %. The mean was 1.21 ± 0.12% and the variation coefficient 0.1 (Fig. 4.22a). This profile followed a diminishing trend towards the bottom.

IC content profile showed an increment with depth that varied between <0.003 and 0.01% (Fig. 4.22b). The average was 0.005 ± 0.003 and the variation coefficient 0.53. $CaCO_3$ content minimum and maximum values were 0 and 0.07%, respectively (Fig. 4.22c). The mean was 0.04 ± 0.2%.

OC content values changed between 1.02 and 1.52% (Fig. 4.22d). The average was 1.2 ± 0.13% and the variation coefficient 0.1. OC was more than 99% of the TC.

N content decreased towards the bottom. N profile ranged from 0.12 to 0.25% (Fig. 4.22e). The mean was 0.17 ± 0.03 and the variation coefficient 0.17.

BSi content profile showed two peaks at both the top and the bottom of the core. BSi values varied between 15.01 and 20.74 (Fig. 4.22f). They averaged 17.44 ± 1.38 and the variation coefficient 0.08.

The SML was 11-cm thick and the SAR 1750 ± 80 g $m^{-2}y^{-1}$ or 3.11 ± 0.14 mm y^{-1} (Table 4.1). Mean OC, N, $CaCO_3$, and BSi content values within the SML were 1.31 ± 0.06, 0.19 ± 0.02, 0.03 ± 0.01, and 18.4 ± 1.1%, respectively. In the same order mean values below this layer were 1.09 ± 0.05, 0.14 ± 0.02, 0.05 ± 0.02, and 16.43 ± 0.8%. The accumulation rates for each biogenic variable and the associated burial efficiencies are listed in Table 4.1.

Sand content minimum and maximum values were 1.66 and 31.70%, respectively (Fig. 4.23a). The average was 10.04 ± 9.36 and the variation coefficient 0.93. The sand content decreased towards the bottom.

4.2.6.2. Associations between variables

Atomic OC/N ratio values varied between 7.21 and 10.35 (Fig. 4.23c). The average was 8.59 ± 0.73 and the variation coefficient 0.09. This ratio profile showed an increasing trend towards the bottom. BSi/OC weight ratio curve followed an increasing

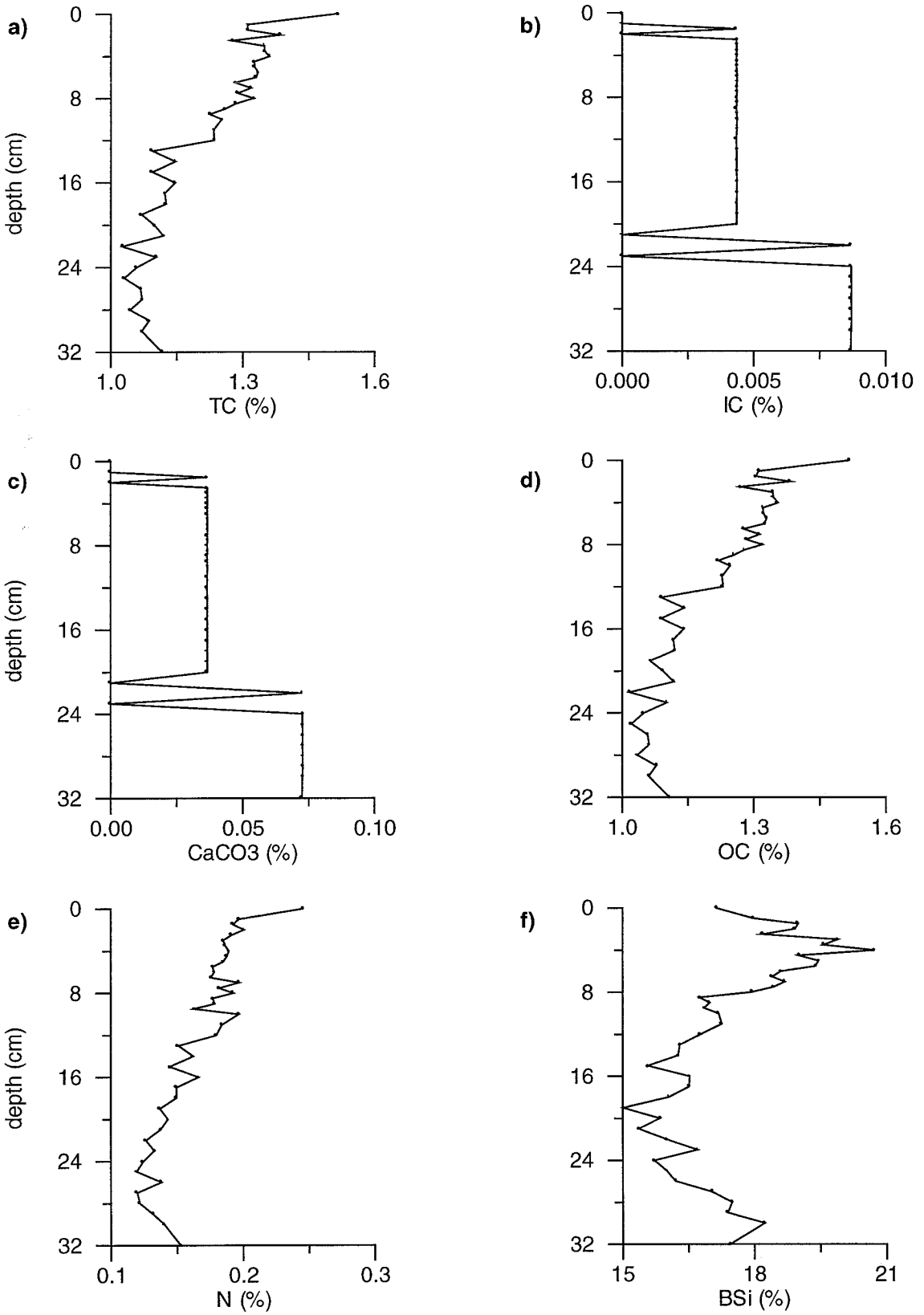

Fig. 4.22. (a) Total carbon (TC), (b) inorganic carbon (IC), (c) calcium carbonate (CaCO3), (d) organic carbon (OC), (e) nitrogen (N) and (f) biogenic silica (BSi) concentrations along multicore B7 in central Gerlache Strait.

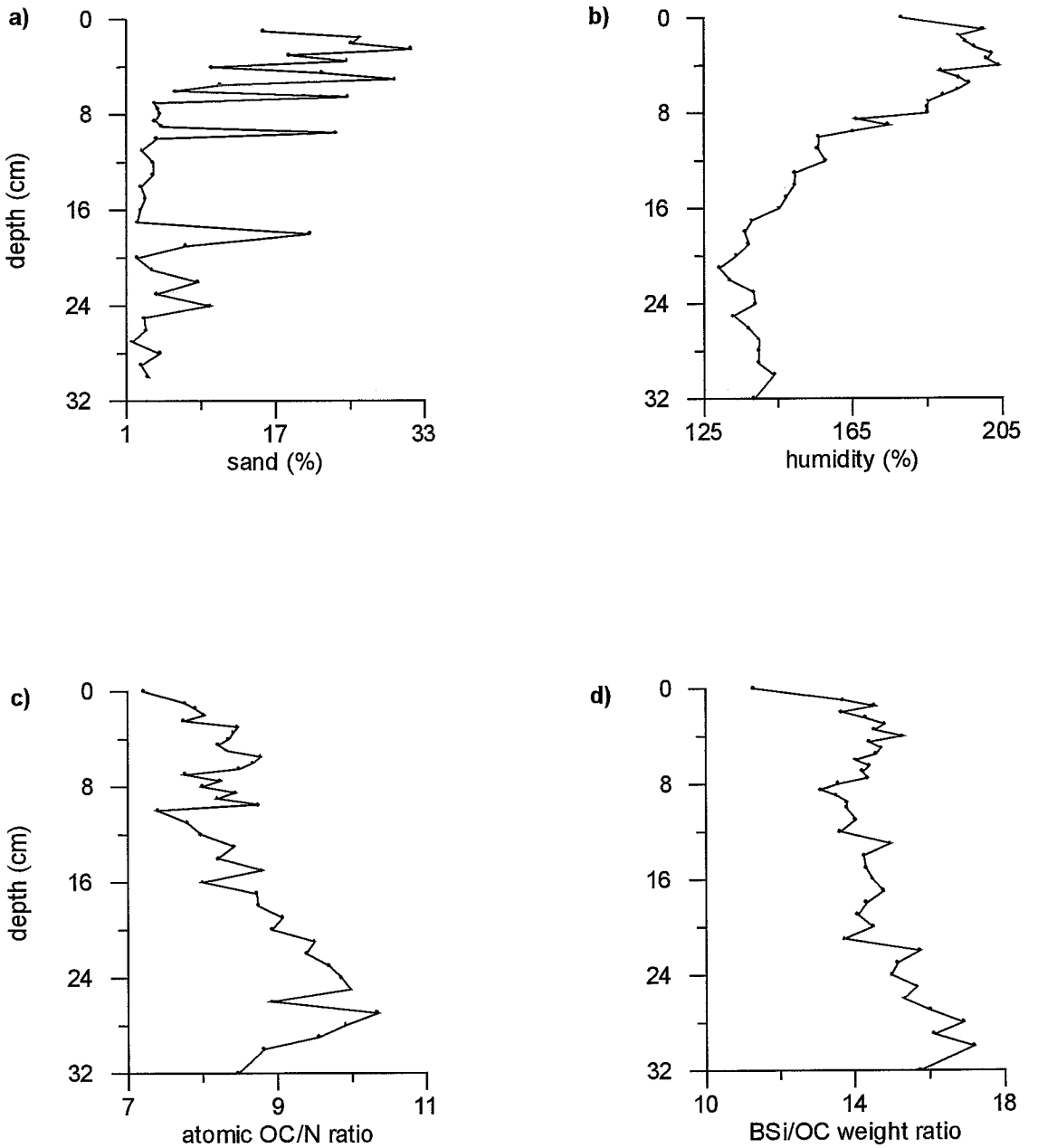

Fig. 4.23. (a) Sand and (b) humidity contents and (c) atomic organic carbon to nitrogen (OC/N) and (d) biogenic silica to organic carbon (BSi/OC) weight ratios along multicore B7 in central Gerlache Strait. Note: sand content in sample of cm 32 is not available.

downcore tendency that ranged from 11.31 to 17.18 (Fig. 4.23d). The mean value was 14.56 ± 1.04 and the variation coefficient 0.07.

The BSi had the highest burial efficiency among the remaining variables. Sand content was not clearly related to any variable.

4.3. BELLINGSHAUSEN SEA

Two multicores, B214 and B223, were recovered in the vicinities of the Bellingshausen Sea with the adjacent Bransfield Strait.

4.3.1. Multicore B214

4.3.1.1. Major biogenic constituents, SAR, and sand content

It was taken at 192-m water depth between Smith and Snow Islands (Fig. 2.3). It consisted in sandy mud and it was 34-cm long.

TC content varied between 0.16 and 0.42%. The average was 0.26 ± 0.08% and the variation coefficient 0.29 (Fig. 4.24a). The TC content profile followed a diminishing trend towards the bottom.

IC content had a variation coefficient of 0.29 and a mean value of 0.01 ± 0.003% (Fig. 4.24b). IC content percentage minimum value was <0.003 and the maximum 0.02. IC content profile showed a slight increasing trend towards the bottom. $CaCO_3$ content values ranged from 0 to 0.13%. The mean value was 0.09 ± 0.03% (Fig. 4.24c).

OC was more than 91% of the TC. OC content values varied between 0.15 and 0.42%. They averaged 0.25 ± 0.08% and their variation coefficient was 0.31 (Fig. 4.24d).

N content profile showed a diminishing trend towards the bottom. Its values ranged from 0.01 to 0.05%. The mean value was 0.03 ± 0.01% and the variation coefficient 0.42 (Fig. 4.24e).

BSi content minimum and maximum values were 4.46 and 7.43%, respectively. The average was 5.69 ± 0.71% and the variation coefficient 0.13 (Fig. 4.24f). This profile showed a slight decreasing trend towards the bottom, though there were two evident peaks close to the extremes of the core.

The SAR, the SML, and the biogenic variables accumulation rates are listed in Table 4.1.

Sand content showed a clear increasing trend towards the bottom that varied between 24.06 and 73.37%. The mean value was 49.95 ± 14.23% and the variation coefficient 0.29 (Fig. 4.25a).

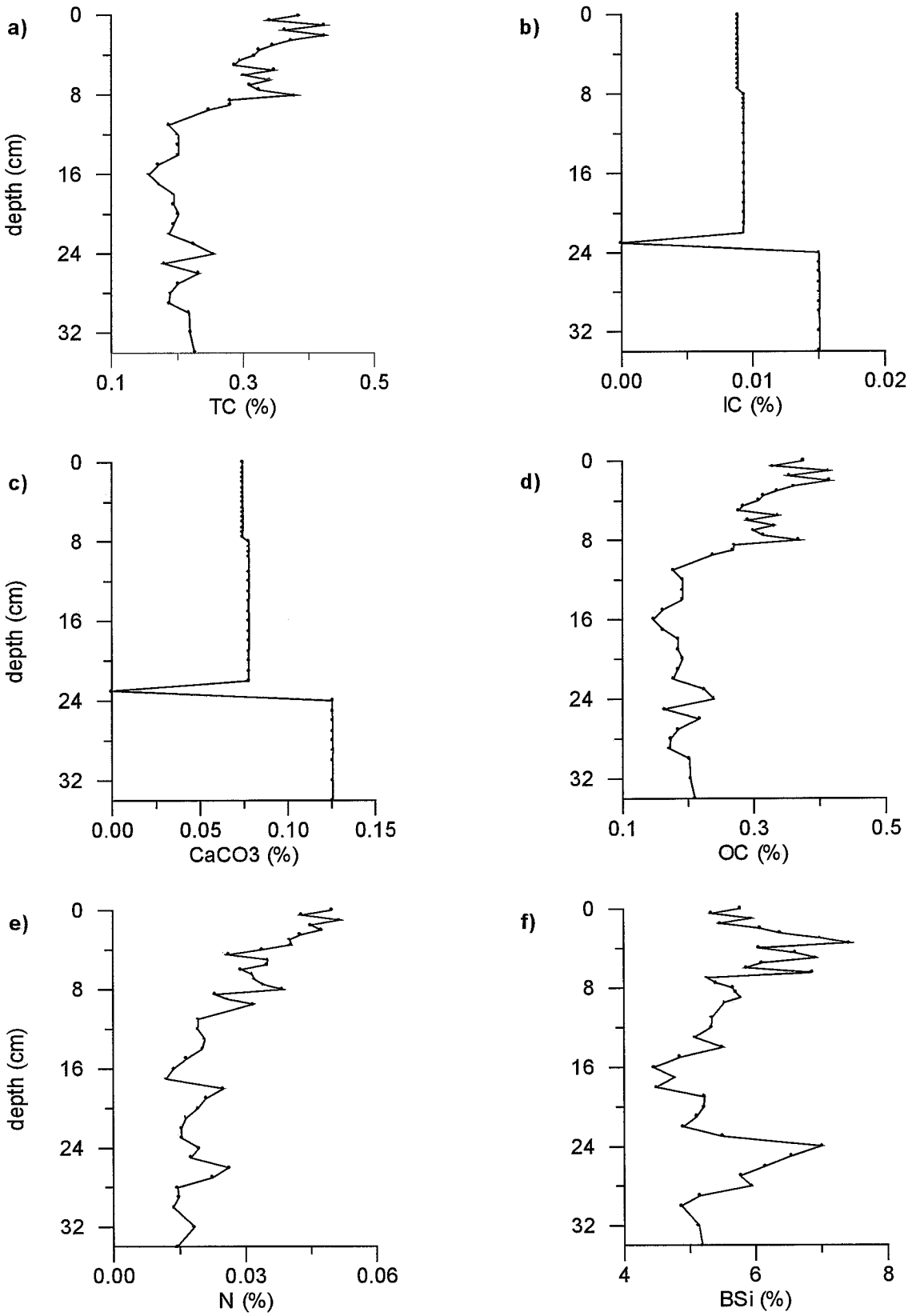

Fig. 4.24. (a) Total carbon (TC), (b) inorganic carbon (IC), (c) calcium carbonate (CaCO3), (d) organic carbon (OC), (e) nitrogen (N) and (f) biogenic silica (BSi) concentrations along multicore B214 in the Bellingshausen Sea.

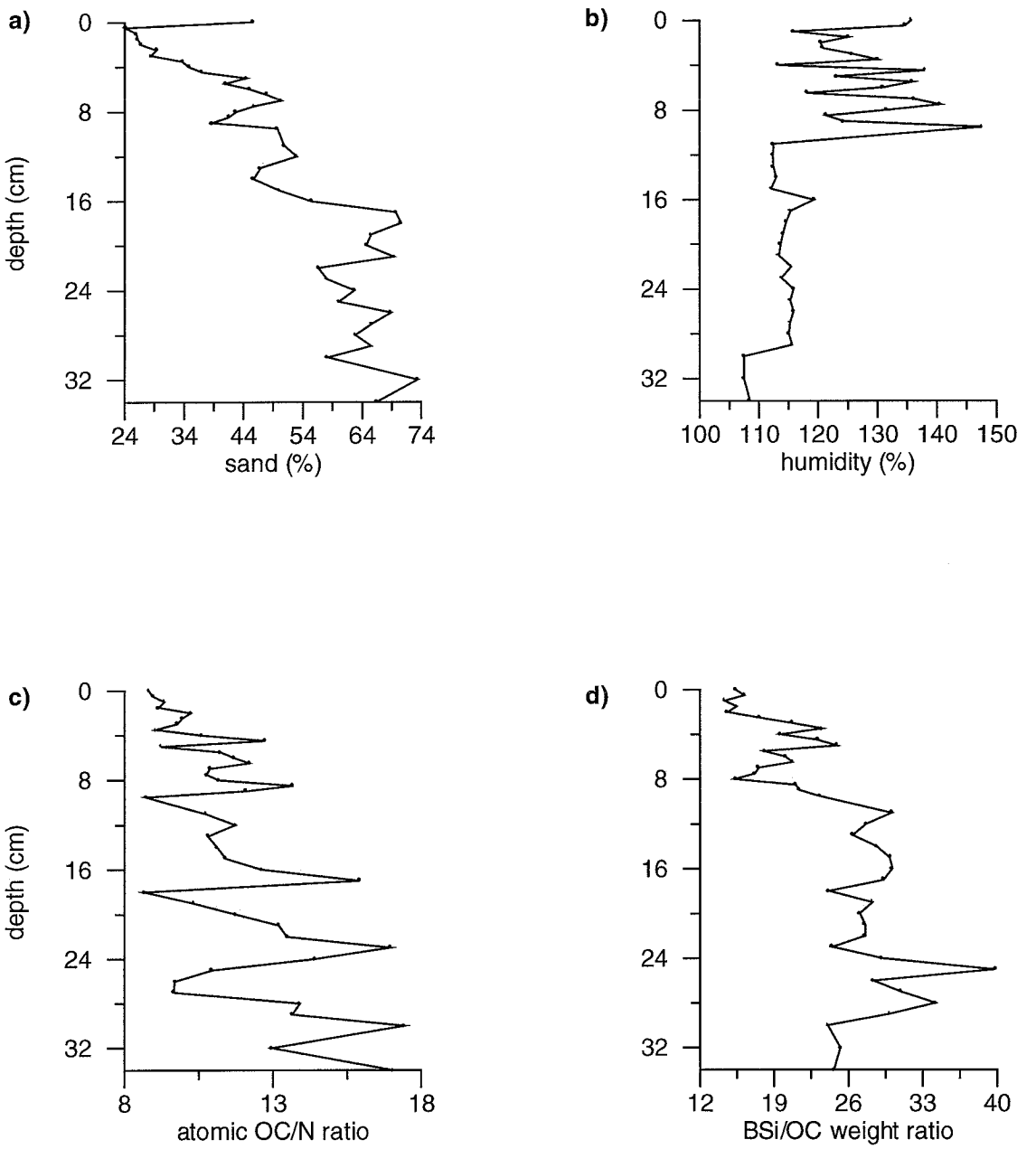

Fig. 4.25. (a) Sand and (b) humidity contents and (c) atomic organic carbon to nitrogen (OC/N) and (d) biogenic silica to organic carbon (BSi/OC) weight ratios along multicore B214 in the Bellingshausen Sea.

4.3.1.2. Associations between variables

Atomic OC/N ratio increased towards the bottom. These values varied between 8.65 and 17.41. The mean value was 11.63 ± 2.32 and the variation coefficient 0.2 (Fig. 4.25c). BSi/OC weight ratio values ranged from 14.35 to 39.82. The average was 24.03 ± 5.89 and the variation coefficient 0.25 (Fig. 4.25d). BSi was better preserved than the other biogenic variables.

4.3.2. Multicore B223

4.3.2.1. Description of constituents

This 16-cm core was taken at a water depth of 1180-m on the continental rise in front of the Smith and Snow Islands in the Bellingshausen Sea (Fig. 2.3). It consisted in sandy mud.

TC content profile showed a clear decreasing trend towards the bottom. These values ranged from 0.15 to 0.64%. The average was 0.4 ± 0.11% with a variation coefficient equal to 0.27 (Fig. 4.26a).

IC content values varied between <0.003 and 0.02%, the mean value was 0.007 ± 0.006% and the variation coefficient 0.9 (Fig. 4.26b). $CaCO_3$ content minimum and maximum values were 0 and 0.18%, respectively. The average was 0.06 ± 0.05% (Fig. 4.26c).

OC content ranged from 0.13 to 0.62%. The mean value was 0.39 ± 0.11% with a variation coefficient equal to 0.27 (Fig. 4.26d). OC content accounted for more than 86% of the TC, though the average OC percentage in TC was 98 ± 2.28.

N content values varied between 0.02 and 0.09%. This profile followed a clear diminishing trend towards the bottom. The mean was 0.06 ± 0.02% with a variation coefficient of 0.3 (Fig. 4.26e).

BSi content curve was quite constant with a sharp decrease at the bottom of the core. BSi minimum and maximum values were 3.99 and 10.26%, respectively and they averaged 9.4 ± 0.66% with a variation coefficient equal to 0.07 (Fig. 4.26f).

SAR, SML, and the biogenic variables accumulation rates are listed in Table 4.1.

Sand content increased towards the bottom, markedly after cm 9. Sand content values ranged from 10.39 to 73.13%. The mean was 23.83 ± 14.39% and the variation coefficient 0.6 (Fig. 4.27a).

4.3.2.2. Associations between variables

Atomic OC/N ratio curve described an increasing trend towards the bottom with values between 7.12 and 10.96. The mean was 8.33 ± 0.92 and the variation coefficient 0.11 (Fig. 4.27c). BSi/OC weight ratio minimum and maximum values were 15.55 and

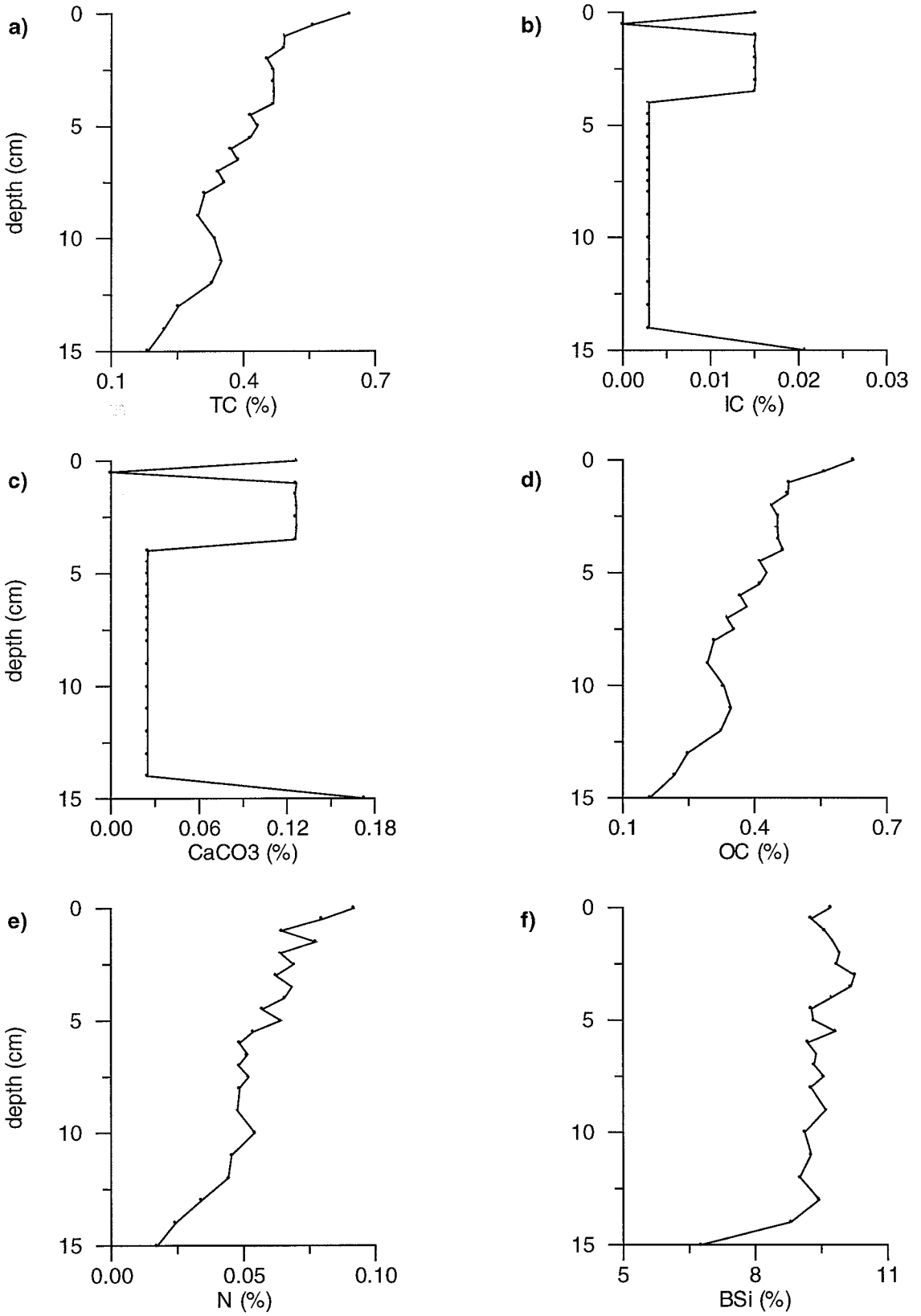

Fig. 4.26. (a) Total carbon (TC), (b) inorganic carbon (IC), (c) calcium carbonate (CaCO3), (d) organic carbon (OC), (e) nitrogen (N) and (f) biogenic silica (BSi) concentrations along multicore B223 in the Bellingshausen Sea.

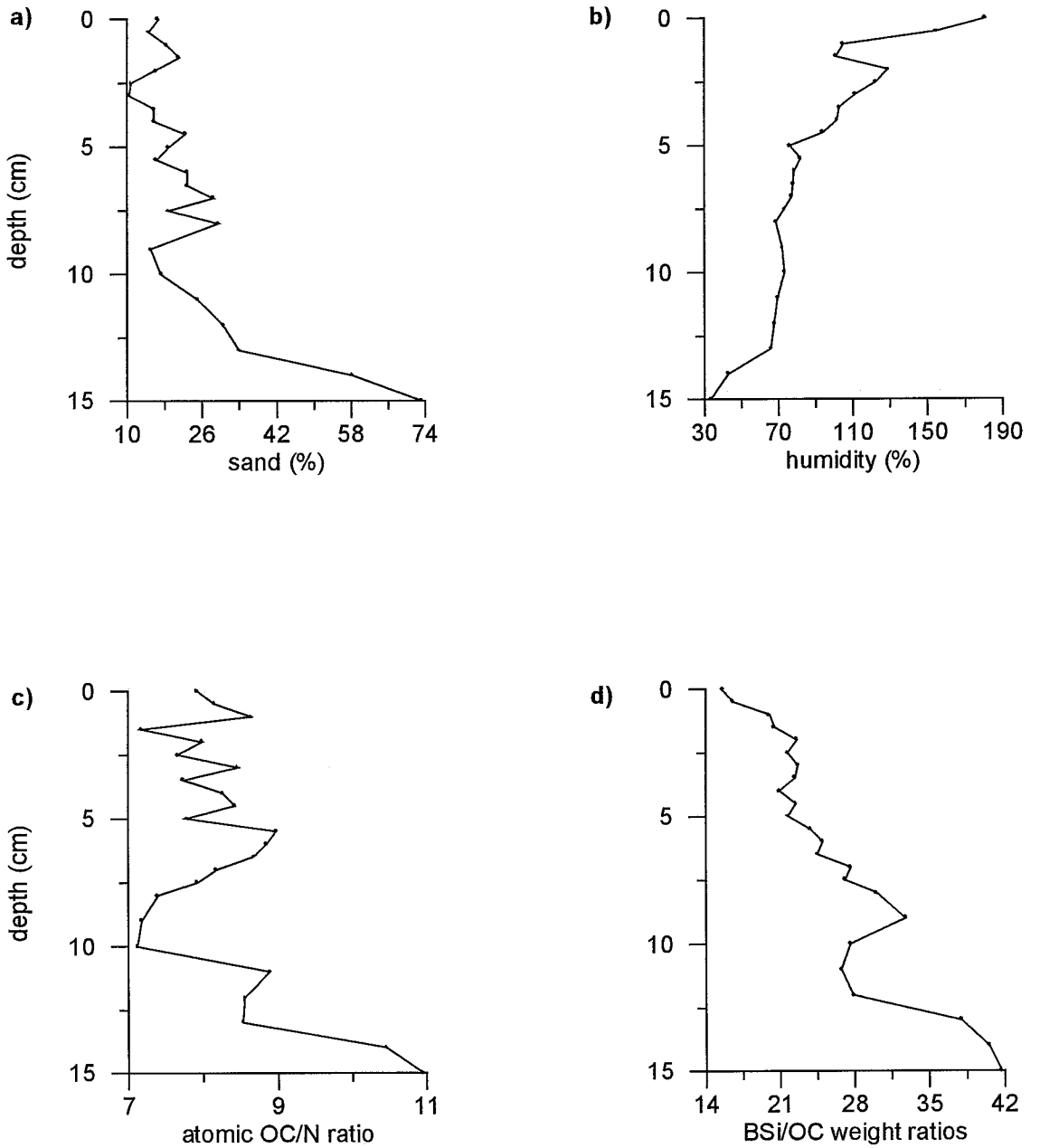

Fig. 4.27. (a) Sand and (b) humidity contents and (c) atomic organic carbon to nitrogen (OC/N) and (d) biogenic silica to organic carbon (BSi/OC) weight ratios along multicore B223 in the Bellingshausen Sea.

41.76, respectively. The average was 25.88 ± 6.78 and the variation coefficient 0.26 (Fig. 4.27d). This profile followed an increasing trend towards the bottom.

Sand content was inversely related to OC (R^2= 0.63) and BSi (R^2= 0.85). This relation was more evident after cm 11, where sand content showed a sharp increment from 17 to 25%.

4.4. STATISTICAL ANALYSIS

After the statistical analysis it was found that with a confidence value of 0.05 there were large differences in the OC, N, and BSi content between the SML and the rest of the core (Table 4.2). $CaCO_3$ did not differ significantly along the core.

4.5. SUMMARY OF SEDIMENT CORES DESCRIPTION

All the analysed samples consisted mainly in olive green and black mud sediments. The lowest sand content values -between 0.49 and 8.98%- corresponded to samples from more than 700-m water depth. Nevertheless, no correlation between sand content and water depth was found (R^2=0). These samples came from the western and central Bransfield Strait (core B2 and core A3), and the western Gerlache Strait (core B187) (Figs. 4.2, 4.10, and 4.13). The highest sand content -up to 70%- corresponded to the cores B214 and B223 both from the Bellingshausen Sea. These cores were taken from shelf and deep basin environments, respectively (Figs. 4.25 and 4.27). When sand content was higher than 40%, the OC content diminished evidently almost in every case. The highest determination coefficient between these two variables was 0.6.

Organic carbon content accounted for more than 71% of the TC and it ranged from 0.13 to 1.61% (Figs. 4.1, 4.5, 4.9, 4.12, 4.14, 4.16, 4.18, 4.20, 4.22, 4.24, and 4.26). The samples with the lowest OC content came from the Bellingshausen Sea (cores B214 and B223). The highest OC content values were measured in samples from the eastern Gerlache Strait (core B6). The N content values varied between 0.01 and 0.31% (Figs. 4.1, 4.5, 4.9, 4.12, 4.14, 4.16, 4.18, 4.20, 4.22, 4.24, and 4.26). The N content followed the OC distribution pattern along the study area. In all the cores collection both variables showed a diminishing trend towards the bottom of the core. Both variables were reasonably well related. The determination coefficient was always above 0.56 with the exception of core B187 (R^2= 0.47).

$CaCO_3$ was not clearly related to any other variable and its values varied between <0.003 and 1.23% (Figs. 4.1, 4.5, 4.9, 4.12, 4.14, 4.16, 4.18, 4.20, 4.22, 4.24, and 4.26). The highest values were related to samples from western Bransfield Strait basin (core A6), western Bransfield Strait (core B2) and central Gerlache Strait (B192). High sand and high $CaCO_3$ content were coincident in some cases. Usually the highest $CaCO_3$ content values occurred toward the bottom of the core.

Biogenic silica ranged from 3.99 to 25.49% (Figs. 4.1, 4.5, 4.9, 4.12, 4.14, 4.16, 4.18, 4.20, 4.22, 4.24, and 4.26). The highest values corresponded to the samples from the central Bransfield Strait (core A3) and the western Gerlache Strait (B187). The lowest

values were associated to samples from the Bellingshausen Sea (cores B214 and B223). BSi and OC were not clearly related. The best correspondence values (R^2>=0. 51) were found in the samples with the highest BSi content.

The mean sediment accumulation rates (SAR) varied between 220 ± 16 and 1750 ± 80 g $m^{-2}y^{-1}$ (Table 4.1). The highest sedimentation rates were measured in the central and eastern Gerlache Strait (cores B7 and B5). The lowest SAR corresponded to central Bransfield Strait sediments (core A6). OC, N and BSi lowest and highest SAR values were associated to the same areas as well. $CaCO_3$ SAR lowest values were measured in the western Gerlache Strait samples (core B187) and the highest values corresponded to the central area of the Strait (core B192).

Atomic OC/N ratio values varied between 4.27 and 17.41 (Figs. 4.2, 4.6, 4.10, 4.13, 4.15, 4.17, 4.19, 4.21, 4.23, 4.25, and 4.27). The lowest values were associated to samples from the Bransfield and Gerlache Straits confluence (core B2) and the highest corresponded to Belllingshausen Sea sediments (core B214). BSi/OC weight radio minimum and maximum values were 10.47 and 41.59 (Figs. 4.2, 4.6, 4.10, 4.13, 4.15, 4.17, 4.19, 4.21, 4.23, 4.25, and 4.27). The lowest values were found in central Gerlache Strait samples (core B6) and the highest were related to the central Bransfield Strait sediments (core A6).

Central Gerlache Strait sediments had the highest biogenic variable concentrations and mean accumulation rate values and the lowest sand content within the sampled area (Table 4.1). The Bellingshausen Sea sediments had the highest sand percentage and the lowest biogenic component contents. The sampled site at the continental shelf (core B214) had relatively medium SAR and the site at a deep-sea environment (B223) showed the lowest SAR values. The central and western Bransfield Strait basins had mean over all values.

There were no clear relations between any variable with water depth or sand content with the exception of samples with high (>40%) sand percentage. Usually these samples showed an evident decrease in the biogenic component contents, but no as a general rule.

After the statistical analysis it was found that with a confidence value of 0.05 there were large differences in the OC, N, and BSi content between the SML and the rest of the core (Table 4.2). $CaCO_3$ did not differ significantly along the core.

Table 4.1. Surface mixed layer (SML) depth and mean values for organic carbon (OC), nitrogen (N), calcium carbonate (CaCO3) and biogenic silica (BSi), within and below the SML. All expressed as weight percentage. Apparent mean accumulation rate (AR) and burial efficiency (BE) for each variable. Apparent mean sediment accumulation rate (SAR) at each site expressed as grams per square centimetre per year (g m-2y-1) and millimetre per year (mm y-1). g m-2y-1 denotes gram per square meter per year.

CORE	SML		avg. OC	avg. N	avg. CaCO3	avg. BSi	OC AR	BE	N AR	BE	CaCO3 AR	BE	BSi AR	BE	SAR	SAR
	cm		%	%	%	%	g/m2y	%	g/m2y	%	g/m2y	%	g/m2y	%	g/m2y	mm/y
B187	-	surface	1.26	0.20	0	20.17	8.06 ± 0.38	79	1.28 ± 0.06	70	0	-	129.09 ± 6.05	101	640 ± 30	1.71 ± 0.07
		core avg.	1.00 ± 0.03	0.14 ± 0.03	0.06 ± 0.06	20.39 ± 1.34	6.40 ± 0.30		0.90 ± 0.04		0.38 ± 0.02		130.50 ± 6.12			
B191	2	within	0.84 ± 0.04	0.12 ± 0.01	0.10 ± 0.06	11.13 ± 0.89	7.81 ± 0.42	80	1.12 ± 0.06	75	0.97 ± 0.05	86	103.51 ± 5.57	99	930 ± 50	1.17 ± 0.07
		below	0.67 ± 0.06	0.09 ± 0.01	0.09 ± 0.05	11.04 ± 0.63	6.23 ± 0.33		0.84 ± 0.05		0.83 ± 0.05		102.67 ± 5.52			
B192	6.5	within	0.75 ± 0.04	0.12 ± 0.01	0.62 ± 0.12	10.27 ± 0.33	4.73 ± 0.22	75	0.76 ± 0.04	75	3.89 ± 0.19	89	64.70 ± 3.08	83	630 ± 30	0.65 ± 0.03
		below	0.56 ± 0.11	0.09 ± 0.01	0.55 ± 0.31	8.53 ± 0.83	3.53 ± 0.17		0.57 ± 0.03		3.47 ± 0.17		53.74 ± 2.56			
B7	11	within	1.31 ± 0.06	0.19 ± 0.02	0.03 ± 0.01	18.4 ± 1.10	22.93 ± 0.11	83	3.33 ± 0.15	74	0.54 ± 0.02	159	322.00 ± 14.72	89	1750 ± 80	3.11 ± 0.14
		below	1.09 ± 0.05	0.14 ± 0.02	0.05 ± 0.02	16.43 ± 0.80	19.08 ± 0.87		2.45 ± 0.11		0.86 ± 0.04		287.53 ± 13.14			
B6	3	within	1.32 ± 0.13	0.17 ± 0.02	0.06 ± 0.05	17.03 ± 0.37	14.52 ± 1.18	71	1.87 ± 0.15	71	0.62 ± 0.05	204	187.33 ± 15.33	86	1100 ± 90	1.57 ± 0.13
		below	0.94 ± 0.14	0.12 ± 0.02	0.12 ± 0.06	14.65 ± 1.61	10.34 ± 0.84		1.32 ± 0.11		1.28 ± 0.11		161.15 ± 13.19			
B5	11	within	1.13 ± 0.07	0.14 ± 0.02	0.08 ± 0.04	17.39 ± 0.88	12.54 ± 1.35	81	1.55 ± 0.17	86	0.90 ± 0.01	85	193.03 ± 20.87	98	1110 ±120	1.8 ± 0.2
		below	0.91 ± 0.09	0.12 ± 0.01	0.07 ± 0.03	16.96 ± 0.74	10.10 ± 1.09		1.33 ± 0.14		0.76 ± 0.08		188.26 ± 20.35			
A3M	12	within	1.23 ± 0.05	0.18 ± 0.01	0.12 ± 0.04	18.38 ± 0.77	7.38 ± 0.37	92	1.08 ± 0.05	89	0.72 ± 0.04	83	110.28 ± 5.51	103	600 ± 30	1.17 ± 0.05
		below	1.13 ± 0.05	0.16 ± 0.01	0.10 ± 0.06	18.95 ± 1.73	6.78 ± 0.34		0.96 ± 0.05		0.60 ± 0.03		113.7 ± 5.69			
A6M	8.5	within	0.96 ± 0.11	0.14 ± 0.02	0.08 ± 0.06	14.27 ± 0.61	3.37 ± 0.10	68	0.49 ± 0.01	65	0.28 ± 0.01	214	50.09 ± 1.43	91	351 ± 10	0.57 ± 0.02
		below	0.65 ± 0.18	0.09 ± 0.02	0.17 ± 0.05	12.97 ± 1.61	2.28 ± 0.07		0.32 ± 0.01		0.60 ± 0.02		45.53 ± 1.30			
B2	10	within	0.85 ± 0.09	0.12 ± 0.01	0.08 ± 0.02	14.63 ± 1.35	7.91 ± 0.26	74	1.12 ± 0.04	83	0.74 ± 0.02	176	136.06 ± 4.39	95	930 ± 30	1.56 ± 0.05
		below	0.63 ± 0.04	0.10 ± 0.02	0.14 ± 0.12	13.85 ± 1.24	5.86 ± 0.19		0.93 ± 0.03		1.30 ± 0.04		128.81 ± 4.16			
B214	3.5	within	0.36 ± 0.04	0.05 ± 0.01	0.07 ± 0.01	6.18 ± 0.72	2.48 ± 0.22	64	0.34 ± 0.03	41	0.48 ± 0.04	129	42.52 ± 3.71	90	688 ± 60	0.52 ± 0.05
		below	0.23 ± 0.06	0.02 ± 0.01	0.09 ± 0.03	5.57 ± 0.67	1.58 ± 0.14		0.14 ± 0.01		0.62 ± 0.05		38.32 ± 3.34			
B223	5	within	0.48 ± 0.06	0.07 ± 0.01	0.09 ± 0.06	9.72 ± 0.34	1.06 ± 0.08	64	0.15 ± 0.01	60	0.20 ± 0.01	45	21.38 ± 1.56	94	220 ± 16	0.25 ± 0.02
		below	0.31 ± 0.07	0.04 ± 0.01	0.04 ± 0.04	9.13 ± 0.75	0.68 ± 0.05		0.09 ± 0.01		0.09 ± 0.01		20.09 ± 1.46			

Table 4.2. One-way ANOVA analysis of OC, N, BSi, and $CaCO_3$ content (%) and OC/N ratio within the surface mixed layer (SML) and below it, with a significance level of 0.05. Degrees of freedom are expressed as DF. Significant difference: ** ($p<0.01$), *** ($p<0.001$); n.s. Non-significant difference ($p>0.05$).

variable	F test	DF	% within the SML	% below the SML
OC	98.36***	1	1.06	0.82
N	126.52***	1	0.15	0.11
BSi	24.99***	1	15.81	14.11
$CaCO_3$	0.0001 n.s.	1	0.14	0.14
atomic OC/N	6.78**	1	7.18	7.37

5. DOWNWARD PARTICLE FLUXES

5.1. WESTERN BRANSFIELD STRAIT (SITE A6)

5.1.1. Mid-depth trap (530 mab on a site at 1066m water depth)

Fecal pellets and fine particulate matter mainly composed the collected particulate matter at this depth, almost no coarse clastic material was found. Particles >1mm were rare and consisted mainly in clasts and crustaceans moults. The total mass flux and the content and fluxes of the major constituents (OC and IC, $CaCO_3$, organic matter, BSi, N, fecal pellets, and aluminosilicates) collected during each sampling interval are listed in Tables 5.1 and 5.2. Annual fluxes are listed in Table 5.3a.

Total mass flux (TMF) ranged from 0.09 to 112.5 mg $m^{-2}d^{-1}$ (Fig. 5.1a). The minimum flux was trapped during April and May (austral winter) and the maximum was associated to late November (austral spring). The annual TMF was 3.89 g m^{-2} (Table 5.3a). The four evident 15-day period peaks that occurred during late November, late December, early January, and early February concentrated 98% of the annual TMF and these values were between 2 and 3 orders of magnitude higher than those from the rest of the year.

Due to material availability IC analyses were performed only in the three samples that collected the highest TMF. In these samples OC was always more than 94% of the TC. Thus, in the remaining samples TC content values were treated as OC content values. Following this assumption, OC content varied between 6.85% in March (autumn) and 18.75% during August and September (winter) (Fig. 5.2a). The OC content in the three highest TMF periods was constant around 8%. It was evident that the samples from the coldest season, from April to October, had higher OC content than those from the rest of the year.

The minimum OC flux, 0.01 mg/m^2d, was sampled during April and May (autumn) and the maximum, 9.8 mg/m^2d, was related to late November (spring) (Fig. 5.3a). Both values coincided with TMF minimum and maximum values, respectively. OC flux followed the TMF pattern. 98% of the OC flux was concentrated in the same three periods of highest TMF and their values were about 2 orders of magnitude higher than the rest. The OC annual flux was 0.34 g m^{-2}.

IC content measurements were performed only to late-November, late December and early January samples (spring and summer). Their values were 0.15, 0.5, and 0.21%, respectively (Fig. 5.2b). $CaCO_3$ content values were, in the same order, 1.21, 4.17, and 1.77% (Fig. 5.2c). The $CaCO_3$ flux measurements were 1.36, 2.09, and 1.2 mg $m^{-2}d^{-1}$ (Fig. 5.4a). The annual $CaCO_3$ flux during the sampling period was 0.07 g m^{-2} (Table 5.3a).

The sample from the last days of the spring in late November had the highest OC/IC ratio, 60.21. The lowest, 16.4, was associated to the late December sample (summer), during early January the ratio was 39.35 (Fig. 5.5a).

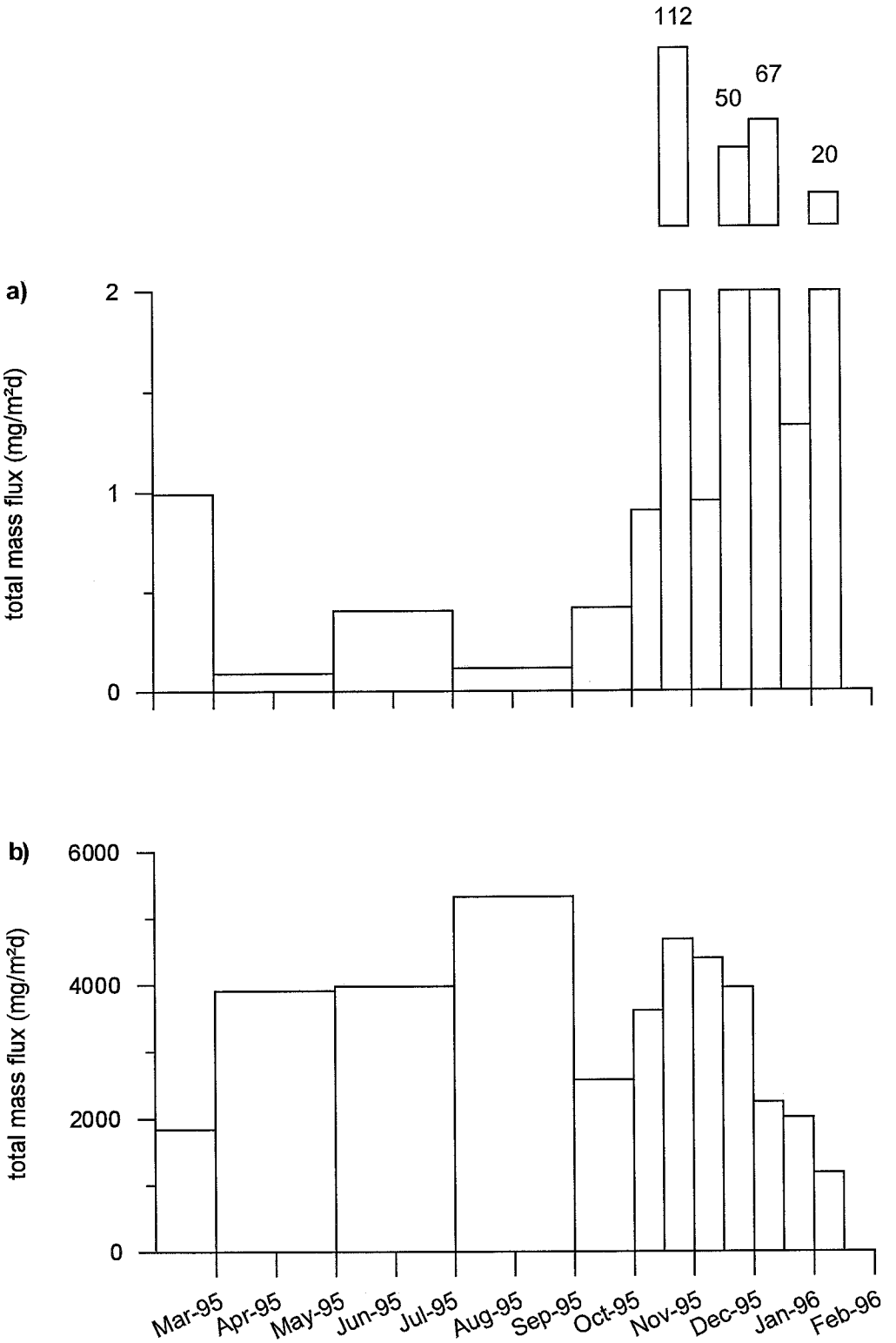

Fig. 5.1. Total mass flux temporal series at (a) mid-depth and (b) near-bottom traps at site A6 in central Bransfield Strait.

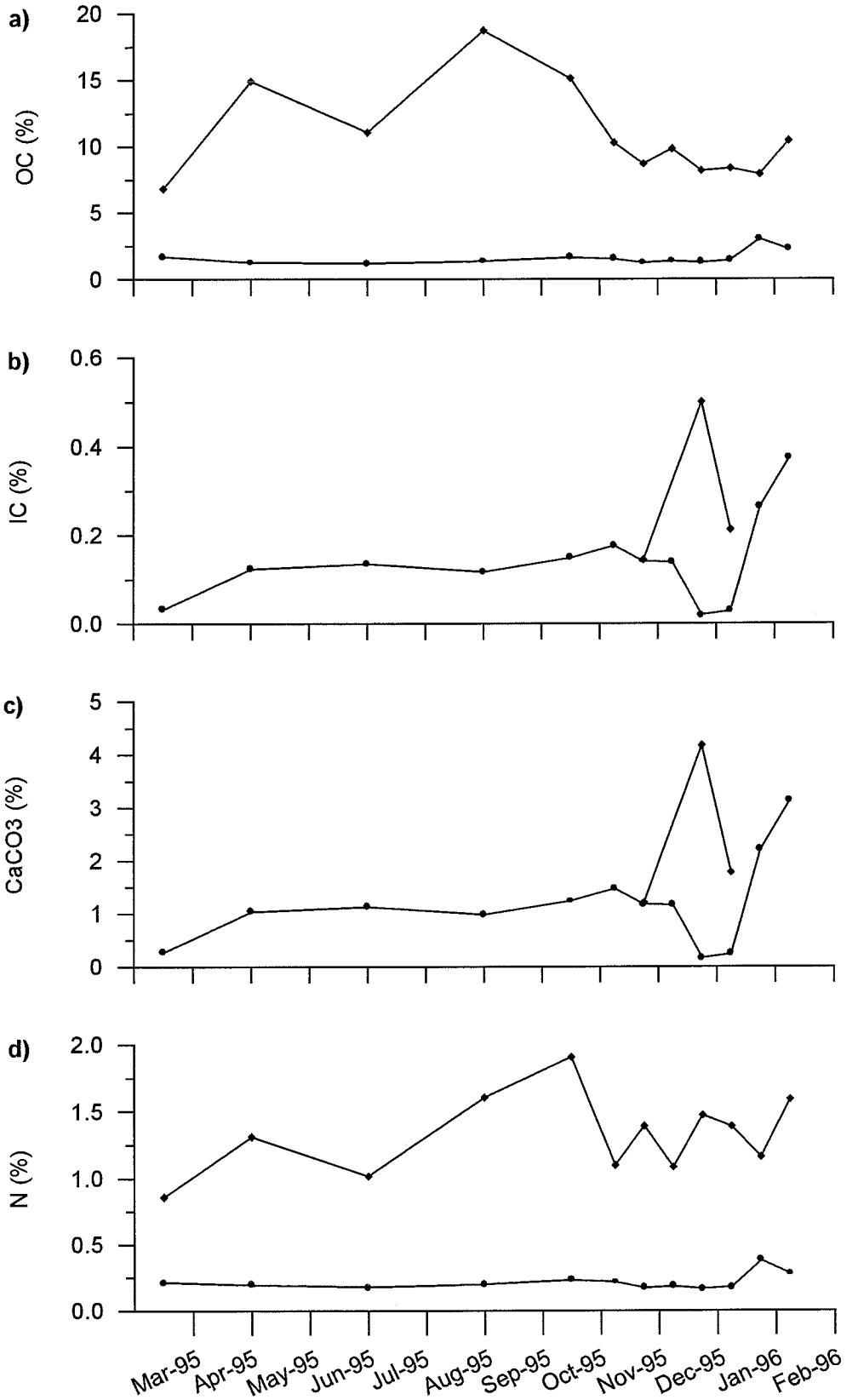

Fig. 5.2. Temporal series of (a) organic carbon (OC), (b) inorganic carbon (IC), (c) calcium carbonate (CaCO3) and nitrogen (N) contents at mid-depth (squares) and near-bottom (filled circles) traps at site A6 in central Bransfield Strait.

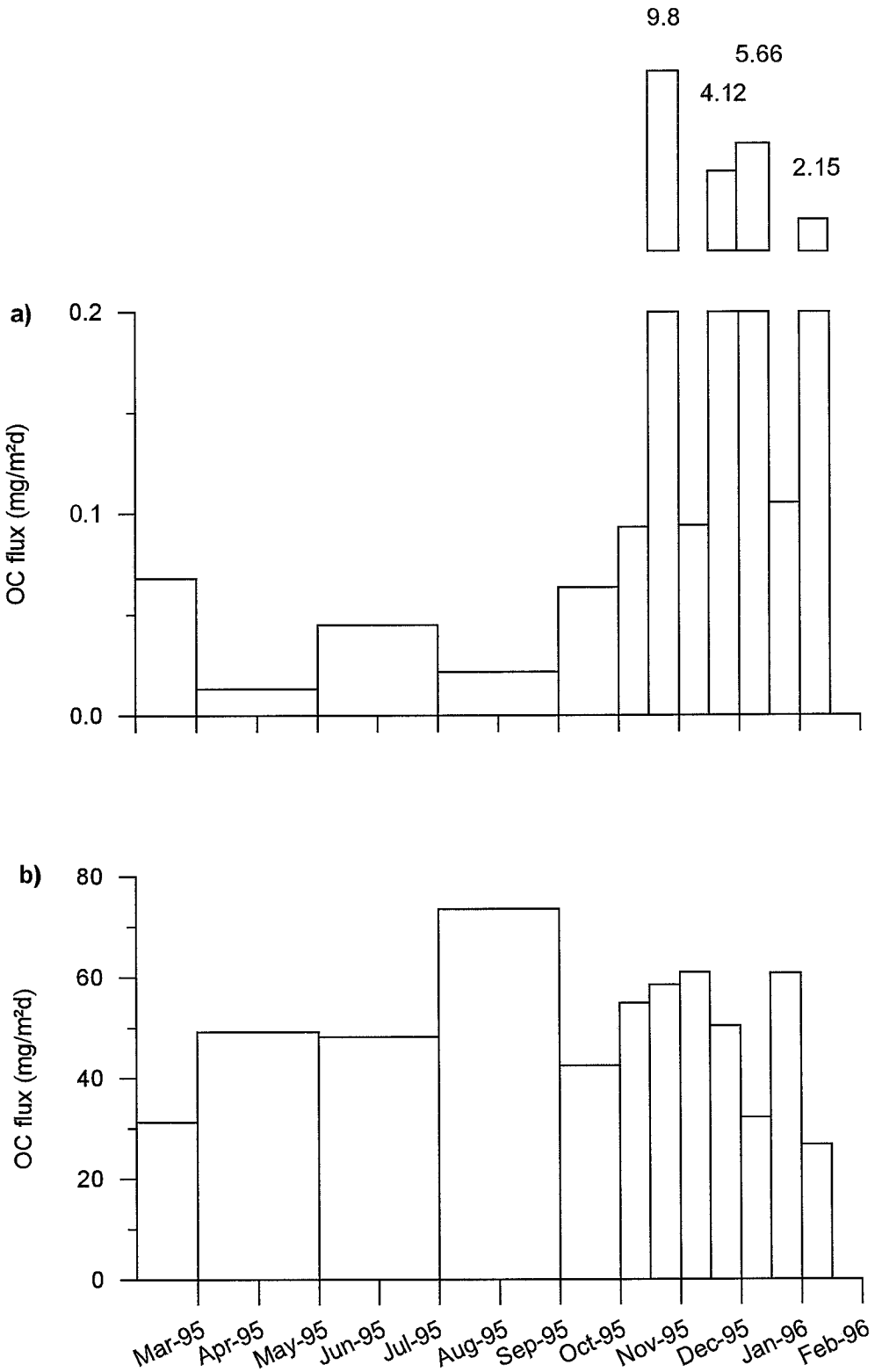

Fig. 5.3. Organic carbon (OC) flux temporal series at (a) mid-depth and (b) near-bottom traps at site A6 in central Bransfield Strait.

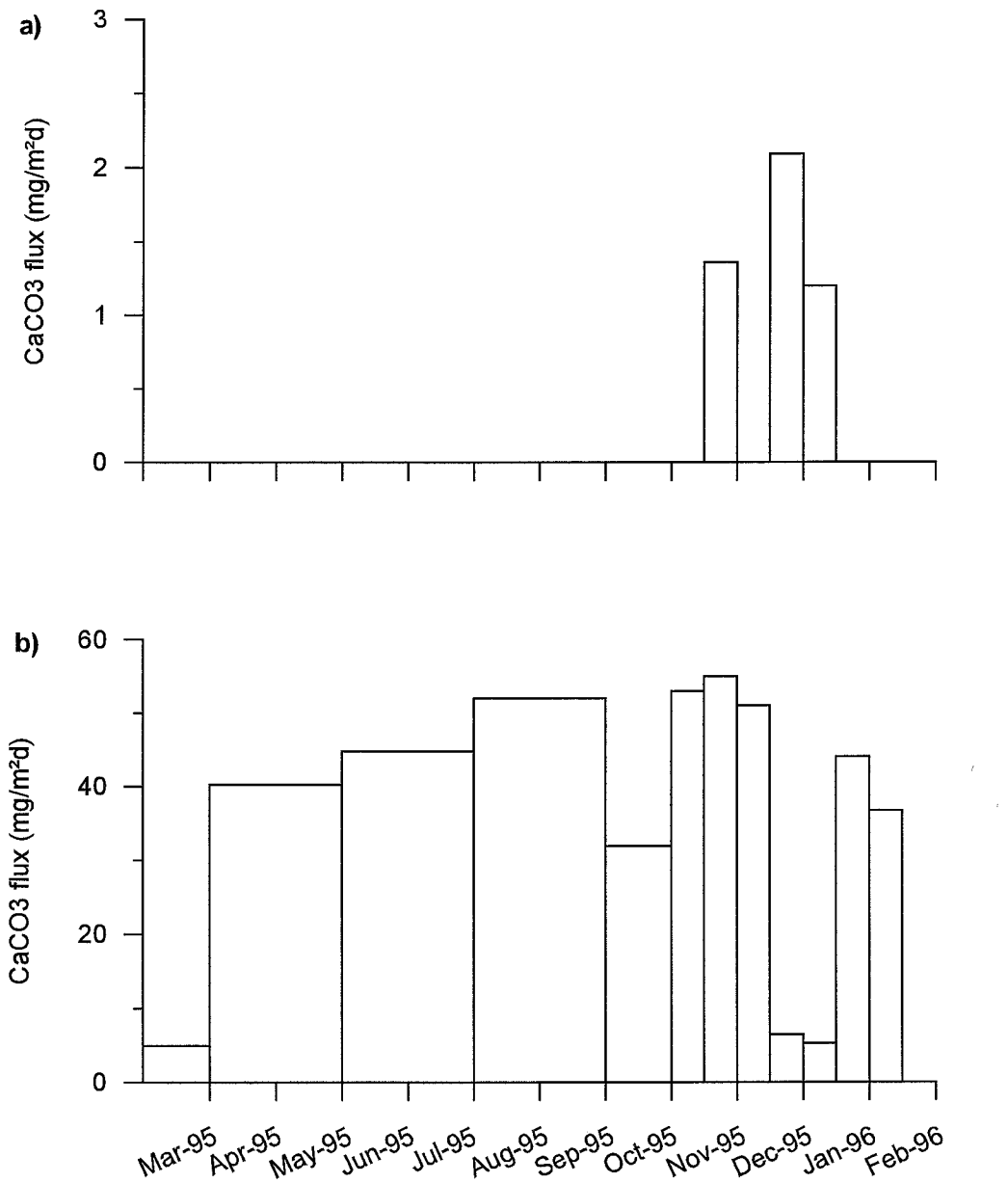

Fig. 5.4. Calcium carbonate (CaCO3) flux temporal series at (a) mid-depth and (b) near-bottom traps at site A6 in central Bransfield Strait.

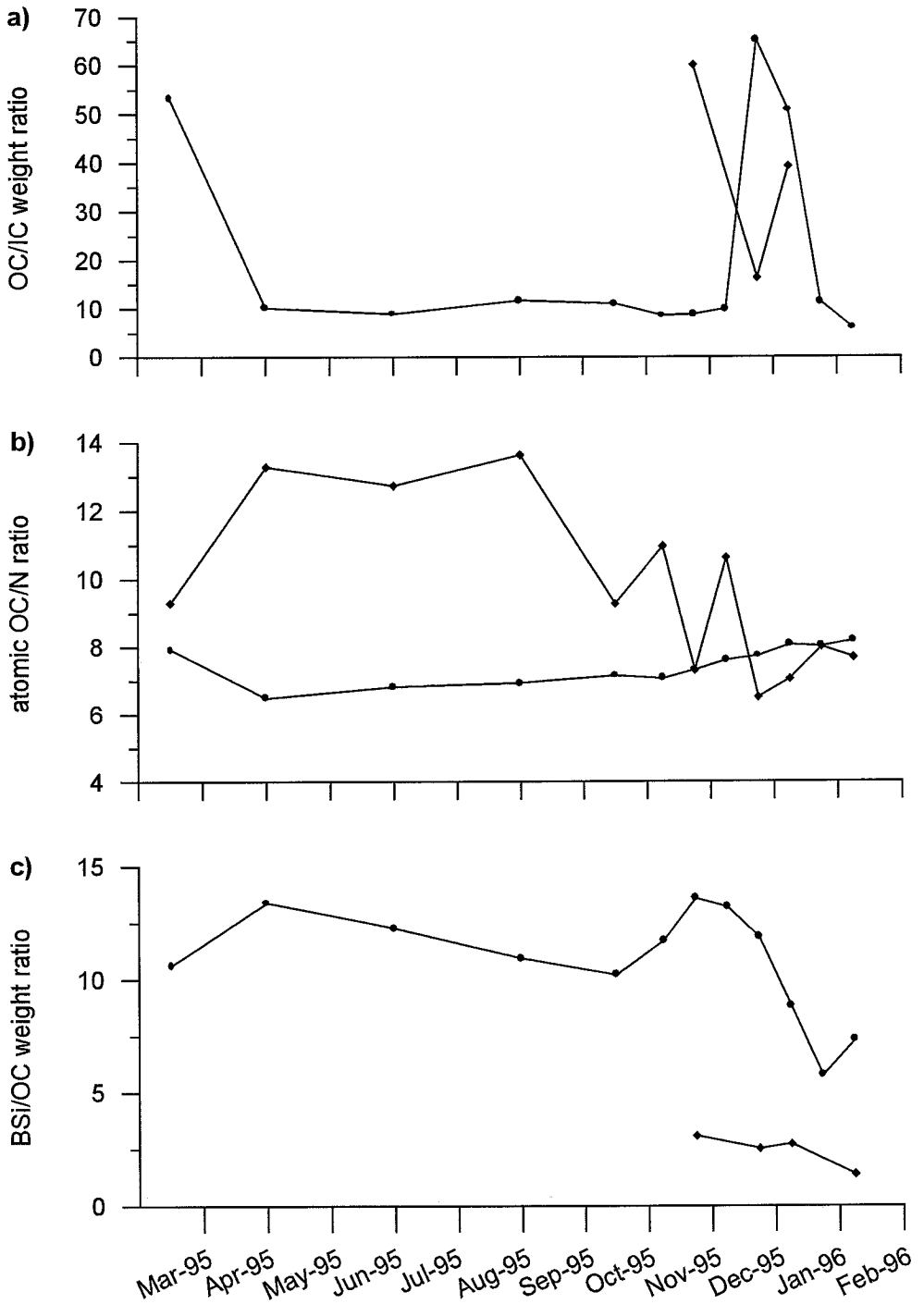

Fig. 5.5. (a) Organic to inorganic carbon (OC/IC) weight ratio, (b) atomic organic carbon to nitrogen ratio (OC/N) and (c) biogenic silica to organic carbon (BSi/OC) ratio at mid-depth (squares) and near-bottom (filled circles) traps at site A6 in central Bransfield Strait.

N content values varied between 0.86% during the autumn in March and 1.91% during the late winter in October (Fig. 5.2d). The minimum N flux, 0.002 mg $m^{-2}d^{-1}$, was collected during the winter in August and September, the maximum value was 1.56 mg $m^{-2}d^{-1}$ and corresponded to a spring sample trapped in late November (Fig. 5.6a). The flux variation along the year was about 3 orders of magnitude. The samples with highest N flux values were concentrated in the spring and summer, following the TMF pattern. The annual N flux was 0.06 g m^{-2}.

The atomic OC/N ratio varied from 6.5 in late December to 13.63 in the wintertime from August to September (Fig. 5.5b). The ratio values were quite constant around 6 during the spring and summer months. During that time they reached the lowest levels while the TMF was higher. An evident decreasing trend towards the summertime was noticed.

BSi measurements were performed only to the four samples with the highest total mass flux. BSi was the most abundant biogenic constituent in the trapped material. The BSi content values were 14.38, 20.64, 22.78, and 26.87% for early February, late December, early January and late November, respectively (Fig. 5.7a). This curve showed a decreasing trend from the spring to the summer, which was very similar to that of BSi/OC weight ratio (Fig. 5.5c). BSi flux values varied between 2.95 mg $m^{-2}d^{-1}$ in early February and 30.22 mg $m^{-2}d^{-1}$ in late November (Fig. 5.8a). During late December and early January the flux values were 10.36 and 15.41 mg $m^{-2}d^{-1}$, respectively. BSi flux changed like TMF and it had an annual value of 0.88 g m^{-2}. BSi/OC weight ratio minimum and maximum values were 1.37 and 3.09, respectively.

Aluminosilicates (lithogenics) were only measurable on the three samples associated to the highest total mass fluxes on which other major constituents were analysed. Lithogenic contents composed the major fraction of the settled particulate matter. The lithogenic (LG) contents during late November was 54.51%, during late December and early January 58.8 and 58.7%, respectively (Fig. 5.7c). A slight increasing trend was noticed. In the same order, the LG flux was 61.32, 29.52, and 39.72 mg $m^{-2}d^{-1}$, respectively. LG flux followed the TMF pattern (Fig. 5.9a). Considering that most of the mid-depth flux settled during three sampling periods (90%) the annual LG flux was 1.96 g m^{-2} (Table 5.3a).

Total fecal pellets (FP) content varied from 2 units in the April-May (late autumn) and the October (late winter) samples to 1608 units in early February (summer) (Fig. 5.7b). There was an evident difference of two orders of magnitude between the cold and the warm seasons. Nevertheless, there was a sharp decrease in the FP content during the second half of January. The minimum FP flux (Fig. 5.10a), 1 fp $m^{-2}d^{-1}$ (real value 0.4), corresponded to the winter months, June-July and August-September samples and the maximum value, 858 fp $m^{-2}d^{-1}$, was associated to the first half of February during the summer. 96% of the FP flux was concentrated during the four periods of highest TMF. The annual FP flux was 31 960 fp m^{-2} (Table 5.3a).

The only three available ^{210}Pb concentration measurements ranged from 1200 to 1500 Bq kg^{-1}, the lowest value was related to late November sample and the highest to that from late December (Fig. 5.7d). These data followed an increasing trend along the summer. The ^{210}Pb flux followed the same TMF temporal variation (Fig. 5.11a). The ^{210}Pb flux varied between 0.07 and 0.13 Bq $m^{-2}d^{-1}$. After this flux values and assuming

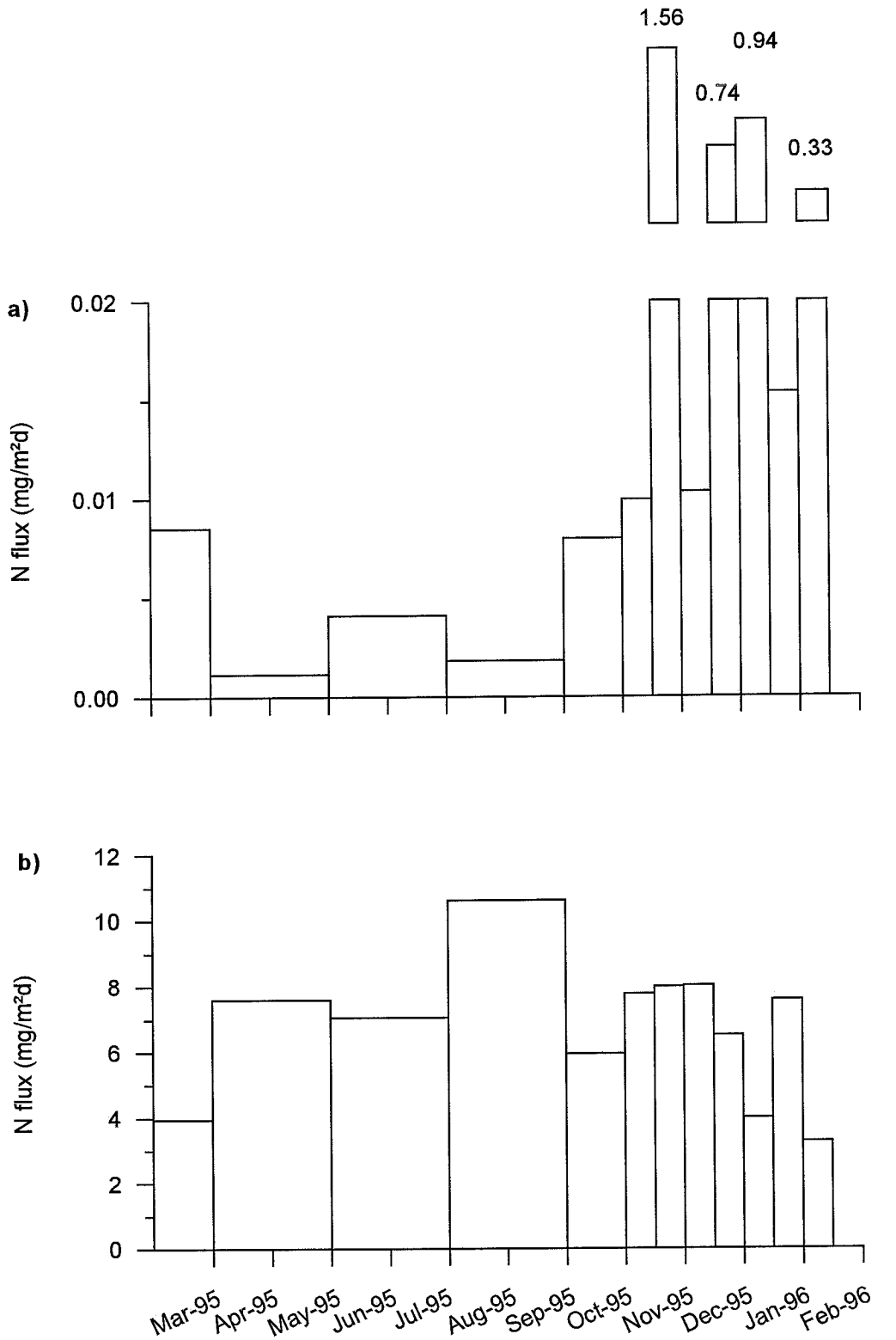

Fig. 5.6. Nitrogen (N) flux temporal series at (a) mid-depth and (b) near-bottom traps at site A6 in central Bransfield Strait.

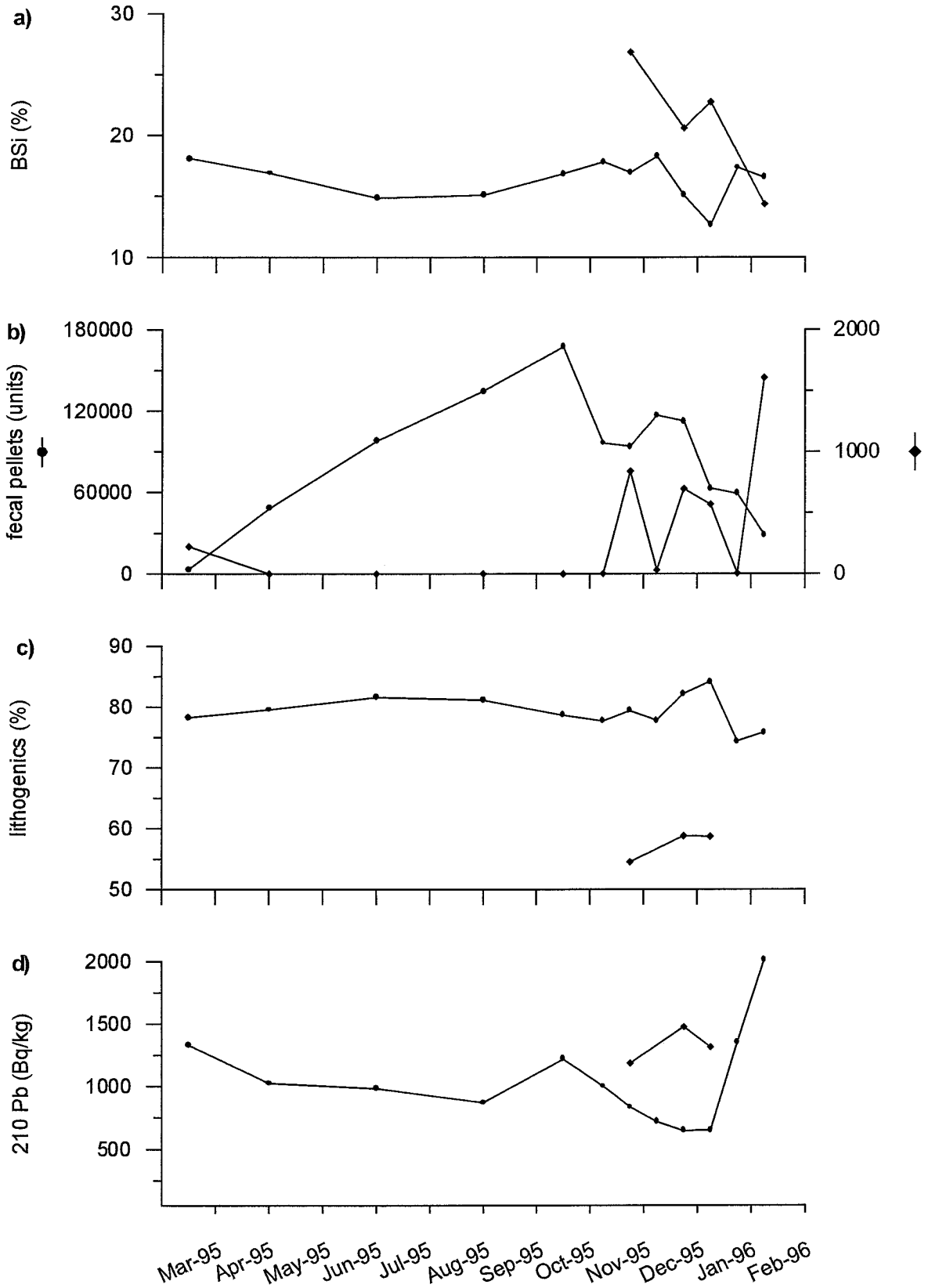

Fig. 5.7. Temporal series of (a) biogenic silica (BSi), (b) fecal pellets, (c) lithogenics and (d) 210 Pb contents at mid-depth (squares) and near-bottom (filled circles) traps at site A6 in central Bransfield Strait.

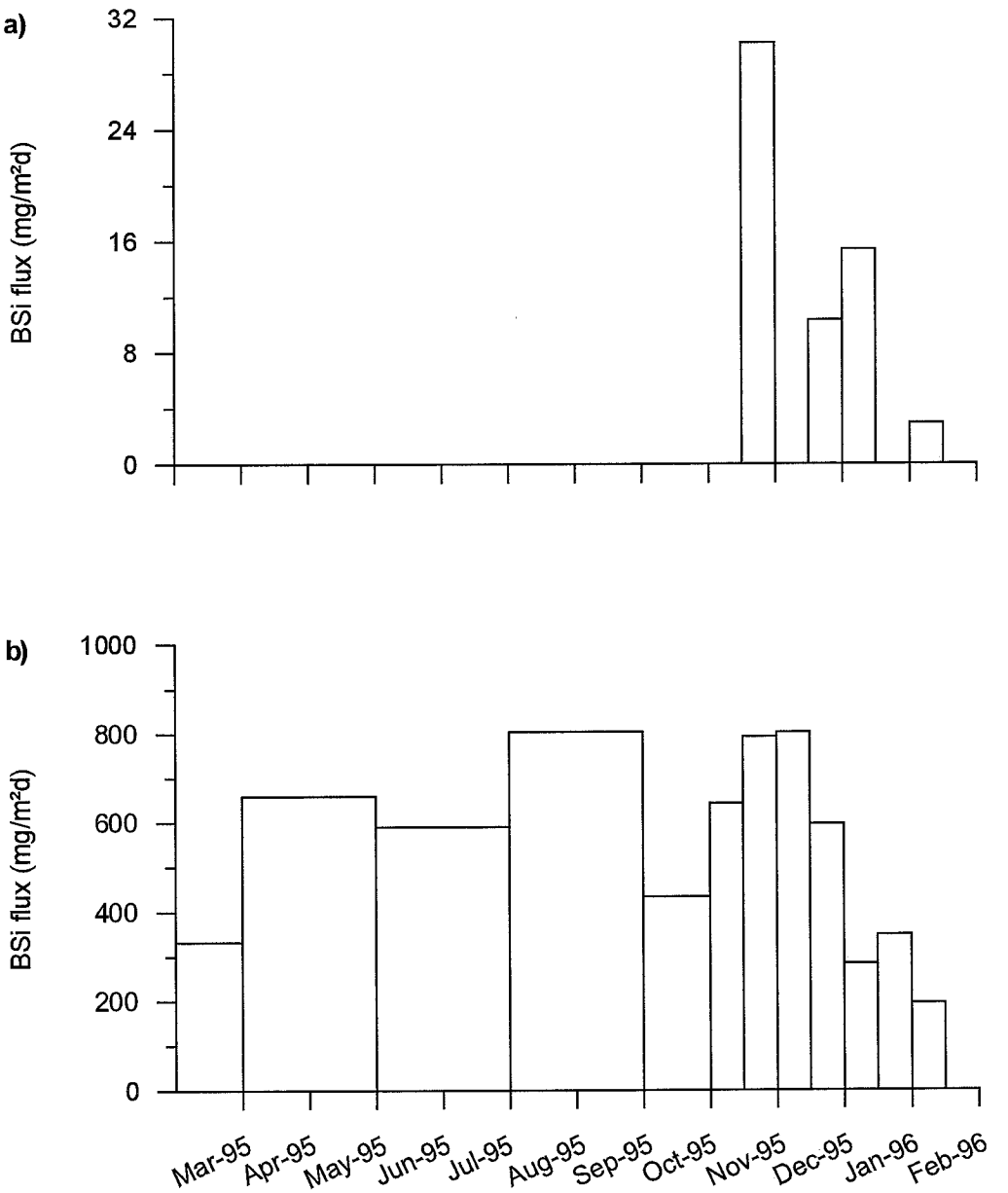

Fig. 5.8. Biogenic silica (BSi) flux temporal series at (a) mid-depth and (b) near-bottom traps at site A6 in central Bransfiel Strait.

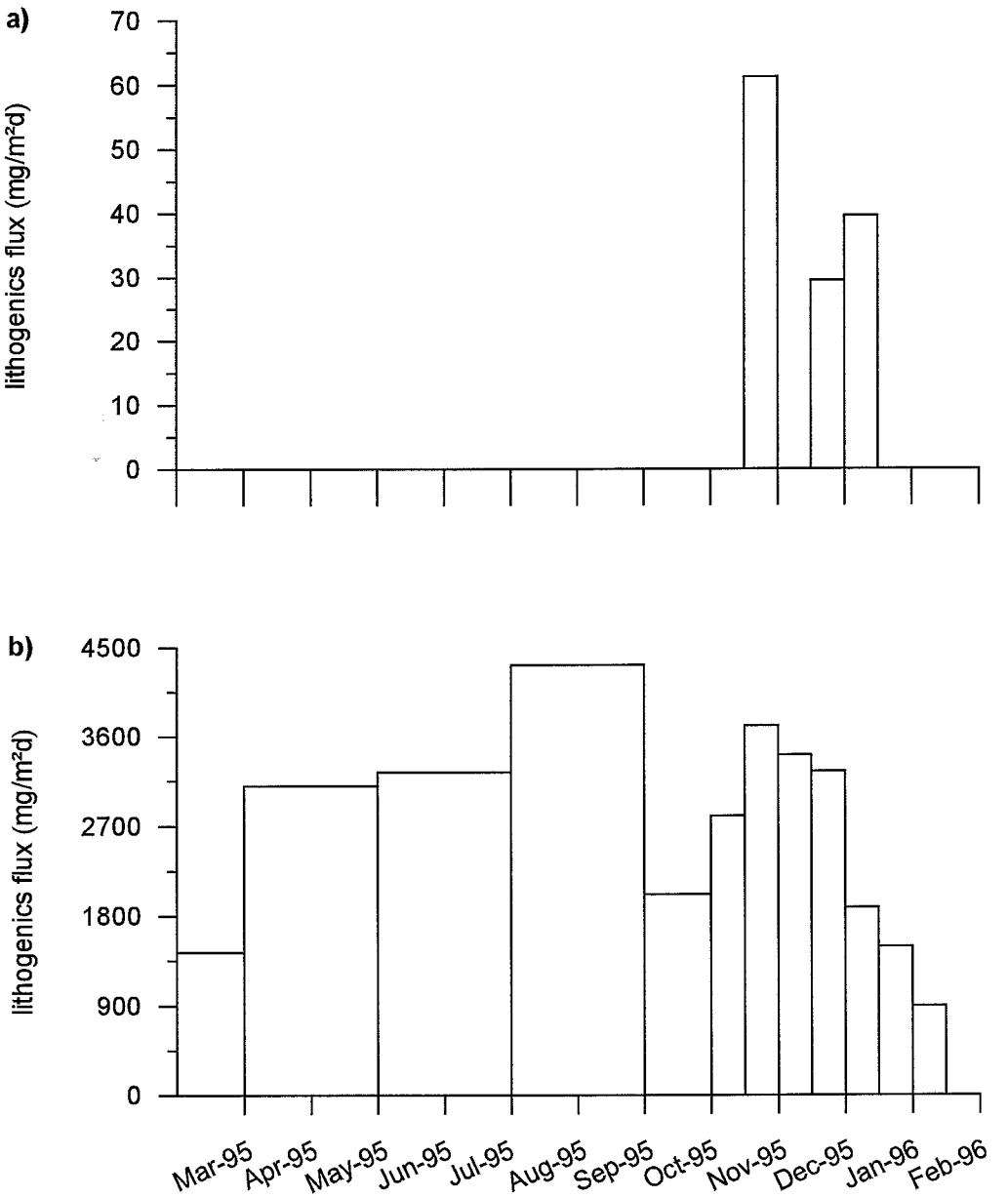

Fig. 5.9. Lithogenics flux temporal series at (a) mid-depth and (b) near-bottom traps at site A6 in central Bransfield Strait.

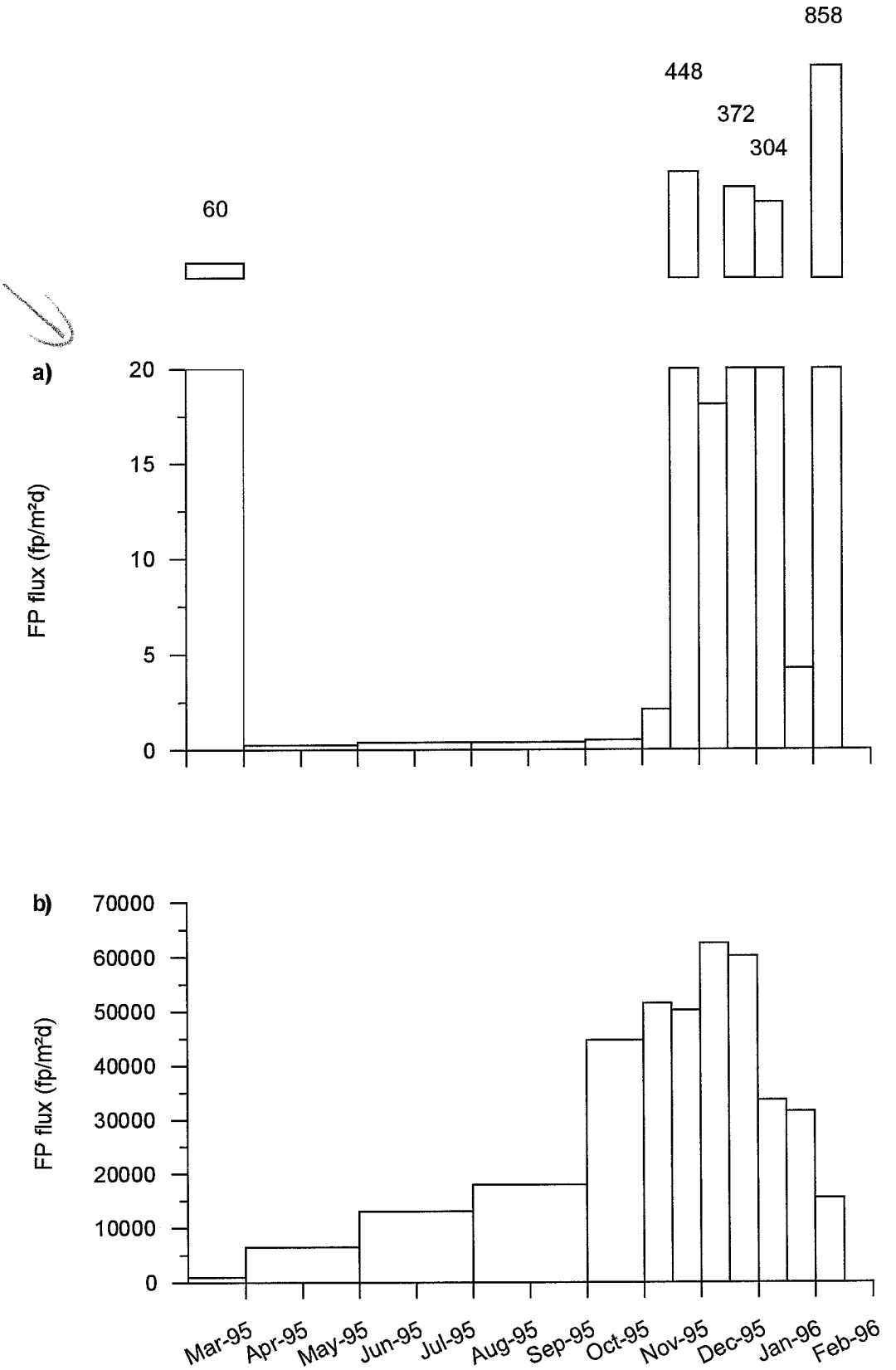

Fig. 5.10. Fecal pellets flux temporal series at (a) mid-depth and (b) near-bottom traps at site A6 in central Bransfield Strait.

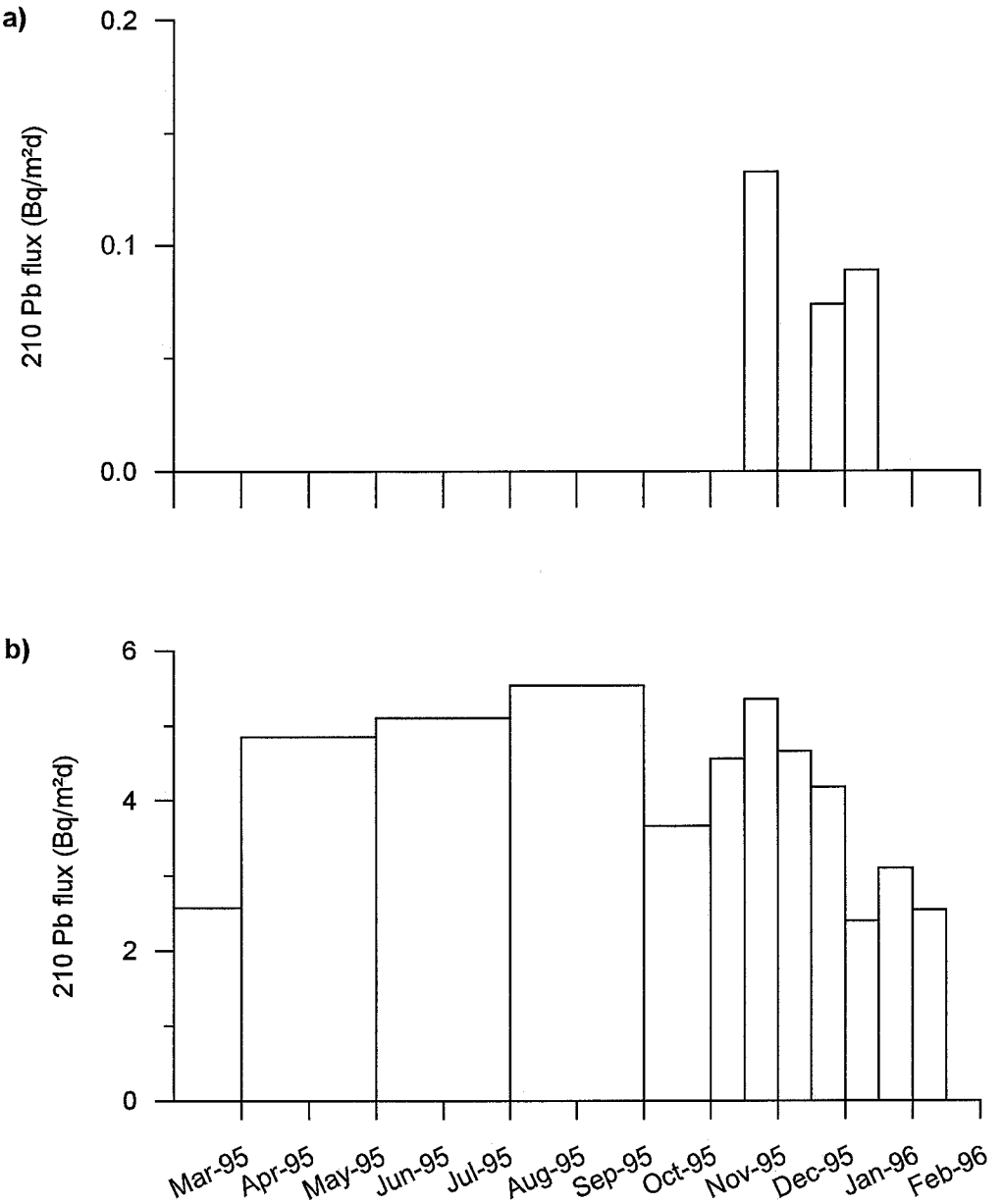

Fig. 5.11. 210 Pb flux temporal series at (a) mid-depth and (b) near-bottom traps at site A6 in central Bransfield Strait.

a mean concentration of 1320 Bq kg^{-1} for the collected particulate matter, the annual ^{210}Pb flux was estimated around 5.3 Bq m^{-2}.

5.1.2. Near-bottom trap (30 mab on a site at 1066m water depth)

The material collected in the near bottom trap was composed mainly by fecal pellets and fine particulate matter. Particles >1mm were principally clasts and crustaceans moults.

TMF minimum and maximum values were 1179 mg $m^{-2}d^{-1}$ during early February and 4672 mg $m^{-2}d^{-1}$ in the August-September period, respectively (Fig. 5.1b). TMF at this water depth was between 1 and 4 orders of magnitude higher than the flux during the same sampling periods at the mid-depth trap. The temporal evolution at both depths was very different as well. The highest near-bottom TMF was collected during the winter and not in the spring and summer like in the mid-depth trap. The annual flux was not concentrated in a short period of time but it was distributed along the year. The annual TMF was 1254 g m^{-2} (Table 5.3a).

OC content was always more than 85% of the TC. OC content varied between 1.21 and 3.03% (Fig. 5.2a). The highest value was measured during the summer in late January and the lowest in the early winter during the June-July sampling period. The rest of the year the OC content was quite constant between 1.2 and 1.7%. OC content near the bottom was significantly lower than at mid depth trap. Nevertheless, OC flux near the bottom was between 1 and 2 orders of magnitude higher than at the mid-depth trap (Fig. 5.3b). OC flux maximum, 73.5 mg $m^{-2}d^{-1}$, was associated to the August-September period during the winter. The lowest OC flux, 26.7 mg $m^{-2}d^{-1}$, was measured during the summer in early February. Both values coincided with the lowest and highest measurements of TMF. OC flux followed almost the same pattern of TMF. The annual OC flux was 17.62 g m^{-2} (Table 5.3a).

IC content changed between 0.02 and 0.37% (Fig. 5.2b). Both extremes were measured during the summer, the former within late December and the latter in early February. $CaCO_3$ content fluctuated between 0.16 and 3.12% (Fig. 5.2c). Although the $CaCO_3$ content was similar during late November in both traps (when TMF was highest in the mid depth trap), during the following periods the difference at both depths increased to one order of magnitude. The $CaCO_3$ flux values ranged from 4.88 to 54.94 mg $m^{-2}d^{-1}$ (Fig. 5.4b). The minimum value was for the late March sample (autumn) and the maximum for the late November one (spring). $CaCO_3$ flux followed TMF trend although extreme values of both parameters did not coincide in time and the two $CaCO_3$ flux peaks during the summer in late January and early February did not corresponded with TMF peaks. This was due to the relatively high variability in $CaCO_3$ content during the spring and summer months and the quite constant levels during the rest of the year. The annual $CaCO_3$ flux was 13.1 g m^{-2} (Table 5.3a).

OC/IC ratio lowest and highest values, 6.06 and 65.39, were measured in the samples from late February and late December (both during summer time), respectively (Fig. 5.5a). The IC content and the OC/IC ratio curves of both traps were clearly opposite.

The N content varied from 0.17 to 0.38%, both measurements were related to summer samples (Fig. 5.2d). They corresponded to the material trapped during late December and late January, respectively. N content values were constant during the rest of the year. The difference in N content between samples from both depths was within one order of magnitude.

The lowest N flux, 3.27 mg $m^{-2}d^{-1}$, occurred in summer during early February. The highest, 10.6 mg $m^{-2}d^{-1}$, occurred in the winter during the August-September period (Fig. 5.6b). The N flux temporal variation along the year was similar to that of the TMF. N flux was higher at mid-depth during the spring and summer months and near the bottom the highest N fluxes were registered during the winter. The annual N flux near the bottom was 2.49 g m^{-2} (Table 5.3a).

Atomic OC/N ratio in near-bottom samples showed relatively little variation along the year when compared with mid-depth results. The minimum value was 7.57 in the autumn sample from the April-May period and the maximum was 9.53 in the summer sample from early February (Fig. 5.5b). The atomic OC/N ratio curve showed an inverse relation to TMF pattern and an evident increasing trend towards the summer.

BSi content ranged from 12.69% during early January (summer) to 18.29% during early December (spring) (Fig. 5.7a). As in the upper trap, BSi constituted the biggest fraction of the biogenic material. BSi content highest variation occurred during the spring and summer months. The annual changes in BSi flux fluctuated between 195.2 mg $m^{-2}d^{-1}$ during early February (summer) and 803.9 mg $m^{-2}d^{-1}$ during the August-September period (winter) (Fig. 5.8b). BSi and OC flux temporal variation along the year was similar. They both were different from TMF pattern during the spring and summer months although BSi and total mass fluxes tended to decrease during the same summer periods. BSi flux near the bottom was about two orders of magnitude higher than at mid-depth trap. The annual flux was 201 g m^{-2} (Table 5.3a). BSi/OC weight ratio lowest and highest values were 5.74 and 13.56 (Fig. 5.5c). The former was measured in the late January sample and the latter in the late November material. The BSi/OC weight ratio curve showed a decreasing trend towards the summer interrupted by a peak in the spring (November and December). The BSi/OC weight ratio values near the bottom were between four and seven times higher than those obtained at mid-depth during the same sampling periods.

LG content, as in the upper trap, represented the major constituent of the collected material. It varied between 74.37% during late January and 84.2% during the first half of the same summer month (Fig. 5.7c). A slight increment occurred at the beginning of the summer. LG content was quite constant over the year and higher than in the upper trap. LG flux minimum and maximum values were 893.28 and 4318.43 mg $m^{-2}d^{-1}$, respectively (Fig. 5.9b). They were associated to early February (summer) and to the August-September period (winter), respectively. LG flux followed the TMF pattern. LG flux near the bottom was about two orders of magnitude higher than in the upper trap for the same sampling periods. The annual LG flux was 1005 g m^{-2} (Table 5.3a).

FP content changed between 3 600 units at the beginning of the autumn (March) and 167 430 units during the late winter (October) (Fig. 5.7b). FP content curve showed a sharp increasing trend after March and an evident diminishing tendency towards the summer after October. FP content near the bottom was about five orders of magnitude

higher than at mid-depth. FP flux was higher in spring than in summer and it did not reflect the mid-depth trap pattern (Fig. 5.10b). The maximum value, 62 432 mg $m^{-2}d^{-1}$, was sampled during early December. The minimum value was 960 mg $m^{-2}d^{-1}$ and corresponded to the autumn sample of March. There was not clear influence of TMF on the annual temporal evolution of the FP flux. Although the four near-bottom FP flux peaks were associated to the spring and early summer (November and December period) they did not represent more than 58% of the total annual flux. Near the bottom FP flux was, like during the winter, up to 5 orders of magnitude higher than in the mid-depth trap. The annual flux was 8 185 856 fp m^{-2} (Table 5.3a).

The ^{210}Pb concentration showed a decreasing trend from 1300 to 870 Bq kg^{-1} during autumn and winter (March to September period), a peak in October, followed by a sharper decrease during the spring and summer (October to January period) when the minimum value, 650 Bq kg^{-1}, was measured (Fig. 5.7d). The maximum value, 2 000 Bq kg^{-1} was observed in February. This peak was also observed in the OC and $CaCO_3$ content curves. The ^{210}Pb concentration in mid-depth samples was about 2 times higher than that found in the bottom trap for the same sampling periods.

As all the major constituents, ^{210}Pb flux showed a temporal variation similar to that of the TMF. ^{210}Pb flux ranged from 1.5 Bq $m^{-2}d^{-1}$ in early January to 4.6 Bq $m^{-2}d^{-1}$ in the August-September and early December sampling periods (Fig. 5.11b). The annual ^{210}Pb flux near the bottom was 1310 Bq m^{-2} (Table 5.3a).

5.2. JOHNSON'S DOCK (SITE BAE)

The trap was moored on a site at 19.5 m water depth, 4.5 m above the bottom (Fig. 2.3).

The total mass flux and the content and fluxes of the major constituents (OC and IC, $CaCO_3$, organic matter, BSi, N, fecal pellets, and aluminosilicates) collected during each sampling interval are listed in Tables 5.4 and 5.5. All the samples were a mixture of fine particles with poorly classified clastic material. The total fluxes during the study period are listed in Table 5.3b.

Time series of total mass flux (TMF) showed a relatively constant value throughout the study period, although four peaks were recognisable (Fig. 5.12). The maximum value, 89 073 mg $m^{-2}d^{-1}$, was registered in late January and the minimum value, 23 235 mg $m^{-2}d^{-1}$, in mid-late December (Fig. 5.12). The total TMF during the study period (two thirds of the summer) was 3325.26 g m^{-2} (Table 5.3b).

The OC content ranged from 0.3 to 0.8% (Fig. 5.13a). Maximum OC values in late February, early January and in mid-February coincided with low TMF values. Minimum values corresponded to mid-late January when TMF was high. There was a clear inverse relation between OC content and TMF.

OC flux values showed similar trends to those of the TMF except in mid-January and in early February (Fig. 5.13a). OC fluxes ranged from a minimum of 125 mg $m^{-2}d^{-1}$, during the first week of February to a maximum of 315 mg $m^{-2}d^{-1}$, during the fourth week of January. The total OC flux during the study period was 16.04 g m^{-2} (Table 5.3b).

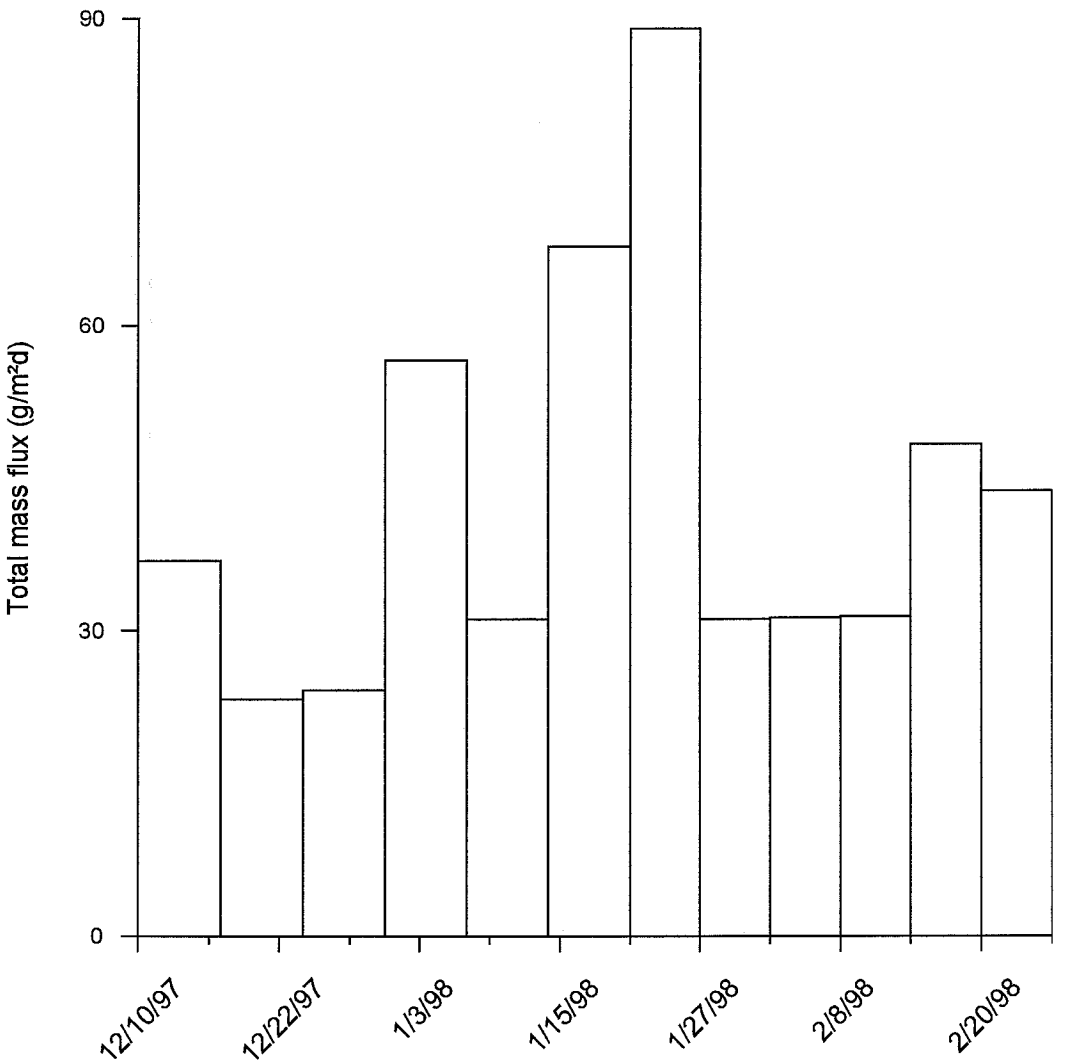

Fig. 5.12. Total mass flux temporal series at Johnson's Dock, Livingston Island

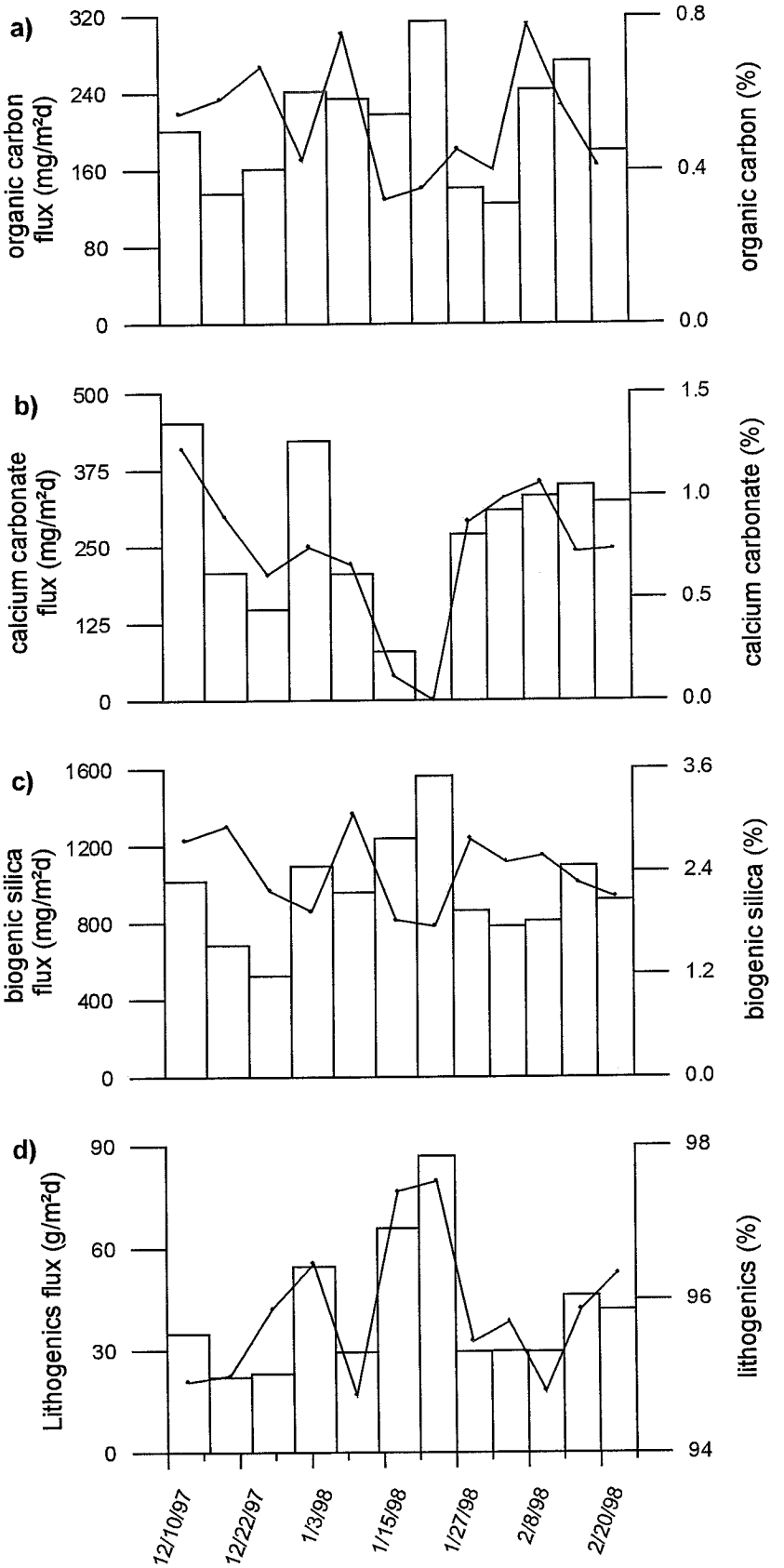

Fig. 5.13. (a) Organic carbon, (b) calcium carbonate, (c) biogenic silica and (d) lithogenic fraction concentrations (filled circles) and total fluxes (histograms) at Johnson's Dock, Livingston Island.

N content varied between 0.02 and 0.12%. N flux minimum and maximum values were 15 and 44 mg $m^{-2}d^{-1}$, respectively (Fig. 5.14a). The lowest N flux was collected in first week of February when the OC flux reached its lowest value and the TMF was low as well. The highest N flux occurred during the third week of February. The total N flux during the study period was 2.15 g m^{-2} (Table 5.3b).

The atomic OC/N ratio showed low values ranging from 7.16 to 10.56, except in late January when it increased to 22.98 (Fig. 5.15a). The average value was 9.46 ± 4.41 and the variation coefficient 0.47. The OC/IC ratio ranged from 3.71 to 9.55 except in mid- and late January when it increased sharply to 23.2 (Fig. 5.15b). The mean value was 7.15 ± 5.63 and the variation coefficient 0.79. Both atomic OC/N and OC/IC increases were produced by a decrease in N and IC contents.

$CaCO_3$ content in the trapped sediment was very low, ranging between 0 and 1.23% (Fig. 5.13b). The mean $CaCO_3$ content was only 0.72%. The maximum content was measured in the mid-December and mid-February samples, whereas during late January was practically null (when the IC values were below the detection level, 0.003%). The $CaCO_3$ flux maximum values (greater than 400 mg $m^{-2}d^{-1}$) occurred in mid-December and early January and minimum values (approximately 0 mg $m^{-2}d^{-1}$) in late January just when TMF was maximum. The total $CaCO_3$ flux during the study period was 20.09 g m^{-2}.

The BSi content ranged from 1.75 to 3.08% (Fig. 5.13c). The sample with the maximum BSi content corresponded to the second week of January and it coincided with a peak of the OC content. The material with the minimum BSi content was trapped in mid-late January, it also had low OC content and coincided with maximum TMF values. The BSi flux was influenced by the TMF and it showed an opposite trend to that of the BSi content. The BSi flux ranged from 524 mg $m^{-2}d^{-1}$ in late December to 1562 mg $m^{-2}d^{-1}$ in late February. The total BSi flux during the sampling period was 74.76 g m^{-2}.

The BSi/OC weight ratio varied between 3.25 during late December and 6.24 in early February (Fig 5.15c). The minimum values were measured during late December and early January while the maximum occurred in the first week of February.

The lithogenic (LG) constituents were the major fraction of the settling particulate matter ranging from 94.75 to 97.54%. Maximum lithogenic content values were registered in mid- and late January (Fig. 5.13d). The lithogenic flux clearly controlled the total mass flux and ranged from 22 074 mg/m^2d in late December to 86 881 mg $m^{-2}d^{-1}$ in late January, with an average value of 41 225 ± 19 473 mg $m^{-2}d^{-1}$. The total LG flux during the study period was 3198.34 g m^{-2}.

The fecal pellets (FP) flux showed a clear decreasing trend along the study period that ranged from approximately 100 000 to 10 000 FP $m^{-2}d^{-1}$ (Fig. 5.14b). Nevertheless, there was a peak of 288 571 FP $m^{-2}d^{-1}$ in early January, apparently not associated to any other measured variable. The minimum value (7 200 FP $m^{-2}d^{-1}$), in mid-January, corresponded to the highest TMF period. FP content did not show clear associations to any major constituent. The total FP flux during the sampling period was 5 350 680 FP m^{-2}.

The sediment trap also collected coarse detritic clasts. The number and flux of the clasts coarser than 1 mm showed an increasing trend along the sampling period from 10 to more than 800 and from 5 to 9143 mg $m^{-2}d^{-1}$, respectively. Minimum values were recorded at the beginning of the experiment and maximum peaks in early and late February (Fig. 5.14c).

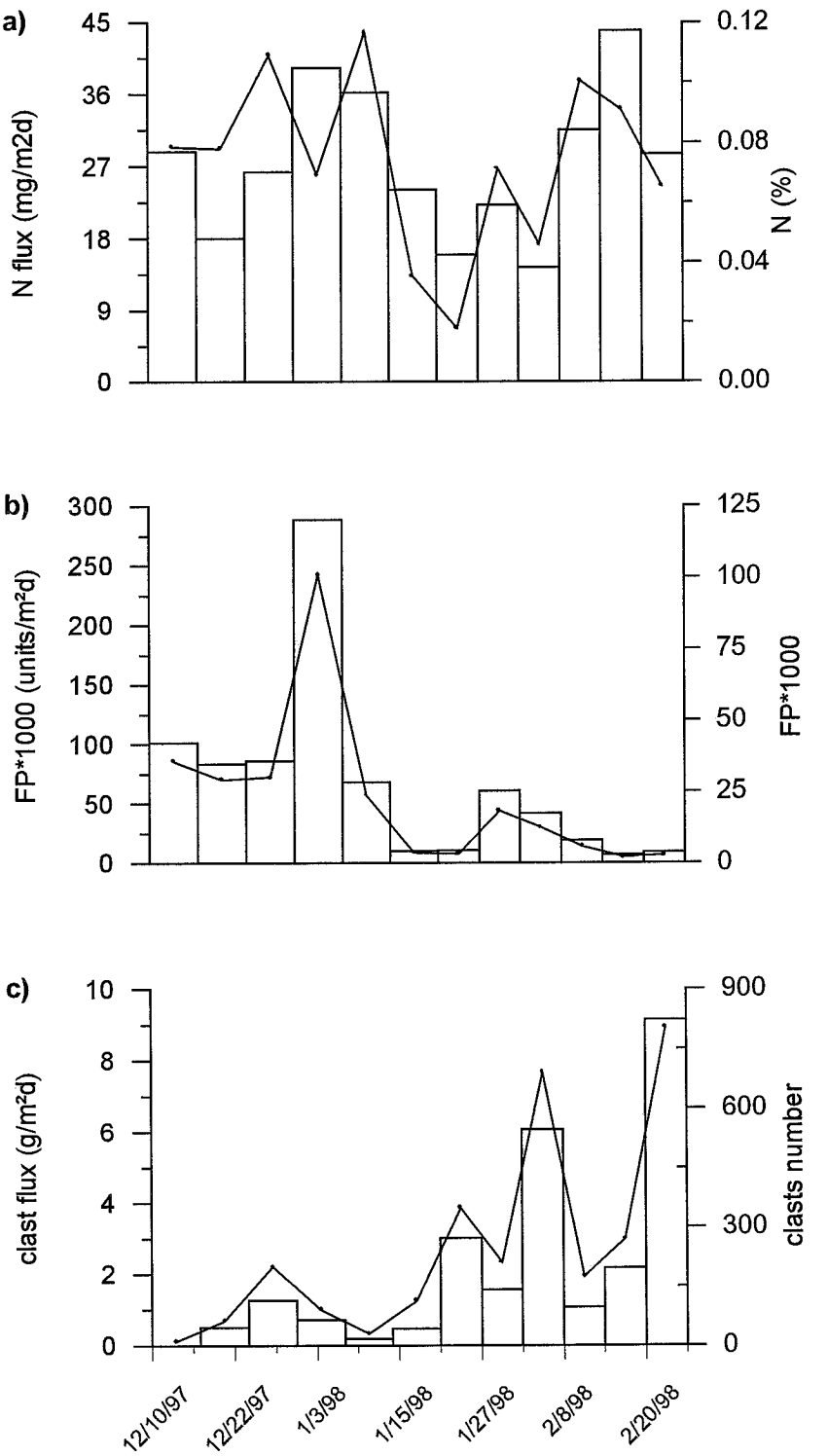

Fig. 5.14. Time series of (a) nitrogen (N), (b) fecal pellets (FP) and (c) clasts contents (filled circles) and fluxes (histogram) at Johnson's Dock, Livingston Island.

Table 5.1. Organic carbon, calcium carbonate ($CaCO_3$), nitrogen, biogenic silica, lithogenics and fecal pellets contents and atomic organic carbon to nitrogen (OC/N) and biogenic silica to organic carbon (BSi/OC) weight ratios of each sampling interval for the two traps at site A6. MD and NB mean mid-depth and near-bottom, respectively. All values expressed as weight percentage (%), except those referring to fecal pellets, which are fecal pellets units. Note: * concentration estimated after the 2.4 mean BSi/OC weight ratio averaged between the four analysed samples.

starting date	organic carbon %		$CaCO_3$ %		nitrogen %		biogenic silica %		lithogenics %		atomic OC/N		weight BSi/OC		fecal pellets units	
A6	MD	NB	MD	NB	MD	NB	MD	NB	MD	NB	MD	NB	MD	NB	MD	NB
1/3/95	6.85	1.7	nd	0.27	0.86	0.215	16.44*	18.1	nd	78.23	9.3	9.3	2.4*	10.6	225	3600
1/4/95	14.92	1.26	nd	1.03	1.31	0.195	35.78*	16.89	nd	79.56	13.3	7.6	2.4*	13.4	2	48120
1/6/95	11.09	1.21	nd	1.13	1.016	0.178	26.54*	14.87	nd	81.58	12.7	8	2.4*	12.3	3	97740
1/8/95	18.75	1.38	nd	0.98	1.605	0.199	45*	15.11	nd	81.15	13.6	8.1	2.4*	10.9	3	134900
1/10/95	15.15	1.65	nd	1.24	1.907	0.231	36.36*	16.86	nd	78.59	9.3	8.3	2.4*	10.2	2	167430
1/11/95	10.3	1.52	nd	1.47	1.096	0.216	24.72*	17.83	nd	77.66	11	8.2	2.4*	11.7	4	96444
16/11/95	8.71	1.25	1.21	1.18	1.39	0.171	26.87	16.96	54.51	79.37	7.3	8.5	3.1	13.6	840	94050
1/12/95	9.85	1.39	nd	1.16	1.082	0.183	23.64*	18.29	nd	77.77	10.6	8.9	2.4*	13.2	34	117060
16/12/95	8.2	1.27	4.17	0.16	1.471	0.165	20.64	15.08	58.8	82.21	6.5	9	2.5	11.9	697	112710
1/1/96	8.37	1.44	1.77	0.24	1.386	0.179	22.78	12.69	58.7	84.2	7.1	9.4	2.7	8.8	569	63048
16/1/96	7.93	3.03	nd	2.2	1.158	0.379	19.03*	17.38	nd	74.37	8	9.3	2.4*	5.7	8	59130
1/2/96 (15 days)	10.47	2.27	nd	3.12	1.591	0.278	14.38	16.56	nd	75.79	7.7	9.5	1.4	7.3	1608	29000

Table 5.2. Mean flux rates for each sampling interval for sediment traps at western Bransfield Strait (siteA6). MD and NB mean mid-depth and near-bottom, respectively. All values expressed as miligrams per square meter per day (mg $m^{-2}d^{-1}$), except those referring to fecal pellets, which are fecal pellets $m^{-2}d^{-1}$.

starting date	total mass mg $m^{-2}d^{-1}$		organic carbon mg $m^{-2}d^{-1}$		$CaCO_3$ mg $m^{-2}d^{-1}$		nitrogen mg $m^{-2}d^{-1}$		biogenic silica mg $m^{-2}d^{-1}$		lithogenics mg $m^{-2}d^{-1}$		fecal pellets units $m^{-2}d^{-1}$	
A6	MD	NB	MD	NB	MD	NB	MD	NB	MD	NB	MD	NB	MD	NB
1/3/95	0.992	1834	0.068	31.25	nd	4.88	0.009	3.94	nd	331.91	nd	1435	60	960
1/4/95	0.089	3901	0.013	49.19	nd	40.26	0.001	7.59	nd	658.69	nd	3104	1	6416
1/6/95	0.405	3974	0.045	48.18	nd	44.82	0.004	7.07	nd	590.79	nd	3242	1	13032
1/8/95	0.115	5321	0.026	73.48	nd	52.1	0.002	10.6	nd	803.93	nd	4318	1	17987
1/10/95	0.419	2567	0.063	42.44	nd	31.9	0.008	5.94	nd	432.8	nd	2017	1	44648
1/11/95	0.907	3600	0.093	54.76	nd	52.94	0.01	7.76	nd	641.94	nd	2796	2	51437
16/11/95	112.5	4672	9.8	58.4	1.36	54.94	1.56	7.99	30.22	792.27	61.32	3708	448	50160
1/12/95	0.955	4387	0.094	60.83	nd	50.98	0.01	8.01	nd	802.32	nd	3412	18	62432
16/12/95	50.21	3949	4.12	50.28	2.09	6.41	0.738	6.51	10.36	595.55	29.52	3247	372	60112
1/1/96	67.66	2234	5.66	32.1	1.20	5.25	0.938	3.99	15.41	283.55	39.72	1881	304	33626
16/1/96	1.33	2002	0.105	60.6	nd	44.03	0.015	7.58	nd	347.94	nd	1489	4	31536
1/2/96 (15 days)	20.54	1179	2.15	26.72	nd	36.72	0.327	3.27	2.95	195.17	nd	893	858	15467

Table 5.3a. Total downward fluxes during the whole sampling period in sediment traps at site A6. MD and NB mean mid-depth and near-bottom, respectively. All values expressed as grams per square meter (g m^{-2}), except those referring to fecal pellets, which are fecal pellets m^{-2}.

	total mass g m^{-2}		organic carbon g m^{-2}		$CaCO_3$ g m^{-2}		nitrogen g m^{-2}		biogenic silica g m^{-2}		lithogenics g m^{-2}		fecal pellets units m^{-2}	
A6	MD	NB	MD	NB	MD	NB	MD	NB	MD	NB	MD	NB	MD	NB
	3.89	1254	0.34	17.62	0.07	13.1	0.06	2.49	0.88	201.03	1.96	1005	31960	8185856

Table 5.3b. Total downward fluxes during the summer sampling period for the sediment trap at Johnson's Dock (BAE site). All values expressed as grams per square meter (g m^{-2}), except those referring to fecal pellets, which are fecal pellets m^{-2}.

	total mass g m^{-2}	organic carbon g m^{-2}	$CaCO_3$ g m^{-2}	nitrogen g m^{-2}	biogenic silica g m^{-2}	lithogenics g m^{-2}	fecal pellets units m^{-2}
BAE	3325.26	16.04	20.09	2.15	74.76	3198.34	5350680

Table 5.4. Organic carbon, calcium carbonate ($CaCO_3$), nitrogen, biogenic silica, lithogenics, and fecal pellets contents and atomic organic carbon to nitrogen (OC/N) and biogenic silica to organic carbon (BSi/OC) weight ratios of each sampling interval for the sediment trap at Johnson's Dock (BAE site). All values expressed as weight percentage (%), except those referring to fecal pellets, which are fecal pellets units.

starting date	organic carbon %	$CaCO_3$ %	nitrogen %	biogenic silica %	lithogenics %	atomic OC/N	weight BSi/OC	fecal pellets units
BAE 12/10/97	0.55	1.23	0.078	2.77	94.92	8.1	5.1	35520
12/17/97	0.58	0.89	0.078	2.94	95	8.8	5	29150
12/24/97	0.67	0.61	0.109	2.17	95.88	7.2	3.3	30100
12/31/97	0.43	0.75	0.069	1.93	96.47	7.2	4.5	101000
1/7/98	0.76	0.66	0.117	3.08	94.75	7.6	4.1	23694
1/14/98	0.32	0.12	0.036	1.83	97.41	10.6	5.7	3600
1/21/98	0.35	0	0.018	1.75	97.54	23	5	3200
1/27/98	0.45	0.87	0.071	2.77	95.45	7.4	6.1	18200
2/2/98	0.40	0.99	0.046	2.5	95.7	10.1	6.2	12450
2/8/98	0.78	1.06	0.101	2.58	94.8	9	3.3	5760
2/14/98	0.57	0.72	0.091	2.26	95.88	7.3	4	2160
2/20/98 (6 days)	0.41	0.74	0.065	2.1	96.34	7.4	5.1	2700

Table 5.5. Mean flux rates for each sampling interval for sediment trap at Johnson's Dock (site BAE). All values expressed as miligrams per square meter per day (mg $m^{-2}d^{-1}$), except those referring to fecal pellets, which are fecal pellets $m^{-2}d^{-1}$.

starting date	total mass mg $m^{-2}d^{-1}$	organic carbon mg $m^{-2}d^{-1}$	$CaCO_3$ mg $m^{-2}d^{-1}$	nitrogen mg $m^{-2}d^{-1}$	biogenic silica mg $m^{-2}d^{-1}$	lithogenics mg $m^{-2}d^{-1}$	fecal pellets units $m^{-2}d^{-1}$
BAE 12/10/97	36819	201.07	451.53	28.87	1018.31	34947	101486
12/17/97	23235	135.7	207.9	18.08	682.05	22074	83286
12/24/97	24125	161.39	148.1	26.31	524.16	23130	86000
12/31/97	56620	242.11	422.37	39.34	1094.9	54618	288571
1/7/98	31081	234.95	205.09	36.3	957.41	29449	67697
1/14/98	67711	218.58	78.51	24.14	1239.7	65956	10286
1/21/98	89073	315.05	0	16	1562.73	86881	10667
1/27/98	31072	141.07	270.01	22.2	862.07	29658	60667
2/2/98	31188	125.14	308.4	14.46	781.14	29847	41500
2/8/98	31310	244.26	331.7	31.54	808.56	29681	19200
2/14/98	48336	274.15	349.7	44.03	1094.09	46344	7200
2/20/98 (6 days)	43708	180.16	322.12	28.57	915.93	42110	9000

PART IV. DISCUSSION

6. MAJOR BIOGENIC CONSTITUENTS IN BOTTOM SEDIMENT, PRESERVATION, AND BURIAL EFFICIENCIES

6.1. MAJOR BIOGENIC CONSTITUENTS

Overall values for OC (0.13-1.61%), $CaCO_3$ (<0.003-1.23%), N (0.01-0.31%) and BSi (3.99-25.49%) content lied within the same range found by previous works in the Bransfield Strait (Warnke et al., 1973; DeMaster et al., 1987; Gersonde and Wefer, 1987; Nelson, 1988; Harden, 1989; DeMaster et al., 1991; Yoon et al., 1994; Bárcena et al., 1998; Fabrés et al., 2000) and in other Antarctic areas (Ledford-Hoffman, et al., 1984; Ledford-Hoffman, 1986; Dunbar et al., 1989; De Master et al., 1992; De Master et al., 1996; Hulth et al., 1997; Langone et al., 1998).

Within the study area, the finer sediment and the material with the highest OC, N and BSi content within the surface mixed layer (SML) corresponded to the end of the Orleans trough, western Bransfield Strait (core A3), and to the Gerlache Strait (cores B187, B5, B6 and B7) (Fig. 6.1, 6.2, and 6.3). The samples from the western and central sectors of the Gerlache Strait (cores B191 and B192) and from the central (core A6) -close to Deception Island- and western (core B2) -between Low and Trinity Islands- Bransfield Strait basins showed relatively medium OC, N, and BSi concentrations. The sediments with the lowest OC, N, and BSi content values and with the highest sand percentage were taken at Bellingshausen Sea (cores B214 and B223).

There was no evident correlation between organic matter content within the SML (recently deposited material) and water depth (Fig. 6.4). Hulth et al. (1997) found a similar pattern with the OC concentration in sediments from the Weddell Sea.

The BSi, followed by the organic carbon, composed the main fraction of the biogenic matter content, according to previous works in the Antarctic Ocean (DeMaster et al., 1987; Nelson, 1988; Yoon et al., 1994; DeMaster et al., 1996; Dunbar et al., 1998; Langone et al., 1998). The high BSi content in the bottom sediment related to the apparent mean annual low productivity in the surface waters of the Southern Ocean is known as the "opal paradox ". This fact has been explained by the good preservation of BSi in the bottom sediment promoted at least in part by low temperatures (DeMaster et al., 1996). Nevertheless, a recent proposal (Pondaven et al., 2000) suggests that opal production has been underestimated and opal accumulation rates overestimated.

Reports on Bransfield and Gerlache Straits sediment showed that $CaCO_3$ content is very low or undetectable and it has no relation to any other variable (Warnke et al., 1972; Harden et al., 1992; Yoon et al., 1994). Results in the present work agree with previous research but contrary to Yoon et al. (1994) the highest carbonate concentration was found toward the bottom of the cores. Hulth et al., (1997) found the similar trend in southern Weddell Sea sediment and they attributed it to a higher inorganic carbon deposition in the past. It is possible to suggest that in the Bransfield and Gerlache Straits similar events could happen. Further evidence will be

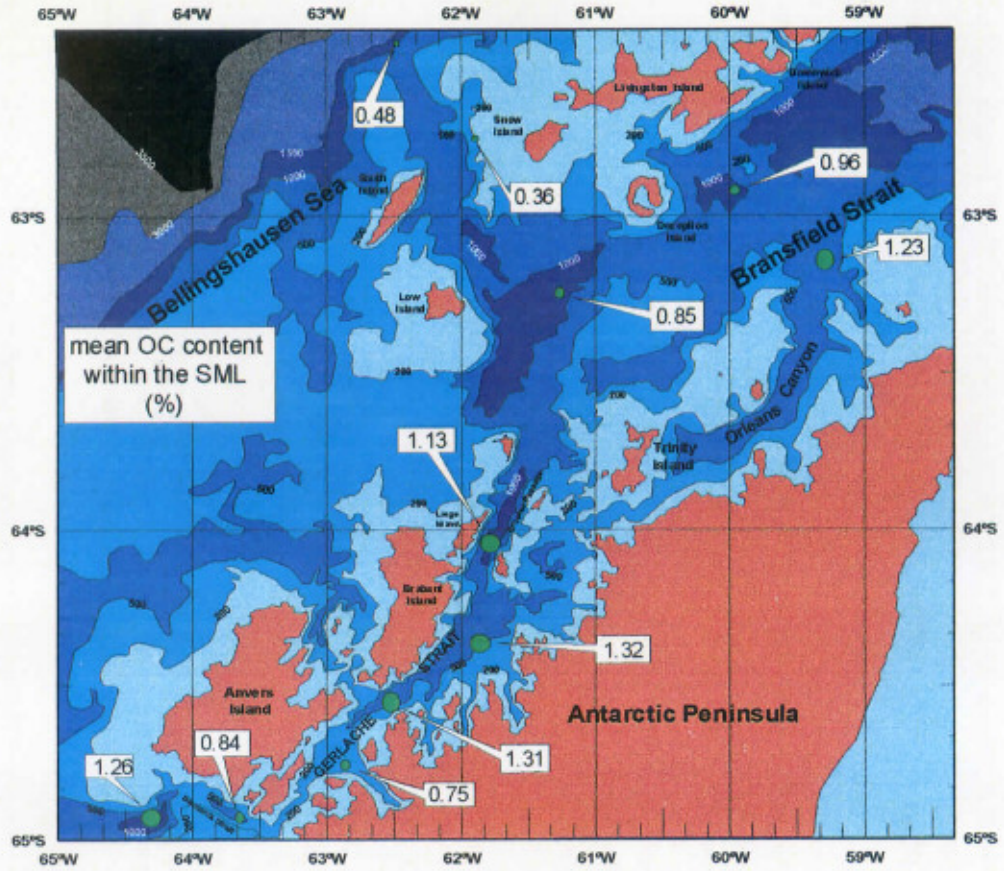

Fig. 6.1. Organic carbon (OC) content expressed as weight percentage (%) within the surface mixed layer (SML) of the sediment in both Bransfield and Gerlache Straits and the Bellingshausen Sea.

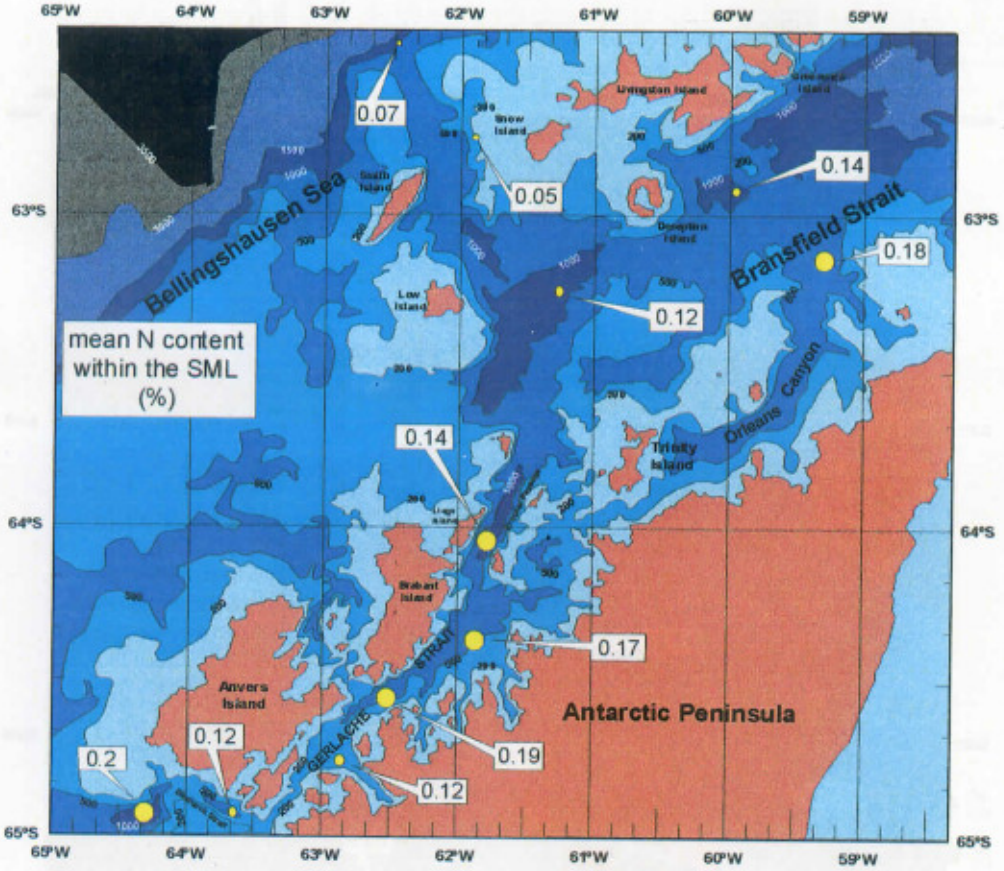

Fig. 6.2. Nitrogen (N) content expressed as weight percentage (%) within the surface mixed layer (SML) of the sediment in both Bransfield and Gerlache Straits and the Bellingshausen Sea.

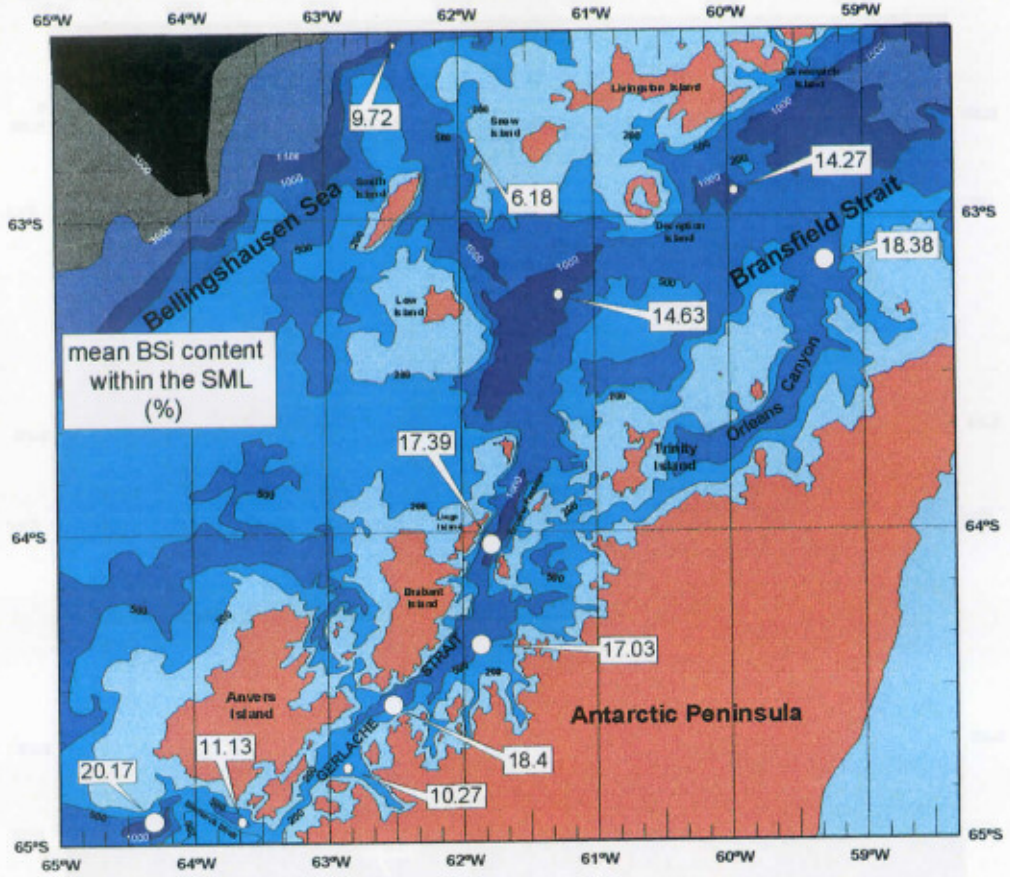

Fig. 6.3. Biogenic silica (BSi) content expressed as weight percentage (%) within the surface mixed layer (SML) of the sediment in both Bransfield and Gerlache Straits and the Bellingshausen Sea.

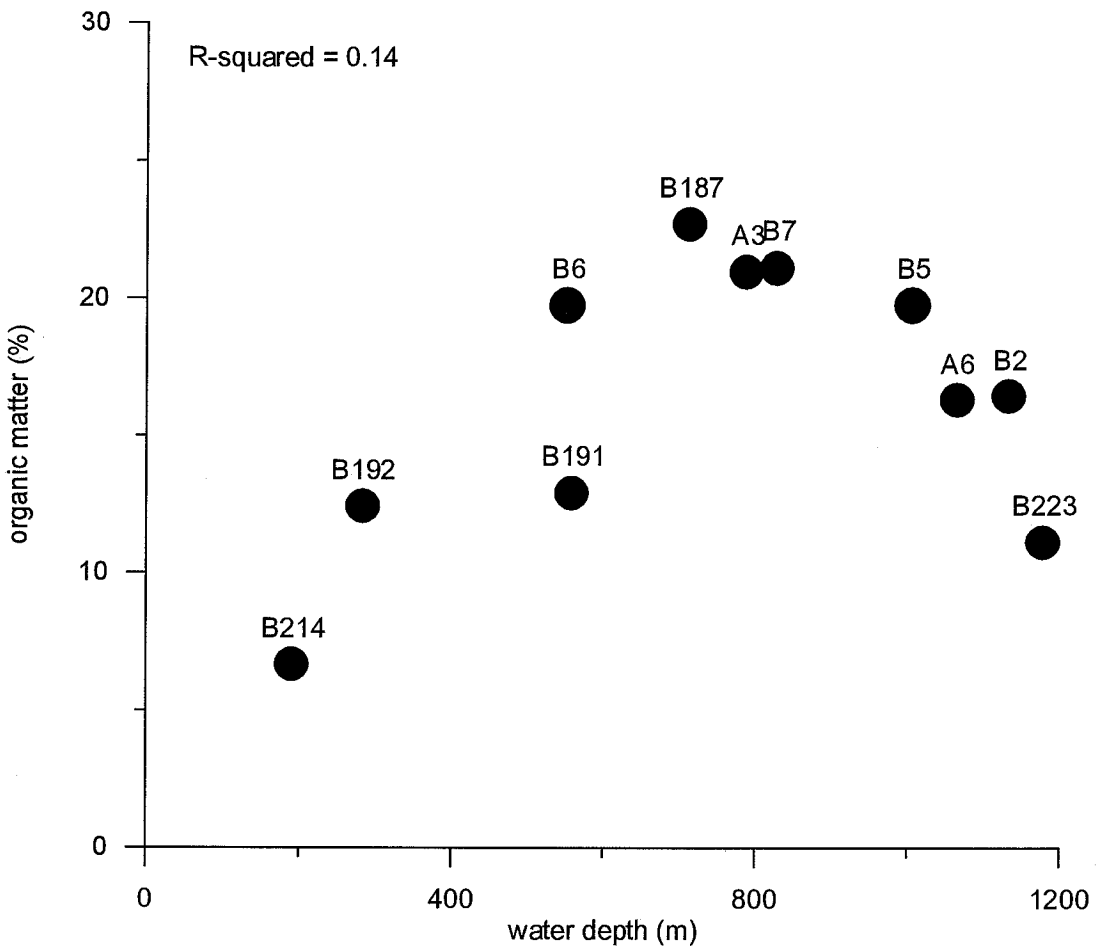

Fig. 6.4. Organic matter (expressed in dry weight percentage) within the surface mixed layer (SML) versus water depth (expressed in meters) from cores data from the Bellingshausen Sea (B214 and B223) and both the Gerlache (B187, B191, B192, B5, B6, and B7) and Bransfield Straits (A3, A6, and B2).

detailed in the burial efficiency section. The highest carbonate concentration was measured in the shallowest sampled site at central Gerlache Strait but no correlation was found between carbonate content and water depth in all the analysed cores (R^2= 0). Thus, high carbonate uptake within the sediment prevents the sedimentary record to keep a clear $CaCO_3$ signal, as it will be discussed in the sediment traps section.

6.2. ZONES OF RELATIVELY HIGH ORGANIC MATTER CONCENTRATION

The higher organic matter concentrations were found in the samples from the central and eastern part of the Gerlache Strait (sites B7, B6, and B5) and from the Orleans Trough in the central Bransfield Strait (site A3).

The relatively high OC, N and BSi content in the bottom sediments from the central and eastern part of the Gerlache Strait is a consequence of the high phytoplankton biomass and primary production rates in the euphotic layer of these zones (Burkholder and Sieburth, 1961; Mandelli and Burkholder, 1966; Holm-Hansen and Mitchell, 1991; Huntley et al., 1991; Karl et al., 1991). This correspondence between surface waters and bottom sediment could be due to: a) the rapid sinking of diatom resting spores (Karl et al., 1991; Von Bodungen et al., 1986) during the phytoplankton demise experienced at the end of the austral summer (Karl, et al.,1991; Holm-Hansen and Mitchell, 1991) and, b) the transport of biogenic material packed in fecal pellets (Wefer et al., 1988). The former mechanism has an estimated sinking rate of 50-1500 m day^{-1} (Karl et al., 1991), and the latter between 100-300 m day^{-1} (Eppley and Peterson, 1979; Billett, et al., 1983). Although, the persistent water current flowing eastwards in the middle of the strait (Niiler et al. 1990) is strong enough to transport fine particulate material out to the Bransfield Strait (Karl et al., 1991), the relatively high OC, N and BSi content in the bottom sediment of the Gerlache Strait, verifies that a considerable fraction of the primary produced organic matter finally deposits in this area. The major part of the organic particulate matter settling at the bottom of the central and eastern part of the Gerlache Strait should be produced in the euphotic layer above it, since there are no such productive waters toward the west. Thus, an important part of the biogenic particulate matter exported from the euphotic layer of the central and eastern Gerlache Strait settles in the same area and is kept within the strait. In this part of the Southern Ocean the primary productivity signal is transferred to the sea bottom by settling particles yielding a good coupling between the surface and the deep ocean. These results agree with reports from other basins in the Atlantic Ocean (Deuser et al., 1981; Lampitt, 1985; Asper et al., 1992).

The correspondence between bottom sediments (OC, N and BSi concentration) at the Orleans trough and the surface waters above them (plankton biomass content and primary production rates) is not like in the Gerlache Strait. Although, the bottom sediment in the central and western Bransfield Strait showed relatively high organic matter concentration the euphotic layer in that area is not so rich and productive in organic carbon as in the Gerlache Strait. The highest biomass and primary production values are related to Deception Island rather than to the Antarctic Peninsula coast (Burkholder and Sieburth, 1961; Mandelli and Burkholder, 1966; Hernandez-Leon et al., 1999). Therefore, a different organic matter input than that of the local

primary productivity is expected. One current coming out from the Gerlache Strait and another coming along the western coast of the Antarctic Peninsula from the Weddell Sea converge between Trinity and Tower Islands, in the vicinities of the Orleans trough (García, et al., 1994, Niiler, et al., 1991). The relatively high concentration of OC, N and BSi in the bottom sediment might be explained by the fact that the Orleans trough is acting as a sediment trap. The trough is collecting particulate material from both the Gerlache Strait (as suggested in Karl et al., 1991) and the western coast of the Antarctic Peninsula. This deep area, as Nelson (1988) found in the Bransfield Strait basins, has fine grained and high organic content sediments due to focusing processes caused by lateral transport (Karl et al., 1991; Palanques et al., in press). Thus, within the study area two main processes could be leading to the production of relatively high organic matter concentration in the bottom sediment: 1) the rapid settling of the organic matter in high primary productivity environments (Gerlache Strait), and 2) the focusing of particulate matter produced away from the final deposition area due to currents and topographic structures, (central Bransfield Strait).

6.3. ZONES OF RELATIVELY MEDIUM ORGANIC MATTER CONCENTRATION

The relatively medium organic matter concentrations were found in the samples from the western part of the Gerlache Strait (sites B187, B191, and B192) and from the western Bransfield Strait (sites B2 and A6).

The relatively medium organic matter concentration in the bottom sediment of the western Gerlache Strait (core 191 and 192) could be due to 1) the relatively medium primary productivity in the euphotic layer of this area and 2) the general water circulation pattern.

Holm-Hansen and Vernet (1992) showed that there was an interannual variation in phytoplankton abundance and distribution within the Gerlache Strait and the highest values could be reached in the western part. However, when this part of the strait had the highest phytoplankton abundance, it was about one fifth of the highest values reported for the eastern part. A fraction of this relatively medium primary production probably is flushed by the main current that flows toward the east (Niiler et al., 1990). Nevertheless, as in the eastern part of the strait, the organic matter content decreases with depth, in the same direction of the current. It is possible to suggest that the rapid settling of particulate matter has major influence on bottom sediment composition than the local water currents. However, both mechanisms should be considered.

At both sides of Deception Island, the sediment at central and western subbasins of the Bransfield Strait (sites A6 and B2, respectively) have very similar OC, N and BSi content and relatively medium concentrations when compared with the rest of the study area. The primary production in the euphotic layer at Deception Island vicinities has been identified as moderate (Burkholder and Sieburth, 1961; Mandelli and Burkholder, 1966;Hernández-León et al., 1999; Varela et al., in press). It is an area where waters coming from the Gerlache Strait and from both the Bellingshausen and Weddell Seas converge. These water masses flow toward the east along the South Shetland Archipelago margin (García, et al., 1994, Niiler, et al., 1991). Both

sampling sites in this zone were located in deep basins, which apparently are acting as the final deposition area for particulate matter. In addition, the sand content in the sediment from these areas was relatively low (less than10%). These results agree with the work of Nelson (1988) that suggests sorting and current winnowing processes in the Bransfield Strait basins as the cause of fine grained, low bulk density sediments with a high biogenic fraction. The organic matter content at western Bransfield Strait is higher than at the central part probably due to its proximity to the Gerlache Strait.

6.4. ZONES OF RELATIVELY LOW ORGANIC MATTER CONCENTRATION

The relatively low organic matter concentrations were found in the sediment from the Bellingshausen Sea at the vicinities with the western Bransfield Strait (sites B214 and B223).

The low organic matter concentration and the high sand content in the Bellingshausen Sea samples might be the effect of two main facts. The low plankton biomass and primary productivity rates (Mandelli and Burkholder, 1966; Hernández-León et al., 1999) and the winnowing of fine particulate organic matter by both the Bellingshausen Sea Antarctic Superficial Water and the Circumpolar Deep Water. These water masses get into the Bransfield Strait between the Snow and Smith Islands over the Boyd Strait and between Smith and Low Islands. In both cases, the current flows toward the east surrounding Deception Island (Sievers, 1982; Capella, et al., 1992), preventing the organic matter to settle in the area. The relatively high sand content in cores B214 and B223, from 10 to 70% (Figs. 4.25 and 4.27), indicates that the fine particulate matter is transported probably to the adjacent western Bransfield Strait.

6.5. RELATIONSHIP AMONG THE MAJOR BIOGENIC CONSTITUENTS

The relatively high, medium and low concentrations of OC, N and BSi were associated among them. This means that high OC and N values coexisted with high BSi content. The sediment from the most western part of the Gerlache Strait (core B187) was the exception. These samples had the highest BSi concentration but not the highest OC and N content, in addition they had almost the lowest carbonate concentration. This unusual result could be due to: 1) the transport of organic matter, richer in BSi rather than in OC, through diatom aggregates (Smetacek, 1985) and 2) the better burial efficiency in the bottom sediment for BSi relative to OC.

6.6. ATOMIC OC/N AND BSI/OC WEIGHT RATIOS

The atomic OC/N ratio along every core was very constant (variation coefficients always less than 0.2). Average values (7.61-11.63) were higher than the 6.625 Redfield atomic ratio for marine plankton (Redfield et al. 1963) but within the same range for sea bed sediment in the Ross Sea (DeMaster et al., 1996). Von Bodungen et al. (1986) found that for the austral summer

in shallow waters of the Bransfield Strait, phyto- and zooplankton were the dominant producers of both suspended and settling organic matter. Since there are not important river inputs in the studied area and the main organic matter downward flux from surface waters occurs during the austral summer (see sediment traps section of this work) (Wefer et al., 1988; Cripps and Clarke, 1998; Palanques et al., in press), is possible to assume that the settling organic matter is mainly planktonic. Thus, the difference between the atomic OC/N ratios in the sediment and the Redfield ratio in marine plankton suggest that the biological and chemical processes in the water column and in the bottom sediment remove preferentially nitrogen relative to organic carbon from the organic matter. The atomic OC/N ratio in the overall studied surface sediment ranged between 7.06 and 8.82. This fact gives further evidence of its marine origin if the terrestrial plant ratio is considered (10 to 100 and 100 to 1000 for soft and woody tissues, respectively) (Ruttenberg and Goñi, 1997).

The BSi/OC weight ratio values (10.47 and 41.59) agreed with results obtained in the Ross Sea (DeMaster et al., 1992; DeMaster et al., 1996) and the Bransfield Strait (DeMaster et al., 1991). The common increasing trend towards the bottom of the cores evidenced the decoupling between BSi and OC within the sediments (Figs. 4.2, 4.6, 4.10, 4.13, 4.15, 4.17, 4.19, 4.21, 4.23, 4.25, and 4.27). Regarding the decay of organic matter it is not possible to state that in the studied area the OC and the N are decoupled within the sediment. The degradation of OC relative to BSi is more clear (Figs. 6.5 and 6.6). DeMaster et al. (1996) found in the Ross Sea that in general, little fractionation between OC and N occurred within the water column or in sediment. Nevertheless, burial efficiency percentages evidence fractionation to some degree, as it will be discussed in the biogenic variables mean accumulation rates and burial efficiency section.

6.7. ^{210}PB BASED APPARENT SEDIMENT ACCUMULATION RATES

The sediment accumulation rates of the present study agree with those ^{210}Pb based results of DeMaster et al. (1987 and 1991) in the Bransfield Strait and of Harden et al. (1992) for both Bransfield and Gerlache Straits.

6.7.1 Gerlache Strait

Apparent sediment accumulation rate (SAR) and water depth were not related when analysing the studied area (figs. 6.7a and 6.7b) as a whole (R^2=0), or when divided in sub-areas as Gerlache Strait (R^2=0.29), Bransfield Strait (R^2=0.07), and the Bellingshausen Sea (R^2 not determined because there were only two values).

Nevertheless, in the Gerlache Strait the low determination coefficient value could be much higher (R^2=0.63) without the effect of points B7 (central part of the strait) and B187 (western extreme of the strait). The exceptionally high sediment accumulation rate in the central part of the strait (core B7) is due to the correspondence with the highly productive waters of this area.

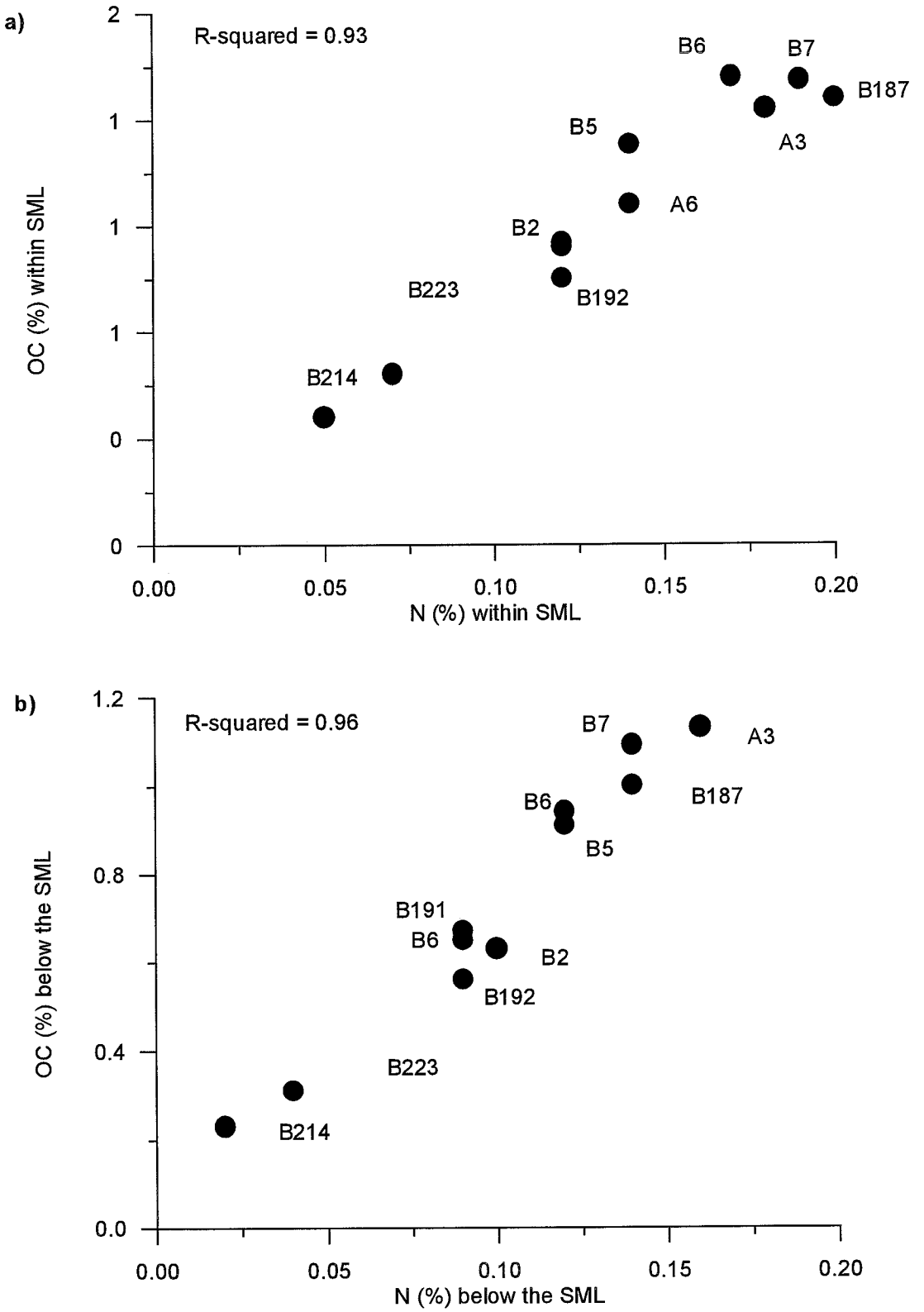

Fig. 6.5. Organic carbon (OC) versus nitrogen (N) concentrations (expressed in dry weight percentage), (a) within and (b) below the surface mixed layer (SML) with cores data from the Bellingshausen Sea (B214 and B223) and both the Gerlache (B187, B191, B192, B5, B6, and B7) and Bransfield Straits (A3, A6, and B2).

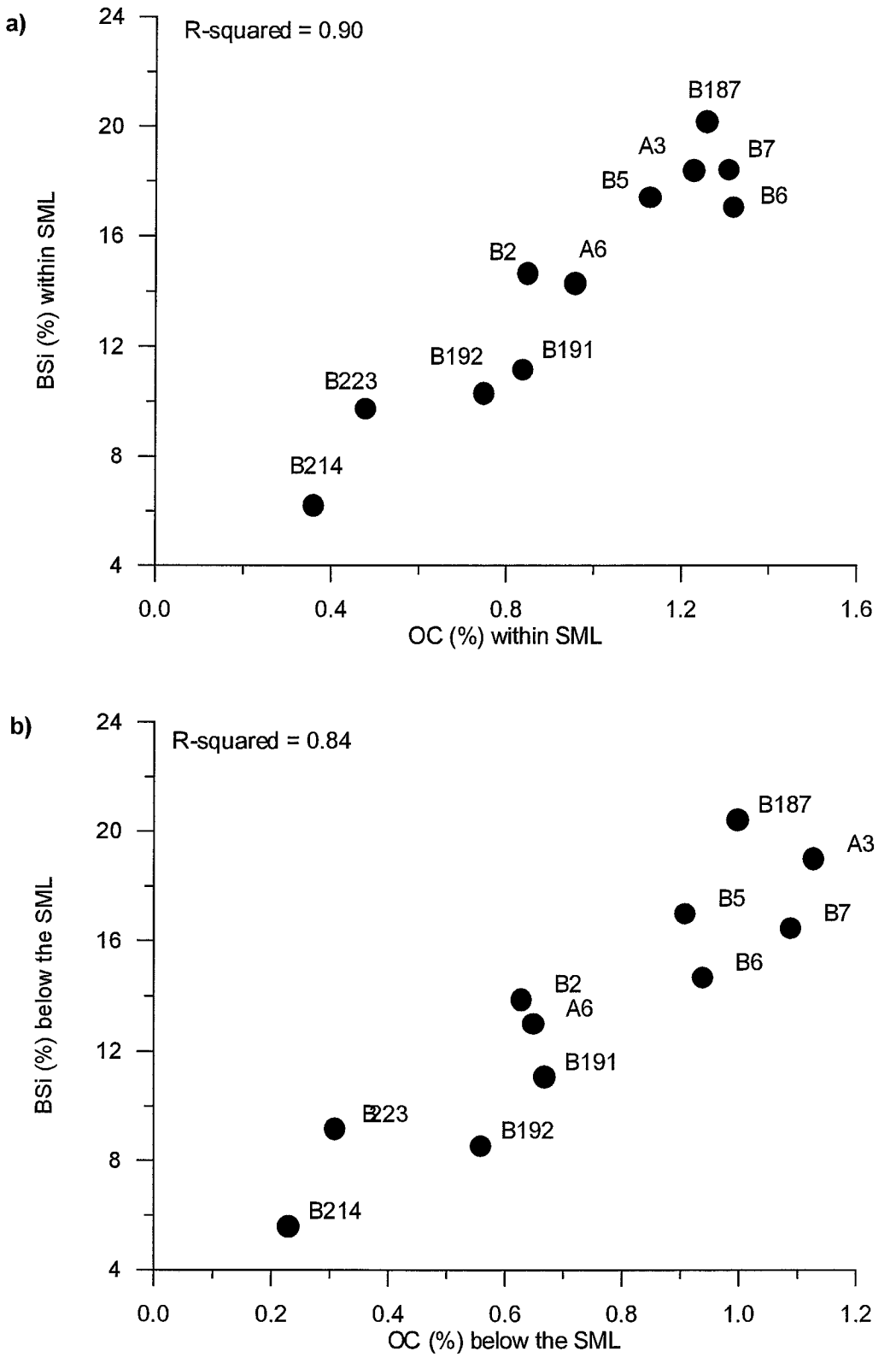

Fig. 6.6. Organic carbon (OC) versus biogenic silica (BSi) concentrations (expressed in dry weight percentage), (a) within and (b) below the surface mixed layer (SML) with cores data from the Bellingshausen Sea (B214 and B223) and both the Gerlache (B187, B191, B192, B5, B6, and B7) and Bransfield Straits (A3, A6, and B2).

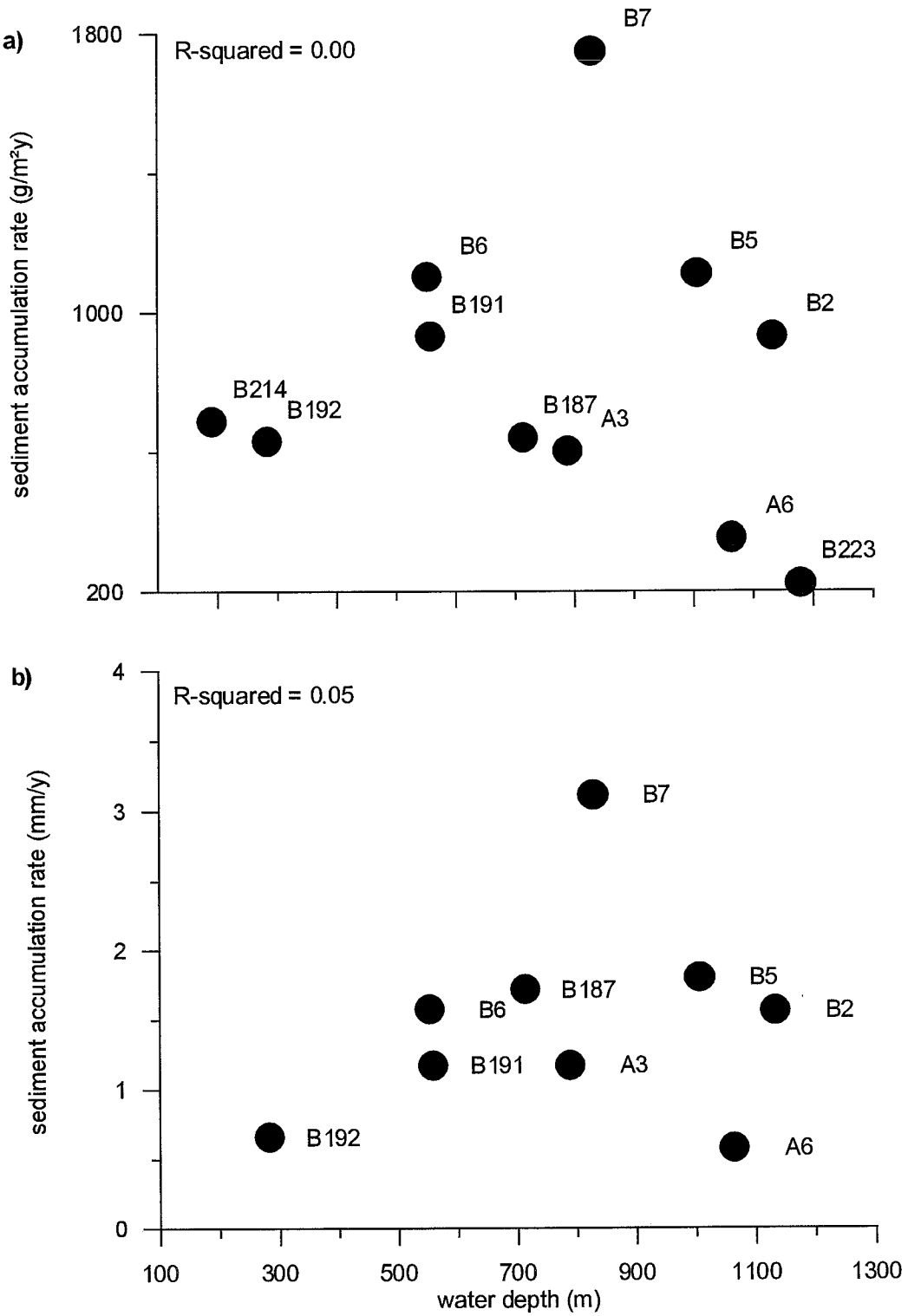

Fig. 6.7. Water depth (expressed in meters) versus sediment accumulation rate expressed in (a) g/m²y and (b) mm/y with cores data from the Bellingshausen Sea (B214 and B223) and both the Gerlache (B187, B191, B192, B5, B6, and B7) and Bransfield Straits (A3, A6, and B2).

Thus, in this part of the strait sediment accumulation rate gives additional evidence of the linkage through settling particle matter between the surface waters and the seabed. The evident decrease of the SAR value at point B187 when expressed in g m^{-2} y^{-1} (fig. 6.7a) and compared to mm y^{-1} (fig. 6.7b) is due to the relatively low density of this sediment.

The highest SAR values corresponded to the samples of the eastern part of the Gerlache Strait (Table 4.1). This deep part of the strait is probably acting as a settling particulate matter collector of that material produced on the shelf and the slope just as Palanques et al. (in press) and Nelson (1988) found in the Bransfield Strait. Due to the main circulation pattern of the strait this area should be receiving material from the western part as well. The high variability between local conditions (both in hydrographic and biological controls) prevents to establish a clear relation between SAR and water depth in the Gerlache Strait.

6.7.2. Western Bransfield Strait

In the central basin of the Bransfield Strait SAR values are higher at site A3 than at site A6 (figs. 6.7a and 6.7b). As it was pointed out, site A3 should be receiving material from the Gerlache Strait through the Orleans canyon and from the western coast of the Antarctic Peninsula. The water front at the middle of the strait (García, et al., 1994) and the circulation pattern of the Circumpolar Deep Water (CDW) (Capella, et al., 1992) might be keeping part of the settling particulate matter from the Orleans trough to reach the site A6.

^{14}C (1000yr time scales) and ^{210} Pb (100 yr time scales) based SAR were comparable (Masquè et al., in press) in Bransfield Strait sediment (sites A3 and A6) and agreed well with those results from Harden et al. (1992). The latter authors proposed that sedimentary processes in the area have been more or less constant during the last 1000 yr. The highest SAR within the studied portion of the Bransfield Strait was related to site B2. This point is located in the deepest area of the western basin. Due to the circulation pattern this zone should be receiving material from both the Gerlache Strait and the Bellingshausen Sea. The sand content at this point is very low (1.29-2.5%) (Fig. 4.10), so this deep basin might be acting as a sediment trap and the final settling area of very fine particulate material transported from both margins of the strait. Thus, bottom topography and currents are influencing the SAR in this area. Nelson (1988) found in other basins of the Strait similar characteristics as consequence of focusing processes.

6.7.3. Bellingshausen Sea

The lowest SAR value corresponded to the sediment from a deep-sea environment (core B223). This is probably the effect of winnowing by both the Bellingshausen Sea Antarctic Superficial Water (BSW) and the Circumpolar Deep Water (CDW) (Sievers, 1982; Capella, et al., 1992). These water streams get into the Strait over the Boyd Strait between Smith and Snow Islands and flow northeastward, surrounding Deception Island. The high sand content in the sediment evidence the action of the current over the fine particles.

At the continental shelf of Snow Island (core B214), out of the Bransfield Strait, the sand percentage of the sediment was relatively high as well (Fig. 4.25) and the SAR relatively medium and higher than at the Orleans canyon (Table 4.1). Site B214 is exposed to the action of both BSW and CDW so, winnowing could be expected. Nevertheless, its relatively shallow (at 192 m water depth) and current ward position allow those particles supplied by the iceberg melting to settle and not to be transported into the Bransfield Strait, like it should be happening with fine particles that might settle at site B2 in the western basin of the Strait.

6.8. BIOGENIC CONSTITUENTS APPARENT MEAN ACCUMULATION RATES AND BURIAL EFFICIENCIES

OC and BSI accumulation rates exposed in (Table 4.1) agree with previous results in the Bransfield Strait (Nelson, 1988) and the southwestern Ross Sea (DeMaster et al., 1996).

Relative high or low values of OC, BSi, and N mean accumulation rates corresponded to the same areas with relative high or low SAR values (Table 4.1). The $CaCO_3$ mean accumulation rate and SAR were not in accordance. The former value was determined by the large differences in the little amount of carbonate within all the cores.

The biogenic variables burial efficiency was not clearly related to accumulation rates (Fig. 6.8) or to any biogenic constituent content in the sediment. The depth of the SML was not related to the burial efficiency either (R^2=0.06) (Fig. 6.9). DeMaster et al. (1996) found an evident correlation between burial efficiencies and accumulation rates (expressed as cm kyr^{-1}) for both BSI and OC in sediments from the broad continental shelf of the Ross Sea. It seems that in Gerlache and western Bransfield Straits the high oceanographic and bathymetric variability within small areas, with a relatively narrow and incised continental shelf is leading to differences in the biogeochemical processes affecting the settling particulate matter.

The best-preserved biogenic constituent in the sediment of the studied area was the BSi (Table 4.1). This is a common phenomena observed in the Southern Ocean sediment (DeMaster et al., 1996; Nelson et al., 1996). Although Müller and Suess (1979) proposed that accumulation rates seems to be the parameter that better explains the organic matter preservation efficiency, no correlation between these two variables was found in the present study (Fig. 6.8). The conjunction of local characteristics as temperature, the nature of the siliceous assemblages, the mechanisms by which they reach the seabed (DeMaster et al., 1996) and dissolution (Schlüter et al., 1998) among other might be what better explains the amount of siliceous material that is finally kept within the sediment. Apparently microbial activity is very important in OC and N reutilization but has little to deal with BSi uptake (Canfield, 1994; DeMaster et al., 1996; Schlüter et al., 1998).

OC and N burial efficiencies were not clearly related to any parameter. In addition, OC was not always better preserved than N, although atomic OC/N ratio was quite constant along every core. An example of this is the sediment at sites B5 and B2 (Table 4.1). In sites B6 and B192

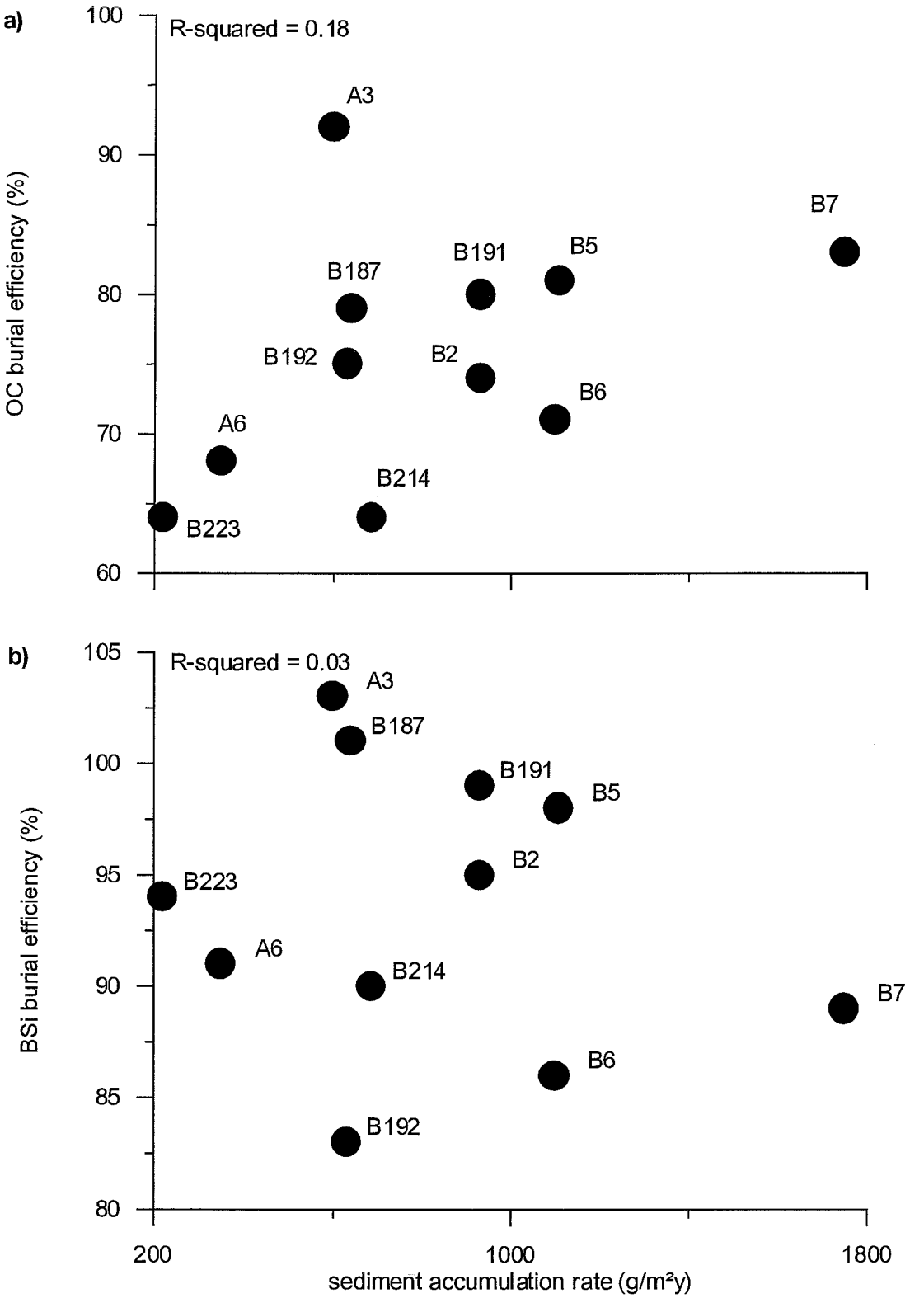

Fig. 6.8. Sediment accumulation rate expressed in g/m²y versus (a) organic carbon (OC) and (b) biogenic silica (BSi) burial efficiencies with cores data from the Bellingshausen Sea (B214 and B223) and both the Gerlache (B187, B191, B192, B5, B6, and B7) and Bransfield Straits (A3, A6, and B2).

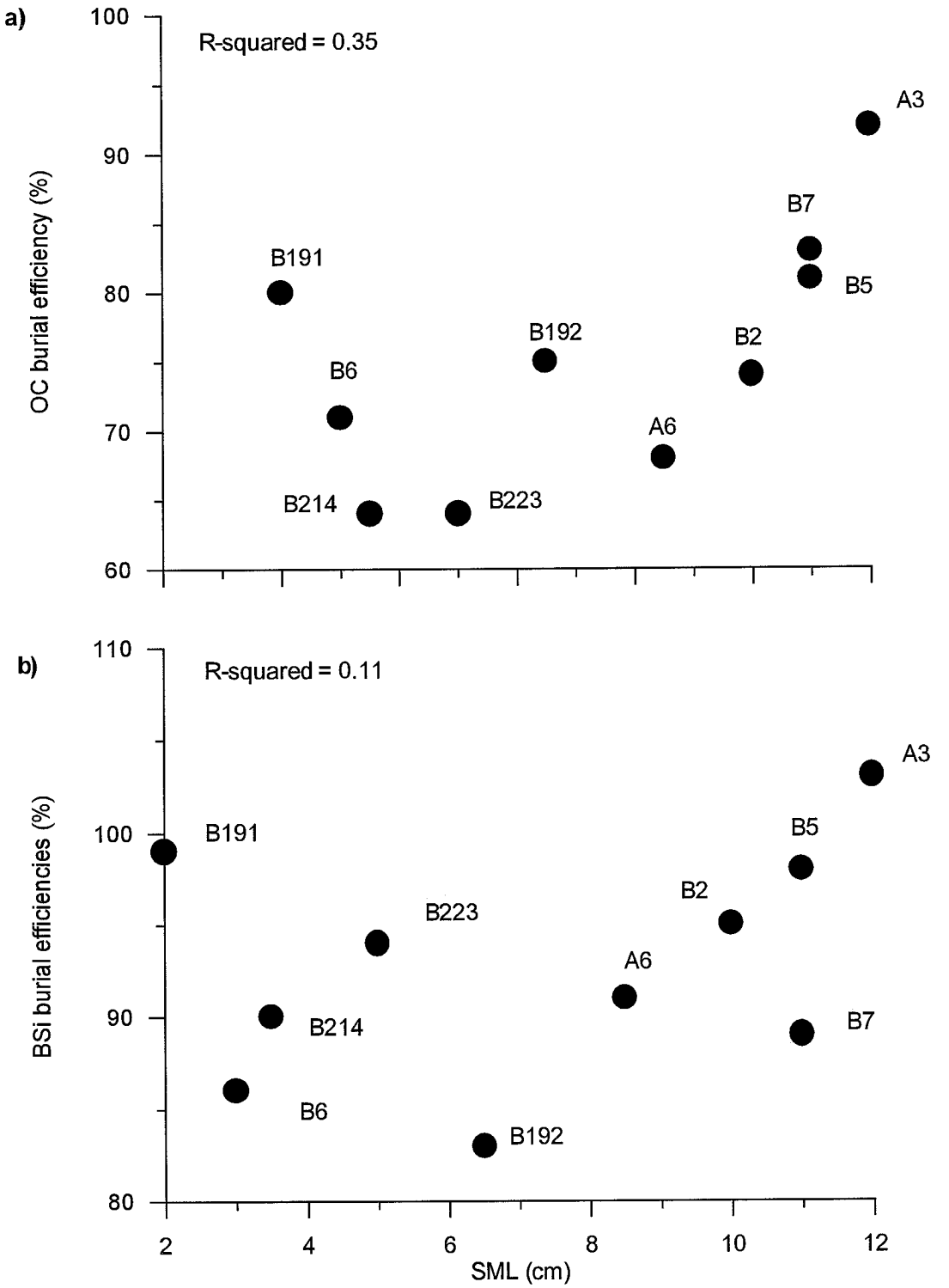

Fig. 6.9. a) Organic carbon (OC) and b) biogenic silica (BSi) burial efficiencies expressed in percentage versus depth of the surface mixed layer (SML) expressed in cm with cores data from Bellingshausen Sea (B214 and B223) and both the Gerlache (B187, B191, B192, B5, B6, and B7) and Bransfield (A3, A6, and B2) Straits.

burial efficiency for both OC and N were the same. It can not be stated a realistic explanation for this non-homogeneous pattern. Nevertheless, is possible to suggest that biogenic material uptake from the sediments depends largely on local and particular environmental characteristics rather than in one main parameter. The highest OC, N, and BSi burial efficiency was measured at the Orleans Trough followed by the Gerlache Strait (Table 4.1). Although the Orleans Trough did not have the highest biogenic matter concentrations and the highest accumulation rates, it seems to have special environmental conditions that are promoting high burial efficiencies.

$CaCO_3$ was better preserved at the eastern Gerlache Strait. Nevertheless, at the central part of the strait, at the western basin of the Bransfield Strait and at the Bellingshausen Sea, the carbonate concentration was lower within the SML than below it, yielding to burial efficiencies higher than 100% (Table 4.1). This fact suggests two mechanisms: 1) higher inorganic carbon deposition during past times and/or 2) better preservation conditions. Hulth et al. (1997) found an increase in inorganic carbon concentration toward the bottom of sediment cores from the Weddell Sea. These authors proposed higher inorganic carbon deposition during past (1) as the possible cause. It is highly probable that same conditions might occur on the western side of the Antarctic Peninsula as well.

A similar pattern was found with the BSi burial efficiency percentages at western Gerlache Strait and at the Orleans Trough (Table 4.1). Both high BSi productive (site B187) and high burial efficiency environments (site A3) may explain this fact. However, greater BSi deposition in the past should be considered.

The Bellingshausen Sea had the lowest burial efficiencies percentages for organic carbon and nitrogen because the relatively low amount of organic matter in the sediment. Therefore, a little uptake in both OC and N represent a high percentage of the concentration in the originally settled particulate matter. Although BSi content was also relatively low, it did not follow this trend. This fact evidences the higher preservation of BSi over OC and N. The preferential remineralisation order of the organic matter within the sediment of the studied area was N, OC, and BSi. This trend agrees with the rest of the Antarctic deep-sea and continental margin environments that preferentially preserve BSi relative to OC in the sedimentary record (DeMaster et al., 1991).

For the scope of this study, organic matter preservation processes remain unclear in this area in accordance to Hedges and Keil (1995) results in other marine environments, probably due to the interaction of several environmental conditions.

6.9. PRESERVATION EFFICIENCIES AND PRIMARY PRODUCTIVITY

6.9.1. Gerlache Strait

The mean primary production over spring and summer months in the Gerlache Strait range from 2 to 5 g C $m^{-2} d^{-1}$ and during the rest of the year is negligible (Cochlan, 1993). Supposing that the growing period is proportional to the solar intensity for about 150 austral spring and summer days (from November to April) (DeMaster et al., 1987), the annual primary production in the study area should range between 300 and 750 g C m^{-2}. Multiplying the mean sedimentation rate (assumed as constant) by the average OC content below the SML, we can calculate the amount of OC buried in the bottom floor (approximately between 3.5 and 19 g OC $m^{-2} y^{-1}$) (Table 4.1). If the eastern Gerlache Strait has the maximum primary production values (750 g C $m^{-2} y^{-1}$), then in the bottom sediments below this area (stations B7, B6 and B5) approximately between 1.3 and 2.5% (approx. mean 2%) of the primary produced OC remains below the SML. By using the minimum primary production values (300 g C m^{-2} y^{-1}) this stock goes to an average value of 4.9%. These values are compatible with those estimated by Nelson (1988) and DeMaster et al. (1991) in the Bransfield Strait. Assuming for the western part of the Gerlache Strait (stations B187, B191 and B192) a mean annual primary production of 300 g C m^{-2} the percentage of the primary produced OC that remains in the sedimentary record ranges between 1.2 and 2.1% (3.53 and 6.40 g OC $m^{-2} y^{-1}$). Thus, about 1.5% of the OC produced in the euphotic layer of the western Gerlache is finally buried in the same area.

Unfortunately, there are no available BSi production values for this area, at least to this author's knowledge. Nelson (1988) proposed a mean annual BSI production for the Bransfield Strait equal to 154 g BSi m^{-2} based in the BSi/OC ratio of local phytoplankton equal to 2 (Jennings et al., 1984; Nelson and Smith, 1986). If the same value is assumed for the Gerlache strait a low (perhaps-underestimated) budget can be calculated. Thus, for western Gerlache Strait the minimum amount of primary produced BSi buried in the sediment should be approximately between 35 and 85%. This agrees with Nelson (1988) results for the Bransfield Strait. Nevertheless, in the eastern part of the strait the amount of BSi buried would be almost twice the amount of the BSi produced. Another estimation of the annual BSi production could be obtained by multiplying the value of the primary produced OC in the area by the BSI/OC weight ratio of local phytoplankton, approximately equal to 2 (Jennings et al., 1984; Nelson and Smith, 1986). In the Gerlache Strait the mean annual BSi production would be approximately varying between 600 and 1500 g BSi m^{-2}. Then, the percentage of the primary produced BSi preserved within the sediment would be around 9 and 22% in the western part of the strait. In the eastern side the fraction of primary produced BSi that finally remains in the bottom sediment would range between 11 and 19%. In both parts the values are lower than the expected percentage of around 80 found in the Bransfield Strait (Nelson, 1988) and in the Ross Sea sediment (DeMaster et al., 1996), but close to the 50% found by DeMaster et al. (1987) in the Bransfield Strait.

The annual primary production estimated from 150 days of solar intensity (DeMaster, 1987) could be overestimated because cloudy and stormy days were not subtracted. Therefore, it is possible to suggest that burial percentages reported in the present work could be underestimated. Thus, minimum burial percentages should be considered.

Sediment trap studies in the Bransfield Strait have demonstrated that more than 90% of organic matter flux at mid depth in water column occurred within a 60 days period (Wefer et al., 1988; Palanques et al., in press; the present study). Therefore, is possible to calculate preservation efficiencies on the basis of a shorter, and perhaps more realistic, period of annual primary production. Nevertheless, it should be stated that primary production could be underestimated and the preservation efficiencies overestimated. Then, in the western part of the Gerlache Strait the annual primary productivity would be around 120 g C m^{-2} and in the eastern part about 300 g C m^{-2}. The amount of primary produced OC finally buried in the bottom sediment of the western part would be between 3 and 5% and in the eastern part between 3 and 6%. In the case of BSi the primary production values would be approximately 240 g BSi m^{-2} and 600 g BSi m^{-2} for the western and eastern parts, respectively. Thus, preservation efficiencies for BSi would vary between 22 and 54% and 27 and 48%, in the same order. These values are closer to previous studies in the Bransfield Strait (DeMaster et al., 1987; Nelson, 1988).

6.9.2. Western Bransfield Strait

Varela et al. (in press) estimated a rate of primary productivity in the west of Bransfield Strait approximately equal to 1 g C $m^{-2}d^{-1}$ during the 95-96-summer period. Thus, for this area it is considered a mean annual OC production of 150 g m^{-2}.

The percentage of the primary produced OC buried in this area, sites A3, A6 and B2, would be 5, 2, and 4, respectively. BSi burial values would be 38, 15, and 43% in the same order. Overall values are two to four times lower than those proposed by Nelson (1988). The annual OC and BSi production values used by Nelson (1988) were extrapolated for the whole Bransfield Strait from local measurements compiled from the literature. His annual budgets are about one half of those calculated in the present work from local measurements. The difference in annual primary production budgets is leading to differences in preservation efficiency percentages. This difference demonstrates in part the large interannual primary production variability of the region. In consequence, it is necessary the use of local measurements in order to elaborate accurate local budgets. The preservation efficiency percentages for both the OC and the BSi are about two times larger in the Bransfield Strait than in the Gerlache Strait. The difference is because probably the values of primary productivity (5 g C m^{-2} d^{-1}) in the Gerlache Strait are overestimated for an annual budget and because the high organic matter preservation efficiencies at the Orleans Trough.

Considering the assumption of 60 productive days along the year, the annual primary production would be approximately 60 g m^{-2}. Thus, the preservation efficiency for the OC would be 11% for site A3, 4% for site A6, and, 10% B2. In the case of the BSi the primary production would be approximately 120 g m^{-2}. Then, preservation efficiency values would be 95% for site A3, 38% for site A6, and for site B2 the amount of BSi preserved in the bottom sediment would be higher than that produced above it. This means that the annual BSi production is understimated or there is an important BSi input from a different source at site B2. Since the rest of the calculated values for both the Gerlache and Bransfield Strait on the basis of 60 productive days did not showed this behaviour is possible to suggest that site B2 is receiving BSi from some other place

different than the euphotic layer above it. It is probable that the OC preservation efficiencies are not reflecting this kind of inputs because of its the relatively small percentages.

The eastern Gerlache Strait was the only region in the studied area where SAR and the percentage of primary produced OC (R^2=0.99) and BSi (R^2=0.97) finally buried in the bottom sediment were strongly related. It seems that high productivity environments in Gerlache Strait lead to high organic matter preservation efficiency percentages (Figs. 6.10a and 6.10b).

6.9.3. Bellingshausen Sea

According to Varela et al. (in press) the primary produced organic carbon over the studied area at the Bellingshausen Sea varied between 0.2 and 1 g C $m^{-2}d^{-1}$ during the 1995-96 spring-summer season. The seasonal mean value would be approximately 0.6 g C $m^{-2}d^{-1}$. Considering this as the average primary produced OC during the most productive season of 150 days per year, the annual mean value would be 90 g C $m^{-2}d^{-1}$. Thus, the annual budget of BSi produced by phytoplankton would be around 180 g $m^{-2}d^{-1}$. Therefore, the amount of primary produced OC and BSi finally kept in the sedimentary record might be 1.8 and 0.8% (cores B214 and B223, respectively) and 21 and 11% (cores B214 and B223 in the same order), respectively. If it is consider the value of 60 productive days to calculate the annual production the quantity of OC produced in one year over this area would be around 36 g m^{-2} and the preservation efficiency for OC would be 4% for site B214 and 2% for site B223. In the case of the BSi, the annual production in the euphotic layer would be 72 g m^{-2} and the preservation efficiency 53% for site B214 and 28% for site B223.

The eastern part of the Gerlache Strait is the portion of the study area where more OC is produced, settled, and buried.

The preservation efficiency results agree well with those found by DeMaster et al. (1991) in Antarctic sediment, except those values from the Bellingshausen Sea, where primary productivity rates are relatively low.

6.10. BURIAL PERCENTAGES WITHIN A GLOBAL CONTEXT

Estimates of the global oceanic OC production rate are about $2.7*10^{16}$ g y^{-1} (Eppley and Peterson, 1979). The seabed accumulation rate is approximately $0.02*10^{16}$ g C y^{-1} (Broecker and Peng, 1982; Romankevich, 1984). Therefore, about 0.7 % of the OC produced in the upper layers of the oceans is buried in the bottom sediments (DeMaster et al., 1992). This means that the portion of the Antarctic Peninsula studied in this work is able to keep in the sediment, at least, up to 3 times more primary produced OC when compared with the global oceanic burial rate. Focusing on the continental margins and specially comparing to other Antarctic highly productive regions the percentage of primary produced OC buried in the bottom sediment is similar to that of the Bransfield Strait -about 9%- (DeMaster, et al., 1991) and the Ross Sea

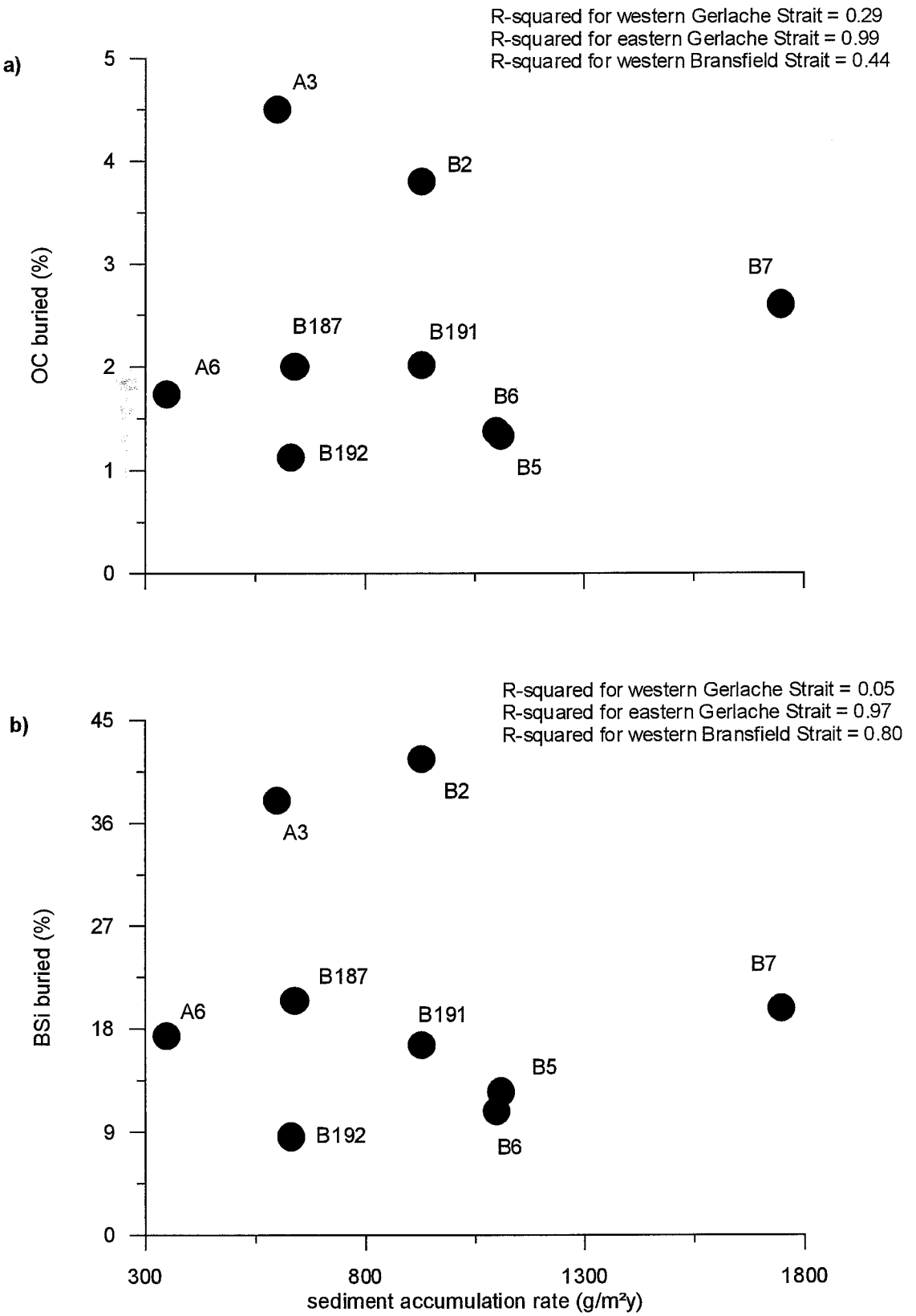

Fig. 6.10. Sediment accumulation rate (expressed in grams per square meter per year) versus a) percentage of primary produced organic carbon (OC) and b) biogenic silica (BSi) finally buried in the bottom sediment at both the Gerlache (B187, B191, B192, B5, B6, and B7) and Bransfield Straits (A3, A6, and B2).

-about 4.9%- (DeMaster et al., 1996). However, the amount of primary produced OC buried in the eastern Gerlache Strait sediment -between 3 and 19 g $m^{-2}y^{-1}$- is about twice the amount buried in the Bransfield Strait and the Ross Sea -between 3 and 8 g $m^{-2}y^{-1}$- (DeMaster, et al., 1991; Nelson et al., 1996). Thus, the bottom sediment in the Gerlache Strait is keeping a relatively high amount of OC and it can be considered as an important carbon sinking area within the Antarctic context. It is possible, as Karl et al. (1991) suggested that the Gerlache Strait is exporting particulate OC to the adjacent western Bransfield Strait, enhancing the OC accumulation rate of this latter area. Then, high primary productivity environments of the Southern Ocean, as the Gerlache Strait, could be acting as important OC exporting areas as well.

The approximate BSi production for the world oceans is $1.2*10^{16}$ g y^{-1} (Calvert, 1983; Brzezinsky, 1985) and the seabed accumulation rate is only $0.04*10^{16}$ g y^{-1} (DeMaster, 1981), which means that approximately 4% of the BSi produced in the euphotic layer is finally buried in the bottom sediments. Tréguer et al., (1995) reestimate this percentage in about 3%. The bottom sediment at Gerlache Strait and the western part of the Bransfield Strait is keeping, at least, between two and twenty times more BSi than the global mean. This burial efficiency agrees with those from other Antarctic regions as the Ross Sea (DeMaster et al., 1992; Nelson et al., 1996).

In the studied area at the Bellingshausen Sea the percentages are lower than the global budgets. In this area relatively low primary productivity and winnowing are generating organic matter-poor sediments. The opposite mechanism was observed in the rest of the study area where relatively high primary productivity and focusing promote organic matter-rich sediment. However, in both cases bottom sediment is reflecting the primary production activity in the euphotic layer above them.

7. MID-DEPTH AND NEAR-BOTTOM TOTAL MASS, CARBON, AND BIOGENIC SILICA FLUXES

7.1. SEDIMENT TRAP AT MID-DEPTH IN SITE A6

7.1.1. Collection efficiency

Sediment trap efficiency has been considered as well. Numerous studies have addressed the influence of hydrodynamic effects on trap collection biases (Butman et al., 1986, Gust et al. 1992, Gust et al., 1994), that would also explain the low amount of particles collected in the mid-depth trap. However, a field experiment by Gardner et al. (1997) using sediment traps with a geometry similar to that of PPS 3 showed no decrease in collection efficiency at mean velocities of 1-22 cm s^{-1}. In addition, another field experiment conducted by Heussner et al. (1999) with PPS 3 sediment traps also demonstrated the absence of relationship between total mass flux of particles and trap Reynolds number at mean speeds ranging from few cm s^{-1} to 12 cm s^{-1}. There are no current speed measurements available for the present work. Previous current meter data obtained at 400 m depth in the Bransfield Strait (López et al., 1994) showed that currents at mid-depths in summer were tidally dominated, with maximum values of about 25-30 cm s^{-1} and typical residual currents of 15 cm s^{-1}. Based on the results obtained by Gardner et al. (1997) and Heussner et al. (1999), little effect on collection efficiencies can be expected for this study. Although, due to the slightly higher current regime, the mid-depth fluxes could be affected by hydrodynamic biasses to some degree.

7.1.2. Total mass flux

The annual total mass flux at the study site during the experiment (3.89 g m^{-2}) (Table 5.3a) is one to two orders of magnitude lower than those recorded previously in the Central basin of the Bransfield Strait south of King George Island (Wefer et al., 1988; Wefer et al., 1990). At that site, annual fluxes at mid-depth (500 m deep) were about 120 g m^{-2} in 1984 and 11.9 g m^{-2} in 1985. This difference shows the high interannual variability of mid-depth fluxes in the Bransfield Strait. South of King George Island, mean total mass fluxes at mid-depth were 3 to 27 times higher than that at the study site (close to Livingston and Deception Islands). In addition, the highest fluxes (809-1901 mg m^{-2} d^{-1}) were one order of magnitude higher than in the present work (112 mg m^{-2} d^{-1}). In both areas, the maximum fluxes occurred in 3 or 4 sampling periods of the austral summer related to late November-December and/or December-January. On site A6 the total mass flux peaks occurred in three pulses, from late November to early February (which represented 98% of the total annual flux), separated by periods with fluxes about two orders of magnitude lower (Fig. 5.1). The lithogenic component was approximately 50% of the TMF (Table 5.1). South of King George Island the highest fluxes occurred mainly in one pulse of 30 days at the early summer. In both areas, the transfer of particles at mid-depth was mainly through fecal pellets, and the particulate matter that settled during the periods of maximum fluxes accounted for more than 95% of the annual budget. A similar event was found in the Gerlache Strait, at 100-m water depth, where the plankton bloom promoted a seasonal pulse in the downward flux of particulate organic matter Karl and Asper (1990).

In the present study the low downward particle flux at mid-depth should be related to the moderate primary production in the area (Burkholder and Sieburth, 1961; Mandelli and Burkholder, 1966; Hernández-León et al., 1999; Varela et al., in press), together with hydrologic controls. Bellingshausen Sea Antarctic Superficial Water (BSW) and the Circumpolar Deep Water (CDW) (Sievers, 1982; Capella et al., 1992) get into the Bransfield Strait over the Boyd Strait between Smith and Snow Islands and flow northeastward, surrounding Deception Island. These currents should be bathing the trap and preventing the downward particle flux to settle in it.

7.1.3. Major biogenic constituent fluxes

The mean OC content of the settled particles at mid-depth south of King George Island (3%) was lower than at site A6 (11%), but the mean BSi content (29-50%) was higher (21%) (Table 5.1). However, both the annual OC and BSi fluxes were up to one order of magnitude higher at south of King George Island than at site A6, due to the higher settling particle flux. Thus, in addition to the interannual variability, among different regions of the Bransfield Strait there are not only differences in the magnitude of the particle flux but also in its chemical composition. Phyto and zooplankton abundance and distribution, together with physical features should be involved in the development of these dissimilarities.

The peaks of total mass flux at mid-depth in late November, late December and early January were coupled to peaks of OC, BSi and fecal pellet fluxes (Fig. 5.1, 5.3, 5.8, and 5.10). During these periods, the settling particulate matter had the highest BSi content (>20%), the lowest OC content (about 8.5%), the lowest atomic OC/N (6.5-7.5) and fecal pellets peaks. This fact leads to conclude that most of the biogenic components during these high flux periods were diatom frustules and their debris. Thus, these flux peaks could be related to phytoplankton blooms. Based in other works, during these periods, swarms were probably feeding on phytoplankton blooms (Wefer et al., 1990) and most of the vertical OC flux from surface water could be attributed to krill fecal material (von Bodungen, 1986). During these events the organic particulate matter mainly settled through fecal pellets as is suggested by its high concentration (Fig 5.7b).

The biogenic silica flux, followed by the OC, was the main biogenic component of the TMF, like in other Bransfield Strait areas (Wefer et al., 1988).

During early February, there was a fecal pellets flux maximum at mid-depth with a high fecal pellet concentration (Fig. 5.7b) combined with a relatively medium OC content and relatively low BSi concentration and atomic OC/N values (Figs. 5.2a, 5.5b, and 5.7a). These characteristics might be related to a zooplankton bloom. Nevertheless, the BSi/OC weight ratio in this sample was similar to the local plankton, approximately 2, so a high phytoplankton content in the fecal pellets is reflected (Fig. 5.5c). During the winter, the mid-depth total mass fluxes were very low and showed the highest carbon content and the highest atomic OC/N values. These data indicate that degraded organic matter composed the major fraction of the downward flux during this period. This material was probably laterally transported from shallower areas as suspended matter with low settling velocity, thereby enhancing chemical decay and remineralization (Wefer et al., 1990). In addition, the fecal pellet flux measured during

winter was the lowest of the study period. Then, in wintertime, a major fraction of the captured organic matter was not packed.

The mean primary production measured by Varela et al. (in press) in the Western Bransfield Strait during the spring was about 1 g C m^{-2} d^{-1}. Thus, the highest OC fluxes at mid-depths (Fig. 5.3 and Table 5.2) varied between 0.22 and 0.98% of the mean primary production. If we consider the annual productivity around 150 g C m^{-2}, the annual OC flux at mid-depth (Table 5.3a) represented only 0.2% of the annual productivity, but on the basis of 60 productive days this fraction would be 0.6% (annual productivity around 60 g C m^{-2}). Regarding the BSi, the highest fluxes (which were coincident with OC peaks as well) ranged between 0.15 and 1.5% of the mean primary production (Fig. 5.8). These values were obtained assuming a BSi production of 2 g m^{-2} d^{-1} after considering the mean BSi/OC weight ratio of local phytoplankton equal to 2 (Jennings et al., 1984; Nelson and Smith, 1986). Hence, the annual BSi flux at mid depth (Table 5.3a) should represents about 0.3% of the annual production in the euphotic layer, estimated in 300 g BSi m^{-2}. Taking into account a productive period of 60 days the annual production would be 120 BSi g m^{-2} and the fraction trapped at mid depth approximately 0.7% of it. Therefore, more than 98% of the primary produced OC and BSi is consumed within the first 500 m of the water column in western Bransfield Strait. Both the OC and BSi are affected and fractionated to a degree that no decoupling between these phases could be stated. The atomic OC/N and BSi/OC weight ratios in the trapped material (Figs. 5.5b and 5.5c) are similar to the 6.685 atomic OC/N Redfield ratio (Redfield et al. 1963) and to the mean BSi/OC weight ratio for this area (between 1 and 3), respectively (Jennings et al., 1984; Nelson and Smith, 1986). Consequently, at this depth of the water column, the organic matter trapped is planktonic and it had undergo negligible loss of either organic or siliceous material as Nelson et al. (1996) found in the Ross Sea below 250-m water depth.

7.2. SEDIMENT TRAP NEAR THE BOTTOM AT SITE A6

7.2.1. Collection efficiency

Although there are no near-bottom current data available for this particular area of the Bransfield Strait, either in this experiment or in the scientific literature, there are some evidences indicating that bottom currents were not strong enough to induce significant biases in the collection efficiency of the bottom trap. The atomic OC/N ratio (7-9) and the mean ^{210}Pb activity (987 Bq kg^{-1}) (Masqué et al., in press) of the settling particulate matter collected near the bottom correspond to relatively fresh material and are similar to those of the surface sediment at the mooring site. Their OC and BSi contents are very similar as well (1.3% and 14.3, respectively) (Figs. 4.5 and 4.6 and Table 5.1). Thus, the trapped material and that which reaches the sea floor have the same nature. At Bransfield Strait, Dunbar et al. (1985) found that as depth increases the material in vertical transit becomes more similar in composition to that already settled. In addition, the particle fluxes measured near the bottom could be related to the present sediment accumulation rates. The mean SAR determined by ^{210}Pb analysis was 351 ± 14 g m^{-2} y^{-1} (Table 4.1) (Masqué et al., in press). This accumulation rate is one fourth of the annual flux measured by the near-bottom trap, 1254 g m^{-2} (Table 5.3a). Direct comparison between bottom sediment and trap data must be done with caution, because time scales differ by a factor of about 100 (from 1 year to 100 years). The

higher total mass flux of the near-bottom trap suggests that at least this trap did not underestimate downward particle fluxes. However, it is difficult to discern whether the near-bottom trap flux was inflated by hydrodynamic biases causing overtrapping. Based on the results obtained in field experiments by Gardner et al. (1997) and Heussner et al. (1999), little hydrodynamic effects on trap collection efficiency might be expected, unless high near-bottom currents operate in the deeper part of the basin at 1000 m depth. Taking into account the bottom topography, the grain size (less than 5% of sand content), and the high accumulation rates at the mooring site, bottom currents in the deep basin should not be high. Thus, negligible hydrodynamic effects on trap collection efficiency for the near-bottom trap were expected.

7.2.2 Total mass flux

In the Bransfield Strait, studies of near-bottom fluxes during annual cycles had never been conducted before. The near-bottom TMF was about one to four orders of magnitude higher than at mid-depth (Figs. 5.1a and 5.1b). The annual total mass flux increased from 500 m to 1000-m water depth (30 m above bottom) by a factor of 322 (Table 5.3a). These near-bottom TMF were about two times higher than that measured in the Ross Sea (50 mab at 700-m water depth on the continental shelf) by Dunbar et al. (1998) and similar to the results of a 22.5 days deployment at King George Basin (60 mab at 1890-m water depth) (Gersonde and Wefer, 1987). The large difference with the TMF measured in the mid-depth trap is due to the extremely low flux at that depth. On other latitudes, around 1000-m depth, similar near-bottom TMF were only found in submarine canyons (Puig and Palanques, 1998). It is probable that these near-bottom fluxes, relatively high and constant during most of the year, are maintained by the action of near-bottom currents that resuspend and/or transport sediment basinward. The site A6 is located at the end of a trough similar and parallel to the Orleans Canyon (Fig. 2.3). Thus, sediment supply through these channels and from the Livingston and Deception Islands margin could explain these results.

Results from the trap at Johnson's Dock verified that there is an important supply of fine material to the littoral zone. However, bottom sediment on most of the continental shelves around the study site consists of sand and gravels (Yoon et al., 1992) and the sand content in the surface sediment at site A6 was relatively little (Fig. 4.6). This indicates that most of the fine particulate matter is transferred offshore from the shelf. A near-bottom nepheloid layer extending from the Orleans canyon head to the traps site was observed through transmissometer profiles (Fig. 7.1). This confirms that there is a lateral transport of suspended particulate matter close to the bottom and that near-bottom fluxes are probably related to a downbasin transport, at least in part, through this canyon. Most of the suspended particulate matter transferred offshore along the Antarctic Peninsula shelf and slope close to the Orleans Canyon was probably collected and reoriented basinward, generating this bottom nepheloid layer and high total mass fluxes near the bottom. The differences in the lithogenic component content in the TMF between both traps at this site (Table 5.3a) show that a major fraction of the lithogenic material travels near the bottom. Thus, almost no lithogenic matter is collected at mid-depths.

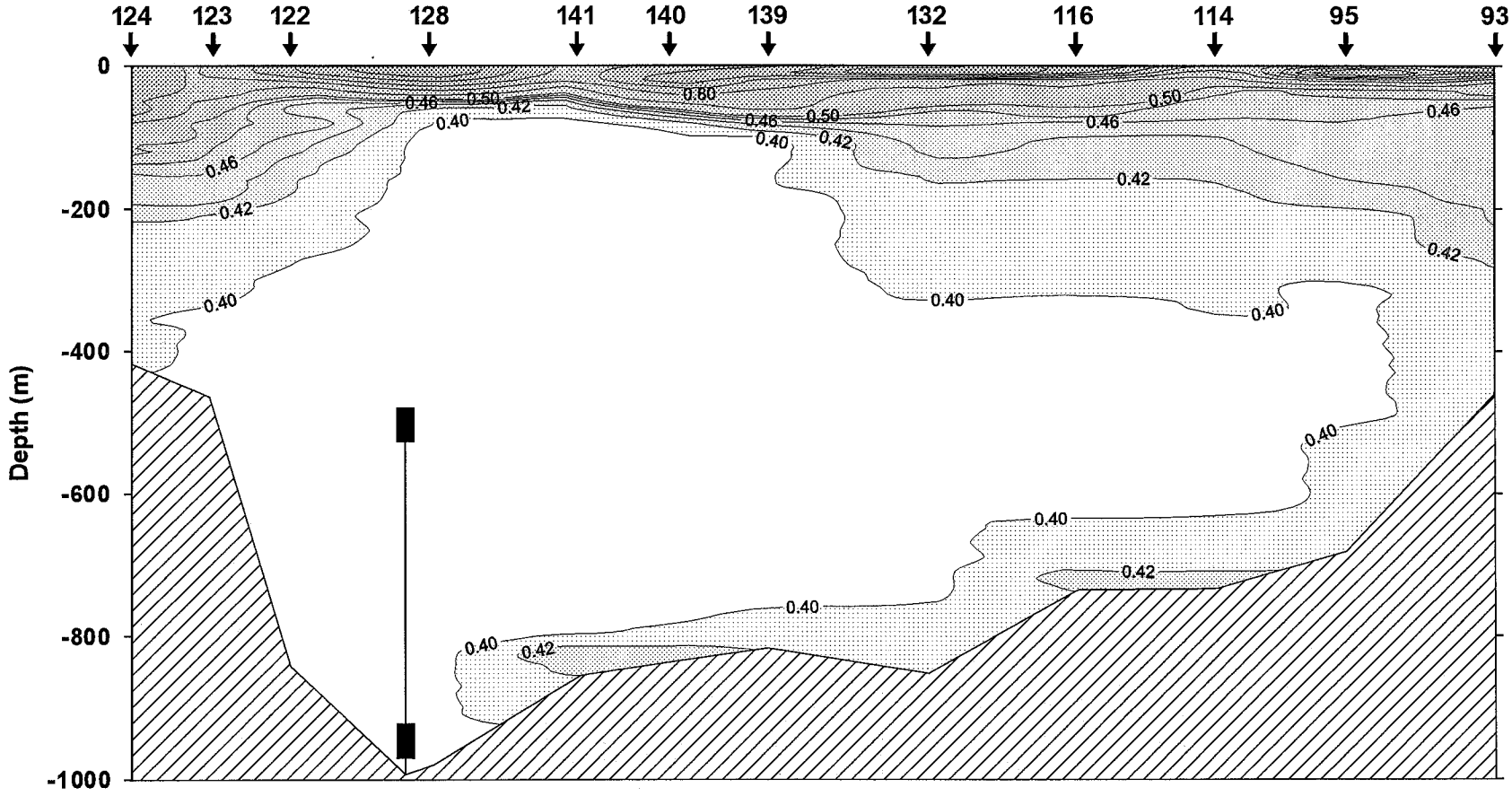

Fig. 7.1. Transect of beam attenuation coefficient across the western Bransfield Strait and along the Orleans Canyon (station positions are shown in Fig. 58). Note the presence of a wide bottom nepheloid layer developed along the Orleans Canyon towards the basin where the sediment traps (black rectangles) were deployed.

Swimmers and diatoms in the samples of the near-bottom trap also provided some indications of downbasin transport (Palanques et al., in press). Among the collected amphipod fauna, there were some species not common (*Orchomenella pinguides*), or never found in the water column (*Hirondella antarctica, Opisa sp.* and *Epimeriidae gen. sp.*). Similarly, benthic polychaete fauna like *Scalibregmatids*, which live buried in the sediment were found. Regarding the collected diatoms, the most significant species and genus were *Amphora, Cocconeis* (*C. fasciolata*), and *Grammatophora (G. angulosa*), which are also benthic. Other groups of common littoral species frequently trapped during the year were *Actinocyclus actinochilus, Navicula directa, N. glaciei, Thalasiosira antarctica and Fragiliariopsis kergelensis.*

Many of the species collected in the near-bottom trap are abundant in shallow bays of the South Shetland Islands (Ahn et al., 1997). Thus, the presence of these polychaetes, benthic amphipoda and diatoms in the near-bottom trap at 1000 m depth (approximately 30 mab) indicate that this fauna was resuspended in shallow environments and transported laterally basinward along with the non-living particles. The atomic OC/N ratio, 7.5-9.5 (Table 5.1) of near-bottom settling particles in the study area throughout the year could also be related to resuspension and lateral transport of benthic or recently settled planktonic organic matter. The relatively high near-bottom fluxes of major organic constituents along the year cannot be explained by vertical transit at the mooring site. Therefore, lateral transport from more productive zones is what better justifies these fluxes. The highest primary productivity areas close to the mooring site are located around Deception Island. In addition, the mooring site might be also receiving material exported from the high productive waters of the Gerlache Strait through to the canyons in the vicinities between them.

The maximum TMF was measured during the August-September period. At this time the near-bottom temperature in the central basin of the Bransfield Strait decreased from –0.8 to –1.55 º C (Canals, 1996). This temperature decrease probably corresponded to the sinking of cold dense water formed on the shelf, during the autumn and winter months. The downflow of dense bottom water could winnow the particles from shallow environments towards the deep basin (Domack et al., 1994). This mechanism could also flush out newly deposited unconsolidated sediment from the floor, causing a winter maximum of sediment transport, as it was suggested for the Barents Sea by Honjo (1990). This hypothesis is also supported by the fact that the deep water of the Bransfield basins must be formed by sinking of surface waters, because the advection of deep water into the strait basins is prevented by the presence of shallow sills (Gordon and Nowlin, 1978).

Resuspension in shallow Antarctic environments might be related to several processes, such as friction of icebergs against the seabed, formation of dense water (Domack et al., 1994), wind storms over ice free areas, and even internal waves. However, only these processes cannot explain high and constant near-bottom fluxes during the whole year and a permanent mechanism must be causing them. Time series of current data taken during the summer by López et al. (1994) showed that the local circulation in the Bransfield Strait is strongly influenced by tides and that surface (10-50 m water depth) maximum currents south of Deception Island were 30-40 cm s^{-1} toward the northeast. These maximum tidal currents are strong enough to resuspend continuously fine sediment and benthic organisms on the continental shelves of the study area. The

narrow continental shelves and the steep slopes of this area can favour the shelf-slope sediment transfer mechanism toward the Bransfield Strait basins.

7.2.3. Major biogenic constituent fluxes

The OC and N fluxes increased with depth up to 3 orders of magnitude during the winter and between one and three during the spring and summer (Figs. 37a and b). The annual OC and N fluxes were 52 and 42 times larger than at mid-depth, respectively (Table 5.3a). In the mid-depth trap BSi measurements were only available in four samples from spring and summer (Fig. 5.7a) due to the little amount of material captured during the rest of the study period. Differences between BSi fluxes at both depths varied between one and four orders of magnitude, being always higher near the bottom. The annual BSi flux increased with depth 218 times (Table 5.3a). In the Ross Sea, Leventer and Dunbar (1986) reported an increase of about 30 times between 100 and 600-m water depth. This increment was attributed to resuspension events and lateral transport in addition to dissolution processes (up to 80% of the diatom frustules within the first 220-m water depth) in the upper water column. Liebzeit and von Bodungen (1987) also found an increase in TMF with depth at the King George's Basin (central Bransfield Strait). They explained it as the admixture of resuspended lithogenic material. It is highly probable that at site A6, the significant increase in BSi flux could be due to both, lateral transport and resuspension events, enhanced by the neighbouring troughs. Apparently, dissolution has a little effect in the BSi captured at mid-depth because the 2.4 mean BSi/OC weight ratio (Fig. 5.5c) is similar to that of the local phytoplankton. Furthermore, the great difference between OC and BSi fluxes with depth (Table 5.3a) remarks the evident better preservation of BSi over OC in the water column of the Bransfield Strait. The annual OC and BSi fluxes captured near the bottom represented 12 and 67% of the production in the euphotic layer, respectively (on the basis of 150 productive days) (Table 5.3a). Comparing with the amount of OC and BSi that is finally buried in the bottom sediment at site A6 the trap values drop around 6 and 4 times, respectively (2 and 17%, in the same order). This fact represents the Antarctic tendency to preserve preferentially BSi to OC in the sediment (DeMaster et al., 1991) and showed that there are intense losses in organic matter and biogenic silica within the upper centimetres of the sea bottom. Emerson et al., (1985) found similar results in the deep Pacific Ocean regarding the OC.

In the autumn-winter period and near the bottom, relatively high TM, OC, BSi, and N fluxes were coupled to relatively low atomic OC/N and high weight BSi/OC ratios that coexisted with relatively low fluxes and high atomic OC/N ratios at mid-depth (Figs. 5.1, 5.3, 5.5, 5.6, and 5.8). This coexistence suggests that there was a major and dominant lateral input of particles with fresh benthic organic matter near the bottom during the autumn-winter season. This biogenic material was probably deposited in shallower areas the previous spring and summer season. In addition, the ^{210}Pb activity is relatively low when compared to spring-summer values (Fig. 5.7). FP fluxes were relatively high at both depths during spring and summer months. This reflects an increase in the supply of rapid sinking biogenic particulate matter from October to February.

After the August-September peak, the total mass flux decreased sharply in October. In this sampling period, ^{210}Pb, OC, and BSi content increased, whereas lithogenic content decreased (Figs. 5.1, 5.2, and 5.7). This could be caused by the lower particulate

matter availability after the previous winnowing of particles and unconsolidated sediment that might occurred during the sinking of cold dense water. This winnowing would have washed out most of the relatively old and remineralised particulate matter. Therefore, the material reaching the study site was relatively new and fresh from the beginning of the productive season.

In late November, total mass, BSi, and $CaCO_3$ fluxes increased together with slight increases in lithogenic content and the atomic OC/N and BSi/OC weight ratios and decreases in ^{210}Pb activity (Figs. 5.1, 5.4, 5.5, 5.7, and 5.8). These relations indicate that the November peak is produced by increases in lithogenic inputs, probably associated with ice melting and raises in biogenic components as a consequence of the spring bloom. During spring and summer, at mid-depth, both atomic OC/N and BSi/OC weight ratios decrease to lower values (in the former case even more than near the bottom). This trend was coupled near the bottom to an increase in atomic OC/N ratio and a decrease in the weight BSi/OC ratio. Both phenomema might reflect that the organic matter that arrives to the bottom trap contains fresh primary produced material that had undergo an evident decay in N content but little in BSi during its vertical transit. This fact is supported by the relatively high ^{210}Pb activity in the bottom samples at that time. Then, organic particles travelling through water column experienced little BSi dissolution and high N uptake.

During December and January, the lithogenics, TMF, OC, N, BSi, and FP fluxes near the bottom coupled to the ^{210}Pb content decreased (Figs. 5.1, 5.3, 5.6, 5.7, 5.9, and 5.10). However, at the same time in the mid-depth trap high fluxes and relatively low atomic OC/N and weight BSi/OC ratios were detected. In order to explain these differences the following process is suggested. During the warm months, the mechanisms that promote the bottom currents and consequently the resuspension of particles during the cold season (e. g. sinking of cold dense water) loss energy. Therefore, the high fluxes collected near the bottom decrease during the spring and summer months.

In late January and February, lithogenic and total mass flux decreased, whereas OC, BSi, ^{210}Pb, and calcium carbonate contents increased. Fecal pellets concentration and atomic OC/N and BSi/OC weight ratios showed the same trend. The rapid sink of fresh organic matter incorporated in fecal pellets could produce these peaks near the bottom. This could be the consequence of a zooplankton bloom.

At late December and early January calcium carbonate flux at both depths was almost the same. The $CaCO_3$ content at mid-depth was similar to that near the bottom and both were close to the content measured in the surface sediment at Johnson's Dock. This means that carbonate dissolution is more effective within the upper layer of the bottom sediment (Fig. 4.11) than in the water column (Fig. 5.2) and that the material reaching the bottom trap was recently resuspended.

7.3. SEDIMENT TRAP IN SITE BAE

7.3.1. Collection efficiency

Sediment trap collection efficiency has been discussed in detail in the site A6 section. However, it should be stated that current measurements in the area, done by the Base Antártica Española (BAE) crew, indicate that the maximum current speeds were about 8 cm s^{-1} and these magnitudes are not strong enough to produce hydrodynamic biases.

7.3.2. Total mass flux

Johnson's Dock is a shallow closed system that receives icebergs and water from the Johnson's glacier (Fig. 2.3). The interchange with the open sea is restricted and it takes place only by its narrow and shallow mouth. The settling total mass fluxes of this bay had the same order of magnitude than those measured in other Antarctic coastal environments (Cripps and Clarke, 1998). The TMF collected during the summer period was higher than 20,000 mg $m^{-2}d^{-1}$ with a very high lithogenic component (94-97.5%) (Table 5.4) and showed an inverse relation to the organic variables content (Figs. 5.12, 5.13 and 5.14). The TMF increased by a factor of 2 during mid-December and mid-February and by a factor of 3-4 in early and late January (Fig. 5.12). Those TMF increments were linked to increases of the lithogenic content and to decreases of OC, N and BSi contents. The increase in both lithogenics and TMF should be related to ice melting. However, the fluxes of the organic components increased with the TMF, suggesting that the increase in the lithogenic content caused the decrease in the organic components content.

Lithogenic inputs come mainly from erosive action and melting of the glaciers, since there are not any river system in the area. The clasts coarser than 1 mm must have been transported by icebergs and settled into the trap during the ice melting. The clast flux showed an increasing trend with time, indicating that ice-melting development was accentuated during summer, but this flux was not directly related to the TMF trends. This is because the flux of fine lithogenic component is more than 5 times higher than that of >1mm-lithogenic clasts, so the former flux is dominant and it masks the latter (Figs. 5.13d and 5.14c). The fine lithogenic material has a different dynamics to coarse lithogenic material, because fine particles can remain suspended in the water column along density gradients (Domack et al., 1994), and their sinking is controlled by other hydrographic processes.

7.3.3. Major biogenic constituent fluxes

Regarding the organic components (Figs. 5.13 and 5.14), their fluxes were similar or significantly higher than those measured in deeper regions of the Bransfield Strait (DeMaster et al., 1987; Wefer et al., 1988; Karl et al., 1991; Palanques et al., in press). However, their relative contents were much lower than those from offshore. This is not because there were low organic inputs, but because they were diluted by the high lithogenic inputs of this bay.

The chlorophyll-a in the surface water is related to primary productivity and to biogenic component inputs. The temporal evolution of chlorophyll-a in the bay did not show a direct relation to the content and fluxes of organic components and fecal pellets during the study period (Isla et al., 2001). The apparent lack of connection between chlorophyll-a curve and the organic matter fluxes collected by the trap is due to the fact that the water sampling was performed once per day at the South Bay and not on the point above the trap. However, the peaks of chlorophyll-a in mid-January and late February corresponded to increases in organic carbon content. Both, chlorophyll-a peaks coincided with low atomic OC/N ratio values, suggesting that the settling organic matter was fresher during these periods of time (Isla et al., 2001). The peak value of fecal pellets indicates that a bloom of zooplankton could have happened in early January before the-mid January chlorophyll-a peak. The February peak could have some relation to the biomass bloom that tends to happen in the open water of the Bransfield Strait during this month (Holm-Hansen and Mitchell, 1991).

The higher atomic OC/N values corresponded to the samples from the periods with the highest lithogenic fluxes (Fig. 5.13d and 5.15a). Probably, an increase in nitrogen remineralisation processes is related to these fluxes and/or they bore an evident fraction with already remineralised organic matter because IC input during this time was very low (Fig. 5.15b).

Settling OC was dominant over IC and ranged from 77 to 100% of the total carbon. Organic carbon and calcium carbonate content in the surface sediment of the study site showed similar values to those of the settling particles (Fig. 4.11b and Table 5.4). This means that the particles in this shallow system reach the sediment without being significantly altered. The residence time of the particles in shallow environments is probably too short to allow the transformations that happen in Antarctic deeper environments, where carbonate in sediments is lower than in the settling particulate matter (see PART III in the present study)(Palanques et al., in press). At Johnson's Dock, the carbonate content in the sediment column decrease with depth indicating that dissolution is gradual from the surface to about 8-cm depth, where the $CaCO_3$ content was approximately null (Fig. 4.11a). This indicates that in Antarctic shallow coastal environments the shells of carbonated organisms settle and accumulate in the bottom sediment where they are dissolved after buried. Atomic OC/N ratio of the surface sediment (the first cm) is similar to that of the material collected in the trap so it is possible to suggest that settled and trapped material is the same (Fig. 4.11b and Table 5.4). Atomic OC/N ratio increases with depth indicating higher N uptake relative to OC (Fig. 4.11b).

The results obtained in this deployment revealed that even though there are no large river systems in the Bransfield Strait, high sediment fluxes occurred in the shallow environments mainly due to sediment supplies from the action of ice. The lithogenic fine sediment fraction is the dominant contributor to these fluxes, but it is important to note that the input of coarse clasts from iceberg melting is also very relevant in the study area. However, not only the processes associated with the ice melting seem to control the temporal variability of the settling fluxes of particles, and hydrodynamic processes should be studied in these shallow environments to understand the mechanisms that control their particle fluxes.

PART V. SUMMARY AND CONCLUSIONS

8. SUMMARY OF THE MAIN FINDINGS

8.1. MAJOR BIOGENIC CONSTITUENTS IN THE BOTTOM SEDIMENT

The OC, $CaCO_3$, N, and BSi concentrations and accumulation rates in the bottom sediment of the Gerlache and western Bransfield Straits and the Bellingshausen Sea are in accordance with the ranges of other Antarctic areas.

Within the study area the finer sediment and the material with the highest OC, N, and BSi content corresponded to the end of the Orleans trough, western Bransfield Strait (core A3), and to the Gerlache Strait (cores B187, B5, B6, and B7). The sediments with the lowest OC, N, and BSi content values and with the highest sand percentage were taken at Bellingshausen Sea (cores B214 and B223) (Figs. 6.1, 6.2, and 6.3). There was no evident correlation between organic matter content within the SML (recently deposited material) and water depth (Fig. 6.4).

An important part of the biogenic particulate matter, exported from the euphotic layer of the central and eastern Gerlache Strait, should be settling vertically rather than horizontally and is kept within the strait. This is confirmed by the opposite distribution of the organic matter concentration to the main circulation pattern. The current flows toward the east (Niiler et al., 1990), and the biogenic variable contents decrease in the same direction (Figs. 6.1, 6.2, and 6.3). In this part of the Southern Ocean the primary productivity signal is transferred to the sea bottom by settling particles yielding a good coupling between the surface and the deep ocean.

Within the study area two main processes could be leading to the production of relatively high organic matter concentration in the bottom sediment. The rapid settling of the organic matter in high primary productivity environments (Gerlache Strait) and the focusing of biogenic particles produced away from the final deposition area due to circulation and bottom topographic controls (central Bransfield Strait).

It is possible to suggest that in the Gerlache Strait the rapid settling of particulate matter has major influence on bottom sediment composition than the local water currents. In the Bransfield Strait the inverse situation was observed and focusing is acting as an important agent in the developing of organic matter rich sediment in the deep basins and troughs.

The low organic matter concentration and the high sand content in the Bellingshausen Sea samples might be the effect of two main facts. The low plankton biomass and primary productivity rates (Mandelli and Burkholder, 1966; Hernández-León et al., 1999) and the winnowing of fine particulate organic matter by both the Bellingshausen Sea Antarctic Superficial Water and the Circumpolar Deep Water (Sievers, 1982; Capella, et al., 1992).

Reports on Bransfield and Gerlache Straits sediment showed that $CaCO_3$ content is very low or undetectable and it has no relation to any other variable (Warnke et al., 1972; Harden et al., 1992; Yoon et al., 1994). Results in the present work agree with previous research but contrary to Yoon et al. (1994) the highest carbonate concentration was found toward the bottom of the cores. Hulth et al., (1997) found the similar trend in southern Weddell Sea sediment and they attributed it to a greater

inorganic carbon deposition in the past. It is possible to suggest that in the Bransfield and Gerlache Straits similar events could happen.

8.2. ATOMIC OC/N AND BSI/OC WEIGHT RATIOS

The atomic OC/N ratio along every core was quite constant (variation coefficients always less than 0.2). Average values (7.61-11.63) were higher than the 6.625 Redfield atomic ratio for marine plankton (Redfield et al. 1963) but within the same range for sea bed sediment in the Ross Sea (DeMaster et al., 1996). It is possible to assume that the settling organic matter is mainly planktonic. Thus, the difference between the atomic OC/N ratios in the sediment and the Redfield ratio in marine plankton suggest that, the biological and chemical processes in the water column and in the bottom sediment remove preferentially nitrogen relative to organic carbon.

The BSi/OC weight ratio values (10.47 and 41.59) agreed with results obtained in the Ross Sea (DeMaster et al., 1992; DeMaster et al., 1996) and the Bransfield Strait (DeMaster et al., 1991). The common decreasing trend towards the bottom of the cores evidenced the decoupling between BSi and OC within the sediments (Figs. 4.2, 4.6, 4.10, 4.13, 4.15, 4.17, 4.19, 4.21, 4.23, 4.25, and 4.27). Regarding the decay of organic matter is possible to state that in the studied area the OC and the N are decoupled within the sediment but in an evident minor degree than the BSi and the OC.

8.3. ^{210}PB BASED APPARENT SEDIMENT ACCUMULATION RATES

8.3.1. Gerlache Strait

The high OC and BSi accumulation rates in the central part of the Gerlache Strait (core B7) (Table 4.1) is due to the correspondence with the highly productive waters of this area. Thus, in this part of the strait accumulation rates give additional evidence of the linkage through settling particle matter between the surface waters and the sea-bottom. The high variability between local conditions (both in hydrographic and biological controls) prevents to establish a clear relation between SAR and water depth in the Gerlache Strait.

8.3.2. Bransfield Strait

In both, central and western Bransfield Strait basins, focusing due to water circulation and bottom topography is contributing to enlarge the apparent sediment accumulation rates in the deep basins and is also the cause of SAR differences between different areas. The deep basins of the studied area are acting as sediment traps.

8.3.3. Bellingshausen Sea

The apparent SAR at the Bellingshausen Sea area was relatively low at 1180-m water depth due to the winnowing by both the Bellingshausen Sea Antarctic Superficial Water and the Circumpolar Deep Water. This phenomenon is preventing the fine particles to

settle at that point. The sampled site over the continental shelf (192 m water depth) had a relatively medium apparent SAR value. This fact might be due to the contribution of coarse material supplied by the iceberg melting that due to the currents is not allow to travel basin ward outside the Strait and it is not transported between Smith and Snow Islands either.

8.4. MAJOR BIOGENIC CONSTITUENTS APPARENT MEAN ACCUMULATION RATES AND BURIAL EFFICIENCIES

The OC, BSi, and N apparent mean accumulation rates trend was similar than that of SAR (Table 4.1). The $CaCO_3$ mean accumulation rate and SAR were not in accordance due to its little concentration along the cores.

However, biogenic constituents burial efficiency was not clearly related to sediment (expressed as mm y^{-1} or g $m^{-2}y^{-1}$) or biogenic variables accumulation rates (Fig. 6.8) neither to any measured concentration in the sediment. The depth of the SML was not related to the burial efficiency either. It seems that in Gerlache and western Bransfield Straits the high oceanographic and bathymetric variability within small areas is leading to differences in the biogeochemical processes affecting the settling particulate matter. The best-preserved biogenic constituent in the sediment of the studied area was the BSi (Table 4.1). Organic matter preservation processes remain unclear in this area in accordance to Hedges and Keil (1995) results in other marine environments. Nevertheless, is possible to suggest that biogenic material uptake from the sediments depends largely on local and particular environmental characteristics rather than in one main parameter. The highest OC, N, and BSi preservation efficiency was measured at the Orleans trough followed by the Gerlache Strait. Although the Orleans trough did not have the highest biogenic matter concentrations and the highest accumulation rates, it is acting as an efficient organic matter final deposit. The preferential remineralisation order of the organic matter within the sediment of the studied area was N, OC, and BSi.

8.5. PRESERVATION EFFICIENCIES AND PRIMARY PRODUCTIVITY

8.5.1. Gerlache Strait

In the eastern Gerlache Strait (stations B7, B6, and B5) approximately between 1.3 and 2.5% (approx. mean 2%) of the primary produced OC remains below the SML. In the western part of the Gerlache Strait (stations B187, B191, and B192) the percentage of the primary produced OC kept in the sedimentary record ranges between 1.2 and 2.1%. Thus, about 1.5% of the OC produced in the euphotic layer of the western Gerlache is finally buried in the same area. The percentage of the primary produced BSi preserved within the sediment would be around 9 and 22% in the western part of the strait. In the eastern side the fraction of primary produced BSi that finally remains in the bottom sediment would range between 11 and 19%. Considering an annual productive period of 60 days the OC preservation efficiency would vary between 3 and 5% and between 3 and 6% in the western and eastern parts, respectively. Regarding the BSi this values would vary between 22 and 54% in the western part and between 27 and 48% in the eastern section.

8.5.2. Western Bransfield Strait

The percentage of the primary produced OC buried in sites A3, A6, and B2 would be 5, 2, and 4, respectively. BSi burial values would be 37.9, 17.29, and 41.55% in the same order.

The burial budgets for both straits should be considered as minimum values because a high annual primary productive season was considered (150 days per year). The necessity to use local primary productivity measurements in order to elaborate accurate local burial budgets is remarked. On the basis of a 60 days annual productive period the OC values would be 11, 4, and 10% for sites A3, A6, and B2, respectively. In the case of BSi preservation efficiency would be 95% in site A3, 38% in site A6, and in site B2 the amount of BSi would be higher than that produced. The possibility of inputs from a different areas is considered.

8.5.3. Bellingshausen Sea

The amount of primary produced OC and BSi finally kept in the sedimentary record might be approximately 1.8-0.8% (cores B214 and B223, respectively) and 21-11% (cores B214 and B223, in the same order), respectively. A 60 days annual productive period would change these values to 4 and 2% for OC and 53 and 28% for BSi in sites B214 and B223, respectively. Relatively low primary productivity and current circulation pattern prevent the area to preserve organic matter within the bottom sediment.

The eastern Gerlache Strait was the only region in the studied area where SAR and the buried OC (R^2=0.99) and BSi (R^2=0.97) were strongly related. It seems that high productivity environments in Gerlache Strait lead to high organic matter burial percentages. The eastern part of the Gerlache Strait is the portion of the study area where more OC is produced, settled, and buried.

In the studied area the OC burial efficiency varied between 71 and 92% and between 83 and 99% of the BSi that reach the sea bottom is finally buried (Table 4.1).

8.6. BURIAL PERCENTAGES WITHIN A GLOBAL CONTEXT

The portion of the Antarctic Peninsula studied in this work is able to keep in the sediment, at least, up to 3 times more primary produced OC when compared with the global oceanic burial rate (0.7%). Within the Antarctic Ocean their role is only comparable to the highly productive Ross Sea (DeMaster, et al., 1992). However, the area could be considered as continental margin and in this areas this preservation efficiencies are similar.

It is possible that the Gerlache Strait is exporting particulate organic matter to the Bransfield Strait. Thus, high primary productivity environments of the Southern Ocean, as the Gerlache Strait, could be acting as important OC exporting and sinking areas.

The bottom sediment at Gerlache Strait and the western part of the Bransfield Strait is keeping, at least, between two and twenty times more BSi than the global mean

(around 3-4%). The budgets reported in the present work represent minimum values and this should be bare in mind.

In the studied area at the Bellingshausen Sea the percentages are lower that the global budgets. In this area relatively low primary productivity and winnowing are generating organic matter-poor sediments. The opposite mechanism was observed in the rest of the area of study where relatively high primary productivity and focusing promote organic matter-rich sediment. Nevertheless, in both cases bottom sediment is reflecting the primary production activity in the euphotic layer above them.

8.7. MID-DEPTH TOTAL MASS FLUX IN THE WESTERN BRANSFIELD STRAIT

The annual total mass fluxes at the study site during the experiment (3.89 g m^{-2}) (Table 5.3a) is one to two orders of magnitude lower than those recorded previously in the Central Basin of the Bransfield Strait south of King George Island (Wefer et al., 1988; 1990). 98% of the annual flux was measured during three pulses from late November to early February. The lithogenic component was approximately 50% of the TMF (Table 5.1). In the present work the low downward particle flux at mid-depth was related to the moderate primary production in the area (Burkholder and Sieburth, 1961; Mandelli and Burkholder, 1966; Hernández-León et al., 1999; Varela et al., in press), together with hydrologic controls.

8.8. MID-DEPTH MAJOR BIOGENIC CONSTITUENT FLUXES IN THE WESTERN BRANSFIELD STRAIT

Among different regions of the Bransfield Strait, there are not only variations in the magnitude of the particle flux but also in its chemical composition. The peaks of total mass flux at mid-depth in late November, late December and early January were coupled to peaks of OC, BSi, and fecal pellet fluxes (Figs. 5.1, 5.3, 5.8, and 5.10), they could be related to phytoplankton blooms. During these events the particulate matter mainly settled as single particles and aggregates, as is suggested by the lower fecal pellet concentration (Fig. 5.7b).

The biogenic silica flux, followed by the OC, were the main biogenic component of the TMF, like in other Bransfield Strait areas (Wefer et al., 1988). During early February the annual fecal pellets flux maximum at mid-depth was associated to a zooplankton bloom. During the winter, the highest carbon content and the highest atomic OC/N values indicate that degraded, not packed, organic matter composed the major fraction of the downward flux during this period. This material was probably laterally transported from shallower areas as suspended matter with low settling velocity, thereby enhancing chemical decay and remineralization (Wefer et al., 1990). During the spring, the highest OC fluxes at mid-depths (Fig. 5.3 and Table 5.2) varied between 0.22 and 0.98% of the mean primary production. The annual OC flux at mid-depth represented only 0.23% of the annual productivity (around 150 g C m^{-2}) but on the basis of 60 productive days this fraction would be 0.57%. The highest BSi fluxes (which were coincident with OC peaks as well), ranged between 0.15 and 1.5% of the mean primary production (Fig. 5.8). The annual BSi flux at mid depth represented 0.3% of the annual production in the euphotic layer, estimated in 300 g m^{-2}. Taking into account a productive period of 60 days the

annual production would be 120 BSi g m^{-2} and the fraction trapped at mid depth approximately 0.7% of it. Therefore, more than 98% of the primary produced OC and BSi is consumed within the first 500-m of the water column in western Bransfield Strait. Both the OC and BSi are affected and fractionated to a degree that no decoupling between these phases could be stated. At this depth of the water column, the trapped organic matter is planktonic and it had suffered negligible loss of either organic or siliceous material.

8.9. NEAR-BOTTOM TOTAL MASS FLUX IN THE WESTERN BRANSFIELD STRAIT

The near-bottom TMF was about one to four orders of magnitude higher than at mid-depth (Figs. 5.1a and 5.1b) with a lithogenic content of approximately 80% (Table 5.1). The annual total mass flux increased from 500 m to 1000-m water depth (30 m above bottom) by a factor of 322 (Table 5.3a). The large difference with the TMF measured in the mid-depth trap is because this latter is extremely low. As it is verified by the results of the trap at Johnson´s Dock fine particulate matter is supplied from glaciers. Most of this material is transferred offshore. Transmissometer profiles (Fig. 7.1) and the differences in the lithogenic components content in the TMF between the three traps (Tables 5.1 and 5.4) evidenced that suspended particulate matter is transported laterally close to the bottom. These near-bottom fluxes are probably related to a downbasin transport, at least in part, through submarine troughs. Suspended particulate matter transferred offshore along the Antarctic Peninsula shelf and slope close to the Orleans Canyon was probably collected and reoriented basinward, generating a bottom nepheloid layer and high total mass fluxes near the bottom. Analysed swimmers and diatoms in the samples of the near-bottom trap also provided some indications of downbasin transport. This lateral transport from more productive zones is what better justifies the relatively high near-bottom fluxes of major organic constituents along the year.

8.10. MAJOR BIOGENIC CONSTITUENT FLUXES NEAR THE BOTTOM IN THE WESTERN BRANSFIELD STRAIT

The OC and N fluxes increased with depth up to 3 orders of magnitude during the winter and between one and three during the spring and summer (Figs. 5.3 and 5.6). The annual OC and N fluxes were 52 and 42 times larger than at mid-depth, respectively. The annual BSi flux increased 218 times with depth (Table 5.3a). It is highly probable that at site A6, the significant increase in BSi flux could be due to both, lateral transport and resuspension events, enhanced by the neighbouring troughs. Apparently, dissolution has a little effect in the BSi captured at mid-depth because the 2.4 mean BSi/OC weight ratio (Fig. 5.5c) is similar to that of the local phytoplankton. Furthermore, the great difference between OC and BSi fluxes with depth (Table 5.3a) remarks the evident better preservation of BSi over OC in the water column of the Bransfield Strait. The annual OC and BSi fluxes captured near the bottom represent 12 and 67% of the production in the euphotic layer, respectively. Comparing with the amount of OC and BSi that is finally buried in the bottom sediment at site A6 the trap values drop around 7 and 4 times, respectively. This fact represents the Antarctic tendency to preserve preferentially BSi to OC in the sediment (DeMaster et al., 1991)

and showed that there are intense losses in organic matter and biogenic silica within the upper centimetres of the sea bed.

There was a major and dominant lateral input of particles with fresh benthic organic matter near the bottom during the autumn-winter period. This biogenic material was probably deposited in shallower areas the previous spring and summer seasons. From October to February FP fluxes were high at both depths. This reflects an increase in the supply of rapid sinking biogenic particulate matter. During spring and summer, the bottom trap contains fresh primary produced material that had undergo an evident decay in N content but little in BSi during its vertical transit. This fact is supported by the relatively high ^{210}Pb activity in the bottom samples at that time. Then, organic particles travelling through water column experienced little BSi dissolution and high N uptake. During the autumn and the winter, the mechanisms that promote the bottom currents (e. g. sinking of cold dense water) and consequently the resuspension of particles loss energy at the beginning of the productive season. Therefore, slightly lower fluxes were collected near the bottom during spring and summer.

In late January and February, the lithogenic and total mass flux decreased, whereas OC, BSi, ^{210}Pb and calcium carbonate contents increased. The fecal pellets concentration and the atomic OC/N and BSi/OC weight ratios showed the same trend. The rapid sink of fresh organic matter incorporated in fecal pellets could produce these peaks near the bottom. This could be the consequence of a zooplankton bloom.

At late December and early January calcium carbonate flux at both depths was almost the same. The $CaCO_3$ content at mid-depth was similar to that near the bottom and both were close to the content measured in the surface sediment at Johnson's Dock. This means that carbonate dissolution is more effective within the upper layer of the bottom sediment (Fig. 4.11) than in the water column (Fig. 5.2) and that the material reaching the bottom trap was recently resuspended.

8.11. TOTAL MASS FLUX IN JOHNSON'S DOCK

The settling total mass fluxes of this bay had the same order of magnitude than those measured in other Antarctic coastal environments (Cripps and Clarke, 1998). The TMF collected during the summer period was higher than 20,000 mg $m^{-2}d^{-1}$ with a very high lithogenic component (94-97.5%) (Table 5.4). Those TMF increments were linked to increases of the lithogenic content and to decreases of OC, N, and BSi contents. The increase in both lithogenics and TMF should be related to ice melting. However, the fluxes of the organic components increased with the TMF, suggesting that the increase in the lithogenic content caused the decrease in the organic components content.

The clast flux showed an increasing trend with time, indicating that ice melting increased during summer, but this flux was not directly related to the TMF trends. The flux of the fine lithogenic component was more than 5 times higher than that of >1mm-lithogenic clasts. The fine lithogenic material has a different dynamics to coarse lithogenic material.

8.12. MAJOR BIOGENIC CONSTITUENT FLUXES IN JOHNSON'S DOCK

OC, N, and BSi fluxes (Figs. 5.13 and 5.14) were similar or significantly higher than those measured in deeper regions of the Bransfield Strait (DeMaster et al. 1987; Wefer et al. 1988; Karl et al. 1991; Palanques et al., in press). However, the relative organic matter contents were much lower than those from offshore because the former were diluted by the high lithogenic inputs of this bay. Due to the sampling strategy the temporal evolution of chlorophyll-a in the bay did not show a direct relation to the content and fluxes of organic components and fecal pellets during the study period (Isla et al., 2001). However, the peaks of chlorophyll-a occurring in mid-January and late February corresponded to increases in organic carbon content. The peak value of fecal pellets indicates that a bloom of zooplankton could have happened in early January before the-mid January chlorophyll-a peak.

The higher atomic OC/N values corresponded to the samples from the periods with the highest lithogenic fluxes (Figs. 5.13d and 5.15a). Probably, an increase in nitrogen remineralisation processes is related to these fluxes and/or they bore an evident fraction with already remineralised organic matter because IC input during this time was very low (Fig. 5.15b).

Settling OC was dominant over IC and ranged from 77 to 100% of the total carbon. Organic carbon and calcium carbonate content in the surface sediment of the study site showed similar values to those of the settling particles (Fig. 4.11a and Table 5.4). This means that the particles in this shallow system reach the sediment without being significantly altered. At Johnson's Dock, the carbonate content in the sediment column decreased with depth indicating that dissolution is gradual from the surface to about 8-cm depth, where the $CaCO_3$ content was approximately null (Fig. 4.11a). In Antarctic shallow coastal environments the shells of carbonated organisms settle and accumulate in the bottom sediment where they are dissolved after buried.

The high sediment fluxes in these kind of shallow environments are mainly due to sediment supplies from the action of ice. The lithogenic fine sediment fraction is the dominant contributor to these fluxes.

8.13. CARBON AND BIOGENIC SILICA BUDGET

On the basis of a 60 productive days along the year the Figure 8.1 shows the organic carbon and biogenic silica fluxes for mooring site A6 and a compilation for the Gerlache Strait. This is an approach to the biogenic silica and organic carbon budgets in the water column and the bottom sediment. The decoupling between both biogenic variables is evident from the fluxes decrease and the BSi/OC weight ratio increase from the euphotic layer to the sediment. At site A6 in the first 500 m of the water column, dissolution and uptake remove more than 99% of the BSi and OC surface production. In this layer there is not an evident separation between both fluxes. 30 meters above the bottom (mab) both fluxes increase due to an evident lateral input of particles with little OC content and a very important BSi component. This is resuspended material from shallower environments that present a similar BSi/OC weight ratio than that of the bottom sediment. In the case of the BSi flux this lateral input is more obvious. At both Gerlache and western Bransfield Straits decoupling

between BSi and OC is accentuated within the sediment where preservation of BSi is higher relative to the OC. At both Straits the percentage of primary produced BSi and OC buried in the bottom sediment is about 40 and 5%, respectively.

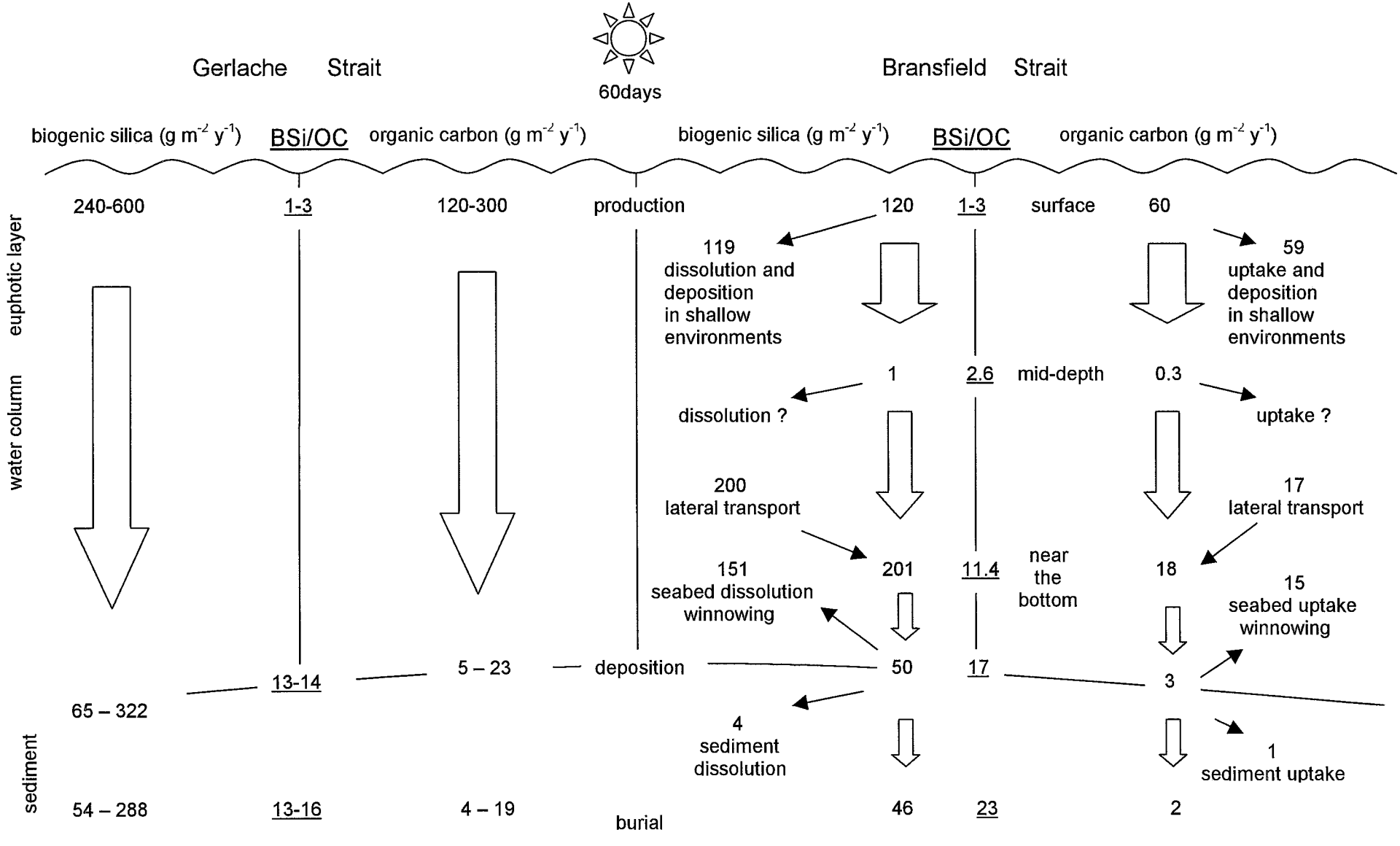

Fig. 8.1. Summary of organic carbon and biogenic silica fluxes at Gerlache and Bransfield Straits (mooring site A6) on the basis of a 60 productive days period per year. All numbers represent grams per square meter per year. Biogenic silica to organic carbon weight ratio (BSi/OC) values are underlined.

9. CONCLUSIONS OF THE STUDY

- The bottom sediment at eastern Gerlache Strait has relatively high organic matter content yielding a good connection between the surface primary production and the deep sea through the high amount of rapid sinking biogenic particulate matter. Vertical transport is generating relatively rich organic matter sediments and high accumulation rates of biogenic constituents.
- The Orleans trough is acting as a sediment funnel that collects and transports biogenic matter from the Antarctic Peninsula and the Gerlache Strait due to focusing by currents and bottom topography. Lateral transport is generating relatively rich organic matter sediments and high accumulation rates.
- The Gerlache Strait is probably exporting particulate organic matter to the adjacent Bransfield Strait.
- The Bottom sediment in the Bellingshausen Sea at its vicinities with the Bransfield Strait has relatively little organic matter content due to both low primary productivity and winnowing by currents.
- The carbonate content in the bottom sediment of the study area is irregular and very low due to the high dissolution rate within the upper layers of the sediment and the water column.
- The preferential remineralisation order in the sediment of the studied area is nitrogen over organic carbon and this latter over biogenic silica.
- The biogenic silica is the best-preserved constituent of the organic matter in the bottom sediment of the studied area.
- The Orleans Trough has the highest organic carbon, nitrogen and biogenic silica burial efficiencies.
- The biogenic material loss from the bottom sediment depends largely on local and particular characteristics rather than in one main parameter.
- Approximately between 2 and 11% of the primary produced organic carbon is buried in the western part of the Bransfield Strait.
- Approximately between 15 and 95% of the primary produced biogenic silica is buried in the western part of the Bransfield Strait.
- Approximately between 1 and 5% of the primary produced organic carbon is buried in the western part of the Gerlache Strait.
- Approximately between 1 and 6% of the primary produced organic carbon is buried in the eastern part of the Gerlache Strait.
- Approximately, between 9 and 54% of the primary produced biogenic silica is preserved in the bottom sediment at the western part of the Gerlache Strait and between 11 and 48% in the eastern part.
- The eastern part of the Gerlache Strait is the portion of the study area where more organic carbon is produced, settled, and buried.
- The eastern part of the Gerlache Strait is the portion of the study area where more biogenic silica is produced and buried. The western Gerlache Strait is the portion of the studied area where more biogenic silica is settled.
- The sediment trap moored at Johnson's Dock (coastal environment) collected sediment supplied by ice.
- In coastal environments coarse and fine lithogenic particle fluxes are not coupled. The latter is more constant through the summer season because it remains suspended in the water column.

- The sediment trap moored at an Antarctic deep basin reflects the lateral transport of the sediment from shallower environments.
- At mid-depth in the water column 98% of the annual particle flux occurred in three pulses during 60 days of the austral spring and summer season.
- The low downward particle flux at mid-depth in the water column is related to moderate primary production together with hydrologic controls.
- During the austral spring and summer season the very little downward flux is related to plankton activity.
- During the austral autumn and winter season the very little downward flux is related to ice covering.
- The biogenic silica followed by the organic carbon is the main biogenic component of the organic matter flux.
- The annual organic carbon flux at mid-depth represents between 0.2 and 0.6% of the surface production.
- The annual biogenic silica flux at mid-depth represents between 0.3 and 0.7% of the surface production.
- The total mass flux near the bottom is one to four orders of magnitude higher than at mid-depth.
- In the Bransfield Strait most of the fine particulate matter is transferred laterally and near the bottom from shallow to deep environments.
- The lithogenic component in the total mass flux is higher in coastal environments than in the deep basins.
- The high near bottom total mass flux is maintained through the year by physical controls (e.g. the sinking of cold dense water) and reflect seasonal changes.
- The organic carbon and biogenic silica trapped near the bottom represent 12 and 67% of the primary production, respectively.
- Approximately 78 and 72% of the organic carbon and the biogenic silica, trapped 30 meters above the bottom do not settle in the sediment.

10. FUTURE RESEARCH

During the development of this study some ideas appeared as I realised that some information was missing. Some other emerged when the work was finished and new questions arose. From this point of view, it will be helpful to improve the knowledge in the downward particle flux dynamics and the organic carbon and biogenic silica cycles in the Gerlache and Bransfield Straits with the following suggestions:

- To complement the study of the water current regime with the measurements of the streams in the deep water column of both the Bransfield and Gerlache Straits.

- To study the development of resuspension events on the continental shelf environments to better understand the processes that might promote the flux of organic matter to the basins.

- To complement the study of carbon and silicon biogeochemical cycles with the analysis of the pore water in the upper layers of the bottom sediment.

- To study with more resolution the transport dynamics of resuspended material to the deep basins with the deployment of near-bottom sediment traps, transmisometers and current meters on the continental shelf and slope.

- To measure the magnitude of the organic matter exportation from the Gerlache to the Bransfield Strait with sediment traps and sediment cores along the Orleans Trough and the parallel canyon.

  To relate the sediment and organic matter downward fluxes and their dynamics to the benthic communities.

PART VI. REFERENCES

11. REFERENCES

Abelmann, A. and R. Gersonde, 1991. Biosiliceous particle flux in the Southern Ocean. Marine Chemistry, 35, 503-536.

Ahn I-Y., H. Chung, J-S. Kang, S-H. Kang, 1997. Diatom composition and biomass variability in nearshore waters of Maxwell Bay, Antarctica, during the 1992/1993 austral summer. Polar Biology, 17, 123-130.

Anadón Alvarez, R., 1996. Flujo de carbono en un área de elevada productividad: Cuenca Occidental del Estrecho de Bransfield y Estrecho de Gerlache, Antártida. Informe sobre las actividades científicas de España en la Antártida durante la campaña 1995-96. Comisión Interministerial de Ciencia y Tecnología. Juan Ramón Vericad y Javier Cacho, eds.

Anadón R. and M. Estrada, in press. The FRUELA cruises: a carbon flux study in productive areas in the Antarctic Peninsula (December 1995 – January 1996). Deep-Sea Research II.

Anderson J.B., D.D. Kurtz, E.W. Domack and K.M. Balshaw, 1980. Glacial and glacial marine sediments of the Antarctic continental shelf. Journal of Geology, 88, 399-414.

Asper, V. L., W. G. Deuser, G. A. Knauer and S. E. Lohrenz, 1992. Rapid coupling of sinking particle fluxes between surface and deep ocean waters. Nature, 357, 670-672.

Bárcena, M.A., E. Isla, A. Plaza, J.A. Flores, F.J. Sierro and A. Palanques, in press. Bioaccumulation record and its relation with paleoclimatic evolution in the Western Bransfield Strait. Deep-Sea Research II

Bárcena, M.A., R. Gersonde, S. Ledesma, J. Fabrès, A.M. Calafat, M. Canals, F.J. Sierro and J.A. Flores, 1998. Record of Holocene glacial oscillations in the Bransfield Basin as revealed by siliceous microfossil assemblages. Antarctic Science, 10, 3, 269-285.

Basterretxea, G. and J. Arístegui, 1999. Phytoplankton biomass and production during late austral spring (1991) and summer (1993) in the Bransfield Strait. Polar Biology, 21, 11-22.

Berdalet E., D. Vaqué, L. Arin, M. Estrada, M. Alcaraz and J.A. Fernández, 1997. Hydrography and biochemical indicators of microplankton biomass in the Bransfield Strait (Antarctica) during January 1994. Polar Biology, 17, 31-38.

Billett, D. S .M., R. S. Lampitt, A. L. Rice and R. F. C. Mantoura, 1983. Seasonal sedimentation of phytoplankton to the deep-sea benthos. Nature, 302, 520-522.

Biscaye P. E. and R. F. Anderson, 1994. Fluxes of particulate matter on the slope of the southern Middle Atlantic Bigth: SEEP-II. Deep-Sea Research II, 41, 459-509.

Bodungen, B. v, 1986. Phytoplankton growth and krill grazing during spring in the Bransfield Strait, Antarctica – Implications from sediment trap collections. Polar Biology, 6, 153-160.

Bodungen, B. v, V. S. Smetacek, M. M. Tilzer and B. Zeitzschel, 1986. Primary production and sedimentation during spring in the Antarctic Peninsula region. Deep-Sea Research, 33, 2, 177-194.

Broecker, W. S and T. H. Peng, 1982. Tracers in the sea. Columbia University Press, Palisades, NY, 687 pp.

Brzezinsky, M. A., 1985. The Si:C:N ratio of marine diatoms: interspecific variability and the effect of some environmental variables. Journal of Phycology, 21, 347-357.

Burkholder, P. R. and J. M. Sieburth, 1961. Phytoplankton and chlorophyll in the Gerlache and Bransfield Straits of Antarctica. Limnology and Oceanography, 6, 1, 45-52.

Butman, C. A., W. D. Grant and K. D. Stolzenbach, 1986. Predictions of sediment trap biases in turbulent flows: a theoretic analysis based on observations from the literature. Journal of Marine Research, 44, 601-644.

Calvert, S. E., 1983. Sedimentary geochemistry of silicon. In: Silicon geochemistry and biogeochemistry. S. R. Aston, ed., Academic Press, London, 143-186.

Canals, M., 1996. Detección de posibles fuentes hidrotermales submarinas en la cuenca de Bransfield (Antártida): Proyecto GEBRATERM. In: Informe sobre las acitividades científicas de España en la Antártida durante la Campaña 1995-1996. J. R. Vericad and J.Cacho, eds. Comisión Interministerial de Ciencia y Tecnología (CICYT). Madrid, pp. 85-88.

Canfield, D. E., 1994. Factors influencing organic carbon preservation in marine sediments. Chemical Geology, 114, 315-329.

Capella, J. E., R. M. Ross, L. B. Quetin and E. E. Hofmann, 1992. A note on thermal structure of the upper ocean in the Bransfield Strait-South Shetland Islands region. Deep-Sea Research, 39, 7-8, 1221-1229.

Clarke, A., 1988. Seasonality in the Antarctic marine environment. Comparative Biochemistry and Physiology, 90B, 3, 461-473.

Clowes A. J., 1934. Hydrology of the Bransfield Strait. Discovery Reports, 9, 1-64.

Cochlan, W. P., J. Martinez and O. Holm-Hansen, 1993. RACER: Primary production in Gerlache Strait, Antarctica, during austral winter. Antarctic Journal of United States, 28, 5, 172-174.

Cripps, G. C. and A. Clarke, 1998. Seasonal variation in the biochemical composition of the particulate material collected by sediment traps at Signy Island, Antarctica. Polar Biology, 20, 414-423.

DeMaster, D. J., 1981. The supply and accumulation of biogenic silica in the marine environment. Geochimica et Cosmochimica Acta, 45, 1715-1732.

DeMaster, D. J., T. M. Nelson, C. A. Nittrouer and S. L. Harden, 1987. Biogenic silica and organic carbon accumulation in modern Bransfield Strait sediments. Antarctic Journal of United States, 12, 5, 108-110.

DeMaster, D. J., T. M. Nelson, S. L. Harden and C. A. Nittrouer, 1991. The cycling and accumulation of biogenic silica and organic carbon in Antarctic deep-sea and continental margin environments. Marine Chemistry, 35, 489-502.

DeMaster, D. J., R. B. Dunbar, L. Gordon, A. Leventer, J. M. Morrison, D. M. Nelson, C. A. Nittrouer and W. O. Smith Jr., 1992. Cycling and accumulation of biogenic silica and organic matter in high-latitude environments: The Ross Sea. Oceanography, 5, 3, 146-153.

DeMaster, D. J., O. Ragueneau and C. A. Nittrouer, 1996. Preservation efficiencies and accumulation rates for biogenic silica and organic C, N and P in high-latitude sediments: The Ross Sea. Journal of Geophysical Research, 101, C8, 18501-18518.

Deuser, W. G., E. H. Ross and R. F. Anderson, 1981. Seasonality in the supply of sediment to the deep Sargasso Sea and implications for the rapid transfer of matter to the deep ocean. Deep-Sea Research, 28A, 5, 495-505.

Domack, E. W., D. J. P. Foss, J. P. M. Syvitsky and C. E. McClennen, 1994. Transport of suspended particulate matter in an Antarctic fjord. Marine Geology, 121, 161-170.

Drewry, D. J. and P. R. Cooper, 1981. Processes and models of Antarctic glaciomarine sedimentation. Annals of Glaciology, 2, 117-122.

Dunbar, R. B., A. J. Macpherson and G. Wefer, 1985. Water-column particulate flux and seafloor deposits in the Bransfield Strait and southern Ross Sea, Antractica. Antarctic Journal of United States, 20, 98-100.

Dunbar, R.B., A.R. Leventer and W.L. Stockton, 1989. Biogenic sedimentation in McMurdo Sound, Antarctica. Marine Geology, 85, 155-179.

Dunbar, R.B., A.R. Leventer and D.A. Mucciarone, 1998. Water column sediment fluxes in the Ross Sea, Antarctica: Atmospheric and sea ice forcing. Journal of Geophysical Research, 130, C13, 30741-30759.

Emerson, S., K. Fischer, C. Reimers and D. Heggie, 1985. Organic carbon dynamics and preservation in deep-sea sediments. Deep-Sea Research, 32, 11-21.

Eppley, R. W. and B. J. Peterson, 1979. Particulate organic matter flux and planktonic new production in the deep ocean. Nature, 282, 677-680.

Fabrés, J., A. Calafat, M. Canals, M.A. Bárcena, and J.A. Flores, 2000. Bransfield Basin fine-grained sediments: late-Holocene sedimentary processes and Antarctic oceanographic conditions. The Holocene, 10, 6, 703-718.

García, M. A., O. López, J. Sospedra, M. Espino, V. Gràcia, G. Morrison, P. Rojas, J. Figa, J. Puigdefàbregas and A. S.-Arcilla, 1994. Mesoscale variability in the Bransfield Strait region (Antarctica) during Austral summer. Annales Geophysicae, 12, 856-867.

García, M.A., C. Castro, A.F. Ríos, M.D. Doval, G. Rosón, D Gomis and O. López, 1999. Water masses and distribution of physico-chemical properties in the western Bransfield Strait and Gerlache Strait during austral summer 1995/96. Deep-Sea Research II

Gardner W. D., P. E. Biscaye and M.J. Richardson, 1997. A sediment trap experiment in the Vema channel to evaluate the effect of horizontal particle fluxes on measured vertical fluxes. Journal of Marine Research, 55, 995-1028.

Gersonde R. and G. Wefer, 1987. Sedimentation of biogenic siliceous particles in Antarctic waters from the Atlantic sector. Marine Micropaleontology, 11, 311-332.

Gordon, A.L. and W.D. Nowlin Jr., 1978. The Basin waters of the Bransfield Strait. Journal of Physical Oceanography, 8, 258-264.

Griffith, T. W. (1988) A geological and geophysical investigation of sedimentation and recent glacial history in the Gerlache Strait region, Graham Land, Antarctica. M.A. Thesis. Rice University, Houston, Texas. 449 pp.

Griffith, T. W. and J. B. Anderson, 1989. Climatic control on sedimentation in bays and fjords of the northern Antarctic Peninsula. Marine Geology, 85, 181-204.

Gundersen, K., 1988. Degradation of organic matter in sediment traps, In Sediment Trap Studies in the Nordic Countries 1, P. Wassmann and A.S. Heiskanen, eds.,22-37.

Gundersen, K. and P. Wassmann, 1990. Use of choloroform in sediment traps: caution advised. Marine Ecology Progress Series, 64,187-195.

Gust, G., R. H. Byrne, R. E. Bernstein, P. R. Betzer and W. Bowles, 1992. Particle fluxes and moving fluids: experience from synchronous trap collections in the Sragasso Sea. Deep Sea Research, 39, 1071-1083.

Gust, G., A. F. Michaels, R. Johnson, W. G. Deuser and W. Bowles, 1994. Mooring line motions and sediment trap hydromechanics: in situ intercomparison of three common deployment designs. Deep-Sea Research I, 41, 5/6, 831-857.

Harden, S. L., 1989. Establishing rates of sediment accumulation on 100-years and 1000-years time scales for glacial-marine deposits of the continental shelf of the western Antarctic Peninsula: a radiochemical approach. M.S. Thesis. North Carolina State University, Raleigh, NC. 87 pp.

Harden, S.L., D.J. DeMaster and C.A. Nittrouer, 1992. Developing sediment geochronologies for high-latitude continental shelf deposits: a radiochemical approach. Marine Geology, 103, 69-97.

Hedges, J. I. and R. G. Keil, 1995. Sedimentary organic matter preservation: an assessment and speculative synthesis. Marine Chemistry, 49, 81-115.

Hernández-León, S., S. Torres, M. Gómez, I. Montero and C. Almeida, 1999. Biomass and metabolism of zooplankton in the Bransfield Strait (Antarctic Peninsula) during austral spring. Polar Biology, 21, 214-219.

Heussner, S. C. Ratti and J. Carbonne, 1990. The PPS 3 time-series sediment trap and the trap sample processing techniques used during the ECOMARGE experiment. Continental Shelf Research, 10, 943-958.

Heussner, S., X. Durrieu de Madron, O. Radakovitch, L. Beaufort, P. E. Biscaye, J. Carbonne, N. Delsaut, H. Etcheber, and A. Monaco, 1999. Spatial and temporal patterns of downward particle fluxes on the continental slop of the Bay of Biscay (northeastern Atlantic). Deep-Sea Research Part-II, 46, 2101-2146.

Holm-Hansen, O. and B.G. Mitchell, 1991. Spatial and temporal distribution of phytoplankton and primary production in the western Bransfield Strait region. Deep-Sea Research, 38, 8/9, 961-980.

Holm-Hansen, O. and M. Vernet, 1992. RACER: Distribution, abundance, and productivity of phytoplankton in Gerlache Strait during austral summer. Antarctic Journal of United States, 27, 5, 154-157.

Honjo S., 1990. Particle fluxes and modern sedimentation in the polar oceans. In: Polar Oceanography. part B: Chemistry, Biology and Geology. W. O. Smith, Jr., editors, Academic Press, Inc. pp. 687-739.

Hulth S., A. Tengberg, A. Landén and P.O.J. Hall, 1997. Mineralization and burial of organic carbon in sediments of the southern Weddell Sea (Antarctica). Deep-Sea Research I, 44, 6, 955-981.

Huntley, M., D.M. Karl, P. Niiler and O. Holm-Hansen, 1991. Research on Antarctic Coastal Ecosystems Rates (RACER): an interdisciplinary field experiment. Deep-Sea Research, 38, 8/9, 911-941.

Isla, E., A. Palanques, V. Alvà, P. Puig and J. Guillén, 2001. Fluxes and composition of settling particles during summer in an Antarctic shallow bay of Livingston Island, South Shetlands. Polar Biology.

Jeffers, J.D. and J.B. Anderson, 1990. Sequence stratigraphy of the Bransfield Basin, Antarctica: Implications for tectonic history and hydrocarbon potential. In: Antarctica as an exploration frontier: Hydrocarbon potential, geology and hazards. John, B. S. (Ed.), AAPG studies in Geology, 13-29.

Jennings, J. C., L. I. Gordon and D. M. Nelson, 1984. Nutrient depletion indicates high primary productivity in the Weddell Sea. Nature, 308, 51-54.

Karl, D. A. and V. L. Asper, 1990. RACER: Particle flux measurements during the 1989-1990 austral summer. Antarctic Journal of United States, 25, 5, 167-169.

Karl D. M., B. D. Tilbrook and G. Tien, 1991. Seasonal coupling of organic matter production and particle flux in the western Bransfield Strait, Antarctica. Deep-Sea Research, 38, 8/9, 1097-1126.

Knauer, G. A., D. M. Karl, J. H. Martin and C. N. Hunter, 1984. *In situ* effects of selected preservatives on total carbon, nitrogen and metals collected in sediment traps. Journal of Marine Research, 42, 445-462.

Lamb, H.H., 1965. The early medieval warm epoch and its sequel. Palaeogeography, Palaeoclimatology, Palaeoecology, 1, 13-37.

Lampitt, R. S., 1985. Evidence for the seasonal deposition of detritus to the deep-sea floor and its subsequent resuspension. Deep-Sea Research, 32, 8, 885-897.

Langone, I. Frignani, M. Labbrozzi, L. and Ravaioli, M., 1998. Present-day biosiliceous sedimentation in the northwestern Ross Sea, Antarctica. Journal of Marine Systems 17, 459-470.

Ledford-Hoffman, P. A., D. J. DeMaster and C. A. Nittrouer, 1984. Biogenic-silica accumulation in the Ross Sea and the importance of Antarctic continental shelf deposits in the marine silica budget. EOS, 65, 45, 916.

Ledford-Hoffman, P. A., D. J. DeMaster and C. A. Nittrouer, 1986. Biogenic-silica accumulation in the Ross Sea and the importance of Antarctic continental shelf deposits in the marine silica budget. Geochimica et Cosmochimica Acta, 50, 2099-2110.

Leventer, A. and R. B. Dunbar, 1986. Dissolution and transport of particulate silica in McMurdo Sound, Antarctica. Antarctic Journal of United States, 21, 134-137.

Leventer, A., 1991. Sediment trap diatom assemblages from the northern Antarctic Peninsula region. Deep-Sea Research, 38, 8-9, 1127-1143.

Liebzeit, G. and B. v Bodungen, 1987. Biogenic fluxes in the Bransfield Strait: planktonic versus macroalgal sources. Marine Ecology Progress Series, 36, 23-32.

López O., M. A. García and A. Sánchez-Arcilla, 1994. Tidal and residual currents in the Bransfield Strait, Antarctica. Annales Geophysicae, 12, 887-902.

Mandelli, E. F. and P. R. Burkholder, 1966. Primary productivity in the Gerlache and Bransfield Straits of Antarctica. Journal of Marine Research, 24, 1, 15-27.

Masqué, P., E. Isla, J. A. Sánchez-Cabeza, A. Palanques, J.M. Bruach, P. Puig and J. Guillén, in press. Sediment accumulation rates and carbon fluxes to bottom sediments at the Western Bransfield Strait Basin (Antarctica). Deep Sea-Research II

McCarthy, J. J., 2000. The evolution of the Joint Global Ocean Flux Study project. In: The changing ocean carbon cycle. A midterm synthesis of the Joint Global Ocean Flux Study, ed. R. B. Hanson, H. W. Ducklow and J. G. Field, pp.1-15. Cambridge University press.

McGinnis, J. P., D. E. Hayes and N. W. Driscoll, 1997. Sedimentary processes across the continental rise of the southern Antarctic Peninsula. Marine Geology, 141, 91-109.

Mortlock, R. A. and Froelich, P. N., 1989. A simple method for the rapid determination of biogenic opal in pelagic marine sediments. Deep-Sea Research 36, 9, 1415-1426.

Müller, P. J. and E. Suess, 1979. Productivity, sedimentation rate, and sedimentary organic matter in the oceans-I. Organic carbon preservation. Deep-Sea Research, 26A, 1347-1362.

Nelson, D. M. and W. O. Smith Jr., 1986. Phytoplankton bloom dynamics of the western Ross Sea ice edge. II. Mesoscale cycling of nitrogen and silicon. Deep-Sea Research, 33, 1389-1412.

Nelson, D. M., 1988. Biogenic silica and carbon accumulation in the Bransfield Strait, Antarctica. M.S. Thesis, North Carolina State University, Raleigh NC, 89 pp.

Nelson, D. M., D. J. DeMaster, R. Dunbar and W. O. Smith Jr., 1996. Cycling of organic carbon and biogenic silica in the Southern Ocean: Estimates of water-column and sedimentary fluxes on the Ross Sea continental shelf. Journal of Geophysical Research, 101, C8, 18519-18532.

Niiler, P., J. Illeman and J.H. Hu, 1990. RACER: Lagrangian drifter observations of surface circulation in the Gerlache and Bransfield Straits. Antarctic Journal of United States, 24, 134-137.

Niiler, P.P., A. Amos and J.H. Hu, 1991. Water masses and 200 m relative geostrophic circulation in the western Bransfield Strait region. Deep-Sea Research, 38, 8-9, 943-959.

Palanques A., E. Isla, P. Puig, J. A. Sánchez-Cabeza, P. Masquè, in press. Annual evolution of settling particle fluxes during the FRUELA experiment (Western Bransfield Strait, Antarctica). Deep-Sea Research

Pelayo, A.M. and D.A. Wiens, 1989. Seismotectonics and relative plate motions in the Scotia Sea region. Journal of Geophysical Research, 94, 7293-7320.

Pondaven, P., O. Ragueneau, P. Tréguer, A. Hauvespre, L. Dezileau and J. L. Reyss, 2000. Resolving the "opal paradox " in the Southern Ocean. Nature, 405, 168-172.

Prieto, M. J., G. Ercilla, M. Canals and M. de Batist, 1999. Seismic stratigraphy of the Central Bransfield Basin (NW Antarctic Peninsula): interpretation of deposits and sedimentary processes in a glacio-marine environment. Marine Geology, 157, 47-68.

Puig, P. and A. Palanques, 1998. Temporal variability and composition of settling particle fluxes on the Barcelona continental margin (Northwestern Mediterranean). Journal of Marine Research, 56, 639-654.

Raymont, J.E.G., 1980. Plankton and productivity in the oceans. Volume 1: Phytoplankton. Pergamon Press, 2nd edition. Oxford, England.

Redfield, A.C., B.H.Ketchum and F.A. Richards, 1963. The influence of organisms on the composition of sea-water. In: The Sea. R.N. Hill (Ed). Vol. II, 554 pp. John Wiley and sons, N.Y.

Rickert, D., 2000. Dissolution kinetics of biogenic silica in marine environments. Berichte zur Polarforschung. Reports on Polar Research, 351. Alfred Wegener Institute for Polar and Marine Research. Bremerhaven, Federal Republic of Germany.

Romankevich, E.A., 1984. Goechemistry of organic matter in the ocean. Springer-Verlag, New York, 334 pp.

Ruttenberg, K. C. and M. A. Goñi, 1997. Phosphorous distribution, C:N:P ratios, and $\delta^{13}C_{oc}$ in arctic, temperate, and tropical coastal sediments: tools for characterizing bulk sedimentary organic matter. Marine Geology, 139, 122-145.

Sánchez-Cabeza, J.A., P. Masqué and I. Ani-Ragolta, 1998. Pb-210 and Po-210 analysis in sediments and soils by microwave acid digestion. Journal of Radioanalytical and Nuclear Chemistry, 227, 19-22.

Schlosser, P., E. Suess, R. Bayer and M. Rhein, 1988. ^{3}He in the Bransfield Strait waters: Indication for local injection from back-arc rifting. Deep-Sea Research, 35, 1919-1935.

Schlüter, M., M. M. Rutgers van der Loeff, O. Holby and G. Kuhn, 1998. Silica cycle in the surface sediments of the South Atlantic. Deep-Sea Research I, 45, 1085-1109.

Schrader, H.J. and R. Gersonde, 1978. Diatoms and silicoflagellates. In: Zachariasse W. J. et al. (Eds.), Micropaleontological counting methods and techniques- an

exercise on an eight metres section of the lower Pliocene of Capo Rossello, Sicily. Utrecht Micropaleontological Bulletins, 17, 129-176.

Siegenthaler, U. and J. L. Sarmiento, 1993. Atmospheric carbon dioxide and the ocean. Nature, 365, 119-125.

Sievers C., H.A., 1982. Descripción de las condiciones oceanográficas físicas, como apoyo al estudio de la distribución y comportamiento del krill. Instituto Antártico Chileno serie científica, 28, 87-136.

Singer, J. K., 1987. Terrigenous, biogenic, and volcaniclastic sedimentation patterns of the Bransfield Strait and bays of the northern Antarctic Peninsula: Implications for Quaternary glacial history. Ph. D. dissertation, Rice University, Houston, Texas, U. S. A.

Smetacek, V.S., 1985. Role of sinking in diatom life-history cycles: ecological, evolutionary and geological significance. Marine Biology, 84, 239-251.

Sokal R. R. and F. J. Rohlf, 1981. Biometry. The principles and practice of statistics in biological research. W. H. Freeman and company, 2nd ed. NY, U. S. A.

Steemann Nielsen, E., 1975. Marine Photosynthesis with special emphasis on the ecological aspects. Elsevier Oceanography Series, 13. Elsevier Scientific Publishing Company, The Netherlands.

Stein R., 1990. Organic Carbon content/sedimentation rate relationship and its paleoenvironmental significance for marine sediments. Geo-Marine Letters, 10, 37-44.

Tréguer P., D. M. Nelson, A. J. van Bennekom, D. J. DeMaster, A. Leynaert and B. Quéguiner, 1995. The silica balance in the world ocean: A reestimate. Science, 268, 375-379.

Thunell R.C., 1998. Seasonal and annual variability in particle fluxes in the Gulf of California: A response to climate forcing. Deep-Sea Research I, 45, 2059-2083.

Varela, M., E. Fernández and P. Serret, in press. Size-fractioned phytoplankton biomass and primary production in the Gerlache and South Bransfield Straits (Antarctic Peninsula) in the austral summer 95-96. Deep-Sea Research.

Warnke, D. A., J. Richter and C. H. Oppenheimer, 1973. Characteristics of the near shore environment off the south coast of Anvers Island, Antarctic Peninsula. Limnology and Oceanography, 18, (1), 131-142.

Wefer, G., G. Fischer, D. Füetterer and R. Gersonde, 1988. Seasonal particle flux in the Bransfield Strait, Antarctica. Deep-Sea Research, 35, 6, 891-898.

Wefer G., G. Fisher, D. K. Fütterer, R. Gersonde, S. Honjo and D. Ostermann, 1990. Particle sedimentation and productivity in Antarctic waters of the Atlantic sector. In: Geological History of the Polar Oceans: Arctic Versus Antarctic, U. Beil and J. Thiede, editors, Kluwer Academic Publishers, The Netherlands, pp. 363-379.

Wefer, G. and G. Fischer, 1991. Annual primary production and export flux in the Southern Ocean from sediment trap data. Marine Chemistry, 35, 597-613.

Yoon H. I., M. W. Han, B. K. Park, S. J. Han and J. K. Oh, 1992. Distribution, provenance, and dispersal pattern of clay minerals in surface sediment, Bransfield Strait, Antarctica, Geo-Marine Letters, 12, 223-227.

Yoon H.I., M.H. Han, B.K. Park, J.K. Oh, S.K. Chang, 1994. Depositional environment of near-surface sediments, King George Basin, Bransfield Strait, Antarctica. Geo-Marine Letters, 14, 1-9.

PART VII. RELATED STUDIES

FLUXES AND COMPOSITION OF SETTLING PARTICLES DURING SUMMER IN AN ANTARCTIC SHALLOW ENVIRONMENT: JOHNSON'S DOCK (LIVINGSTON ISLAND, SOUTH SHETLANDS).

Enrique Isla*, Albert Palanques, Victor Alvà, Pere Puig and Jorge Guillén.

Institut de Ciències del Mar (CSIC). Passeig Joan de Borbò s/n. Barcelona 08039, Spain.

Polar Biology (in press)

*To whom correspondence should be addressed:
e-mail: isla@icm.csic.es
fax: 34 93221 7340

Fluxes and composition of settling particles during summer in an Antarctic shallow environment: Johnson's Dock (Livingston Island, South Shetlands).

E Isla*, A Palanques, V Alvà, P Puig and J Guillén.

Institut de Ciències del Mar (CSIC). Passeig Joan de Borbò s/n. Barcelona 08039, Spain.

*To whom correspondence should be addressed:
e-mail: isla@icm.csic.es
fax: 34 93221 7340

Abstract

A moored experiment using a sediment trap was conducted at Johnson's Dock, Livingston Island from December 11th 1997 to February 24th 1998, as part of the EASIZ Program activities carried out at the Juan Carlos I Spanish Antarctic base. Total mass vertical fluxes ranged from 23,235 mg/m^{2}d to 89,073 mg/m^{2}d during the experiment, with a mean value of 42,856 mg/m^{2}d. Lithogenic components were the major contributors to the settling particulate flux. Organic components accounted for a low fraction of the settling particulate matter because they were diluted by the high lithogenic inputs, showing an inverse relation to total mass flux. Nevertheless, the fluxes of organic components at Johnson's Dock are as high as in open sea. The increases in chlorophyll-a in water were related to increases in the organic carbon content. Organic carbon content dominated over inorganic carbon during the complete experiment. Calcium carbonate particles settle without being significantly altered in the water column and are dissolved in the upper centimetres of the bottom sediments, once they are buried. The settling material consisted of fine particles with coarse clasts transported by icebergs. Antarctic shallow environments receive important sediment fluxes from the erosion and transport action of ice.

Introduction

Particle fluxes in polar oceans show a high seasonal variability linked to the sea-ice coverage dynamics and its relation to living organisms and glacier melting events. Maximum activity takes place mainly during the polar spring and summer when the ice sheets break and melt and the ocean surface becomes ice-free (Wefer and Fischer 1991; Huntley et al. 1991).

Most of the research carried out in Antarctic areas has focused on offshore coastal and oceanic environments and very little has been done in the small bays and water inlets along the enormous coastal line of the Antarctic continent and its surrounding islands.

These in-shore coastal waters have very peculiar oceanographic and climatic conditions (Klöser et al., 1994; Kowalewski and Wielbinska, 1983; Pruszak, 1980) and are different environments to offshore oceanic waters. In contrast to Arctic coastal systems, Antarctic shallow environments show weak estuarine circulation, little riverine input and low sedimentation rates (Klöser et al. 1994). These conditions, however, should not be understood as a rule for the whole Antarctic. The singular relations between many factors such as biological productivity, sediment inputs and sea-ice give unique characteristics to the small bays. Settling particle flux behaviour in Antarctic shallow nearshore environments is poorly known. Most of the continental shelves in the Bransfield Strait are mainly covered by coarse sediment (sand and gravels) (Yoon et al. 1992). Accumulation of fine sediment is restricted to fjords and bays (Griffith and Anderson 1989), so coastal settling sediments fluxes can only be studied in these confined environments. The existing data are mainly qualitative (Griffith and Anderson 1989) and the few experimental measurements do not include identification of the major components of the fluxes (Cripps and Clarke 1998).

This paper studies the settling particles fluxes and its composition in order to quantify and characterise the particle inputs entering the Antarctic coastal ecosystem.

Johnson's Dock, a semi-enclosed and well-controlled small bay was chosen to study these fluxes. Johnson's Dock is in Livingston Island's South Bay (South Shetland islands), beside the Spanish Antarctic Base (Fig.1). This dock is approximately 750-m long and 550-m wide. It has several depressions of more than 20-m depth that are confined by the till deposits of the frontal morraine of the Contell glacier and is connected to Livingston Island South Bay through a small mouth about 75-m wide and 40-cm deep.

Materials and methods

As part of the EASIZ Program activities carried out at the Juan Carlos I Spanish Antarctic base, a mooring line equipped with a Technicap pps 4 sediment trap installed 4.5 m above the bottom, from December 11th 1997 to February 24th 1998, was deployed at 60° 23.2' W and 62° 39,5' S in Johnson's Dock at 19.5 m water depth (Fig. 1). The sediment trap used in this study has a carrousel with 12 rotary collectors and the sample-collecting intervals were preselected at 6-7 days. The upper part of the internal-collecting hull is cylindrical and has an inner diameter of 25 cm. At the mooring site, water samples were collected at 10 m depth and a sediment core was taken using a grab.

The sample tubes were filled with 5% formalin solution to avoid organic matter degradation in the sediment trap. The collected samples were processed according to Heussner et al. (1990). Zooplankton organisms that entered into the trap, also called "swimmers", were removed by hand picking and stored for further analysis. Sample dry weight was determined using three subsamples filtered onto 47-mm diameter and 0.45 µm pore preweighed Millipore cellulose filters. Total mass flux was calculated from the sample dry weight, the collecting trap area and the time sampling interval.

Organic carbon, calcium carbonate and nitrogen of the settling particles and bottom sediment were analysed by duplicate using a LECO CN2000 analyser. Two subsamples were used to determine the total carbon and the nitrogen content and another two subsamples were digested with HCl 6M in a LECO CC100 measuring the inorganic carbon delivered by this reaction in the analyser. The difference between total and inorganic carbon was considered as the organic carbon content. Biogenic silica was analysed using a wet alkaline extraction with sodium carbonate following the method described by Mortloch and Froelich (1989).

The lithogenic component was estimated as the difference between the total mass and the sum of the biogenic components: organic matter (twice the percentage of organic carbon), calcium carbonate (inorganic carbon percentage multiplied by 8.3331) and opal.

Fecal pellets were counted under a dissection microscope from the subsample used for major components analysis. Fecal pellets flux was calculated from the fecal pellets number, the collecting trap area and the time sampling interval.

Clasts coarser than 1mm were separated by sieving and counted also from the subsample used for major components analysis.

The Chlorophyll-a content in water samples taken from 10 m depth was analysed fluorometrically (Strickland and Parsons 1972). Samples (100 ml) were filtered through 25-mm GF/F glass fibre filters and immediately frozen at -70°C. The filters were then left for 12 h in 90% acetone at 4°C in the dark for pigment extraction. The fluorescence of the extract (before and after acidification) was measured using a Turner Designs fluorometer.

Results

Settling particulate matter

The mean total mass flux collected by the sediment trap and the mean content and fluxes of the major components (organic and inorganic carbon, calcium carbonate, organic matter, biogenic opal, total nitrogen, fecal pellets and aluminosilicates) are listed in Table 1. All the samples were a mixture of fine particles with poorly classified clastic material.

Time series of total mass flux (TMF) show a relatively constant value throughout the study period, although four peaks can be recognised (Fig. 2). The maximum value, 89,073 mg/m^{2}d, was registered in late January and the minimum value, 23,235 mg/m^{2}d, in mid-late December (Fig. 2). The mean total mass flux during the study period was about 43,000 mg/m^{2}d.

The organic carbon (OC) content ranged from 0.3 to 0.8% (Fig. 3a). Maximum OC values were in late February and in mid-February coinciding with low TMF values, whereas minimum values were in mid-late January when TMF was high. In fact, taking into account all the samples, there is a clear inverse relation between OC content and TMF.

OC flux values showed similar trends to those of the TMF except in mid-January and in early February (Fig. 3a). OC fluxes ranged between a minimum of 125 mg/m^{2}d, during the first week of February and a maximum of 315 mg/m^{2}d, during the fourth week of January.

Calcium carbonate content in the trapped sediment was very low, ranging between 0 and 1.23 % (Fig. 3b). The mean $CaCO_3$ content was only 0.72% , showing the maximum contents in mid-December and mid-February, whereas in late January it was practically null (when the inorganic carbon (IC) values were below the detection level (0.003%)). The calcium carbonate flux showed a different pattern to TMF, with maximum values of more than 400 mg/m^{2}d in mid-December and early January and minimum values (0 mg/m^{2}d) in late January just when TMF was maximum (Fig 3b).

The OC/N relation showed low values ranging between 6 and 8, except in late January when it increased to about 20. The OC/IC ratio was also relatively constant ranging between 3.3 and 8 except in mid- and late January when it increased sharply to 23.2.

Both OC/N and OC/IC increases were produced by a decrease in N and IC contents (Fig. 4a and 4b).

The opal content ranged from 1.75 to 3.08%. The maximum opal content corresponded to the second week of January, coinciding with a peak of the OC content. Minimum opal content occurred in mid-late January and also coincided with minimum OC values and maximum TMF. The opal flux was influenced by the TMF and shows trends opposite to those of the opal content (Fig 3c). The opal flux ranged from 524 mg/m^{2}d in late December to 1562 mg/m^{2}d in late February. Mean opal flux was 962 mg/m^{2}d.

The lithogenic components were the major fraction of the settling particulate matter ranging from 94.75 to 97.54 %. Maximum lithogenic values were registered in mid- and late January (Fig. 3d). The lithogenic flux clearly controlled the total mass flux and ranged from 86,881 mg/m^{2}d in late January to 22,074 mg/m^{2}d in late December, with an average value of 41,225 mg/m^{2}d.

The fecal pellets (FP) flux showed a decreasing trend with time from 100,000 to 10,000 fp/m^{2}d, but with a maximum peak of 288,571 fp/m^{2}d in early January and a minimum peak of 7,200 fp/m^{2}d in mid-January which corresponded to the highest TMF period (Fig. 5a). However, FP content did not show a clear relation to any major component.

The sediment trap also collected detritic clasts. The number and flux of the clasts coarser than 1 mm showed an increasing trend with time from 10 to more than 800 and from 5 mg/m^{2}d to 9143 mg/m^{2}d. Minimum values were recorded at the beginning of the experiment and maximum peaks in early February and late February (Fig. 5b).

Water samples

There were relatively constant chlorophyll-a content values during the sampling period (Fig. 6). These values ranged between 0.3 and 0.5 mg/m^{3}d with two peaks of 0.9 and 1 mg/m^{3}d which corresponded to mid-January and mid-February respectively. These two peaks ocurred when organic carbon content was high and OC/N ratio had relatively low values.

Bottom sediment

The organic carbon content in the bottom sediment varied between 0.28 and 1.38%, with an average value of 0.42% (Fig. 7). The calcium carbonate content ranged from 0 to 0.86%, with a mean value of 0.51% (Fig. 7). The OC content remains quite constant in the upper centimetres of the sediment record and increases at the same depth where the carbonate content decreases to zero.

Discussion and conclusions

Johnson's Dock is a shallow closed system that receives icebergs and water from the Contell glacier. The interchange with the open sea is restricted and it takes place only by its narrow and shallow mouth. The settling total mass fluxes of this bay have the

same order of magnitude than those measured in other Antarctic coastal environments (Cripps and Clarke, 1998). The TMF collected during the summer period, is higher than 20,000 mg/m^{2}d with a very high lithogenic content and shows an inverse relation to the organic components content. In the Johnson's Dock, TMF increased by a factor of 2 in mid-December and in mid-February and by a factor of 3-4 in early and late January. Those TMF increments were linked to increases of the lithogenic content and to decreases of organic carbon and biogenic opal contents. However, the fluxes of the organic components increased with the TMF, suggesting that the increase in the lithogenic content caused the decrease in the organic components content by dilution.

Lithogenic inputs come mainly from erosive action and melting of the glaciers. Clasts coarser than 1 mm must have been transported by icebergs and settle into the trap during the ice melting. The clasts flux shows an increasing trend with time, indicating that ice melting increases during summer, but the clasts flux trend is not directly related to the TMF trends. This is because the flux of fine lithogenic components is more than 5 times higher than that of >1mm-lithogenic clasts, so fine lithogenic flux is dominant. The fine lithogenic material has a different dynamics to coarse lithogenic material, because fine particles can remain suspended in the water column along density gradients (Domack et al., 1994), and their sinking is controlled by other hydrographic processes.

Regarding the organic components, their fluxes were similar to, or significantly higher than, those measured in deeper regions of the Bransfield Strait (DeMaster et al. 1987; Wefer et al. 1988; Karl et al. 1991; Palanques et al. in press), even though their relative contents were much lower than those from off-shore. This is not because there are low organic inputs, but because they are diluted by the high lithogenic inputs of this bay.

The chlorophyll-a in the surface water is related to primary productivity and to biogenic component inputs. The temporal evolution of chlorophyll-a in the bay does not show a direct relation to the content and fluxes of organic components and fecal pellets during the study period (Fig. 6). However, the peaks of chlorophyll-a occurring in mid-January and late February correspond to increases in organic carbon content. Both chlorophyll-a peaks coincide with low OC/N values, suggesting that settling organic matter was fresher during these periods of time. The peak value of fecal pellets indicates that a bloom of zooplankton could have happened in early January before the-mid January chlorophyll-a peak. The February peak could have some relation to the biomass bloom that tends to happen in the open water of the Bransfield Strait during this month (Holm-Hansen and Mitchell, 1991). The higher OC/N values correspond to the highest lithogenic fluxes, which probably indicates that organic matter during these events could has been recycled and /or degraded.

Settling OC was dominant over IC and ranged from 77 to 100% of the total carbon. Organic carbon and calcium carbonate content in the surface sediment of the study site showed similar values to those of the settling particles (Fig. 7). This means that the particles in the water column reach the sediment without being significantly altered. The residence time of the particles in shallow environments is probably too short to allow the transformations that happen in Antarctic deeper environments, where carbonate in sediments is lower than in the settling particulate matter (Palanques et al. in press). In the Johnson's Dock, the carbonate content in the sediment column decrease with depth indicating that dissolution is gradual from the surface to about 8-

cm depth, where the $CaCO_3$ content is null (Fig. 7).This indicates that the shells of carbonated organisms settle and accumulate in the bottom sediment where they are dissolved after buried.

The results obtained from this experiment reveal that even though there are not large river systems in the Bransfield Strait, high sediment fluxes occurred in the shallow environments mainly due to sediment supplies from the action of ice. The lithogenic fine sediment fraction is the dominant contributor to this fluxes, but it is important to note that the input of coarse clasts from iceberg melting is also very relevant in the study area. However not only the processes associated with the ice melting seem to control the temporal variability of the settling fluxes of particles, and hydrodynamic processes should be studied in these shallow environments to understand the mechanisms that control their particle fluxes.

Acknowledgements This research was supported by the project MAR96-1781-CO2-01 funded by the "Comisión Interministerial de Ciencia y Tecnología" and by the "Plan Nacional de Investigación en la Antártida" as a Spanish contribution to EASIZ-SCAR program. It was benefited also by the fellowship 92766 from the Consejo Nacional de Ciencia y Tecnologia (México).

References

Cripps GC, Clarke A (1998) Seasonal variation in the biochemical composition of the particulate material collected by sediment traps at Signy Island, Antarctica. Pol Biol 20:414-423

DeMaster DJ, Nelson TM, Nittrouer CA, Harden SL (1987) Biogenic silica and organic carbon accumulation in modern Bransfield Strait sediments. Ant Jour U S 12:108-110

Domack EW, Foss DJP, Syvitski JPM, McClennen CE (1994) Transport of suspended particulate matter in an Antarctic fjord. Mar Geol 121:161-170.

Griffith TW, Anderson JB (1989) Climatic control of sedimentation in bays and fjords of the northern Antarctic Peninsula. Mar Geol 85:181-204

Heussner S, Ratti C, Carbonne J (1990) The PPS 3 time-series sediment trap and the trap sample processing techniques used during the ECOMARGE experiment. Cont Shelf Res 10:943-958

Holm-Hansen O, Mitchell BG (1991) Spatial and temporal distribution of phytoplankton and primary production in the western Bransfield Strait region. Deep-Sea Res 38:961-980

Huntley M, Karl DM, Niiler P, Holm-Hansen O (1991) Research on Antarctic Coastal Ecosystems Rates (RACER): an interdisciplinary field experiment. Deep-Sea Res 38:911-941

Karl DM, Tilbrook BD, Tien G (1991) Seasonal coupling of organic matter production and particle flux in the western Bransfield Strait, Antarctica. Deep-Sea Res 38:1097-1126

Klöser H, Ferreyra G, Schloss I, Mercuri G, Laturnus F, Curtosi A (1994) Hydrography of Potter Cove, a small fjord like inlet on King George Island (South Shetlands). Est Coast Shelf Sci 38:523-537

Kowalewski J, Wielbinska D (1983) Characteristics of variation of meteorological elements in Ezcurra inlet during the Polish Academy of Sciences' second Antarctic expedition from 20 December 1977 to 16 March 1978. Oceanologia 15:7-19

Mortlock RA, Froelich PN (1989) A simple method for the rapid determination of biogenic opal in pelagic marine sediments. Deep-Sea Res 36:1415-1426

Palanques A, Isla E, Puig P, Sanchez-Cabeza JA, Masqué P (in press) Annual evolution of settling particle fluxes during the FRUELA experiment (Western Bransfield Strait, Antarctica)

Pruszak Z (1980) Currents circulation in the waters of Admiralty Bay (region of Arctowski station on King George Island). Pol Polar Res 1:55-74

Strickland JDH, Parsons TR (1972) A practical handbook of sea-water analysis. Fish Res Board Can Bull (2nd edn) 167:1-326

Wefer G, Fischer G (1991) Annual primary production and export flux in the Southern Ocean from sediment trap data. Mar Chem 35:597-613

Wefer G, Fischer G, Füetterer D, Gersonde R (1988) Seasonal particle flux in the Bransfield Strait, Antarctica. Deep-Sea Res 35:891-898

Yoon HI, Han MW, Park BK, Han SJ, Oh JK (1992) Distribution, provenance, and dispersal pattern of clay minerals in surface sediment, Bransfield Strait, Antarctica. Geo-Mar Let 12:223-227

Figure captions.

Fig. 1 Map showing the location of the sediment trap site at Johnson's Dock, Livingston Island, South Shetland Islands, Antarctica

Fig. 2 Time series of the total mass flux at Johnson's Dock, Livingston Island during the study period

Fig. 3 Time series of organic carbon (a), calcium carbonate (b), opal (c) and lithogenics (d) fluxes (histograms) and contents (filled circles) during the study period

Fig. 4 Temporal variation of the organic carbon (OC) to total nitrogen (N) ratio (a) and organic carbon to inorganic carbon (IC) (b) ratio. (* Missing point because inorganic carbon content in that sample was below detection level (0.003%))

Fig. 5 Time series of clasts (a) and fecal pellets (b) fluxes (histogram) and contents (filled circles) during the study period

Fig. 6 Temporal variation in chlorophyll-a at 10-m depth during the study period

Fig. 7 Vertical profile of organic carbon (filled circles) and calcium carbonate (crosses) content in the bottom sediment at the mooring site

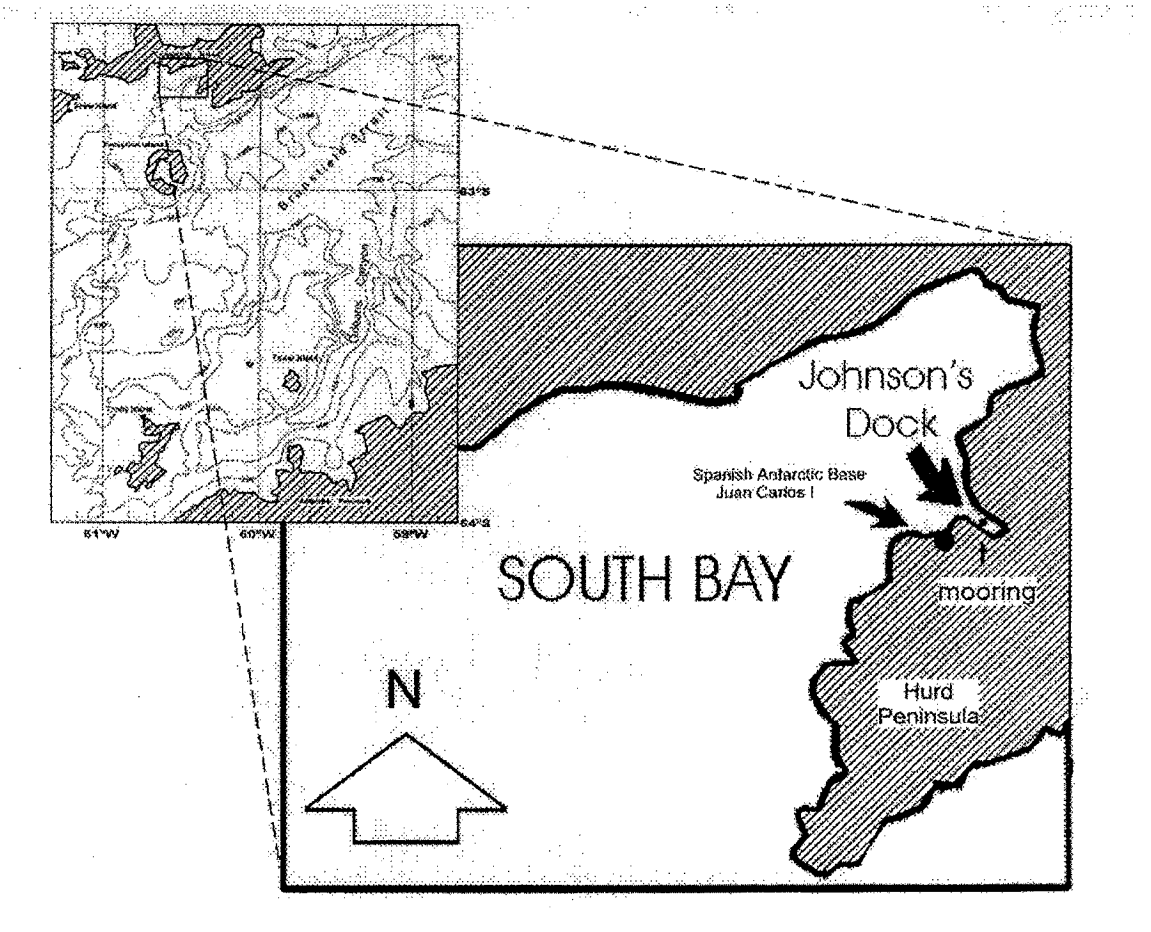
Johnson's
Dock
Spanish Antarctic Base
Juan Carlos I
SOUTH BAY
mooring
N
Hurd
Peninsula

Fig. 1

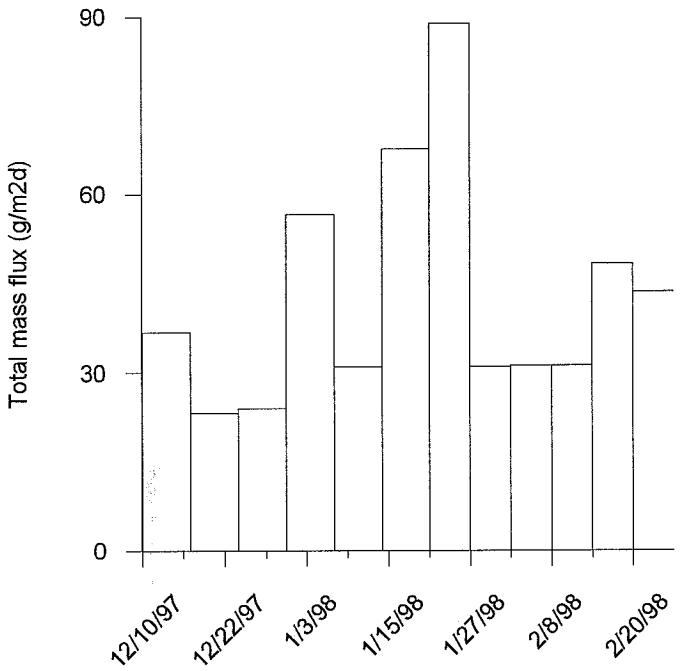

Fig. 2 , Isla et al.

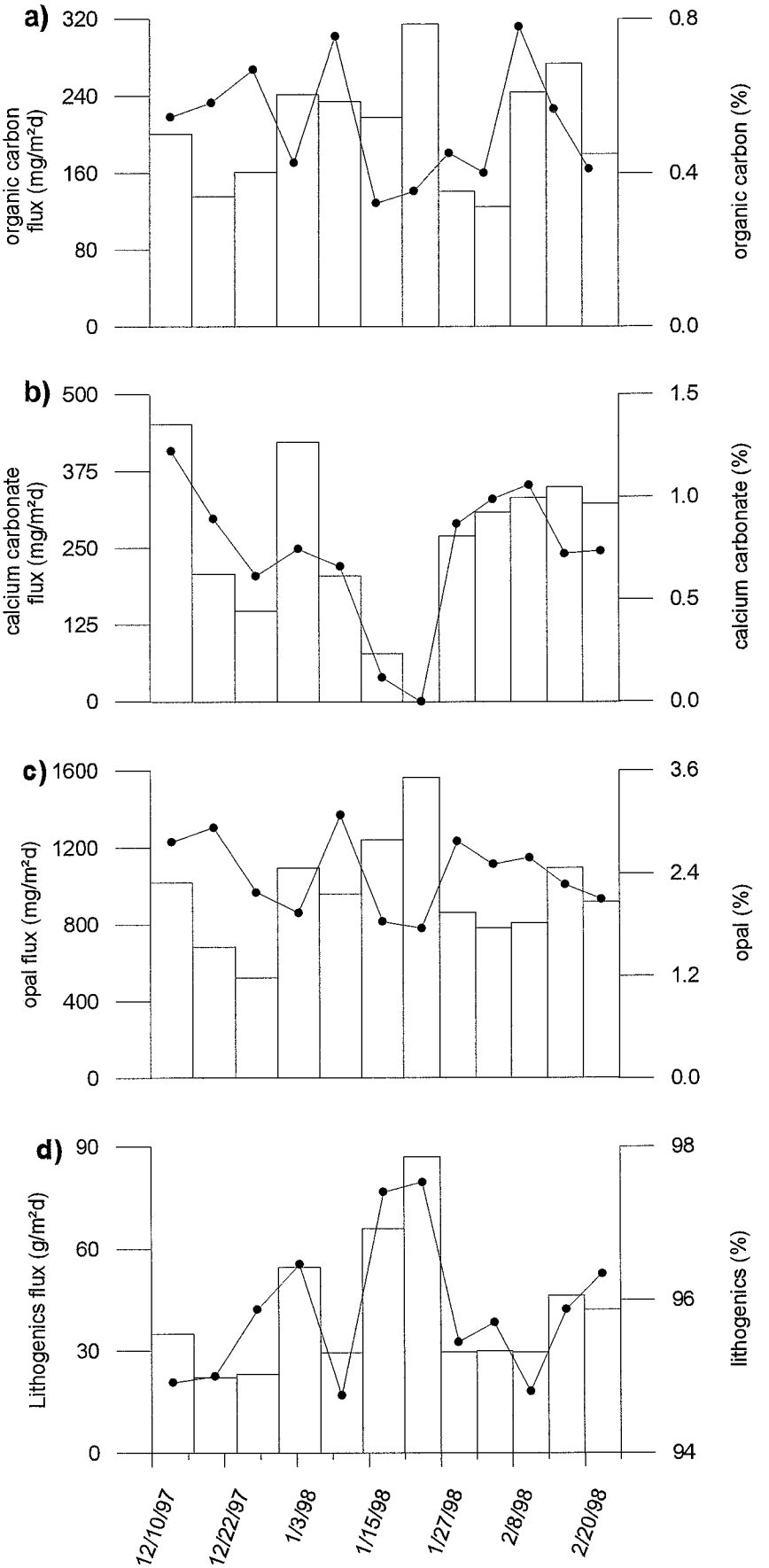

Fig. 3, Isla et al.

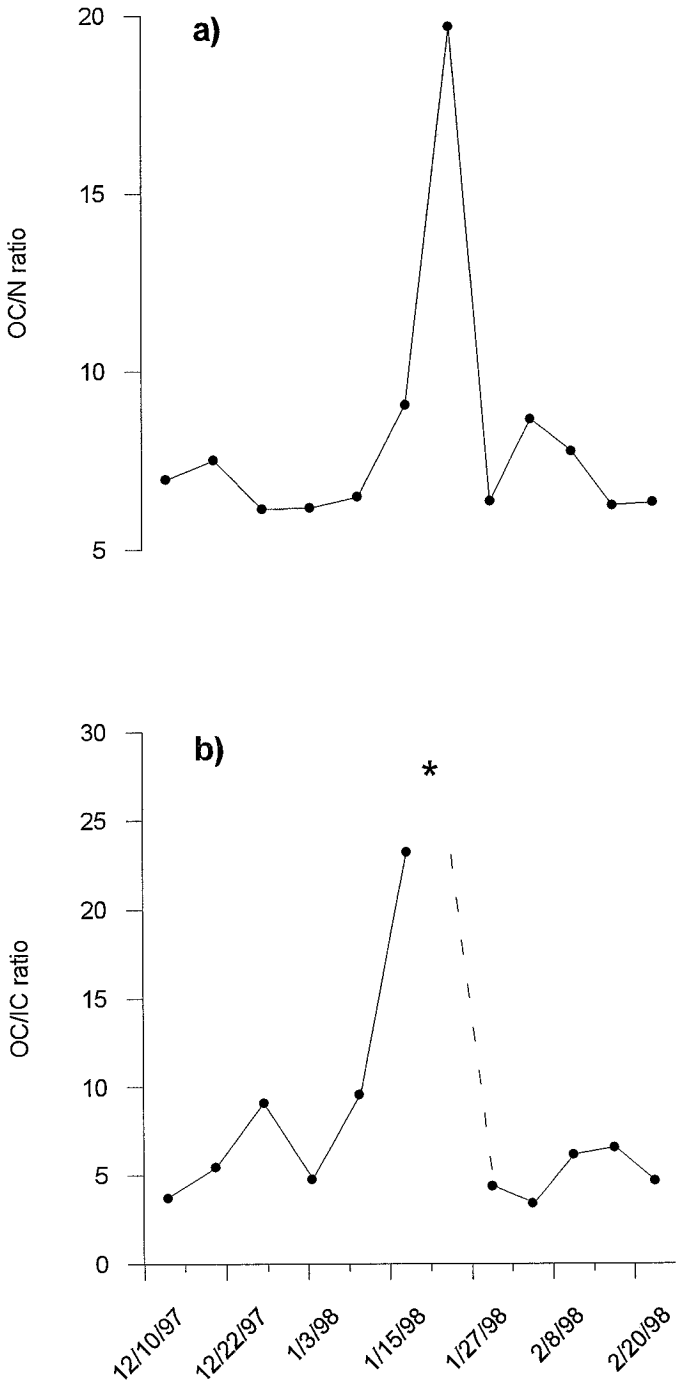

Fig. 4 , Isla et al.

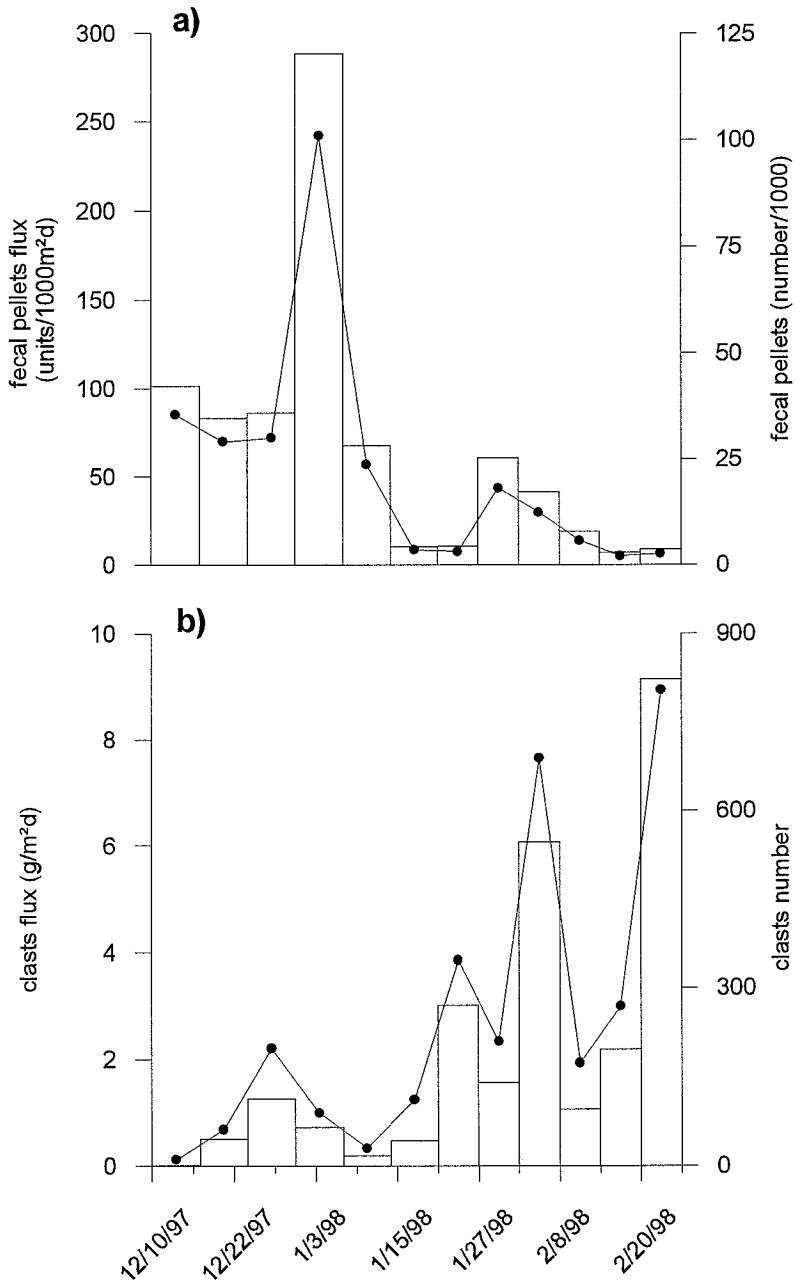

Fig. 5, Isla et al.

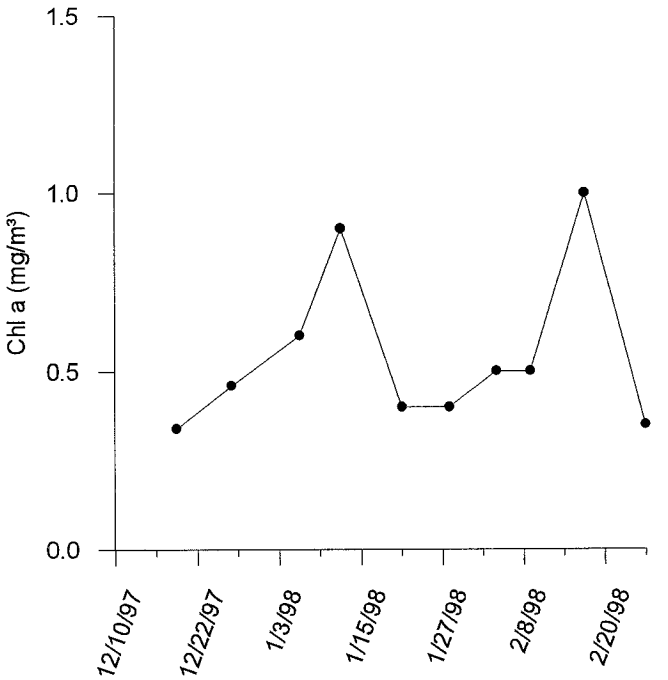

Fig. 6, Isla et al.

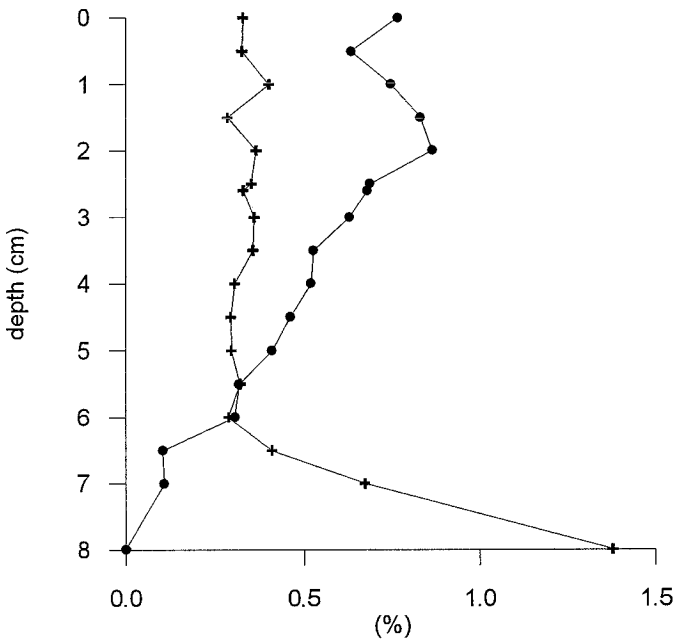

Fig. 7, Isla et al.

SEDIMENT ACCUMULATION RATES AND CARBON BURIAL EFFICIENCY IN THE BOTTOM SEDIMENT OF A HIGH PRODUCTIVITY AREA: GERLACHE STRAIT (ANTARCTICA)

Enrique Isla[1*], Pere Masqué[2,3], Albert. Palanques[1], Joan Albert Sanchez-Cabeza[2], Joan M. Bruach[2], Jorge Guillén[1] and Pere Puig[1]

[1] Unitat de Geologia Marina i Oceanografia Física, Institut de Ciències del Mar-CSIC. Passeig Joan de Borbó s/n, Barcelona E-08039, Spain.

[2] Departament de Física, Universitat Autònoma de Barcelona, E-08193 Bellaterra, Spain.

[3] Present address: Marine Science Research Center, State University of New York, Stony Brook, NY 11794-5000, USA.

Deep-Sea Research II (accepted)

*To whom correspondence should be addressed:
e-mail: isla@icm.csic.es
fax: 34 93221 7340

SEDIMENT ACCUMULATION RATES AND CARBON BURIAL EFFICIENCY IN THE BOTTOM SEDIMENT OF A HIGH PRODUCTIVITY AREA: GERLACHE STRAIT (ANTARCTICA)

Isla, E.[1*], P. Masqué[2,3], A. Palanques[1], J.A. Sanchez-Cabeza[2], J.M. Bruach[2], J. Guillén[1] and P. Puig[1]

[1]*Unitat de Geologia Marina i Oceanografia Física, Institut de Ciències del Mar-CSIC. Passeig Joan de Borbó s/n, Barcelona E-08039, Spain.*

[2]*Departament de Física, Universitat Autònoma de Barcelona, E-08193 Bellaterra, Spain.*

[3]*Present address: Marine Science Research Center, State University of New York, Stony Brook, NY 11794-5000, USA.*

[*]To whom correspondence should be addressed:
e-mail: isla@icm.csic.es
fax: 34 93221 7340

Abstract

Recent (100 yr) sediment, carbon, and nitrogen accumulation rates at six different sites along a high productivity area, Gerlache Strait, Antarctica, have been assessed.
Organic carbon (OC) content in the sampled sediments along the strait accounted for more than 90 % of the total carbon, which ranged from 0.7 to 1.2 % of the total mass. Bottom sediments from the northern part of the Strait had the highest mean OC content and apparent mean sediment accumulation rates. These last values ranged between 630 ± 30 and 1750 ± 80 g $m^{-2}y^{-1}$ (0.65 ± 0.03 to 3.11 ± 0.14 mm y^{-1}). The organic carbon sedimentation rates during the recent 100 y were significant and varied between 5 and 23 g $m^{-2}y^{-1}$, with the highest values at the center of the Strait. Bottom topography and both hydrographic and biologic controls make the eastern half of the Strait a deposit of material produced farther to the west. Burial efficiency of OC in the bottom sediments was estimated between 71 and 83%, which represented about 2.5 % of the OC produced in the euphotic layer. Thus, Gerlache Strait is keeping at least 3 times more primary produced OC if compared with the global oceanic burial rate but no more than in other Antarctic areas as the Ross Sea. The Strait can be considered as an area that could export particulate OC to the adjacent western Bransfield Strait.

Introduction

During the last three decades studies concerning the carbon cycle have multiplied substantially due to the changes in the global climate after the increase of the green house gasses concentration in the earth's atmosphere. The study of the global carbon cycle is complex and it should be supported by modeling (Liu et al., 2000). The challenge in constructing the global carbon cycle comes from the great diversity of the marine environment. Thus, the accuracy of any model is related to the diversity of information from where it is feed by. The contribution of the knowledge of the carbon cycle in particular areas is basic to the global model development.

The Southern Ocean has special interest in the global carbon cycle due to its great extension (one fifth of the world ocean surface) and because generally the primary production is not limited by the availability of nutrients.

The net amount of primary produced organic carbon sequestered from the upper layers of the water column and buried in the Southern Ocean sediments is still poorly known. The percentage of primary produced carbon that finally remains in the bottom sediments is very little, between <1 and 5 %, when compared with biogenic silica values that ranged between 12 and 50 % (DeMaster et al., 1991; DeMaster et al., 1992; Nelson et al., 1996; Masqué et al., in press). The ocean surrounding Antarctica does not remove atmospheric CO_2 in a uniform manner along its whole extension. Several areas have been detected as a sink or source regions due to different factors (Karl et al., 1991; Metzl et al., 1991; Murphy et al., 1991). This "patchy" behaviour is experienced in the euphotic zone by the biological activity as well; so it is possible to identify high and low productivity areas even within one particular region, i.e. RACER studies (Huntley et al., 1991) and FRUELA studies (Anadón and Estrada, in press). The seabed should behave in a similar patchy fashion, in which it reflects the primary production conditions in the euphotic layer above it as well as lateral transport, deposition and preservation processes. The particular attention to the study of the sediment below those areas of high productivity or high atmospheric CO_2 uptake is therefore needed in

order to develop a better understanding of the carbon cycle in the Southern Ocean and its position in the global context.

The aim of the present work is to contribute to the knowledge of the organic carbon accumulation rates to the bottom sediments below a high productivity area where this kind of information is scarce: the Gerlache Strait, Antarctic Peninsula.

Background

The Gerlache Strait is located approximately between 61° W, 64° S and 64° W, 65° S (Fig. 1). It is a very narrow passage -between 8 and 60 km wide- limited by the northern margin of the Antarctic Peninsula and the southern margin of the Palmer Archipelago. It extends about 180 km from Hoseason and Trinity Islands in the north to Wiencke and Anvers Islands at Bismarck Strait in the south. Several small islands are present throughout the strait. The Palmer Archipelago margin is steeper than that of the Antarctic Peninsula where four major bays incise the continental shelf. Because of their shape these bays were probably glacially developed. The troughs of three of these bays on the eastern half descend until 500-m depth to a central basin. The Crocker Passage at the northeastern end of the strait is the deepest access with more than 1000-m depth. The western half of the strait has a mean depth of approximately 300-m.

Like in the adjacent Bransfield Strait (Jeffers and Anderson, 1990; Yoon et al., 1994), biogenic sedimentation and glacial deposition act as the main material suppliers. Griffith (1988) found that the bottom mud in both the Palmer Archipelago and the Antarctic Peninsula margins is mainly terrigenous (<15% of biogenic silica content). Nevertheless, on the Peninsula margin the diatomaceous content of the bottom sediment is higher, though the terrigenous component is the larger fraction. This latter sediment is deposited quickly and is not transported outside the strait.

Regarding the general circulation, there is a persistent surface current in the middle of the strait of about 10–18 cm s^{-1} that transports water northeastward to the Bransfield Strait. Mesoscale features on both sides of the current increase water residence time on the sheltered bays of the Antarctic Peninsula (Niiler et al. 1990).

Biomass and productivity values in the Gerlache Strait (both in its sheltered bays and the open waters at its center) during the austral summer are quite high and greater than in surrounding regions such as the Bransfield Strait (Burkholder and Sieburth, 1961; Mandelli and Burkholder, 1966; Holm-Hansen and Mitchell, 1991; Basterretxea and Arístegui, 1999). Summer chlorophyll-a concentrations in surface waters have been reported to be between 500-700 mg m^{-2} (20-25 mg Chl a m^{-3}) and primary productivity estimated rates within the euphotic zone range between 2-5 g C $m^{-2}d^{-1}$ (Cochlan et al., 1993). This high productivity values are due, partially, to the water residence time -up to several months- in the sheltered bays of the Antarctic Peninsula, increased by eddies development (Niiler et al., 1990). The nutrient-rich waters of the peninsula coast become nursery grounds from where substantial quantities of dissolved and particulate organic matter are transported to the western Bransfield Strait and downwards, specially to those regions where water depth is less than or equal to 250-m water depth (Karl et al., 1991). The usually extraordinary phytoplankton bloom experienced in the Gerlache Strait during mid-December and January is followed by an abrupt decline in February (Clarke, 1988; Karl et al., 1991). This bloom demise generates

a rain of non-living cells and resting spores that reaches the seabed. This mechanism enriches deeper zones with organic matter (V. Bodungen et al. 1986).

Sample collection and analytical methods

Bottom sediments

Six sediment cores were taken along the Gerlache Strait from Anvers Island to the Crocker passage during January and February 1996 as part of the research expedition FRUELA-96 on board the Spanish R/V Hespérides (Fig. 1). Cores were collected using a multiple corer (Bowers and Connelly) designed to recover up to 8 replicates, of 10-cm diameter each. Core lengths ranged from 16 to 34 cm (Table 1). Bottom sediment was recovered from the deepest subbasins along the Strait.

One core from each station was subsampled on board, at 0.5 to 2-cm intervals from top to bottom. Sections were stored and frozen in sealed plastic bags until analysis. The outer 2 mm ring was removed from each section to eliminate the effects of sediment smearing downward during core insertion. Wet and dry masses were determined before and after drying samples at 40°C, dry bulk densities were calculated as well. About half of dried sample were homogenized to carry out carbon, nitrogen and ^{210}Pb analysis. The remaining non-homogenized sediment was used to determine the sand content.

Carbon and nitrogen

Total carbon (TC) and nitrogen (N) were measured twice in a LECO CN-2000 analyzer. Two other subsamples were treated with HCl in a LECO CC-100 digester and the resultant CO_2 was detected in the LECO CN-2000 analyzer yielding the inorganic carbon (IC) content. The difference between TC and IC is equal to the organic carbon percentage (OC). Calcium carbonate content ($CaCO_3$) was calculated multiplying IC by 8.33.

Sand content

The sand percentage was obtained by sieving through a 63-µm-mesh screen a pre-weighed sample pre-treated with peroxide (20%). The material collected on the sieve was rinsed with distilled water and then placed in an oven at 90°C for 24 h. The difference between dried and sifted matter weight and the initial dry weight was used to calculate the sand percentage.

Radiometric analysis

^{210}Pb concentration profiles in the sediment cores were used as a basis for determining the apparent mean sediment accumulation rates onto the seabed during the last ca. 100 years. ^{210}Pb analyses of the sediment samples were performed following the methodology described by Sanchez-Cabeza *et al.* (1998), by total digestion of 200-300 mg sample aliquots. ^{209}Po were added to each sample before digestion as internal tracer. After digestion, samples were made 1 N HCl and ^{209}Po and ^{210}Po were deposited onto silver disks at 60-70

°C for 8 hours while stirring. α-Alpha-spectrometers equipped with low background SSB detectors (EG&G Ortec) were used for counting polonium isotopes. The elapsed time span between sediment sampling and analyses, allowed ^{210}Pb to be in radioactive equilibrium with ^{210}Po (half-life = 138 d) in the sediment samples. For each batch of 10 samples, a reagent blank analysis was also carried out and subtracted for activity determination.

Excess ^{210}Pb was obtained by subtracting the supported ^{210}Pb calculated from the deeper parts of each core, where ^{226}Ra and ^{210}Pb are in equilibrium, assuming that it is constant along the core. This procedure is relatively usual in the literature (Langone *et al.*, 1998) and was recently checked by Masqué *et al.* (in press) in the neighboring Bransfield Strait by determining the ^{226}Ra concentrations along several sediment cores by gamma spectrometry, obtaining a good agreement between both approaches.

Apparent mean sediment accumulation rates

We applied the widely used advection-diffusion model first proposed by Goldberg and Koide (1962), who stated that the main processes governing excess ^{210}Pb profiles are sediment accumulation, radioactive decay and particle mixing. This can be expressed as (Cochran, 1985):

$$\frac{\partial A}{\partial t} = \frac{\partial}{\partial m} E \frac{\partial A}{\partial m} - r \frac{\partial A}{\partial m} - \lambda A \qquad (1)$$

where t is the time (years), A (Bq kg^{-1}) is the excess ^{210}Pb concentration at depth (accumulated mass) m (kg·m^{-2}), λ is the ^{210}Pb decay constant (0.03114 y^{-1}) and r and E are the sediment accumulation rate (in kg·m^{-2}·y^{-1}) and the sediment mixing coefficient (in kg^2·m^{-4}·y^{-1}) respectively, which are assumed to be constant. The mixing coefficient is then computed as $D_B = E \cdot \rho^2$ (kg·m^{-2}) where ρ is the dry-bulk density of the material (calculated as dry weight divided by the core volume section). Under steady-state conditions ($\partial A/\partial t = 0$), equation (1) is solved considering there is a constant mixing coefficient at the SML observed in the top part of a core. The sediment accumulation rate, r (or the correspondent sedimentation rate S in terms of cm·y^{-1}), can be calculated from the excess ^{210}Pb profile below it, where mixing is considered to be negligible. The term apparent sediment accumulation rate is generally used to emphasize that deep mixing is neglected. Thus, the accumulation rate corresponds to a maximum value. This magnitude of the sediment accumulation rate is then used to determine D_B in the surface mixed layer (SML). This is a common procedure used by many researchers in the marine environment (i.e. Guinasso and Shink, 1975; DeMaster and Cochran, 1982; Cochran, 1985; Roberts *et al.*, 1997; Zuo *et al.*, 1997; Langone *et al.*, 1998; Sanchez-Cabeza *et al.*, 1999; Masqué *et al.*, in press).

It is usually recommended to check the obtained results by using this procedure with other evidences such as ^{137}Cs profiles. However, as shown by Harden *et al.* (1992) and Masqué *et al.* (in press), this approach has a limited utility due to the very low concentrations of ^{137}Cs in the Southern Ocean sediments. ^{14}C dating has been also proposed as a tool to investigate the validity of the ^{210}Pb derived sedimentation rates (i.e. Nozaki *et al.*, 1977). In recent works in Antarctica, several comparisons between both methodologies have been carried out (Ledford-Hoffman *et al.*, 1986, DeMaster *et al.*, 1991; Harden *et al.*, 1992; DeMaster *et al.*,

1996; Nelson *et al.*, 1996; Langone *et al.*, 1998; Masqué *et al.*, in press). Good agreement is observed in some cases, but also some discrepancies are reported. These discrepancies can be related to overestimation of the ^{210}Pb derived sedimentation rates due to mixing processes. However, they may be faced with caution, as some important aspects should be taken into account. First, temporal spans covered by the two methodologies are very different (about 100 y for ^{210}Pb and up to several thousands of years for ^{14}C). Therefore, ^{14}C dates for very recent sediments are usually an extrapolation with large associated uncertainties. Second, the assumption of a constant sedimentation rate for the last some thousand years in a given area can be too severe, as changes in recent sedimentation rates should not be discarded systematically. Moreover, Langone *et al.* (1998) pointed out that comparison of ^{210}Pb and ^{14}C dates corresponding to samples obtained from the same area but not from exactly the same site can lead to important discrepancies due to the large spatial variability in sediment accumulation. Also, sampling methodologies must be taken into account: for instance, losses of the most top sediment or compaction when using piston or gravity corers for obtaining the samples could favour differences between ^{210}Pb and ^{14}C sediment accumulation rates calculation. Maximum accumulation rates during the last ca. 100 years were obtained by multiplying the average element content value by the apparent sediment accumulation rates derived from ^{210}Pb profiles. The depth of the SML was determined from the slope change in the ^{210}Pb-concentration profile along each core. Within this zone both mixing and sedimentation control the 210Pb profile. Below this layer the sediment accumulation term has more importance in determining the shape of the ^{210}Pb profile. It is assumed that within the SML recent sediment is mixed with that already settled and there is no way to establish differences between both kinds of material. Sediment within the SML has more chemical and biological activity than that below it. The sediment below the SML is considered as buried.

Burial efficiencies within the bottom sediment

In this work we consider the burial efficiency as equivalent to the percentage that represents any variable accumulation rate below the SML of the same variable accumulation rate within the SML. In this case the burial efficiency percentage expresses the quantity of material that was not removed from the sediment after its residence within the SML and it is finally buried. The material lost by uptake or by dissolution in the pore water was not measured.

Statistical analysis

One-way analysis of variance (ANOVA) was performed to test for differences in the mean concentration of OC and N and the OC/N ratio within the SML layer and below it. The squared root of the OC and N content and OC/N ratio values was used in order to apply this parametric test.

Results

All of the studied sediment samples consisted mainly of mud. The highest sand content in bottom sediment, 63%, was found in the central region of the strait and corresponded to the shallowest station (site B192, at 283-m depth) (Fig. 2). The samples with lowest sand content (between 1 and 5%) were from deep stations (sites B187 and B5 at 714 and 1008-m depth, respectively) indicating that the finer sediment feeds deep areas. No clear relation was found

between sand and OC contents (R^2□0.45), though in some samples decreases in OC and N content coincided with sand percentage increases. The rapid changes in the sand content profiles (Fig. 2) indicate that particles □ 0.63 μm are supplied to the bottom by pulses and not by constant processes.

OC accounted for more than 90% of the total carbon in every sample. OC content in the surface sediment varied between 0.72 ± 0.01 and 1.61 ± 0.02% (Fig. 3). Below the SML average OC content ranged from 0.56 ± 0.11 to 1.11 ± 0.05% (Table 2). Every core showed a common OC content diminishing trend with depth along the uppermost 10-12 cm (Fig. 3). Below this layer the OC content profiles were almost constant. The eastern half of the strait had the highest OC content and the highest apparent mean sediment accumulation rates as well (Table 2). These values ranged, all over the strait, from 630 ± 30 to 1750 ± 80 g $m^{-2}y^{-1}$ (0.65 ± 0.03 to 3.11 ± 0.14 mm y^{-1}). Calcium carbonate content varied in the surface sediment between < 0.003 and 0.7% and the average below the SML between 0.05 ± 0.02% and 0.55 ± 0.31%. The shallowest station had the highest calcium carbonate content levels. Nevertheless, the correlation between $CaCO_3$ content and water depth was not strong enough (R^2=0.55) to state clear conclusions. No association was found between calcium carbonate with any other variable. Nitrogen content in the surface sediment varied between 0.12 ± 0.01 and 0.25 ± 0.01% (Fig. 3). The average values below the SML were between 0.09 ± 0.01% and 0.14 ± 0.03% (Table 2). Nitrogen content was closely related to OC content, and it showed a diminishing trend with depth along each core as well. The lowest values of the OC/N ratio (6.14 and 6.18) in the surface sediment corresponded to the samples from the central portion of the strait (stations B192 and B7, respectively), the rest of the values varied between 6.4 and 7.6. Average OC/N ratio below the SML ranged from 6.6 to 7.8.

^{210}Pb and mean sediment accumulation rates

Profiles of excess ^{210}Pb concentration along each core are plotted in Figure 4 and dry bulk densities in Figure 5. The excess ^{210}Pb profiles were used to determine the apparent mean sediment accumulation rate at each station during the last ca. 100 years. Depths of SML and apparent mean sediment accumulation rates are listed in Table 2. In most cases, there was a continuous decrease in ^{210}Pb activity as depth increased. This distribution would correspond to a constant sediment accumulation rate during approximately the last 100 years. However, some features must be taken into account. First, in all cores but in B-187, a change in the slope of the excess ^{210}Pb concentration is observed in the topmost part. This fact, as argued below, is usually attributed to a certain degree of sediment mixing due to the effect of inhabiting living organisms. The second peculiarity to be considered is the identification of specific deep layers in some cores where excess ^{210}Pb concentrations were higher than expected (i.e. at about 10-12 g·cm^{-2} in core B-5, or at the basis of the excess ^{210}Pb profiles in cores B-191 and B-187). We assigned the ^{210}Pb increments to the presence of benthonic organisms rich in ^{210}Pb that cause the modification of the excess ^{210}Pb profiles. However, this slight interference was not taken into account for the calculations of the apparent mean sediment accumulation rate at each station, as they were not important enough when considering the whole profile.

Both maximum and minimum apparent mean sediment accumulation rates (SAR) values were associated to the central area of the strait. At one of the deepest stations (site B7) the SAR was 1750 ± 80 g m^{-2} y^{-1}; the lowest value, 630 ± 30 g m^{-2} y^{-1}, was detected in the shallowest station (site B192) (Table 2).

Statistical analysis

There were significant differences in the mean concentrations of OC and N within the SML and below it ($P<0.001$) (Table 3). In contrast with the other variables, the OC/N ratio did not differ significantly between both layers ($p>0.05$).

Discussion

The OC content and the OC and sediment accumulation rates obtained in this study agree with previous reports for the Bransfield and Gerlache Straits (Nelson, 1988; DeMaster et al., 1991). In addition, our sediment accumulation rates agree with the results of Harden et al. (1992). In the Gerlache Strait the finer sediment and the material with the highest OC and N content was found in the eastern sector. The highest apparent mean sediment accumulation rates corresponded to the samples of this area as well. Within this zone the maximum OC concentrations are located in front of Arctowski Peninsula (AP) and Charlotte Bay (ChB) (sites B7 and B6). The surface waters in this region have also the highest phytoplankton biomass and primary production values in the Strait (Burkholder and Sieburth, 1963; Holm-Hansen and Mitchell, 1991; Karl et al., 1991). This correspondence between surface waters and bottom sediments values could be due to the rapid sinking of diatom resting spores (V. Bodungen et al., 1986; Karl et al., 1991) during the phytoplankton demise experienced at the end of the austral summer (Holm-Hansen and Mitchell, 1991; Karl et al., 1991) and to the transport of biogenic material from the euphotic layer to the bottom packed in fecal pellets (Wefer et al., 1988). The former mechanism has an estimated sinking rate of 50-1500 m day^{-1} (Karl et al., 1991), and the latter between 100-150 m day^{-1} (Billett, et al., 1983).

Excess ^{210}Pb inventories in the bottom sediment cores were calculated from the excess ^{210}Pb concentration profiles. The excess ^{210}Pb inventories significantly enough increased with water column depth ($R^2 = 0.66$) (Fig. 6a). The estimation of the annual fluxes of excess ^{210}Pb to the sea floor at each station gave a range of values between 339 ± 5 and 1804 ± 14 Bq $m^{-2}y^{-1}$. These values are significantly greater than those estimated taking into account the atmospheric supply and the in situ production of ^{210}Pb due to disintegration of ^{226}Ra in the water column, which would be less than 100 Bq $m^{-2}y^{-1}$ in this area (Ku and Lin, 1976; Broecker and Peng, 1982; Rutgers van der Loeff and Berger, 1991; Masqué et al., in press). The excess ^{210}Pb concentrations at the surface of the sediment cores also followed this trend of increasing with depth ($R^2 = 0.86$) (Fig. 6b). Hence, these patterns may be explained by considering advection processes and focussing of material to the deep basins along the Gerlache Strait, allowing to the ^{210}Pb enrichment of the particles during their transport. At the most eastern extreme of the Strait (site B5) both the bottom topography and the main circulation pattern might explain the relatively high accumulation rates and OC concentrations in the bottom sediment. This is the deepest part of the strait and is probably acting as a settling particulate matter collector of part of the material produced farther to the west and on the adjacent shelf and the slope. Palanques et al. (in press) found similar transfers in the western basin of the Bransfield Strait from shallow environments to deep areas. The main current in the middle of the Gerlache Strait (Niiler et al., 1990) could be carrying farther to the east a fraction of the organic matter produced in the west and the center of the Strait. Karl et al. (1991) considered a probable particulate organic matter exportation out from the Gerlache Strait since the current velocities could be strong enough to produce this kind of transport.

From our results the OC burial efficiency varied between 71 and 83%. Thus, around one third and one fifth of the OC that arrives to the bottom is recycled (Table 2). We found no relation between SML depth and the amount of OC recycled. The nitrogen burial efficiency varied within the same range than the OC, between 70 and 86 % (Table 2). The burial efficiency was not clearly related to any other variable. The OC/N ratio was around 7 along each studied core. This value is very close to the 6.625 Redfield ratio results in the plankton analysis (Redfield 1958) and similar to those found by DeMaster et al. (1996) in the bottom sediments of the Ross Sea. The OC/N ratio average below the SML (6.6 and 7.8) is between 2 and 11% higher than the OC/N ratio within the SML (6.5 and 7.0). Although, there was a little increase in the OC/N ratio below the SML there is no statistical evidence to establish a preferential nitrogen uptake relative to OC. In addition, the burial efficiencies for both elements were similar. DeMaster et al. (1996) found similar results in the Ross Sea where in general, OC and N experienced little fractionation between them along the water column or in the sediment. Burial efficiency in the Gerlache Strait bottom sediment was not clearly related to any variable and seems that is controlled by several processes rather than by one main factor.

The annual value of primary production can be estimated from the mean production over spring and summer months, which in the study area ranges from 2 to 5 g C m^{-2} d^{-1} (Cochlan, 1993). Considering that these values are representative of the mean primary production over about 150 days, from November to April (DeMaster et al., 1987), and assuming that the primary production is negligible during the rest of the year (Cochlan, 1993), we estimated that the annual primary production in the study area ranges between 300 and 750 g C m^{-2}. Multiplying the apparent mean sediment accumulation rate by the average OC content below the SML we can calculate the amount of OC buried in the sediments (between 3.5 and 19 g OC m^{-2} y^{-1}). Assuming that the maximum primary production values (750 g C m^{-2} y^{-1}) take place in the central Gerlache Strait, we obtain that in the bottom sediments below this area (stations B7 and B6) a maximum of 2.5% of the primary produced OC remains below the SML. With the minimum primary production values (300 g C m^{-2} y^{-1}) the buried fraction would represent 6.3%. These values are compatible with those estimated by Nelson (1988) and DeMaster *et al.* (1991) in the Gerlache Strait and Masqué et al. (in press) in the Bransfield Strait. In the western part of the Gerlache Strait, where the primary productivity values would be around 300 g C m^{-2} y^{-1}, the amount of OC buried in the bottom sediment would vary between 1 and 2% of that produced in the surface layers. Sediment trap studies in the Bransfield Strait have demonstrated that more than the 90% of the annual organic particles flux at mid depth in the water column is restricted to a period of approximately 60 days (Wefer et al., 1988, Palanques et al., in press). Thus, we consider that a calculation with a productive period of 150 days could be underestimating the percentage of primary produced OC finally buried in the bottom sediment. If we recalculate on the basis of a 60 productive days period we obtain for the western part of the Gerlache Strait that the amount of primary produced OC buried within the sediment would vary between 2 and 5% and in the eastern part between 3 and 6%. Therefore, the OC content in the bottom sediment of the Gerlache Strait is reflecting the spatial differences of primary productivity in the euphotic zone. The eastern part of the Gerlache Strait is the portion of the study area where more OC is produced, settled, and buried. This is the result of bottom topography and both hydrodynamic and biologic controls.

Within a global context the approximate primary produced OC rate is 2.7×10^{16} g C y^{-1} (Eppley and Peterson, 1979) and the seabed accumulation rate about 0.02×10^{16} g C y^{-1} (Broecker and Peng, 1982; Romankevich, 1984). Therefore, about 0.7 % of the OC produced in the upper layers of the oceans is buried in the bottom sediments. This means that the Gerlache

Strait is able to keep in the sediment at least up to 3 times more primary produced OC when compared with the global oceanic burial rate. Focusing on the continental margins and specially comparing to other Antarctic highly productive regions the percentage of primary produced OC buried in the bottom sediment is similar to that of the Bransfield Strait -about 9%- (DeMaster, et al., 1991) and the Ross Sea -about 4.9%- (DeMaster et al., 1996). However, the amount of primary produced OC buried in the eastern Gerlache Strait sediment -between 3 and 19 g $m^{-2}y^{-1}$- is about twice the amount buried in the Bransfield Strait and the Ross Sea -between 3 and 8 g $m^{-2}y^{-1}$- (DeMaster, et al., 1991; Nelson et al., 1996). Thus, the bottom sediment in the Gerlache Strait is keeping a relatively high amount of OC and it can be considered as an important carbon sinking area within the Antarctic context.

Acknowledgements

The Comisión Interministerial de Ciencia y Tecnología of Spain funded this research under contracts ANT94-1010, MAR96-1781-CO2-01 and ANT96-1346-E. This sudy was also benefited with a pre-doctoral fellowship from CONACYT (México), reference 92766. We thank the officers, managers, technicians and crew of the BIO Hespérides and the UGBO (CSIC) for their assistance during the cruise. We also thank M. Farrán for his support during fieldwork. André Monaco and two anonymous referees contributed with valuable comments and suggestions.

References

Anadón, R and M. Estrada (in press) The FRUELA cruises. A carbon flux study in productive areas of the Antarctic Peninsula (December 1995 - February 1996). Deep Sea-Research II

Basterretxea, G. and J. Arístegui (1999) Phytoplankton biomass and production during late austral spring (1991) and summer (1993) in the Bransfield Strait. Polar Biology, **21**, 11-22.

Billett D.S.M., R.S.Lampitt, A.L. Rice and R.F.C. Mantoura (1983) Seasonal sedimentation of phytoplankton to the deep-sea benthos. Nature, **302**, 520-522.

Bodungen, B. v, V.S.Smetacek, M.M.Tilzer and B. Zeitzschel (1986) Primary production and sedimentation during spring in the Antarctic Peninsula region. Deep-Sea Research, **33**, 2, 177-194.

Broecker, W.S. and T.H. Peng (1982) Tracers in the sea. Columbia University Press, Palisades, New York, 687 pp.

Burkholder, P.R. and J.M. Sieburth (1961) Phytoplankton and chlorophyll in the Gerlache and Bransfield Straits of Antarctica. Limnology and Oceanography, **6**, 1, 45-52.

Clarke A. (1988) Seasonality in the antarctic marine environment. Compendium of Biochemistry and Physiology, **90B**, 3, 461-473.

Cochlan W., J. Martinez and O. Holm-Hansen (1993) RACER: Primary production in Gerlache Strait, Antarctica, during austral winter. Antarctic Journal of United States, **28**, 5, 172-174.

Cochran, J.K. (1985) Particle mixing rates in sediments of the eastern equatorial Pacific. Evidence from ^{210}Pb, $^{239,240}Pu$ and ^{137}Cs distributions at MANOP sites. Geochimica et Cosmochimica Acta, **49**, 1195-1210.

DeMaster, D.J. and J.K. Cochran (1982) Particle mixing rates in deep-sea sediments determined from excess ^{210}Pb and ^{32}Si profiles. Earth and Planetary Science Letters, **61**, 257-271.

DeMaster, D.J., T.M. Nelson, C.A. Nittrouer and S.L. Harden (1987). Biogenic silica and organic carbon accumulation in modern Bransfield Strait sediments. Antarctic Journal of United States, **12**, 5, 108-110.

DeMaster, T.M. Nelson, S.L. Harden and C.A. Nittrouer (1991) The cycling and accumulation of biogenic silica and organic carbon in Antarctic deep-sea and continental margin environments. Marine Chemistry, **35**, 489-502.

DeMaster, D.J., R. Dunbar, L.I. Gordon, A.R. Leventer, J.M. Morrison, D.M. Nelson, C.A. Nittrouer and W.O. Smith Jr. (1992) Cycling and accumulation of biogenic silica and organic matter in high-latitude environments: The Ross Sea. Oceanography, **5**, 3, 146-153.

DeMaster, D.J., O. Ragueneau and C. Nittrouer (1996) Preservation efficiencies and accumulation rates for biogenic silica and organic C, N and P in high-latitude sediments: The Ross Sea. Journal of Geophysical Research, **101**, C8, 18501-18518.

Eppley R.W. and B.J. Peterson (1979) Particulate organic matter and planktonic new production in the deep ocean. Nature, **282**, 677-680.

Goldberg, E.D. and M. Koide (1962) Geochronological studies of deep-sea sediments by the ionium-thorium method. Geochimica et Cosmochimica Acta **26**, 417-450.

Griffith, T.W. (1988) A geological and geophysical investigation of sedimentation and recent glacial history in the Gerlache Strait region, Graham Land, Antarctica. M.A. Thesis. Rice University, Houston, Texas. 449 pp.

Guinasso, N.L. and D.R. Shink (1975) Quantitative estimates of biological mixing rates in abyssal sediments. Journal of Geophysical Research, **80**, 21, 3032-3043.

Harden S.L., D.J. DeMaster and C.A. Nittrouer (1992) Developing sediment geochronologies for high-latitude continental shelf deposits: a radiochemical approach. Marine Geology, **103**, 69-97.

Holm-Hansen, O. and B.G. Mitchell (1991) Spatial and temporal distribution of phytoplankton and primary production in the western Bransfield Strait region. Deep-Sea Research, **38**, 8/9, 961-980.

Huntley, M., D.M. Karl, P. Niiler and O. Holm-Hansen (1991) Research on Antarctic Coastal Ecosystems Rates (RACER): an interdisciplinary field experiment. Deep-Sea Research, **38**, 8/9, 911-941.

Jeffers, J.D. and J.B. Anderson (1990) Sequence stratigraphy of the Bransfield Basin, Antarctica: Implications for tectonic history and hydrocarbon potential. In: Antarctica as an exploration frontier: Hydrocarbon potential, geology and hazards. John, B. S. (Ed.), AAPG studies in Geology, 13-29.

Karl D.M., B.D. Tilbrook and G. Tien (1991) Seasonal coupling of organic matter production and particle flux in the western Bransfield Strait, Antarctica. Deep-Sea Research, **38**, 8/9, 1097-1126.

Ku, T.-L. and M.-C. Lin (1976) ^{226}Ra distribution in the Antarctic Ocean. Earth and Planetary Science Letters, **32**, 236-248.

Langone, l. Frignani, M. Labbrozzi, L. and Ravaioli, M. (1998) Present-day biosiliceous sedimentation in the northwestern Ross Sea, Antarctica. *Journal of Marine Systems* **17**, 459-470.

Ledford-Hoffman, P.A., D.J. DeMaster and C.A. Nittrouer (1986) Biogenic-silica accumulation in the Ross Sea and the importance of Antarctic continental-shelf deposits in the marine silica budget. Geochimica et Cosmochimica Acta, **50**, 2099-2110.

Liu, K.-K., K. Iseki and S.-Y. Chao (2000) Continental margin carbon fluxes. In: The changing ocean carbon cycle. A midterm synthesis of the Joint Global Ocean Flux Study, R. B. Hanson, H. W. Ducklow and J. G. Field, editors, Cambridge University Press, Cambridge, U. K., pp. 187-239.

Mandelli, E.F. and P.R. Burkholder (1966) Primary productivity in the Gerlache and Bransfield Straits of Antarctica. Journal of Marine Research, **24**, 1, 15-27.

Masqué, P., E. Isla, J.A.. Sanchez-Cabeza, A. Palanques, J.M. Bruach, P. Puig and J. Guillén (in press) Sediment accumulation rates and carbon fluxes to bottom sediments at the Western Bransfield Strait Basin (Antarctica). Deep Sea-Research II

Metzl, N., C. Beauverger, C. Brunet, C. Goyet and A. Poisson (1991) Surface water carbon dioxide in the southwest Indian sector of the Southern Ocean: a highly variable CO_2 source/sink region in summer. Marine Chemistry, **35**, 85-95.

Murphy, P.P., R.A. Feely, R.H. Gammon, K.C. Kelly and L.S. Waterman (1991) Autumn air-sea disequilibrium of CO_2 in the South Pacific Ocean. Marine Chemistry, **35**, 77-84.

Nelson, T.M. (1988) Biogenic silica and carbon accumulation in the Bransfield Strait, Antarctica, M.S. Thesis, North Carolina State University, Raleigh NC, 89 pp.

Nelson, D.M., D.J. De Master, R. Dunbar and W. O. Smith Jr. (1996) Cycling of organic carbon and biogenic silica in the Southern Ocean: Estimates of water-column and sedimentary fluxes on the Ross Sea continental shelf. Journal of Geophysical Research, **101**, C8, 18519-18532.

Niiler, P., J. Illeman and J.H. Hu (1990) RACER: Lagrangian drifter observations of surface circulation in the Gerlache and Bransfield Straits. Antarctic Journal of United States, **24**, 134-137.

Nozaki, Y., J.K Cochran, K.K. Turekian and G.Keller (1977) Radiocarbon and Pb-210 distribution in submersible-taken deep-sea cores from project FAMOUS. Earth and Planetary Science Letters, **34**, 167-173.

Palanques A., E. Isla, P. Puig, J.A. Sanchez-Cabeza and P. Masqué (in press) Annual evolution of settling particle fluxes during the FRUELA experiment (Western Bransfield Strait, Antarctica). Deep-sea Research II

Redfield, A.C. (1958) The biological control of chemical factors in the environment. American Scientist, **46**, 3, 205-220.

Roberts, K.A., J.K. Cochran and C. Barnes (1997) ^{210}Pb and $^{239,240}Pu$ in the Northeast Water Polynya, Greenland: particle dynamics and sediment mixing rates. Journal of Marine Systems, **10**, 401-413.

Romankevich, E.A. (1984) Geochemistry of organic matter in the ocean. Springer-Verlag, New York, 334 pp.

Rutgers van der Loeff, M.M. and G.W. Berger (1991) Scavenging and particle flux: seasonal and regional variations in the Southern Ocean (Atlantic sector). Marine Chemistry **35**, 553-567.

Sanchez-Cabeza, J.A., P. Masqué and I. Ani-Ragolta (1998) Pb-210 and Po-210 analysis in sediments and soils by microwave acid digestion. Journal of Radioanalytical and Nuclear Chemistry, **227**, 19-22.

Sanchez-Cabeza, J.A., P. Masqué, I. Ani-Ragolta, J. Merino, M. Frignani, F. Alvisi, A. Palanques and P. Puig (1999) Sediment accumulation rates in the southern Barcelona continental margin (NW Mediterranean Sea) derived from ^{210}Pb and ^{137}Cs chronology. Progress in Oceanography, **441**, 1-3, 313-332.

Wefer, G., G. Fischer, D. Füetterer and R. Gersonde (1988) Seasonal particle flux in the Bransfield Strait, Antarctica. Deep-Sea Research, **35**, 6, 891-898.

Yoon H.I., M.H. Han, B.K. Park, J.K. Oh, S.K. Chang (1994) Depositional environment of near-surface sediments, King George Basin, Bransfield Strait, Antarctica. Geo-Marine Letters, **14**, 1-9.

Zuo, Z., D. Eisma, R. Gieles and J. Beks (1997) Accumulation rates and sediment deposition in the northwestern Mediterranean. Deep-Sea Research Part II, **44**, (3-4), 597-609.

Figure captions

Fig.1 Study area and sampling stations at Gerlache Strait, Antarctic Peninsula. AC means Arctowsky Peninsula and ChB, Charlotte Bay.

Fig 2. Sand content profiles in bottom sediments from the Gerlache Strait, expressed in dry weight percentage.

Fig. 3 OC (solid line) and N (dotted line) content profiles in bottom sediments from the Gerlache Strait, expressed in dry weight percentage.

Fig. 4 Excess ^{210}Pb activity profiles versus depth in bottom sediments from the Gerlache Strait. The dotted line indicates the surface mixed layer (SML) depth.

Fig. 5 Dry bulk densities in bottom sediments from the Gerlache Strait, expressed in grams per cubic centimeter.

Fig. 6 Excess ^{210}Pb inventories (a) and surface activities (b) versus water column depth in bottom sediment cores from the Gerlache Strait.

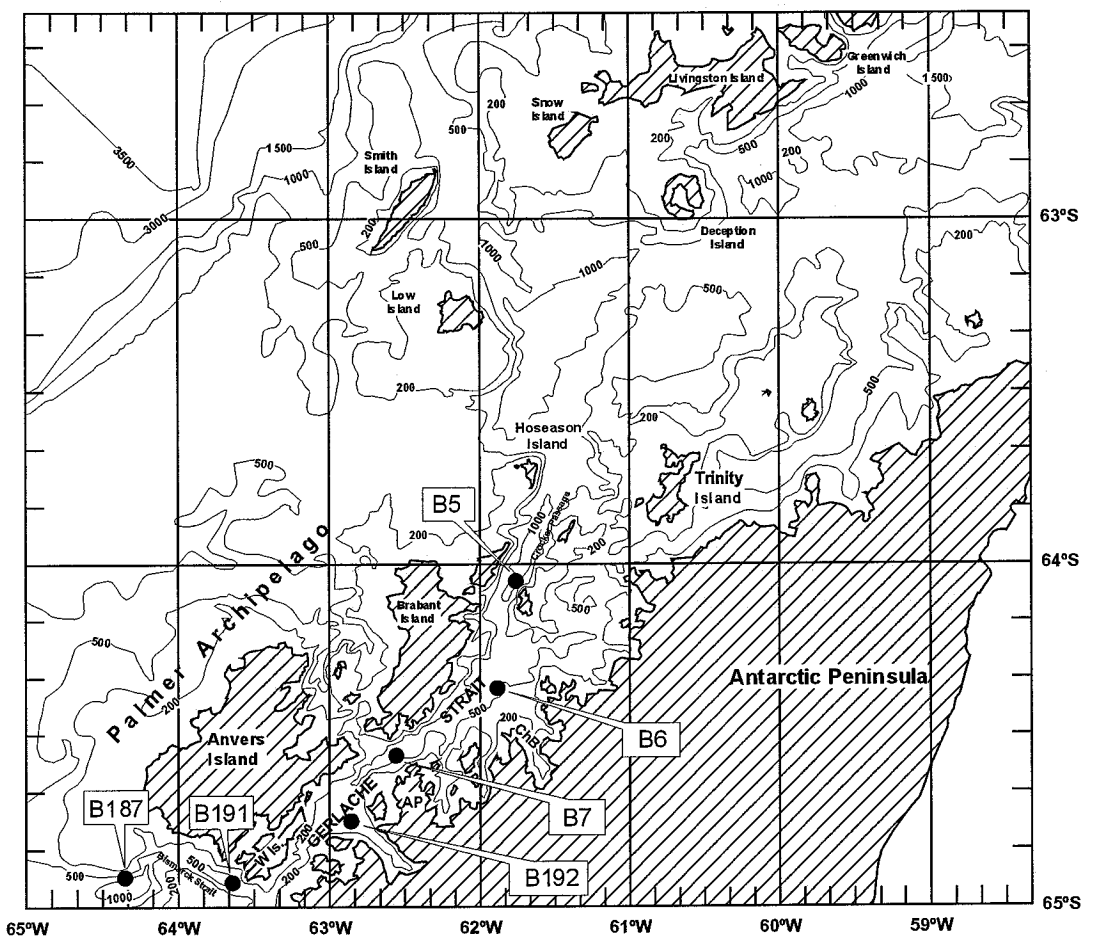
Greenwich Island
Livingston Island
Snow Island
Smith Island
Deception Island
Low Island
Hoseason Island
Trinity Island
B5
Brabant Island
Palmer Archipelago
Antarctic Peninsula
Anvers Island
B187
B191
B6
B7
B192
63°S
64°S
65°S
65°W
64°W
63°W
62°W
61°W
60°W
59°W

Fig. 1

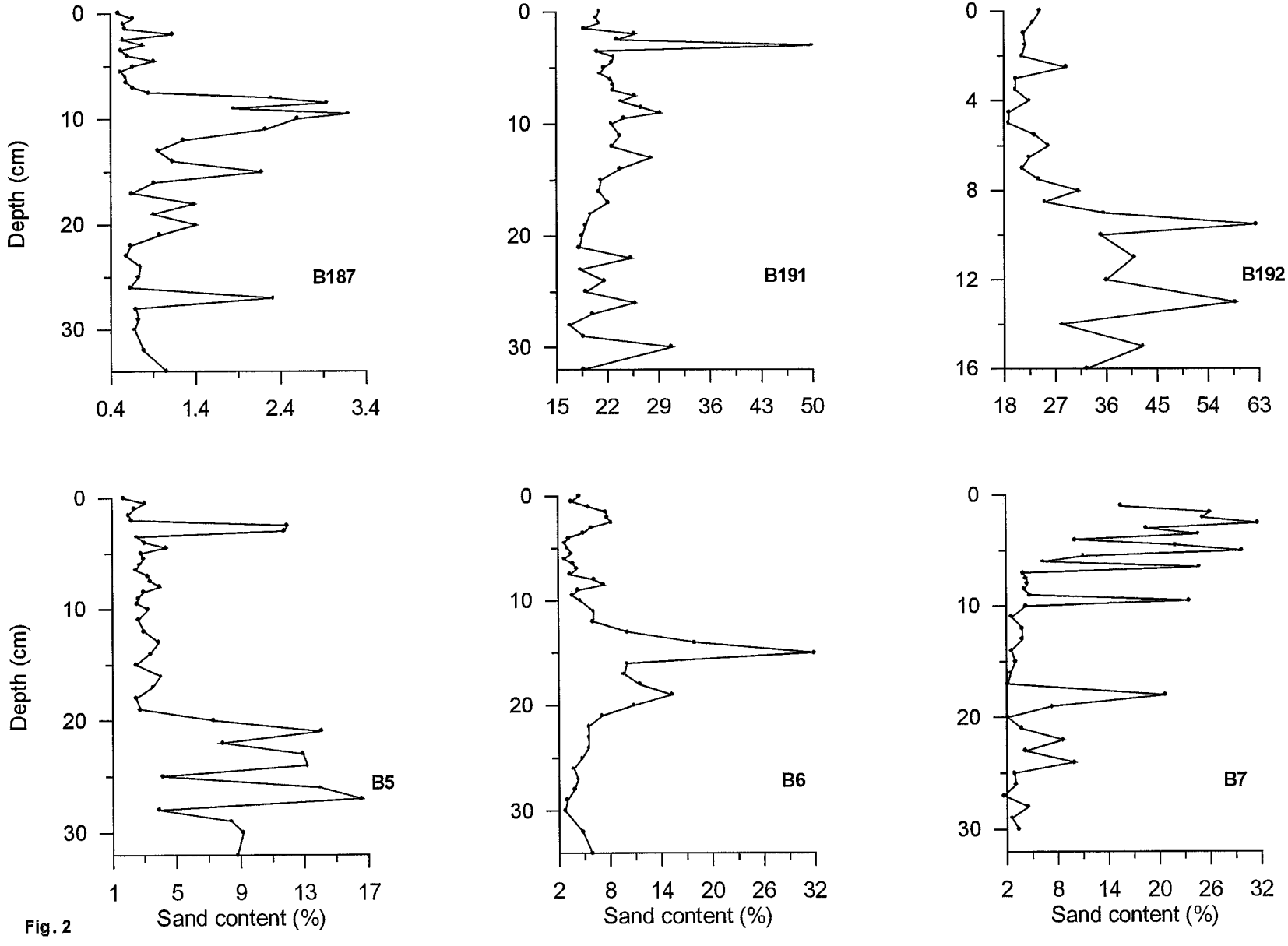
Depth (cm)
0
10
20
30
B187
0.4
1.4
2.4
3.4
B191
15
22
29
36
43
50
4
8
12
16
B192
18
27
36
45
54
63
B5
1
5
9
13
17
Sand content (%)
B6
2
8
14
20
26
32
B7

Fig. 2

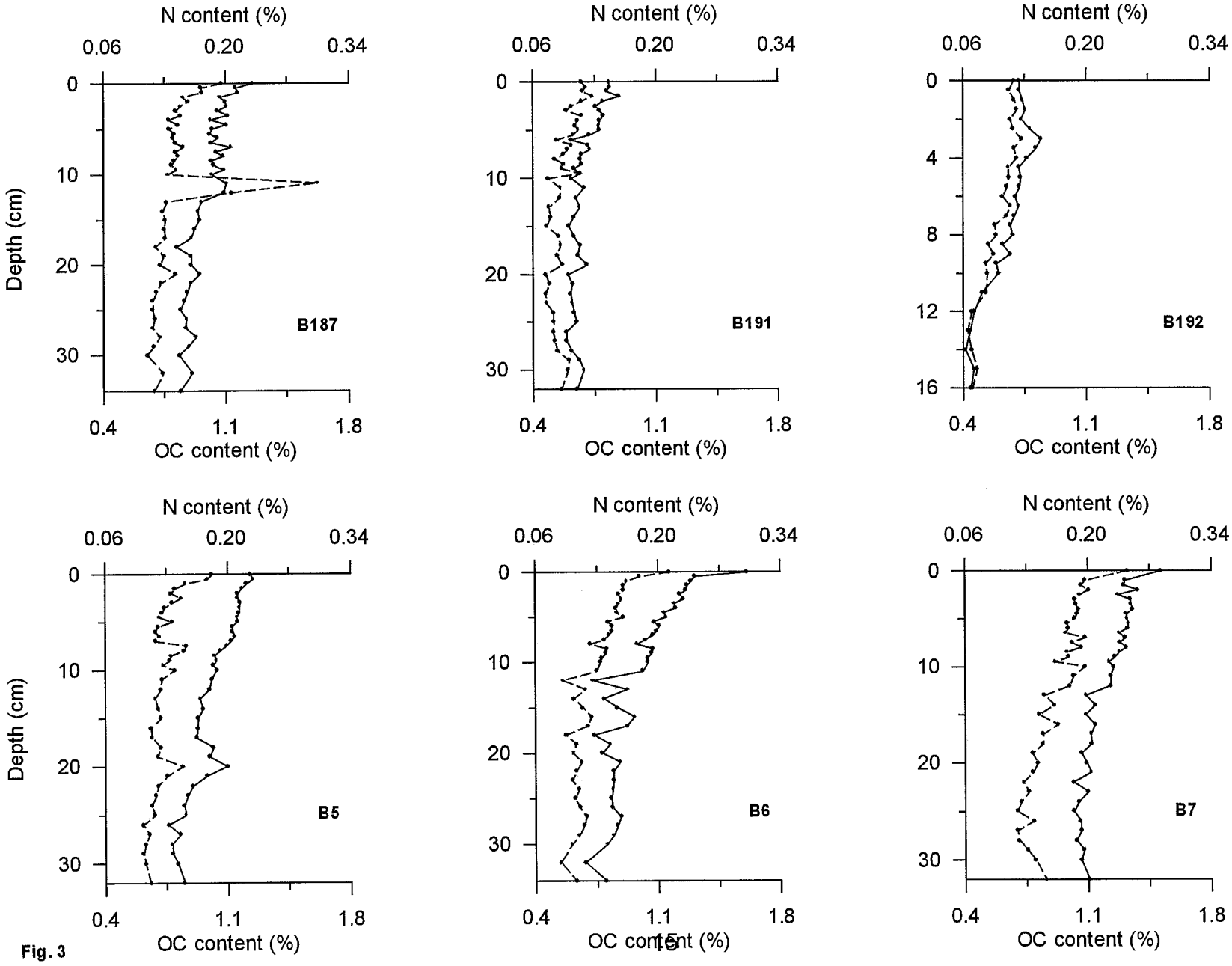
N content (%)
0.06
0.20
0.34
Depth (cm)
0
10
20
30
B187
0.4
1.1
1.8
OC content (%)
N content (%)
0.06
0.20
0.34
0
10
20
30
B191
0.4
1.1
1.8
OC content (%)
N content (%)
0.06
0.20
0.34
0
4
8
12
16
B192
0.4
1.1
1.8
OC content (%)
N content (%)
0.06
0.20
0.34
Depth (cm)
0
10
20
30
B5
0.4
1.1
1.8
OC content (%)
N content (%)
0.06
0.20
0.34
0
10
20
30
B6
0.4
1.1
1.8
OC content (%)
N content (%)
0.06
0.20
0.34
0
10
20
30
B7
0.4
1.1
1.8
OC content (%)

Fig. 3

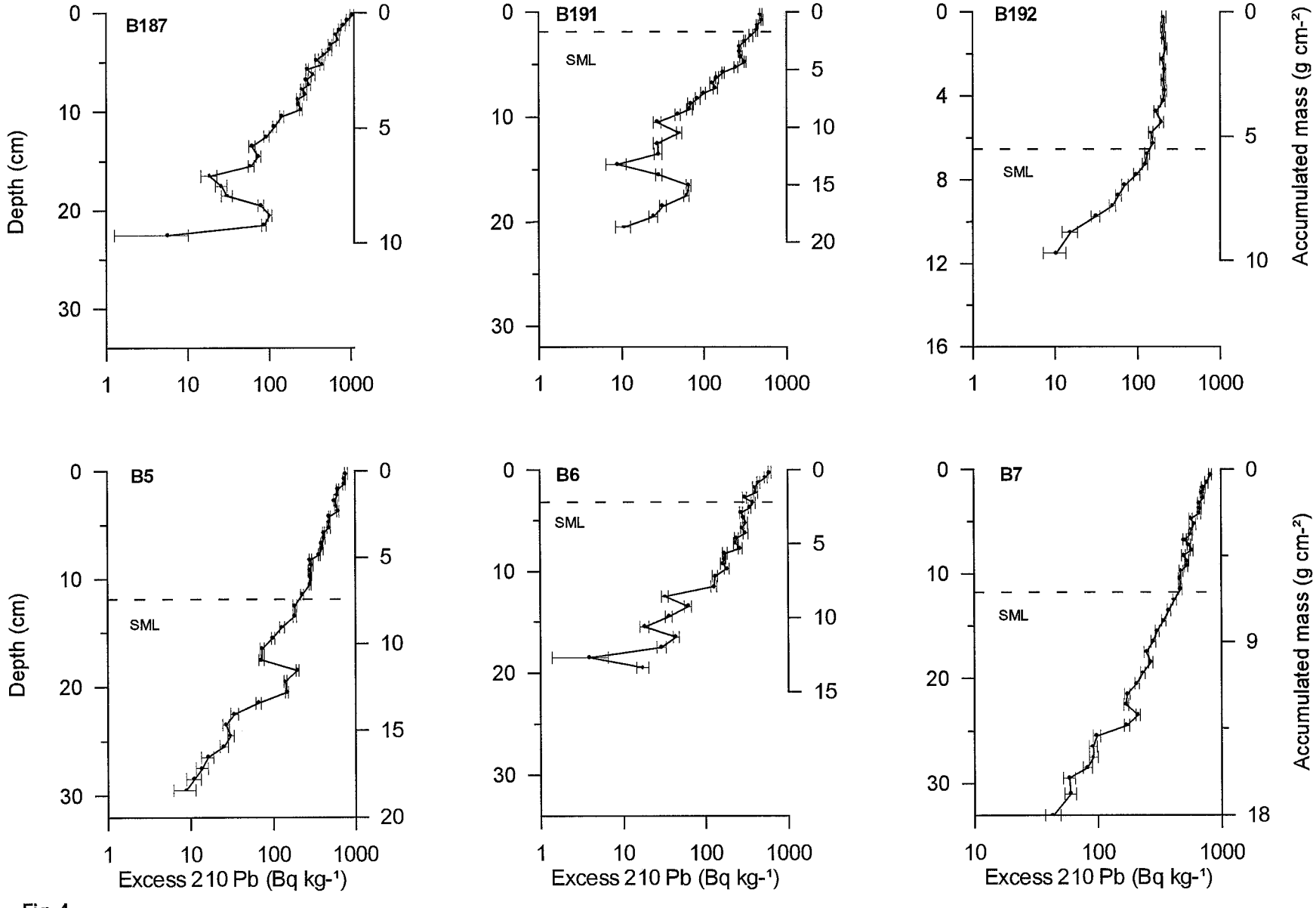
B187
B191
B192
B5
B6
B7
SML
Depth (cm)
Accumulated mass (g cm-2)
Excess 210 Pb (Bq kg-1)
1
10
100
1000

Fig. 4

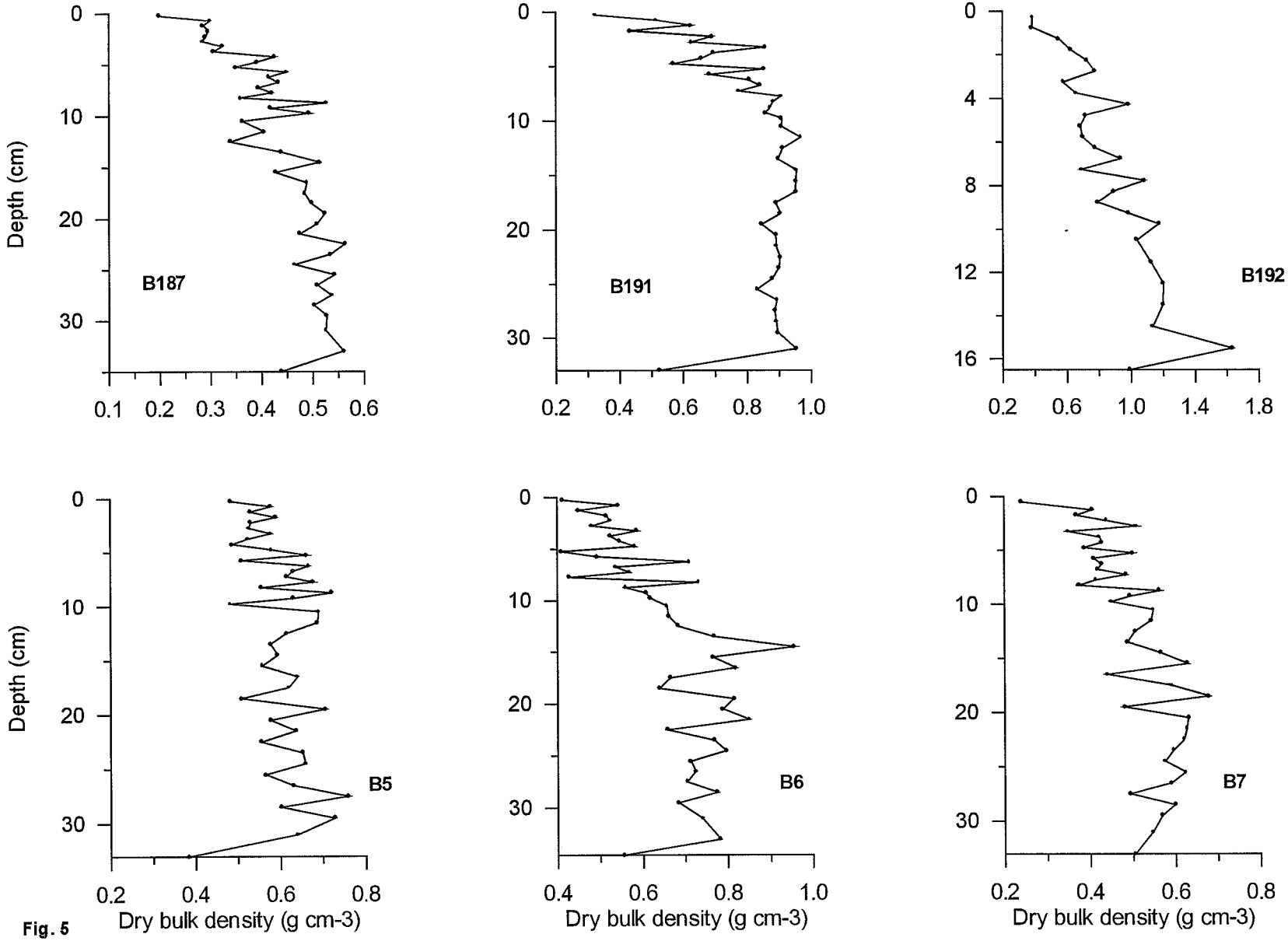
Depth (cm)
B187
B191
B192
B5
B6
B7
Dry bulk density (g cm-3)
Dry bulk density (g cm-3)
Dry bulk density (g cm-3)

Fig. 5

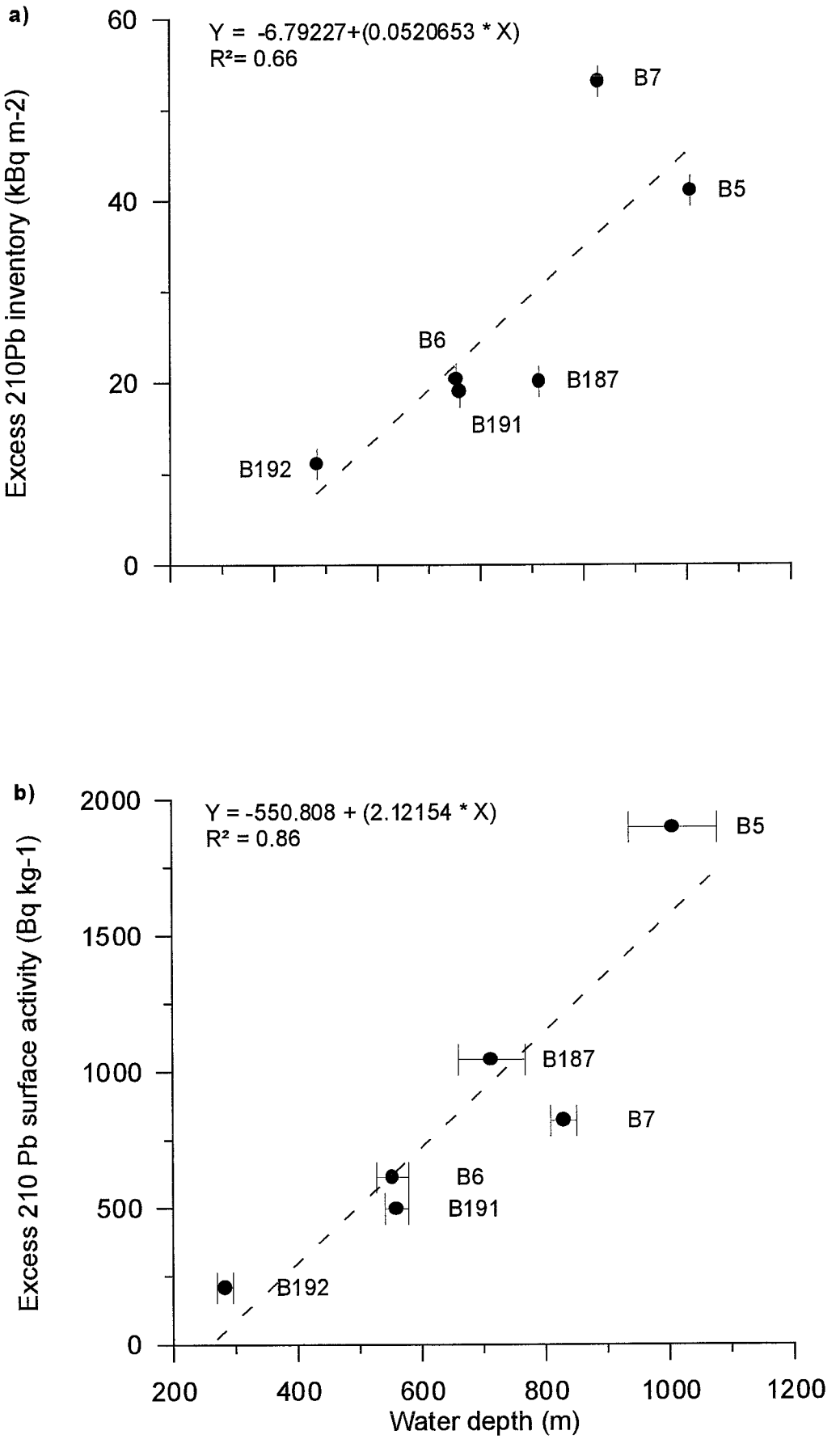
a)
Y = -6.79227+(0.0520653 * X)
R²= 0.66
Excess 210Pb inventory (kBq m-2)
60
40
20
0
B7
B5
B6
B187
B191
B192
b)
Y = -550.808 + (2.12154 * X)
R² = 0.86
Excess 210 Pb surface activity (Bq kg-1)
2000
1500
1000
500
0
B5
B187
B7
B6
B191
B192
200
400
600
800
1000
1200
Water depth (m)

Fig. 6

Table 1. Date, location coordinates, depth of recovery, and length of the core set taken at Gerlache Strait (Antarctic Peninsula) during the Fruela 95/96 expedition.

station	date	latitude (S)	longitude (W)	water depth (m)	length (cm)
B187	19/01/96	64º 54.05'	64º 27.52'	714	34
B191	04/02/96	64º 56.47'	63º 33.37'	560	32
B192	04/02/96	64º 45.21'	62º 51.44'	283	16
B7	20/01/96	64º 33.53'	62º 33.49'	830	32
B6	20/01/96	64º 22.38'	61º 53.23'	553	34
B5	19/01/96	64º 03.05'	61º 45.60'	1008	32

Table 2. Organic carbon (OC), nitrogen (N) and calcium carbonate ($CaCO_3$) average content and accumulation rate (AR), within and below the surface mixed layer (SML), burial efficiencies (BE), and mean apparent sediment accumulation rate (SAR) at each station. No SML was found in core 187.

core	SML		avg. OC	avg. N	avg. CaCO3	OC AR	BE	N AR	BE	CaCO3 AR	BE	SAR	SAR
	cm		%	%	%	g/m2y	%	g/m2y	%	g/m2y	%	g/m2y	mm/y
B187	—	surface	1.26	0.20	< 0.003	8.06 ± 0.38	79	1.28 ± 0.06	70	0.00	—	640 ± 30	1.71 ± 0.07
		core avg	1.00	0.14	0.06	6.40 ± 0.30		0.90 ± 0.04		0.38 ± 0.02			
B191	2	within	0.84	0.12	0.10	7.81 ± 0.42	80	1.12 ± 0.06	75	0.97 ± 0.05	86	930 ± 50	1.17 ± 0.07
		below	0.67	0.09	0.09	6.23 ± 0.33		0.84 ± 0.05		0.83 ± 0.05			
B192	6.5	within	0.75	0.12	0.62	4.73 ± 0.22	75	0.76 ± 0.04	75	3.89 ± 0.19	89	630 ± 30	0.65 ± 0.03
		below	0.56	0.09	0.55	3.53 ± 0.17		0.57 ± 0.03		3.47 ± 0.17			
B7	11	within	1.31	0.19	0.03	22.93 ± 0.11	83	3.33 ± 0.15	74	0.54 ± 0.02	159	1750 ± 80	3.11 ± 0.14
		below	1.09	0.14	0.05	19.08 ± 0.87		2.45 ± 0.11		0.86 ± 0.04			
B6	3	within	1.32	0.17	0.06	14.52 ± 1.18	71	1.87 ± 0.15	71	0.62 ± 0.05	204	1100 ± 90	1.57 ± 0.13
		below	0.94	0.12	0.12	10.34 ± 0.84		1.32 ± 0.11		1.28 ± 0.11			
B5	11	within	1.13	0.14	0.08	12.54 ± 1.35	81	1.55 ± 0.17	86	0.90 ± 0.01	85	1110 ± 120	1.80 ± 0.20
		below	0.91	0.12	0.07	10.10 ± 1.09		1.33 ± 0.14		0.76 ± 0.08			

Table 3. One-way ANOVA analysis of OC and N content and OC/N ratio within the surface mixed layer (SML) and below it, with a significance level of 0.05. Degrees of freedom are expressed as DF, mean square root as MSR. *** Significant difference ($p < 0.001$). n.s. Non-significant difference ($p > 0.05$).

variable	F test	DF	MSR within the SML	MSR below the SML
OC	65.30***	1	1.04	0.91
N	87.37***	1	0.38	0.33
OC/N	1.81 n.s.	1	2.71	2.74

Table 3. One-way ANOVA analysis of OC and N content and OC/N ratio within the surface mixed layer (SML) and below it, with a significance level of 0.05. Degrees of freedom are expressed as DF, mean square root as MSR. *** Significant difference ($p < 0.001$). n.s. Non-significant difference ($p > 0.05$).

variable	F test	DF	MSR within the SML	MSR below the SML
OC	65.30***	1	1.04	0.91
N	87.37***	1	0.38	0.33
OC/N	1.81 n.s.	1	2.71	2.74

ANNUAL EVOLUTION OF DOWNWARD PARTICLE FLUXES IN THE WESTERN BRANSFIELD STRAIT (ANTARCTICA) DURING THE FRUELA EXPERIMENT

Albert Palanques[1*], Enrique Isla[1], Pere Puig[1], Joan Albert Sanchez-Cabeza[2], Pere Masqué[2]

[1] Institut de Ciències del Mar (CSIC) Av. Joan de Borbó, s/n E-08039 Barcelona Spain.

[2] Departament de Física Universitat Autònoma de Barcelona E-08193 Bellaterra Spain.

Deep-Sea Research II (accepted)

*Corresponding author. Fax 34 93 221 73 40; e-mail: albertp@icm.csic.es

ANNUAL EVOLUTION OF DOWNWARD PARTICLE FLUXES IN THE WESTERN BRANSFIELD STRAIT (ANTARCTICA) DURING THE FRUELA EXPERIMENT

Albert Palanques[1*], Enrique Isla[1], Pere Puig[1], Joan A. Sanchez-Cabeza[2], Pere Masqué[2]

[1] Institut de Ciències del Mar (CSIC) Av. Joan de Borbó, s/n E-08039 Barcelona Spain.

[2] Departament de Física Universitat Autònoma de Barcelona E-08193 Bellaterra Spain.

[*]Corresponding author. Fax 34 93 221 73 40; e-mail: albertp@icm.csic.es

ABSTRACT

Particle fluxes in the SW Bransfield Strait basin were determined by means of sediment traps deployed at intermediate and near-bottom water depths. Sampling was carried out during a complete year, from March 1995 to February 1996, during the FRUELA experiment. Total mass fluxes, major constituents and 210Pb were analyzed to study the temporal evolution of downward particle fluxes and to determine the origin of particles transferred to this basin. Mid-depth particle fluxes were much lower than, and showed a different temporal evolution to, those near the bottom. Particle flux variability was mainly related to processes associated with ice dynamics and biological productivity. The particulate matter transfer and export at mid-depth was very low and most of it took place between November and February during four 15-day sampling periods of the year. Downward carbon export at mid-depths was produced mainly by fecal pellets. The near-bottom fluxes were high (1.1-5.3 g m-2 d-1) during the whole year, and the greatest carbon transfer took place by lateral transport of resuspended and winnowed particulate matter. This study provides a better understanding of sedimentation processes in glacial environments and the role of near-bottom particle fluxes in the carbon cycle.

Keywords: downward particle fluxes, sediment trap, carbon fluxes, lateral transport, Antarctic Peninsula

1. Introduction

The southern ocean occupies a position of special interest because of its role in atmospheric pCO2 control (Knox and McElroy, 1984). This interest has increased due to the urgent need to understand the biogeochemical cycle of carbon in relation to the recent anthropogenic increase of atmospheric CO2 (Bewer *et al.* 1986). Despite this interest, fewer direct flux measurements have been made in Antarctic seas than in low and mid-latitude oceans (Dunbar, 1984; Wefer *et al.*, 1990). Polar Oceans are strongly influenced by the extent of ice coverage, particularly of dynamic marginal ice zones (Smith and Nelson, 1986). Seasonal variation in primary production in these regions is great because short-lived blooms of phytoplankton take place when ice cover opens, supplying a significant amount of the annual production of biogenic particles (Honjo, 1990).

Most of the experiments concerning annual particle fluxes in polar oceans have been measured at least 300 m below the surface to avoid collision with ice, and always 300 m above the sea floor to avoid collecting the near-bottom fluxes affected by lateral transport of particles. As annual downward particle flux data from the upper 300 m of the water column are not available, there are limitations to relating deep-ocean particulate carbon (POC) flux data to surface productivity. However, the processes and fate of oceanic particles in the polar oceans are closely controlled by the high seasonal variability of primary production, with the exception of lithogenic particles, although light clay and organic particles are also aggregated by biological mediators and are strongly coupled in polar oceans (Honjo, 1990).

In the Antarctic oceans particle fluxes and pelagic organic carbon and calcium carbonate fluxes are smaller than in other oceans. However, in some Antarctic nearshore environments such as the Ross Sea and the Antarctic Peninsula, fluxes of biogenic and lithogenic particles were orders of magnitude higher than in the pelagic areas of the Weddell Sea (Wefer *et al.*,

1982; Dunbar *et al.*, 1995; Honjo 1990). One of these nearshore environments is the Bransfield Strait, a semienclosed sea bounded by the Antarctic Peninsula and the South Shetland Islands. There are three major basins in the western, central and eastern parts of the Bransfield Strait, separated by sills of about 500 m depth. The maximum depth of these basins increases from the western part (about 1000 m) to the eastern part (about 2500 m) (Huntley *et al.*, 1991, Gracia *et al.*, 1997; Canals *et al.*, 2000).

Previous experiments involving four-season time-series traps were conducted for several years at a 1900 m deep site in the central Bransfield basin south of King George Island (Dunbar, 1984; Dunbar *et al.*, 1985; Gersonde and Wefer, 1987; Wefer *et al.*, 1988; Wefer *et al.*, 1990; Abelmann and Gersonde, 1991). These studies indicated that over 95% of the annual flux at mid-depths occurred during December and January and that the annual flux could range from 11.9 g m-2 to 107.7 g m-2. About 50% of the mid-depth flux consisted of biogenic constituents (Wefer *et al.*, 1988; 1990) and the mode of sedimentation was characterized by the fact that 100% of the particles were transported downward by *Euphausia superba* fecal pellets (Wefer *et al.*, 1982, 1988; Dunbar, 1984). The flux of biologically produced particles can have an important lateral component, especially near the bottom in continental margins (Biscaye and Anderson 1994; Monaco, *et al.*, 1990; Heussner, *et al.*, 1999; Puig and Palanques, 1998). In Antarctic seas, there are practically no measurements of near-bottom fluxes transported laterally and their contribution to the carbon cycle is largely unknown.

During the "FRUELA" research project, downward particle fluxes were collected by sediment traps in the western Bransfield Strait south of Livingston Island during a year cycle at mid-depths and also near the seabed. The aim of this paper is to study the composition and annual variability of the downward fluxes of particulate matter in the western Bransfield Strait, and to analyze the contribution of the biogenic particles exported vertically out of the photic zone and the role of the lithogenic and biogenic particles transported laterally from shallower environments.

2. Methods

A mooring line equipped with two sequential sediment traps was deployed south of Livingston Island and west of Deception Island at 1000 m depth (Fig. 1). This area is located at the mouth of the Orleans canyon, which is incised along the northern Antarctic Peninsula slope. One sediment trap was placed 30 meters above bottom (mab), and the other trap was installed in mid-depth waters, 500 mab. Unfortunately, other moorings deployed in the surrounding area and equipped with additional sediment traps and current meters could not be recovered.

The sediment traps used in this study were Technicap model PPS3. The upper part of the traps' internal sample-collecting hull is cylindrical and has an inner diameter of 40 cm (a collecting area of 0.125 m2) and a height of 190 cm. These traps incorporate a carousel with 12 sampling bottles, which is controlled by a programmable motor to preset variable sampling intervals for each of the 12 sampling tubes (Heussner *et al.*, 1990). The sampling period comprised almost a complete year (345 days) from March 1st 1995 to February 15th 1996. In this experiment, the sample collecting interval was set to different time intervals: 60 days during late autumn-winter months (from April to September), 30 days in March and October and 15 days in spring and summer months (from November to February) in order to have a higher resolution during the spring and summer months.

Before the trap deployments, the sampling tubes were rinsed and filled with a 5% (~1.7 M) formalin solution prepared from Carlo Erba analytical grade 40% formaldehyde mixed with 0.2 µm filtered seawater to avoid the degradation of organic matter in the trapped particles. The solution was buffered (7.5<pH< 8) with Carlo Erba analytical grade sodium borate. After the trap recovery, the pH was checked and it indicated that the solutions remained buffered.

The collected samples were processed in the laboratory according to the method described by Heussner *et al.* (1990). The total sample was divided into several aliquots to obtain different subsamples for analyzing total mass flux, major constituents (organic carbon, calcium carbonate, opal and lithogenic components) and 210Pb. However, most of the mid-depth samples only had material for analyzing the total mass flux and the total carbon. The other analyses on the mid-depth samples could only be done in the three richest samples (late November, late December and early January). Zooplankton organisms, also called "swimmers", were removed by hand picking under a dissecting microscope using forceps and were stored for further analysis.

Sample dry weight was determined using three subsamples filtered onto 47 mm diameter, 0.45 µm preweighed Millipore filters rinsed with distilled water and dried at 40° C for 24 hours. Total mass flux was calculated from the sample dry weight, the collecting trap area and the sampling interval. Mean mass fluxes were weighted by time and mean concentrations of constituents were weighted by time and flux.

For carbon and nitrogen analyses, four subsamples were filtered onto 47 mm diameter preweighed Whatman GF/F glass microfiber filters that had previously been combusted at 550°C for 24 hours. Two subsamples were used to determine the total carbon (TC) and nitrogen percentages in a LECO CN 2000 analyzer. Another two subsamples were digested with HCl in a LECO CC 100 digestor and the resulting CO2 was analyzed in the same CN analyzer and assigned to inorganic carbon (IC) content. The difference between the two values (TC-IC) is the percentage of organic carbon (OC). The calcium carbonate (CaCO3) percentage is calculated by multiplying the IC content by 8.33.

Biogenic silica (opal) was analyzed using a wet-alkaline extraction with sodium carbonate using the method described by Mortlock and Froelich (1989). This analysis consists of a differential wet-chemical extraction into a 2 M Na2CO3 solution at 85 °C for 5 h. The wet-chemical dissolution technique appears to be the most versatile in its application to marine samples of various types and compositions (DeMaster, 1991).

The lithogenic component was computed as the difference between the total mass and the sum of the biogenic components (organic matter [twice the percentage of organic carbon], calcium carbonate and opal), as lithogenic components or aluminosilicates.

210Pb, a member of the 238U decay series with a half-life of 22.3 years, enters the oceans mainly via the atmosphere and through in situ production from radioactive decay of dissolved 226Ra. In addition, inputs from rivers could also be considered in coastal areas. The higher affinity of 210Pb for fine-grained particles and organic matter compared to that of 226Ra causes an excess of 210Pb with respect to 226Ra in the settling particles that are subsequently deposited on the sea floor. The 210Pb content in the downward particulate matter can be related with its origin. Particles newly settling from the surface can have a higher 210Pb content than those resuspended and transported laterally. 210Pb analyses were performed following the methodology described in Sanchez-Cabeza *et al.* (1998),

assuming that 210Pb was in secular equilibrium with its daughter 210Po. An aliquot of each sample was spiked with 209Po and totally digested using a microwave oven. After digestion, samples were made 1 N HCl and 209Po and 210Po were deposited onto silver disks, previously coated on one side with a plastic lacquer, and left at 60-70°C for 8 hours while stirring. Polonium isotopes were counted with α-spectrometers equipped with low-background SSB surface barrier detectors in vacuum conditions (EG&G Ortec). Chemical recoveries ranged from 93 to 100% and several reagent blank analyses were also carried out and subtracted for activity determination.

3. Results

Time series of total mass fluxes are shown in Figure 2 and time series of contents and fluxes of major constituents (organic carbon, calcium carbonate, biogenic silica and aluminosilicates) are shown in Figures 3 and 4 respectively. Mean annual total mass fluxes and mean annual contents and fluxes of major constituents measured by the sediment traps during the experiment are listed in Table 1.

3.1. Total mass fluxes

Total mass fluxes in the study site ranged from a minimum of about 0.1 mg m-2 d-1 recorded at mid-depth to a maximum of about 5000 mg m-2 d-1 recorded near the bottom (Fig. 2). The maximum total mass flux at mid-depth was 112 mg m-2 d-1 and occurred in spring (late November sampling period), whereas near the bottom it was 5321 mg m-2 d-1 and occurred in winter (August-September sampling period). Minimum values were 0.08 mg m-2 d-1 in intermediate waters and 1178 mg m-2 d-1 near the bottom, and occurred in early winter (April-May sampling period) and in late summer (early February sampling period) respectively. Total mass fluxes near the bottom were 1 to 4 orders of magnitude higher than those at mid-depth during the same sampling periods.

The temporal evolution of the total mass fluxes at the two depths was also very different (Fig. 2). Whereas the near-bottom fluxes were always within the same order of magnitude, at mid-depth 95% of the annual mass flux occurred within four 15-day periods of the experiment year (late November, late December, early January and early February), when particle fluxes were 2 to 3 orders of magnitude higher than during the rest of the year. For this reason, we assume the mean contents and the mean fluxes of major constituents during these sampling periods to be the mean annual contents and the mean annual fluxes of these constituents at mid-depth.

3.2. Organic Carbon

At the study site, the carbon content of the particulate matter was essentially organic (90 to 99% of the total carbon). In intermediate waters, the organic matter (OC) content during the three 15-day sampling periods with the highest total mass flux was quite constant (8.2 to 8.7%) and higher than that of near-bottom settling particles (Fig. 3A). During the rest of the year, only the TC content was available at mid-depth. However, considering the high OC/IC ratios (20 to 60) of the analyzed samples (Fig. 5B), we can assume the TC content as OC content for the periods of the lowest total mass flux at mid-depth. Following this assumption,

the estimated OC content at mid-depth could range from 6.8 to 18.7%. The highest OC content occurred during the August-September period, when the total mass flux was minimum (0.1 mg m-2 d-1). However, the lowest values of OC content (6 to 8%) were common to periods of different total mass flux. Thus, there was no clear relationship between the two parameters. The near-bottom OC content was relatively constant, ranging from 1.2 to 1.7% during most of the year, and only increasing to 3% in late summer (late January sampling period) (Fig. 3A).

Assuming the TC contents as OC contents during periods of low total mass, the OC fluxes at mid-depths ranged from 0.01 mg m-2 d-1 in early winter (April-May), when the total mass flux was minimum, to 9.8 mg m-2 d-1 in late spring (late November sampling period), when the total mass flux was maximum (Fig. 4B). In spite of this variability, the OC flux followed the same temporal pattern as the total mass flux (Fig. 2). This is because the variability of the total mass flux is much higher (within a factor of 100-1000) than that of the OC flux (within a factor of 2).

The OC flux near the bottom showed the same temporal pattern as the near-bottom total mass flux, because of the low variability of the OC content in the near-bottom settling particulate matter during the whole experiment. The near-bottom OC fluxes were 1 to 3 orders of magnitude higher than those measured at mid-depth during the same sampling periods. Near-bottom OC fluxes ranged from 26.7 mg m-2 d-1 in late summer (early February sampling period) to 73.5 mg m-2 d-1 in late winter (August-September sampling period), (Fig 4A).

3.3. Organic carbon to nitrogen ratio (mol/mol)

The OC to Nitrogen ratio (OC/N) of the settling material also showed a different pattern at the two depths (Fig. 5A). In intermediate waters this ratio reached the highest values (12.7 to 14.6) in winter, when total mass flux was minimum, and the lowest values (6.9 to 7.9) in the summer periods of highest total mass and OC fluxes (Fig. 5A). In October and November the OC/N increased to a value of about 10.

Near bottom, the OC/N of settling particulate matter ranged from 7.5 to 9.5 and was more constant than at mid-depths (Fig. 5A). The lowest ratios occurred in winter, coinciding with the highest ratios in intermediate waters. In summer, the near-bottom OC/N increased, reaching maximum values of about 9.5 in January and February, when the mid-depth ratios fell below near-bottom values (Fig. 5A).

3.4. Calcium Carbonate

The calcium carbonate is a major component of the particle flux that is estimated from the IC content. The IC percentaje in the study area was very low ranging between only 0.02% and 0.5%. Thus, the calcium carbonate in the settling particulate matter of the study area was also low and varied from 0.2% to 4.1% (Fig. 3B). In intermediate waters, the calcium carbonate content could only be determined in the three 15-day sampling periods of highest total mass flux. The late November sample, which corresponded to the highest total mass flux in intermediate waters, showed the same content (1.2%) as the one recorded near the bottom in the same period. However, in the late December-early January samples at mid-

depth the calcium carbonate content (4.1 and 1.8% respectively) were one order of magnitude higher than those recorded near the bottom during the same sampling periods, which were the lowest calcium carbonate values recorded during this study (about 0.2%). Near the bottom, the calcium carbonate content was quite constant (1 to 1.5) during most of the year, except in summer when both the lowest (0.16%) and the highest (3.11%) values were recorded, the former between mid-November and mid-January and the latter in March (Fig. 3B).

The calcium carbonate fluxes at mid-depth ranged from non-detectable to a maximum of 2.09 mg m-2 d-1 in mid-summer (late December sampling period). The maximum calcium carbonate fluxes did not correspond to maximum total mass fluxes (Fig. 4D). The calcium carbonate flux near the bottom had the same temporal evolution as the total mass flux, except in summer (Fig. 4C). This was due to the high carbonate content variations in summer. The calcium carbonate flux during the other seasons showed similar trends to the total mass flux because of its relatively constant content. The near-bottom calcium carbonate fluxes ranged from 4.8 mg m-2 d-1 in early autumn (March sampling period) to 54.9 mg m-2 d-1 in late spring (late November sampling period), coinciding with the maximum total mass flux (Fig. 4C).

3.5. Biogenic silica (opal)

Opal is the most abundant biogenic component in the particulate matter of the study area at both depths. At mid-depths, the opal content of the four sampling periods with highest total mass flux ranged from 12 to 26% (Fig. 3C). Near the bottom, the opal content ranged from about 14% in winter to about 17% in summer, except in late December and early January, when it fell to 12% (Fig. 3C).

At mid-depth, the opal fluxes during the four sampling periods of highest total mass flux ranged from 2.9 mg m-2 d-1 in late January to 30.2 mg m-2 d-1 in late November (Fig. 4F). The near-bottom opal fluxes were 1 to 2 orders of magnitude higher than those at mid-depth during the same sampling periods and ranged from 195 mg m-2 d-1 in early February to about 800 mg m-2 d-1 in late November and August-September (Fig. 4E). The opal flux had the same temporal pattern as the total mass flux because the variability of the total mass flux was much higher than that of the opal content.

3.6. Lithogenic components

The lithogenic components represent the major fraction of the settling particulate matter, both at mid-depth and near the bottom (Fig. 3D). At mid-depth, the lithogenic components during the three 15-day periods of highest total mass flux ranged from 54 to 58% (Fig 3D). Near the bottom, the lithogenic content ranged from a minimum of 75% to a maximum of 85% in early January.

The lithogenic flux had a relatively low variability and showed the same temporal pattern as the total mass flux. During the three periods of highest total mass flux at mid-depth, the lithogenic flux ranged from 29 to 61 mg m-2 d-1 (Fig. 4H). Near the bottom, the lithogenic flux ranged from 893 mg m-2 d-1 in the early February period to 4318 mg m-2 d-1 in the August-September period (Fig. 4G). The near-bottom lithogenic flux was 1 to 2 orders of magnitude higher than the lithogenic flux at mid-depth during the same sampling periods.

3.7. Lead-210

The concentration of 210Pb ranged from about 650 to 2000 Bq/kg (Fig. 6A). The only three available 210Pb measurements at mid-depth were obtained in summer. They ranged from 1200 to 1500 Bq/kg (Fig 6A) and were 1.4 to 2.3 times higher than the near-bottom ones during the same sampling periods. Near the bottom there was a decreasing trend from 1300 to 870 Bq kg-1 during autumn and winter (March to September), and a peak in October, followed by a sharper decrease during spring and summer (October to January), when the minimum value was recorded (650 Bq kg-1). The maximum value (2000 Bq kg-1) was recorded in February. This maximum peak was also observed for the calcium carbonate and the organic carbon contents. The mean near-bottom 210Pb concentration was 987 Bq kg-1.

210Pb fluxes (Fig. 6) show a temporal pattern similar to that of the total mass flux (Fig. 2), as all the fluxes of major constituents did. At mid-depth, the 210Pb flux during the three available periods ranged from 0.07 to 0.13 Bq m-2 d-1. From these fluxes, assuming a mean concentration of 1288 Bq/kg for the particulate matter collected by the intermediate trap during the rest of the year, the annual 210Pb flux at mid-depth was estimated at around 5.3 Bq m-2. Near the bottom, the 210Pb flux ranged from 1.5 Bq m-2 d-1 in early January to 4.6 Bq m-2 d-1 in the August-September and early December sampling periods (Fig. 6C). The mean near-bottom Pb flux was 3.5 Bq m-2 d-1 and the annual 210Pb flux near the bottom was 1310 Bq m-2.

4. DISCUSSION

Downward particle fluxes at the studied depths are fundamentally different. Mid-depth fluxes are largely biological and controlled mainly by settling of fecal pellets, whereas near-bottom fluxes are more dynamic, being mainly controlled by lateral transport of material supplied from shallower environments. These fluxes and the processes generating them are discussed in this section.

4.1. Mid-depth downward particle fluxes

The mid-depth downward fluxes at the study site were about 2 orders of magnitude lower than those of continental margins from other latitudes at similar depths (e.g. Biscaye, *et al.* 1988; Biscaye and Anderson, 1994; Heussner *et al.* 1996; Puig and Palanques, 1998). Even in the same Bransfield Strait, our annual total mass flux at mid-depth (4.11 g m-2) was up to one order of magnitude lower than that collected south of King George Island in 1984 (107 g m-2) (Wefer *et al.*, 1988, 1990). However, the measured annual flux was similar to that collected in 1985 (11.9 g m-2) and reported by Wefer *et al.* (1990), which is indicative of the high interannual variability of the mid-depth fluxes in the Bransfield Strait. The low downward particle fluxes at mid-depth could be related to the moderate primary production in this area (Varela *et al.*, this issue), and probably also to the morphology and hydrology of the study area. Numerous studies have addressed the influence of hydrodynamic effects on trap collection biases (e.g. Butman 1986, Gust *et al.* 1992, 1994), which would also explain the low amount of particles collected in the mid-depth trap. However, a field experiment by Gardner *et al.* (1997) using sediment traps with a geometry similar to that of PPS3 showed no decrease in collection efficiency at mean velocities of 1-22 cm s-1. In addition, another field experiment conducted by Heussner *et al.* (1999) with PPS3 sediment traps also

demonstrated the absence of relationship between total mass flux of particles and trap Reynolds number at mean speeds ranging from few cm s-1 to 12 cm s-1. Unfortunately, no current measurements were available for this deployment, but previous current meter data obtained at 400 m depth in the Bransfield Strait (Lopez *et al.*, 1994) showed that currents at mid-depths in summer were tidally dominated, with some maximum values of about 25-30 cm s-1 and typical residual currents of 15 cm s-1. Based on the results obtained by Gardner *et al.* (1997) and Heussner *et al.* (1999), little effect on collection efficiencies can be expected for this study, although due to the slightly higher current regime, the mid-depth fluxes could be affected by hydrodynamic bias to some degree.

During the mooring deployment, drifting sediment traps were used south of Livingston Island in the FRUELA cruises. These traps collected fluxes of 115 mg C m-2 d-1 and 175 mg C m-2 d-1 at the end of December 1995 and in January 1996 respectively (Anadon *et al.*, this issue). The carbon flux measured with the sequential trap at 500 m depth in late December and January represents about 3.3% of the surface fluxes measured by the drifting traps. However, we should consider that sequential traps cover 15-day sampling periods.

On the other hand, the mean primary production measured in the study area in spring was about 1 g C m-2 d-1 (Varela *et al.*, this issue). Thus, carbon fluxes at mid-depths in late December 1995 and January 1995 were less than 1% of the mean primary production. However, if we consider the annual productivity to be about 100 g C m2 (Varela *et al.*, this issue), the annual OC flux at mid depth represents only 0.35% of the annual productivity.

4.2. Near-bottom downward particle fluxes

In the Bransfield Strait, near-bottom fluxes had hardy been studied previously, and never during a complete annual cycle. The near-bottom fluxes found in this study were significantly high (from 1178 to 5321 mg m-2 d-1) and similar to those measured near the bottom in the eastern Bransfield Strait during only a one-month deployment (Gersonde and Wefer, 1987; Liebezeit and Bodungen, 1987). Compared to near-bottom fluxes in other areas at similar depths, our near-bottom sediment fluxes are only similar to those measured in the southern middle Atlantic Bight (Biscaye and Anderson, 1994) and within some submarine canyons, (e.g. Puig and Palanques 1998; Heussner *et al.*, 1996).

Although there are no near-bottom current data available for this particular area of the Bransfield Strait either in this experiment or in the scientific literature, there are some evidences indicating that bottom currents were not strong enough to induce significant biases in the collection efficiency of the bottom trap. The OC/N ratio, the OC content and the mean 210Pb activities of the settling particulate matter collected near the bottom are very similar to those of the surface sediment at the mooring site, which is mud (95% silt+clay) with a 210Pb activity of 987 Bq kg-1 (Masqué *et al.*, this issue) a OC/N ratio of 6-7 and an OC content of 1.3%. This indicates that the material collected by the sediment trap is of the same nature as that which ultimately accumulates on the sea floor, and that the near-bottom trap measured particle fluxes that may be representative of present sediment accumulation. The mean sediment accumulation rate determined from 210Pb was 351 ± 14 g m-2 y-1 (Masqué *et al.*, this issue). This accumulation rate, which is relatively high for these depths, indicates that the mooring site is a clear depositional environment of fine sediment. This is one fourth of the mean annual flux measured by the near-bottom trap (1326 g m-2). However, direct comparison between bottom sediment and trap data must be done with caution, as time

scales differ by a factor of about 100 (from 1 year to 100 years). Several factors, including interannual variability in downward particle fluxes, biological activity, and dynamics in the uppermost sediment column, might be a source of discrepancy between the two fluxes. The higher total mass flux of the near-bottom trap suggests that at least this trap did not underestimate downward particle fluxes. However, it is difficult to discern whether the near-bottom trap flux was inflated by hydrodynamic biases causing overtrapping. Based on the results obtained in field experiments by Gardner *et al.*, (1997) and Heussner *et al.*, (1999), few hydrodynamic effects on trap collection efficiency for the near bottom trap might be expected, unless high near-bottom currents operate in the deeper part of the basin at 1000 m depth. Taking into account the bottom morphology and the high accumulation rates of very fine sediment at the mooring site, bottom currents in the deep basin should not be high. All this suggests few hydrodynamic effects on trap collection efficiency for the near-bottom trap.

Besides the small hydrodynamic biases that may affect the collection efficiency of the two traps, the near-bottom fluxes at the study site were much higher than those at mid-depth. The annual total mass and OC fluxes increased from 500 to 1000 m water depth (30 m above bottom) by a factor of 324 and 53 respectively (Table 1). This great difference is not because the near-bottom fluxes of the Bransfield Strait are especially high but because mid-depth fluxes are extremely low.

During December 1995 and January 1996, the OC near-bottom flux was about 5% of the mean primary productivity during the same months estimated by Varela *et al.* (this issue) (about 1 g C m-2 d-1). If we consider the deployment period, the annual near-bottom OC flux represents 18% of the annual productivity of 100 g C m-2 estimated by Varela *et al.* (this issue). However, we should take into account that the Bransfield Strait can receive organic matter exported from the Gerlache Strait, where primary production is higher (Varela *et al*, this issue).

4.3 Sedimentary processes

Downward particulate matter has different characteristics during the year, which generally are not common to both sampling depths. The periods of highest fluxes at mid-depths were in spring when settling particulate matter had the highest opal content (>20%) and the lowest OC/N ratio (5.5-6.5), suggesting that they were related to phytoplankton blooms.

Near the bottom, between spring and summer there was an increase in terrigenous inputs, with lower organic matter content and 210Pb activity and higher OC/N ratio, indicating more degraded organic matter. This was probably caused by the effects of thaw, and perhaps by the effect of wave storms without ice cover supplying sediment particles from nearshore areas. In summer, the lithogenic flux decreased, whereas the organic carbon, the OC/N ratio, the 210Pb activity and the calcium carbonate increased, probably due to the rapid sinking of new material incorporated in fecal pellets. The increase in the OC/N could be due to grazing and degradation of pellets by meso and macro zooplankton in subsurface levels (Gonzalez and Smetacek, 1994; Noji et al., 1991).

In winter, the high near-bottom fluxes of low OC/N and the decreasing trend of the Pb activity occurring simultaneously with extremely low mid-depth fluxes of high OC/N ratio (Figs. 2 and 5A) suggest that there was a major and dominant lateral input of particles with fresh organic matter near the bottom. The maximum total mass flux in winter occurred in the August-

September period, coinciding with a decrease in the 210Pb activity. During these months, the near-bottom temperature in the central basin of the Bransfield Strait decreased dramatically from –0.8 to –1.55 °C (Canals, 1996). This temperature decrease probably corresponded to the sinking of dense water formed on the shelf by a winter cooling mechanism. The down-flow of dense bottom water could winnow the particles from shallow environments towards the deep basin. This mechanism could also flush out newly deposited unconsolidated sediment from the floor, causing a winter maximum of sediment transport, as was suggested for the Barens Sea by Honjo (1988).

The near-bottom Pb activity versus OC/N ratio show an inverse covariation during the year except in summer (samples 11, 12, and 1). This suggest a dominant lateral input from shallower environments during most of the year and a higher influence of fecal pellets newly settled and transported laterally in summer.

Swimmers and diatoms in the samples of the near-bottom trap were studied (Palanques *et al.*, in press), and also provided some indications for sedimentary processes. Among the amphipod fauna collected in this trap, there were some species not commonly found in the water column (*Orchomenella pinguides*) or never found in the water column (*Hirondella antarctica, Opisa sp. and Epimeriidae gen. sp.*). Similarly, polychaete fauna consisted of benthic species, which in the case of the *Scalibregmatids* live inside the sediment. Among the collected diatoms, the most significant species and genus were *Amphora, Cocconeis* (*C. fasciolata*), and *Grammatophora (G. angulosa*), which also are benthic. Another group of common species frequently trapped during the year are *Actinocyclus actinochilus, Navicula directa, N. glaciei, Thalasiosira antarctica and Fragiliariopsis kergelensis*, which are littoral species.

Many of the species collected in the near-bottom trap are abundant in shallow bays of the South Shetland Islands (Ahn *et al.*, 1997). Thus, the presence of these polychaetes, benthic amphipoda and diatoms in the near-bottom trap at 1000 m depth indicate that this fauna was resuspended in shallow environments and transported laterally basinward along with the non-living particles. The low OC/N ratio of near-bottom settling particles in the study area throughout the year could also be related to resuspension and lateral transport of benthic or recently sedimented planktonic organic matter. The relatively high near-bottom fluxes of major organic constituents cannot be explained by vertical fluxes at the mooring site, and must be due to lateral transport from more productive zones. The highest primary productivity of the study area is found on the Antarctic shelf and slope around the Orleans Canyon (Holm-Hansen and Mitchell, 1991), which may also receive material exported from the high productive waters of the Gerlache Strait (Varela *et al.*, this issue).

Near-bottom total mass flux and lithogenic content show an inverse correlation ($r = -0.7$; N:12) with Pb activity and OC/N ratio (Fig. 7A,B,C), indicating that increases of lithogenic supplies are related to material transported laterally from shallow environments with fresher organic matter. This also suggests an input of resuspended material from shallower environments with either benthic organisms and/or recently sedimented planktonic organic matter.

Resuspension in shallow Antarctic environments can occur due to several processes, such as friction of icebergs against the seabed, formation of dense water and polynyas, wind storms when there is no ice cover, and even internal waves. However, high and constant near-bottom fluxes during the whole year cannot be explained only by these processes, and

a continuously operating mechanism must be causing them. Time series of current data taken in the summer season by López *et al.* (1994) show that the local circulation in the Bransfield Strait is strongly influenced by tides and that surface (10-50 m water depth) maximum currents south of Deception Island were 30-40 cm s-1 towards the northeast. These maximum tidal currents are energetic enough to continuously resuspend fine sediment and benthic organisms on the continental shelves of the study area.

Bottom sediment on most of the continental shelves around the study site consists of sand and gravels. (Yoon *et al.*, 1992), which confirms that most of the fine particulate matter is transferred offshore. The narrow continental shelves and steep slopes of the study area can favor the shelf-slope sediment transfer mechanism towards the Bransfield Strait basins. The geostrophic current in the study area during summer is predominantly towards the northeast, and it has typical velocities of 15 cm s-1 and maximum velocities of around 20 cm s-1 (López *et al.*, 1994 Gomis *et al.*, this issue), This geostrophic current is energetic enough to winnow and transport fresh and resuspended particles advectively from the shelf towards the slope. In addition, the presence of a bottom nepheloid layer extending along the Orleans canyon axis towards the study site was observed in transmissometer profiles recorded during the December 95 FRUELA cruise (Fig. 8). These data indicate that there is an active mechanism transporting suspended particulate matter near the bottom through this canyon. Thus, suspended particulate matter transferred from the Antarctic shelf and upper slope around this canyon is probably collected and reoriented basinward, helping to maintain the high and permanent downward particle fluxes observed near the bottom in the western Bransfield Strait basin.

5. CONCLUSIONS

In the Western subbasin of the Central Branfield Strait, the mid-depth annual total mass flux during the year of deployment was extremely low (4.11 g m-2). Most of this flux settled in summer during a time period no longer than 60 days. The maximum mid-depth fluxes of all the major constituents also occurred during these periods and were associated with planktonic blooms. Vertical carbon export was mainly by fecal pellets, although mid-depth settling fluxes were very low in winter and contained degraded organic matter.

The annual near-bottom total mass fluxes were three orders of magnitude higher than those at mid-depth. Near-bottom fluxes were high during the whole year of experiment and in winter they were up to 4 orders of magnitude higher than those at mid-depth during the same sampling periods. The constantly high near-bottom fluxes of the study area indicate a permanent high transfer of sediment from shallow to deep environments. The most likely mechanism supplying this material is sediment resuspension by tidal currents over the shelf regions. Other mechanisms, such as ice friction with the seabed, ice melting or sinking of dense water, may contribute more sporadically to high near-bottom fluxes. The geostrophic current could winnow and transport particulate matter basinward, and the Orleans Canyon appears to funnel particles transferred from the continental shelf of the Antarctic Peninsula, reorienting them basinward.

The annual carbon flux at mid-depths and near the bottom represents 0.35% and 18% of the annual primary production respectively. Near-bottom flux includes benthic organisms and lithogenic particles that were resuspended from shallow environments and transported laterally basinward.

Thus, in Antarctic marginal seas and continental margins, lateral advection, resuspension and associated processes in the benthic boundary layer must be taken seriously into account in the study of biogeochemical cycles.

Acknowledgements. This research was supported by the project ANT94-1010 and MAR96-1781-CO2-01 funded by the "Comisión Interministerial de Ciencia y Tecnología". It also benefited from a pre-doctoral fellowship from CONACYT (Mexico), reference 92766. We thank the officers and crew of the RV Hespérides and all participants in the FRUELA cruises for their help and support during the surveys. We also express our gratitude to the "Unidad de Gestión de Buques Oceanográficos" (UGBO) for their logistic support and to the coordinator of the FRUELA project, R. Anadón.

REFERENCES

Abelmann A. and Gersonde, R. (1991) Biosiliceous particle flux in the Southern Ocean. *Marine Chemistry*, **35**, 503-536.

Ahn I-Y., H. Chung, J-S. Kang, S-H. Kang (1997) Diatom composition and biomass variability in nearshore waters of Maxwell Bay, Antarctica, during the 1992/1993 austral summer. *Polar Biology*, **17**,123-130

Amos A. F. (1987) RACER: physical oceanography of the western Bransfield Strait. *Antarctic Journal of the United States*, **22**, 137-140.

Anadón R., F. Alvarez-Marqués, E. Fernandez, M. Varela, M. Zapata, J.M. Gasol, D. Vaqué (2001). Vertical biogenic particle flux during austral summer in the Antarctic Peninsula area. *Deep sea Research*, **this issue**.

Biscaye P.E. and R.F. Anderson (1994) Fluxes of particulate matter on the slope of the southern Middle Atlantic Bigth: SEEP-II. *Deep-Sea Research II*, **41**, 459-509.

Biscaye, P.E., R.F. Anderson and B.L. Deck (1988) Fluxes of particles and constituents to the eastern United States continental slope and rise: SEEP-I. *Continental Shelf Research*, **8**, 855-904.

Bodungen B. V. (1986) Phytoplankton growth and krill grazing during spring in the Bransfield Strait, Antarctica-Implications from sediment trap collections, *Polar Biology*, **6**, 153-160.

Brewer P.G. K.W. Bruland, R.W. Eppley and J.J. McCarthy (1986) The Global Ocean Flux Study: Status of the U.S. GOFS program. *Eos*, **67**, 827-832.

Butman, C.A., Grant, W.D, Stolzenbach, K.D., (1986) Predictions of sediment trap biases in turbulent flows: a theoreticla analysis based on observations from the literature. Journal of Marine Research, **44**, 601-644.

Canals M. (1996) Detección de posibles fuentes hidrotermales submarinas en la cuenca de Bransfield (Antártida): Proyecto GEBRATERM. In: *Informe sobre las actividades científicas de España en la Antártida durante la Campaña 1995-1996*. J.R. Vericad and J. Cacho, editors, Comision Interministerial de Ciencia y Tecnología (CICYT). Madrid , pp. 85-88.

Canals, M., Urgeles, R., Calafat, M.A. (2000) Deep sea-floor evidence of past ice streams of the Antarctic Peninsula. *Geology*, **28**, 31-34.

DeMaster D.J. (1991) Measuring biogenic silica in marine sediments and suspended matter. In: *Marine particles: Analysis and Characterization*, D.C. Hurd and D.W. Spencer, editors, American Geophysical Union, pp. 363-367.

Dunbar R. B. (1984) Sediment trap experiments on the Antarctic continental margin, *Antarctic Journal of the United States*, **19**, 70-71.

Dunbar R. B., A. J. Macpherson and Wefer, G. (1985) Water-column particulate flux and seafloor deposits in the Bransfield Strait and southern Ross Sea, Antarctica. *Antarctic Journal of the United States*, **20** (5), 98-100

Garcia M.A., O. López, J. Sospedra, M. Espino, V. Gràcia, G. Morrison, P. Rojas, J. Figa, J. Puigdefàbregas, A.S.-Arcilla, (1994) Mesoscale variability in the Bransfield Strait region (Antarctica) during Austral summer. *Ann. Geophysicae*, **12**, 856-867.

Gardner W.D., P.E. Biscaye and M.J. Richardson, (1997) A sediment trap experiment in the Vema channel to evaluate the effect of horizontal particle fluxes on measured vertical fluxes. *Journal of Marine Research*, **55**, 995-1028.

Gersonde R. and G. Wefer (1987) Sedimentation of biogenic siliceous particles in Antarctic waters from the Atlantic sector. *Marine Micropaleontology*, **11**, 311-332.

Gomis D., M.A. García, O. López, A. Pascual (2001). Quasi-geostrophic 3D Circulation and mass transport in the Western Bransfield Strait during Austral summer. *Deep Sea Research*, **this issue**

Gonzalez, H.E. and V. Smetacek (1994) The possible role of the cyclopoid copepod Oithoma in retarding vertical flux of zooplancton faecal material. *Marine Ecology Progress Series*, **113**, 233-246.

Gordon A. L. and W. D. Nowlin (1978) The basin waters of the Bransfield Strait. *Journal of Physical Oceanography*, **8**, 258-264.

Gràcia, E. Canals, M., Farràn, M., Sorribas, J, and Pallàs, R. 1997. Central and Eastern Bransfield Basins (Antarctica) from high resolution swath-bathymetry data. *Antarctic Science* **9**, 168-180.

Grelowski, A., A. Majewicz and M. Pastuszak (1986) Mesoscale hydrodynamic processes in the region of Bransfield Strait and the southern part of Drake Passage during BIOMASS – SIBEX 1983/84, *Polish Polar Reseach*, **7**, 353-369.

Gust, G., Byrne, R.H., Bernstein, R.E., Betzer, P.R., Bowles, W. (1992) Particle fluxes and moving fluids: experience from synchronous trap collections in the Sragasso Sea. *Deep Sea Research*, **39**, 1071-1083.

Gust, G., Michaels, A.F., Johnson, R., Deuser, W.G., Bowles, W. (1994) Mooring line motions and sediment trap hydromechanics: in situ intercomparison of three common deployment designs. *Deep Sea Research Part-I*, **41**, 831-857.

Heussner S., C. Ratti and J. Carbonne (1990) The PPS 3 time-series sediment trap and the trap sample processing techniques used during the ECOMARGE experiment. *Continental Shelf Research*, **10**, 943-958.

Heussner, S., A.M. Calafat and A. Palanques (1996) Quantitative and qualitative features of particle fluxes in the North-Balearic Basin. In: EUROMARGE-NB Final Report, MAST II Programme, E. U., M. Canals, J. L. Casamor, I. Cacho, A. M. Calafat and A. Monaco (editors), Barcelona, Vol. II, pp. 43-66.

Heussner, S., Durrieu de Madron, X., Radakovitch, O., Beaufort, L., Biscaye, P.E., Carbonne, J., Delsaut, N., Etcheber, H., Monaco, A. (1999) Spatial and temporal patterns of downward particle fluxes on the continental slop of the Bay of Biscay (northeastern Atlantic). *Deep-Sea Research Part-II*, **46**, 2101-2146.

Holm-Hansen O. H. and B. G. Mitchell (1991) Spatial and temporal distribution of phytoplankton and primary production in the western Bransfield Strait region. *Deep-Sea Research Part-II*, **38**, 961-980.

Honjo S. (1990) Particle fluxes and modern sedimentation in the polar oceans. In: *Polar Oceanography. part B: Chemistry, Biology and Geology.* W. O. Smith, Jr., editors, Academic Press, Inc. pp. 687-739.

Honjo S., S.J. Manganini and G. Wefer (1988) Annual particle flux and a winter outburst of sedimentation in the northern Norwegian Sea. *Deep Sea Research*, **35**, 1223-1234.

Huntley, M., Karl. D.M., Niler, P. and Holm-Hansen, O. 1991. Research on Antarctic Ecosystem Rates (RACER): an interdisciplinary field experiment. *Deep-Sea Research Part-II*, **38**, 911-941.

Knox F. and McElroy, B. 1984. Changes in atmospheric CO_2: Influence of the marine biota at high latitudes. *Journal of Geophysical Research* , **89**, 4629-4337.

Leventier A., (1991) Sediment trap diatom assemblages from the northern Antarctic Peninsula region. *Deep-Sea Research*, **38 (8/9)**, 1127-1143.

Liebezeit G., and B. von Bodungen (1987) Biogenic fluxes in the Bransfield Strait: planktonic versus macroalgal sources. *Marine Ecology-Progress serie*,**36**, 23-32.

Lipski M. (1982) The distribution of chlorophyll a in relation to the water masses in the southern Drake Passage and Bransfield Strait (BIOMASS-FIBEX, February-March 1981). *Polish Polar Research*, **3**, 143-152.

López O., M.A. García and A. S.-Arcilla (1994). Tidal and residual currents in the Bransfield Strait, Antarctica. *Annales Geophysicae*, **12**, 887-902.

Masqué P., E. Isla,, J.A. Sanchez-Cabeza, A. Palanques, J.M. Bruach, P. Puig and J. Guillén (2001) Sediment accumulation rates and carbon fluxes to bottom sediments at the Western Bransfield basin (Antarctica). *Deep Sea Research*, **this issue**.

Monaco, A., P. E. Biscaye, J. Soyer, R. Pocklington and S. Heussner (1990) Particle fluxes and ecosystem response on a continental margin: the 1985-1988 Mediterranean ECOMARGE experiment. *Continental Shelf Research*, **10**, 809-839.

Mortlock R.A. and P.N. Froelich (1989) A simple method for the rapid determination of biogenic opal in pelagic marine sediments. *Deep-Sea Research*, **36**, 1415-1426.

Noji T.T., K.W. Estep, F. MacIntyre and F. Norrbin (1991) Image analysis of faecal material grazed upon three species of copepods: Evidence for coprohexy, coprohagy and coprochaly. *Journal Marine Biological Association UK*, **71**, 465-480.

Puig P. and A. Palanques (1998) Temporal variability and composition of settling particle fluxes on the Barcelona continental margin (Northwestern Mediterranean). *Journal of Marine Research*, **56**, 639-654.

Rojas R.(1986) Thermal Structure and heat fluxes at Bransfield Strait during SIBEX 1985 (SIBEX – Phase II, Chile), *INACH Serie Científica*, **35**, 39-63.

Sánchez-Cabeza, J.A., Masqué, P., Ani-Ragolta, I. (1998) 210Pb and 210Po analysis in sediments and soils by microwave acid digestion. *Journal of Radioanalytical and Nuclear Chemistry*, **227**, 19-22.

Sievers H. A. (1982) Descripción de las condiciones oceanográficas físicas, como apoyo al estudio de la distribución y comportamiento del krill. *INACH Serie Científica*, **28**, 87-136.

Smith, W.O., Jr. and D.M. Nelson (1986) The importance of ice edge phytoplankton blooms in the Southern Ocean. *BioScience*, **36**, 251-257.

Varela M., E. Fernandez, P. Serret (2001) Size-fractionated phytoplancton biomass and primary production in the Gerlache and South Bransfield Straits (Antarctic Peninsula) in austral summer 95-96. *Deep Sea Reseach*, **this issue**.

Wefer G., G. Fisher, D.K. Fütterer, R. Gersonde, (1988) Seasonal particle flux in the Bransfield Strait, Antarctica. *Deep Sea Research*, **35** (6), 891-898.

Wefer G., G. Fisher, D.K. Fütterer, R. Gersonde, S. Honjo and D. Ostermann, (1990) Particle sedimentation and productivity in Antarctic waters of the Atlantic sector. In: *Geological History of the Polar Oceans: Arctic Versus Antarctic,* U. Beil and J. Thiede, editors, Kluwer Academic Publishers, The Netherlands, pp. 363-379.

Wefer G., E. Suess, W. Balzer, G. Liebezeit, P. J. Muller, A. Ungerer and W. Zenk (1982). Fluxes of biogenic components from sediment trap deployment in circumpolar waters of the Drake Passage. *Nature* (London), **299**, 145-147.

White J. The use of sediment traps in high-energy environments. *Marine Geophysical Researches*, **12**, 145-152.

Yoon H.I., M.W. Han, B.K. Park, S.J. Han and J.K. Oh, (1992) Distribution, provenance, and dispersal pattern of clay minerals in surface sediment, Bransfield Strait, Antarctica, *Geo-Marine Letters*, **12**, 223-227.

FIGURES

Figure 1: Bathymetric map of the western Bransfield Strait showing the position of sediment traps (triangle) and the locations of hydrographic stations (dots) distributed in a hydrographic transect (Fig. 8) across the Bransfield Strait and along the Orleans Canyon.

Figure 2: Times series of total mass fluxes of settling particulate matter collected at (A) mid-depth (500 m water depth) and (B) near the bottom (1000 m water depth and 30 m above bottom) during the FRUELA experiment.

Figure 3: Time series of major constituents contents of settling particulate matter during the FRUELA experiment: organic carbon (A), calcium carbonate (B), opal (C) and lithogenic fraction (D) at mid-depth (open squares) and near the bottom (black dots).

Figure 4: Time series of the major constituents fluxes of settling particulate matter at mid-depth and near the bottom during the FRUELA experiment. Near-bottom organic carbon (A), mid-depth calculated organic carbon (B), calcium carbonate (C, D), opal (E, F) and lithogenic fraction (G, H).

Figure 5: Time series of ratios of biogenic components on the settling particulate matter during the FRUELA experiment. OC/N (mol/mol) (A), OC/IC (B), OC/Opal (C), at mid-depth (open squares) and near the bottom (black dots).

Figure 6: Time series of ^{210}Pb concentration (A), at mid-depth (open squares) and near the bottom (black dots), and ^{210}Pb fluxes at mid-depth (B) and near the bottom (C) during the FRUELA experiment.

Figure 7: Concentration of near-bottom ^{210}Pb plotted against near-bottom total mass flux (A), Lithogenic content (C) and OC/N ratio (D). Near-bottom OC/N ratio plotted against total mass flux (B). Numbers indicate the sequential number of samples as they were collected by the sediment trap. 1: March, 2: April and May, 3: June and July, 4: August and September, 5: October, 6: 1-15 November, 7: 16-30 November, 8: 1-15 December, 9: 16-31 December, 10: 1-15 January, 11: 16-31 January, 12: 1-15 February.

Figure 8: Transect of beam attenuation coefficient across the western Bransfield Strait and along the Orleans Canyon (station positions are shown in Fig. 1). Note the presence of a wide bottom nepheloid layer developed along the Orleans Canyon towards the basin where the sediment traps (black rectangles) were deployed.

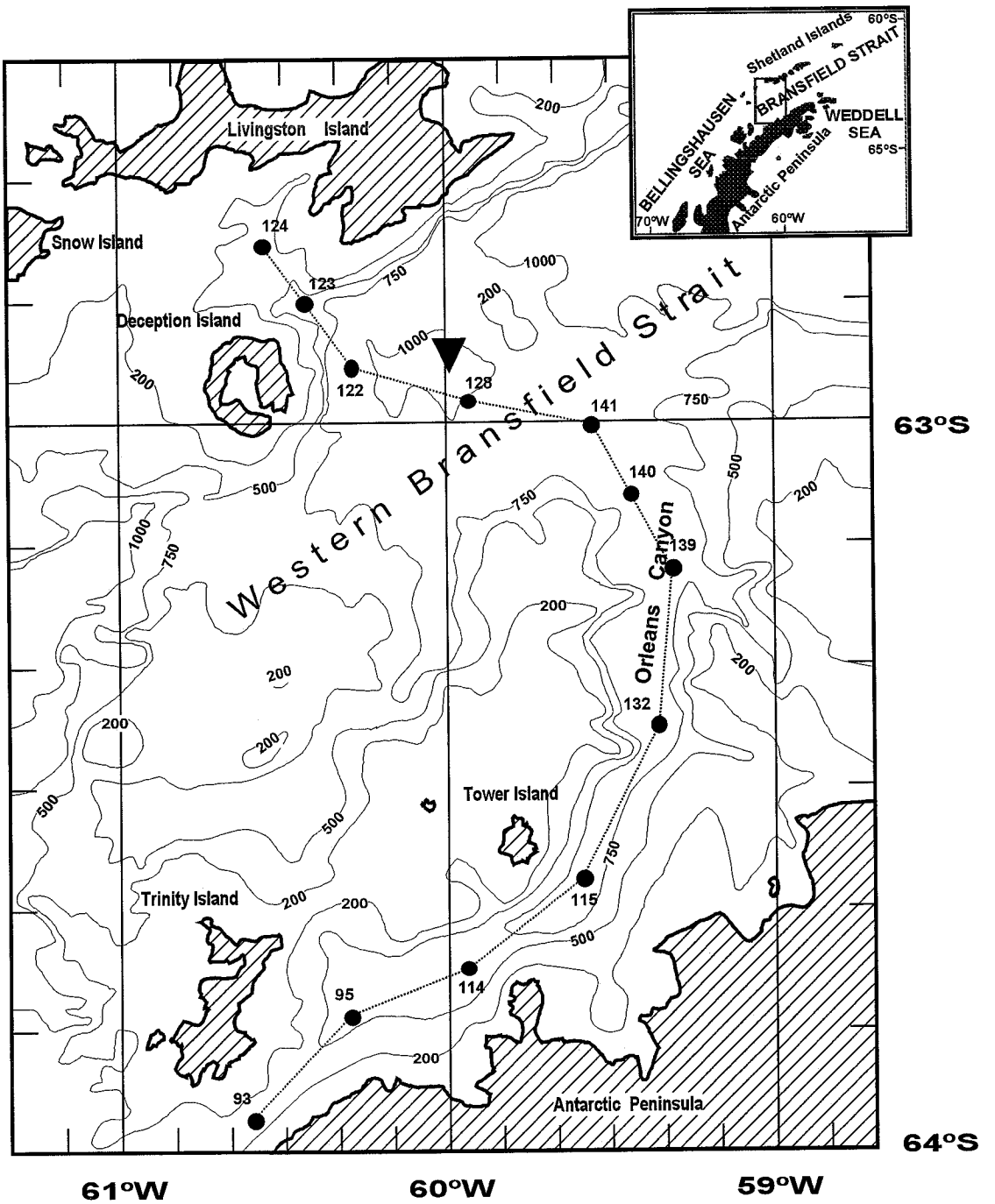
Livingston Island
Snow Island
Deception Island
Western Bransfield Strait
Orleans Canyon
Tower Island
Trinity Island
Antarctic Peninsula
124
123
122
128
141
140
139
132
115
114
95
93
200
500
750
1000
63°S
64°S
61°W
60°W
59°W
Shetland Islands
60°S
BRANSFIELD STRAIT
WEDDELL SEA
65°S
BELLINGSHAUSEN SEA
Antarctic Peninsula
70°W
60°W

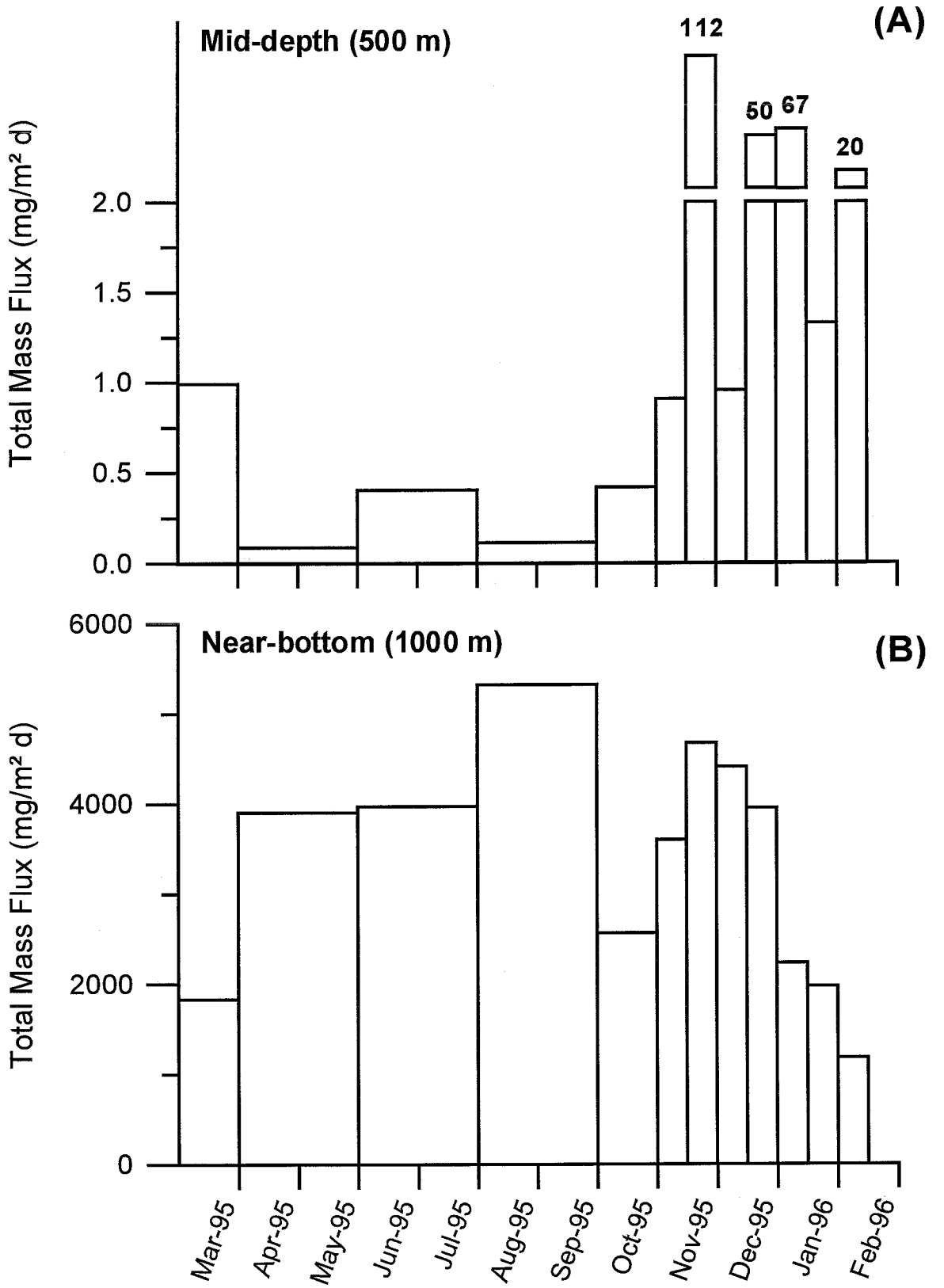
(A)
Mid-depth (500 m)
Total Mass Flux (mg/m² d)
112
50
67
20
2.0
1.5
1.0
0.5
0.0
(B)
Near-bottom (1000 m)
Total Mass Flux (mg/m² d)
6000
4000
2000
0
Mar-95
Apr-95
May-95
Jun-95
Jul-95
Aug-95
Sep-95
Oct-95
Nov-95
Dec-95
Jan-96
Feb-96

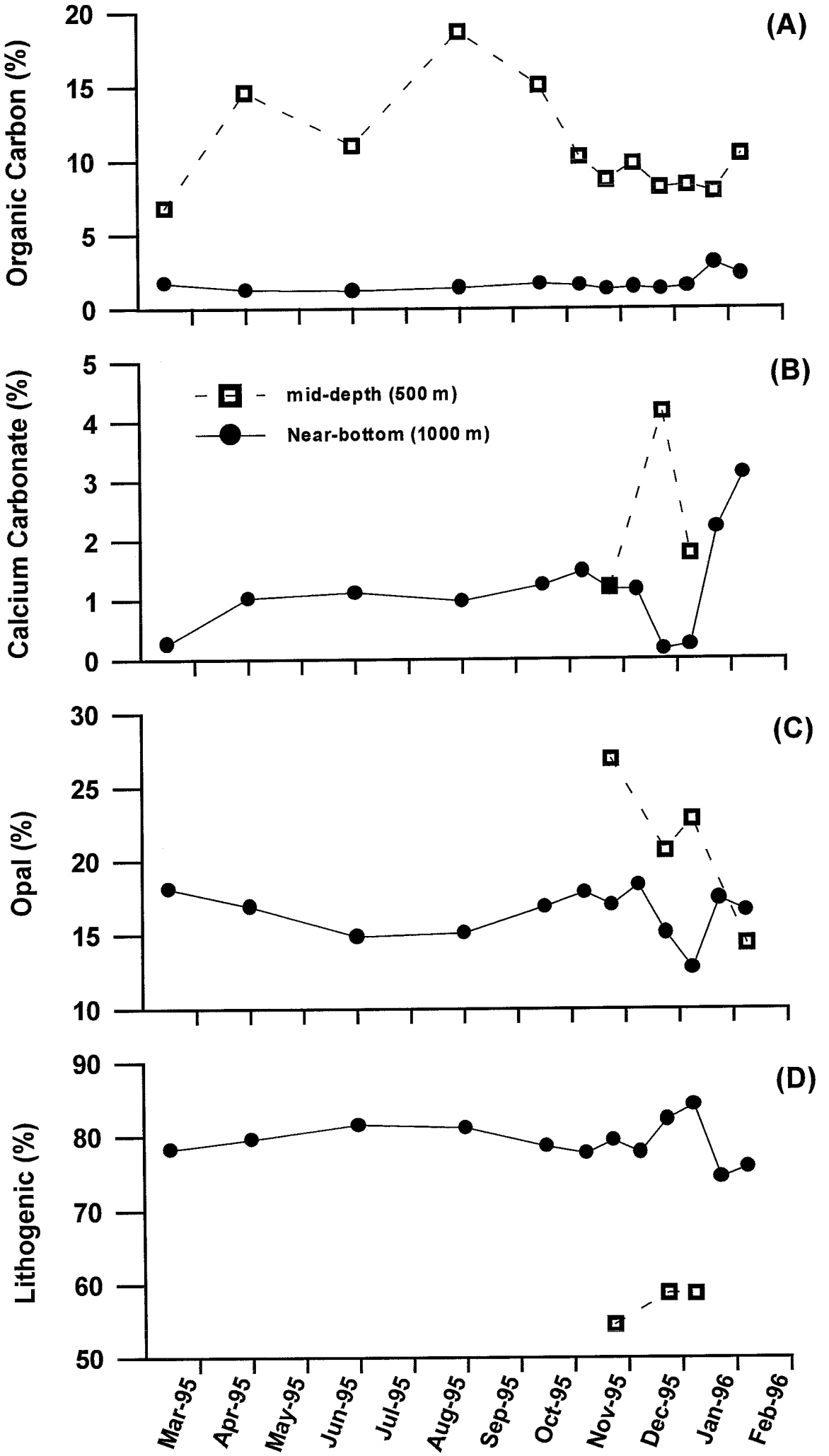
(A)
Organic Carbon (%)
20
15
10
5
0
(B)
Calcium Carbonate (%)
5
4
3
2
1
0
mid-depth (500 m)
Near-bottom (1000 m)
(C)
Opal (%)
30
25
20
15
10
(D)
Lithogenic (%)
90
80
70
60
50
Mar-95
Apr-95
May-95
Jun-95
Jul-95
Aug-95
Sep-95
Oct-95
Nov-95
Dec-95
Jan-96
Feb-96

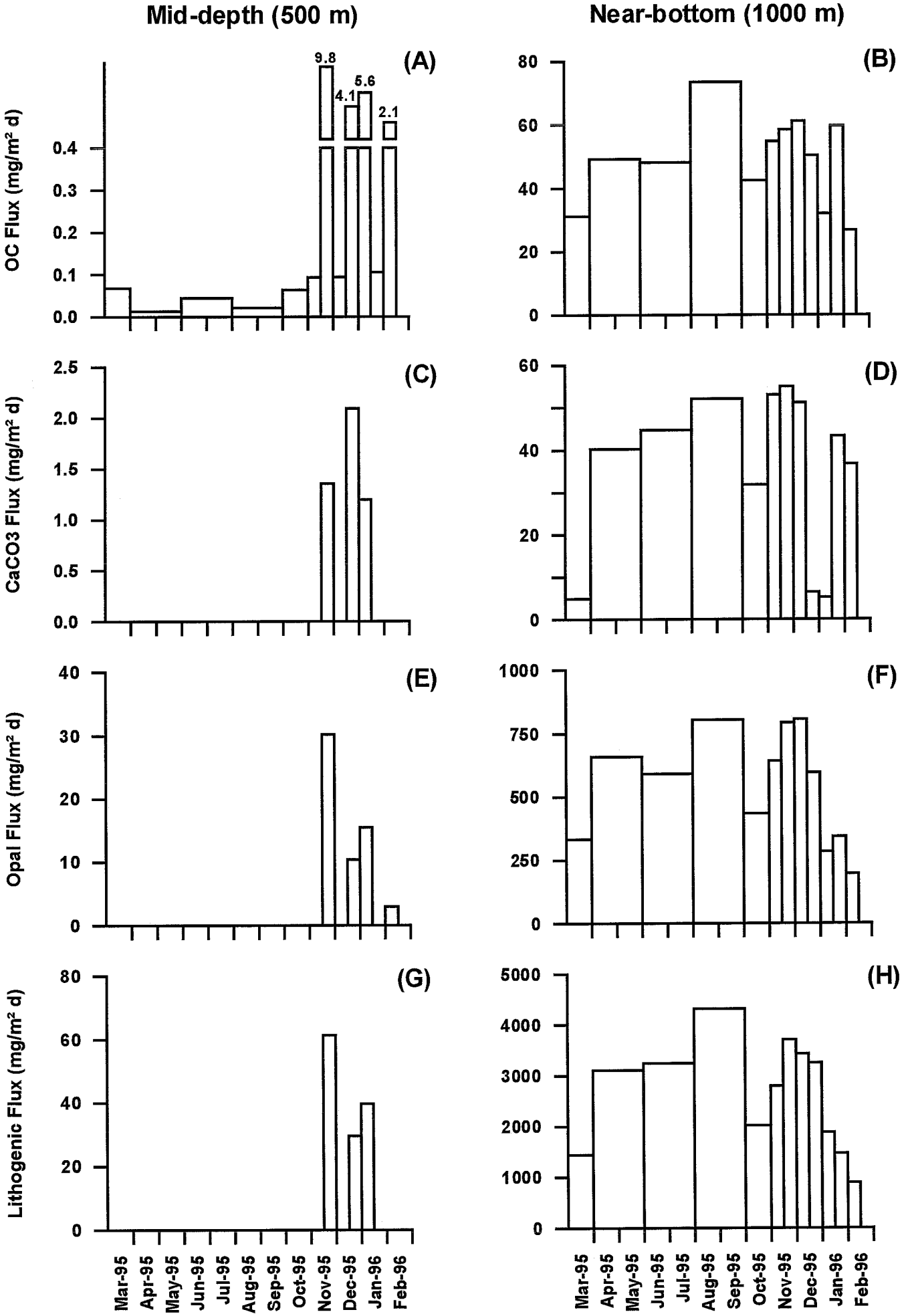
Mid-depth (500 m)
Near-bottom (1000 m)
(A)
(B)
(C)
(D)
(E)
(F)
(G)
(H)
OC Flux (mg/m² d)
CaCO3 Flux (mg/m² d)
Opal Flux (mg/m² d)
Lithogenic Flux (mg/m² d)
9.8
5.6
4.1
2.1
0.0
0.1
0.2
0.3
0.4
0
20
40
60
80
0.5
1.0
1.5
2.0
2.5
10
30
250
500
750
1000
2000
3000
4000
5000
Mar-95
Apr-95
May-95
Jun-95
Jul-95
Aug-95
Sep-95
Oct-95
Nov-95
Dec-95
Jan-96
Feb-96

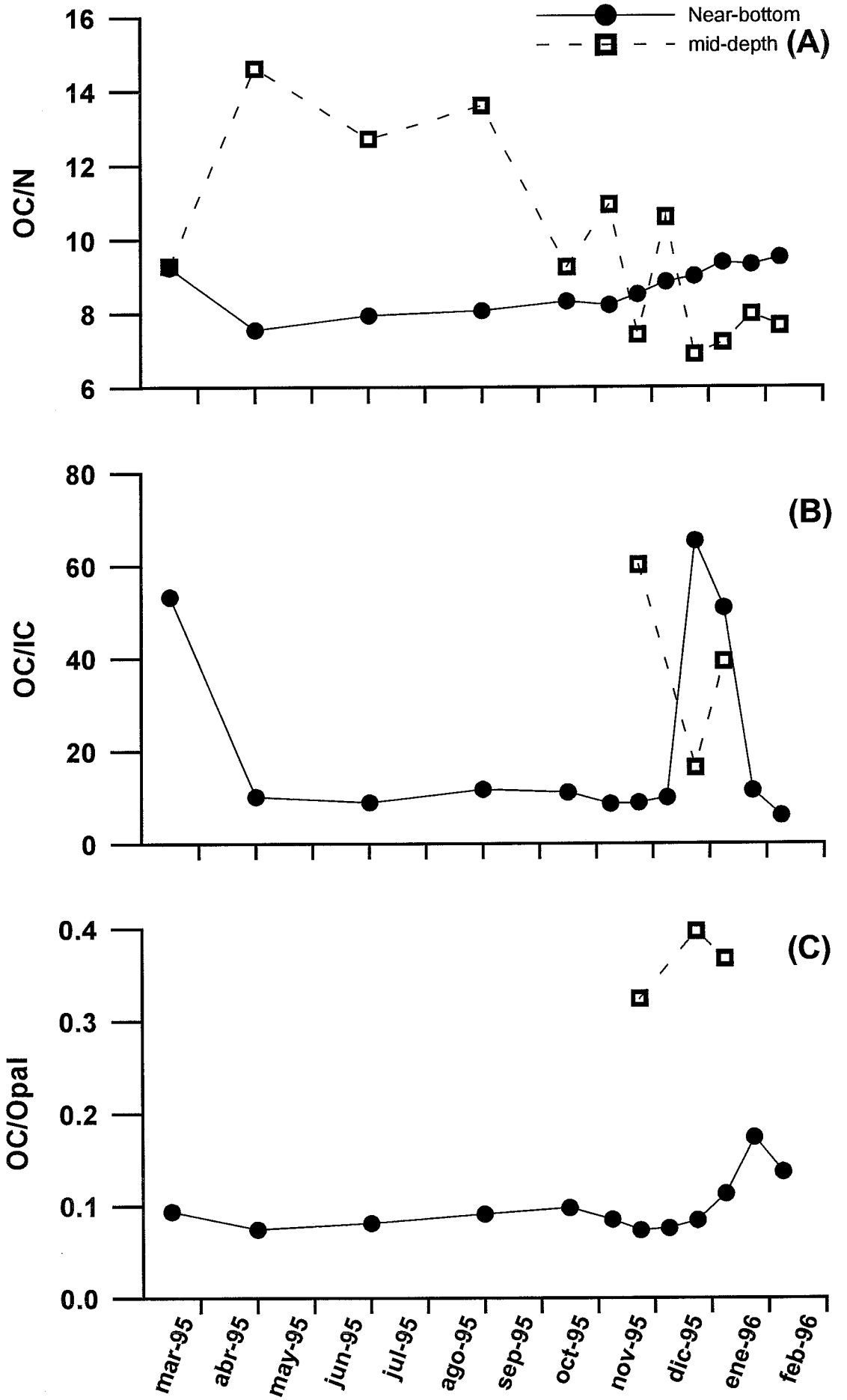
Near-bottom
mid-depth
(A)
OC/N
16
14
12
10
8
6
(B)
OC/IC
80
60
40
20
0
(C)
OC/Opal
0.4
0.3
0.2
0.1
0.0
mar-95
abr-95
may-95
jun-95
jul-95
ago-95
sep-95
oct-95
nov-95
dic-95
ene-96
feb-96

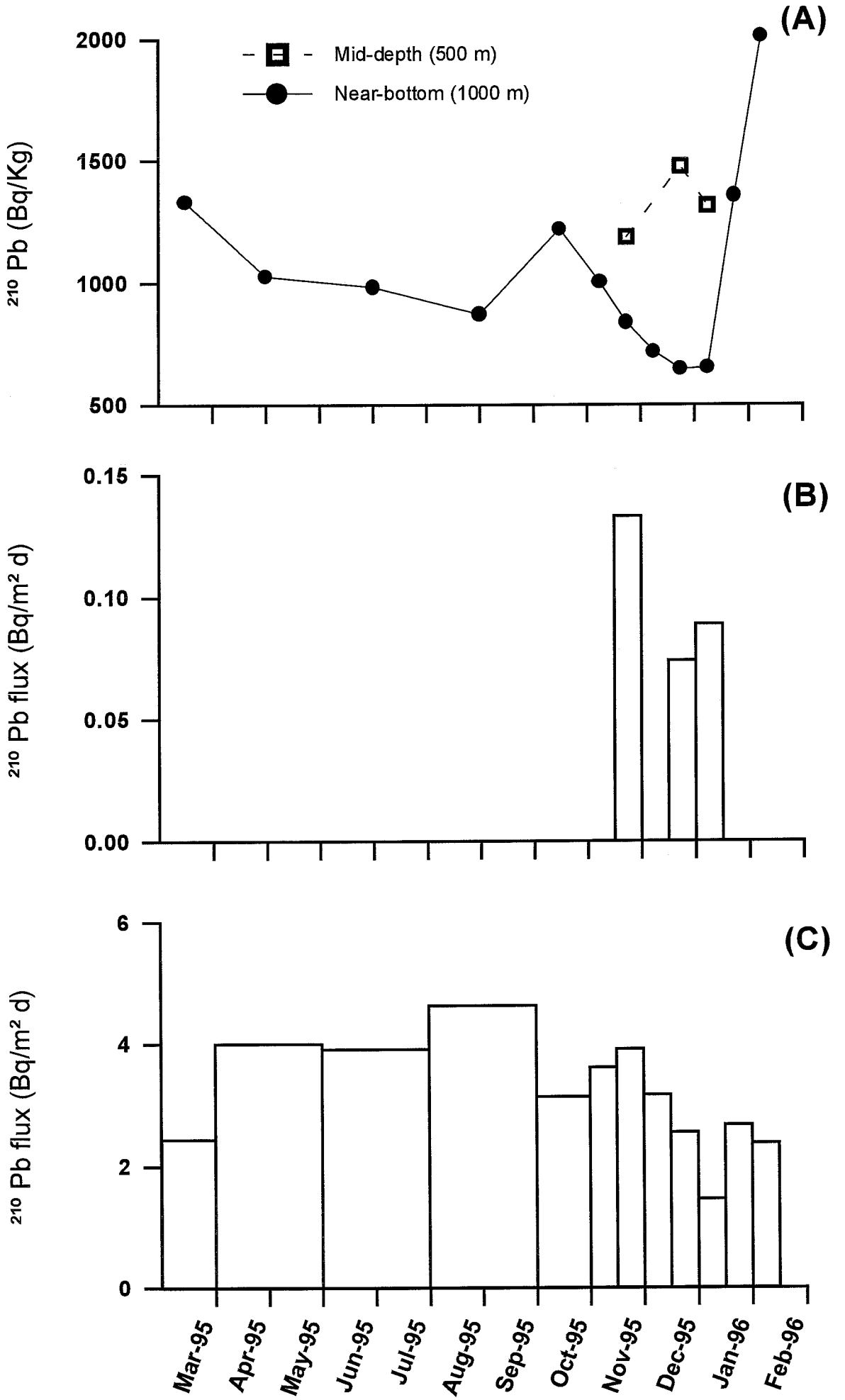
(A)
2000
1500
1000
500
Mid-depth (500 m)
Near-bottom (1000 m)
210 Pb (Bq/Kg)
(B)
0.15
0.10
0.05
0.00
210 Pb flux (Bq/m2 d)
(C)
6
4
2
0
210 Pb flux (Bq/m2 d)
Mar-95
Apr-95
May-95
Jun-95
Jul-95
Aug-95
Sep-95
Oct-95
Nov-95
Dec-95
Jan-96
Feb-96

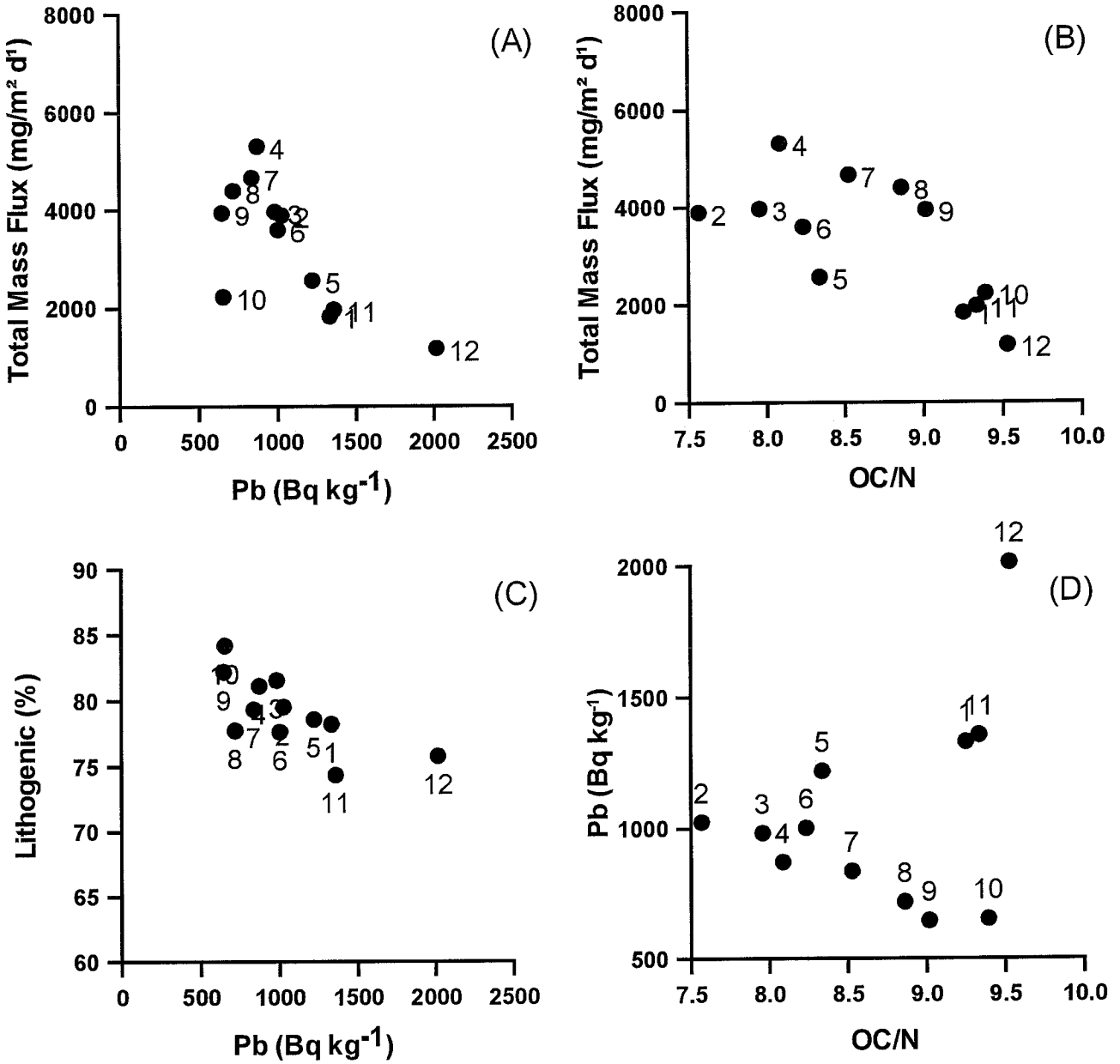
(A)
Total Mass Flux (mg/m² d⁻¹)
Pb (Bq kg⁻¹)
(B)
Total Mass Flux (mg/m² d⁻¹)
OC/N
(C)
Lithogenic (%)
Pb (Bq kg⁻¹)
(D)
Pb (Bq kg⁻¹)
OC/N

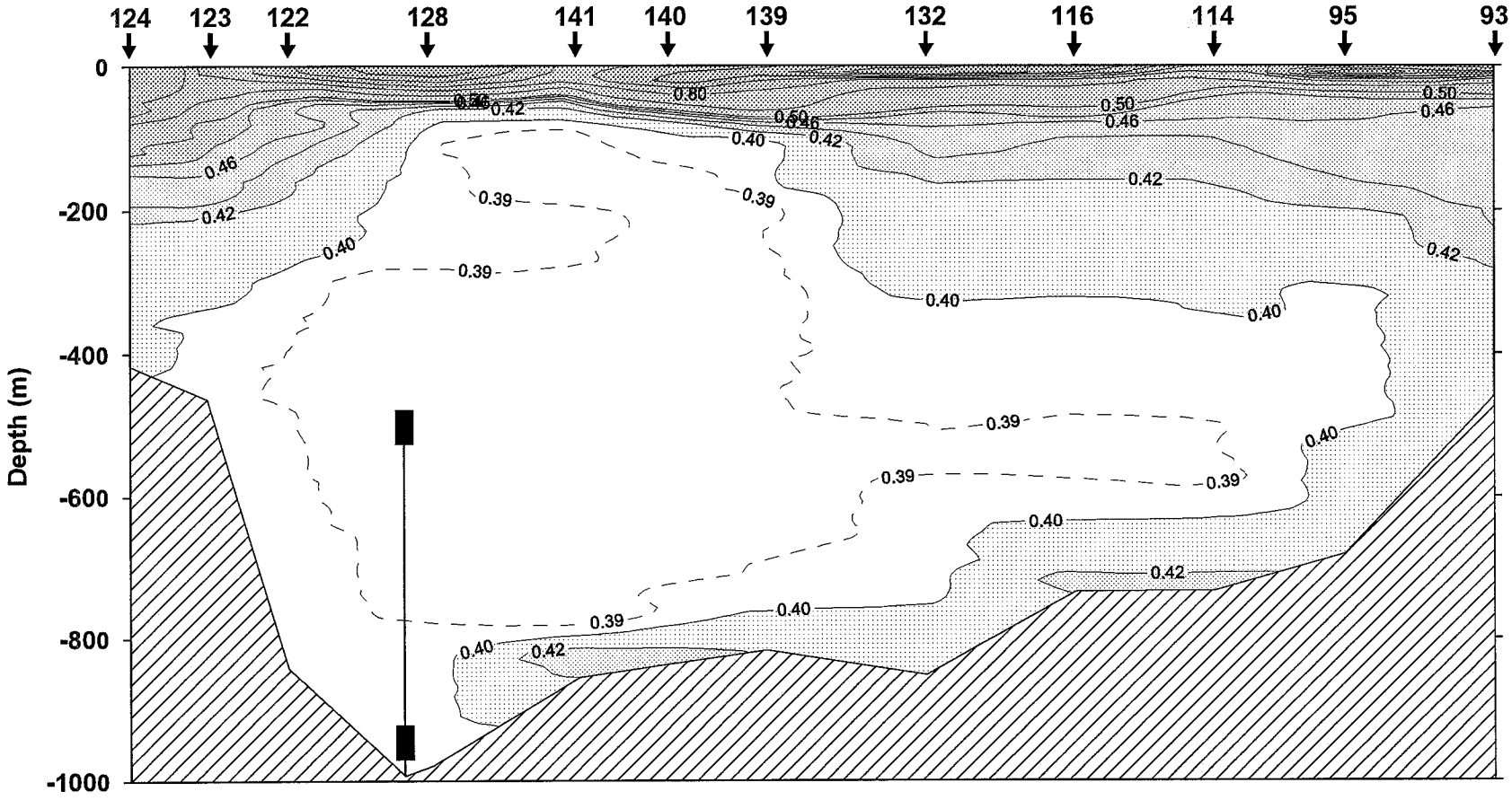
124
123
122
128
141
140
139
132
116
114
95
93
0
-200
-400
-600
-800
-1000
Depth (m)
0.80
0.50
0.46
0.42
0.40
0.39

	Total mass		Organic Carbon		Calcium Carbonate		Biogenic Silica		Lithogenic	
	MD	**NB**	**MD**	**NB**	**MD**	**NB**	**MD**	**NB**	**MD**	**NB**
Mean concentration (%)			8.70	1.4	1.78	1.04	16.03	22	57.	80.
Mean flux (mg m^{-2} d^{-1})	11.27	3634	0.98	51.03	0.19	37.9	2.56	582.68	6.44	2912
Annual flux (g m^{-2})	4.11	1326	0.35	18.62	0.73	13.84	0.922	212.6	2.3	1075

Table 1: Mean annual concentration and fluxes of the total mass and the major constituents of the settling particulate matter in the western Bransfield Strait. MD: Mid-depth, NB near-bottom.

DOWNWARD PARTICLE FLUXES AND SEDIMENT ACCUMULATION RATES IN THE WESTERN BRANSFIELD STRAIT: IMPLICATIONS FOR CARBON CYCLE STUDIES IN ANTARCTIC MARGINAL SEAS.

Albert Palanques[1], Enrique Isla[1], Pere Masqué[2], Pere Puig[1], Joan-Albert Sánchez-Cabeza[2], Josep M. Gili[1] and Jorge Guillén[1]

[1] Institut de Ciències del Mar (CSIC) Av. Joan de Borbó, s/n, E-08039 Barcelona, Spain. ***email: albertp@icm.csic.es***

[2] Departament de Física, Universitat Autònoma de Barcelona, E-08193 Bellaterra, Spain.

Journal of Marine Research (submitted)

DOWNWARD PARTICLE FLUXES AND SEDIMENT ACCUMULATION RATES IN THE WESTERN BRANSFIELD STRAIT: IMPLICATIONS FOR CARBON CYCLE STUDIES IN ANTARCTIC MARGINAL SEAS.

Albert Palanques[1], Enrique Isla[1], Pere Masqué[2], Pere Puig[1], Joan-Albert Sánchez-Cabeza[2], Josep M. Gili[1] and Jorge Guillén[1]

[1] Institut de Ciències del Mar (CSIC) Av. Joan de Borbó, s/n, E-08039 Barcelona, Spain. ***email: albertp@icm.csic.es***

[2] Departament de Física, Universitat Autònoma de Barcelona, E-08193 Bellaterra, Spain.

ABSTRACT

Downward particle and carbon fluxes were studied along with sediment and carbon accumulation fluxes in the Western Bransfield Strait. Near-bottom particle fluxes at 1000 m depth included well-preserved organic matter with benthic diatoms, amphipoda and polychaetes that were resuspended and/or winnowed and transported laterally basinward from shallow high-production environments. Near-bottom fluxes and biogenic components also indicate that most of the carbon accumulated in the seabed at the study site is transported laterally from shallow environments.

High near-bottom particle and carbon fluxes were in agreement with high sediment and carbon accumulation fluxes. The carbon burial efficiency is higher (80-90 %) near the mouth of the Orleans canyon than at the deeper part of the basin (40-50%). The percentage of the carbon produced in the euphotic layer of the Western Bransfield Strait preserved in the sediment represents about 9% near the mouth of the canyon and about 3% at the deeper part of the basin. However, if most of the organic carbon (OC) is transported laterally, the higher primary productivity from nearby shallower areas should be considered and the percentage of the OC preserved in the sediment would account only for 4.5% and 1.5% at each of the study sites.

The results show that resuspension in shallow environments, lateral transport and near-bottom downward fluxes must be considered in addition to surface primary production mid-water downward fluxes and accumulation rates in order to better understand the carbon dynamics in Antarctic marginal seas.

Keywords: near-bottom carbon fluxes, lateral transport, carbon burial and preservation, Antarctica, resuspension

1.Introduction

Understanding the biogeochemical cycling of carbon in the oceans is important in the context of the removal of man-made carbon dioxide from the atmosphere (Heinze *et al.*, 1999). Processes in the sea-atmosphere interface and the dynamics of primary production in the oceans are an essential part of this cycle. However, near-bottom processes and carbon burial and recycling also play an important role that must be understood in order to elucidate whether burial of organic matter removes a significant fraction of carbon dioxide from the ocean-atmosphere system and at what rates (Walsh, 1985). Two aspects that may improve this understanding are the study of near bottom sediment fluxes and the interpretation of the signal of the carbon cycle in the marine sediment.

The Antarctic continental margin is considered to be one of the most sensitive areas to climatic change, and bottom sediments are therefore considered to be important records for investigation. In the Antarctic oceans, particle fluxes and pelagic organic carbon and calcium carbonate fluxes are smaller than in other oceans (Honjo, 1990). However, in some Antarctic nearshore environments such as the Ross Sea and the Antarctic Peninsula, fluxes of

biogenic and lithogenic particles are orders of magnitude higher than in Antarctic pelagic areas. One of these environments is the Bransfield Strait, which is characterized by its high productivity (Huntley *et al.*, 1991) and its potential as a sink for atmospheric CO_2.

Previous studies carried out in the Central Bransfield Strait south of King George Island indicate that over 95% of the annual flux at mid-depths occurs during December and January and that 50% of the mid-depth flux consists of biogenic particles (Wefer *et al.*, 1988; 1990). The mode of vertical sedimentation at mid-depth in the Antarctic Peninsula is characterized by the fact that 100% of the particles are transported downward by Euphasia Superba fecal pellets (Wefer *et al.*, 1982; 1988; Dunbar, 1984). However, the near-bottom downward fluxes in the Bransfield Strait, as in most of the Antarctic marginal seas, were unknown.

Near-bottom particle fluxes play a key role in the deep compartment of the carbon cycle and are important for benthic ecology. Grebmeier and Barry (1991) suggested that lateral advection could be a more relevant process for pelagic-benthic coupling than previously though. In addition, the high variability of ice cover and its effects on hydrographic processes, which influence plankton primary production throughout the year, suggest that other mechanisms besides vertical flux may control benthic biomass and diversity (Arntz et al 1994). In areas with ice cover or during the dark winter period benthic organisms must also survive by consuming organic debris resuspended in the water column near the bottom.

Typical carbon content in bottom sediment from the Bransfield Strait has been reported to range from 0.5 to 1.7%. (Dunbar *et al.*, 1985; De Master *et al.*, 1987; Yoon *et al.*, 1994; Fabrés *et al.*, 1997). Sedimentation rates of 1.2 to 2.3 mm yr^{-1} were estimated in this area (Nelson, 1988; DeMaster *et al.* 1991).

This paper deals with downward particle and carbon fluxes at mid and near-bottom depths and carbon accumulation rates in sediment from the Western Bransfield Strait, providing new insights into the role of near-bottom particle and carbon fluxes and giving estimations of carbon preservation and carbon burial rates in marginal Antarctic seas.

2. Methods

The Bransfield Strait is a semi-enclosed sea bounded by the Antarctic Peninsula and the South Shetland Islands, with a volcanic basin that can be divided into different sub-basins separated from each other by sills shallower than 1000 m (Huntley *et al.*, 1991, Gracia *et al.*, 1997; Canals *et al.*, 2000). The study area is located in the western sector of the Bransfield Strait, south of Livingston Island (Fig. 1). This region has narrow (20-50 km wide) continental shelves and steep slopes, especially on the northern perimeter of the Antarctic Peninsula where the Orleans submarine canyon incises the continental slope down to 800 m depth.

Downward particle and carbon fluxes were measured by one sediment trap installed 30 meters above bottom (mab) at 1000 m water depth and another trap installed in the same mooring array at 500 mab. These traps were deployed south of Livingston Island and west of Deception Island at the A6 site (Fig. 1). In this deployment, the sample-collecting interval was set to different time intervals and the sampling period comprised almost a complete year (345 days) from March 1st 1995 to February 15th 1996. Bottom currents in the study area are not strong enough to induce significant biases in the collection efficiency of the bottom trap (see Palanques *et al.*, 2001 for further details).

The samples collected with the sediment trap were processed in the laboratory according to the method described by Heussner *et al.* (1990). Sample dry weight was determined using three subsamples filtered onto 47 mm diameter, 0.45 μm porous preweighed Millipore cellulose filters. Total mass flux was calculated from the sample dry weight, the collecting trap area and the time sampling interval. Zooplankton organisms, also called "swimmers", were removed by hand picking under a dissecting microscope using forceps and stored for analysis.

Bottom sediment cores from the Western Bransfield Strait basin were collected in January 1996 using a multiple corer (Bowers and Connelly), and a gravity corer. Cores nearby the mooring site at 1066 m depth (A6 site) and at the mouth of the Orleans canyon at 810 m depth (A3 site) were selected for this study (Fig. 1). The multicores from each site were subsampled at 0.5 to 2 cm intervals from top to bottom, whereas gravity cores were sampled every 5 cm. For each sample wet and dry masses were determined before and after drying at 40°C, and dry bulk densities were calculated. About half of the sample was homogenized and used for geochemical analysis.

Carbon and Nitrogen were measured in duplicate using a Leco CN 2000 analyzer. Two subsamples were used to determine the total carbon percentage (TC%) after combustion at 1050°C. Another two subsamples were digested with HCl in a LECO CC 100 digestor and the resulting CO_2, was analyzed in the same LECO CN 2000 analyzer and assigned to inorganic carbon content (IC%). The difference between the two values is the percentage of organic carbon (OC%).

Sediment accumulation rates were estimated by ^{210}Pb in the multicores and by ^{14}C in the gravity cores. ^{210}Pb concentrations were also determined at each cm of depth in the top 20 cm of the gravity cores. ^{210}Pb analyses of the sediment samples were performed following the methodology described by Sánchez-Cabeza *et al.* (1998) and Masqué *et al.* (2001) by total digestion of 200-300 mg sample aliquots. ^{209}Po was added to each sample before digestion as an internal tracer. After digestion, samples were made 1 N HCl and ^{209}Po and ^{210}Po were deposited onto silver disks at 60-70°C for 8 hours while stirring. Polonium isotopes were counted with α-spectrometers equipped with low background SSB detectors (EG&G Ortec). In this study we consider the ^{210}Pb profiles as a two-layer system with a surface mixed layer (SML) extending to a distance L below the water-sediment interface and a second layer below L where no mixing takes place. Radiocarbon dating by accelerator mass spectrometry (^{14}C AMS) was done

on total organic carbon by "Beta Analytic INC". Conventional radiocarbon ages of three stratigraphic levels in gravity core A3 and two in gravity core A6 were analyzed.

3. Results

a. *Downward particle and accumulation fluxes*

Downward total mass fluxes measured during the sediment trap deployment are represented in Fig. 2. At mid-depth, total mass fluxes ranged from 0.08 mg m^{-2} d^{-1} to 112 mg m^{-2} d^{-1}, the weighted mean value was 11.27 mg m^{-2} d^{-1}, and 95% of the mid-depth annual mass flux (4.11 g m^{-2}) occurred during summer. Near the bottom, total mass fluxes were between 1178 and 5321 mg m^{-2} d^{-1} with a weighted mean value of 3634 mg m^{-2} d^{-1}, and the annual flux was 1326 g m^{-2}. Total mass fluxes near the bottom remained high during the whole year and the annual flux was between 2 and 3 orders of magnitude higher than that at mid-depth.

The linear sedimentation rates measured by ^{210}Pb were 1.17 ± 0.05 mm y^{-1} for A-3, and 0.57 ± 0.02 mm y^{-1} for A-6. These values correspond to an accumulation flux of 600 ± 30 g m^{-2} y^{-1} for A3 site, at the mouth of the Orleans canyon, and of 351 ± 14 g m^{-2} y^{-1} for A6 site, at the mooring location. ^{210}Pb activity indicates a SML of 12 cm for A3 site and 8.5 cm for A6 site.

^{14}C derived linear sedimentation rates calculated for gravity cores, were 2.08 mm y^{-1} at A3 site, and 1.15 mm y^{-1} at A6 site. These rates should be considered only as an approach because severe changes in sedimentation rates can occur in the time scale of millennia. However, ^{14}C is commonly used to check the validity of the sediment accumulation rates inferred from ^{210}Pb profiles. Taking into account the different time scales addressed by the two dating techniques, the two sedimentation rates agree reasonably well.

b. *Carbon in settling particulate matter*

Organic carbon (OC) in settling particulate matter ranged from 1.2% to 18.7% whereas inorganic carbon (IC) in the study area was very low, ranging from only 0.02% to 0.5% (Fig. 3). Thus, OC accounted for most of the total carbon content (90-99%) of the settling particulate matter in the study area.

At mid-depth the IC content ranged from non-detectable values, due to the low amount of sample, to 0.5% in late December, when the IC fluxes reached a maximum of 0.25 mg m^{-2} d^{-1} (Fig. 4). The mean annual IC flux at mid-depth can be estimated to be about 0.02 mg m^{-2} d^{-1} and the annual IC flux about 8.84 mg m^{-2}.

Near the bottom, the IC content was quite constant throughout the year, decreasing between mid-November and mid-January and increasing in March (Fig. 3). The weighted mean annual IC content near the bottom was 0.12%. Near-bottom IC fluxes ranged from 0.58 mg

$m^{-2}\,d^{-1}$ in March to 6.59 mg $m^{-2}\,d^{-1}$ in late November (Fig. 4). The mean annual IC flux near the bottom was 4.55 mg $m^{-2}\,d^{-1}$, which represents an annual IC flux of 1.66 g m^{-2}.

At mid-depth, the OC content of settling particles ranged from 6.8% to 18.7% with a weighted mean value of 8.7% (Fig. 3). The OC fluxes at mid-depth ranged from 0.01 mg $m^{-2}\,d^{-1}$ in April-May to 9.8 mg $m^{-2}\,d^{-1}$ in late November (Fig. 4). The OC weighted mean value was 0.98 mg $m^{-2}\,d^{-1}$, which corresponds to an annual OC flux at mid-depth of 0.35 g m^{-2}.

Near the bottom, the OC content of the settling particles was relatively constant, ranging from 1.2% to 1.7% during most of the year with a mean annual content of 1.4% (Fig. 3). Near-bottom OC fluxes ranged from 26.7 mg $m^{-2}\,d^{-1}$ in early February to 73.5 mg $m^{-2}\,d^{-1}$ in August-September (Fig. 4). Near-bottom OC fluxes were 1 to 3 orders of magnitude higher than those measured at mid-depth during the same sampling periods. The weighted mean near-bottom OC flux was 51.03 mg $m^{-2}\,d^{-1}$ and the near-bottom annual OC flux was 18.62 g m^{-2}.

The Organic Carbon to Nitrogen molar ratio (OC/N) of the mid-depth settling particles ranged from 12.7 to 14.6 during winter and from about 6 to 7 during the summer periods of higher total mass flux, whereas the near-bottom OC/N ratio ranged from 7.5 to 9.5 throughout the year (Fig. 5).

c. Swimmers and diatoms collected near the bottom

Swimmers and diatoms in the samples of the near-bottom traps were also studied. The swimmer fauna was dominated by polychaetes and amphipods although other groups such as medusa and euphausids (mainly their exuvia) were also present.

The amphipod fauna was a mixture of well-known pelagic species (*Parandania boecki*, *Cyphocaris* sp. and *Eusirus propeperdentatus*) benthopelagic species occurring on the bottom and in the water column (*Eusirus antarcticus*, *Eurythenes gryllus* and *Abyssorchomene* sp.) and other species uncommonly found in the water column (*Orchomenella pinguides*). It is relevant to note that other amphipod species recorded mainly in winter months (*Hirondella Antarctica*, *Opisa* sp. and *Epimeriidae* gen. sp.) were never found in the water column.

The polychaete fauna was characterized by the presence of relatively few truly pelagic species (*Tomopteris* spp. and *Pelagobia longicirrata*). The rest of species collected throughout the year sampled were benthic species, which in the case of the *Scalibregmatids* live inside the sediment and lack swimming appendages. The species *Scalibregma inflatum* was the most abundant one in all months while other exclusively benthic species were present in all samples (*Pseudoscalibregma brabsfieldium* and *Laonice cirrata*).

Diatoms were very diverse. Some of the most frequent species in the samples are truly pelagic and common in Antarctic surface waters such as the species of the genus

Chaetoceros and *Pseudonitzschia*. However, the most significant common and frequent components of diatom species were benthic species and genus such as *Amphora*, *Cocconeis* (*C. fasciolata*), and *Grammatophora* (*G. angulosa*) and also littoral species abundant in shallow waters such as *Actinocyclus actinochilus*, *Navicula directa*, *N. glaciei*, *Thalasiosira antarctica* and *Fragiliariopsis kergelensis*.

d. Carbon in bottom sediment

The carbon in bottom sediment is mainly composed of the organic fraction. IC ranged from non-detectable to 0.04%. The vertical OC distribution in the uppermost sediment column sampled from multicores A3 and A6 is shown in Figure 6. The vertical OC distribution of the gravity cores (Fig.7) shows the OC variability for a longer period of time, though they do not show the most modern sediment because the uppermost centimeters were lost during sampling operations. Comparison of ^{210}Pb activities between the two types of cores indicate that A3 and A6 gravity cores lost about 20 cm of the uppermost sediment.

OC content in the uppermost surface sediment of the multicores was 1.28% for A3 site and 1.38% for A6 site (Fig. 6) with OC/N ratios of 8.2 and 7 respectively (Fig 8). OC contents and the OC/N ratio change from the surface to reach a more constant value approximately below the SML. In multicore A3, the OC content below the SML remains between 1.1 and 1.2 and in multicore A6, it decreases to between 0.6 and 0.7%. The OC/N ratio increases downwards to values of 8 to 9 in A3 and of 7.8 to 9.5 in A6 (Fig. 8).

Deeper in the sediment column, the OC content is not constant, ranging from 0.8 to 1.2% for A3 gravity core, and from 0.2 to 0.8% for A6 gravity core. Mean values were 1% and 0.5% for A3 and A6 respectively.

OC accumulation fluxes in the uppermost sediments estimated from the ^{210}Pb accumulation rates in the multicores are 7.68 g m^{-2} y^{-1} for A3 and 4.84 g m^{-2} y^{-1} for A6. These fluxes decrease with depth beyond the SML, to values about 6.9 g m^{-2} y^{-1} for A3 site and 2.28 g m^{-2} y^{1} for A6 site.

Considering the OC content of the gravity cores and extrapolating the accumulation rates estimated by ^{210}Pb for longer periods of time, the OC accumulation fluxes ranged from 4.8 to 7.2 g m^{-2} y^{-1} for A3 site and from 1.05 to 2.45 g m^{-2} y^{-1} for A6 site. Taking into account the accumulation rates estimated by ^{14}C, these values would increase by a factor of 2.

4. Discussion

The downward particle fluxes and the sediment accumulation rates indicate the importance of the near-bottom processes and the benthic zone in the sediment and carbon cycles of the Western Bransfield Strait. The role of resuspension and lateral transport along with sedimentation and carbon preservation is discussed in this section.

a. Resuspension and lateral transport

The much higher particle and OC fluxes near the bottom in comparison with those at mid-depth indicates that most of the sediment and carbon reaching the seabed at the studied site is transported laterally. In addition, the fauna found in the near-bottom sediment trap also give clues about particle sources and transport processes.

One relevant aspect is that many of the species collected in the near-bottom trap are not commonly found in the water column. Some examples are: 1) polychaetes of the group *Scalibregmatids*, which always live inside the sediment and lack swimmer anatomical structures (Fauchald and Jumars 1979); 2) benthic amphipods, which were rarely found in the antarctic water column (De Broyer and Jazdzewski, 1996); and 3) benthic diatoms that were found in shallow waters near the bottom (Dunbar *et al.,* 1989), but never so high as 30 m above the bottom in Antarctic waters.

Another very relevant aspect is that most of the pelagic and benthic species collected in the near-bottom trap are abundant in shallow bays of the South Shetland Islands (Ahn *et al.*, 1997) and that some of them, such as Navicula glaciei, are specifically littoral benthic diatoms.

These facts indicate that not all the fauna found in the near-bottom sediment trap samples were pelagic organisms that settled from the surface or that swam into the trap sample, but there were swimmers and benthic organisms that behaved as passive particulate matter, being resuspended and transported along with inorganic particles.

Sediment resuspension is a common phenomenon that has already been documented in near-shore environments surrounding Antarctica (e.g. Klöser *et al.,* 1994). Resuspension may be particularly relevant during the austral winter and in sublittoral areas, increasing the occurrence of sediment particles in the water column. For example, in Maxwell Bay and Marion Cove, an important source of suspended particulate matter seemed to be resuspension of benthic material through a year cycle (Kang *et al.,* 1997). In these bays, daily tidal currents make benthic diatoms regularly available to benthic communities (Ahn *et al.,* 1997). The same tidal water movements could be also responsible for the transport of benthic diatoms and other biogenic material far away from the shallow areas. Berkman *et al.,* (1986) demonstrated that resuspended sediments in the vicinity of McMurdo Station contained viable algal material throughout the winter darkness period. From these

sediments, organic material is introduced into the water column providing an alternative food source for primary and secondary consumers, which rely on the transport of allochthonous or resuspended organic material during the Antarctic winter.

The presence of swimmers and benthic diatoms from shallow environments at the deep trap site indicates resuspension and lateral transport of particles from these environments, and suggests that tidal currents and internal tides could resuspend and transport part of the spring primary producers' blooms from the shelf areas to surrounding depths. This transport would include plankters and detritus settled in the seabed, the latter mainly from macroalgal beds. These processes would explain the high and continuous near-bottom fluxes throughout the year.

Preservation of organic matter (OC/N ratio) is also coherent with this pattern. In contrast to the downward mid-depth particles that showed high OC/N ratios in winter (12.7 to 14.6) and low ones in summer (6 to 7), the downward near-bottom particles showed relatively low OC/N ratios throughout the year (7.5 to 9.5). These low OC/N ratios could be related to continuous resuspension of sedimented planktonic or benthic organic matter and lateral transport.

The narrow continental shelves and steep slopes of the study area would help to enlarge the shelf-slope sediment transfer. In addition, the Orleans canyon, which is incised almost parallel to the foot of the slope, can receive particle supplies from the shelf and slope of the northern Antarctic Peninsula and probably redirect near-bottom particle fluxes basinward.

b. Sedimentation and carbon preservation

Once the OC is accumulated in the seabed, the OC burial efficiency and the percentage of the primary production preserved in the sediment must be evaluated to integrate them in the framework of the carbon cycle.

The similar low OC/N ratios of the uppermost sediment and the near-bottom settling particulate matter suggests that the organic matter accumulated on the seafloor have the same origin as that settling near the bottom. However, only 26% of the annual downward OC flux at A6 (18.6 g m^{-2}) accumulates in the seafloor (4.8 g m^{-2}). The remaining 74% of the near-bottom OC flux is probably recycled or advected from this site. The role of benthic organisms consuming and transforming OC can also be an important mechanism, as suggested by Gili *et al.* (2001).

Downward, in the first centimeters of the sediment column, there is a decreasing trend of the OC content and an increasing trend of the OC/N ratio due to mixing, remineralization and degradation processes. These trends are clearer for A6 than for A3. Comparing the annual accumulation fluxes in surface sediment (7.6 g m^{-2} for A3 and 4.8 g m^{-2} for A6) with those below the SML where values become more constant (6.9 g m^{-2} for A3 and 2.3 g m^{-2} for A6),

we can estimate an OC burial efficiency of about 80-90% for A3 and 40-50% for A6. Remineralization occurring when OC has been deposited accounts for the remaining percentage. Thus, the higher accumulation rate at A3 (by a factor of 2) contributes to a better preservation of the organic matter at the mouth of the Orleans Canyon than in the center of the basin.

The fraction of the primary produced OC that is preserved in the sediment can not be estimated very accurately. However, the accuracy of this relationship cannot be very high, mainly because of the different time scale of the variables and the particle dynamics. On the one hand, OC accumulation fluxes are related to Pb^{210} accumulation rates that result from the integration of Pb^{210} activity in sediment accumulated during several tens of years. On the other hand, the primary production measurements normally correspond to time periods of days and must be properly extrapolated to year periods. In addition, the particle dynamics depends on the interaction with currents that can transport particles far away from where they were produced.

In the Western Bransfield Strait, average primary productivity values during spring are of the order of 1 g C m^{-2} d^{-1} (Holm-Hansen and Mitchell, 1991; Moran and Estrada, 2001; Varela *et al.*, 2001). As primary production is negligible with ice cover, the annual primary production can be estimated from the primary production during spring months. Mid-depth carbon fluxes in the study area were only significant during about 60 spring days when about 95% of the mid-depth annual mass flux took place (Fig. 4b). The same period of about 60 days was observed by Wefer *et al.*, (1988; 1990). This suggests that primary production in the Bransfield Strait is significant only for no longer than 60 days per year during the spring-summer period. Thus, the average annual productivity in the study area could be about 60 g C m^{-2}. Particulate carbon exportation measured with drifting sediment traps in the western Bransfield strait in summer 1996 was about 175 mg C m^{-2} d^{-1} (Anadón *et al.*, 2001), which allows one to estimate an annual exportation form the euphotic zone of about 10 g C m^{-2} for that year.

Taking into account the average annual primary production in the Western Bransfield Strait, the annual carbon accumulation flux in the uppermost sediments estimated from ^{210}Pb accumulation rates (7.68 g m^2 for A3 and 4.84 g m^2 for A6) represents about 12.8% and 8% of the annual primary production in the photic layer for stations A3 and A6 respectively. Considering the deeper and more constant values of the multicores below the SML (6.9 g m^2 for A3 and 2.28 g m^2 for A6), this percentage decreases to about 11.5% for A3 and 3.8 % for A6 due to degradation processes within the sediment column. The OC preservation estimated near the mouth of the Orleans Canyon (A3) is slightly higher than that estimated by Nelson (1988) and DeMaster *et al.* (1991) for sediments of the continental margin of the Bransfield Strait, which accounted for a 9% of the total production in surface waters. The lower preservation in the deeper part of the system (A6) is probably related to the lower accumulation rates, which could allow a greater organic matter degradation due to a longer residence time at the sediment-water interface.

These estimations fit into a classical model of vertical exportation from the surface water to the seabed. However, if we consider that the annual mid-depth downward OC flux represents only 0.3 to 0.6% of the annual primary production in the Western Bransfield Strait and that the annual near-bottom OC flux represents 20 to 30% of it, it is evident that most of the near-bottom downward OC flux is transported laterally from the shelf and slope of the surrounding areas. Thus, it would be more correct to consider the average annual productivity in these areas in order to estimating the carbon preserved in the sediment, although the model including lateral transport would be more complex due to recycling, resuspension and advection of particles from these zones. Nephelometric data indicates that an important source area is the continental margin of the Antarctic Peninsula around the New Orleans Canyon (Palanques *et al.*, 2001). The Gerlache Strait also exports material towards the western Bransfield Strait (Isla *et al.*, 2001). Assuming that the average primary production during spring in these zones is 2.1 g C m^{-2} d^{-1} (Varela *et al.*, 2001), the annual primary production can also be estimated considering that it is significant only for no longer than 60 days per year. Thus, the average annual productivity in these zones could be estimated as around 126 g C m^{-2}. Particulate carbon exportation measured with drifting sediment traps in the Gerlache Strait during spring 1996 was about 0.5 g C m^{-2} d^{-1} (Anadón *et al.*, 2001), which allows one to estimate an annual exportation of 30 g C m^{-2}.

Taking into account the primary production of these zones (126 g C m^{-2}), the annual near-bottom carbon flux represents about 15 % of the annual primary production in the carbon source areas and the annual carbon accumulation flux in the uppermost sediments represents about 6.5% and 4% of this annual primary production for stations A3 and A6 respectively. Considering the deeper and more constant values of the multicores below the SML, this percentage is about 5.7% for A3 and 1.9 % for A6. Thus, without entering into the complexity of particle recycling, resuspension and advection, the percentage of the primary production preserved in the sediment of the study area changes if we consider the productivity in the potential source areas of the sediment transported laterally in stead of that of the same study area.

In marginal seas dominated by lateral transport such as the Bransfield Strait, both the OC burial efficiency and the percentage of the primary produced OC preserved in the sediment change in space and the latter should be estimated in relation to the primary production at the source area. A schematic diagram of the carbon budget in the study area summarizing the results obtained is shown in Figure 9. This diagram includes both vertical and lateral supplies.

Regarding the longer carbon record of the gravity cores, the changes in the OC content are related to the temporal evolution of the primary production and the OC preservation in the study area. The primary productivity of this area has been decreasing during the last two millennia, with variations on this trend related to cold (neoglacial) stages (Wigley and Kelly, 1990; Leventier *et al.,* 1996 and Bárcena *et al.*, 1998). Primary production decreased during cold periods because ice remained for longer periods of time (Abelmann and Gersonde, 1991). However, Bárcena *et al.,* (1998) concluded that, in spite of this decrease of primary

production, the OC content in sediment increased during neoglacial periods as a response to a higher preservation (Bárcena *et al.*, 1998). Relationships between primary production and carbon preservation should be more studied in order to better understand the spatial and temporal variability of the OC record.

5. Conclusions

In the Western Bransfield Strait, south of Livingston Island, one quarter of the near-bottom OC flux accumulates in the seafloor, and the remaining OC flux is advected or recycled. At this site, only 40-50 % of the OC in the surface sediment was buried under the SML. This percentage is higher (80-90%) in the margin at the mouth of the Orleans Canyon where the higher sedimentation rate probably helped to increase the OC preservation. Remineralization accounts for the remaining percentage lost in the SML. The OC preserved in the sediment (under the SML) of the deep basin is about 3% of the average annual primary production in the Western Bransfield Strait.

However near-bottom fluxes and the presence of benthic organisms from shallow environments indicate sediment resuspension and basinward transport in these environments, and suggest that most of the carbon accumulated in the deep basin was transported laterally from shallower environments. Considering that laterally-transported OC is produced mainly in shallower environments where primary production is higher (such as the shelf and slope surrounding the Orleans Canyon, the Gerlache Strait and the bays in the south of the Shetland Islands), the percentage of OC carbon preserved at the deep basin is 1.5% of the average primary production of these areas. The OC preserved at the mouth of the Orleans canyon represents 9% of the primary production in the Western Bransfield Strait and 4.5% of that in the shallower OC source areas.

Thus, the fraction of carbon removed from the ocean in marginal seas and preserved by burial of organic matter should take into account lateral transport of organic matter and primary production in the source areas from where material is laterally transported. Resuspension, lateral advection and associated processes in the benthic boundary layer must be considered in the studies of the carbon cycle and are a key phenomena for understanding the functioning of Antarctic marginal ecosystems.

Acknowledgements. This research was supported by the project ANT94-1010 and MAR96-1781-CO2-01 funded by the "Comisión Interministerial de Ciencia y Tecnología". It also benefited from a pre-doctoral fellowship from CONACYT (Mexico) reference 92766. We thank the officers and crew of the RV Hespérides for their help and support during surveys. We also wish to thank Prof. Claude De Broyer, Dr. Brigitte Hilbig and Dr. Martha Ferrario for their valuable help in the identification of Amphipoda, Polycheta and Diatoms respectively, and Covadonga Orejas for her help in the preparation of this manuscript.

References

Abelmann A. and R. Gersonde. 1991. Biosiliceous particle flux in the Southern Ocean. Mar. Chem., *35*, 503-536.

Ahn I-Y., H. Chung, J-S. Kang and S-H. Kang. 1997. Diatom composition and biomass variability in nearshore waters of Maxwell Bay, Antarctica, during the 1992/1993 austral summer. Polar Biol., *17*, 123-130.

Anadón R., F., Alvarez-Marqués, E. Fernandez, M. Varela, M. Zapata, J.M. Gasol and D. Vaqué. 2001. Vertical biogenic particle flux during austral summer in the Antarctic Peninsula area. Deep-Sea Res. II, in press.

Arntz W.E., T. Brey and V.A. Gallardo. 1994. Antarctic zoobenthos. Ocean. Mar. Biol. Ann. Rev., *32*, 241-304.

Bárcena M.A., R. Gersonde, S. Ledesma, J. Fabrés, A.M. Calafat, M. Canals, F.J. Sierro and J.A. Flores. 1998. Record of Holocene glacial oscillations in the Bransfield Basin as revealed by siliceous microfossil assemblages. Antarctic Sci., *10 (3)*, 269-285.

Berkman P.A., D.S. Marks and G.P. Shreve. 1986. Winter sediment resuspension in McMurdo Sound, Antarctica, and its ecological implications. Polar Biol., *6*, 1-3

Canals M., R. Urgeles and A.M. Calafat. 2000. Deep sea-floor evidence of past ice streams off the Antarctic Peninsula. Geology, 28(1), 31-34.

De Broyer C. and K. Jazdzewski. 1996. Biodiversity of the Southern Ocean: towards a new synthesis for the Amphipoda (Crustacea). Boll. Mus. Civ. Sci. Nat. Verona, *20*, 547-568.

Demaster D. J., T.M. Nelson, C.A. Nittrouer and S.L. Harden. 1987. Biogenic silica and organic carbon accumulation in modern Bransfield Strait sediments. Antarctic J. United States, *22*, 108-110.

DeMaster D.J., T.M. Nelson, S.L. Harden and C.A. Nittrouer. 1991. The cycling and accumulation of biogenic silica and organic carbon in Antarctic deep-sea and continental margin environments. Mar. Chem., *35*, 489-502.

Dunbar R. B. 1984. Sediment trap experiments on the Antarctic continental margin, Antarctic J. United States, *19*, 70-71.

Dunbar R. B., A. J. Macpherson and G. Wefer. 1985. Water-column particulate flux and seafloor deposits in the Bransfield Strait and southern Ross Sea, Antarctica. Antarctic J. of the United States, *20 (5)*, 98-100.

Dunbar R.B., A.R. Leventer and W.L. Stockon. 1989. Biogenic sedimentation in McMurdo Sound, Antarctica. Symposium on Glaciomarine Environments, INQUA XII International Congress. Mar. Geol., *85*, 155-179.

Fabrés, J., A.M. Calafat, M. Canals, G. Francés, M. A. Bárcena, S. Ledesma and J. A. Flores. 1997. Identificación de procesos sedimentarios en la Cuenca de Bransfield (Antártida Occidental). Bol. Real Soc. Española de Hist. Nat., *93 (1-4)*, 85-94.

Fauchald K and P.A. Jumars. 1979. The diet of worms: a study of Polychaete feeding duilds. Oceanogr. Mar. Biol. Ann. Rev., *17*, 193-284.

Gili J.M., R. Coma, C. Orejas, W.E. Arntz, P. López-González and M. Zabala. 2001. Antarctic benthic suspension feeder communities within a world-wide approach: a short review. Polar Biol., in press.

Gràcia, E. M. Canals, M. Farràn, J. Sorribas and R. Pallàs. 1997. Central and Eastern Bransfield Basins (Antarctica) from high resolution swath-bathymetry data. Antarctic Sci., 9, 168-180.

Grebmeier J.M. and J.P. Barry. 1991. The influence of oceanographic processes on pelagic-benthic coupling in polar regions: A benthic perspective. J. Mar. Systems, *2*, 495-518.

Heinze, C., E. Jansen, O. Ragueneau, C.M.G. van den Berg and A.K. Watson. 1999. Global carbon balance. *in* Air-sea and Sea-ice Interactions, W. Oost and E. Lipiatou, eds., Research in enclosed seas series – 7. EUR 18638 EN, pp 36.

Heussner S., C. Ratti and J. Carbonne. 1990. The PPS 3 time-series sediment trap and the trap sample processing techniques used during the ECOMARGE experiment. Cont. Shelf Res., *10*, 943-958.

Holm-Hansen O. and B.G. Mitchell. 1991. Spatial and temporal distribution of phytoplankton and primary production in the western Bransfield Strait region. Deep-Sea Res., *38 (8/9)*, 961-980.

Honjo S. 1990. Particle fluxes and modern sedimentation in the polar oceans. *in* Polar Oceanography. part B: Chemistry, Biology and Geology. W. O. Smith, Jr., ed., Academic Press, Inc., 687-739.

Huntley M., D.M. Karl, P. Niler and O. Holm-Hansen. 1991. Research on Antarctic Ecosystem Rates (RACER): an interdisciplinary field experiment. Deep-Sea Res., *38 (8/9)*, 911-941.

Isla, E., P. Masqué, A. Palanques, J.A. Sanchez-Cabeza, J.M. Bruach, J. Guillén and P. Puig. 2001. Sediment accumulation rates and carbon fluxes to bottom sediments in a high productivity area: Gerlache Strait (Antarctica). Deep-Sea Res II, in press.

Kang J-S., S-H. Kang, J.H. Lee, K.H. Chung, and M-Y. Lee. 1997. Antarctic micro- and nano-sized Phytoplankton assemblages in the surface water of Maxwell Bay during the 1997 Austral Summer. Korean J. Polar Res., *8*: 35-45.

Klöser H., G.A. Ferreyra, I.R. Schloss, G. Mercuri, F. Laturnus and A. Curtosi. 1994. Hydrography of Potter Cove, a small fjord-like inlet on King George Island (South Shetlands). Estuar. Coastal Shelf Sci., *38*: 523-537.

Leventer A., E. Domack, S.E. Ishman, S. Brachfeld, C.E. Mcclennen and P. Manley. 1996. Productivity cycles of 200-300 years in the Antarctic Peninsula region: Understanding linkages among the sun, atmosphere, oceans, se ice, and biota. Geol. Soc. Am. Bull., *108 (12),* 1626-1644.

Masqué P. E. Isla, J.A. Sanchez-Cabeza, A. Palanques, J.M. Bruach, P. Puig and J. Guillén. 2001. Sediment accumulation rates and carbon fluxes to bottom sediments at the Western Bransfield basin (Antarctica), Deep-Sea Res. II, in press.

Moran X.A.G. and M. Estrada. 2001. Phytoplanktonic DOC and POC in the Bransfield and Gerlache Straits as derived from kinetic experiments of ^{14}C incorporation. Deep Sea Res. II, in press.

Nelson T.M.1988. Biogenic silica and carbon accumulation in the Bransfield Strait, Antarctica, M.S. Thesis, North Carolina State University, Raleigh NC, 89 pp.

Palanques A., E. Isla, P. Puig, J.A. Sanchez-Cabeza and P. Masqué. 2001. Annual evolution of settling particle flux during FRUELA experiment (Western Bransfield Strait, Antarctica). Deep-Sea Res II, in press.

Rosenberg R. 1995. Benthic marine fauna structured by hydrodynamic processes and food availability. Netherlans J. of Sea Res., *34*, 303-317.

Sánchez-Cabeza J.A., P. Masqué, and I. Ani-Ragolta. 1998. Pb-210 and Po-210 analysis in sediments and soils by microwave acid digestion. J. Radioanalytical and Nuclear Chem., *227*, 19-22.

Varela M., E. Fernandez and P. Serret. 2001. Size-fractionated phytoplancton biomass and primary production in the Gerlache and South Bransfield Straits (Antarctic Peninsula) in austral summer 95-96. Deep-Sea Res. II, in press.

Walsh J.J., E.T. Premuzic, , J.S. Gaffney, G.T. Rose, T. Harbottle, R.W. Stoenner, W.L. Balsam, , P.R. Betzer and S.A. Macko. 1985. Organic storage of CO_2 on the continental slope off the mid-Atlantic Bight, the southeastern Bering Sea and the Peru Coast. Deep-Sea Res., *32*, 853-883.

Wefer G., E. Suess, W. Balzer, G. Liebezeit, P. J. Muller, A. Ungerer and W. Zenk. 1982. Fluxes of biogenic components from sediment trap deployment in circumpolar waters of the Drake Passage. Nature, *299*, 145-147.

Wefer G., G. Fisher, D.K. Fütterer and R. Gersonde. 1988. Seasonal particle flux in the Bransfield Strait, Antarctica. Deep-Sea Res., *35 (6)*, 891-898.

Wefer G., G. Fisher, D.K. Fütterer, R. Gersonde, S. Honjo and D. Ostermann. 1990. Particle sedimentation and productivity in Antarctic waters of the Atlantic sector, *in* Geological History of the Polar Oceans: Arctic Versus Antarctic, U. Beil and J. Thiede, eds., Kluwer Academic Publishers, The Netherlands, 363-379.

Wigley T. M. L. and P. M. Kelly (1990) Holocene climatic change, 14C wiggles and variations in solar irradiance. Phil. Trans. R. Soc. Lond., *330*, 547-560.

Yoon H.I., M.W. Han, B.K. Park, J.K. Oh, and S.K. Chang. 1994. Depositional environment of near-surface sediments, King George Basin, Bransfield Strait, Antarctica. Geo-Mar. Let., *14*, 1-9.

FIGURES

Figure 1. Bathymetric map of the western Bransfield Strait showing the position of the stations where selected multicores and gravity cores were taken. The mooring was located at site A6.

Figure 2. Times series of total mass fluxes of settling particulate matter collected at mid-depth (A) and near the bottom (B) during the experiment.

Figure 3. Time series of organic carbon contents (A) and inorganic carbon content (B) in the settling particulate matter at mid-depth (open squares) and near the bottom (black dots) during the experiment.

Figure 4. Time series of Organic Carbon fluxes (A, B) and inorganic carbon fluxes (C, D) in the settling particulate matter near the bottom and at mid-depth during the experiment.

Figure 5. Time series of the OC/N ratio (mol/mol) on the settling particulate matter at mid-depth (open squares) and near the bottom (black dots) during the experiment.

Figure 6. Vertical distribution of organic carbon content in multicores A-3 and A-6.

Figure 7. Vertical distribution of organic carbon content in gravity cores A-3 and A-6.

Figure 8. Vertical distribution of the OC/N ratio (mol/mol) in multicores A-3 and A-6.

Figure 9. Diagram of the carbon budget to show carbon burial and preservation of the primary production in the sediment, taking into account both vertical and lateral inputs in the study area during the field work. Ph. Z.: photic zone. Ex.: Carbon exportation from the photic zone. Ad/Rc: advected/recycled. SML: surface mixed layer. Rm: remineralized. Br: buried.

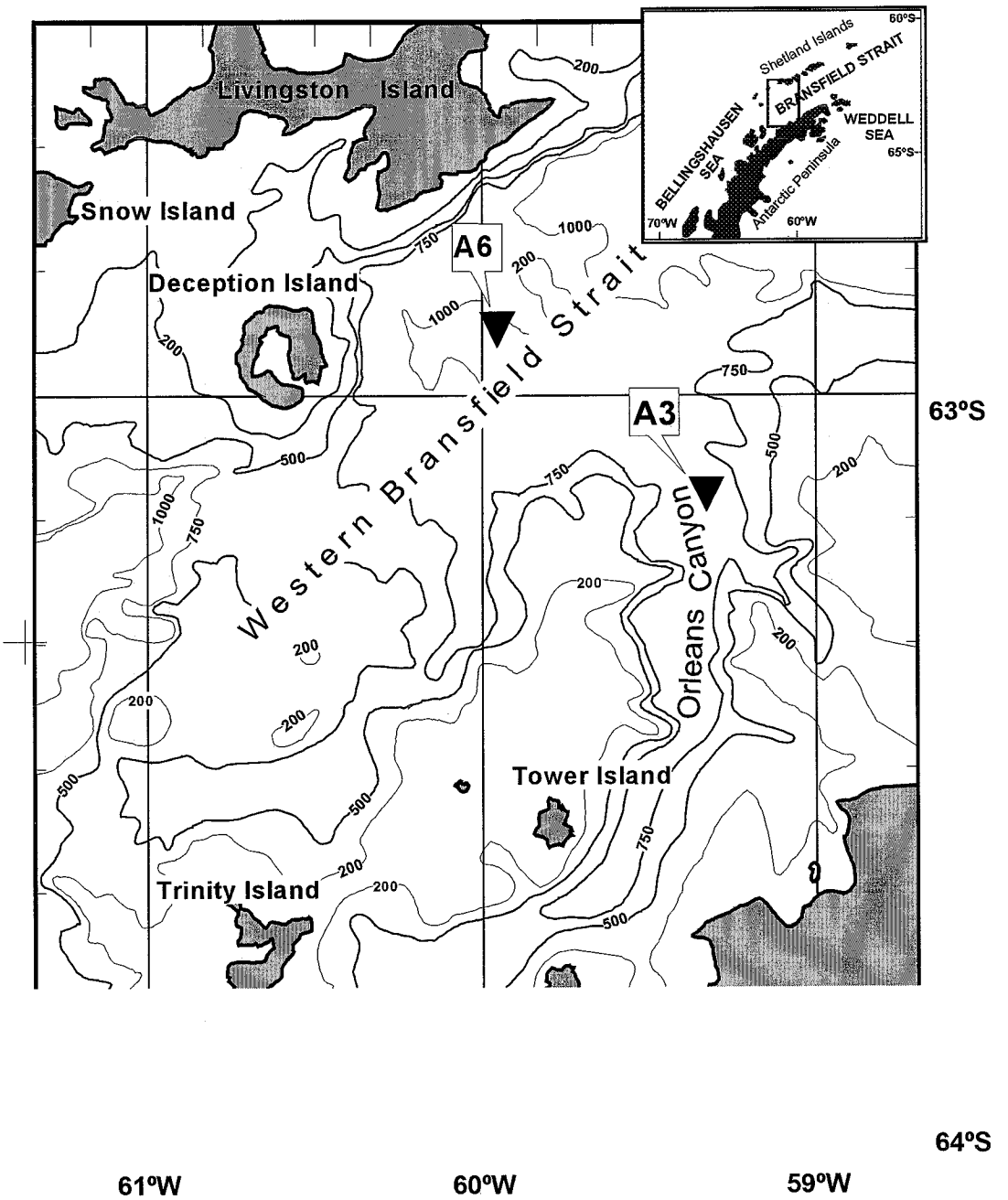
Livingston Island
Snow Island
Deception Island
A6
A3
Western Bransfield Strait
Orleans Canyon
Tower Island
Trinity Island
63°S
64°S
61°W
60°W
59°W
Shetland Islands
BRANSFIELD STRAIT
WEDDELL SEA
BELLINGSHAUSEN SEA
Antarctic Peninsula
60°S
65°S
70°W
60°W

Figure 1

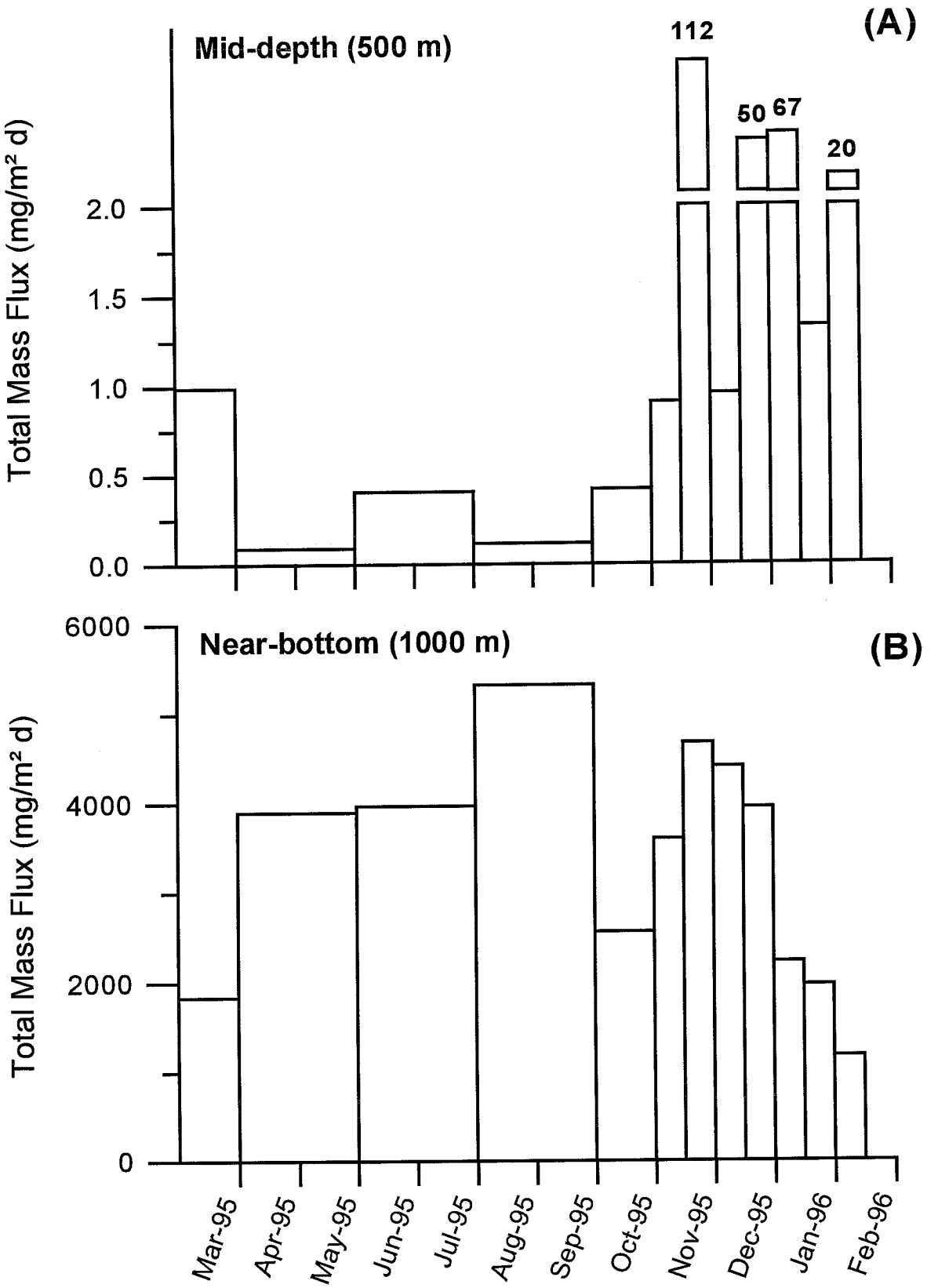
(A)
Mid-depth (500 m)
112
50
67
20
Total Mass Flux (mg/m² d)
2.0
1.5
1.0
0.5
0.0
(B)
Near-bottom (1000 m)
Total Mass Flux (mg/m² d)
6000
4000
2000
0
Mar-95
Apr-95
May-95
Jun-95
Jul-95
Aug-95
Sep-95
Oct-95
Nov-95
Dec-95
Jan-96
Feb-96

Figure 2

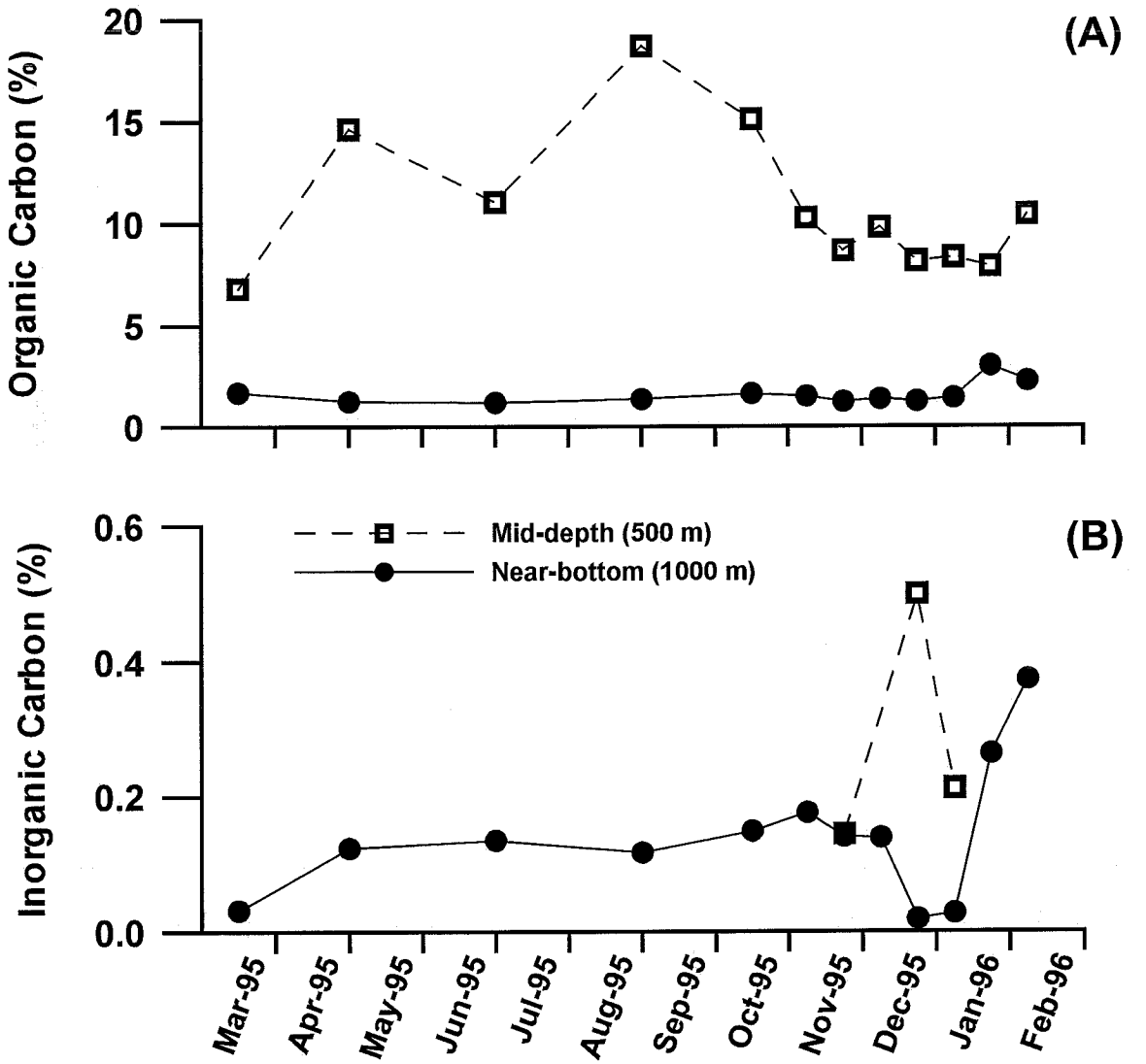
(A)
Organic Carbon (%)
20
15
10
5
0
(B)
Inorganic Carbon (%)
0.6
0.4
0.2
0.0
Mid-depth (500 m)
Near-bottom (1000 m)
Mar-95
Apr-95
May-95
Jun-95
Jul-95
Aug-95
Sep-95
Oct-95
Nov-95
Dec-95
Jan-96
Feb-96

Figure 3

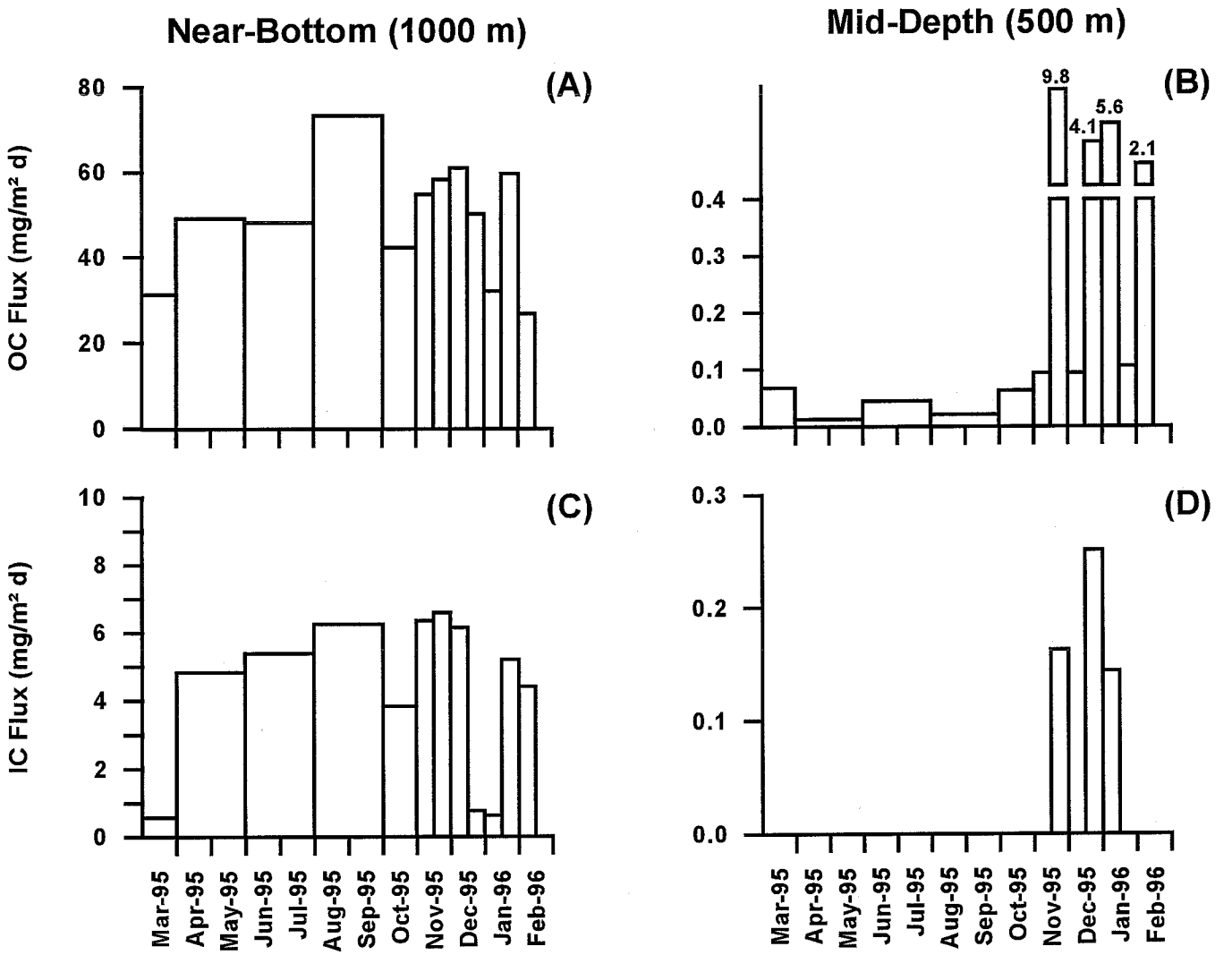
Near-Bottom (1000 m)
Mid-Depth (500 m)
(A)
(B)
(C)
(D)
OC Flux (mg/m² d)
IC Flux (mg/m² d)
80
60
40
20
0
0.4
0.3
0.2
0.1
0.0
9.8
5.6
4.1
2.1
10
8
6
4
2
0
0.3
0.2
0.1
0.0
Mar-95
Apr-95
May-95
Jun-95
Jul-95
Aug-95
Sep-95
Oct-95
Nov-95
Dec-95
Jan-96
Feb-96

Figure 4

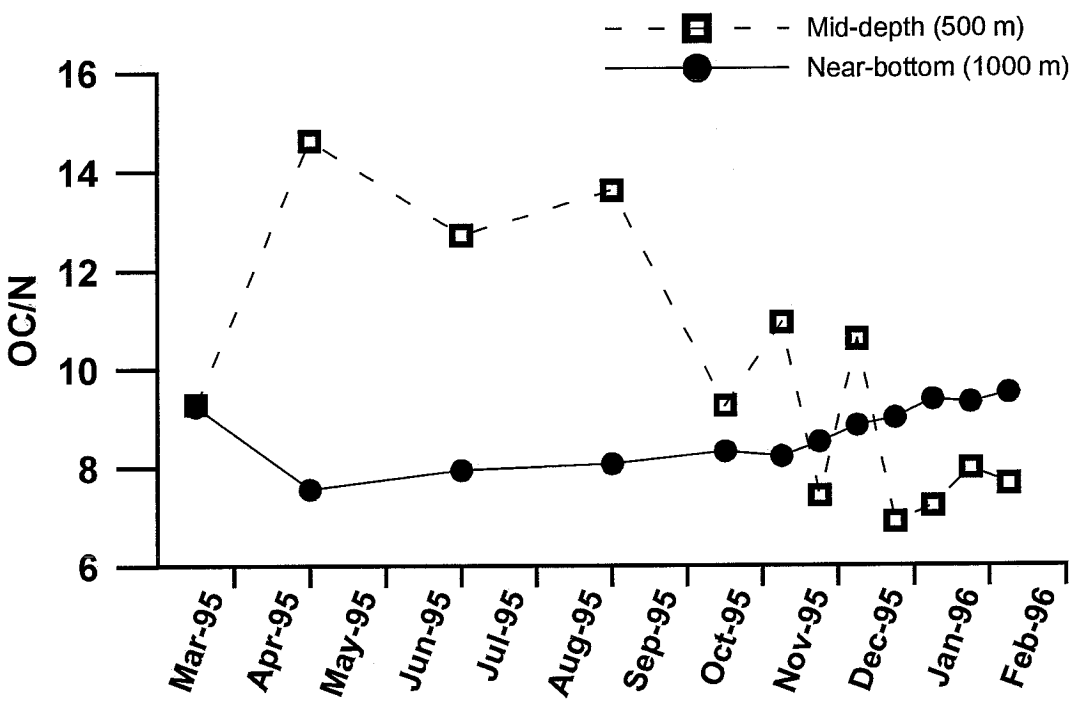
Mid-depth (500 m)
Near-bottom (1000 m)
OC/N
16
14
12
10
8
6
Mar-95
Apr-95
May-95
Jun-95
Jul-95
Aug-95
Sep-95
Oct-95
Nov-95
Dec-95
Jan-96
Feb-96

Figure 5

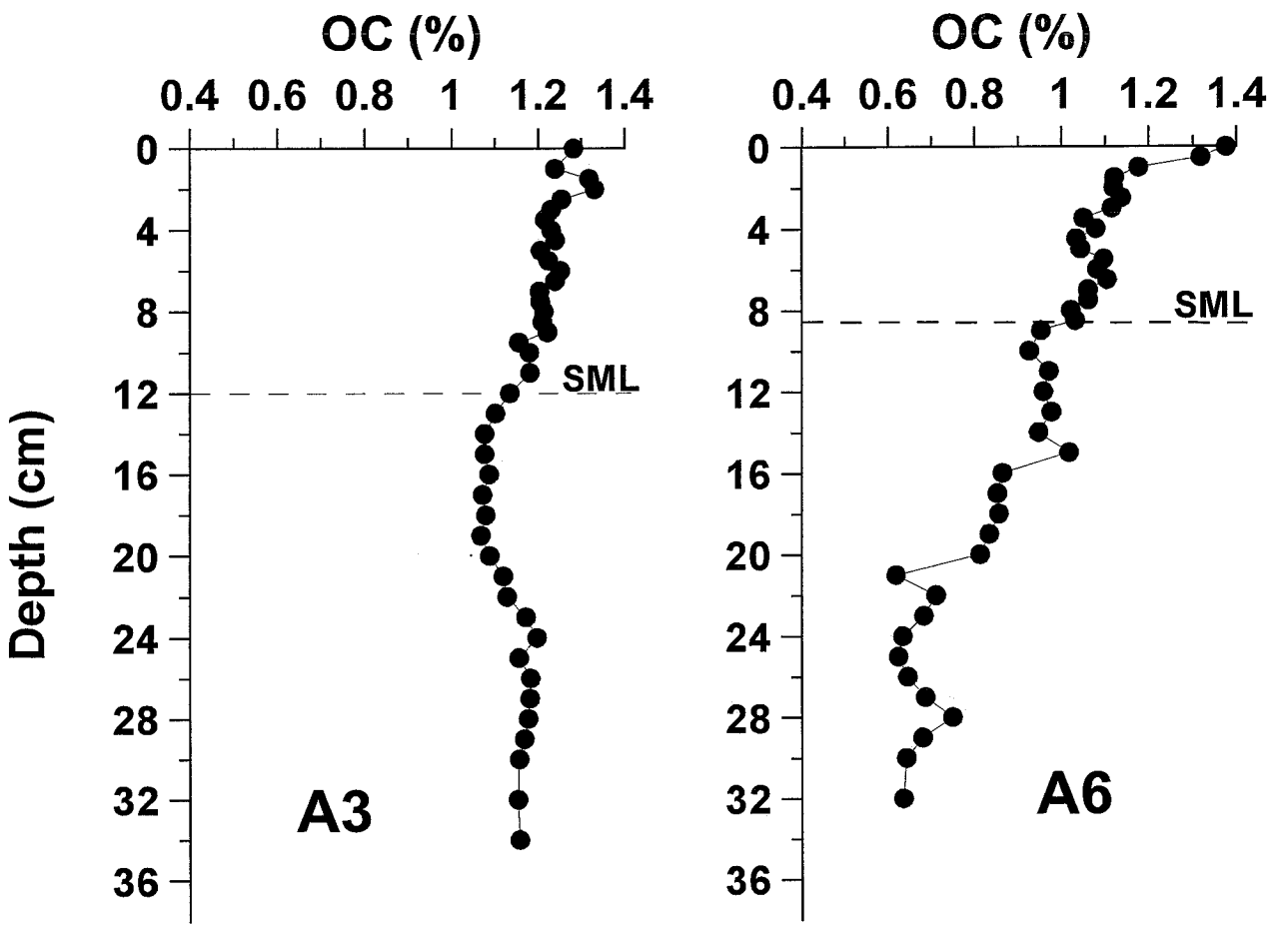
OC (%)
0.4 0.6 0.8 1 1.2 1.4
Depth (cm)
0 4 8 12 16 20 24 28 32 36
SML
A3
OC (%)
0.4 0.6 0.8 1 1.2 1.4
0 4 8 12 16 20 24 28 32 36
SML
A6

Figure 6

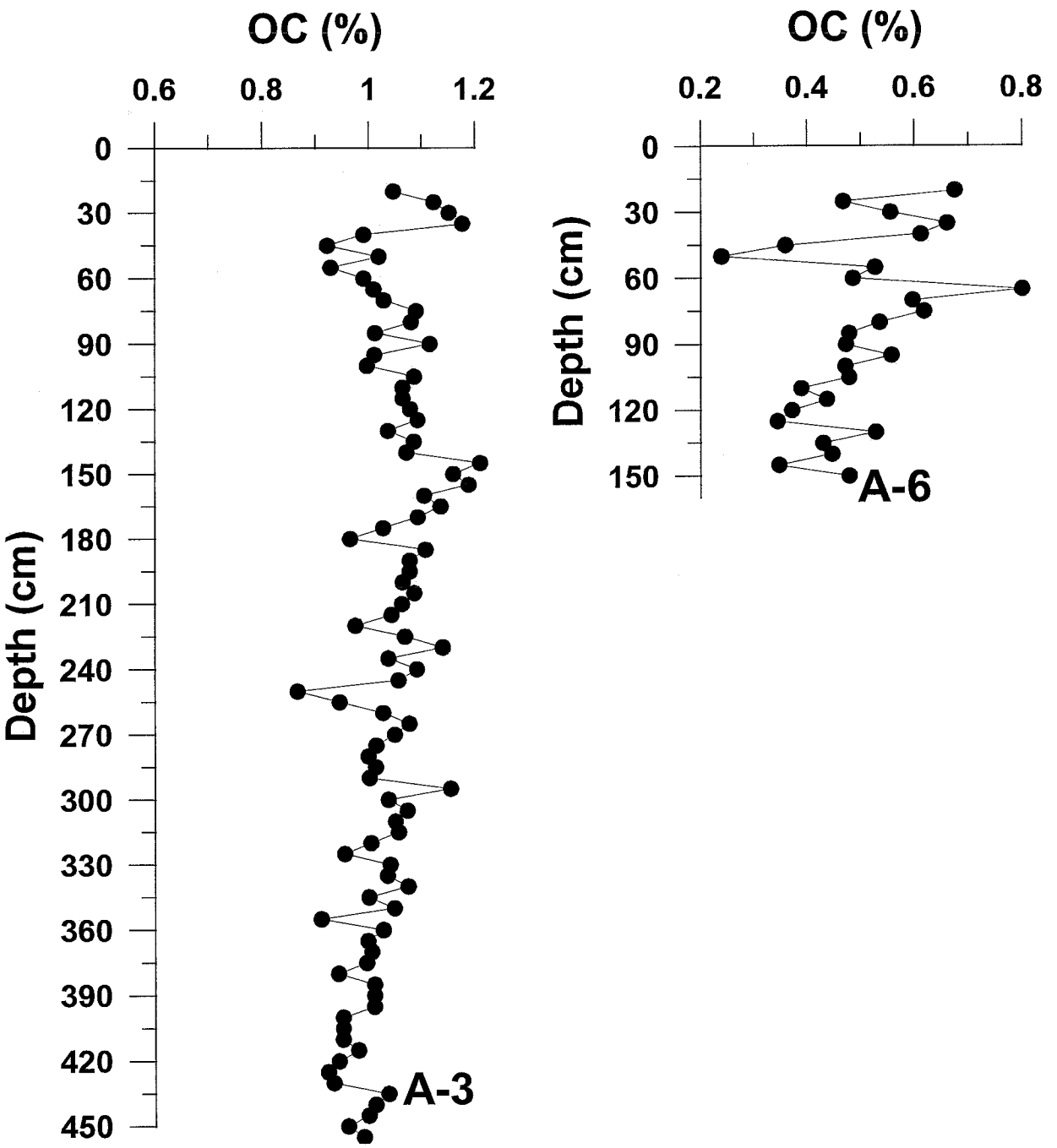
OC (%)
0.6
0.8
1
1.2
0
30
60
90
120
150
180
210
240
270
300
330
360
390
420
450
Depth (cm)
A-3
OC (%)
0.2
0.4
0.6
0.8
0
30
60
90
120
150
Depth (cm)
A-6

Figure 7

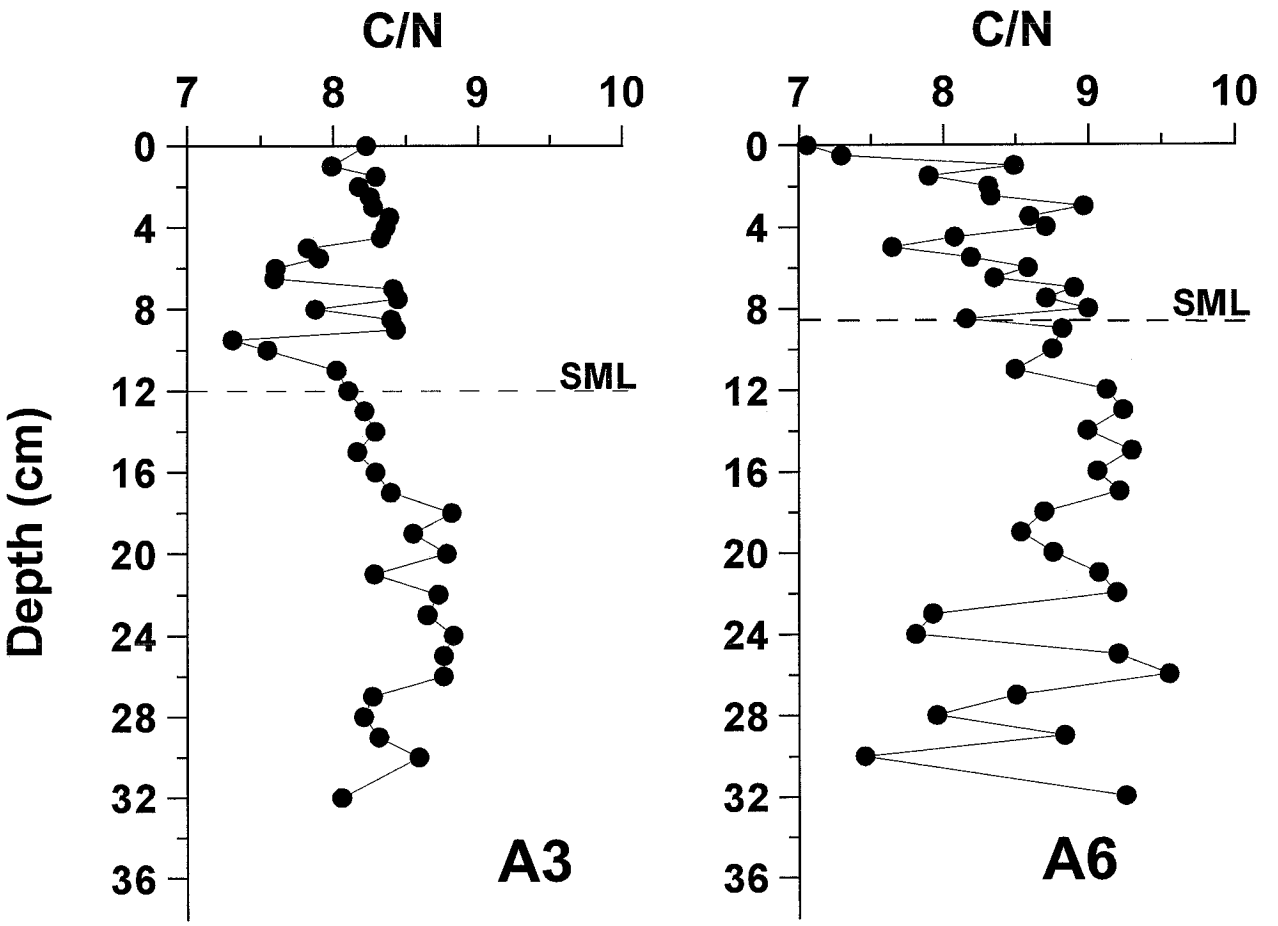

Figure 8

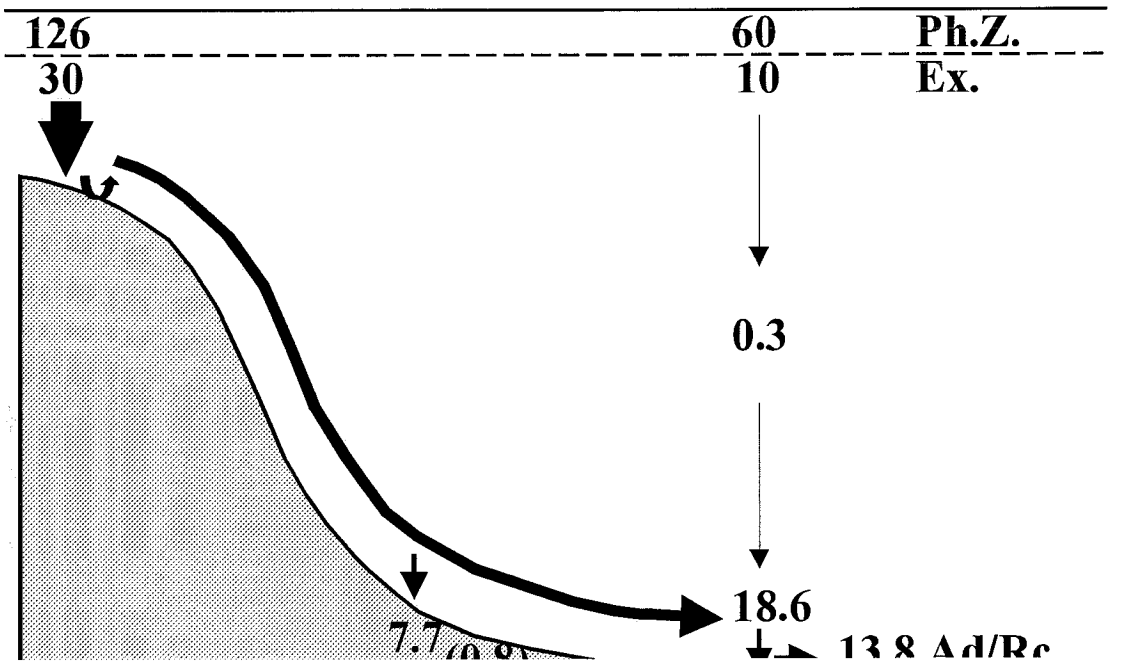

Figure 9

SEDIMENT ACCUMULATION RATES AND CARBON FLUXES TO BOTTOM SEDIMENTS AT THE WESTERN BRANSFIELD STRAIT (ANTARCTICA)

Pere Masqué.[1,3*], Enrique Isla.[2], Joan Albert Sanchez-Cabeza[1], Albert Palanques.[2], Joan M, Bruach[1], Pere Puig[2,4] and Jorge Guillén[2].

[1] Departament de Física, Universitat Autònoma de Barcelona, E-08193 Bellaterra, Spain.

[2] Departament de Geologia Marina i Oceanografia Física, Institut de Ciències del Mar, Av. Joan de Borbó, s/n, E-08039 Barcelona, Spain.

[3] Present address: Marine Science Research Center, State University of New York, Stony Brook, NY 11794-5000, USA.

[4] Present address: School of Oceanography, University of Washington, Box: 357940, Seattle, WA 98195, USA.

Deep-Sea Research II (accepted)

* Corresponding author. Fax: 34-93-5812155; E-mail: pmasque@einstein.uab.es

SEDIMENT ACCUMULATION RATES AND CARBON FLUXES TO BOTTOM SEDIMENTS AT THE WESTERN BRANSFIELD STRAIT (ANTARCTICA)

Masqué, P.[1,3*], Isla, E.[2], Sanchez-Cabeza, J.A.[1], Palanques, A.[2], Bruach, J.M.[1], Puig, P.[2,4] and Guillén, J.[2].

[1] Departament de Física, Universitat Autònoma de Barcelona, E-08193 Bellaterra, Spain.

[2] Departament de Geologia Marina i Oceanografia Física, Institut de Ciències del Mar, Av. Joan de Borbó, s/n, E-08039 Barcelona, Spain.

[3] Present address: Marine Science Research Center, State University of New York, Stony Brook, NY 11794-5000, USA.

[4] Present address: School of Oceanography, University of Washington, Box: 357940, Seattle, WA 98195, USA.

* Corresponding author. Fax: 34-93-5812155; E-mail: pmasque@einstein.uab.es

ABSTRACT

Mean sediment and carbon accumulation rates in the western Bransfield Strait, during the last circa 100 years, were determined at three sites by using ^{210}Pb as a radiotracer of sedimentation processes. ^{210}Pb profiles showed moderate mixing in the upper 8.5-12 cm, which was attributed to bioturbation. Sediment accumulation rates calculated assuming no mixing below the Surface Mixed Layer (SML) were found to be relatively high (between 0.03 and 0.09 g cm^{-2} y^{-1}), and in good agreement with previously reported data based on both ^{210}Pb and ^{14}C dating methodologies in surrounding areas. These results, together with the calculated excess ^{210}Pb fluxes to the bottom sediments and the ^{210}Pb and ^{210}Po distributions in the water column, indicated the presence of a large net advective flux of material in the area, highlighting the importance of glacial related sedimentation processes in this semi-enclosed sea. Carbon in bottom sediments was mainly organic and its content was moderately low (0.65-1.25 %), being slightly higher within the SML, in accordance with the presence of inhabiting organisms. However, OC accumulation fluxes (3.1-6.7 g C m^{-2} y^{-1}) were considerable, due to the high sediment accumulation rates. ^{210}Pb dated profiles allowed us to estimate the amount of carbon exported from the water column and buried in the bottom sediment, which represents about 3-7 % of the mean annual primary production in the euphotic layer of the Bransfield Strait. Finally, the burial efficiency of OC in the sediment was estimated to be approximately 60 to 80 %.

Keywords: sediment accumulation rate, mixing, ^{210}Pb, carbon fluxes, carbon burial, Antarctica.

INTRODUCTION

Studies from ice core measurements have allowed to estimate that the atmospheric partial pressure of CO_2, the most important greenhouse gas in the atmosphere after water vapour, has increased by about 32% from the beginning of the industrial revolution (Neftel *et al.*, 1985). From emission estimates (Marland *et al.*, 1999) and tropospheric pCO_2 measurements (Keeling and Whorf, 1999) it can be deduced that the oceans and the terrestrial biosphere take up about 50% of anthropogenic emissions. The ocean alone presumably takes up about 35% of the anthropogenic emissions. Therefore, the understanding of the biogeochemical cycling of carbon in the oceans is important in the context of the removal of man made carbon dioxide from the atmosphere. Heinze *et al.* (1999) recently stated that advances in marine carbon cycle research are urgently needed for both the inorganic as well as the biological CO_2 pumps to assess the role that the oceans play in the CO_2 cycle. In particular, it is considered essential to improve, among other aspects, the quantitative interpretation of the marine sediment signal of the carbon cycle and climate changes. This is, to elucidate whether bottom sediments act as a sink for atmospheric CO_2 and, hence, whether burial of organic matter removes a significant fraction of carbon dioxide from the ocean-atmosphere system (Walsh *et al.*, 1985). Therefore, one important aspect is the determination of present and past fluxes of carbon to the sea floor on the basis of recent sediment accumulation rates.

Sarmiento and Toggweiler (1984) suggested that both biogeochemical cycles and water circulation in the Southern Ocean play an important role in controlling atmospheric carbon dioxide levels, which in turn affect global climate. Field measurements and numerical models suggest that the Southern Ocean is currently a net sink for CO_2, with the region south of 50° S accounting for circa 20% of the global marine sink. The Antarctic continental margin is considered to be one of the most sensitive areas to climatic change, and therefore bottom sediments are considered to be important archives for the investigation of past climatic transitions. The Bransfield Strait, characterised by its high productivity (Huntley *et al.*, 1991; Álvarez *et al.*, this issue), has a potential as a sink for atmospheric CO_2, thus being an interesting area for studies on carbon fluxes (Anadón and Estrada, this issue).

The Bransfield Strait is a semi-enclosed Antarctic sea comprising an area of about 50.000 km^2 between the South Shetlands archipelago and the Antarctic Peninsula (Figure 1). Gràcia *et al.* (1997) described the Bransfield Strait as a narrow, volcanic and seismically active extensional basin. It can be divided into three sub-basins which are separated from each other by sills shallower than 1000 m. Maximum depths in the Bransfield Strait are deeper than 2500 m in the eastern basin, 1950 m in the central basin and 1200 m in the western basin (Gràcia *et al.*, 1997; Canals *et al.*, 2000). The western Bransfield Strait is connected to the neighbouring Bellingshausen Sea to the west through passages between the westernmost South Shetland Islands and the Gerlache Strait, and to the Drake Passage to the north via the Boyd Strait. Connections also exist between interinsular passages, and through the northern mouth of the eastern Bransfield Basin.

The western basin has narrow (20-50 km wide) continental shelves and steep slopes, especially on the northern perimeter of the Antarctic Peninsula margin (Canals *et al.*, 2000). The continental shelf is mainly covered by coarse sediments, whereas the

deep basin receive fine sediments probably winnowed by bottom currents transported laterally (Anderson *et al.*, 1991; Palanques *et al.*, this issue). The near-bottom particle fluxes are about three orders of magnitude higher than those of the middle depth, supplying most of the organic components by advective transport (Palanques *et al.*, this issue). From the hydrographic point of view, the Bransfield Strait is best defined as a transition zone between the Bellingshausen Sea and the Weddell Sea.

Radionuclides can be used to obtain sediment geochronologies and accumulation rates at different time scales. Therefore, they can be used to provide the temporal frame for the assessment of the evolution of parameters such as organic carbon (OC), which is a requirement to set up the carbon balance in a particular area. Naturally occurring radionuclides that are particle-reactive are useful for quantification of mixing and accumulation rates in marine sediments (i.e. Koide *et al.*, 1972; Guinasso and Shink, 1975; Benninger *et al.*, 1979; Cochran, 1985). ^{210}Pb, a member of the ^{238}U decay series with a half-life of 22.3 years, enters the oceans mainly *via* the atmosphere and through *in situ* production from radioactive decay of dissolved ^{226}Ra. In addition, inputs from rivers could also be considered in coastal areas. The higher affinity of ^{210}Pb for fine-grained particles and organic matter compared to that of ^{226}Ra causes an excess of ^{210}Pb with respect to ^{226}Ra in the settling particles that are subsequently deposited on the sea floor. Under the assumption of a constant flux of ^{210}Pb to the sea bed, excess ^{210}Pb in the sediments can be used as a tool to estimate recent (*ca.* 100 y) sediment accumulation rates and the degree of mixing produced by the action of living organisms inhabiting the sediments or by physical agents (i.e. Goldberg, 1963; Appleby and Oldfield, 1978; 1992; DeMaster and Cochran, 1982; Zuo *et al.*, 1997; Sanchez-Cabeza *et al.*, 1999).

In this work we selected three stations in the western Bransfield Basin to determine the recent (*ca.* 100 years) sediment accumulation and mixing rates, and the OC fluxes to bottom sediments, burial rates and the fraction preserved with respect to production. In addition, the ^{210}Pb and ^{210}Po behaviour in the water column at one of these stations was also investigated in order to obtain a simple model for balancing ^{210}Pb in the overlying water column and to verify some of the hypotheses.

FIELD AND LABORATORY METHODS

Bottom sediments

Bottom sediments from the western Bransfield Strait were collected using a multiple corer (Bowers and Connelly) designed to recover up to 8 replicates of 10 cm diameter. All studied samples presented a layer of clear sea water over the top of the sediment, thus indicating that very low, if any, disturbance of the samples were induced due to insertion of the tube. Cores were collected in January and February 1996 during the research expedition FRUELA-96 on board the Spanish research vessel BIO Hespérides. Three cores (A3, A6 and B2) were selected for ^{210}Pb analysis. Core locations are shown in Figure 1. Station A-3 was located at the mouth of the Orleans Canyon, while station A-6 was south of Livingston Island and west of Deception Island and at the end of the Orleans Canyon.

Sediment core lengths ranged from 34 to 40 cm. One core from each station was subsampled at 0.5 to 2-cm intervals from top to bottom and sections were stored and frozen in sealed plastic bags until analysis. The outer 2 mm ring was removed from each section to discard the sediment possibly smeared downward during core insertion. For each section, wet and dry masses were determined before and after drying samples at 40°C, and dry bulk densities were calculated. About half of the sample was homogenised to carry out carbon, nitrogen and radionuclide analyses, which included ^{210}Pb and gamma-emitters. The remaining non-homogenised sediment was used to determine the sand content.

Determination of sand content

The sand percentage was obtained by sieving through a 63-µm mesh sieve a pre-weighed sample previously treated with peroxide (20%). The material collected on the sieve was rinsed with distilled water and then placed in an oven at 90°C for 24 h. The dry weight of this fraction was used to calculate the sand percentage.

Water column

At station A-6, 30 l water samples were collected with 12-litre Niskin bottles with an oceanographic rosette, from eight depths (10, 20, 150, 250, 500, 650, 950 and 1059 m) to determine ^{210}Pb and ^{210}Po concentrations. Samples were immediately filtered through Schleicher&Schuell membrane filters to separate dissolved (< 0.2 µm) and particulate (> 0.2 µm) fractions. From each sample, an aliquot of 3-5 litres was filtered through a 0.2 µm pore pre-weighted Nuclepore polycarbonate filter to determine the concentration of suspended particulate matter (SPM). The fraction for the determination of the dissolved species was immediately acidified to pH = 1 using HCl. Known amounts of ^{209}Po (half-life = 102 y) and stable Pb^{2+} were added as internal tracers, as well as Fe^{3+} as a carrier for co-precipitation of lead and polonium isotopes as hydroxides after addition of NaOH. Filters containing the retained particulate matter and precipitates were stored in sealed plastic bags and plastic containers respectively until analysis in the laboratory.

Radiometric analysis

^{210}Pb analyses of the sediment samples were performed following the methodology described by Sanchez-Cabeza *et al.* (1998), by total digestion of 200-300 mg sample aliquots. ^{209}Po was added to each sample before digestion as internal tracer. After digestion, samples were made 1 N HCl and ^{209}Po and ^{210}Po were deposited onto silver disks at 60-70 °C for 8 hours while stirring. Polonium isotopes were counted with α-spectrometers equipped with low background SSB detectors (EG&G Ortec). Due to the elapsed time span between sediment sampling and analyses, ^{210}Pb was assumed to be in radioactive equilibrium with ^{210}Po (half-life = 138 d) in the sediment samples.

Some dried and homogenised samples of each core were counted by gamma spectrometry in calibrated geometries for 2-3 10^5 seconds. This was done by using a high purity intrinsic Ge detector, surrounded by a 12 cm lead shield, lined with 1 cm

copper and 2 mm cadmium, and linked to an 8K MCA. Spectra were analysed with a modified version of the SAMPO family of programs (Koskelo *et al.*, 1981). ^{226}Ra activities were determined through ^{214}Pb (351.92 keV) and ^{214}Bi (609.4 keV) lines of gamma emissions, assuming secular equilibrium with ^{226}Ra. No ^{137}Cs was detected along the cores by gamma spectrometry, due to the combined effects of low concentrations and small amounts of sample available.

Filters containing SPM for ^{210}Pb and ^{210}Po analyses were digested using *aqua regia* after addition of ^{209}Po, while precipitates were centrifuged in order to reduce volumes. All samples were made 1 N with HCl and the same procedure described for sediment samples was followed. As analyses were carried out within 3 months after sample collection, equilibrium between ^{210}Po and ^{210}Pb was not yet reached. One year after the first analyses, samples were reanalysed for ^{210}Po, present by *in situ* disintegration of ^{210}Pb, thus permitting us to determine both ^{210}Pb and ^{210}Po activities at the sample collection date after appropriate decay corrections.

Chemical recoveries of all radiochemical separations ranged from 85 to 100%. For each batch of 10 samples, a reagent blank analysis was also carried out and subtracted for activity determination.

Carbon and nitrogen

Total carbon (TC%) and nitrogen (N%) were measured in duplicate using a Leco CN 2000 analyser. Two subsamples were used to determine the total carbon percentage (TC%). Two other subsamples were digested with HCl in a LECO CC 100 digester and the resultant CO_2 was analysed in the LECO CN 2000 analyser and assigned to inorganic carbon content (IC%), which was used to calculate the calcium carbonate concentration ($CaCO_3$%). The difference between the two values was assumed to represent the percentage of organic carbon content (OC%).

RESULTS AND DISCUSSION

Cores A3 and B2 consisted of muds with very low sand contents (2.8 ± 0.2% and 1.8 ± 0.2% respectively) whereas at station A6 the sand content was higher (13.2 ± 0.4%). The major components of the mud fraction were lithogenic minerals coming from weathering of the volcanic terrain forming the Antarctic Peninsula and the islands of the Bransfield Strait. The mud also showed a relatively high content of biogenic components, especially biogenic opal (Holler, 1989; Yoon *et al.*, 1994; Banfield and Anderson, 1995).

Excess ^{210}Pb concentration profiles in bottom sediments

Supported ^{210}Pb in bottom sediments was calculated from the constant activity of the deepest samples in the cores and was subtracted from the ^{210}Pb total activities to

obtain the excess ^{210}Pb. Good agreement was found between the supported ^{210}Pb mean activities derived from alpha measurements (63.3 ± 2.8, 46.2 ± 0.7 and 31.3 ± 1.1 Bq kg^{-1} for cores A-3, A-6 and B-2 respectively) and ^{226}Ra mean activities obtained by gamma counting at several depths, which were found to range from 35.5 to 54.4 Bq kg^{-1}. Excess ^{210}Pb profiles for each of the three sediment cores are shown in Figure 2. All data are plotted *versus* accumulated mass, to avoid the shape of the profile being affected by variation in porosity along the core.

Excess ^{210}Pb extended to different depths at the three sites (maximum of 36 cm for core B-2, 25 cm and 16 cm for cores A-3 and A-6 respectively), which is a preliminary indication of the different sediment accumulation rates at the three sites. In all cores, a Surface Mixed Layer (SML) ranging from 8.5 to 12 cm was present in the upper part of the sediment (Table 1), as deduced from the change in the ^{210}Pb slopes when plotted in a semi-logarithmic scale (Figure 2). In fact, the SML presence led to an almost constant excess ^{210}Pb activity, especially in the case of core B-2, thus indicating that the degree of mixing in this core was the highest. However, an exponential decrease of ^{210}Pb activity below the SML was observed in all cases, and was used to determine the mean sediment accumulation rates.

Surface excess ^{210}Pb concentrations in cores A-6 and B-2, which were collected from similar depths, were comparable (1046 ± 54 and 1010 ± 59 Bq kg^{-1} respectively) and higher than in core A-3 (676 ± 32 Bq kg^{-1}) (Table 1). Excess ^{210}Pb inventories, *A(0)*, ranging from 26.3 to 42.3 kBq m^{-2}, were calculated by summing the excess ^{210}Pb activity of each section. These results agree well with those given by Harden *et al.* (1992) for the Bransfield Strait, who reported a range of surface excess ^{210}Pb from 268 to 1610 Bq kg^{-1} and of excess ^{210}Pb inventories from 15 to 66 kBq m^{-2}. The annual excess ^{210}Pb fluxes to the sediment, *q*, were obtained by applying the expression proposed by Sanchez-Cabeza *et al.* (2000):

$$q = \frac{\quad}{\Delta t} \qquad (1)$$

The use of this formula instead of the usual one *($q=\lambda \cdot A(0)$)* permits to consider a more general hypothesis, by which the flux of ^{210}Pb to the sediments is constant during a period of time *Δt (order of magnitude of years)*, instead of being continuously constant. In this work, *Δt* was taken as one year assuming that the *unsupported* ^{210}Pb flux to the sediment is time dependent, though the annual variations are possibly small (Turekian *et al.*, 1977; Tsunogai *et al.*, 1988; Heussner *et al.*, 1990; Thunell and Moore, 1994). From equation (1), the highest excess ^{210}Pb annual flux was obtained for core B-2 (1293 ± 11 Bq m^{-2} y^{-1}), it being significantly lower for the other two stations (Table 1).

Sediment accumulation rates

Sediment reworking due to physical or biological agents may affect the excess ^{210}Pb distribution along the sediment. Therefore, when building up a sedimentation model basic hypotheses must take into account this factor so as not to overestimate sedimentation rates (Benninger *et al.*, 1979; Nittrouer *et al.*, 1984; Cochran, 1985). Goldberg and Koide (1962) pointed out that the main processes governing excess ^{210}Pb profiles in the seabed are sediment accumulation, radioactive decay and particle

mixing. They proposed a one-dimensional advection-diffusion model to calculate the sedimentation rate (S, in cm y^{-1}) and the mixing coefficient (D_B, in cm^2 y^{-1}) that describes the intensity of particle reworking:

$$\partial t \quad - \quad _B \quad \partial x^2 \quad \quad \partial x \quad \quad (2)$$

where A (Bq kg^{-1}) is the excess ^{210}Pb concentration at depth x (cm), and S and D_B are assumed to be constant.

Many researchers have used this procedure in continental margins and deep-sea sediments (i.e. Guinasso and Shink, 1975; DeMaster and Cochran, 1982; Roberts *et al.*, 1997). As D_B and S cannot be determined independently, a solution for D_B can be obtained if S is known or assumed to be negligible. When the latter is not the case or no evidence supporting this is available, S can be determined from other evidences, such as ^{14}C dating or ^{210}Pb from the non-mixed layer, where D_B is assumed negligible. In this respect, although comparison of ^{210}Pb sedimentation rates with those calculated from ^{14}C date may be useful, it must be done with caution because the two methodologies involve different time-scales.

Assuming steady state conditions and when mixing is not present, equation (2) can be solved under the boundary conditions of $A = A_0$ (x=0) and $A \rightarrow 0$ ($x \rightarrow \infty$), by means of the equation

$$A = A_0 e \quad \quad (3)$$

This is usually done by least-squares fitting of the logarithm of excess ^{210}Pb versus depth for the strata below the SML. Then, the sedimentation rate calculated by using equation (3) or from ^{14}C data can be introduced as a constant in equation (4) to determine D_B, also using least-square fitting for the SML:

$$A = A_0 e \quad \quad (4)$$

In fact, as one cannot know for sure that deep mixing is not present, equation (3) allows us to obtain an apparent sediment accumulation rate which may be an upper limit (Benninger *et al.*, 1979; Nittrouer *et al.*, 1984; Ledford-Hoffman *et al.* 1986). Some authors (i.e. Roberts *et al.*, 1997) also simplify equation (4) by assuming that sediment accumulation is negligible in the mixed layer, and the obtained mixing coefficient D_B is also an upper limit.

In this study we consider the ^{210}Pb profiles as a two layer system with an upper mixed layer extending to a distance L below the water-sediment interface (SML) and a second layer below L where no mixing takes place. Nelson (1988), DeMaster *et al.* (1991) and Harden *et al.* (1992) also used this procedure for determining accumulation rates and mixing coefficients when studying some cores in the Antarctic Peninsula area.

The largest sediment accumulation rate was obtained for core B-2 (0.093 ± 0.003 g cm^{-2} y^{-1}, or 1.56 ± 0.05 mm y^{-1}), being slightly higher than at station A-3 (0.060 ± 0.003 g cm^{-2} y^{-1}, or 1.17 ± 0.05 mm y^{-1}) and almost three times higher than that observed at station A-6 (0.0351 ± 0.0014 g cm^{-2} y^{-1}, or 0.57 ± 0.02 mm y^{-1}). Therefore, sedimentation is relatively high at all three stations, with particular emphasis at B-2.

The mixing coefficient was also higher at station B-2 (40 $cm^2\ y^{-1}$), which is fed by fines coming from the highly productive Gerlache Strait and adjacent fjords, than at stations A-3 and A-6 (12 and 2 $cm^2\ y^{-1}$ respectively).

In general, ^{210}Pb derived accumulation rates must be taken with prudence, and independent methods, such as ^{14}C dates or ^{137}Cs or $^{239,240}Pu$ chronologies, should be used to verify the results. This has been remarked on by various authors for southern high latitude environments (Ledford-Hoffman *et al.*, 1986; DeMaster *et al.*, 1991; 1996; Harden *et al.*, 1992). ^{137}Cs, present in the environment as a consequence of the atmospheric detonation of nuclear weapons, has been in the seabed sediments since the early 1950s. Therefore, it can be used to quantify the mixing processes in the surface sediments and to study how they affect the ^{210}Pb profiles. However, we were not able to detect ^{137}Cs by gamma spectrometry because levels are very low. Indeed, Harden *et al.* (1992) found that ^{137}Cs chronologies have a limited usefulness due to the fact that activities are too close to detection limits in the sediments of the Antarctic region. Nevertheless, DeMaster *et al.* (1991) stated that in the Bransfield Strait the ^{137}Cs-penetration depth confirmed that deep mixing would be negligible in most cases, although this assertion was made with caution, due to the above mentioned limitations regarding to detection limits.

^{14}C is commonly used to check the validity of the sediment accumulation rates inferred from ^{210}Pb profiles, due to the fact that its longer half-life (5730 y) allows it to be detected deeper in the sediment, presumably not affected by recent mixing processes (e.g. Nozaki *et al.*, 1977). In a companion paper (Bárcena *et al.*, this issue), ^{14}C derived sediment accumulation rates have been calculated for stations A-3 (2.08 mm y^{-1}) and A-6 (1.15 mm yr^{-1}). Taking into account the different time scales addressed by both dating techniques, these values agree reasonably well with those obtained using the ^{210}Pb method. This finding is of particular interest, as in some cases the differences between the two dating methods can be as high as one order of magnitude. For instance, Harden *et al.* (1992) reported discrepancies between ^{210}Pb and ^{14}C sediment accumulation rates at two particular stations in Marguerite Bay (Pacific margin of the Antarctic Peninsula, 2.5 mm y^{-1} and 0.4 mm y^{-1} respectively) and the Bransfield Strait (2.0 mm y^{-1} and 0.9 mm y^{-1} respectively). In fact, in the latter case, the ^{14}C derived sediment accumulation rate could range from 0.5 to 2.1 mm y^{-1}, depending on the ranges in the ^{14}C ages used. Nevertheless, these authors and DeMaster *et al.* (1991) concluded that sediment accumulation rates on 100-yr (^{210}Pb, 0.8 - 3.4 mm y^{-1}) and 1000-yr (^{14}C, 0.6 to 4.9 mm y^{-1}) time scales were in good agreement in the Bransfield Strait, at least in a factor of two. Moreover, the results for sedimentation rates reported by these authors for the studied area of the Bransfield Strait (1.2 - 2.3 mm y^{-1}) also compare well with ours. Sedimentation rates obtained from ^{14}C in gravity cores at stations A-3 and A-6 were introduced in equation (4) to calculate the mixing rates for the cores collected using the maxicorer system, confirming that they were not significantly different (10 $cm^2\ y^{-1}$ for A-3 and 12 $cm^2\ y^{-1}$ for A-6) from those derived by using the ^{210}Pb sedimentation rates. For core B-2, as no ^{14}C derived accumulation rates were available, both the accumulation rate and the mixing coefficient derived from ^{210}Pb data were assumed to be reliable.

Palanques *et al.* (this issue) reported mass fluxes and ^{210}Pb data obtained from a sediment trap deployed 30 meters above the sea floor at station A-6 during one year. The estimated mass flux was 0.13 g $cm^{-2}\ y^{-1}$, the mean ^{210}Pb activity was found to be

987 ± 9 Bq kg^{-1}, and the annual ^{210}Pb flux was 1310 ± 12 Bq m^{-2} y^{-1}. The mean ^{210}Pb activity in the material collected by the sediment trap and the surface ^{210}Pb activity in core A-6 (1046 ± 54 Bq kg^{-1}) are similar (ratio trap/core = 0.94), thus indicating that the material collected by the sediment trap is of the same nature as that which ultimately accumulates on the sea floor. It is worth mentioning that although corrections for ^{226}Ra contents in sediment trap material were not carried out, they would not be critical given that concentrations usually found in sinking material (between 30-60 Bq kg^{-1}) are low compared to excess ^{210}Pb.

On the contrary, some discrepancies are observed when comparing both mass and ^{210}Pb fluxes, as annual trap values were respectively 3.8 and 1.6 times higher than those derived from ^{210}Pb dating of bottom sediments. Direct comparison between sediment and trap data must be done with caution, as time scales differ by a factor of about 100 (from 1 year to 100 years). However, an important conclusion is that sediment trap fluxes confirmed that sediment accumulation in this area is high, of the order of that observed in bottom sediments, and sufficient to discard the hypothesis that mixing is the only process that accounts for the presence of excess ^{210}Pb downcore to 20-25 cm depth.

^{210}Pb and ^{210}Po in the water column

^{210}Pb and ^{210}Po concentrations in the dissolved fraction were almost constant along the entire water column, with 210Pb systematically in excess (ratio $^{210}Po/^{210}Pb$ = 0.48 ± 0.02) at all depths (Table 2). In the particulate fraction, ^{210}Pb concentration increased almost monotonically with depth, from 0.071 ± 0.006 Bq m^{-3} (4% of the total ^{210}Pb) at the surface to 0.28 ± 0.02 Bq m^{-3} (14% of the total ^{210}Pb) at 10 m above the sea floor. As ^{210}Pb is scavenged by sinking particles, this suggests that the residence time of particles is responsible for this enrichment. Particulate ^{210}Po, representing about 25% of the total ^{210}Po, showed a similar pattern with the exception of concentrations observed in surface waters (10 and 20 meters), where maximum activities were found.

The $^{210}Po/^{210}Pb$ ratios in the particulate fraction at 10 and 20 m were 4.5 ± 0.5 and 5.3 ± 0.6 respectively. It is usually accepted (Heyraud and Cherry, 1983) that average values for the $^{210}Po/^{210}Pb$ ratio are 0.5 in surface waters, 1 in sediments, 2 in zooplankton faecal pellets, 7 in phytoplankton and 30 in zooplankton. Hence, $^{210}Po/^{210}Pb$ ratios higher than unity are expected to be found in fresh biogenic material, while $^{210}Po/^{210}Pb$ ratios close to unity would correspond to old material in which ^{210}Po and ^{210}Pb are in radioactive equilibrium. Our results indicate that SPM in the upper part of the water column was mainly composed of biogenic particles, whilst at greater depths the $^{210}Po/^{210}Pb$ ratio close to unity would indicate that the material is relatively old. In this discussion it is recognised that the particulate matter collected in Niskin bottles may not be exactly the same as that which sinks to the sea floor, but in our opinion this approximation can be accepted at least as a first approximation. In any case, along the entire water column the $^{210}Po/^{210}Pb$ ratio was slightly higher than unity (mean 1.25 ± 0.04), indicating that, to some extent, a contribution of biogenic material characterised by a high $^{210}Po/^{210}Pb$ ratio can be inferred.

Imposing steady state conditions, for station A-6 a balance equation can be written as:

$$F_{atm} + F_{Ra} = D + T_{sink} \quad (5)$$

where F_{atm} is the atmospheric flux of ^{210}Pb to the sea surface, F_{Ra} is the *in situ* ^{210}Pb production by ^{226}Ra disintegration, D accounts for ^{210}Pb decay and T_{sink} is the flux of ^{210}Pb due to particle sinking. Broecker and Peng (1982) estimated the atmospheric flux of ^{210}Pb (F_{atm}) for these latitudes as 25 Bq m^{-2} y^{-1}, and more recently Rutgers van der Loeff and Berger (1991) reported a range of 2-33 Bq m^{-2} y^{-1}. From the works of Ku and Lin (1976) and Rutgers van der Loeff and Berger (1991), an average concentration of ^{226}Ra in the water column of 3.3 Bq m^{-3} can be used. Then, the ^{210}Pb flux to the sea floor was estimated to be in the range 38-69 Bq m^{-2} y^{-1}. These values are less than 10% of the ^{210}Pb flux calculated from the ^{210}Pb inventory in the sedimentary column at station A-6 (803 ± 11 Bq m^{-2} y^{-1}). Therefore, an important net input of ^{210}Pb to the sea floor, not associated to vertical sinking of particles from the surface waters, is needed and, as a consequence, a large net advective flux of material should occur.

The findings of Palanques *et al.* (this issue) support this conclusion, as the flux in a trap at 30 m above the bottom (mab) is about 300 times larger than that found at 500 mab. Then, it was concluded that lateral currents near the sea floor drive the lateral transport of particles from shallow areas, causing sediment focussing in the deepest parts of the basin. This confirms the findings reported by DeMaster *et al.* (1991), who observed that excess ^{210}Pb inventories in the basins (mean = 45 kBq m^{-2}) were three times greater than on the shallow flanks (mean = 15 kBq m^{-2}).

Organic carbon

Concentrations of organic carbon (OC) along the three sediment cores presented slight variations with depth (Figure 3). Mean OC contents for each core were 1.20 ± 0.07 % (A-3), 0.94 ± 0.11 % (A-6) and 0.75 ± 0.13 % (B-2) if all data from the individual profiles were considered. However, and as stated before, a certain degree of mixing is present at the topmost part of the sea floor. In fact, OC contents decrease from the core surface until reaching a constant value approximately at the SML lower limit. This is especially evident in core B-2 (Figure 3). Therefore, mean values were recalculated for the SML and below it. For stations A-3 and A-6 mean concentrations are similar for both parts of the profiles taking into account associated uncertainties (Table 3), although still slightly higher in the SML. At station B-2, this difference is more pronounced. We attribute the higher contents of OC in the SML to the presence of inhabiting organisms, being noticeable that for station B-2 the mixing coefficient was correspondingly higher. The OC/N mean ratios in cores A-3, A-6 and B-2 were 7.1 ± 0.3, 7.4 ± 0.5 and 7.0 ± 0.4 respectively (Isla, in preparation), indicating that this material was close to fresh marine organic matter. It was observed that, as expected, no significant differences were obtained when calculating separately these mean values for the SML and below it. OC/N values were very similar to those observed in near-bottom settling particulate matter, which contains fresh organic matter that was transported laterally (Palanques *et al.*, this issue). As mid water mean settling fluxes are negligible (0.19 mg C m^{-2} d^{-1}, Palanques *et al.*, this issue), we concluded that the

organic matter accumulated in bottom sediment has the same origin as that transported laterally near the bottom. Moreover, mean OC concentrations in particulate matter settling at 500 and 30 mab over one year at station A-6 were 8.7 and 1.4% respectively, while OC content at the surface of the sediment core A-6 was 1.3%. All these considerations agree well with the results of ^{210}Pb concentrations obtained in both the trapped sediment and the bottom sediment at station A-6 and discussed before.

Once accumulated at the surface of the bottom sediments, OC undergoes deep burial and is affected by degradation processes within the sediment column. A fraction of OC is not affected by these degradation processes and remains preserved in the sediments over geological time scale. Maximum OC burial rates can be obtained by multiplying OC contents by sediment accumulation rates derived from ^{210}Pb profiles. According to the preceding remarks, we made these calculations using the OC mean values below the SML, obtaining accumulation fluxes of 6.7 ± 0.4, 3.1 ± 0.2 and 6.1 ± 0.4 g C m^{-2} y^{-1} in cores A-3, A-6 and B-2 respectively (Table 3). If OC values from the SML were used, accumulation fluxes would be consequently slightly higher. These results are coherent with those of DeMaster *et al.* (1991), who reported OC contents ranging from 0.56 to 1.7 % along the whole Bransfield Strait and a mean OC net flux to the bottom sediments of 7.5 g C m^{-2} y^{-1}.

The annual value of primary production can be estimated from the mean production over spring months, which in the study area ranges from 0.86 g C m^{-2} d^{-1} to 1 g C m^{-2} d^{-1} (Holm-Hansen and Mitchell, 1991; Moran and Estrada, this issue). Considering that these values are representative of the mean primary production over about 100 spring days, and assuming that the primary production is negligible during the rest of the year (Estrada, pers. comm.), we estimated that the annual primary production in the study area is of the order of 100 g C m^{-2}. Thus, the fraction of the annual carbon accumulation flux in the sediment represented around 6-7 % of the mean annual primary production in the euphotic layer for stations B2 and A3, and about 3 % for core A6. These values are compatible with those estimated by DeMaster *et al.* (1991) for the Bransfield Strait. They concluded that about 9% of the total production in surface waters (considered as 77 g C m^{-2} y^{-1}) was preserved in the seabed.

The OC burial efficiency, or the percentage of deposited OC that is preserved in the sediment, can be estimated comparing the concentration at the surface of the core and the constant concentration at depth where it already underwent some diagenesis. In doing so, we obtained OC burial efficiencies of about 80% at station A-3 and 60% at stations A-6 and B-2. Another way to face this estimation could be as follows: annual OC fluxes calculated from sediment trap data at 500 and 30 mab at station A-6 (Palanques *et al.*, this issue) were 0.35 and 18.6 g C m^{-2} y^{-1} respectively. Taking into account that the sediment flux measured by the near bottom sediment trap was apparently almost 4 times higher than the accumulation rate derived by ^{210}Pb in bottom sediments, the annual OC accumulation rate could be near 5 g C m^{-2} y^{-1}. Therefore, both organic carbon contents and the burial rate calculated from ^{210}Pb sedimentation rates in the sea floor below the SML would be a factor 1.6 lower than the expected levels from sediment trap measurements, indicating that the OC burial efficiency would be about 60%. Remineralisation (consumption of organic matter mainly by microbial processes) occurring in the SML once OC has been deposited on

the seafloor would account for remaining 40%, turning to be less efficient as depth increases in the sedimentary column

ACKNOWLEDGEMENTS

This research was funded by the Comisión Interministerial de Ciencia y Tecnología of Spain, under contracts ANT94-1010, MAR96-1781-CO2-01 and ANT96-1346-E. It also benefited from a pre-doctoral fellowship from CONACYT (México), reference 92766. We thank the officers, managers, technicians and crew of the BIO Hespérides and the UGBO (CSIC) for their assistance during the cruise. We also thank M. Farrán for his support during fieldwork. Comments and suggestions by O. Radakovitch and two anonymous reviewers helped to improve the manuscript.

REFERENCES

Álvarez, M., Ríos, A.F. and Rosón, G. 2001. Spatio-temporal variability of Air-Sea carbon dioxide and oxygen fluxes in the Bransfield and Gerlache straits during Austral summer 1995-1996. Deep-Sea Research II, this issue.

Anadón, R. and Estrada, M. 2001. The FRUELA cruises: a carbon flux study in productive areas in the Antarctic peninsula (December 1995 – January 1996). Deep-Sea Research II, this issue.

Anderson, J.B., Bartek, L.R. and Thomas, M.A. 1991. Seismic and sedimentological record of glacial events on the Antarctic Peninsula shelf. In: Thomson, M.R.A., Crame, J.A., Thomson, J.W. (Eds.), Evolution of Antarctica. Cambridge University Press, Cambridge, pp. 687-691.

Appleby, P.G. and Oldfield, F. 1978. The calculation of Lead-210 dates assuming a constant rate of supply of unsupported Pb-210 to the sediment. Catena 5, 1-8.

Appleby, P.G. and Oldfield, F. 1992. Application of lead-210 to sedimentation studies. In: Ivanovich, M. and Harmon, R.S. (Eds), Uranium-Series Disequilibrium - Applications to Earth, Marine and Environmental Sciences. Oxford University Press, pp. 731-338.

Banfield, L.A. and Anderson, J.B. 1995. Seismic facies investigation of the Late Quaternary glacial history of Bransfield Basin, Antarctica. In: Cooper, A.K., Barker, P.F., Web, P.N. and Brancolini, G. (Eds.), Geology and Seismic Stratigraphy of the Antarctic Margin. American Geophysical Union, Washington D.C., pp. 123-140.

Bárcena, M. A., Isla, E., Plaza, A., Flores, J. A., Sierro, F.J., Masqué, P., Sanchez-Cabeza, J.A. and Palanques, A. 2001. Bioaccumulation record and paleoclimatic significance in the Western Bransfield Strait. Deep-Sea Research II, this issue.

Benninger, L.K., Aller, R.C., Cochran, J.K. and Turekian, K.K. 1979. Effects of biological mixing on the ^{210}Pb chronology and trace metal distribution in a Long Island Sound sediment core. Earth and Planetary Science Letters 43, 241-259.

Broecker, W.S. and Peng, T.-H. 1982. Tracers in the Sea. Lamont-Doherty Geological Observatory, Columbia University, NY.

Canals, M., Urgeles, R. and Calafat, A.M. 2000. Deep sea-floor evidence of past ice streams off the Antarctic Peninsula. Geology 28 (1), 31-34.

Cochran, J.K. 1985. Particle mixing rates in sediments of the eastern equatorial Pacific. Evidence from ^{210}Pb, ^{239,240}Pu and ^{137}Cs distributions at MANOP sites. Geochimica et Cosmochimica Acta 45, 1155-1172.

DeMaster, D.J. and Cochran, J.K. 1982. Particle mixing rates in deep-sea sediments determined from excess ^{210}Pb and ^{32}Si profiles. Earth and Planetray Science Letters 61, 257-271.

DeMaster, D.J., Nelson, T.M., Harden, S.L. and Nittrouer, C.A. 1991. The cycling and accumulation of biogenic silica and organic carbon in Antarctic deep-sea and continental margin environments. Marine Chemistry 35, 489-502.

DeMaster, D.J., Ragueneau, O. and Nittrouer, C.A. 1996. Preservation efficiencies and accumulation rates for biogenic silica and organic C, N, and P in high-latitude sediments: The Ross Sea. Journal of Geophysical Research 101 (C8), 18051-18518.

Goldberg, E.D. and Koide, M. 1962. Geochronological studies of deep-sea sediments by the ionium-thorium method. Geochimica et Cosmochimica Acta 26, 417-450.

Goldberg, E.D. 1963. Geochronology with ^{210}Pb in radioactive dating. IAEA, Vienna, 121-131.

Gràcia, E., Canals, M., Farràn, M., Sorribas, J., and Pallàs, R. 1997. Central and Eastern Bransfield Basins (Antarctica) from high resolution swath-bathymetry data. Antarctic Science 9, 168-180.

Guinasso, N.L. and Shink, D.R. 1975. Quantitative estimates of biological mixing rates in abyssal sediments. Journal of Geophysical Research 80 (21), 3032-3043.

Harden, S.L., DeMaster, D.J. and Nittrouer, C.A. 1992. Developing sediment geochronologies for high-latitude continental shelf deposits: a radiochemical approach. Marine Geology 103, 69-97.

Heinze, C., Jansen, E., Ragueneau, O., van den Berg, C.M.G. and Watson, A.K. 1999. Global carbon balance. In: Oost, W. and Lipiatou, E. (Eds.), Air-sea and Sea-ice Interactions. Research in enclosed seas series – 7. EUR 18638 EN, pp 36.

Heussner, S., Cherry, R.D. and Heyraud, M. 1990. Po-210, Pb-210 in sediment trap particles on a Mediterranean continental margin. Continental Shelf Research 10, 989-1004.

Heyraud, M. and Cherry, R.D. 1983. Correlation of Po-210 and Pb-210 enrichments in the sea-surface microlayer with neuston biomass. Continental Shelf Research 1, 283-293.

Holm-Hansen, O. and Mitchell, B.G. 1991. Spatial and temporal distribution of phytoplankton and primary production in the western Bransfield Strait region. Deep-Sea Research 38 (8/9), 961-980.

Holler, P. 1989. Mass physical properties of sediments from Bransfield Strait and Northern Weddell Sea. Marine Geotechnology 8, 1-18.

Huntley, M., Karl. D.M., Niler, P. and Holm-Hansen, O. 1991. Research on Antarctic Ecosystem Rates (RACER): an interdisciplinary field experiment. Deep-Sea Research, 38 (8/9) 911-941.

Isla, E. 2001. Estudio sobre los flujos sedimentarios en los estrechos de Bransfield y Gerlache (Antártida). PhD Thesis, Universitat Politècnica de Catalunya, Barcelona, Spain, in preparation.

Keeling, C.D. and Whorf, T.P. 1999. Atmospheric CO_2 records from sites in the SIO air sampling network. In: Trends: A Compendium of Data on Global Change. Carbon Dioxide Information Analysis Center, Oak Ridge National Laboratory, U.S. Department of Energy, Oak Ridge, Tenn., U.S.A.

Koide, M., Soutar, A. and Goldberg E.D. 1972. Marine geochemistry with ^{210}Pb. Earth and Planetary Science Letters 14, 442-446.

Koskelo, M.J., Aarnio, P.A. and Routti, J.T. 1981. SAMPO80: Minicomputer program for gamma spectrum analysis with nuclide identification. Computer Physics Communications 24, 11-35.

Ku, T.-L. and Lin, M.-C. 1976. ^{226}Ra distribution in the Antarctic Ocean. Earth and Planetary Science Letters 32, 236-248.

Ledford-Hoffman, P.A., DeMaster, D.J. and Nittrouer, C.A. 1986. Biogenic-silica accumulation in the Ross Sea and the importance of Antarctic continental-shelf deposits in the marine silica budget. Geochimica et Cosmochimica Acta 50, 2099-2110.

Marland, G., Boden, T.A., Andres, R.J., Brenkert, A.L. and Johnston. C. 1999. Global, Regional, and National CO_2 Emissions. In: Trends: A Compendium of Data on Global Change. Carbon Dioxide Information Analysis Center, Oak Ridge National Laboratory, U.S. Department of Energy, Oak Ridge, Tenn., U.S.A.

Gutierrez-Moran, X. and Estrada, M. 2001. Phytoplanktonic DOC and POC production in the Bransfield and Gerlache Straits as derived from kinetic experiments of ^{14}C incorporation. Deep-Sea Research II, this issue.

Neftel, A., Moor, E., Oeschger, H. and Stauffer, B. 1985. Evidence from polar ice cores for the increase in atmospheric pCO_2 in the past two centuries. Nature 315, 45-47.

Nelson, T.M. 1988. Biogenic silica and carbon accumulation in the Bransfield Strait, Antarctica, M.S. Thesis, North Carolina State University, Raleigh NC, 89 pp.

Nittrouer C.A., DeMaster, D.J., McKee, B.A., Custhall, N.H. and Larsen, L.I. 1984. The effect of sediment mixing on ^{210}Pb accumulation rates for the Washington continental shelf. Marine Geology 31, 297-316.

Nozaki, Y., Cochran, J.K., Turekian, K.K. and Keller, G. 1977. Radiocarbon and Pb-210 distribution in submersible-taken deep-sea cores from project FAMOUS. Earth and Planetary Science Letters 34, 167-173.

Palanques, A., Isla, E., Puig, P., Sanchez-Cabeza, J.A. and Masqué, P. 2001. Annual evolution of downward particle fluxes in the Western Bransfield Strait (Antarctica). Deep-Sea Research II, this issue.

Roberts, K.A., Cochran, J.K. and Barnes, C. 1997. ^{210}Pb and $^{239,240}Pu$ in the Norheast Water Polynya, Greenland: particle dynamics and sediment mixing rates. Journal of Marine Systems 10, 401-413.

Rutgers van der Loeff, M.M. and Berger, G.W. 1991. Scavenging and particle flux: seasonal and regional variations in the Southern Ocean (Atlantic sector). Marine Chemistry 35, 553-567.

Sanchez-Cabeza, J.A., Masqué, P. and Ani-Ragolta, I. 1998. Pb-210 and Po-210 analysis in sediments and soils by microwave acid digestion. Journal of Radioanalytical and Nuclear Chemistry 227, 19-22.

Sanchez-Cabeza, J.A., Masqué, P., Ani-Ragolta, I., Merino, J., Frignani, M., Alvisi, F., Palanques, A. and Puig, P. 1999. Sediment accumulation rates in the southern Barcelona continental margin (NW Mediterranean Sea) derived from ^{210}Pb and ^{137}Cs chronology. Progress in Oceanography 441 (1-3), 313-332.

Sanchez-Cabeza, J.A., Ani-Ragolta, I. and Masqué, P. 2000. Some considerations of the ^{210}Pb Constant Rate of Supply (CRS) dating model. Limnology and Oceanography 45 (4), 990-995.

Sarmiento, J.L. and Toggweiler, J.R. 1984. A new model for the role of the oceans in determining pCO_2. Nature 308, 621-624.

Thunell, R. C. and Moore, W.S. 1994. Elemental and isotopic fluxes in the Southern California Bight: a time-series sediment trap study in the San Pedro Basin. Journal of Geophysical Research 99, 875-889.

Tsunogai, S., Kurata, T., Suzuki, T. and Yokota, K. 1988. Seasonal Variation of Atmospheric ^{210}Pb and Al in the Western North Pacific Region. Journal of Atmospheric Chemistry 7, 389-407.

Turekian, K. K., Nozaki, Y. and Benninger, L.K. 1977. Geochemistry of atmospheric radon and radon products. Ann. Rev. Earth and Planetary Science Letters 5, 227-255.

Walsh, J.J., Premuzic, E.T., Gaffney, J.S., Rose, G.T., Harbottle, T., Stoenner, R.W., Balsam, W.L., Betzer, P.R. and Macko, S.A. 1985. Organic storage of CO_2 on the continental slope off the mid-Atlantic Bight, the southeastern Bering Sea and the Peru Coast. Deep-Sea Research 32, 853-883.

Yoon H.I., Han, M.W., Park, B.K., Oh, J.K. and Chang, S.K. 1994. Depositional environment of near-surface sediments, King George Basin, Bransfield Strait, Antarctica. Geo-Marine Letters 14, 1-9.

Zuo, Z., Eisma, D., Gieles, R. and Beks, J. 1997. Accumulation rates and sediment deposition in the northwestern Mediterranean. Deep-Sea Research Part II, 44(3-4), 597-609.

FIGURE CAPTIONS

Figure 1. Bottom sediment sampling stations in the western Bransfield Strait. Water samples at different depths were also collected at station A-6.

Figure 2. Excess ^{210}Pb profiles versus mass accumulation in three cores from the western Bransfield Strait. Error bars denote the uncertainty in the activities determined from counting statistics ($\pm 1\sigma$). Dotted lines indicated the depth to which a Surface Mixed Layer (SML) was estimated to be present.

Figure 3. Organic carbon (OC) profiles versus mass accumulation in three cores from the western Bransfield Strait.

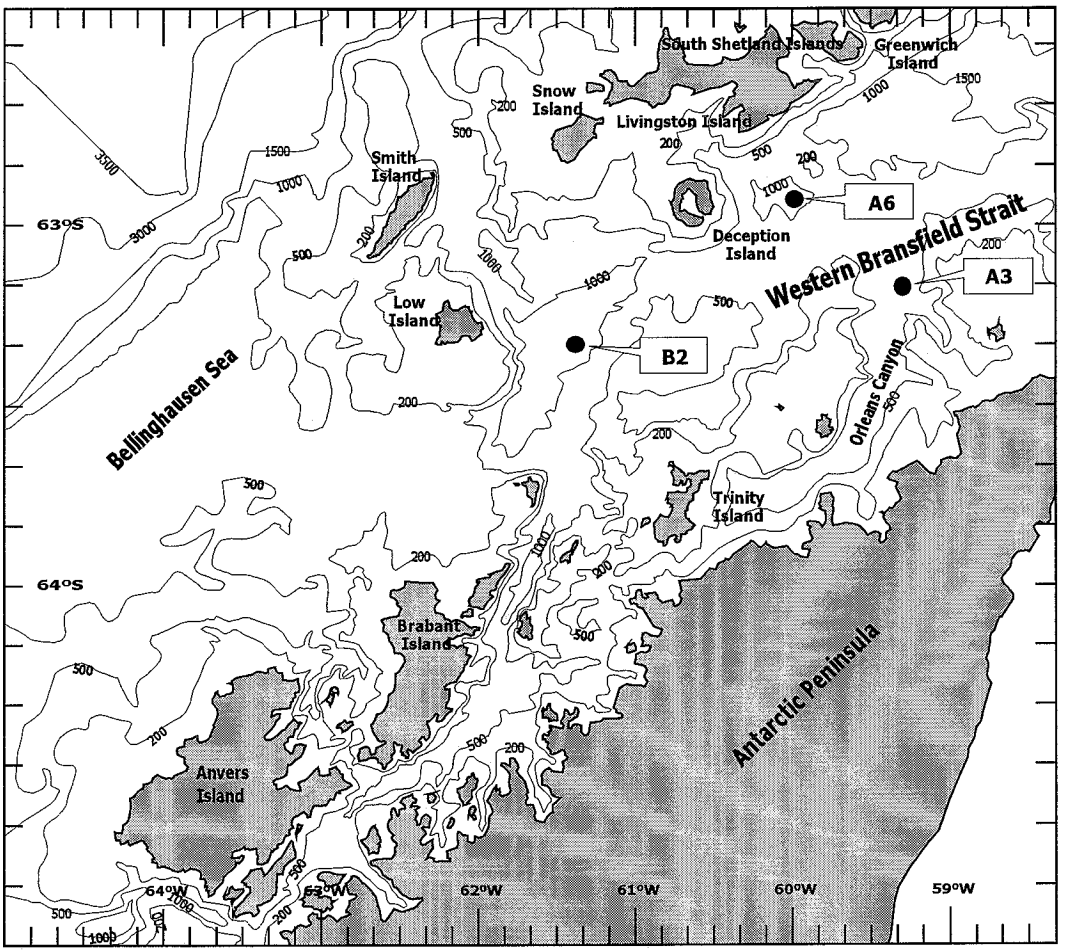
South Shetland Islands
Greenwich Island
Snow Island
Livingston Island
Smith Island
A6
Deception Island
Western Bransfield Strait
A3
Low Island
B2
Bellinghausen Sea
Orleans Canyon
Trinity Island
Brabant Island
Antarctic Peninsula
Anvers Island
63°S
64°S
64°W
63°W
62°W
61°W
60°W
59°W

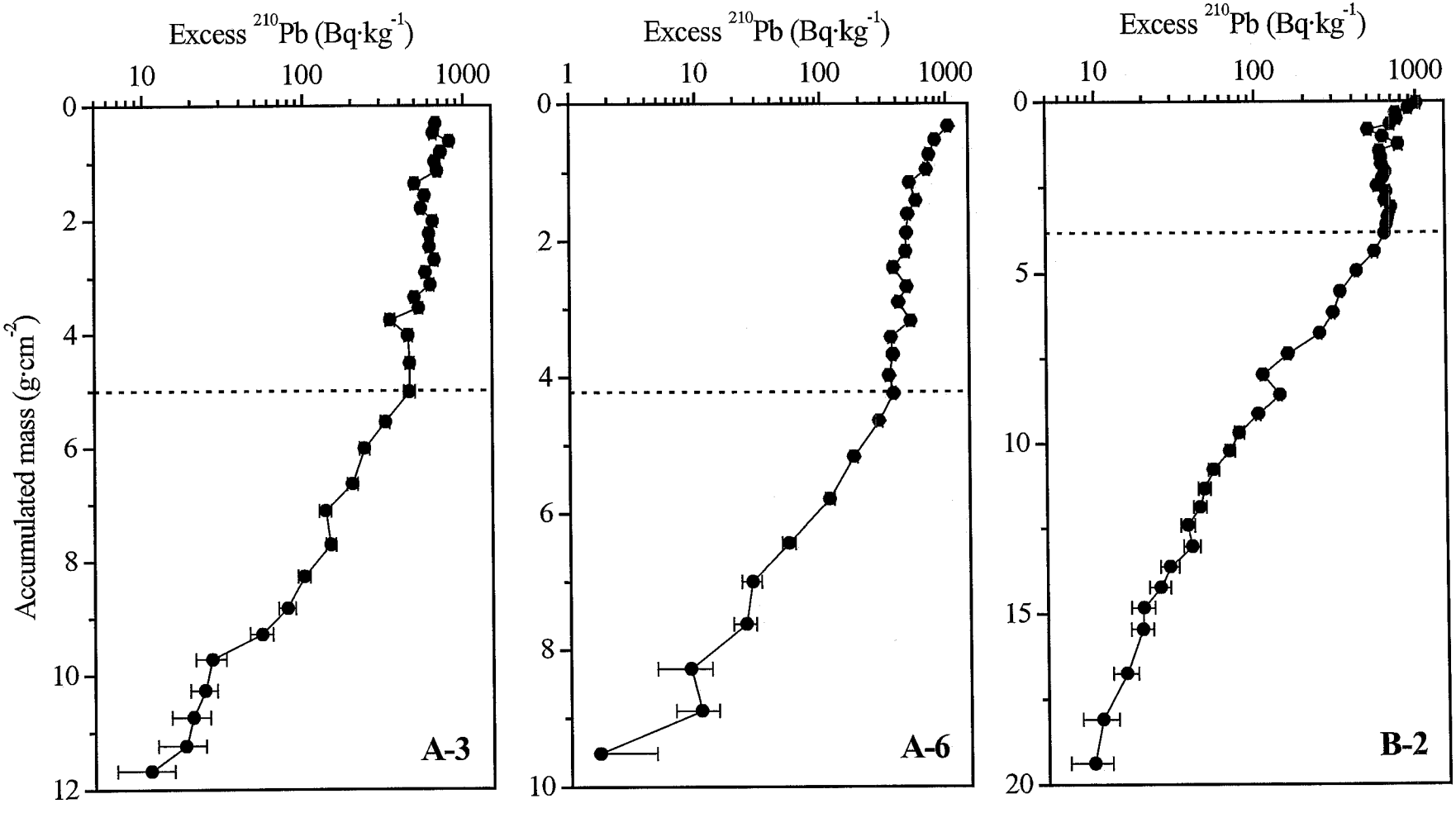
Excess ^{210}Pb (Bq·kg^{-1})
10
100
1000
Accumulated mass (g·cm^{-2})
0
2
4
6
8
10
12
A-3
Excess ^{210}Pb (Bq·kg^{-1})
1
10
100
1000
0
2
4
6
8
10
A-6
Excess ^{210}Pb (Bq·kg^{-1})
10
100
1000
0
5
10
15
20
B-2

OC (%)
0,0
0,5
1,0
1,5
2,0
Accumulated mass (g·cm-2)
A-3
A-6
B-2

TABLES

Table 1. Sediment accumulation rates and main ^{210}Pb results for sediment cores A-3, A-6 and B-2 collected from the western Bransfield Strait.

Core	Location		Depth	Excess ^{210}Pb			Mixed layer		Mean sedimentation rate	
				Surface	Inventory	Flux	Depth (SML)	D_B		
	Latitude S	Longitude W	(m)	(Bq kg^{-1})	(kBq m^{-2})	(Bq m^{-2} y^{-1})	(cm)	(cm^2 y^{-1})	(g cm^{-2} y^{-1})	(mm y^{-1})
A-3	63° 10'	59° 20'	790	676 ± 32	35.9 ± 0.4	1097 ± 13	12	12	0.060 ± 0.003	1.17 ± 0.05
A-6	62° 56'	60° 00'	1066	1046 ± 54	26.3 ± 0.3	803 ± 11	8.5	2	0.0351 ± 0.0014	0.57 ± 0.02
B-2	63° 20'	61° 23'	1135	1010 ± 59	42.3 ± 0.3	1293 ± 11	10	40	0.093 ± 0.003	1.56 ± 0.05

Table 2. ^{210}Pb and ^{210}Po vertical profiles in the water column at station A-6.

Depth	^{210}Pb (Bq m^{-3})			^{210}Po (Bq m^{-3})			$^{210}Po/^{210}Pb$ ratio		
(m)	total	particulate	dissolved	total	particulate	dissolved	total	particulate	dissolved
10	1.72 ± 0.11	0.071 ± 0.006	1.65 ± 0.11	0.99 ± 0.08	0.32 ± 0.02	0.67 ± 0.07	0.57 ± 0.06	4.5 ± 0.5	0.40 ± 0.05
20	1.65 ± 0.11	0.066 ± 0.007	1.58 ± 0.11	1.28 ± 0.10	0.35 ± 0.02	0.92 ± 0.09	0.77 ± 0.08	5.3 ± 0.6	0.58 ± 0.07
150	2.14 ± 0.10	0.116 ± 0.008	2.03 ± 0.10	1.00 ± 0.09	0.16 ± 0.02	0.84 ± 0.09	0.46 ± 0.05	1.4 ± 0.2	0.41 ± 0.05
250	3.09 ± 0.14	0.146 ± 0.014	2.95 ± 0.14	0.60 ± 0.08	0.17 ± 0.02	0.43 ± 0.08	0.19 ± 0.03	1.2 ± 0.2	0.15 ± 0.03
500	2.17 ± 0.11	0.173 ± 0.014	1.99 ± 0.11	1.19 ± 0.10	0.23 ± 0.02	0.96 ± 0.10	0.55 ± 0.05	1.3 ± 0.2	0.48 ± 0.06
650	2.04 ± 0.10	0.21 ± 0.02	1.83 ± 0.09	1.18 ± 0.08	0.27 ± 0.02	0.92 ± 0.08	0.58 ± 0.05	1.3 ± 0.2	0.50 ± 0.05
950	2.11 ± 0.09	0.24 ± 0.02	1.87 ± 0.09	1.20 ± 0.09	0.30 ± 0.03	0.90 ± 0.09	0.57 ± 0.05	1.2 ± 0.2	0.48 ± 0.05
1059	1.98 ± 0.09	0.28 ± 0.02	1.70 ± 0.09	1.16 ± 0.10	0.31 ± 0.02	0.85 ± 0.10	0.59 ± 0.06	1.09 ± 0.12	0.50 ± 0.06

Table 3. OC mean contents and estimates of OC burial rates and burial efficiency.

Core	Mean OC contents			OC/N mean ratio	OC burial rate*	OC burial efficiency
	SML	Below SML	All			
	(%)	(%)	(%)		(g C m^{-2} y^{-1})	(%)
A-3	1.25 ± 0.04	1.12 ± 0.04	1.20 ± 0.07	7.1 ± 0.3	6.7 ± 0.4	~ 80
A-6	0.98 ± 0.11	0.87 ± 0.04	0.94 ± 0.11	7.4 ± 0.5	3.1 ± 0.2	~ 60
B-2	0.87 ± 0.08	0.65 ± 0.04	0.75 ± 0.13	7.0 ± 0.4	6.1 ± 0.4	~ 60

*: Obtained from mean OC contents below the SML and ^{210}Pb derived sediment accumulation rates. These values also represent the percentage of the mean annual primary production (100 g C m^{-2} y^{-1}) that accumulates to the sea bed.

BIOACCUMULATION RECORD AND PALEOCLIMATIC SIGNIFICANCE IN THE WESTERN BRANSFIELD STRAIT. THE LAST 2000 YRS

Maria Ángeles Bárcena[1*], Enrique Isla[2], Ana Plaza[2], José A. Flores[1], Francisco J. Sierro[1], Pere Masqué[3], Joan A. Sanchez-Cabeza[3] and Albert Palanques[2]

[1] Dpto. Geologia, Paleontologia. Fac. Ciencias. Universidad de Salamanca. 37008-Spain.

[2] Instituto Ciencias del Mar (CSIC). Passeig Juan de Borbo s/n. 08039 Barcelona. Spain

[3] Departament de Física, Universitat Autónoma de Barcelona, E-08193 Bellaterra, Spain

Deep-Sea Research II (accepted)

[*] Corresponding author. Fax: +34 923 294514
E-mail address: mbarcena@gugu.usal.es

Bioaccumulation record and paleoclimatic significance in the Western Bransfield Strait. The last 2000 yrs

Maria Ángeles Bárcena[1*], Enric Isla[2], Ana Plaza[2], José A. Flores[1], Francisco J. Sierro[1], Pere Masqué[3], Joan A. Sanchez-Cabeza[3] and Albert Palanques[2]

1- Dpto. Geologia, Paleontologia. Fac. Ciencias. Universidad de Salamanca. 37008-Spain.

2- Instituto Ciencias del Mar (CSIC). Passeig Juan de Borbo s/n. 08039 Barcelona. Spain

3- Departament de Física, Universitat Autónoma de Barcelona, E-08193 Bellaterra, Spain

Received 17 June 1999; received in revised form 6 May 2000; accepted 5 September 2000

---

* Corresponding author. Fax: +34 923 294514
E-mail address: mbarcena@gugu.usal.es

Abstract

Two gravity cores, A-3 and A-6, from the western basin of the Bransfield Strait, Antarctica, were recovered during the BIO Hespérides expedition FRUELA 96. Both cores consist mainly of hemipelagic and laminated muds with black layers rich in sand-sized volcanic ash. Geochemical analyses (TOC and opal), radiometric dating techniques (AMS ^{14}C and ^{210}Pb), and micropaleontological analyses (diatoms) were performed on both cores. AMS analyses on TOC yielded a ^{14}C age older than expected: 3960±50 yr BP for the core top of A-3 and 3410±50 yr BP for A-6. ^{210}Pb analyses revealed that core top age for both gravity cores could be estimated to be about 100 ± 15 years B.P. The results of diatom analyses were related to the sequence of neoglacial events that have occurred over the last two millennia. The abundance patterns of *Chaetoceros* RS, the biogenic silica content, and the number of diatom valves per gram of dry sediment agree with the high productivity values previously reported for the Bransfield Strait waters. The significant reduction in resting spores of the diatom *Chaetoceros* towards the present is interpreted as a reduction in surface productivity. Trend differences between *Chaetoceros* resting spore abundance and TOC contents are explained in terms of organic matter preservation. Diatom communities from the Bransfield Strait did not play an important role in the global CO_2 cycle during cold periods. Bio and geochemical changes have an overprinted high frequency cyclicity at about 200-300 yr, which might be related to the 200 -yr solar cycle.

Keywords: Diatoms, Geochemistry, Paleoceanography, Neoglacial events, CO_2 cycle, Holocene, Bransfield Strait, Antarctica.

1. Introduction

Coastal waters near the Antarctic Peninsula support highly productive ecosystems where large phytoplankton blooms develop throughout the austral spring and summer. These areas may therefore represent key sites where the *biological pump* transports organic carbon below the mixed layer and consequently sequesters atmospheric CO_2 (Sarnthein *et al.*, 1987; Broecker, 1981, 1982 a, b). Between 10 and 50 % of photosynthetically-fixed carbon may be released by respiratory processes (Aristegui *et al.*, 1996) and respiration rates vary with water temperature, phytoplankton populations and oceanographic fronts and currents (Aristegui and Montero, 1995).

The sedimentary record affords long term information about all these processes occurring in the water column. Siliceous microfossil assemblages, together with carbon and opal stored in the sediments, may offer an efficient tool for identifying paleoclimatic and paleoceanographic changes.

The Holocene is characterised by alternating periods of neoglacial expansions and subsequent ice retreats. Evidence for these events, among others, has been found in Antarctic marine sediments by Leventer and Dunbar (1988), Leventer *et al.* (1996) and Bárcena *et al.* (1998). The Bransfield Strait is unusually sensitive to fine-scale climatic and

oceanographic changes, as well as to changes in local tidewater glaciers. Previous studies have shown that the general trend for the last several thousand years is a reduction in primary productivity towards the present (Bárcena *et al.*, 1998). Overprinted on this trend is a high frequency oscillation in diatom abundance, which correlates with an approximately 250 year cyclicity recognised in the magnetic susceptibility, organic carbon and siliceous microfossil data (Leventer *et al.*, 1996; Bárcena *et al.*, 1998). These changes in primary productivity over time are mainly controlled by sea-ice conditions and surface water stability and stratification. Since over the years vertical fluxes are restricted to a short period, the austral summer (Wefer *et al.*, 1988), paleoclimatic evolution may help to study and better understand the biogenic cycles involved.

The present work addresses the sedimentary record during the last 2000 years and its relationship with paleoceanographic evolution, such as changes in primary production, fluctuations in the sea-ice cover, and surface hydrodynamics. This evolution is studied on the basis of the diatom assemblages preserved in the sedimentary column and biogenic silica and organic carbon stored in the sediments. The relatively high accumulation rates found in this area, estimated as higher than 1,1 cm yr^{-1}, afford sufficient resolution to study the effects of climatic changes over the last two millennia. Study of the changes that took place in the past may help to better understand the carbon cycle and to evaluate the possible causes of present climatic-oceanographic changes. The distinction between the anthropogenic action and natural mechanisms should be studied and verified over longer periods of time.

2. Physical environment

The Bransfield Strait is a semi-enclosed basin limited to the south by the Antarctic Peninsula and the South Shetland Islands to the north. The Bransfield Basin is composed of three separate subbasins which are separated from one another by sills about 500 m deep. The western subbasin is relatively shallow (1000 m) and irregularly shaped and lies south and west of Livingston and Deception Islands. The central subbasin is located south of Robert, Nelson and King George Islands, is deeper (2000 m), and has a more regular shape than the others. The eastern subbasin extends north-eastward, is narrower than the central subbasin, and reaches a depth of 2500 m (Fig. 1).

Surface circulation in the Bransfield Strait has two primary sources, the Bellingshausen and Weddell Sea waters (paths are shown in figure 1). Waters coming from the Bellingshausen Sea are warm and relatively fresh while waters from the Weddell Sea are colder and denser (García et al, this issue). The circulation patterns of both water currents have been described in detail by Gordon and Nowlin (1978) and Gomis et al (this issue). These currents meet in the vicinity of Trinity Island and form a front of biological significance (Amos, 1987). Advection of Circumpolar Deep Water (CDW) into the Strait from the Drake Passage is prevented by the presence of shallow sills. Gordon and Nowlin (1978) suggested in situ deep and bottom water formation through the sinking of surface waters of the Bransfield Strait. These waters are characterised by having lower temperatures and salinity, higher oxygen and lower nutrient concentrations (García et al,

this issue) in comparison with deep waters outside the basin. Additionally, the vertical distribution of these parameters also indicates that there are significant differences within each subbasin (Gordon and Nowlin, 1978).

Seasonal sea-ice distribution in the Bransfield Strait is complex. The information concerning annual sea-ice coverage points to a winter maximal extent of 57°S off the Antarctic Peninsula, but in summer the Bransfield Strait is a completely ice-free area (N.O.C., 1985). Surface productivity, and hence the settling of biogenic particles into sediments, is restricted to periods in which the area is ice-free, reaching one of the highest rates in the entire Southern Ocean being reached during this period (Wefer *et al.*, 1988; Abelmann and Gersonde, 1991; Varela et al, this issue). Since surface productivity is linked to sea-ice coverage, biogenic particle sedimentation, especially that of diatoms and radiolarians, is also directly related to seasonal variations in the sea-ice extension. Using time-series sediment traps, Abelmann and Gersonde (1991) showed that particle flux peaks occur during periods with open water conditions, whereas during sea-ice coverage the vertical flux of siliceous organisms from the surface waters is extremely low.

The sediment distribution in the Bransfield Strait is related to the morphology of the sea floor. Jeffers and Anderson (1990) reported that the characteristic sediments of the deepest basin consists of three main components. In order of abundance, these are: biosiliceous material, mostly diatoms; a terrigenous component, quartz silt; and volcanic ashes.

The sedimentary basins in the Bransfield Strait act as a giant sediment trap as they collect large amounts of resuspended material, resulting in high sedimentation rates for the basin sediments (Abelmann and Gersonde, 1991). Comparison of these high sedimentation rate values with those estimated from surface production indicates that the accumulation rate of opal in the Bransfield Strait accounts for only about half of the surface production rate (DeMaster *et al.*, 1987). Alteration of the assemblages of siliceous organisms during vertical transport through the water column is due to mechanical breakdown by grazing zooplankton and to dissolution (Gersonde and Wefer, 1987). Another factor responsible for the composition of the biosiliceous signal in the sediment record is the input of laterally-transported material (Abelmann and Gersonde, 1991).

3. Material and Methods

Gravity cores A-3 and A-6 were recovered during the RV Hespérides cruise FRUELA 96 in the Bransfield Basin at 63°10.06'S/59°18.13'W and 62°54.71'S/59°58.21'W, respectively (Fig. 1). Water depths at the core locations are 810 m (A-3) and 1066 m (A-6). Samples were taken every 5 cm for Total Organic Carbon (TOC) and opal analyses. For micropaleontological studies, core A-3 was sampled every 10 cm and every 5 cm for A-6. Gravity cores are composed of "basin floor sediments", following the terminology of Jeffers and Anderson (1990), with biosiliceous material as the main component.

Total Organic Carbon was determined by sediment dried at 40°C until constant weight and homogenised in an agate grinder, and analysed on a LECO CN-2000 resistance furnace at 1050°C. All the C was converted into CO_2 and passed through an IR cell, converted to voltage, and transformed into carbon concentration (LECO CN-2000 instruction manual, 1994).

Opal was determined using the alkaline extraction method of Mortlock and Froelich (1989) (extraction of silica in 2M Na_2CO_3 at 85°C for 5h) and measured by molibdate-blue spectrometry. Opal percentages were calculated as the percentages of Si extracted into the solution multiplied by 2.4, which includes the average water content of diatomaceous silica (about 10 % water = SiO_2 x 0.4 H_2O). The contribution of silica from coexisting clay minerals was evaluated by the double leaching method (Eggimann *et al.*, 1980). The relative precision of this technique is 5% and was estimated including sediment inhomogenities and analytical errors. Opal percentages were computed on a dry weight basis without corrections for dry sea-salt contents.

Cleaning of the sediment samples and preparation of permanent mounts for light microscopy were accomplished according to the randomly distributed microfossils method outlined in Bárcena and Abrantes (1998). Absolute diatom numbers were determined from microscope slides with randomly distributed microfossils. For the counting routines, a Leica DMLB microscope at 1000X magnification was used. A counting of at least 100 valves of non-dominant taxa per sample was performed using the method of Schrader and Gersonde (1978). In general, more than 600 valves per sample were considered (Tables 2 and 3). The preservation status of the fossil assemblage was estimated by visual examination.

Chronological Assessment

Two different radiometric dating techniques, ^{14}C AMS and excess ^{210}Pb, were used to determine the age of the sediments. The ^{14}C AMS technique on Total Organic Carbon was carried out to estimate sedimentation rates as well as the age of the cores investigated. The conventional radiocarbon ages of three stratigraphic levels in core A-3 and two in core A-6 were analysed (table 1, Fig. 2).

The ^{14}C AMS methodology yielded a ^{14}C age older than expected: 3960±50 yr BP for the top of core A-3 and 3410±50 yr BP for the top of core A-6 (Table 1). Despite this, the ages indicate a sedimentation rate of 208 cm kyr^{-1} for A-3 and 80,7 cm kyr^{-1} for A-6, in agreement with the accumulation rates given in the literature, which range between 60 to 490 cm kyr^{-1} (DeMaster *et al.*, 1987; Van Enst, 1987; Laban and De Groot, 1986; Venkatesan and Kaplan, 1987; Harder *et al.*, 1992; Domack *et al.*, 1993; Scherer and Leventer, 1995; Leventer *et al.*, 1996; Bárcena *et al.*, 1998) (Fig. 2). These values also agree with the expected high accumulation rate in the area, which receives sediment inputs from the Antarctic Peninsula and is under the influence of the highly productive oceanic front between the cold Weddell Sea water and the warmer water from Gerlache and Bellingshausen areas.

The ^{14}C core top ages of 3960±50 yr BP for the top of core A-3 and 3410±50 yr BP for the top of core A-6 are in the same order as those obtained by Harden *et al.* (1992), Domack *et al.* (1993), Leventer *et al.* (1996) and Bárcena *et al.* (1998) in the Antarctic Peninsula area. Radiocarbon dating of Antarctic sea water samples and marine organisms has yielded anomalously old ages of up to 2860 years (Stuiver *et al.*, 1981). Two main factors have been considered to explain the old age of the sediments: the large and regionally variable reservoir effect of 1200-1400 yrs. (Stuiver *et al.*, 1981; Berkman *et al.*, 1998; Ingólfsson *et al.*, 1998) and possible inputs of older eroded sediment, transported by currents or by ice rafting. Nevertheless, the input of terrestrial organic matter can be considered insignificant since most of the organic matter present in the sediments is derived from primary local producers (Venkatesan and Kaplan, 1987).

Due to its half-life (22.3 years), ^{210}Pb is a suitable indicator of to which extent the tops of the gravity cores are recovered during sampling operations and can thus be used to attribute an age to the surface material (Goldberg and Koide, 1962; Nozaki *et al.*, 1977). ^{210}Pb concentrations were determined at each cm-depth along the top 20 cm of gravity cores A-3 and A-6, following the methodology described in Sánchez-Cabeza *et al.* (1998). Excess ^{210}Pb (taken as the difference between total ^{210}Pb and supported ^{210}Pb) in core A-3 was detected on the top 3 cm, while in core A-6 it was only present in the first section (0-1 cm). Surface excess ^{210}Pb concentrations were 26 ± 6 Bq$\sum$kg-1 and 31 ± 4 Bq$\sum$kg-1 for cores A-3 and A-6 respectively. The fact that excess ^{210}Pb was still detectable indicates that the tops of both gravity cores are not older than approximately 100 years. ^{210}Pb data from the gravity cores was also compared to the ^{210}Pb profiles obtained from multicore samples collected at stations A-3 and A-6 and described in a companion paper by Masqué *et al.* (this issue), in which ^{210}Pb is used to determine recent mixing and sediment accumulation rates in the area. It is concluded that in both cases the top 20-22 cm of gravity cores A-3 and A-6 were lost during collection of the samples. Therefore, by using the mean sediment accumulation rates derived from the multicores, the age of the surface of both gravity cores can be estimated to be about 100 ± 15 years.

The chronological criteria used in this work allowed us to determine the age of the sediments recorded in the A-3 and A-6 gravity cores. We constructed an age model based on a combination of ^{210}Pb determination, radiocarbon ages for the evaluation of sedimentation rates, and biogenic evidence. Thus, we considered that the core tops of both cores could have an age of around 100± 15 yrs B.P. The base of cores A-3 and A-6, as extrapolated from linear sedimentation rates (208 cm $kyr^{-1}$and 80,7 cm kyr^{-1} respectively), were estimated at 2050 and 1760 yrs B.P. respectively.

Furthermore, the regional reservoir effect, as well as local processes, has a strong influence on stratigraphic control. Fine scale differences in sedimentation rates cannot be determined owing to limitations in radiocarbon dating and may undergo some variations. Assuming this, we tentatively link the variations in the organic components of the sediments as well as the siliceous microfossil abundance patterns of A-3 and A-6 to climatic changes (Fig. 5). Based on glacier advances and retreats, ^{14}C anomalies in tree-rings and in marine sediments from the Antarctic Peninsula region, four cold episodes have been recognised in the last two millennia (Wigley and Kelly, 1990; Leventer *et al.*,

1996 and Bárcena *et al.*, 1998). Following the terminology and discussion employed by Bárcena *et al.* (1998), we have recognised the last 4 neoglacial episodes recorded for the last 2000 years (neoglacial stages 4, 3, 2 and 1).

4. Results

Diatoms

A large number of diatom valves per gram of dry sediment was observed in both cores, ranging between $2x10^7$ to $14.7x10^8$ (Fig. 3 a and d). The diatoms are in general well preserved. The diatom assemblages are were dominated by *Chaetoceros* resting spores (RS) (73-89 % of the total) (Tables, 2 and 3). The sea-ice taxa, grouping species such as *Fragilariopsis curta* (V. Heurck) Hasle, *F. cylindrus* (Grun.) and *F. vanheurckii* Hasle, were also frequent (up to 9.48 % of the total) (Tables, 2 and 3). These species are commonly found in the sea-ice, and are dominant in the ice-edge blooms as well as in the marginal ice zone (Gersonde 1986; Leventer *et al.* 1996). *Thalassiosira antarctica* Comber/*T. scotia* Fryxell and Hoban in the spore stage (RS), was another component of the assemblage. This species group has been related to oceanic conditions from the Weddell and Scotia Sea (Klöser, 1990; Abelmann and Gersonde, 1991; Bárcena and Flores 1991; Bárcena and Francés, 1998). Species such as *F. kerguelensis* (O'Meara) Hasle, *Rhizosolenia* spp., *Proboscia alata* (Brightwell) Sundstrom, *Thalassiosira gracilis* (Karsten) Hustedt, *T. gravida* Cleve, *T. oliverana* (O'Meara) Sournia, *T. trifulta* Fryxell and *T. tumida* (Jan.) Hasle are also common components of the fossil diatom assemblage.

The species distributions in both cores as well as their relative abundance are in agreement with the values compiled from the literature for the Bransfield Strait area (Gersonde and Wefer, 1987; Wefer *et al.*, 1988, 1990; Abelmann and Gersonde, 1991; Leventer, 1991; Zielinski, 1993; Zielinski and Gersonde, 1997; Bárcena *et al.*, 1998; Varela *et al.*, this issue).

For core A-3, the total abundance of diatom valves/g of dry sediment tends to decrease towards the top. Maximum values are recorded between a core depth of 370-320 cm and between 220-180 cm, while minima are recorded in the uppermost 50 cm (Fig. 3 a). The abundance pattern of *Chaetoceros* RS follows a similar trend to that observed for total diatom valve abundance. The most striking features were three minima recorded at the base, between 265 and 215 cm, and in the uppermost 100 cm. These minima are bounded by strongly marked maxima (Fig. 3 b). The abundance pattern of the sea-ice taxa group follows the opposite behaviour to that observed for *Chaetoceros* RS. Maximum values in *Chaetoceros* RS correspond to minima in sea-ice taxa (Fig. 3 b and c).

The diatom patterns of cores A-3 and A-6 are remarkably similar given the missing core top for A-6 as well as differences in sedimentation rates. In core A-6 two maxima in *Chaetoceros* RS were seen to coincide with minima in sea-ice taxa (Fig. 3 e and f).

Total Organic carbon and biogenic opal

The mean values in TOC contents were 1.03 % for A-3 (Fig. 4 a) and 0.47 % for A-6 (Fig. 4 c). These values are not high for marine sediments but are typical of siliceous muds in the Bransfield strait area (De Master *et al.*, 1987; Yoon *et al.*, 1994; Leventer *et al.*, 1996; Fabrés *et al.*, 1997 and Bárcena *et al.* (1998). The mean biogenic opal content was higher in A-3 (21.66 %) (Fig. 4 b) than in A-6 (13.2 %) (Fig. 4 d).

The TOC record of A-3 showed three clear minimum values: at 35, 230 and 405 cm. The lowest values of biogenic silica were seem at almost the same depths: 35, 235 and 410 cm. Whereas the biogenic silica minimum followed a decreasing trend, the TOC minimum follows an increasing tendency (Fig. 4). Both variables followed the same trend in core A-6, with TOC peaks at 15 and 45 cm. The maximum in biogenic silica was recorded at 35 cm, separated by a minimum at 30 cm.

The overall patterns of the organic components were well correlated and the most striking features were seen for all three components: TOC, biogenic opal content, and absolute abundance of diatom valves (Tables 2 and 3, Fig. 3 and 4). Biogenic opal contents and diatom valve abundances tend to decrease towards the core top, while TOC mainly increases upwards.

Despite the foregoing, sequences can be identified in the organic components along both cores. In the 360-230 cm and 210-40 sections of core A-3, two main sequences, increasing for TOC and decreasing for biogenic opal, can be identified. These two sequences are bounded by a strongly marked minimum. The concentration logs point to a series of more or less symmetric cycles, with a thickness between 25 and 50 cm. This cyclicity can also be observed in core A-6 (Fig. 4).

5. Discussion

Three well-documented maxima in sea-ice taxa seem to be quite closely related to the neoglacial events described for the Holocene, such as those observed by Bárcena *et al.* (1998). Gersonde (1986) related the presence of sea-ice taxa in surface sediments to areas strongly influenced by sea-ice. Gersonde *et al.* (1992) used this group as a tracer of the sea-ice extent. Zielinski and Gersonde (1997) and Bárcena and Francés (1998) report a coincidence between the winter sea-ice extent in the Weddell and Scotia Seas and the northern boundary of significant occurrences of sea-ice taxa in surface sediments. Abelmann and Gersonde (1991) observed that during periods of sea-ice coverage the vertical flux of biosiliceous particles decreases significantly, both for sea-ice taxa and for the rest of the planktonic communities, and that maximum values of sea-ice taxa are reached during and after ice retreat. Thus, we interpret that the higher values of sea-ice taxa in cores A-3 and A-6 may be related to a more extensive sea-ice cover, both spatially and seasonally. Furthermore, maxima of sea-ice taxa are related to lower values for *Chaetoceros* RS, indicating a reduced, but not arrested, interannual diatom production.

We therefore considered that sea-ice taxa can be used as a good indicator of colder atmospheric conditions involving sea-ice advances and larger sea-ice coverage. Warmer interneoglacial periods are characterised by increases in *Chaetoceros* RS and by decreases in sea-ice taxa. Warmer temperatures and shorter sea-ice coverage periods would have been re-established in the Bransfield Basin during interneoglacial stages and the paleoceanographic regime might have been similar to that observed today.

The abundance patterns of *Chaetoceros* RS in cores A-3 and A-6 agree with the high productivity values reported for the Bransfield Strait waters (Varela *et al.*, this issue). In general, high concentrations in *Chaetoceros* RS in the fossil record have been interpreted as indicating very high primary productivity, and this notion is supported by experimental and field data (Leventer *et al.*, 1996). Sedimentologically, a massive sedimentation of *Chaetoceros* RS may have had a determinant effect on the high accumulation rates of biogenic silica in Antarctic sediments (DeMaster *et al.*, 1987; Bareille *et al.*, 1991). From our data, it seems reasonable to speculate that during the time period recorded in A-3 and A-6 surface productivity in the Bransfield Basin would have been higher than today (Fig. 5). A similar pattern in *Chaetoceros* RS abundance has been observed by Scherer and Leventer (1995), Leventer *et al.* (1996) and Bárcena *et al.* (1998), who reported a reduction in primary siliceous productivity as from the last two thousand years to today. In this sense, Leventer *et al.* (1996) linked enhanced productivity to warmer atmospheric conditions, upper water column stratification, and nutrient depletion. The inferred reduction in paleoproductivity towards the present, together with a progressive increase in sea-ice taxa seems to indicate a cooling trend (Bárcena *et al.*, 1998).

Additionally, the abundance of *Chaetoceros* RS along the core runs parallel to the biogenic silica content and the number of diatom valves per gram of dry sediment, indicating a reduction in paleoproductivity (Fig. 5). Nevertheless, TOC tends to increase towards the present. TOC decays towards the top of neoglacial periods (Fig. 5), where sea-surface paleoproductivity is expected to have been minimum. Also, at the base of the neoglacial events TOC shows slight increases, probably due to preservational factors. Trend differences between *Chaetoceros* RS abundance and TOC contents could be explained in terms of organic matter preservation and/or in terms of the resuspension of sediments from the continental shelf into the Bransfield Basin, as was observed by Bárcena *et al* . (1998) and widely discussed by Fabrés *et al* (2000). As reported by Bárcena *et al.* (1998), higher TOC contents during cold periods could be a response to preservation rather than to annual production. Jordan and Pudsey (1992) and Leventer *et al.* (1996) postulated that a high planktonic cell density occurs close to receding ice edges as a result of the sea-ice melting and increased upper water stratification. This large amount of biogenic material will flocculate and descend rapidly as aggregates to the sea floor, preventing organic matter dissolution. Moreover, Broecker and Peng (1989) considered that during cold periods the nutrient content of Antarctic surface waters could have been similar or even higher than today. Because the extent of nutrient utilisation is larger, the O_2 content of deep Antarctic waters would have been two times lower (Broecker and Peng, 1989). If the scenario proposed by the former authors is true, oxidation of the organic matter would have been lower. During neoglacial events, a similar situation would have occurred over a short time: a large amount of biogenic particles produced and precipitated during sea-ice melting

would have preserved the organic matter an the sea floor. Although during warmer episodes surface productivity is higher for the entire season, the settling of biogenic particles might have been less concentrated and hence more exposed to oxidation.

During the Holocene there has been a number of globally quasi-synchronous neoglacial periods lasting for centuries and followed by warmer periods. The most recent neoglacial period was the Little Ice Age (Lamb, 1965). On a 1000-year time scale, climatic changes are associated with Milankovitch orbital effects. However, during the Holocene a century time scale has been imposed on neoglacial events. The world-wide occurrence of neoglacial events has meant that a primary astronomical forcing has been invoked to account for climate changes. Several studies have proposed a solar forcing with a 200 year rhythm, related to reductions in sunspot activity (Wigley and Kelly, 1990; Leventer *et al.*, 1996). The changes have been well correlated with ^{14}C anomalies (^{14}C maxima correspond to temperature minima) (Wigley and Kelly, 1990). This 200 year periodicity has also been observed in marine sediments around the Antarctic peninsula area by Domack *et al.* (1993), Scherer and Leventer (1995), Leventer *et al.* (1996), and Bárcena *et al.* (1998). Although in the cores of the study area it is not possible to give a precise correction for the ^{14}C ages, the three data points do allow the evaluation of the cyclicity record. The assumption of a constant sedimentation rate between each age control-point and application of Blackman-Tuckey spectral analysis routines (Analyses series 1.1, Paillard *et al.*, 1996) on different records (diatom, TOC, and biogenic silica) result in a period of 200 to 300 years, using a Barllett Window type, a confidence interval of 80%, and a band width of 0,002 (Fig. 6). Cross spectral analyse of the valves per gram of dry sediment, the sea-ice taxa and biogenic silica content demonstrate their spectral density coherence at the 80 and 90% levels, respectively, at 250 years. Also, a cross spectral analysis of the biogenic silica content and sea-ice taxa and TOC contents shows their coherence at the 89 and 80% level, respectively, at 250 years.

This period is in concordance with those observed by Domack *et al.* (1993), Scherer and Leventer (1995), Leventer *et al.* (1996), and Bárcena *et al.* (1998). Such periodicity could be related to the effect of the 200-yr solar cycle on the oceanic system. Little is known about solar influence on these restricted oceanic areas from the Antarctic Continent, but the observed variations in planktonic communities, organic matter and biogenic silica in the same time range as solar cycles does suggest a possible influence.

Atmospheric CO_2 versus Bransfield Strait paleoproductivity

Changes in atmospheric pCO_2 represent an important factor inducing changes in global climate and ice-volumes. Atmospheric pCO_2 fluctuations are largely controlled by the exchange rates of CO_2 between the atmosphere and ocean reservoirs, an exchange which depends strongly upon the primary productivity of plankton in oceanic upwelling regions, where the carbon/carbonate ratio is high (Sarnthein *et al.*, 1987). Additionally, variations in the efficiency with which nutrients are used by marine biota could provide the necessary link between high-latitude insolation and CO_2. If all the nutrients in surface waters were used by biota, the marine biological pump would operate at maximum efficiency, drawing

carbon from the atmosphere to the deep ocean and lowering the level of atmospheric CO_2 (Broecker, 1981, 1982 a, b). However, in coastal Antarctic waters, Estrada *et al.* (1992) and Aristegui *et al.* (1996) considered that the respiratory processes of phytoplankton communities could be responsible for the loss of more than 50% of photosynthetically-fixed carbon. These authors also considered that microbial respiration and air-breathing top predators may return high amounts of photosynthetically-fixed carbon to the atmosphere, causing these coastal Antarctic ecosystems to be inefficient as a carbon sink.

The ice core data suggest that CO_2 levels rose significantly during warmings in the past. On a 100-year time scale, Barnola *et al.* (1995) recorded pre-industrial fluctuations in atmospheric CO_2 over the last millennium. Numerous data point to an intensification in upwelling and therefore enhanced paleoproductivity during glacial periods (Sarnthein *et al.*, 1987 and 1988; Abrantes, 1991 a and b). However, there is also evidence of low paleoproductivity during glacial periods in areas such as the North Atlantic and Catalonian-Balearic Seas (Villanueva, 1996; Flores *et al.*, 1997). Villanueva (1996) addressed the possibility of low sea-surface paleoproductivity as a consequence of sea-ice coverage, which prevents the normal growth of planktonic communities. For the Bransfield Strait area there is also evidence of lower paleoproductivity during Holocene neoglacial periods (Bárcena *et al.*, 1998). During today's winters, sea-ice coverage restricts surface productivity (Wefer *et al.*, 1988; Abelmann and Gersonde, 1991), which is directly related to seasonal variations in sea-ice extents.

As revealed by the data obtained in cores A-3 and A-6 (TOC, biogenic silica content and the diatom assemblage), maximum values in paleoproductivity are recorded during the warmest periods. On comparing our data to the CO_2 curve described by Barnola *et al.* (1995) for the last millennium (Fig. 5), minimum CO_2 atmospheric values are seen to be related to minimum in TOC, biogenic silica, diatoms and *Chaetoceros* RS.

From a global point of view, glacial periods and enhanced paleoproductivity in upwelling regions may rule the drawdown of total CO_2 by photosynthesis (Sarnthein *et al.*, 1987). Nevertheless, for specific areas, such as the Bransfield Strait, diatom communities do not play an important role in the global CO_2 cycle during cold periods. In this sense, Broecker and Peng (1989) proposed that decreases in CO_2 occurring during glacial times is a consequence of an increase in the alkalinity of Antarctic surface waters. They argued that this change is not only due to biologic pump efficiency, but is also a natural consequence of the glacial demise of the Atlantic's conveyor (North Atlantic Deep Water).

6. Conclusions

The ^{14}C AMS chronology yielded an older age than expected for cores A-3 and A-6: 3960±50 yr BP and 3410±50 yr BP, respectively. The ^{14}C AMS ages of both cores display a downcore pattern that indicates a linear sedimentation rate of 208 $cmkyr^{-1}$ for A-3, and 80,7 $cmkyr^{-1}$ for A-6. The last two millennia have been recorded in core A-3 (2050 years), while in core A-6 the last 1760 years are documented, in agreement with the accumulation rates given in the literature. The ^{210}Pb profiles obtained from the uppermost 20 cm of cores

A-3 and A-6 permit the conclusion that in both cases the top 20-22 cm were lost during the coring process. Therefore, both core top ages can be estimated to be about 100 ± 15 years.

The variations in the diatom fossil assemblages recorded in cores A-3 and A-6 respond to known neoglacial events for the Holocene. Changes in species composition reflect changes in environmental conditions, including water masses and sea-ice coverage.

The abundance patterns of *Chaetoceros* RS, biogenic silica contents and the number of diatom valves per gram of dry sediment are consistent with the high productivity values reported for the Bransfield Strait waters. The general trend indicates a reduction in paleoproductivity. Past surface productivity in the Bransfield Basin was higher than today.

Trend differences between *Chaetoceros* RS abundance and TOC contents could be explained in terms of organic matter preservation into the Bransfield Strait.

Bio and geochemical changes have an overprinted high frequency cyclicity at about 200-300 yr, possibly related to the 200 -yr solar cycle.

Diatom assemblages from the Bransfield Strait did not play an important role in the global CO_2 cycle during cold periods.

Acknowledgements

The authors would like to thank Dr. A. Leventer, Dr. R. Anadón and two anonymous referees for their valuable reviews and suggestions. N. Skinner is acknowledged for revising the English version of the m.s, and J. Roncero for technical assistance. Funding for this work was generously supported by the Spanish projects ANT94-1010, ANT94-0277, PB95-0927-C02-00, MAR96-1781-CO2-01 and CLI98-1002-CO2.

REFERENCES

Abelmann A. and R. Gersonde (1991) Biosiliceous particle flux in the Southern Ocean. *Marine Chemistry* **35**, 503-536.

Abrantes F. (1991 a) Increased upwelling off Portugal during the last glaciation: Diatom evidence. *Marine Micropaleontology* **17**, 285-310.

Abrantes F. (1991 b) Variability of upwelling off NW Africa during the latest Quaternary: Diatom evidence. *Paleoceanography* **6** (4), 431-460

Amos A. F. (1987) RACER: Physical oceanography of the western Bransfield Strait. *Antarctic Journal of Unites States*, **22**, 137-140.

Aristegui J. and M.F. Montero (1995) The relationship between community respiration and ETS activity in the ocean. *Journal of Plankton Research*, **17**, 1565-1573.

Aristegui, J., M.F. Montero, S. Ballesteros, G. Basterretxea and K. van Lenning (1996) Planktonic primary production and microbial respiration measured by ^{14}C assimilation and dissolved oxygen changes in coastal waters of the Antarctic Peninsula during austral summer: implications for carbon flux studies. *Marine Ecology Program Series*, **132**, 191-201.

Bárcena M. A. and J.A. Flores (1991) Distribución y microtafonomía de las asociaciones de diatomeas de sedimentos superficiales en el sector Atlántico del Océano Antártico. *Revista Española de Paleontología*, **5**, 53-6.

Bárcena M. A. and F. Abrantes (1998) Evidence of a high-productivity area off the coast of Málaga from studies of diatoms in surface sediments. Marine *Micropaleontology*, **35**, 91-103.

Bárcena M.A. and G. Francés (1998) Análisis multivariante Modo-Q realizado sobre diatomeas de sedimentos superficiales del Mar de Escocia y Shetland del Sur. Campaña "Antártida 8611". *Thalassas*, **13**, 59-72.

Bárcena, M.A., R. Gersonde, S. Ledesma, J. Fabrés, A.M. Calafat, M. Canals, F.J. Sierro and J.A. Flores (1998) Record of Holocene glacial oscillations in the Bransfield Basin as revealed by siliceous microfossil assemblages. *Antarctic Science*, **10** (3), 269-285.

Bareille G., M. Labracherie, L. Labeyrie, J.J. Pichon and J.L. Turon (1991) Biogenic silica accumulation rate during the Holocene in the southeastern Indian Ocean. *Marine Chemistry*, **35**, 537-551.

Barnola, J.M., M. Anklin, J. Porcheron, D. Raynaud, J. Schwander and B. Stauffer (1995) CO_2 evolution during the last millennium as recorded by Antarctic and Greenland ice. *Tellus*, **47B**, 264-272.

Berkman, P. A., J. T. Andrews, S. Björk. *et al.* (1998) Circumantarctic coastal enviromental shifts during the late Quaternary reflected by emerged marine deposits. *Antarctic Science*, **10**, 345-362.

Broecker, W.S. (1981) Glacial to interglacial changes in ocean and atmosphere chemistry. *In* A. Berger (Ed.), Climatic variations and Variability: Facts and Theories, 111-121.

Broecker, W.S. (1982 a) Glacial to interglacial changes in ocean chemistry. *Prog. Oceanogr.*, **11**, 151-197.

Broecker, W.S. (1982 b) Ocean chemistry during glacial times. *Geochim. Cosmochim. Acta*, **46**, 1689-1705.

Broecker, W.S. and T. H. Peng. The cause of the glacial to interglacial atmospheric CO2 Change: A polar alkalinity hypothesis. *Global Biogeochemical Cycles*, **3** (3), 215-239.

DeMaster D. J., T.M. Nelson, C.A. Nittrouer and S.L. Harden (1987) Biogenic silica and organic carbon accumulation in modern Bransfield Strait sediments. *Antarctic Journal of the United States*, **22**, 108-110.

Domack E.W., T.A. Mashiotta and L.A. Burkley (1993) 300-year cyclicity in organic matter preservation in Antarctic fjord sediments. The Antarctic Paleoenvironment: A perspective on Global Change. *Antarctic Research Series*, **60**, 265-271.

Eggimann, D. W., F.T. Manheim and P. R. Betzer (1980) Dissolution and analysis of amorphous silica in marine sediments. *Journal of sedimentary Petrology* **50** (1), 215-225.

Enst Van J. W. A. (1987) 210Pb activities in the Bransfield Strait, additional proof of hydrothermal activity (Abstract). *Fifth International Symposium on Antarctic Earth Sciences*, Cambridge, 166.

Estrada, M., R. Martinez, and S. Mathod (1992) Respiratory electron transport activity in plankton of the Weddell and Scotia Seas during the late spring and early summer: relationships with other biological parameters. *Polar Biology*, **12**, 35-42.

Fabrés, J., A.M. Calafat, M. Canals, G. Francés, M. A. Bárcena, S. Ledesma, and J. A. Flores (1997) Identificación de procesos sedimentarios en la Cuenca de Bransfield (Antártida Occidental). *Boletin de la Real Sociedad Española de Historia Natural* **93** (1-4),85-94.

Fabrés, J., A.M. Calafat, M. Canals, M. A. Bárcena and J. A. Flores (2000). Bransfield Basin fine grained sediments: Late Holocene sedimentary processes and oceanographic and climatic conditions. *Holocene* **10** (5).

Flores J.A., F.J. Sierro, G. Francés, A. Vazquez and I. Zamarreño (1997) The last 100,000 years in the western Mediterranean: sea surface water and frontal dynamics as revealed by coccolithophores. *Marine Micropaleontology* **29**, 351-366.

García, M. A., C. Castro, A. F. Rios, M. D. Doval, G. Rosón, D. Gomis and O. López (this issue) Water masses and distribution of physico-chemical properties in the western Bransfield Strait and Gerlache Strait during austral summer 1995/1996.

Gersonde R. (1986) Siliceous microorganisms in sea-ice and their record in sediments in the Southern Weddell Sea (Antarctica). *Proc. 8th Symp. Living and Fossil Diatoms*, 549-566.

Gersonde R. and Wefer G. (1987) Sedimentation of biogenic siliceous particles in Antarctic waters from the Atlantic sector. *Marine Micropaleontology*, **11**, 311-332.

Gersonde R., A. Abelmann and V. Spiess (1992) Pliocene-Pleistocene paleoceanography in the Weddell Sea - Siliceous microfossil evidence. *In*: Bleid, J and J. Thiede (Eds.) *Geological History of the Polar Oceans: Artic versus Antarctic*, 729-759.

Goldberg E.D. and M. Koide (1962) Geochronological studies of deep-sea sediments by the ionium-thorium method. *Geochimica et Cosmochimica Acta* **26**, 417-450.

Gomis D. , M. A. García, O. López and A. Pascual (this issue) Quasy-geostrophic 3-D circulation and water mass transport in the western Bransfield Strait during austral summer 1995-96.

Gordon A L. and W.D. Nowlin (1978) The basin waters of the Bransfield Strait. *Journal of Physical Oceanography*, **8**, 258-264.

Harden S.L., D.J. DeMaster, and C.A. Nittrouer (1992) Developing sediment geochronologies for high-latitude continental shelf deposits: a radiochemical approach. *Marine Geology*, **103**, 69-97.

Ingólfsson, Ó, C. Hjort, P. A. Berkman, S. Björk, E. Colhoun, I. D. Goodwin, B. Hall, K. Hirakawa, M. Melles, P. Möller and M. L. Prentice (1998). Antarctic glacial history

since the Last Glacial Maximum: an overview of the record on land. *Antarctic Science*, **10**, 326-345.

Jeffers J. D. and J.B. Anderson (1990) Sequence stratigraphy of the Bransfield Basin, Antarctica: Implications for Tectonic History and Hydrocarbon Potential. *In* B. S. John (Ed), Antarctica as an exploration frontier-Hydrocarbon potential, Geology, and hazards. *AAPG Studies in Geology*, **31**, 13-29.

Jordan, R.W. and C. J. Pudsey (1992) High-resolution diatom stratigraphy of Quaternary sediments from the Scotia Sea. *Marine Micropaleontology*, **19**, 201-237.

Klöser H. (1990) Distribution of microplankton organisms north and west of the Antarctic Peninsula according to changing ecological conditions in autumn. *Reports on Polar Research*, **77**, 1-255.

Lamb H. H. (1965) The early medieval warm epoch and its sequel. *Palaeogeography, Palaeoclimatology, Palaeoecology*, **1**, 13-37.

Leco CN-2000 (1994) Instruction manual. Edited in: St. Joseph, Michigan.

Leventer A. (1991) Sediment trap diatom assemblages from the northern Antarctica Peninsula region. *Deep-Sea Research*, **38** (8/9), 1127-1143.

Leventer A., E. Domack, S.E. Ishman, S. Brachfeld, C.E. McClennen and P. Manley (1996) Productivity cycles of 200-300 years in the Antarctic Peninsula region: Understanding linkages among the sun, atmosphere, oceans, se ice, and biota. *Geological Society of America Bulletin*, **108** (12), 1626-1644.

Leventer A. and R.B. Dunbar (1988) Recent diatom record of McMurdo Sound, Antarctica: Implications for history of sea-ice extent. *Paleoceanography*, **3** (3), 259-274.

Masqué, P., E. Isla, J. A. Sanchez-Cabeza, A. Palanques, J. M. Bruach, P. Puig and J. Guillén (this issue) Sediment accumulation rates and carbon fluxes to bottom sediments at the western Bransfield Strait Basin (Antarctica).

Mortlock, R. A. and P. N. Froelich (1989) A simple method for the rapid determination of biogenic opal in pelagic marine sediments. *Deep Sea Research*, **36** (9), 1415-1426.

N.O.C. (1985) Naval Oceanography Command Detachment, Asheville. *Sea Ice Climatic Atlas*, **1**: Antarctic.

Nozaki Y., J.K.Cochran, K.K. Turekian and G. Keller (1977) Radiocarbon and Pb-210 distribution in submersible-taken deep-sea cores from project FAMOUS. *Earth and Planetary Science Letters* **34**, 167-173.

Paillard, D., L. Labeyrie, and P. Yiou (1996) Macintosh program performs time-series analyses. *Eos Trans, AGO*, **77**, 379.

Sánchez-Cabeza J.A., P. Masqué, and I. Ani-Ragolta (1998) Pb-210 and Po-210 analysis in sediments and soils by microwave acid digestion. *Journal of Radioanalytical and Nuclear Chemistry* **227**, 19-22.

Sarnthein M., K. Winn, and R. Zahn (1987) Paleoproductivity of oceanic upwelling and the effect on atmospheric CO_2 and climatic changes during deglaciation times. *In* Berger W.H. and L.D. Labeyrie (Eds.) *Abrupt Climate Change*, Proceedings of the NATO/NSF A. R. W. Symposium at Biviers/Grenoble 1985, 311-337.

Sarnthein M., K. Winn, J.C. Duplessy and M.R. Fontugne (1988) Global variations of surface Ocean Productivity in Low and Mid Latitudes: Influence on CO_2 reservoirs of the Deep Ocean and Atmosphere during the last 21,000 years. *Paleoceanography* **3**, 361-399.

Scherer R. and A. Leventer (1995) Holocene diatom productivity along the northern Antarctic Peninsula (Abstract). *5th International Conference on Paleoceanography*, Halifax, Canada.

Schrader H.J. and R. Gersonde (1978) Diatoms and silicoflagellates. *In* Zachariasse W. J. *et al.* (Eds.), Micropaleontological counting methods and techniques- an exercise on an eight metres section of the lower Pliocene of Capo Rossello, Sicily. *Utrecht Micropaleontological Bulletins*, **17**, 129-176.

Stuiver M., G.H. Denton, T.J. Hughes and J.L. Fastook (1981) History of the marine ice sheet in west Antarctica during the last glaciation: A working hypothesis. *In*: Denton G. and T. Hughes (Eds.) *The Last Great Ice Sheets*, Wiley, New York, 319-436.

Varela M., E. Fernandez and P. Serret (this issue). Size-fractionated phytoplankton biomass and primary production in the Gerlache and South Bransfield Straits (Antarctic Peninsula) in the austral summer 95-96.

Venkatesan M. I. and I.R. Kaplan (1987) The lipid geochemistry of Antarctic marine sediments: Bransfield Strait. *Marine Chemistry*, **21**, 347-375.

Villanueva J. (1996) Estudi de les variacions climàtiques y oceanogràfiques a l'Atlantic Nord durant els últims 300.000 anys mitjançant l'anàlisi de marcadors moleculars. Ph.D. dissertation, Ramon Llull University, 186 pp.

Wefer G., G. Fischer, D.K. Fütterer and R. Gersonde (1988) Seasonal particle flux in the Bransfield Strait, Antarctica. *Deep-Sea Research*, **35** (6), 891-898.

Wefer G., G. Fischer, D.K. Fütterer, R. Gersonde, S. Honjo, S. and D. Ostermann (1990) Particle sedimentation and productivity in Antarctic waters of the Atlantic Sector. *In:* Bleil, U. and Thiede, J. *Eds.* Geologic History of the Polar Oceans: Arctic versus Antarctic. *NATO ASI Ser. C*, **308**, 363-379.

Wigley T. M. L. and P. M. Kelly (1990) Holocene climatic change, ^{14}C wiggles and variations in solar irradiance. *Phil. Trans. R. Soc. Lond.*, **330**, 547-560.

Yoon, H.I., Han, M.W., Park, B.K., Oh, J.K. and Chang S.K. (1994) Depositional environment of near-surface sediments, King George Basin, Bransfield Strait, Antarctica. *Geo-Marine Letters*, **14**, 1-9.

Zielinski U. (1993) Quantitative estimation of paleoenviromental parameters of the Antarctic Surface Water in the Late Quaternary using transfer functions with diatoms. *Reports on Polar Research*, **126**, 148 p.

Zielinski U. and R. Gersonde (1997) Diatom distribution in Southern Ocean surface sediments (Atlantic sector): Implications for paleoenvironmental reconstructions. *Palaeogeography, Palaeoclimatology, Palaeoecology*, **129**, 213-250.

Figure Legends

Figure 1: A-3 and A-6 core locations in the Bransfield Basin (closed circles). Open circles indicate locations for Gebra-1 and Gebra-2, cores previously studied by BÁRCENA *et al.* (1998).

Figure 2: Age- depth curve for cores A-3. and A-6. See also Table-1.

Figure 3: Diatom abundance (% of assemblage) in cores A-3 and A-6-. Thicker line indicates a three-point smoothing.

Figure 4: Total organic carbon and biogenic silica values obtained from cores A-3 and A-6. Thicker line indicates a three-point smoothing.

Figure 5: Diatom and geochemical data in cores A-3 and A-6 and their relationships to Holocene neoglacial episodes. The neoglacial events recognised have been labelled with numbers (1 to 4) after BÁRCENA *et al.* (1998). Maximum values in paleoproductivity are recorded during the warmest periods. Comparison of sedimentological data with the CO_2 curve produced by BARNOLA *et al.* (1995) for the last millennium. Minimum CO_2 atmospheric values are related to minima in TOC, biogenic silica, diatoms, and *Chaetoceros* RS.

Figure 6: Spectral analysis of Biogenic silica content and TOC content calculated for core A-3. The signal has a statistically significant (80% level) concentration of variance in a ≈ 250 yr periodicity. The x-axis shows periodicity in years. The y-axis shows spectral density (logarithmic scale). Blackman-Tuckey spectral analysis routines were done according Analyses series 1.1 routines (PAILLARD *et al.*, 1996).

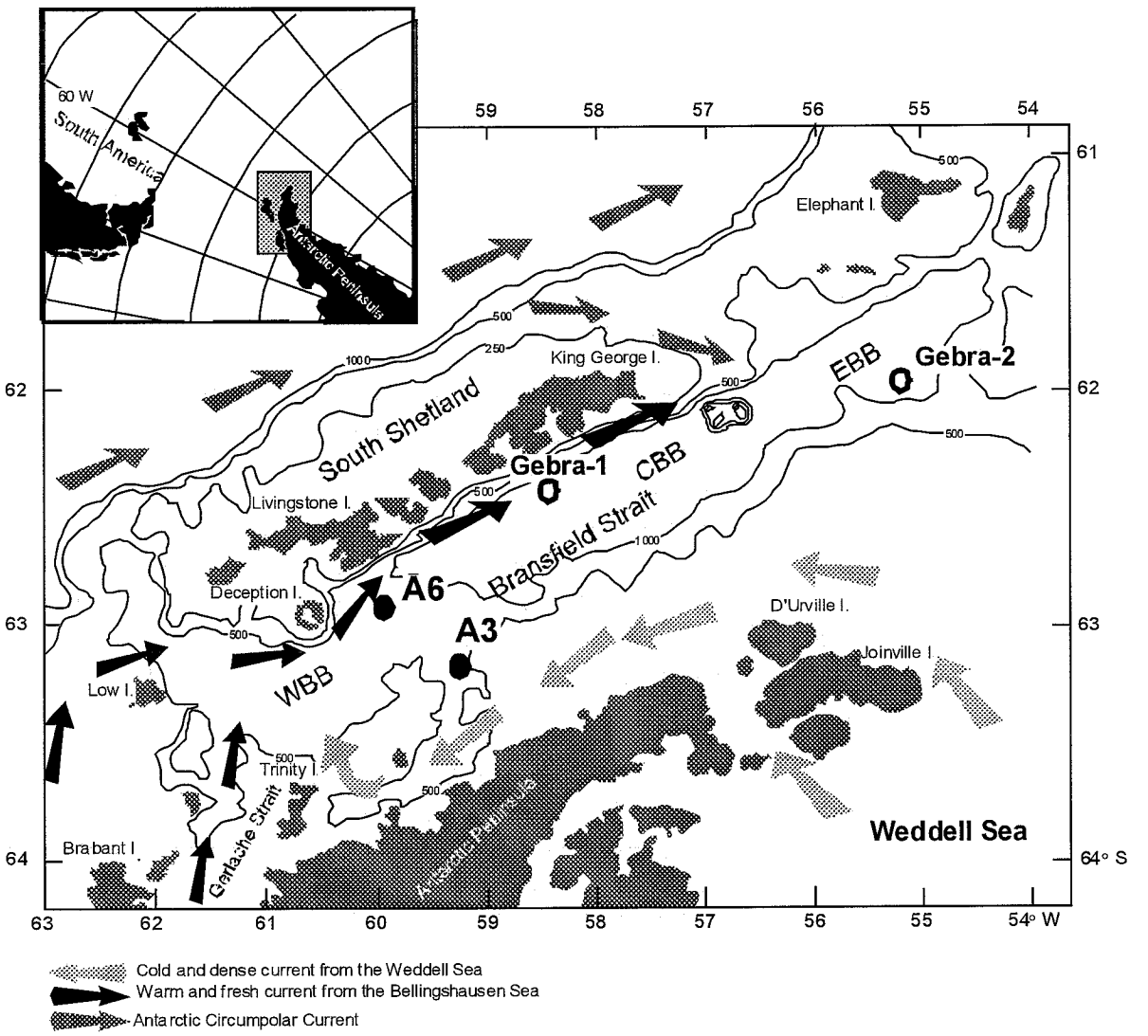
60 W
South America
Antarctic Peninsula
59
58
57
56
55
54
61
62
63
64
64° S
63
62
61
60
59
58
57
56
55
54° W
Elephant I.
King George I.
South Shetland
Livingstone I.
Deception I.
Low I.
Brabant I.
Trinity I.
Gerlache Strait
Antarctic Peninsula
D'Urville I.
Joinville I.
Weddell Sea
Gebra-1
Gebra-2
A6
A3
EBB
CBB
WBB
Bransfield Strait
500
1000
250
Cold and dense current from the Weddell Sea
Warm and fresh current from the Bellingshausen Sea
Antarctic Circumpolar Current

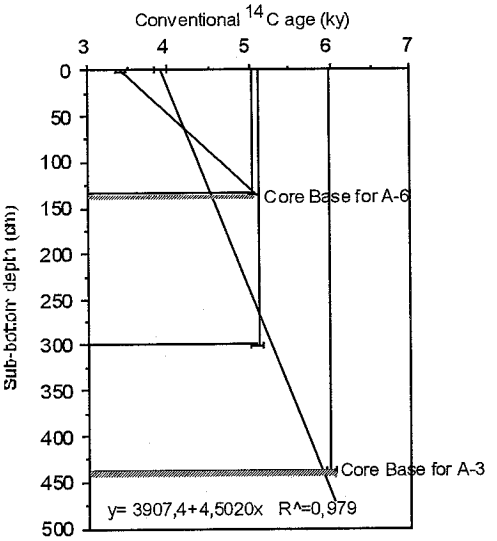
Conventional 14C age (ky)
3
4
5
6
7
0
50
100
150
200
250
300
350
400
450
500
Sub-bottom depth (cm)
Core Base for A-6
Core Base for A-3
y= 3907,4+4,5020x R^=0,979

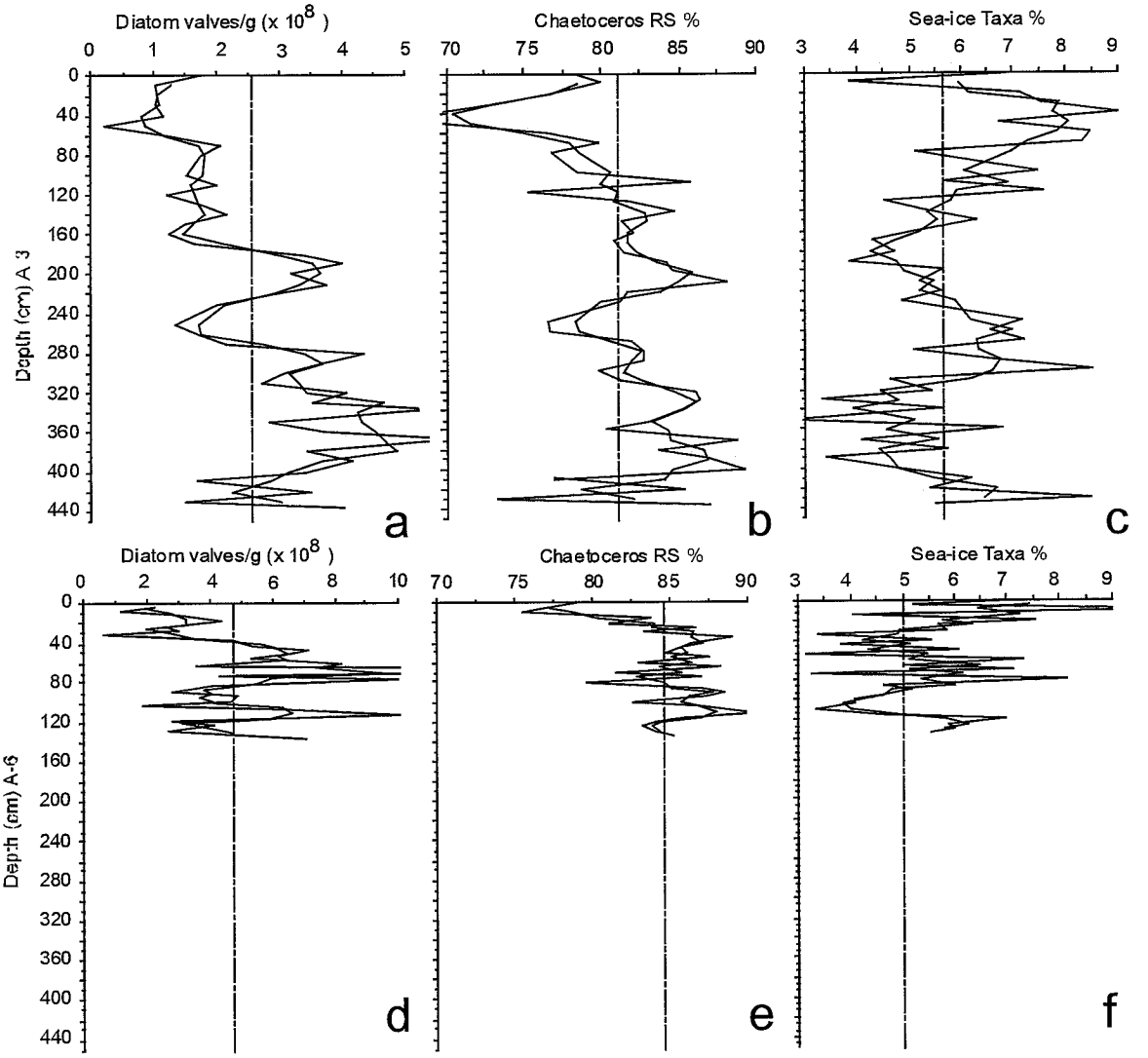
Diatom valves/g (x 10^8)
Chaetoceros RS %
Sea-ice Taxa %
Depth (cm) A-3
a
b
c
Diatom valves/g (x 10^8)
Chaetoceros RS %
Sea-ice Taxa %
Depth (cm) A-6
d
e
f

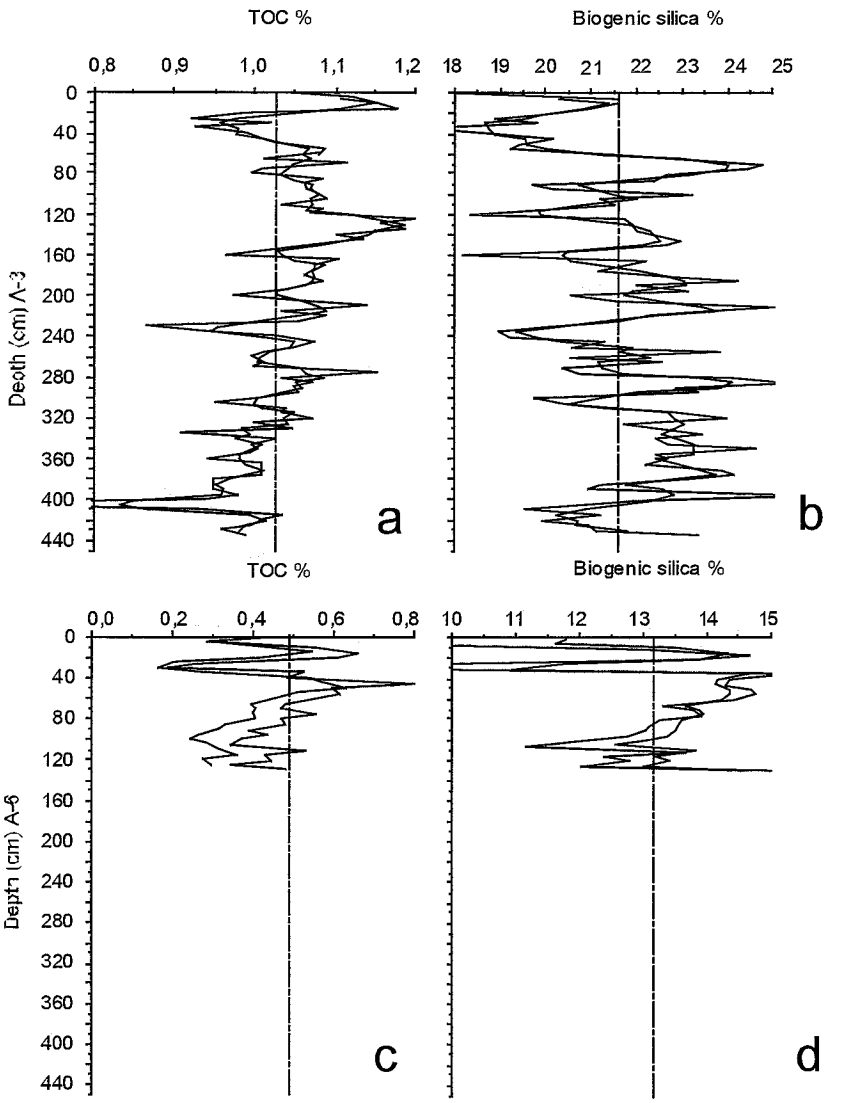
TOC %
Biogenic silica %
0,8 0,9 1,0 1,1 1,2
18 19 20 21 22 23 24 25
0 40 80 120 160 200 240 280 320 360 400 440
Depth (cm) A-3
a
b
TOC %
Biogenic silica %
0,0 0,2 0,4 0,6 0,8
10 11 12 13 14 15
0 40 80 120 160 200 240 280 320 360 400 440
Depth (cm) A-6
c
d

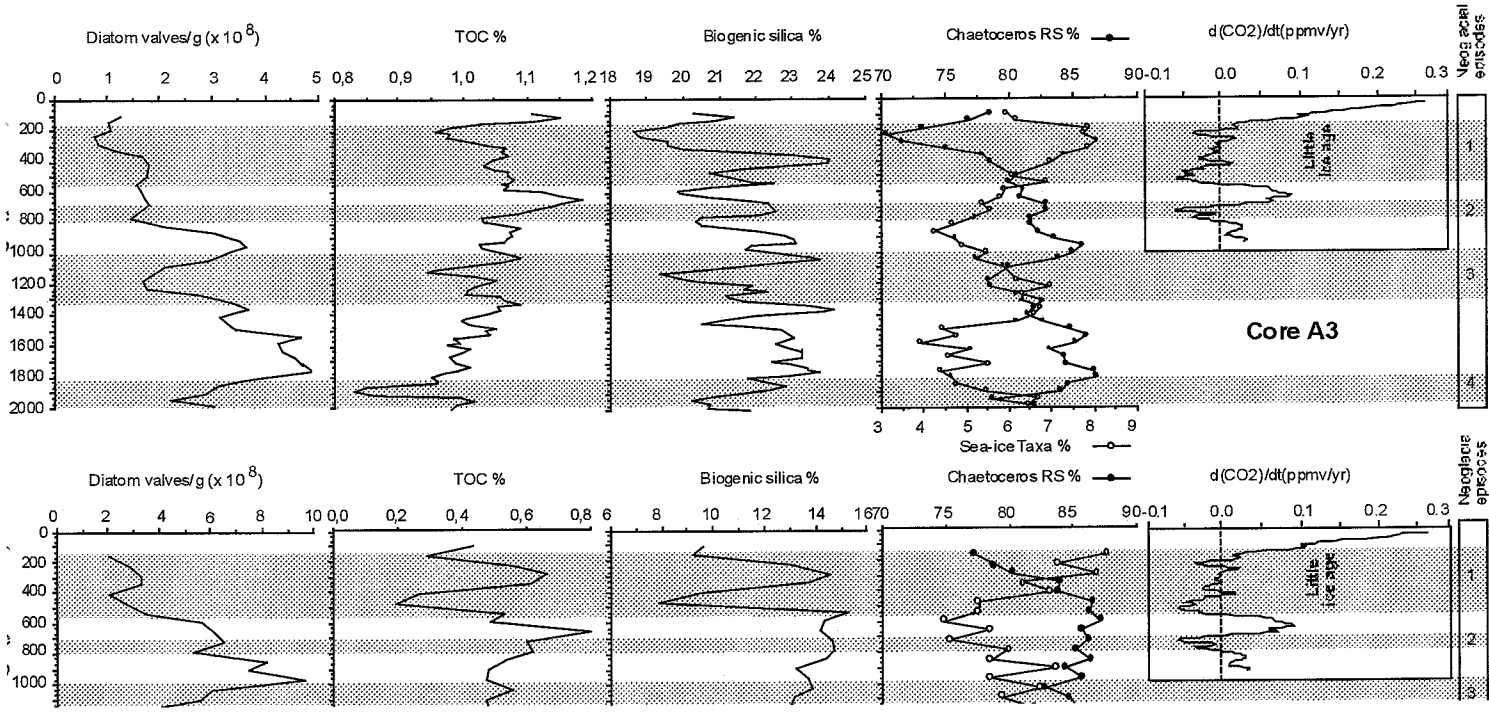
Diatom valves/g (x 10 8)
TOC %
Biogenic silica %
Chaetoceros RS %
d(CO2)/dt(ppmv/yr)
Neoglacial episodes
Little ice age
Core A3
Sea-ice Taxa %
Diatom valves/g (x 10 8)
TOC %
Biogenic silica %
Chaetoceros RS %
d(CO2)/dt(ppmv/yr)
Neoglacial episodes
Little ice age

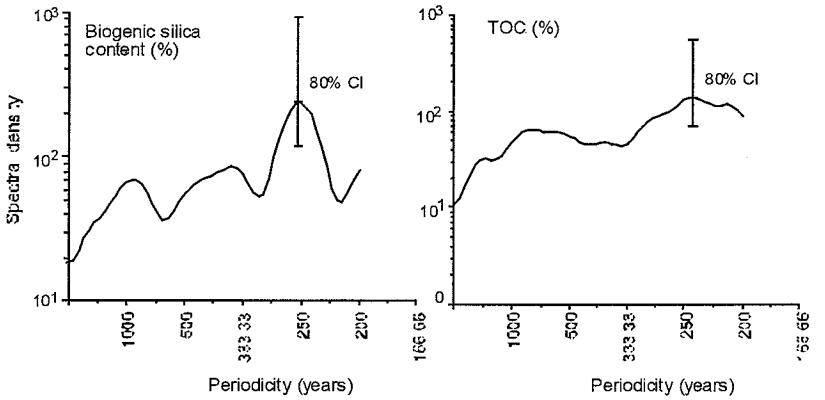
Biogenic silica content (%)
80% CI
Spectra density
Periodicity (years)
TOC (%)
80% CI
Periodicity (years)

Core	Section (cm)	^{14}C Conventional age (yrs)
A-3	0	3960±50
	300	5090±50
	437	5990±50
A-6	0	3410±50
	134	5070±50

DIATOMS				GEOCHEMIC					
Sample	Valves/gr	*Chaetoceros*	Sea-ice	Sample	TOC %	Biogenic	Sample	TOC %	Biogenic
0	1,74	78,52	6,93	0	1,05	17,69	215	1,04	23,53
10	1,04	80,15	3,83	5	1,12	21,57	220	1,09	22,32
20	1,06	76,92	7,12	10	1,15	21,59	225	1,06	21,58
30	1,03	73,54	7,52	15	1,18	20,94	230	0,87	19,9
40	1,15	69,28	9,01	20	0,99	19,86	235	0,94	18,94
50	0,21	68,63	6,75	25	0,92	18,89	240	1,03	19,24
60	1,24	76,78	8,45	30	1,02	19,8	245	1,08	21,29
70	2,07	80,00	8,33	35	0,93	17,32	250	1,05	20,59
80	1,75	77,02	5,11	40	0,99	19,13	255	1,01	23,83
100	1,53	78,63	7,44	45	1,01	20,13	260	1,00	20,52
110	1,99	85,91	5,64	50	1,03	19,39	265	1,01	22,57
120	1,22	75,54	7,58	55	1,09	19,22	270	1,00	20,36
130	1,75	82,02	4,53	60	1,08	21,5	275	1,15	20,76
140	2,15	84,94	5,29	65	1,01	22,81	280	1,04	24,1
150	1,49	81,58	6,30	70	1,12	24,73	285	1,07	25,32
160	1,25	82,28	5,04	75	1,01	24,46	290	1,05	22,86
170	1,66	81,08	4,28	80	1,00	22,66	295	1,06	23,38
180	3,42	81,63	4,71	85	1,09	22,39	300	1,00	19,75
190	4,00	84,39	3,83	90	1,06	19,7	305	0,95	20,45
200	3,18	84,75	5,65	95	1,06	20,13	310	1,04	21,32
210	3,74	88,24	5,19	100	1,08	23,23	315	1,03	22,82
220	2,99	81,92	5,60	105	1,09	21,21	320	1,07	23,95
230	1,99	81,38	4,84	110	1,04	21,53	325	1,00	21,73
250	1,35	76,79	7,14	115	1,09	19,63	330	1,05	
260	1,72	76,90	6,55	120	1,07	18,33	335	0,91	23,44
270	2,17	82,08	7,20	125	1,21	21,74	340	1,03	22,46
280	4,35	82,90	5,10	130	1,16	21,92	345	1,00	22,71
290	3,66	82,90	6,63	135	1,19	21,97	350	1,00	24,64
300	3,06	80,00	8,50	140	1,10		355	1,00	22,45
310	2,72	81,39	4,62	145	1,14	22,94	360	0,94	22,71
320	4,07	86,22	5,41	150	1,09	22,63	365	1,01	22,21
330	3,55	86,51	3,31	155	1,03	20,73	370	1,01	23,89
340	6,36	85,47	5,62	160	0,96	18,17	375	1,01	24,14
350	2,85	83,53	2,83	165	1,11	22,22	380	0,95	23,23
360	3,73	80,52	6,76	170	1,08		385	0,95	21,22
370	7,02	88,86	4,08	175	1,08	21,15	390	0,95	20,95
380	3,43	83,90	5,71	180	1,06	22,85	395	0,98	25,49
390	4,16	87,05	3,39	185	1,09	24,22	400	0,94	21,97
400	3,43	89,51	4,81	190	1,06	22	405	0,62	
410	1,70	77,12	6,17	195	1,04	23,13	410	0,93	19,54
420	3,51	85,52	5,39	200	0,97	20,55	415	1,04	21,21
430	1,50	73,44	8,48	105	1,07	21,55	420	1,01	19,95
437	4,02	87,19	5,47	210	1,14	25,41	425	1,00	20,96
							430	0,96	21,13
							435	0,99	23,37

DIATOMS				GEOCHEMIC	
Sample (cm)	valves/gr (x 10^8)	*Chaetoceros* RS%	Sea-ice Taxa %	TOC %	Biogenic silica %
0	2,16	79,16	6,62	0,43	9,59
5	1,08	76,95	2,6	0,29	9,24
10	2,95	75,36	9,48	0,56	13,01
15	4,34	83,86	3,44	0,66	14,64
20	2,51	81,2	6,96	0,61	13,75
25	2,92	86,79	5,68	0,26	9,54
30	0,54	83,55	5,81	0,19	7,85
35	4,66	89,19	3,01	0,53	15,33
40	5,30	86,44	5,27	0,49	14,33
45	7,01	85,81	3,02	0,8	14,26
50	6,08	85,3	5,86	0,6	14,68
55	6,40	87,68	3,24	0,62	14,73
60	3,50	83,13	6,79	0,54	14,43
65	14,7	88,43	4,48	0,48	13,29
70	4,23	81,68	6,77	0,47	13,75
75	9,93	87,12	3,11	0,56	13,9
80	3,93	79,93	7,99	0,47	13,23
85	2,76	87,24	4,25	0,48	13,08
90	4,76	87,97	4,77	0,39	13,03
95	4,63	87,55	4,29	0,44	12,73
100	1,79	82,68	3,89	0,37	12,07
105	6,28	87,14	3,83	0,34	11,12
110	10,8	90,78	3,06	0,53	13,64
115	2,70	85,71	4,19	0,43	12,36
120	4,06	84,22	6,16	0,45	12,79
125	2,61	83,33	4,9	0,35	12,03
130	4,72	84,18	5,32	0,48	15,07
133	6,95	85,43	5,26		